



**THE EFFECTS OF B CELL DEPLETION ON  
BONE TURNOVER IN RHEUMATOID  
ARTHRITIS**

---

by  
**Gillian Wheeler**

DISSERTATION

Submitted in partial fulfilment of the requirements for the degree of Doctor of  
Philosophy

Musculoskeletal Research Group  
Institute of Cellular Medicine  
The Medical School  
Newcastle University

**MAY 2016**



## Abstract

Rheumatoid arthritis (RA) is the most prevalent inflammatory joint disease. B cells have a role in both the pathogenesis of RA and the regulation of bone cell activity. Depletion of B cells by the anti-CD20 antibody rituximab (RTX) is a highly effective treatment of RA, which is now well established. However, the role of B-cells in bone turnover is controversial. The aim of this thesis was to investigate the effects of B cell depletion on bone turnover in RA. It is postulated that prolonged B cell depletion in patients with RA may have a beneficial effect on the bone loss that would otherwise be expected in active disease. Furthermore, this affect may be direct through modulation of osteoclastogenesis or indirect through attenuation of systemic inflammation and increased physical activity. Preliminary results in forty-six RA patients six months after RTX indicated that there was a significant suppression in bone resorption accompanied to a lesser degree by an increase in bone formation. However, in a second prospective cohort of forty-five RA patients treated with RTX over twelve months, bone mineral density (BMD) fell at the femur sites, but was maintained at the lumbar spine and forearm. There was a significant increase in bone formation, but no significant change in bone resorption or osteocyte markers. Additionally, the effects of RTX on bone turnover were influenced by vitamin D status, gender and menopausal state. Results of *in vitro* osteoclastogenesis with peripheral blood mononuclear cells (PBMCs) isolated from the blood of twelve self-reported healthy volunteers; indicated that *in vitro* B cell depletion via magnetic-activated cell sorting (MACS), significantly increased osteoclast formation. In contrast, PBMCs isolated from the blood of five RA patients, up to twelve months post B cell depletion with RTX, resulted in decreased osteoclast formation using the same standardised culture system. In summary, the results of the pilot study showed that B cell depletion significantly decreased bone resorption and increased bone formation in RA, possibly via a direct effect on osteoclasts and osteoblasts, respectively, or at least partially explained by the decreased inflammation and disease activity. However, this was not confirmed in the prospective study as the results were confounded by a high prevalence of vitamin D deficiency and these patients had significant falls in femur BMD and evidence of higher bone turnover. Furthermore, as there were no control groups it was difficult to establish whether depletion of B cells had in fact slowed down the expected bone loss in these patients. The results of the *in vitro* experiments indicated that under basal conditions i.e. in healthy subjects, the production of osteoprotegerin by B cells outweighed the production of receptor activator of nuclear factor -  $\kappa$ b ligand (RANKL). However, in pro-inflammatory states, where B cells are activated e.g. RA, B cells produce cytokines like RANKL that stimulate osteoclastogenesis resulting in an increased production of osteoclasts. Hence B cell depletion

in this latter situation caused a reduction in osteoclast generation. Further work is now required to investigate if subsets of pathogenic B cells i.e. not found in healthy individuals are specific to inflammatory bone erosion.

## **Dedication**

I would like to dedicate this thesis to “MY PARENTS” who have always loved me unconditionally and have been a source of great encouragement and inspiration. Your good example taught me to work hard for the things that I want to achieve. A very special thank you for all your help and for the immeasurable ways, in which you have supported me in my determination to pursue my ambition throughout my life,

I also dedicate this thesis to “MY HUSBAND” for his encouragement and patience and to “MY DAUGHTERS” for their belief that I would get there in the end.



## **Declaration**

I hereby declare that I am the sole author of this thesis. This is a true copy of my thesis, including any required final revisions, as accepted by my examiners. It has not already been accepted or in the process of being submitted for any other degree.





## Acknowledgements

First and foremost I would like to express my sincere gratitude and thanks to my supervisor Professor Jaap van Laar for his patience, motivation and valuable guidance and support, you have been a tremendous mentor for me. I would also like to express my profound appreciation to my other supervisors; Dr Harish K Datta, Dr Stephen P Tuck and Professor Roger M Francis, for all their assistance and support throughout the project. I would like to thank you all for encouraging my research and for allowing me to grow as a research scientist, your expertise and advice have been priceless.

I would like to express my deep gratitude to Dr John Drury and Tina Porter for believing I could do it and for giving me a chance to start this project, especially to you Tina for your eternal support, for giving me a gentle push when necessary and for always believing that I'd get there in the end.

Thanks are also due to my colleagues in Pathology, especially Andrea Boyce and Anthony Donnelly for their help with the clinical trial samples, to Cheryl Goodrum and Andrew Teggert for help with the bone marker analysis and to Tony Holden and Graeme Singh for their help with the FACS analysis. Also to the Phlebotomy team and members of staff who were always willing to donate samples.

I must extend a very special thank you to Lee Simpson for his assistance with the *in vitro* experiments, for the endless hours counting cells and for always being willing to help and give his best suggestions; it would have been a lonely lab without him. Likewise to Dr Vanessa Hogan for listening and for her helpful guidance at the start of this epic journey. I acknowledge Julie Rowbotham and the R&D department for their guidance and advice managing the clinical trials. I must also acknowledge the patients, investigators and study personnel in The Netherlands who made the pilot study possible and also those in the 10 UK centres who facilitated the prospective 'HORUS' study. My thanks also to Dr Kamran Naraghi and Dr Mohsen Elshahaly for their help with this study.

I recognize that this research would not have been possible without research grants from South Tees R&D and Roche Products Limited (Welwyn Garden City, UK) providing funding for the prospective trial; I express my gratitude to both.

A special thanks to my family. Words cannot express how grateful I am to everyone, for all your support and the sacrifices you've made on my behalf. Finally I would like to express appreciation to my husband and best friend Paul who was always my support in the many moments of absolute panic.



## Abbreviations

<b>1, 25(OH)<sub>2</sub>D<sub>3</sub>:</b>	1, 25-dihydroxy vitamin D3
<b>25OHD:</b>	25- hydroxy cholecalciferol
<b>Ab:</b>	Antibody
<b>ACPA:</b>	Anti-cyclic Citrullinated Peptide Antibody
<b>ACR:</b>	American College of Rheumatology
<b>ALP:</b>	Alkaline Phosphatase (Total)
<b>AP-1:</b>	Activator Protein-1
<b>APRIL:</b>	A PRoliferation-Inducing Ligand
<b>ATF-4:</b>	Activating Transcription Factor-4
<b>Bach2:</b>	Basic leucine zipper transcription factor 2
<b>BAFF:</b>	B cell Activating Factor
<b>BALP:</b>	Bone specific Alkaline Phosphatase
<b>Bcl6:</b>	B cell lymphoma 6
<b>BCR:</b>	B Cell Receptor
<b>βCTX:</b>	Beta-isomerised Carboxy terminal Telopeptide of type I collagen
<b>Be:</b>	B effector cell
<b>BiP:</b>	Immunoglobulin Binding Protein
<b>Blimp1:</b>	B lymphocyte-induced maturation protein 1
<b>BMD:</b>	Bone Mineral Density
<b>BMI:</b>	Body Mass Index
<b>BMP:</b>	Bone Morphogenetic Protein
<b>BSA:</b>	Bovine Serum Albumin
<b>BSAP:</b>	B cell lineage-Specific Activation factor
<b>BTM:</b>	Bone Turnover Marker
<b>Ca:</b>	Calcium
<b>CCa:</b>	Corrected Calcium
<b>CD:</b>	Cluster of Differentiation or Classification Determinant
<b>CE:</b>	Conformité Européenne
<b>c-fms:</b>	colony-stimulating factor 1 receptor
<b>CLL:</b>	Chronic Lymphocytic Leukaemia
<b>CRP:</b>	C-Reactive Protein
<b>CTX:</b>	Carboxy-terminal cross-linked Telopeptides of type I collagen
<b>CTX-MMP:</b>	Carboxy-terminal cross-linked Telopeptide - MMP

<b>CV:</b>	Coefficient of Variation
<b>CXCL12:</b>	C-X-C motif chemokine 12
<b>DAP12:</b>	Dnax-Activating Protein 12
<b>DAS28:</b>	Disease Activity Score using 28 tender or swollen joints
<b>DKK:</b>	DicKKopf- related protein
<b>DMARD:</b>	Disease Modifying Anti Rheumatic Drug
<b>DMP-1:</b>	Dentin Matrix Protein-1
<b>DMSO:</b>	Dimethyl SulfOxide
<b>DPBS:</b>	Dulbecco's Phosphate Buffered Saline
<b>DPD:</b>	DeoxyPyriDinoline
<b>DXA:</b>	Dual-energy X-ray Absorptiometry
<b>ECLIA:</b>	ElectroChemiLuminescent ImmunoAssay
<b>EDTA:</b>	Ethylene Diamine Tetraacetic Acid
<b>eGFR:</b>	estimated Glomerular Filtration Rate
<b>ELISA:</b>	Enzyme Linked ImmunoSorbent Assay
<b>ESR:</b>	Erythrocyte Sedimentation Rate
<b>FACS:</b>	Fluorescence Activated Cell Sorting
<b>FcR<math>\gamma</math>:</b>	Fc Receptor gamma chain
<b>FcRL4:</b>	Fc Receptor-Like protein 4
<b>FCS:</b>	Fetal Calf Serum
<b>FSH:</b>	Follicle Stimulating Hormone
<b>Fz:</b>	Frizzled protein
<b>GC:</b>	Germinal centre
<b>G-CSF:</b>	Granulocyte -Colony Stimulating Factor
<b>G<math>\alpha</math>:</b>	G protein $\alpha$ subunit
<b>HAQ:</b>	Health Assessment Questionnaire
<b>HELP:</b>	type I collagen alpha 1 HELicoidal Peptide
<b>HSC:</b>	Hematopoietic Stem Cell
<b>HBSS:</b>	Hank's Balanced Salt Solution
<b>hsCRP:</b>	high sensitivity C-Reactive Protein
<b>IDS:</b>	Immuno Diagnostic Systems
<b>IFN-<math>\gamma</math>:</b>	InterFeroN-gamma
<b>Ig:</b>	Immunoglobulin
<b>IL:</b>	InterLeukin
<b>IRF:</b>	Interferon Regulatory Factor

<b>ISCD:</b>	International Society for Clinical Densitometry
<b>ITAM:</b>	Immuno receptor Tyrosine-based Activation Motif
<b>JCUH:</b>	The James Cook University Hospital
<b><i>KL</i><sup>-/-</sup>:</b>	<i>Klotho</i> mutant mice
<b>kDa:</b>	kilo Dalton
<b>LH:</b>	Luteinising Hormone
<b>LRP:</b>	Low-density lipoprotein Receptor-related Protein
<b>LS:</b>	Lumbar Spine
<b>LSC:</b>	Least significant change
<b>LT-<math>\alpha</math>:</b>	LymphoToxin-alpha
<b><math>\mu</math>g/L:</b>	micrograms per Litre
<b><math>\mu</math>l:</b>	microlitre
<b><math>\mu</math>m:</b>	micron
<b>ml:</b>	millilitre
<b>MACS:</b>	Magnetic-Activated Cell Sorting
<b>M-CSF:</b>	Macrophage -Colony Stimulating Factor
<b><math>\alpha</math>MEM:</b>	Minimum Essential Medium
<b>MEPE:</b>	Matrix Extracellular Phosphoglycoprotein
<b>MHC:</b>	Major Histocompatibility Complex
<b>MHRA:</b>	Medicines and Healthcare Products Regulatory Agency
<b>MN:</b>	Mean Neck of Femur
<b>MoM:</b>	Multiple of the Median
<b>MSC:</b>	Mesenchymal Stem Cell
<b>MT:</b>	Mean Total Femur
<b>MT1-MMP:</b>	Membrane-Type Matrix MetalloProteinase 1
<b>MTX:</b>	Methotrexate
<b>MZ:</b>	Marginal Zone
<b>n:</b>	number in the sample
<b>ng/L:</b>	nanograms per Litre
<b>NEQAS:</b>	National External Quality Assessment Service
<b>NFATc1:</b>	Nuclear Factor of Activated T cells, cytoplasmic 1
<b>NK-<math>\kappa</math>b:</b>	Nuclear factor kappa-light-chain-enhancer of activated b cells
<b>NICE:</b>	National Institute for Health and Care Excellence
<b>NTX:</b>	amiNo terminal Telopeptide of type I collagen
<b>OB:</b>	Osteoblast

<b>OC:</b>	Osteoclast
<b>OPG:</b>	Osteoprotegerin
<b>OSCAR:</b>	OSteoClast-Associated immunoglobulin-like Receptor
<b>OSTEOC:</b>	Osteocalcin
<b>OSX:</b>	Osterix
<b>Pax5:</b>	Paired box protein 5
<b>pmol/L:</b>	picomoles per Litre
<b>PBMC:</b>	Peripheral Blood Mononuclear Cell
<b>PBS:</b>	Phosphate Buffered Saline
<b>PICP:</b>	Procollagen type 1 Carboxy-terminal Propeptide
<b>PINP:</b>	Procollagen type 1 amiNo-terminal Propeptide
<b>pNPP:</b>	p-NitroPhenyl Phosphate
<b>PO<sub>4</sub>:</b>	Phosphate
<b>PPR:</b>	PTH/ PTHrP Receptor
<b>PSA:</b>	Prostate Specific Antigen
<b>PTH:</b>	ParaThyroid Hormone
<b>PTHrP:</b>	ParaThyroid Hormone related Protein
<b>PYD:</b>	Pyridinoline
<b>QC:</b>	Quality Control
<b>QCT:</b>	Quantitative Computed Tomography
<b>QUS:</b>	Quantitative UltraSound
<b>R<sub>s</sub></b>	Spearman correlation coefficient
<b>RA:</b>	Rheumatoid Arthritis
<b>RANK:</b>	Receptor Activator of Nuclear factor - $\kappa$ b
<b>RANKL:</b>	Receptor Activator of Nuclear factor - $\kappa$ b Ligand
<b>RF:</b>	Rheumatoid Factor
<b>RPM:</b>	Revolutions Per Minute
<b>RPMI:</b>	Roswell Park Memorial Institute
<b>RTX:</b>	Rituximab
<b>RUNX2:</b>	Runt-related transcription factor X2
<b>sRANKL:</b>	soluble Receptor Activator of Nuclear factor - $\kappa$ B Ligand
<b>SCL:</b>	Sclerostin
<b>SD:</b>	Standard Deviation
<b>SDF-1:</b>	Stromal cell-Derived Factor 1
<b>SHBG:</b>	Sex Hormone Binding Globulin

<b>SJC:</b>	Swollen Joint Count
<b>T<sub>FH</sub>:</b>	Follicular T helper cell
<b>TGF-<math>\beta</math>:</b>	Transforming Growth Factor-beta
<b>TJC:</b>	Tender Joint Count
<b>TMB:</b>	3, 3', 5, 5' TetraMethyl Benzidine
<b>TNF-<math>\alpha</math>:</b>	Tumour Necrosis Factor-alpha
<b>TRAF-6:</b>	TNF Receptor-Associated Factor-6
<b>TRAP:</b>	Tartrate Resistant Acid Phosphatase
<b>TRAP5b:</b>	Tartrate Resistant Acid Phosphatase isoform 5b
<b>TREM-2:</b>	Triggering Receptor Expressed on Myeloid cells-2
<b>TSH:</b>	Thyroid Stimulating Hormone
<b>UD Radius:</b>	Ultra-Distal Radius
<b>UK:</b>	United Kingdom
<b>VAS:</b>	Visual Analogue Scale
<b>VCAM 1:</b>	Vascular Cell Adhesion Molecule 1
<b>WHO:</b>	World Health Organisation
<b>Wnt:</b>	Wingless-int
<b>wrCRP:</b>	Wide Range C-Reactive Protein
<b>XBP1:</b>	X-box Binding Protein 1





## Table of Contents

Abstract.....	i
Dedication.....	iii
Declaration.....	v
Acknowledgements .....	vii
Abbreviations .....	ix
List of Figures.....	xix
List of Tables.....	xxi
Chapter 1. General Introduction .....	1
1.1    B cells .....	1
1.1.1 <i>B cell development</i> .....	1
1.1.2 <i>B cell regulation</i> .....	5
1.1.3 <i>Autoantibody production</i> .....	5
1.1.4 <i>Cytokine production</i> .....	6
1.2    Bone .....	7
1.2.1 <i>Bone structure</i> .....	7
1.2.2 <i>Bone mineral density</i> .....	9
1.2.3 <i>Bone metabolism</i> .....	10
1.2.4 <i>Bone cell differentiation and regulation</i> .....	13
1.2.5 <i>Biochemical markers of bone turnover</i> .....	19
1.3    Interactions between the immune and skeletal systems.....	25
1.3.1 <i>Osteoblasts and B cells</i> .....	25
1.3.2 <i>Osteoclasts and B cells</i> .....	26
1.3.3 <i>B cells and the RANK-RANKL-OPG system</i> .....	26
1.4    Rheumatoid arthritis .....	28
1.4.1 <i>Epidemiology</i> .....	28
1.4.2 <i>Pathogenesis of bone loss in rheumatoid arthritis</i> .....	28
1.4.3 <i>Pathway of care</i> .....	32
1.4.4 <i>The role of B cells in rheumatoid arthritis</i> .....	33
1.5    The effect of B cell depletion on bone turnover in rheumatoid arthritis .....	34
1.5.1 <i>Current evidence from clinical trials</i> .....	34
1.6    Project aims.....	35
Chapter 2. Materials and methods .....	37
2.1    Materials .....	37
2.1.1 <i>Biomarker reagents</i> .....	38

2.1.2 <i>In vitro reagents</i> .....	39
2.2 Methods.....	40
2.2.1 <i>Biomarker assays</i> .....	40
2.2.2 <i>In vitro experiments</i> .....	53
2.3 Subjects.....	62
The main characteristics and time-lines of the sub studies are summarised in table 6. ...	62
2.3.1 <i>Pilot study</i> .....	64
2.3.2 <i>Prospective study</i> .....	64
2.3.3 <i>Osteoclast work</i> .....	65
2.4 Statistical analysis.....	66
2.4.1 <i>Pilot study</i> .....	66
2.4.2 <i>Prospective study</i> .....	67
2.4.3 <i>Osteoclast work</i> .....	67
Chapter 3. The effects of B cell depletion on bone turnover in patients with rheumatoid arthritis - the pilot study.....	69
3.1 Introduction.....	69
3.2 Materials and methods.....	69
3.2.1 <i>Patient cohort</i> .....	70
3.2.1 <i>Biomarker measurements</i> .....	70
3.2.2 <i>Statistical analysis</i> .....	70
3.3 Results.....	70
3.3.1 <i>Demographic and clinical characteristics</i> .....	70
3.3.2 <i>Changes in biomarker levels</i> .....	74
3.3.3 <i>Time course of change in bone turnover</i> .....	74
3.3.4 <i>The effect of gender and menopausal status</i> .....	78
3.3.5 <i>The effect of concomitant medication</i> .....	78
3.3.6 <i>Correlations between inflammatory activity and bone turnover</i> .....	78
3.4 Discussion.....	83
3.5 Conclusion.....	84
Chapter 4. The effects of B cell depletion on bone turnover in patients with rheumatoid arthritis - the prospective study.....	87
4.1 Introduction.....	87
4.2 Materials and methods.....	87
4.2.1 <i>Patient cohort</i> .....	88

4.2.2 <i>Clinical and laboratory assessments</i> .....	88
4.2.3 <i>Bone mineral density measurements</i> .....	90
4.2.4 <i>Biomarker measurements</i> .....	90
4.2.5 <i>Statistical analysis</i> .....	90
4.3 Results.....	91
4.3.1 <i>Demographic and clinical characteristics</i> .....	91
4.3.2 <i>Changes in bone mineral density</i> .....	95
4.3.3 <i>Changes in biomarker levels</i> .....	98
4.3.4 <i>Correlations between inflammatory activity and bone density or bone turnover</i> ....	99
4.3.5 <i>The effects of vitamin D</i> .....	104
4.4 Discussion.....	108
4.5 Conclusion.....	110
Chapter 5. <i>In vitro</i> osteoclastogenesis.....	111
5.1 Introduction.....	111
5.2 Osteoclastogenesis protocol.....	115
5.2.1 <i>Methods</i> .....	115
5.2.2 <i>Results</i> .....	116
5.2.3 <i>Discussion</i> .....	123
5.3 The effect of <i>in vitro</i> B cell depletion.....	125
5.3.1 <i>Methods</i> .....	125
5.3.2 <i>Results</i> .....	127
5.3.3 <i>Discussion</i> .....	137
5.4 The effects of <i>ex vivo</i> B cell depletion.....	139
5.4.1 <i>Methods</i> .....	139
5.4.2 <i>Results</i> .....	140
5.4.3 <i>Multiple regression analysis to explore factors affecting osteoclastogenesis</i> .....	150
5.4.4 <i>Discussion</i> .....	151
5.5 Conclusion.....	152
Chapter 6. Discussion.....	153
6.1 Discussion.....	153
6.2 Conclusion.....	156
6.3 Future perspective.....	156
References.....	161
Appendix A. Generic Materials.....	177

General reagents .....	177
General consumables.....	177
General equipment .....	178
Appendix B. Tests for normality of data.....	181
Pilot Study .....	181
Prospective Study .....	209
<i>In vitro</i> unfractionated and CD20 depleted PBMC comparisons.....	353
<i>Ex vivo</i> number of TRAP <sup>+</sup> cells generated per visit.....	385
Appendix C. Multiple regression analysis .....	393
Stepwise regression model 1 – unfractionated mononuclear cells.....	393
Stepwise regression model 2 – CD20 depleted mononuclear cells.....	396
Appendix D. Publications arising from this thesis.....	399
Original publication in peer reviewed journals .....	399
Submitted for publication.....	399
Abstracts.....	400

## List of Figures

Figure 1 Graphical representations of the pathways leading particularly to B cell and osteoclast differentiation from hematopoietic stem cells .....	2
Figure 2 Expression of B cell specific markers during the differentiation of early progenitor B cells into mature memory B cells and/or plasma cells .....	4
Figure 3 Illustration of cortical and trabecular bone .....	8
Figure 4 The bone remodelling cycle .....	12
Figure 5 Graphical representations of the pathways leading particularly to osteoblast and osteocyte differentiation from mesenchymal stem cells.....	15
Figure 6 Osteoclast cells stained with tartrate resistant acid phosphatase .....	17
Figure 7 Osteoclast differentiation .....	18
Figure 8 The effect of age on individual biomarkers for the pilot study.....	46
Figure 9 Ratio of the multiples of the median for a marker of bone formation and bone resorption to signify bone turnover in patients with rheumatoid arthritis .....	47
Figure 10 The effect of age on individual biomarkers for the prospective study.....	52
Figure 11 Diagrammatic representation of the microscope slide showing orientation and counting areas, labelled 1-9 respectively.....	58
Figure 12 Infinity analyse software showing the cell area and circumference measurement for 3 TRAP <sup>+</sup> osteoclast-like cells .....	59
Figure 13 Flowchart showing the pilot study numbers at each time point.....	72
Figure 14 Ratio of bone marker multiples of the median depicting bone turnover in forty-six rheumatoid arthritis patients' pre and 6 months post rituximab.....	76
Figure 15 Change in individual bone markers over the course of the study .....	77
Figure 16 The effects of gender and menopausal status on median biomarker levels .....	80
Figure 17 Location of the ten UK centres recruiting into the prospective study.....	89
Figure 18 Consort flow diagram for the prospective study .....	92
Figure 19 Change in individual bone markers over the course of the study .....	101
Figure 20 Change in individual inflammatory markers over the course of the study .....	102
Figure 21 Ratio of bone marker multiples of the median depicting bone turnover in thirty rheumatoid arthritis patients pre and 3, 6, 9 and 12 months post rituximab .....	103
Figure 22 Comparison with and without the addition of cytokines (×200).....	118
Figure 23 Evaluation of PBMC plating density (×200) showing typical patterns of TRAP <sup>+</sup> cell formation at each concentration.....	119
Figure 24 Evaluation of the time of culture period (×200) showing typical patterns of TRAP <sup>+</sup> cell formation at each day.....	120
Figure 25 Representative TRAP <sup>+</sup> multinucleated cells on a glass coverslip.....	121
Figure 26 Representative actin ring formation on a glass coverslip.....	121
Figure 27 Representative resorption pits on a bone slice, visualised by toluidine blue staining .....	122
Figure 28 The effect of the initial number of monocytes on TRAP <sup>+</sup> cells generated from twelve healthy volunteer peripheral blood mononuclear cells .....	130
Figure 29 The effect of the initial number of B cells on TRAP <sup>+</sup> cells generated from twelve healthy volunteer peripheral blood mononuclear cells.....	131
Figure 30 The effect of the initial number of T cells on TRAP <sup>+</sup> cells generated from twelve healthy volunteer peripheral blood mononuclear cells.....	132
Figure 31 An example of a patient culture at baseline, 3, 6 and 12 months.....	144
Figure 32 The effect of the initial number of monocytes on TRAP <sup>+</sup> cells generated from four rheumatoid arthritis patient cultures .....	146
Figure 33 TRAP <sup>+</sup> cells generated from five rheumatoid arthritis patient cultures before and 3, 6, 12 months post rituximab .....	147

Figure 34 The effect of the initial number of B cells on TRAP<sup>+</sup> cells generated from four  
rheumatoid arthritis patient cultures ..... 148

Figure 35 The effect of the initial numbers of T cells on TRAP<sup>+</sup> cells generated from four  
rheumatoid arthritis patient cultures ..... 149

## List of Tables

Table 1 Major advantages and disadvantages of commonly used bone turnover markers .....	21
Table 2 Types of bone loss in rheumatoid arthritis .....	31
Table 3 Biomarker precision data for the pilot study .....	44
Table 4 Manufacturer defined biomarker reference ranges.....	45
Table 5 Biomarker precision data for the prospective study .....	50
Table 6 Main characteristics of all the sub studies.....	63
Table 7 Baseline characteristics of the forty-six rheumatoid arthritis patients .....	73
Table 8 Change in biomarker concentration for the forty-six rheumatoid arthritis patients ....	75
Table 9 Effect of bisphosphonate treatment on change in biomarker concentration for forty-six rheumatoid arthritis patients from baseline to six months .....	81
Table 10 Correlations between the percentage change from baseline of biomarker values for patients not on bisphosphonates or prednisolone (n=18) .....	82
Table 11 Baseline characteristics of the prospective study patients.....	93
Table 12 Change in bone mineral density from baseline to 12 months .....	96
Table 13 Change in biomarkers from baseline to twelve months .....	100
Table 14 Change in bone mineral density and biomarkers by vitamin D category from baseline to 12 months .....	106
Table 15 Osteoclast culture techniques described in recent literature.....	114
Table 16 Unfractionated and CD20 depleted cultures in twelve healthy volunteers .....	128
Table 17 Comparison of CD20 depleted mononuclear cells using either magnetic-activated cell sorting or <i>in vitro</i> rituximab.....	134
Table 18 Effect of <i>in vitro</i> rituximab on unfractionated and CD14 <sup>+</sup> purified peripheral blood mononuclear cells .....	136
Table 19 Baseline trial data for five rheumatoid arthritis patients .....	141
Table 20 Bone marker and bone mineral density results at each visit for five rheumatoid arthritis patients .....	142
Table 21 Median cell counts at baseline and at 3, 6 and 12 month post-rituximab from four rheumatoid arthritis patient cultures .....	145





# **Chapter 1**

## **General Introduction**



## Chapter 1. General Introduction

Chapter one, the general introduction is divided into six main parts. To begin section one is a brief summary of B cell development, regulation and function. The second section describes bone structure, individual bone cells and the regulation of bone re-modelling, the stages of which can be identified using biochemical markers of bone turnover. Section three describes the interactions between the immune and skeletal system, currently referred to as ‘Osteoimmunology’. Section four is a general overview of rheumatoid arthritis (RA), epidemiology, mechanisms of bone loss and RA management and finally current understanding of the effects of B cell depletion on bone turnover in RA. Taken together the sections form the theoretical basis to this study and the general aims are specified in the final section.

### 1.1 B cells

The immune system is a highly evolved process designed to protect the body from invading pathogens present in the environment, it is typically divided into two main categories; innate and adaptive. B cells are an important component of the adaptive immune system, which allows an individual to develop a specific response to an antigen and remember that antigen, allowing for a faster more robust response to that infection in the future. The adaptive immune response comprises of cell-mediated components; facilitated by T cells that recognise and directly attack foreign antigens that have entered into body cells; and humoral components, mediated by specific antibodies produced by B cells. A simple definition of B lymphocytes is a population of cells that express clonally diverse cell surface immunoglobulin (Ig) receptors recognizing specific antigenic epitopes (LeBien and Tedder 2008).

#### 1.1.1 *B cell development*

B cells develop directly from lymphoid stem cells in the hematopoietic tissue (Figure 1) of the foetal liver from 8-9 weeks gestation in humans, production then transfers into the bone marrow where it continues into adulthood (Asma et al. 1984). B cells initially mature, independently of an antigen, into pro-B cells; then progress through pre-B cells to immature B cells (Figure 2). Thereafter they enter an antigen-dependent phase in the peripheral lymphoid tissues. The B cell receptor (BCR) is activated after encountering exogenous antigen in the extra-follicular region and they progress from ‘naive’ mature to ‘naive activated’ B cells and migrate to the follicular region (Dalakas 2008).

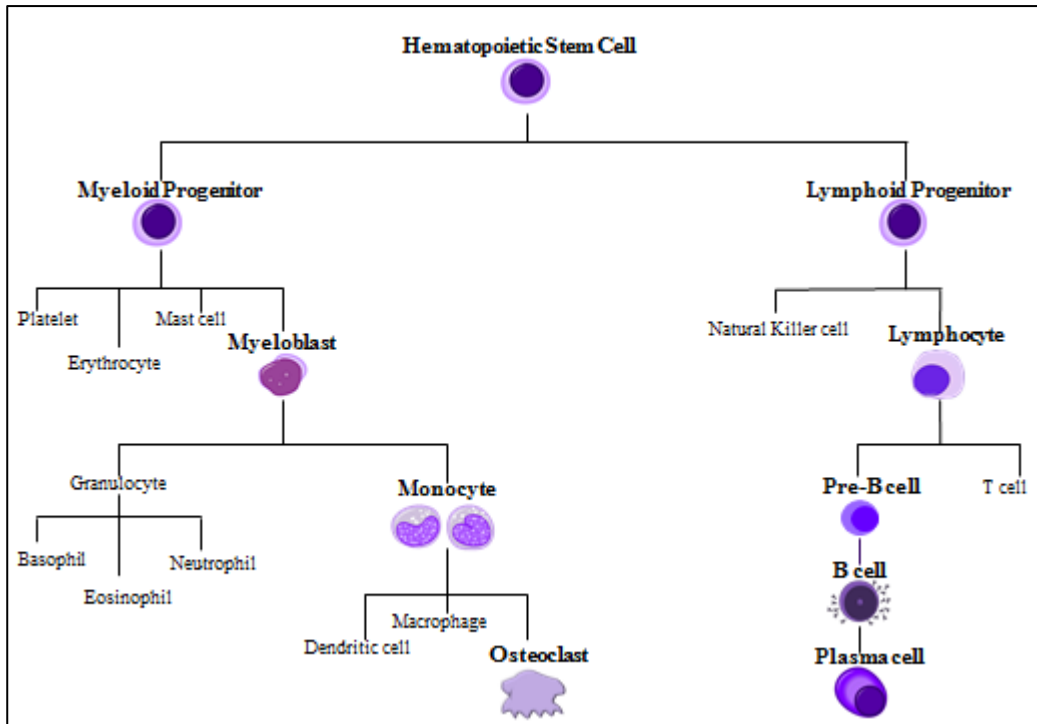


**Figure 1 Graphical representations of the pathways leading particularly to B cell and osteoclast differentiation from hematopoietic stem cells**

Hematopoietic stem cells give rise to both myeloid and lymphoid lineages of blood cells. Myeloid cells include; neutrophils, basophils, eosinophils and monocytes, dendritic cells, macrophages and osteoclasts. Lymphoid cells include; natural killer cells, T cells and B cells.

During the first step of the follicular response, the activated B cells migrate to the inter-follicular foci to receive help for further proliferation and differentiation from activated cluster of differentiation (CD) $4^+$  T helper cells, which start to differentiate into follicular T helper ( $T_{FH}$ ) cells. The activated B cells present processed antigen through direct cell-to-cell contact with the T cell receptor on the surface of  $T_{FH}$  cells via major histocompatibility complex (MHC) class II. The B cells in turn receive co-stimulation via binding of CD40 ligand on T cells to CD40 on B cells leading to full activation, enabling an immediate extra-follicular humoral response as a subset of activated B cells differentiate into short-lived plasmablasts, producing low-affinity antibodies to the antigen (Nera et al. 2015).

Communication between these cells also primes a subset of activated T cells and B cells that then migrate to the B cell follicle and form germinal centres (GC). GCs are made up of dark and light zones; they are checkpoints where both positive and negative selection of B cells for the production of plasmablasts and memory B cells takes place. Additionally, a subset of plasmablasts migrates to the bone marrow where they become long-lived plasma cells (Nera et al. 2015). Specific B cell surface molecules are expressed during differentiation; CD19, CD20, CD27, CD38 and CD138, they identify each of the transitional phases of B cell maturation (Figure 2) and ensure and regulate communication with the extracellular environment and initiate intracellular pathway signalling. Notably the CD19 molecule is expressed on all B lineage cells (Johnsen et al. 2014). In addition naive B cells are generally divided into three subsets; follicular or B-2 cells, classed as the standard type of B cell discussed in this section, plus two minor subsets; B-1 cells, primarily developed from the foetal liver and mainly found in peritoneal and pleural cavities and marginal zone (MZ) B cells particularly located within the spleen (Allman and Pillai 2008).

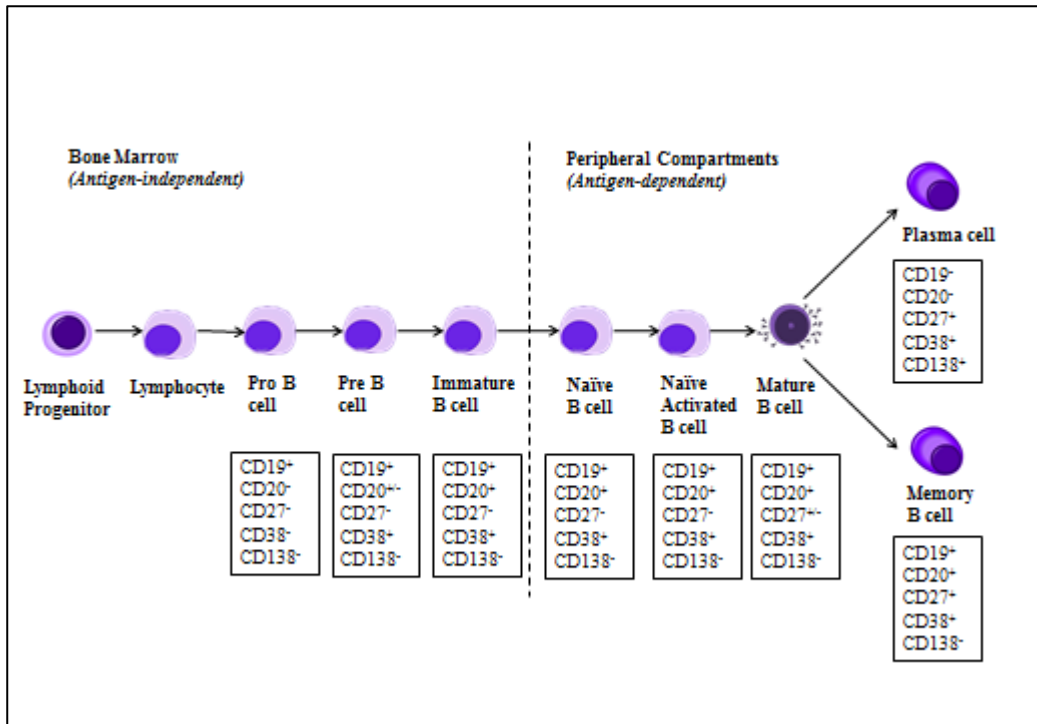


**Figure 2 Expression of B cell specific markers during the differentiation of early progenitor B cells into mature memory B cells and/or plasma cells**

B cells develop from hematopoietic stem cells that originate from bone marrow. When B cells mature they migrate through the blood and become activated when they bind to an antigen. There are many B cell specific membrane-bound proteins expressed during B cell development from early lymphoid progenitor cells to mature memory B cells and/or plasma cells.

### **1.1.2 B cell regulation**

B cell activation and terminal differentiation is a complex mechanism under the influence of two main categories of transcription factors. Those factors promoting B cell phenotype but preventing premature differentiation to plasma cells; paired box protein 5 (Pax5), B cell lymphoma 6 protein (Bcl6), basic leucine zipper transcription factor 2 (Bach2), PU.1 and interferon regulatory factor 8 (IRF8); and those factors driving terminal differentiation into antibody secreting cells; X-box binding protein 1 (XBP1), B lymphocyte-induced maturation protein 1 (Blimp-1) and IRF4 (Nera et al. 2015).

Additionally, BCR signalling typically induces proliferation and differentiation of mature B cells into antibody-secreting cells or memory B cells, but potentially can dictate the functional response and act as a developmental checkpoint for B-cell maturation. Clonal selection mechanisms have evolved to prevent the maturation of B cells that would otherwise produce autoreactive antibodies i.e. blocking the BCR can lead to receptor editing, cellular anergy and/or death by apoptosis of immature B cells (Harnett et al. 2005). Moreover, in the germinal centres, B cells, which have undergone somatic mutation resulting in potentially autoreactive antibodies, are programmed to die (peripheral tolerance) unless rescued by antigen and cognate follicular dendritic cell or T cell-derived signals (Harnett et al. 2005).

### **1.1.3 Autoantibody production**

B cells are unique cells capable of forming terminally differentiated plasma cells producing antibodies (Ab). Antibodies are normally produced in response to a foreign protein or substance, such as an infectious organism within the body; they provide effective protection particularly after re-exposure to a previously encountered pathogen. An autoantibody is an antibody that is directed against one or more of the body's own proteins. In a healthy immune system, B cells only bind to non-self-antigens; immature B cells that recognise self-antigens undergo negative selection by apoptosis or change their antigen specificity. Additionally, B cells that recognise self-antigens lose their ability to respond and are prevented from migrating to the follicular region. Autoimmune diseases develop when these mechanisms fail, and pathogenic, self-reactive B cells are produced (Lipsky 2001). It is clear that the presence of autoantibodies is a feature of rheumatoid arthritis (RA) and a number of autoantibodies have been described including rheumatoid factor (RF), anti-cyclic citrullinated protein antibody (ACPA) and antibodies to immunoglobulin binding protein (BiP). The autoantibodies often appear before overt clinical symptoms and are associated with a more severe disease outcome (Agrawal et al. 2007). Only RA and ACPA are used clinically, but neither factor has one hundred percent specificity e.g. RF is present in fifty to eighty percent

of RA patients, but also around ten percent of the general population and although ACPA is more specific to RA, a limited proportion of 'healthy' individuals also test positive (Mewar and Wilson 2006).

#### **1.1.4 Cytokine production**

The role of B cells in autoimmunity is not restricted to the production of autoantibodies; it is mediated in part by their ability to produce various cytokines that play important roles during infection, autoimmune disease, allergy and cancer (Fillatreau 2012). Moreover, B cell cytokine production is regulated by extrinsic signalling provided by other immune cell types and depends on their differentiation state and activation conditions. Naive B cells do not secrete many cytokines upon activation. In contrast, naive T cells initiate cytokine production almost immediately after activation. Once B cells acquire the capacity to produce cytokines, they become capable of cross-regulating responses via polarization/inhibition and can even negatively regulate the entire immune system (Vazquez et al. 2015). Cytokines produced by B cells (reviewed in Youinou et al. 2009) can be classified as:

- Pro-inflammatory cytokines; such as interleukin (IL)-1, IL-6, tumour necrosis factor-alpha (TNF- $\alpha$ ), interferon-gamma (IFN- $\gamma$ ), lymphotoxin-alpha (LT- $\alpha$ )
- Immunosuppressive cytokines, such as IL-10 and transforming growth factor-beta (TGF- $\beta_1$ )
- Hematopoietic growth factors; such as granulocyte colony-stimulating factor (G-CSF), macrophage colony stimulating factor (M-CSF) and IL-7

Two main B effector (Be) subgroups have been described; Be1 and Be2 that produce distinct patterns of cytokines depending on the cytokine environment in which the cells were stimulated during their primary encounter with antigen and T cells (Harris et al. 2000). Lund further subdivides the pro-inflammatory cytokines into Be subgroups; Be1 primed by Th1 cells and antigen, produce IFN- $\gamma$ , IL-12 associated with type 1 immune responses; and Be2 primed by Th2 cells and antigen, produce IL-2, IL-4, TNF- $\alpha$  and IL-6 often associated with allergic responses (Lund 2008). Furthermore, B cells may also play a regulatory role by modulating the production of IL-10, an anti-inflammatory cytokine that can suppress harmful immune responses (Mauri et al. 2003, Fillatreau 2015) or TGF- $\beta_1$  (Lund 2008).



## 1.2 Bone

### 1.2.1 Bone structure

Bone is a specialised connective tissue hardened by mineralisation with calcium phosphate. The ground substance of bone consists primarily of glycoproteins and proteoglycans, the fibres of bone are composed of type-I collagen impregnated with mineral in the form of hydroxyapatite ( $[\text{Ca}_3(\text{PO}_4)_2] \text{Ca}(\text{OH})_2$ ). The main function of bone is to provide structural support to the human body and locomotion through muscle attachment; however it also serves as a mineral reservoir, shields vital organs and facilitates the production of red and white blood cells. The rate of bone turnover, collagen matrix, size, structure, geometry and density all combine to determine the bone's overall mechanical properties (Datta et al. 2008).

There are two main histological types of bone tissue; cortical and trabecular bone (Figure 3). In general each bone has an outer cortical layer surrounding the trabecular bone in the centre. The cortical bone has an outer membrane called the periosteum consisting of two fibrous layers, the inner layer having osteogenic potential enabling new bone formation. In addition, the inner surface of cortical bone is lined by the endosteum that also contains osteoblasts and osteoclasts. The endosteum is the boundary between the cortical and trabecular bone. Cortical compact bone is dense without any cavities; the fundamental unit is the osteon or Haversian system, a central vascular canal surrounded by concentric lamellae of mineralised fibres, osteocytes are interspersed between lamellae in tiny spaces called lacunae. Volkmann's canals at right angles connect the osteons together. In contrast, the inner trabecular or cancellous bone is spongy with numerous cavities and is made up of a three-dimensional scaffold of pillars which are constantly modified to accommodate load, it is ideally suited to withstand compressive stress. Trabecular bone contains an irregular network of spaces allowing room for blood vessels, bone marrow and hematopoietic stem cells. The rate of bone turnover varies according to the type of bone, being highest in sites such as vertebrae where trabecular bone predominates, and lowest in sites such as the hip composed of cortical bone (Datta et al. 2008).

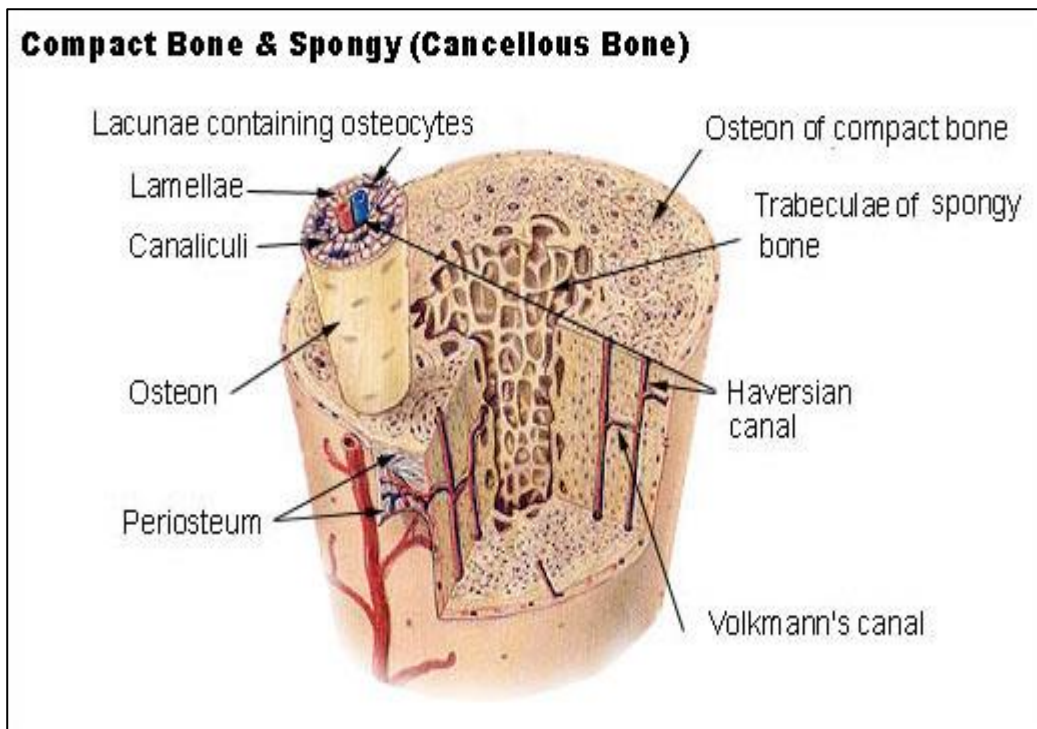


**Figure 3 Illustration of cortical and trabecular bone**

This image was obtained from; SEER - U.S. National Cancer Institute's Surveillance, Epidemiology and End Results (<https://commons.wikimedia.org/w/index.php?curid=378948>)

### 1.2.2 Bone mineral density

Bone mineral density (BMD) can be described as the amount of bone mass per unit volume (volumetric density,  $\text{g}/\text{cm}^3$ ) or per unit area (areal density  $\text{g}/\text{cm}^2$ ), measured *in vivo* by densitometry and reflects the strength of bones characterised by their calcium content (Kanis 2008). BMD measurements have an important clinical role in the diagnosis of osteoporosis, assessment of future fracture risk and monitoring response to treatment (Blake and Fogelman 2010). Many techniques are available to assess BMD, such as quantitative ultrasound (QUS) and quantitative computed tomography (QCT), but the most widely validated technique is dual-energy X-ray absorptiometry (DXA), since the absorption of X-rays are very sensitive to the calcium content of tissue, of which bone is the most important source (Kanis et al. 2008). Nevertheless, the BMD from DXA estimates areal density, the scan is a two-dimensional projection image for any given skeletal site and does not entirely control for bone size among patients e.g. men tend to have higher BMD than women, based on larger bone size (Blake and Fogelman 2010). Additionally, DXA BMD measurement tends to integrate cortical and trabecular changes and explains little about the actual structural properties of bone (Nelson et al. 2005). BMD can be measured at multiple sites e.g. lumbar spine, hip, forearm, each site having unique performance characteristics. The hip being the optimal site for predicting hip fracture risk and the spine, because of the metabolically active trabecular bone in the vertebral bodies, for monitoring response to treatment (Blake and Fogelman 2009). Although severe degenerative changes of the lumbar spine and the presence of compression fractures can result in false elevations in BMD measured by DXA (Nelson et al. 2005). The forearm, mainly cortical bone in the shaft, is considered less responsive to changes in bone and mineral metabolism but should be measured when the other sites are unavailable, when hyperparathyroidism is suspected, or in very obese patients (Nelson et al. 2005). Technical developments in the measurement of BMD have led to its adoption as the standard for diagnosis of osteoporosis, however the relatively poor sensitivity contrasting with high specificity means that many potential fractures will be missed if BMD assessment is used alone (Rabinda et al. 2011). The World Health Organisation (WHO) has defined osteoporosis in postmenopausal women and men above 50 years of age as a femoral neck BMD, measured by DXA, of 2.5 standard deviations (SD) or more below the young female adult mean (T-score), likewise osteopenia is defined as a T-score between  $-1.0$  SD and  $-2.5$  SD below the young female, adult mean (Kanis 2004). However, several studies have reported that the majority of fragility fractures occur in postmenopausal women that don't fit these criteria (Schuit et al. 2004). Other clinical risk factors such as; body mass index (BMI); previous fragility fracture; glucocorticoid therapy; current smoking; alcohol intake exceeding

3units/day; RA and other secondary causes of osteoporosis, independently contribute to fracture risk (Compston 2015). The inclusion of femoral neck BMD and all these risk factors into the fracture risk assessment algorithm (FRAX) 10 year probability of fracture tool, significantly improves prediction of hip and major osteoporotic fracture (Kanis 2004). The effectiveness of osteoporotic therapy can be assessed by serial BMD measurements usually by DXA, but quantifiable changes in bone mass are small and are only apparent after twelve to twenty-four months, furthermore they only measure net balance in a very small portion of the skeleton (Blank et al. 2006). BMD measurement by DXA is affected by; accuracy, largely due to inhomogeneous distributions of adipose tissue in the human body and precision errors as discussed below. The magnitude of these errors is especially important for the interpretation of follow-up measurements. DXA scanners generally have stable calibration and effective instrument quality control procedures to detect any long-term drifts (Blake and Fogelman 2010). However, DXA reproducibility is affected by machine and operator error plus patient variability i.e. weight or degenerative changes (Blank et al. 2006). Therefore BMD changes observed on follow-up scans are interpreted in terms of least significant change (LSC) and only changes greater than the LSC are regarded as clinically significant. Technologists must properly and consistently position patients on initial and subsequent scans and identify and correct errors in analysis. The International Society for Clinical Densitometry (ISCD) states that the minimum acceptable precision for an individual technician should be; 1.9% (LSC 5.3%) at the lumbar spine; 1.8% (LSC 5.0%) at the total hip; and 2.5% (LSC 6.9%) at the femoral neck (ISCD 2007). Intervals between measurements depend on the patient's clinical status, but given the need to exceed the LSC and the relatively modest changes in BMD observed with most treatments it is generally going to be a minimum of twelve months before a significant change can be observed.

### **1.2.3 Bone metabolism**

Bone is a dynamic tissue and is constantly being remodelled throughout an individual's lifetime; beginning before birth and continuing until death. Mature bone tissue is removed from the skeleton i.e. bone resorption and new bone tissue is formed i.e. bone formation. Generally a state of equilibrium is maintained between these processes and they are tightly coupled through a variety of regulatory signals. Approximately twenty percent of bone tissue is replaced annually varying by site and type; however a number of factors such as hormones, cytokines, disease, medication and nutritional status can influence the rate of bone turnover (Carey et al. 2006). In childhood and during the teenage years the balance shifts towards formation as the skeleton develops, peak bone mass is reached during the third decade and

from then onwards resorption predominates. There are sex-specific differences and women normally lose about one to two percent of their bone mass per year as oestrogen levels decline after the menopause however, it has been reported that thirty percent of women lose bone at a much faster rate (Garnero et al. 2000). Bone remodelling is a highly synchronised process, accomplished within basic multicellular units at numerous skeletal sites (Figure 4).

Resorption is a complex procedure requiring dissolution of the bone mineral and degradation of the organic matrix. Initially activated osteoclasts form a sealing zone whereby integrin receptors bind to specific amino acids in the organic matrix. Osteoclasts break down bone by pumping hydrogen ions across their metabolically active ruffled borders to decalcify the inorganic matrix; additionally they release lysosomal enzymes; tartrate resistant acid phosphatase (TRAP) and cathepsin K, plus matrix metalloproteases (MMPs), which effectively digest the exposed type-1 collagen releasing specific degradation products (Schett 2007). Osteoblasts are attracted to this eroded surface and begin to form new osteoid; comprising of type I collagen and non-collagen proteins such as bone sialoprotein, osteocalcin, osteonectin, osteopontin and vitamin D3 receptor. Type 1 procollagen is synthesised by fibroblasts and osteoblasts; it contains both N (amino) and C (carboxy) terminal extensions i.e. propeptides, which are removed by specific proteases during its conversion to collagen and its subsequent incorporation into the bone matrix. Osteoblasts also secrete bone alkaline phosphatase (BALP) to create sites for calcium and phosphate deposition ready for osteoid mineralization (Franz-Odenaal et al. 2006). Initially hydroxyapatite crystals are deposited in the osteoid then a slower mineralisation process continues over several months, followed by a period of quiescence (Wheater et al. 2013).

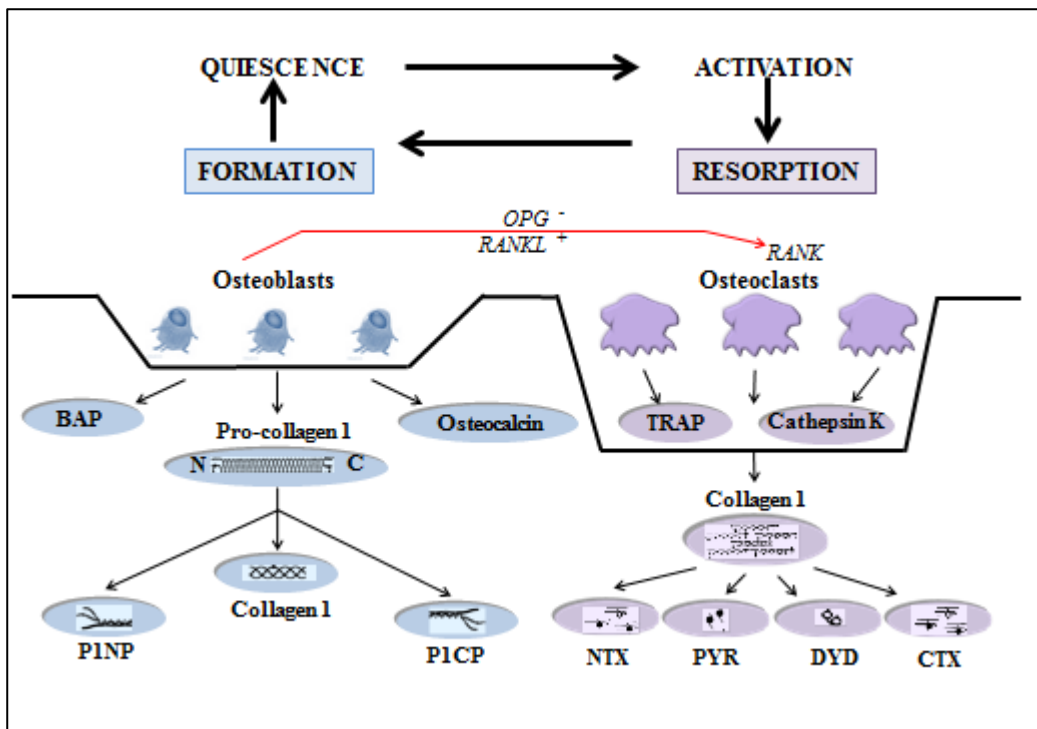


**Figure 4** The bone remodelling cycle

The skeleton is continuously remodelled throughout life. Bone remodelling involves the removal of bone by osteoclasts followed by formation of new bone matrix by osteoblasts. RANKL binds to its cellular receptor RANK on pre-osteoclasts and promotes their differentiation and activation. OPG a decoy receptor for RANKL can reduce bone resorption by binding to RANKL and preventing further osteoclastic activity. Activated osteoclasts create resorption pits with low pH to dissolve the inorganic matrix and lysosomal enzymes, such as TRAP and cathepsin K, effectively digest the exposed type-1 collagen releasing specific degradation products. Osteoblasts are attracted to this eroded surface and begin to form new osteoid. Type-1 pro-collagen is cleaved at the amino- and carboxy-terminals releasing propeptides into the blood. Initially hydroxyapatite crystals are deposited in the osteoid then a slower mineralisation process continues over several months, followed by a period of quiescence (Wheater et al. 2013).

**BALP**: bone alkaline phosphatase; **CTX**: carboxy-terminal cross-linked telopeptides of type I collagen; **DPD**: deoxypyridinoline; **NTX**: amino-terminal cross-linked telopeptide of type I collagen; **OPG**: osteoprotegerin; **PICP**: procollagen type 1 carboxy-terminal propeptide; **PINP**: procollagen type 1 amino-terminal propeptide; **PYD**: pyridinoline; **RANK**: receptor activator of nuclear factor kappa B; **RANKL**: receptor activator of nuclear factor kappa B ligand; **TRAP**: tartrate resistant acid phosphatase

### **1.2.4 Bone cell differentiation and regulation**

There are three basic types of bone cell; osteocytes, osteoblasts and osteoclasts. This brief summary describes their respective differentiation from progenitor cells and local regulation.

#### Osteocytes

Osteocytes are the most abundant cells in bone, it is estimated that there are over forty-two billion osteocytes in the adult human skeleton (Buenzli and Sims 2015). Osteocytes originate from mesenchymal stem cells through osteoblast differentiation (Figure 5), whereby osteoblasts can; become encased in mineralised osteoid as osteocytes, remain inactive osteoblasts, bone-lining cells or undergo programmed cell death (Franz-Odenaal et al. 2006). Osteocytes occupy small pores in the bone called lacunae, they connect with each other, to cells on the mineralised surface or to blood vessels via elongated dendritic processes contained within fluid filled micro-canals or canaliculi. This osteocytic lacunar-canalicular system allows the transport of proteins produced and secreted by osteocytes to act on other cells or tissues. Historically it was believed that osteocytogenesis was a passive process, however recent evidence particularly in a mouse model, suggests that the osteocyte network is a highly complex communication system and osteocytogenesis is an active invasive process, dependent on membrane-type matrix metalloproteinase 1 (MT1-MMP) and continuous cleavage of type-I collagen for maintenance of the osteocyte phenotype (Holmbeck et al. 2005). Recent reviews exploring osteocyte function have also recognised that osteocytes are; mechanosensory cells responsible for the maintenance of bone structure and mass, important regulators of both osteoclastic and osteoblastic activity and key endocrine cells with a role in phosphate and calcium metabolism (Dallas and Bonewald 2010, Bonewald 2011, Buenzli and Sims 2015). *In vivo* studies have shown that osteocyte depletion results in profound loss of trabecular bone mass (Noble et al. 2003, Gross et al. 2005, You et al. 2008), and suggest a close interaction between osteocytes and other bone cells, highlighting their role in the regulation of both bone formation and resorption. Recent research has focused on treatments targeting the Wnt signalling pathway in the management of osteoporosis and related bone diseases.

Osteocytes can regulate osteogenesis through direct contact with osteoblasts via their dendritic processes. The critical signalling pathways described for osteoblast differentiation and maturation are either; canonical wingless-int (Wnt)/  $\beta$ -catenin or non-canonical. Frizzled (Fz), low-density lipoprotein receptor-related protein (LRP)5 and LRP6 are co-receptors for transduction of canonical Wnt signalling that leads eventually to  $\beta$ -catenin stabilization and regulation of gene transcription (Datta et al. 2008). Dickkopf (DKK) proteins and sclerostin

(SCL), a product of the *Sost* gene, are both secreted by osteocytes and bind to LRP5 and LRP6 preventing activation of Wnt signalling in the canonical pathway and also oppose bone morphogenetic protein (BMP) action (Li et al. 2005). Similarly, osteocytes can influence osteoclastogenesis as they are a major source of receptor activator of nuclear factor- $\kappa$ B ligand (RANKL) (Nakashima et al. 2011) and osteoprotegerin (OPG) (Kramer et al. 2010). Additionally research has targeted the complex regulation of osteocyte action by expression of the parathyroid hormone (PTH)/ PTH related protein (PTHrP) receptor's (PPR's). Osteocyte activation of PPR leads to down-regulation of *Sost* and increased Wnt signalling stimulating bone formation, accompanied by up-regulation of RANKL expression and osteoclast number increasing resorption. In contrast the main effect of PPR deletion on osteocytes is reduced osteoclast and osteoblast numbers and decreased bone remodelling (Bellido et al. 2013).



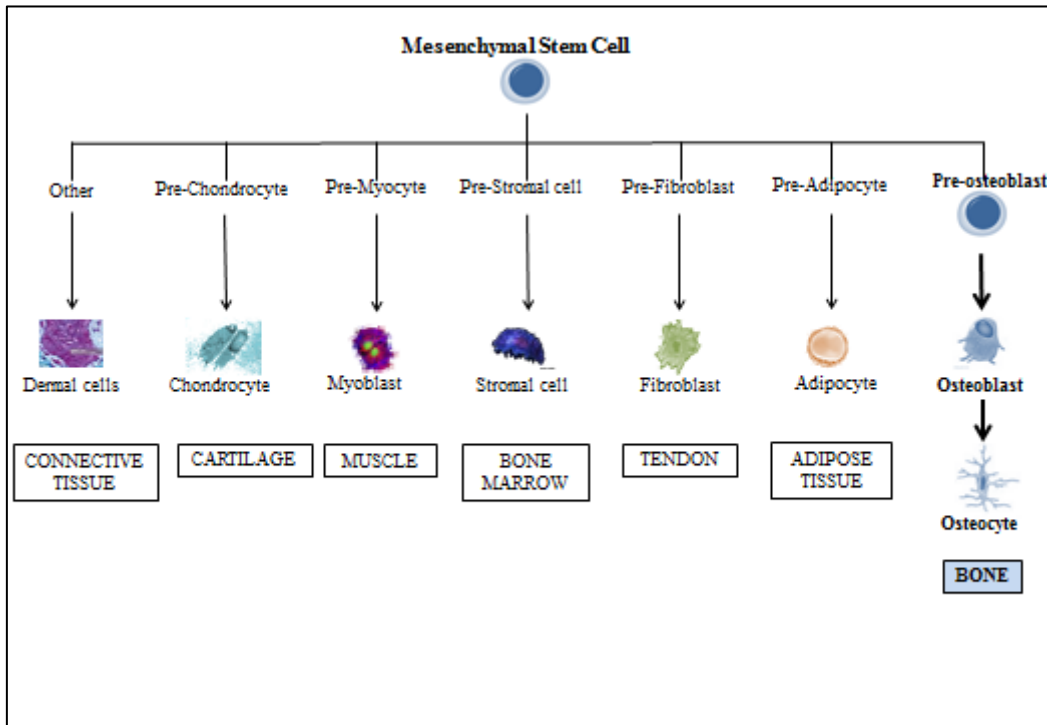


**Figure 5 Graphical representations of the pathways leading particularly to osteoblast and osteocyte differentiation from mesenchymal stem cells**

Mesenchymal stem cells have the capacity to differentiate into a number of cell types including both osteoblasts and osteocytes, in addition to dermal cells, chondrocytes, myoblasts, stromal cells, fibroblasts and adipocytes depending on the local environmental factors to which they are exposed.

### Osteoblasts

Osteoblasts are mononuclear cells of mesenchymal origin (Figure 5) they are committed bone precursor cells responsible for osteogenesis. Osteoblast numbers are therefore dependent on the rate of mesenchymal cell proliferation and differentiation into osteoblasts, which depends on multiple transcription factors and regulatory signals, and also on osteoblast apoptosis. RUNX2, osterix (OSX), homeobox proteins; MSX2, DLX3, DLX5, DLX6 and members of the activator protein-1 (AP-1) family such as Fos and activating transcription factor-4 (ATF4) have all been reviewed and established as critical transcription factors for osteoblast formation (Gonciulea and Jan de Beur 2015). Additionally, Wnt/  $\beta$ -catenin, BMP a transforming growth factor-beta (TGF- $\beta$ ) super-family member and insulin-like growth factor-1 (IGF-1) provide the regulatory signals for osteoblast formation (Gonciulea and Jan de Beur 2015). Osteoblasts are found in the growing portions of bone, including the periosteum and endosteum and they are responsible for making osteoid. Following matrix formation the majority of osteoblasts die by apoptosis or either become incorporated in the matrix as osteocytes or remain on the surface as bone lining cells (Franz-Odenaal et al. 2006).

### Osteoclasts

Osteoclasts are end-differentiated cells formed from circulating precursors of the monocyte/macrophage lineage (Figure 1) from hematopoietic stem cells (HSC). The precursor cells migrate to the bone microenvironment and fuse together depending on local regulatory factors (Schett 2007). Osteoclasts are large, highly specialized, multinucleated cells (Figure 6) and are specialized in bone resorption. Osteoclastogenesis is critically dependent on two factors; macrophage-colony stimulating factor (M-CSF), a polypeptide growth factor and RANKL, a TNF related cytokine. M-CSF binds to colony-stimulating factor 1 receptor (c-fms), on osteoclast precursors and triggers their survival and proliferation (Figure 7). RANKL, expressed on the surface of osteoblasts, binds to its cellular receptor; receptor activator of nuclear factor -  $\kappa$ b (RANK) on pre-osteoclasts and promotes their differentiation and activation (Blair and Zaidi 2006). Conversely, OPG a decoy receptor secreted by osteoblasts and other stromal cells can reduce bone resorption by binding and neutralising RANKL, thus inhibiting osteoclastogenesis and inducing osteoclast apoptosis (Lacey et al 1998).

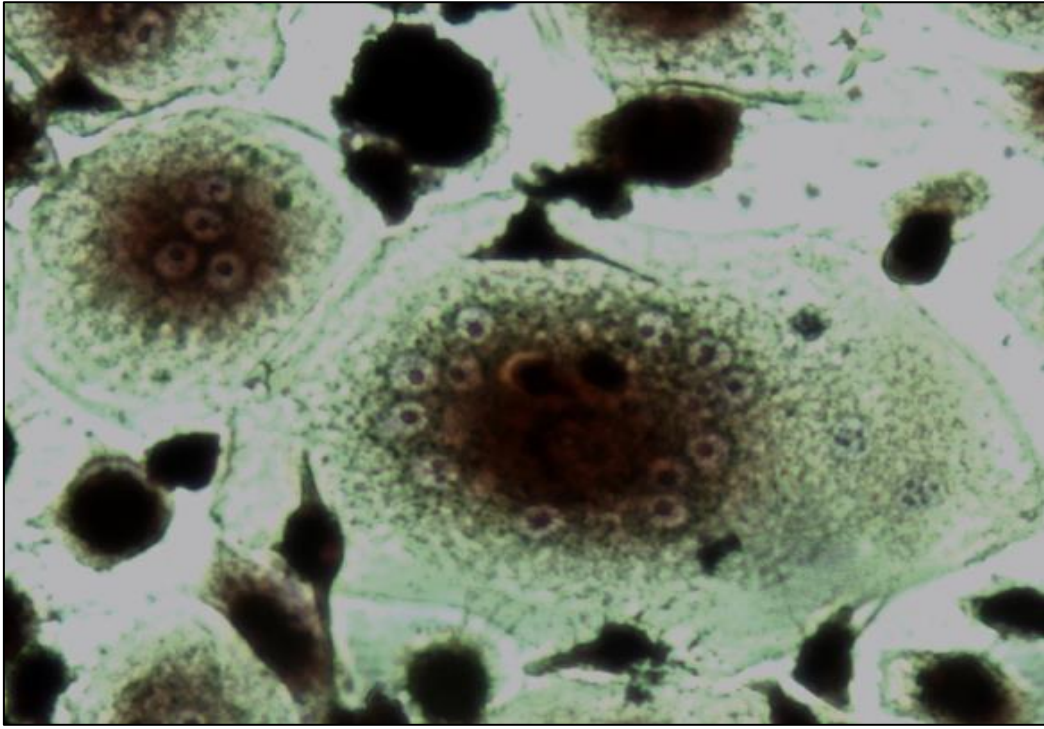


**Figure 6 Osteoclast cells stained with tartrate resistant acid phosphatase**

Osteoclasts are the cells responsible for bone resorption. This image shows giant multinucleated osteoclasts with ruffled borders that have stained positive for tartrate resistant acid phosphatase.

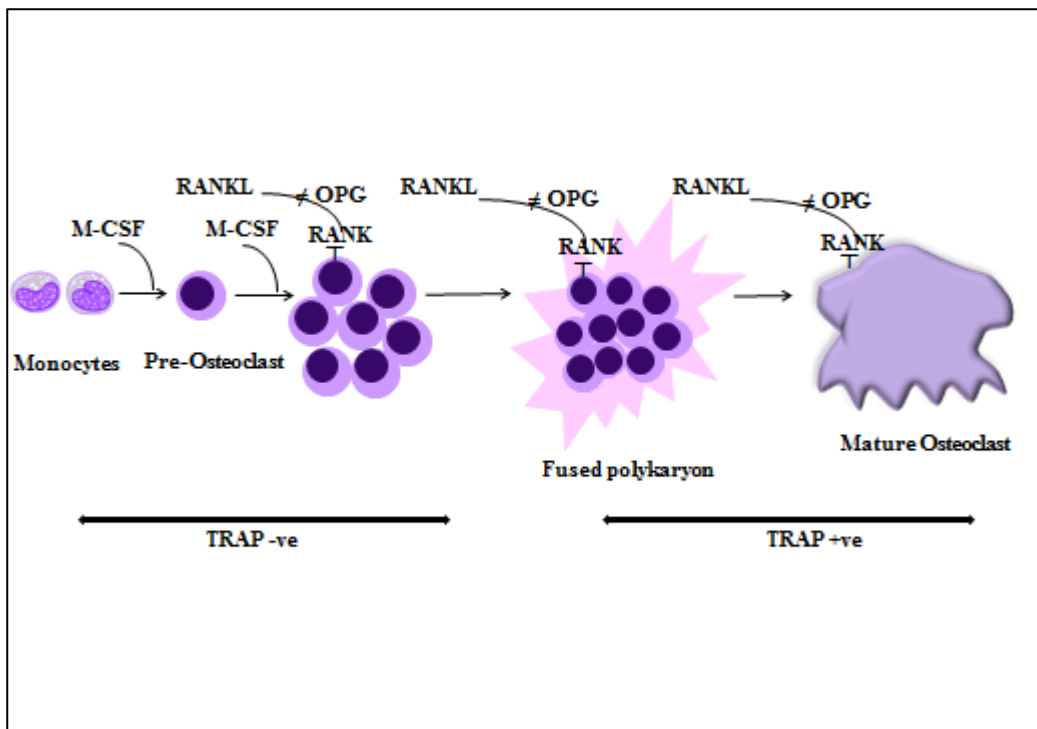


**Figure 7 Osteoclast differentiation**

Osteoclasts are derived from the hematopoietic cell lineage. M-CSF and RANKL are both required and provide the necessary signals enabling promyeloid precursor cells to differentiate into mature osteoclasts. M-CSF acts through its receptor c-Fms and stimulates the proliferation and prevents the apoptosis of early osteoclast precursors. RANKL, a tumour necrosis family member, targets specialized osteoclast differentiation specifically in the bone marrow milieu. RANKL binds and activates its cellular receptor RANK thereby inducing a signalling cascade leading to the differentiation and fusion of osteoclast precursor cells. The effects of RANKL can be counterbalanced by OPG, a soluble decoy receptor which binds and neutralises RANKL, thus inhibiting osteoclastogenesis and inducing osteoclast apoptosis.

M-CSF: macrophage colony- stimulating factor; OPG: osteoprotegerin; RANK: receptor activator of nuclear factor -  $\kappa$ b; RANKL: receptor activator of nuclear factor -  $\kappa$ b ligand; TRAP: tartrate resistant acid phosphatase.

The production of RANKL and OPG by osteoblasts is influenced by hormones (PTH, oestrogen, glucocorticoids); growth factors (BMP, IGF1, TGF- $\beta$ ) and cytokines (TNF- $\alpha$ , IL-1, IL-6, IL-17) and the balance between RANKL and OPG can therefore determine the degree of osteoclastic bone resorption (Geusens 2012, Gonciulea and de Beur 2015). RANKL-RANK interactions also involve downstream signalling molecules; TNF receptor-associated factor-6 (TRAF-6) activates nuclear factor kappa-light-chain-enhancer of activated B cells (NF- $\kappa$ b); a family of dimeric transcription factors that recognise a common DNA sequence called the  $\kappa$ b site, and finally nuclear factor of activated T cells cytoplasmic-1 (NFATc1) leading to an increase in intracellular calcium and tyrosine phosphorylation (Asagiri and Takayanagi 2006). Current evidence suggests that osteoclast-associated receptor (OSCAR) and a triggering receptor expressed on myeloid cells-2 (TREM-2) are also involved (Datta et al 2008). OSCAR is expressed by pre-osteoclasts and signals via an adapter molecule Fc receptor gamma chain (FcR $\gamma$ ) (Barrow et al. 2011), which has an immuno-receptor tyrosine-based activation motif (ITAM) that is critical for the activation of calcium signalling. DNAX activation protein-12 (DAP12), another ITAM –harbouring adaptor is also involved. The precise mechanism is not yet understood however, cooperation between RANK, OSCAR and TREM-2 signalling leads to an increased phosphorylation of ITAM.

### **1.2.5 Biochemical markers of bone turnover**

The rate of bone turnover can be assessed by the measurement of specific proteins/ enzymes generated during the bone remodelling process (Figure 4) and released into the blood. Bone turnover markers (BTMs) have been used in research for a long time but they have only recently found a niche in the clinical management of bone diseases. However, BTMs are not known to control skeletal metabolism and are not disease specific; they reflect the entire skeleton regardless of the underlying cause. Furthermore, several BTMs are present in tissues other than bone and can therefore be influenced by non-skeletal processes (Seibel 2005). BTMs can be measured in blood or urine and are used in selective combinations of formation and resorption markers that express the metabolic activity of osteoblasts or osteoclasts respectively. Over the last few years new markers have been identified and new sensitive assays have been developed that are more specific to the bone matrix, currently there is an extensive list of BTMs available and this makes it very difficult to compare research evidence. Many of these assays have now been automated, improving their reliability, speed and cost effectiveness for clinical practice. Nevertheless, analytical aspects such as within and between batch precision, accuracy and standardisation, remain problematic (Seibel et al. 2001). An American study in 2010 compared six commercial laboratories over an eight month

period and concluded that reproducibility varied substantially for urine NTX and serum BALP (Schafer et al. 2010). The International Osteoporosis Foundation, the International Federation of Clinical Chemistry and Laboratory Medicine (Vasikaran et al. 2011) and the National Bone Health Alliance (Bauer et al. 2012), have recommended that a marker of bone formation; procollagen type 1 amino-terminal propeptide (PINP) and bone resorption: carboxy-terminal cross-linked telopeptides of type I collagen (CTX), are used as reference analytes in all future clinical studies. Furthermore they stipulate that these markers should be measured by standardised assays to minimise immunochemical heterogeneity and recommend that manufacturers adopt international reference standards and minimise batch to batch variability (Vasikaran et al. 2011). Moreover, the regulation of pre-analytical sample collection has also been recognised to minimise the effects of biological variation. Bone turnover shows a circadian rhythm, this is more obvious in markers of bone resorption;  $\beta$ CTX is highest between 01:30 and 04:30 hours and may be more than twice that at the nadir between 11:00 and 15:00 hours (Wichers et al. 1999), but this disparity is diminished with fasting (Bjarnason 2002). Bone formation markers osteocalcin and PICP follow the same diurnal pattern but show only twenty percent difference and BALP has two peaks at 14:00 and 23:30 hours with a nadir thirty percent reduced at 06:30 (Hannon and Eastell 2000). Blood samples should therefore be collected early morning and following an overnight fast to diminish these effects. The advantages and disadvantages of using individual markers of bone formation and resorption have recently been reviewed; a summary is included in Table 1 (Wheater et al. 2013).

**Table 1 Major advantages and disadvantages of commonly used bone turnover markers**

BONE MARKER	ADVANTAGES	DISADVANTAGES	SAMPLE
<b>Bone alkaline phosphatase (BALP)</b>	Low intra-individual variability <10% , not affected by renal function (Brown et al. 2009) Food has little effect (Clowes et al. 2002) Long circulatory half-life 1-2 days (Swaminathan 2001) Sample stability (Quist et al. 2004)	Up to 20% cross reactivity with liver isoforms; 2 peaks at 14:00 and 23:30hrs, nadir 30% ↓ at 06:30 (Seibel 2005) Changes with therapy minimal i.e. less than LSC of 25% (Brown et al. 2009) Multiple methodologies, can measure mass or activity (Vasikaran et al. 2011)	Automated and manual immunoassays Serum, EDTA plasma
<b>Osteocalcin</b>	EDTA sample more stable (Stokes et al. 2011) Late marker of osteoblast activity (Brown et al. 2009)	Intact molecule unstable, Influenced by Vit K status, renal function and circadian variability (Brown et al. 2009) Large inter-lab variation (Vasikaran et al. 2011) Released during formation and resorption (Swaminathan 2001) Short half-life of a few minutes (Blumsohn et al 1995) Osteocalcin gene regulated at transcriptional level by 1,25(OH) <sub>2</sub> D3 (Seibel 2005)	Automated and manual immunoassays Multiplex microarray Serum, EDTA plasma
<b>Procollagen type 1 amino-terminal propeptide (PINP)</b>	Low intra-individual variability and good assay precision (Vasikaran et al. 2011) Small circadian rhythm (Brown et al. 2009) Stable at room temp (Stokes et al. 2011) Change from baseline ↓ up to 80% with anti-resorptive and ↓ up to 200% with PTH medication within 3months (Brown et al. 2009)	Total assay affected by delayed clearance of monomeric fraction e.g. in renal failure or metastatic bone disease (Marin et al. 2011)	Automated and manual immunoassays Multiplex microarray Total or Intact fractions Serum, EDTA plasma
<b>Carboxy-terminal cross-linked telopeptides of type 1 collagen (CTX)</b>	Variability ↓ fasting (Bjarnson et al. 2002) Sample stability, especially EDTA (Stokes et al. 2011) Substantial ↓ post anti-resorptive treatment (Bergmann et al. 2009) Blood sample now preferential	Large circadian variation – highest values between 01:30 – 04:30 of approx. 2x nadir at 11:00-15:00 (Wichers et al 1999)	Automated and manual immunoassays Multiplex microarray Urine , serum, EDTA plasma
<b>Tartrate resistant acid phosphatase –isoform 5b (TRAP5b)</b>	Characteristic of osteoclastic activity (Seibel 2005)	Unstable at room temperature (Halleen et al. 2000) Circadian variability ↑ immediately after exercise (Rogers et al. 2011)	Manual immunoassays. Serum

### Bone formation markers

Bone formation markers are osteoblastic enzymes or by-products of osteoblast formation measured in plasma or serum. The most commonly measured bone formation markers include PINP, osteocalcin and BALP. More than ninety percent of organic bone matrix consists of type I collagen, which is derived from type I procollagen synthesised by fibroblasts and osteoblasts. Type I procollagen contains both N (amino) and C (carboxy) terminal extensions (propeptides), which are removed by specific proteases during the conversion of procollagen to collagen (Figure 7) and its subsequent incorporation into the bone matrix. PINP is widely used and is the marker of choice (Vasikaran et al. 2011), procollagen type I carboxy-terminal propeptide (PICP) has a short half-life of six to eight minutes and is cleared by liver endothelial cells via the mannose receptor so is sensitive to certain hormones, PINP on the other hand is cleared via the scavenger receptor (Hannon and Eastell 2006). Osteocalcin is the most abundant non-collagen protein in the bone matrix and is bound to hydroxyapatite via three vitamin K dependent, gamma-carboxyglutamic acid residues, enabling binding to calcium. During bone synthesis it is produced by osteoblasts and is stimulated by vitamin D3 (Rosenquist et al. 1995). Although osteocalcin is also released during bone resorption and is therefore regarded as a marker of bone turnover (Seibel 2005). BALP is present in osteoblast plasma membranes and is released into the circulation after enzymatic cleavage by phospholipase during mineralisation of osteoid. BALP activity or mass concentration can be measured in serum with comparable results (Avbersek-Luznik et al. 2007).

### Bone resorption markers

The majority of bone resorption markers are degradation products of bone collagen, the exception being tartrate-resistant acid phosphatase (TRAP) and cathepsin K. Historically urinary markers were used and relied on complete twenty-four hour collections or creatinine ratios. Type I collagen has a triple helix structure, the strands are stabilised by intra-molecular covalent cross-links between lysine or hydroxylysine residues that join the non-helical end of one collagen molecule to the helical portion of the adjacent molecule. There are two major cross-link molecules, pyridinoline (PYD) and deoxypyridinoline (DPD), formed extracellularly after the collagen is deposited in the bone matrix. These cross-linked molecules are released into the circulation from bone during the breakdown of mature collagen only and are excreted in the urine as free molecules. DPD is the more bone specific marker as PYD is also found in type II collagen (Hannon and Eastell 2006). Type I collagen alpha 1 helicoidal peptide (HELP) can also be measured, preferably in a twenty-four hour urine sample, it is cleaved from the helical region of type I collagen by cathepsin K during



bone resorption (Seibel 2005). Approximately sixty percent of the cross-links are released in the form of peptide bound molecules, namely carboxy-terminal and amino-terminal cross-linked telopeptides of type I collagen (CTX and NTX respectively). CTX is generated by cathepsin K activity, the CTX epitope contains an aspartyl-glycine motif that is susceptible to spontaneous isomerisation and racemisation generating four isoforms (Swaminathan 2001); the  $\alpha$ -aspartic acid converts to the  $\beta$ -form as the bone ages. Specialized serum immunoassays are now available that target  $\beta$ CTX indicative of the breakdown of mature type I collagen, this is currently the preferred marker of bone resorption (Vasikaran et al. 2011). NTX is also cleaved by cathepsin K and can be measured by specific immunoassays but is less often used. Carboxy-terminal cross-linked telopeptide -MMP (CTX-MMP) cleaved from type I collagen by MMP can also be measured in serum by a manual immunoassay but is less responsive to the usual osteoporotic treatments (Vasikaran et al. 2011). There are at least five different isoforms of acid phosphatase expressed by different tissues and cells in the body and all are inhibited by L(+) tartrate except band 5. The polypeptide chain of TRAP is cleaved by proteases into two distinct sub-forms 5a and 5b, which activate phosphatase activity; TRAP-5a is thought to be expressed by macrophages and TRAP-5b is present in large quantities in the ruffled border of osteoclasts and reportedly reflects osteoclast numbers (Alatalo et al. 2004). Activated osteoclasts secrete TRAP5b which then cleaves type I collagen into fragments. Finally cathepsin K, a cysteine protease present in the ruffled border of actively resorbing osteoclasts that cleaves telopeptide and helical regions of type I collagen can be measured in serum by manual immunoassay. However, it is unstable at room temperature and the clinical validity of the assay needs further investigation (Seibel 2005).

### Osteocyte markers

Osteocytes produce various factors that can be measured in serum such as SCL, DKK-1, dentin matrix protein-1 (DMP-1) and matrix extracellular phosphoglycoprotein (MEPE). Currently these assays are only used in research; their diagnostic importance has yet to be validated due to their large analytical and biological variability (Wheater et al. 2013). SCL levels correlate positively with age, body mass index (BMI) and BMD and negatively with osteocalcin and calcium (Amrein et al. 2012). Serum SCL levels are regulated by both oestrogens and PTH in postmenopausal women (Mirza et al. 2010); levels are decreased in women with postmenopausal osteoporosis compared with non-osteoporotic early postmenopausal women and positively correlated to lumbar spine BMD. Furthermore, levels

are increased after 6 months treatment with risedronate, but remain essentially unchanged after 6 months teriparatide treatment (Polyzos et al. 2012).

### Osteoclastogenesis markers

Osteoclast regulatory proteins are measured in research only. A limited number of commercial assays are available to measure these proteins but with limited success (Bowsher and Sailstad 2008). RANKL is expressed *in vivo* in either a membrane-bound or soluble form. Additionally, in serum it can be either a free molecule or OPG-bound, as a consequence there have been methodological differences between immunoassays making it difficult to compare results. Furthermore, circulating RANKL levels may not reflect the bone microenvironment (Kearns et al. 2008).

### 1.3 Interactions between the immune and skeletal systems

Osteoimmunology is a research field focused on the molecular understanding of the interplay between the skeletal and immune systems. The close interaction between immune progenitors and the skeleton is facilitated by their proximity in the bone marrow and a number of cell surface receptors, cytokines and signalling pathways serve a critical role in both systems (Datta et al. 2008). Crosstalk between bone cells and B cells is bidirectional, in that bone cells can regulate the development and maturation of B cells and B cells can regulate both osteoblastic and osteoclastic activity under different physiological and pathological conditions. The mechanisms that underlie these interactions are only partially understood as is the precise role of B cells in bone turnover. The following section contains a brief overview of the interactions between B cells and bone cells and the factors that influence them.

#### 1.3.1 Osteoblasts and B cells

The differentiation of hematopoietic progenitors in the bone marrow requires specific microenvironments or 'niches' provided by various subsets of stromal cells; osteoblast lineage cells play a supportive role here particularly in the maintenance of B lymphopoiesis. Osteoblasts are mononuclear cells of mesenchymal origin, the transcription factor RUNX2 is required for osteoblastogenesis reinforced by OSX and evidence of osteoblast maturation comes from the expression of BALP, type I collagen and non-collagen proteins; osteocalcin and osteopontin. Panaroni and Wu (Panaroni and Wu 2013) suggest that it is the earlier developmental stages of the osteoblast lineage that are crucial to B lymphopoiesis and these osteoblastic cells are an important source of both C-X-C motif chemokine 12 (CXCL12); necessary for the development of early B cell precursors and their retention in the bone marrow and IL-7; important for progression to pre-B cells. Most of this evidence for the osteoblastic support of B cell development comes from murine studies. One such study has shown that cells of the osteoblastic lineage are both necessary and sufficient for murine B cell commitment and maturation from HSCs via lymphoid progenitors. HSCs cultured on purified osteoblasts *in vitro* stimulated B cell differentiation by; vascular cell adhesion molecule 1 (VCAM-1), stromal cell-derived factor 1 (SDF-1 also known as CXCL12) and IL-7 signalling pathways induced by PTH. To confirm osteoblastic involvement cytokines produced by non-osteoblastic cells i.e. c-Kit ligand, IL-6 and IL-3, were added and the authors found that HSC differentiation shifted towards myelopoiesis. Furthermore, selective elimination of osteoblasts *in vivo* resulted in severely depleted early B cell lineages (Zhu et al. 2007). Expression of both CXCL12 and IL-7 is increased by PTH, in a further study blockade of PTH signalling by ablation of the heterotrimeric G protein  $\alpha$  subunit ( $G_{S\alpha}$ ); a major downstream mediator of

PPR signalling, led to a 59% decrease in the number of B cells in the bone marrow but not in the other hematopoietic lineages and IL-7 expression was diminished in  $G_{S\alpha}$ -deficient osteoblasts (Wu et al. 2008).

### 1.3.2 Osteoclasts and B cells

The role of osteoclasts in B cell development is uncertain. A murine study of zoledronate-induced osteopetrosis in normal mice found a decrease in B cell numbers in the bone marrow which was not directly related to zoledronate. The zoledronate did not directly affect the B cell differentiation, proliferation or apoptosis but induced a decrease in CXCL12 and IL-7 expression by stromal cells associated with osteoblastic activity, the authors further confirmed that the results were due to reduced osteoclastic activity; zoledronate did not directly affect the osteoblasts (Mansour et al. 2011). The authors concluded that osteoclasts can modulate B-cell development in the bone marrow by controlling the bone microenvironment and the osteoblastic activity but they could not rule out the hypothesis that osteoclasts may directly affect B lymphopoiesis. A study by Manabe et al proposed a further link between osteoclast and B cell differentiation; *klotho* mutant mice ( $KL^{-/-}$ ); the mouse model for human ageing that has reduced bone turnover during bone metabolism rather than a decrease in the differentiation potential of osteoclast progenitors, exhibited a decrease in osteoclasts associated with a decrease in B cells (Manabe et al. 2001). Additionally, they reported that early developmental stage B cells have the potential, when stimulated by M-CSF and RANKL, to differentiate into osteoclasts *in vitro* (Manabe et al. 2001). But these findings were later challenged in another study using fluorescence-activated cell sorting (FACS) to identify subsets of bone marrow cells that had osteoclastogenic potential, the authors reported that highly purified  $CD45^{+}$  bone marrow cells were not capable of osteoclastogenesis *in vitro* (Jacquin et al. 2006). The Pax5 gene codes for the transcription factor B cell lineage-specific activation factor (BSAP); Horowitz et al. show that  $Pax5^{-/-}$  mice have a development arrest of B cell lineage at the pro-B cell stage they are also osteopenic with a 100% increase in osteoclast numbers and 60% reduction in their bone mass, the authors suggest that Pax5 is a possible transcription factor for normal regulation of osteoclastogenesis (Horowitz et al. 2004).

### 1.3.3 B cells and the RANK-RANKL-OPG system

Bone homeostasis is delicately balanced between bone resorption by osteoclasts and bone formation by osteoblasts in healthy individuals and osteoclastogenesis is controlled by the ratio of RANKL to its decoy receptor OPG. B cells can produce the pro-osteoclastogenic

cytokine RANKL (Choi et al. 2001) and under pathologic conditions such as RA this process is markedly enhanced by pro-inflammatory cytokines such as TNF- $\alpha$ , IL-1, IL-6 and IL-17 (Schett 2006). Furthermore, in a recent study Yeo et al. assessed the cytokine messenger RNA expression profiles in CD4 and CD8 T cells, B cells, macrophages and neutrophil populations in synovial fluid and in the peripheral blood of twelve RA patients and found that B cells had the highest expression of RANKL (Yeo et al. 2011). However, B cells can also produce OPG; the cytokine that inhibits osteoclast differentiation from the progenitor cells (Weitzmann et al. 2000). *In vivo* animal studies on the role of mature B cells in bone remodelling have been equally inconsistent. In a murine study, five weeks after ovariectomy, bone turnover remained imbalanced with increased osteoclastogenesis and decreased bone formation but there was an increase in B cells expressing RANKL with normal or decreased T cells (Garcia-Perez et al. 2006). In contrast, Li et al report that cells of the B lineage are responsible for 64% of the total bone marrow OPG production, with 45% from mature B cells. Furthermore T cells through CD40 ligand to CD40 co-stimulation promote OPG production by B cells. B-cell knockout mice were consistently osteoporotic and deficient in OPG; the RANKL/OPG ratio had increased in favour of RANKL activated osteoclastogenesis in these mice, generating more TRAP<sup>+</sup> osteoclast-like cells (Li et al. 2007). The authors suggest that the production of OPG by B cells outweighs the production of RANKL under basal conditions (Li et al. 2007). It appears that mature B cells have the capacity to both inhibit and stimulate osteoclastogenesis. It is not therefore surprising that while some studies have shown B cells to stimulate osteoclastogenesis, others have shown that B cells are inhibitory. It is now known that B cells contribute to RANKL production in the inflamed rheumatoid joint (Yeo et al. 2011) and in particular switched memory B cells have the greatest propensity to produce RANKL (Meednu et al. 2015). Meednu et al. hypothesise that the role of B cells in bone erosion is developmental and stage-dependent; they confirmed that stimulated B cells promote *in vitro* osteoclastogenesis from monocytes in a RANKL dependent manner (Meednu et al. 2015). Recently a subset of B cells, expressing FcRL4, has been identified in the rheumatoid synovium that are capable of producing RANKL and TNF- $\alpha$  and these pathogenic B cells are reportedly not found in healthy individuals (Yeo et al. 2015). FcRL4<sup>+</sup> B cells also express high levels of CD20 and are therefore significantly reduced with rituximab (RTX) (Yeo et al. 2015).

## 1.4 Rheumatoid arthritis

### 1.4.1 Epidemiology

RA is a progressive, systemic, autoimmune disease, characterised by widespread and persistent inflammation of the synovial lining of the joints and tendon sheaths. The typical age of onset is 20 to 45yrs and over 75% of patients are female (Silman and Pearson 2002). The prevalence of RA in the United Kingdom (UK) is approximately 1.2% in women and 0.44% in men (Symmons et al. 2002). The skeletal complications of RA consist of focal erosion of marginal and subchondral bone, juxta-articular osteoporosis and generalised bone loss with reduced bone mass. The prevalence of osteoporosis in RA patients ranges from 25 to 50%, depending on the history of prednisone therapy (Kelly et al. 2002). The consequences of this profound bone loss are painful joints, loss of physical function, fatigue and together with the other symptoms of RA have a major impact on social life. The disease is costly to individuals and their families and to society as a whole in both economic and social terms. RA causes significant functional disability by the first decade of onset in about 50% of patients, with an approximate life expectancy reduction of up to 18yrs in 80% of the patients after the second decade of progression (Kosinski et al. 2002). Although the aetiology of RA is largely unknown and no cure exists, treatments have been developed to target pain reduction, improvement in physical function and reduction in disease progression (Scott et al. 1987).

### 1.4.2 Pathogenesis of bone loss in rheumatoid arthritis

Under physiological conditions bone remodelling is a tightly controlled process in which the equilibrium is maintained between bone formation and bone resorption. In pathological states such as RA, there is a shift towards increased resorption. RA is associated with a generalized skeletal bone loss, in addition to periarticular osteopenia and local bone erosions, summarised in Table 2. RA patients have an increased risk of vertebral and non-vertebral fractures compared with age and gender-matched controls; this risk is increased in patients with longstanding disease, low BMI and in those taking oral glucocorticoids (van Staa et al. 2006). Early RA patients have an annual decrease of -2.4% and -4.3% of BMD at the lumbar spine (LS) and femur respectively (Gough et al. 1994). Additionally some studies have reported that the greatest reduction in bone density occurs at the foreram sites and that forearm BMD correlates with clinical features of disease activity and markers of bone turnover (Franck and Gottwalt 2009). Several factors such as disease activity, female gender, older age, glucocorticoid use and decreased mobility are known to promote generalised bone loss with reduced bone mass in RA patients. However disease activity is the major predictor and is

independent of the other factors (Schett 2006). Furthermore, RA patients are reported to have lower levels of total 25-hydroxyvitamin D (25OHD) and this is associated with increased disease activity and musculoskeletal pain (Kostoglou-Athanassiou et al. 2012). Serum 25OHD is also negatively associated with the disease activity score (DAS)28, erythrocyte sedimentation rate (ESR), platelets, IL-17 and IL-23 and patients with osteoporosis and osteopenia have significantly lower levels of 25OHD than those with normal BMD (Hong et al. 2014).

In contrast, the main cause of periarticular bone loss and marginal joint erosions is chronic inflammation of the synovial membranes. Osteoclasts have been highlighted as mediators of this erosive process, additionally inhibition of the Wnt signalling pathway results in impairment of bone formation resulting in a lack of repair of the erosions (Deal 2012). The synovial membrane is transformed into hypertrophic inflammatory tissue, based on the influx of inflammatory cells including B cells and osteoclast differentiation appears to be enhanced leading to increased bone resorption (Jimenez-Boj et al. 2005). These are areas of high bone breakdown, activated osteoclasts secrete TRAP-5b which then cleaves type I collagen into fragments, CTX is released into the circulation and is indicative of this increased breakdown of mature type I collagen. The bone compartment in closest proximity to the inflamed joints suffer the most severe damage (Schett 2006). RANKL is expressed by osteoblasts and activated T and B cells, upregulation of RANKL by pro-inflammatory cytokines such as TNF- $\alpha$ , together with decreased levels of OPG are thought to be responsible for the increased osteoclastogenesis and therefore bone resorption in RA patients (Haynes et al. 2001, Xu et al. 2012). Furthermore, bone formation is also suppressed; DKK-1 is upregulated in the inflamed synovium and in cartilage adjacent to inflammatory tissue, possibly mediated by TNF- $\alpha$  (Diarra et al. 2007). DKK-1 suppresses Wnt signalling leading to decreased bone formation and suppression of OPG contributing to the overall bone loss and decreased levels of bone formation markers such as PINP and BALP in blood. However, these biomarkers represent total bone cell activity and cannot distinguish local from generalised bone loss in RA. BTMs are used in research in selective combinations of formation and resorption markers that express the metabolic activity of osteoblasts or osteoclasts respectively, they are not known to control skeletal metabolism and are not disease specific; they reflect the entire skeleton regardless of the underlying cause (Seibel 2005). Nevertheless, bone resorption and formation markers can be correlated with inflammatory markers (CRP, ESR) and disease activity (DAS28) and with lumbar spine, hip and forearm BMD to help clarify the cause of the bone loss. Additionally, Bieglmayer and Kudlacek (Bieglmayer and Kudlacek 2009) have

suggested combining a marker of formation and resorption to gain a direct insight into the changes in the balance of bone turnover in relation to a reference value.



**Table 2 Types of bone loss in rheumatoid arthritis**

	<b>Focal bone erosions</b>	<b>Periarticular osteopenia</b>	<b>Generalized skeletal bone loss</b>
<b>Clinical features</b> (Deal 2012)	Joint erosions	Loss of trabeculae	Reduced bone mass
<b>Contributing factors</b> (Deal 2012 unless otherwise stated)	Chronic inflammation of synovial membranes Increased osteoclast precursors (monocytes) Inflammatory B and T cells (Jimenez-Boj et al. 2005) Pro-inflammatory cytokines (TNF- $\alpha$ ) (Schett 2006) Pro-osteoclastogenesis factors (RANKL) Up-regulated DKK-1	Inflammatory cytokines from synovium triggering osteoclast-mediated bone loss	Disease activity (Schett 2006) Female gender Older age Glucocorticoid use Decreased mobility Decreased vitamin D (Kostoglou-Athanassiou et al. 2012)
<b>Bone biomarkers</b> (Deal 2012 unless otherwise stated)	↑ bone resorption ↑ DKK-1 (Diarra 2007) ↓ bone formation	Inhibition of bone formation	Bone resorption > bone formation

### 1.4.3 Pathway of care

The presentation of RA and its prognosis are highly variable both within and between individuals, involving genetic and environmental factors and possibly chance (McInnes and Schett 2011). Because of this variety in disease expression the pathway of care for RA is diverse and dependent on individual patient responses to therapies. The current strategy is to start therapy as soon as possible after diagnosis and to escalate the treatment to achieve clinical remission; as assessed by disease activity (McInnes and Schett 2011). Bakker et al. evaluated the results of four clinical trials; FIN-RACo, TICORA, BeSt and the CAMERA study and found that the current concept of 'tight control' resulted in greater improvement and a higher percentage of patients achieving remission compared to placebo (Bakker et al. 2007). Treatment traditionally started with disease modifying anti-rheumatic drugs (DMARD's) including methotrexate (MTX), sulfasalazine, leflunomide and glucocorticoids, however the current strategy is to use a combination of conventional DMARDs and biologics (Bakker et al. 2007). The development of biologic therapies targeting TNF (adalimumab, etanercept and infliximab) resulted in further improvements in outcomes related to the capacity of these treatments to retard radiographic progression of the disease and improve physical function, as reported in the ARMADA trial (Weinblatt et al. 2003). However, their use has been limited by their high costs and the uncertainty about the long term side effects. There is now evidence that B cells contribute significantly to the pathogenesis of RA and the focus of new biological therapies therefore target B cell depletion. RTX was the first B cell depleting agent used in combination with MTX, it is licensed for the treatment of adults with severe active RA who have had an inadequate response to, or intolerance of other DMARD's, including one or more TNF- $\alpha$  inhibitors (NICE technology appraisal guidance - TA195 August 2010). RTX is a genetically engineered, chimeric mouse-human, monoclonal antibody that depletes the B-cell population by targeting cells bearing the CD20 surface marker. This results in significant depletion of peripheral B cells from early pre B cells to mature B cells, sparing other cell lineages (Figure 1) and stem cells, therefore immunoglobulin secretion by plasma cells is maintained. Several control trials have reported that RTX is an effective treatment in RA e.g. DANCER trial (Emery et al. 2006), REFLEX trial (Cohen et al. 2006) and a short course of treatment with RTX has been shown to result in long term improvement of disease activity in patients with previously refractory RA (Teng et al. 2007). However, biologic and clinical responses to RTX vary greatly; RTX induces clinical responses that last for years in some patients whereas in others the benefits last only a few months (Silverman 2006). Silverman proposes that other mechanisms in addition to simple pharmacokinetic clearance of RTX are involved e.g. tissue depots of RTX in the bone marrow resulting in prolonged B cell depletion

(Silverman 2006). Additionally, combination therapy with MTX may diminish the capacity to produce pro-inflammatory cells including B cell survival factors such as B cell activating factor (BAFF) and a proliferation-inducing ligand (APRIL) (Silverman 2006).

#### **1.4.4 The role of B cells in rheumatoid arthritis**

The role of T cells in the pathogenesis of RA is well established but the contribution of B cells is less well defined. Recent research indicates that B cells may play several critical roles (reviewed in Silverman and Carson 2003, Panayi 2005, Mauri and Ehrenstein 2007):

- B cells are the source of autoantibodies, namely RF and ACPA, which contribute to immune complex formation and complement activation in the joints. RF is present in fifty to eighty percent of RA patients, it is reactive against antigenic determinants on the Fc fragment of the IgG molecule, the severity of RA has been correlated with RF levels, 'seropositive' RA being associated with more aggressive articular disease (Panayi 2005). Additionally, it is thought that B cells with RF specificity migrate to the synovium to present a variety of complex antigens to T cells, thus extending the inflammatory response and amplifying RF production in the synovium (Panayi 2005). Although the biologic significance of ACPA is unclear citrullination may be a by-product of abnormal protein metabolism. B cells from RA patients appear to have greater resistance to certain apoptotic stimuli, ACPA titres are increased and could possibly be linked to impaired lymphocyte clonal regulation in these patients (Silverman and Carson 2003).
- B cells are very efficient antigen-presenting cells and can contribute to T cell activation, proliferation and pro-inflammatory activities, through expression of co-stimulatory molecules. A study by Takemura et al. in the rheumatoid synovium of a mouse model proposed that B cells provided a critical function in T cell activation this was later confirmed following B cell depletion (Takemura et al. 2001).
- B cells both respond to and produce the chemokines and cytokines (TNF- $\alpha$ , IL6) that promote leukocyte infiltration into the joints, formation of ectopic lymphoid structures, angiogenesis, and synovial hyperplasia (Mauri and Ehrenstein 2007).
- In contrast to the detrimental effects of B cells in RA described above B cells may also have a protective role. Synovial inflammatory tissue can completely disrupt the cortical bone barrier, exposing and replacing the underlying fat-rich bone marrow with B cell-rich mononuclear cell aggregates. However, new bone formation has been described here and it has been hypothesised that these aggregates have a protective effect providing a physical barrier to shield bone marrow at these sites of pannus penetration (Jimenez-Boj et al. 2005, Hayer et al. 2008).

## **1.5 The effect of B cell depletion on bone turnover in rheumatoid arthritis**

The effectiveness of B cell depletion therapies in RA has demonstrated that B cells play a key role in the perpetuation of RA. RA is associated with chronic inflammation and bone loss and cytokines are recognised as important factors; the joint is infiltrated by multiple inflammatory cell populations including T cells, B cells, macrophages and neutrophils, all of which contribute to the local cytokine network. However, RANKL, the key cytokine driving bone destruction by osteoclast activation, is produced by synovial B cells in RA (Yeo et al. 2011, Meednu et al. 2015). Crosstalk between B cells and bone cells is bidirectional; bone cells can regulate the development and maturation of B cells and B cells can regulate osteoblastic and osteoclastic activity. The mechanisms that underlie these interactions are only partially understood as is the precise role of B cells in bone turnover. Defects in the RANKL-RANK-OPG signalling axis result in altered bone phenotypes. While the role of B cells during normal bone remodelling appears minimal, activated B cells play an important role in RA related skeletal damage (Horowitz 2010).

### **1.5.1 Current evidence from clinical trials**

Keystone et al. provided the first evidence that RTX causes a significant reduction in joint damage progression in patients with severe refractory RA previously enrolled into the REFLEX trial; 287 patients received RTX plus MTX and 192 received placebo plus MTX. After 56 weeks there was a significant improvement in the Genant-modified Sharp score (Keystone et al. 2009). Similar results were reported in patients enrolled into the IMAGE trial; 249 patients received MTX alone, 249 received RTX (2× 500mg) plus MTX and 250 received RTX (2× 1000mg) plus MTX. After 52 weeks there was a significant improvement in the Genant-modified Sharp score in patients treated with RTX (2× 1000mg) in combination with MTX (Tak et al. 2011). A small study of 13 patients with active RA was the first to investigate the effects of RTX on systemic bone remodelling. However, there was no significant difference in serum markers of osteoclastogenesis (OPG, sRANKL), bone formation (PICP, BAP) or bone resorption (TRAP5b), but DPD a urinary marker of bone resorption was significantly reduced after 15 months (Hein et al. 2011). Finally a further group reported that RTX significantly affects the RANK/RANKL/OPG system in the synovium and peripheral blood of 28 patients with active RA. After 16 weeks the number of RANK positive osteoclast precursors in synovial tissue had significantly decreased by 99% and RANKL expression had decreased by 37%, serum RANKL and OPG had both decreased but the OPG/RANKL ratio had increased. These alterations in the RANK/RANKL/OPG

system were not related to radiological progression, as assessed by the Sharp-van der Hijde score of their hands and feet. However, joint destruction was stabilised in a large majority of patients, indicating that RTX's interference with the mediators of osteoclastogenesis resulted in the inhibition of further bone loss. (Boumans et al.2012).

These studies have shown that RTX not only significantly reduces clinical symptoms and inflammation in RA but also inhibits the progression of structural joint damage, highlighting the connection between B cells and bone homeostasis in RA and advocating that B cells may play a key pathogenic role in bone erosion. Some of these effects may be indirect through attenuation of systemic inflammation, while others may be direct as a result of the absence of B cells during osteoclast formation.

### **1.6 Project aims**

This project aims to address the role of human B cells in bone turnover. Given the impact of B-cells in the pathogenesis of RA and apparent importance in regulating bone cell activity it is postulated that prolonged B cell depletion in patients with RA may have a beneficial effect on the bone loss that would otherwise be expected in active disease. Furthermore, this affect may be direct through modulation of osteoclastogenesis or indirect through attenuation of systemic inflammation and increased physical activity. Therefore, the main study aims were:

- 1) To initially explore the effects of B cell depletion on serum biomarkers of bone turnover before and after RTX treatment in a cohort of patients with severe RA.
- 2) To confirm and extend these findings in a second cohort of RA patients to additionally measure the change in bone density and to explore factors that may influence the outcome such as change in disease activity and vitamin D status.
- 3) To evaluate and create a robust, reproducible protocol for osteoclast formation and characterisation from peripheral blood *in vitro*, representative of *in vivo* conditions without the addition of endogenous substances.
- 4) Finally to use this culture system to investigate the potential role of B cells on osteoclastogenesis; using healthy volunteer blood depleted of B cells *in vitro*, plus blood from RA patients following B cell depletion *ex vivo*.



# **Chapter 2**

## **Materials and Methods**





## Chapter 2. Materials and methods

This Chapter contains a general description of all the materials, methods and subjects that were used throughout this study to investigate the aims of this work outlined in Chapter 1. Initially a range of automated and manual bone turnover assays were evaluated for use in the following clinical studies:

1. Pilot study to investigate the effect of *in vivo* B cell depletion on markers of bone turnover pre and 6 months post RTX in RA patients.
2. Prospective study to investigate the effect of *in vivo* B cell depletion on bone mineral density and bone turnover markers pre and 3, 6 and 12 months post RTX in RA patients.

Finally, to investigate *in vitro* osteoclastogenesis, a protocol for osteoclast formation and characterisation from peripheral blood was optimised for use in the following experiments:

1. Potential role of B cells on *in vitro* osteoclastogenesis in healthy volunteer unfractionated and CD20 depleted peripheral blood mononuclear cells (PBMCs).
2. Potential role of B cells on osteoclastogenesis in RA patient PBMCs pre and 3, 6 and 12 months post RTX *ex vivo*.

Throughout this thesis *in vitro* (Latin translation: in glass) experiments are defined as; osteoclast culture, using unfractionated and artificially depleted CD20<sup>-</sup> PBMCs in the laboratory. In contrast, *ex vivo* (Latin translation: out of the living) experiments refer to; osteoclast culture, using PMBCs isolated from RA patient blood pre and post CD20 depletion using RTX administered as a 1000mg intravenous infusion in the Rheumatology clinic i.e. with minimal alteration of natural conditions.

Specific details of any modifications to these general methods are explained in more detail in the relevant sections of the respective Chapters. All the experiments for this research project were carried out in the Research laboratories or Pathology department at The James Cook University Hospital (JCUH), Middlesbrough.

### 2.1 Materials

All the materials used in this research, unless otherwise stated, were obtained from companies or their distributors based in the United Kingdom. All generic reagents, consumables and equipment are listed in appendix A.

### **2.1.1 Biomarker reagents**

- The manual ELISA kits for DKK1; product code BI-20413 and Sclerostin; product code BI-20492 were purchased from Oxford Biosystems Cadama (Wheatley, Oxford, OX33 1NB, UK), a UK distributor for Biomedica Medizinprodukte (1210 Vienna, Austria).
- The manual ELISA kits for ampli sRANKL; product code FS-04PL; OPG; product code FS-01PL were purchased from IDS Ltd. (Boldon, Tyne and Wear, NE35 9PD, UK), a UK distributor for Biomedica Medizinprodukte (1210 Vienna, Austria).

- The manual ELISA kit for TRAP isoform 5b; product code SB-TR201APL and the automated chemiluminescence assays for 25OHD; product code IS-2700PL; 25OHD tri-level control set; product code IS-2730; BALP; product code IS-2800; IDS-iSYS BALP tri-level control set; product code IS-2830;  $\beta$ CTX; product code IS-3000PLV3 2011-11; CTX-I tri-level control set; product code IS-3030 and intact PINP; product code IS-4000PL; PINP tri-level control set; product code IS-4030, were obtained from IDS Ltd. (Baldon, Tyne and Wear, NE35 9PD, UK).
- The automated electrochemiluminescent assays for  $\beta$ CTX; product code 11972308 122; N-MID Osteocalcin; product code 12149133 122; PTH; product code 11972103; total PINP; product code 03141071 190, PreciControl Bone 3 levels; product code 11972227 122 and PreciControl Varia 2 levels; product code 05618860 190 were purchased from Roche Diagnostics Ltd. Burgess Hill, West Sussex, RH15 9RY, UK).
- The latex-enhanced immunoturbidimetric assay for wide range CRP (wrCRP); product code 10494060 was purchased from Siemens Healthcare Diagnostics (Camberley, Surrey, GU16 8QD, UK).
- Multichem S Plus - level 1; product code CH101CRP, level 2; product code CH102CRP and level 3: product code CH103CRP were purchased from Technopath Ltd. (Leatherhead, Surrey KT22 9AD).

### 2.1.2 *In vitro reagents*

- Peripheral blood mononuclear cell isolation: Lymphoprep; product code 1114544 (250ml) was purchased from Axis-Shield Diagnostics (Dundee, DD2 1XA, UK).
- Osteoclast culture: Roswell Park Memorial Institute (RPMI) 1640 medium; product code R0883 (500ml), Corning 6 and 24 well plastic microplate with lid; product codes 353046, 3524 and coverslips (round glass 13mm diameter); product code LABS6310149, were purchased from LabShop<sup>®</sup> (Hartlepool, Cleveland, TS25 2DL, UK). Minimum Essential Medium ( $\alpha$ MEM); product code 225171-020 (500ml) and Glutamax-I supplement; product code 35050-038 (100ml), were purchased from Invitrogen Life Technologies (Paisley PA4 9RF, UK). 13 mm circular bone slices were kindly donated by Dr HK Datta (ICM, Newcastle University).
- Osteoclastogenesis experiments: Human recombinant - Macrophage Colony Stimulating Factor (MCSF); product code 216-MC-025 (25 $\mu$ g@10 $\mu$ g/ml) and human recombinant RANKL; product code 6449-TEC (10 $\mu$ g@500ng/ml), were purchased from R&D Systems (Abingdon, OX14 3NB, UK).

- Osteoclast characterisation: Tartrate Resistant Acid Phosphatase (TRAP) staining kit; product code 386 and Trypan Blue; product code T8154 (20ml), were purchased from LabShop® (Hartlepool, Cleveland, TS25 2DL, UK), a UK distributor for Sigma-Aldrich Company Ltd. (Gillingham, SP8 4XT, UK). Toluidine Blue O Basic Blue 17 CI: 52040; product code S3382 (25g), was purchased from RALamb dry dyes at Fischer Scientific UK Ltd. (Loughborough, Leicestershire, LE11 5RG, UK). Alexa Fluor 488 Phalloidin; product code A12379 (300 units) was purchased from Invitrogen Life Technologies (Paisley PA4 9RF, UK).
- Fluorescence Activated Cell Sorting (FACS) reagents: ONCOMARK CD14/CD64 CE reagent; product code 333179, CD3 PERCP-CY5.5 CE reagent; product code 332771, CD19 PERCP-CY5.5 CE reagent; product code 332780, CD45 APC (2D1) CE reagent; product code 340910 and TruCOUNT tubes; product code 340334, were purchased from BD Biosciences (Oxford, OX4 4DQ, UK).
- B cell depletion: Magnetic-Activated Cell Sorting (MACS) BSA Stock solution; product code 130-091-376 (75ml), autoMACS™ Rinsing Solution; product code 130-091-222 (1.45L), LD columns; product code 130-042-901 (25 pack), MS columns; product code 130-042-201 (25 pack), CD20 MicroBeads human; product code 130-091-104 (2ml) and CD14 MicroBeads human; product code 130-050-201 (2ml), were purchased from Miltenyi Biotec (Bisley, Surrey GU24 9DR, UK).
- RTX (1ml containing 10mg/ml); gratefully donated by ICM, Newcastle University.

## 2.2 Methods

The methods used in this thesis comprised of manual and automated assays of bone turnover markers and osteotropic factors, *in vitro* osteoclastogenesis from PBMCs and following B cell depletion. These studies involved modification of osteoclastogenesis and these experiments are described in detail in subsequent relevant Chapters.

### 2.2.1 Biomarker assays

The following automated and manual biomarkers were considered and evaluated for use in the pilot and prospective studies. The major advantages and disadvantages of individual markers was outlined in Chapter 1 section 1.2.4 and summarised in Table 1, where possible automated assays were used to improve technical variability. The manual enzyme linked immunosorbent assays (ELISA's) were carried out in duplicate and the final absorbance's were read on the Labtech 4000 microplate reader (Labtech International Ltd. Uckfield, East Sussex, TN22

1QQ, UK) in conjunction with automated MANTRA software to calculate the sample concentration from a standard curve using pre-defined linear algorithms. Low and high levels of quality control (QC) material were included in each batch.

Automated electro-chemiluminescent immunoassays (ECLIA) were done in singleton on the Roche Elecsys 2010 (Roche Diagnostics Ltd. Burgess Hill, West Sussex, RH15 9RY, UK) unless otherwise stated. All biomarker experiments were carried out in serum or ethylene diamine tetraacetic acid (EDTA) plasma and following the manufacturer's guidelines, unless stated otherwise. The majority of commercial bone biomarker assays are CE (Conformité Européenne) marked for clinical diagnostic use. The CE marking is the manufacturer's declaration that the product meets the requirements of the applicable European Commission directives. It also shows that the manufacturer has checked that these products meet European Union health, safety or environmental requirements and are 'fit for purpose' i.e. they should only be used within the scope of the manufacturer's instructions. Although technological advances have greatly enhanced the accuracy and reliability of BTM measurement, the assays still vary significantly (Seibel et al. 2001, Schafer et al. 2010). Studies from well-characterised populations have reported BTM reference ranges in large cohorts (Glover et al. 2008, Eastell et al. 2012). However, only reference ranges established using the same assay method with standardised pre-analytical conditions are comparable.

Recommendations by the Bone Marker Standards Working Group have proposed that a marker of bone resorption i.e.  $\beta$ CTX and a marker of bone formation i.e. PINP are used as reference analytes in all research studies (Vasikaran et al. 2011, Bauer et al. 2012) and so these markers were used in both clinical studies described in this Chapter. The majority of bone resorption markers are degradation products of type I collagen and  $\beta$ CTX is the marker of choice (Vasikaran et al. 2011).  $\beta$ CTX was measured in 50 $\mu$ l serum (Kit insert - Roche;  $\beta$ CTX; 11972308 122 V8 2007-07), an automated ECLIA already used diagnostically within Pathology and therefore subject to external validation using samples from the United Kingdom National External Quality Assessment Service (UK-NEQAS). The measurable range of this  $\beta$ CTX assay was 10-6000ng/L.

PINP, a commonly used marker of bone formation measured in 20 $\mu$ l serum (Kit insert - Roche; TPINP; 03141071 190 V6 2008-05), has low inter-individual variability (Vasikaran et al. 2011) and is relatively stable in serum at room temperature (Stokes et al. 2011). The measurable range was 5-120 $\mu$ g/L, so ideal for this work. In addition the following biomarkers were used in the specific studies detailed below.

### Biomarkers for the Pilot study

- Osteocalcin (Kit insert - Roche; N-MID Osteocalcin; 12149133 122 V11 2008-03), a bone turnover marker rather than specific bone formation or bone resorption marker was measured by automated immunoassay in 20µl serum; the measurable range was 0.5-300µg/L. Both intact osteocalcin (amino acids 1-49) and the large N-MID fragment (amino acids 1-43) occur in blood. Intact osteocalcin is unstable due to protease cleavage between amino acids 43 and 44. This assay measured the resulting N-MID fraction, the most stable fraction (Rosenquist et al. 1995) using two monoclonal antibodies specifically directed against the epitopes on the MID region (amino acids 20-42) and the N-terminal region (amino acids 1-19).
- OPG (Kit insert - IDS; OPG; FS-01PL V6 2008-10) a marker of osteoclastogenesis was measured in 50µl serum using a manual IDS ELISA. OPG is a basic glycoprotein comprising of 401 amino acid residues arranged into 7 structural domains. It is found as either a 60kDa monomer or a 120kDa dimer linked by disulphide bonds. This assay measured both the monomeric and dimeric forms of OPG using a sandwich principle. The measurable range was 14-30pmol/L.
- Soluble RANKL (Kit insert - IDS; ampli sRANKL; FS-04PL V3 2008-10) was measured in 100µl serum using a similar manual IDS ELISA. This assay measured free RANKL in sera using a sandwich principle, as the concentration of sRANKL is usually quite low in normal samples the manufacturer added an additional enhancement system to increase the sensitivity. The measurable range was quoted as 0.02-2.0pmol/L. However this assay was problematic as many of the patient samples were below the sensitivity of the assay. The capture antibody was OPG and therefore the assay was only capable of detecting sRANKL not already complexed with OPG in serum and it was felt that any circulating OPG autoantibodies would interfere with this method so it was abandoned.

The reproducibility of the automated assays was established using up to 12 replicates of 3 levels of generic QC material (PeciControl Bone and PeciControl Varia); run in the same batch (intra-assay) and in different batches (inter-assay) to check precision and drift (Table 3). Additionally, thirty-eight spare patient samples (23 females between 27-91yrs, 15 males between 35-82yrs) from general practice that had 'normal' biochemistry results were used to verify the manufacturer stated reference ranges (Table 4) and to investigate age-related changes in these biomarkers (Figure 8). Similarly, for the manual immunoassay kits; up to 8 replicates of QC1 supplied in the kits were included at the beginning, middle and end of the plate in the same batch and in different batches to check precision and drift (Table 3) and 63

patient samples (46 females between 30-91yrs, 17 males between 35-82yrs) to verify the stated reference ranges and age-related changes (Figure 8).

The intra-assay coefficient of variation (CV) was less than 3.7% for the automated assays and less than 11% for the manual ELISA's. As expected the inter-assay CV's were higher reflecting the use of different lot numbers of reagents and calibrations but were deemed acceptable for the study.

The mean values for each biomarker were generally consistent with those reported in the kit inserts by the manufacturer. Notably, the reference ranges for  $\beta$ CTX and PINP in pre-menopausal women agreed with values quoted in the literature for identical methods (Glover et al. 2008, Eastell et al. 2012). However, reference ranges for the other BTMs have yet to be established. There was a trend in OPG results with age this was expected (Kudlacek et al. 2003).

In contrast to the use of reference ranges Bieglmayer and Kudlacek (Bieglmayer and Kudlacek 2009) have suggested combining a marker of formation and resorption to gain a direct insight into the changes in the balance of bone turnover in relation to a reference value. Individual marker concentrations can be expressed as multiples of the median (MoM), defined as

$$\text{MoM} = \frac{\text{Individual marker result}}{\text{Median of the reference population}}$$

The MoM was calculated using the median bone marker values from 72 self-reported healthy volunteers analysed as part of the  $\beta$ CTX, PINP comparison study but for this purpose only the E411 results were used (Wheater et al. 2013). The ratio of MoM formation ( $\text{MoM}_F$ ) and MoM resorption ( $\text{MoM}_R$ ) ( $\text{MoM}_F / \text{MoM}_R$ ) was plotted for each patient to signify bone turnover; a value of 1 indicated equilibrium. The results from 53 RA patients also included in the comparison study (Wheater et al. 2013) were plotted to illustrate the use of this graph (Figure 9). This model was applied to the results of the pilot and prospective studies, before and after RTX treatment.

**Table 3 Biomarker precision data for the pilot study**

	Intra-assay			Inter-assay		
	QC1	QC2	QC3	QC1	QC2	QC3
<b>PINP (µg/L)</b>						
n	12	12	12	3	3	3
Mean	75.8	409.2	825.7	75.2	403.6	781.8
SD	1.4	8.2	28.6	0.7	4.9	38.5
CV	<b>1.9</b>	<b>2.0</b>	<b>3.5</b>	<b>0.9</b>	<b>1.2</b>	<b>4.9</b>
Target mean	81.5	433	820	81.5	433	820
<b>Osteocalcin (µg/L)</b>						
n	12	11	11	3	3	3
Mean	17.7	94.6	194.2	18.6	91.4	184.0
SD	0.5	1.9	3.8	1.8	2.8	9.5
CV	<b>2.7</b>	<b>2.0</b>	<b>2.0</b>	<b>9.7</b>	<b>3.1</b>	<b>5.2</b>
Target mean	19.4	101	198	19.4	101	198
<b>βCTX (ng/L)</b>						
n	3	2	3			
Mean	304	720	2869			
SD	11	10	65			
CV	<b>3.7</b>	<b>1.4</b>	<b>2.2</b>			
Target mean	330	780	2820			
<b>OPG(pmol/L)</b>						
n	8	-	-	6	-	-
Mean	1.8	-	-	2.1	-	-
SD	0.2	-	-	0.4	-	-
CV	<b>11</b>	-	-	<b>21.5</b>	-	-
Target mean	2.2	-	-	2.9	-	-
<b>sRANKL (pmol/L)</b>						
n	7	-	-	5	-	-
Mean	0.65	-	-	0.57	-	-
SD	0.06	-	-	0.07	-	-
CV	<b>9.5</b>	-	-	<b>12.7</b>	-	-
Target mean	0.51	-	-	0.48	-	-

The reproducibility of the automated immunoassays was established using up to 12 replicates of 3 levels of generic QC material; run in the same batch (intra-assay) and in different batches (inter-assay) to check precision and drift. Similarly up to 8 replicates of QC1 included in the kits were used for the manual ELISA's. The mean, SD and CV were calculated for each assay.

βCTX: beta-isomerised carboxy terminal telopeptide of type I collagen; PINP: procollagen type 1 amino-terminal propeptide; sRANKL: soluble receptor activator of nuclear factor κB ligand; OPG: osteoprotegerin.



**Table 4 Manufacturer defined biomarker reference ranges**

	<b>PINP (<math>\mu\text{g/L}</math>)</b>	<b>Osteocalcin (<math>\mu\text{g/L}</math>)</b>	<b>BALP (<math>\mu\text{g/L}</math>)</b>	<b><math>\beta\text{CTX}</math> (<math>\text{ng/L}</math>)</b>	<b>TRAP5b (<math>\text{U/L}</math>)</b>	<b>OPG (<math>\text{pmol/L}</math>)</b>	<b>sRANKL (<math>\text{pmol/L}</math>)</b>	<b>SCL (<math>\text{pmol/L}</math>)</b>	<b>DKK-1 (<math>\text{pmol/L}</math>)</b>
	<b>Median Value</b>	<b>Median value</b>	<b>Median value</b>	<b>Mean value</b>	<b>Mean value</b>	<b>Median value</b>	<b>Median value</b>	<b>Median value</b>	<b>Median value</b>
<b>Pre-menopausal Female</b>	27.8	23.0	10.2	299	2.6	1.8	0.37	24.1	36.0
<b>Post-menopausal Female</b>	37.1	27.0	10.4	556	3.2	1.8	0.37	24.1	36.0
<b>Male &lt;50yrs</b>	-	25.0	10.6	300	3.1	1.8	0.46	24.1	36.0
<b>Male &gt;50yrs</b>	-	24.0	10.6	394	3.3	1.8	0.46	24.1	36.0

The reference ranges included in this Table were taken from the relevant manufacturer kit inserts.

$\beta\text{CTX}$ : beta-isomerised carboxy terminal telopeptide of type I collagen; BALP: bone specific alkaline phosphatase; DKK-1: dickkopf- related protein 1; PINP: procollagen type 1 amino-terminal propeptide; SCL: sclerostin; sRANKL: soluble receptor activator of nuclear factor  $\text{KB}$  ligand; OPG: osteoprotegerin; TRAP5b: tartrate resistant acid phosphatase isoform 5b.

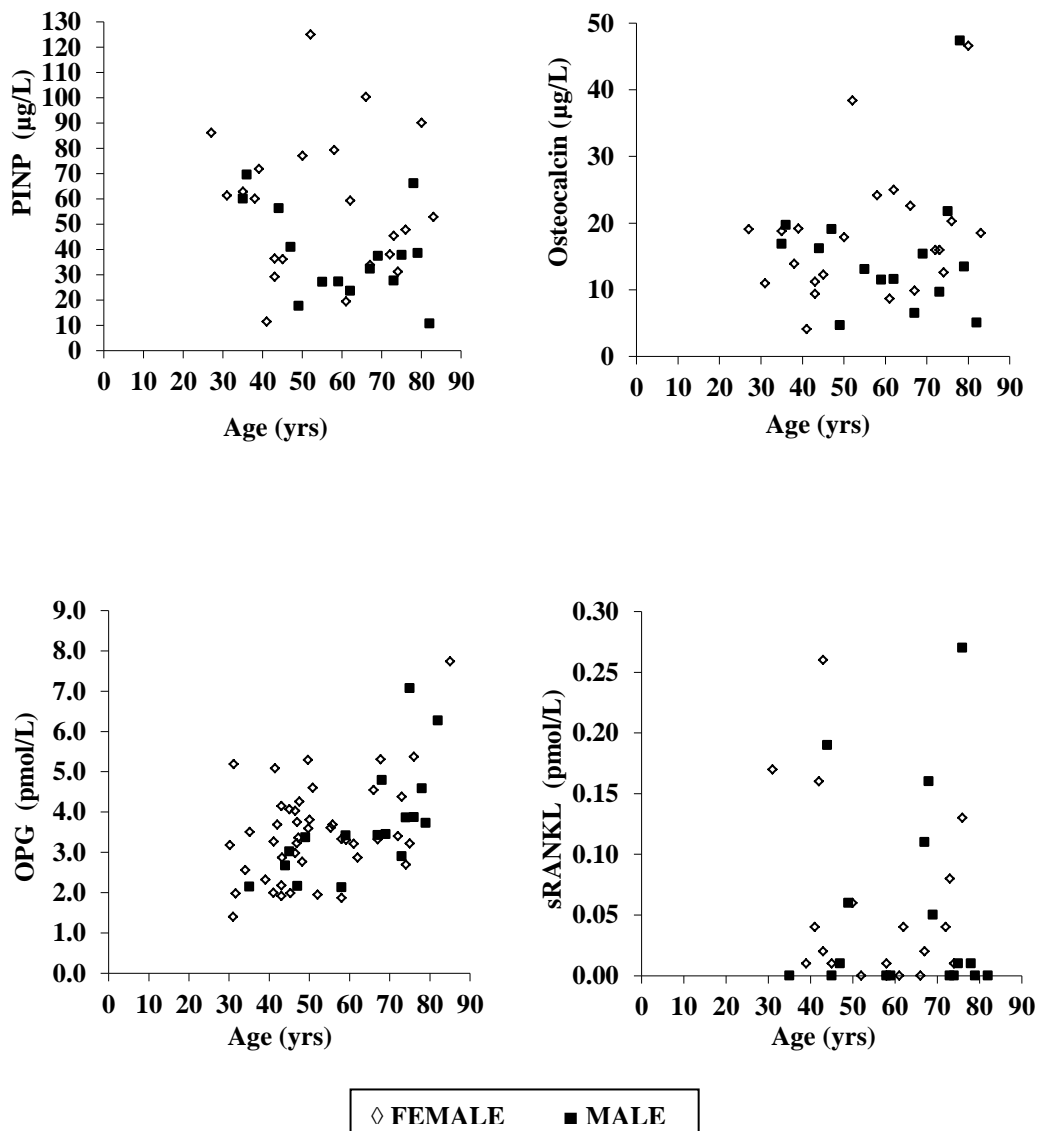


**Figure 8** The effect of age on individual biomarkers for the pilot study

Thirty-eight patient samples (23 females 27-91yrs, 15 males 35-82yrs) from general practice that had 'normal' biochemistry results were used to investigate age-related changes in PINP and osteocalcin. Similarly, 63 patient samples (46 females 30-91yrs, 17 males 35-82yrs) were used to investigate age-related changes in OPG and sRANKL.

PINP: procollagen type 1 amino-terminal propeptide; sRANKL: soluble receptor activator of nuclear factor kB ligand; OPG: osteoprotegerin.

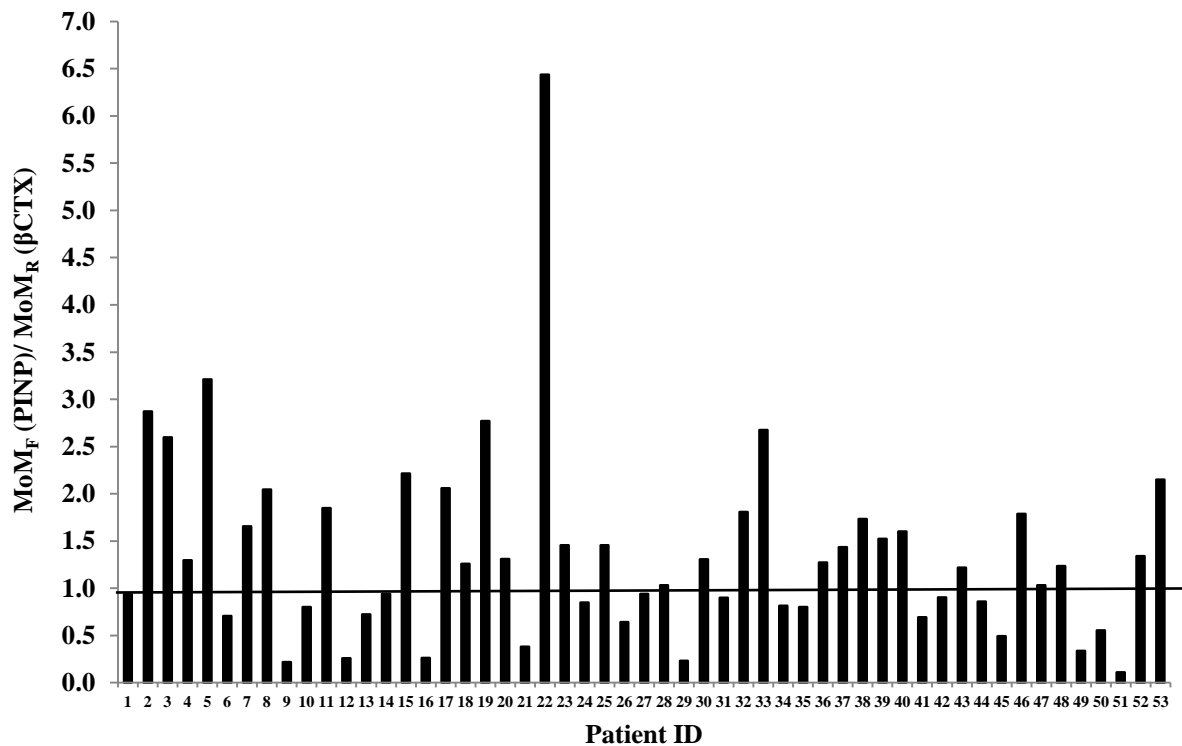


**Figure 9 Ratio of the multiples of the median for a marker of bone formation and bone resorption to signify bone turnover in patients with rheumatoid arthritis**

A marker of bone formation (PINP) and a marker of bone resorption ( $\beta$ CTX) are expressed as multiples of the median MoM<sub>F</sub> and MoM<sub>R</sub> respectively and their ratio plotted for individual patients (MoM<sub>F</sub>/ MoM<sub>R</sub>). MoM is calculated as 'individual marker result/ median of the reference population'. Fifty-three RA patient results from a previous study (Wheater et al. 2013) were used in this plot.

$\beta$ CTX: beta-isomerised carboxy terminal telopeptide of type I collagen; PINP: procollagen type 1 amino-terminal propeptide; MoM: multiple of the median.

### Biomarkers for the Prospective study

Prior to the prospective study analysis, a second automated immunoassay system; IDS iSYS (IDS Ltd, Boldon, Tyne and Wear, NE35 9PD, UK ) in addition to an upgraded Roche Elecsys 2010 renamed E411 became available within Pathology and so both systems were evaluated for  $\beta$ CTX and PINP. The Roche assay parameters remained the same however, the following were specific to the iSYS methods;  $\beta$ CTX Kit insert - IDS; iSYS  $\beta$ CTX; IS-3000PLV3 2011-11) was measured in 45  $\mu$ l serum, the measurable range being 33-6000ng/L; PINP (Kit insert - IDS; iSYS PINP; IS-4000PL V2 2009-12) was measured in 20 $\mu$ l serum, the measurable range was 2-230 $\mu$ g/L. Both  $\beta$ CTX assays were specific for cross-linked isomerised type I collagen fragments, independent of the nature of the crosslink (e.g. pyrrole, pyridinolines). Assay specificity was guaranteed through the use of two monoclonal (capture) antibodies each recognising the Glu-Lys-Ala-His- $\beta$ Asp-Gly-Gly-Arg peptide (Crosslaps antigen). Additionally, PINP is released as a trimeric structure but is rapidly broken down to a monomeric form by thermal degradation (Brandt 1999). The iSYS detects the trimeric 'intact' molecule and the E411 measures both fractions i.e. a total PINP assay. The Roche E411 2-site immunometric assays combine conventional antigen-antibody reactions on the surface of streptavidin coated paramagnetic microparticles, with electrochemical stimulation involving a ruthenium label on the surface of an electrode. The luminescence generated is directly proportional to the amount of analyte. The iSYS methods work on the same principle, however, streptavidin coated microparticles are captured using a magnet and then trigger reagents are added. The resultant light, emitted by an acridinium label, is proportional to the analyte concentration. There was disparity between the methods; there was a progressive deviation with increasing concentration between  $\beta$ CTX assays and the spread of values around the mean increased with increasing PINP concentration (Wheater et al. 2013). For comparison between studies it was decided to continue using the Roche assays for the prospective study but to use plasma rather than serum for these two assays, in addition to the following biomarkers.

- BALP is a glycoprotein found on the surface of osteoblasts, it reflects the metabolic activity of osteoblasts, therefore bone formation. BALP (Kit insert - IDS; iSYS BALP; IS-2800 V1 2011-03) was quantified in 50 $\mu$ l serum by chemiluminescence on the IDS iSYS analyser. The reportable range of this assay was 1-75 $\mu$ g/L.
- TRAP-5b (Kit insert - IDS; TRAP5b; SB-TR201APL V3 2007-03) was measured in 100 $\mu$ l serum by a manual IDS ELISA. This method specifically measured TRAP isoform 5b activity freshly liberated from osteoclasts and so is a marker of bone resorption. The measurable range of this assay was 0.5-10.0U/L.

- DKK-1 levels (Kit insert - Biomedica; DKK-1; BI-20413 rev.no.130823) were measured in 20µl serum using a manual Biomedica ELISA. DKK-1 is a secreted protein that acts as a soluble inhibitor of the Wnt signaling pathway and is an osteocyte marker. The reportable range was 1.7-160pmol/L.
- SCL was quantified in 20µl serum using a manual Biomedica ELISA (Kit insert - Biomedica; SCL; BI-20492 rev.no.131015). SCL, a secreted glycoprotein, is mainly produced in osteocytes. SCL acts by binding to the Wnt co-receptor low-density lipoprotein receptor-related protein 5 (LRP5) thus preventing the binding of Wnt molecules. The measurable range was 7.5-240pmol/L.
- Wide range wrCRP (Kit insert - Siemens; WR-CRP; 10494060\_EN 2011-01) often termed high sensitivity CRP (hsCRP) was quantified in serum by a latex-enhanced immunoturbidimetric assay on the Siemens Advia 2400 analyser (Siemens Healthcare Diagnostics, Camberley, Surrey, GU16 8QD, UK). The assay was based on the principle that CRP concentration was a function of the intensity of the scattered light caused by the agglutination of latex particles coated with anti-CRP in the presence of CRP-forming aggregates. The turbidity was measured at 571nm. The reportable range was 0.03-156 mg/L.
- 25OHD (Kit insert - IDS; iSYS 25OHD; IS-2700PL V6 2012-07) was quantified in 10µl of serum. Samples were subjected to a pre-treatment step to denature the vitamin D binding protein, the treated samples were then neutralised in assay buffer before analysis by chemiluminescence on the IDS iSYS analyser. The reportable range of the assay is 5-140µg/L.
- Intact PTH (Kit insert - Roche; PTH; 11972103 122 V19 2010-02) was quantified in 50µl EDTA plasma by electrochemiluminescent immunoassay on the Roche E411 analyser. This assay works on a sandwich principle; in which a biotinylated monoclonal antibody reacts with the N-terminal fragment (amino acids 1-37) and a monoclonal antibody labelled with a ruthenium complex reacts with the C-terminal fragment (amino acids 38-84). The measurable range of this assay was 1.2-5000ng/L.

**Table 5 Biomarker precision data for the prospective study**

	Intra-assay		Inter-assay	
	Low	High	QC1	QC2
<b>PINP (µg/L)</b>				
n	10	10	7	7
Mean	20.5	805.6	29.3	170.3
SD	0.5	25.1	1.2	5.6
CV	<b>2.6</b>	<b>3.1</b>	<b>4.1</b>	<b>3.3</b>
Target mean	-	-	27.0	181.0
<b>BALP (µg/L)</b>				
n	10	10	2	2
Mean	11.6	22.5	4.8	49.1
SD	0.3	0.5	0.4	0.8
CV	<b>2.4</b>	<b>2.2</b>	<b>7.4</b>	<b>1.6</b>
Target mean	-	-	5.3	49.8
<b>βCTX(ng/L)</b>				
n			3	5
Mean	-	-	280	759
SD	-	-	3.6	17
CV	-	-	<b>1.3</b>	<b>2.3</b>
Target mean	-	-	270	700
<b>TRAP5b (U/L)</b>				
n			7	7
Mean	-	-	1.7	5.6
SD	-	-	0.1	0.2
CV	-	-	<b>4.3</b>	<b>3.4</b>
Target mean	-	-	1.9	6.0
<b>SCL (pmol/L)</b>				
n	8		6	
Mean	80.8	-	89.1	-
SD	2.9	-	8.3	-
CV	<b>3.6</b>	-	<b>9.3</b>	-
Target mean	89.0	-	89.0	-
<b>DKK-1 (pmol/L)</b>				
n	8		6	
Mean	23.3	-	27.3	-
SD	1.3	-	4.3	-
CV	<b>5.4</b>	-	<b>15.8</b>	-
Target mean	27.8	-	27.8	-

The reproducibility of the automated immunoassays was established using up to 10 replicates of 2 levels of generic QC material; run in the same batch (intra-assay) and in different batches (inter-assay) to check precision and drift. Similarly up to 8 replicates of QC material supplied in the kits were used for the manual ELISA's. The mean, SD and CV were calculated for each assay. βCTX: beta-isomerised carboxy terminal telopeptide of type I collagen; BALP: bone specific alkaline phosphatase; DKK-1: dickkopf-related protein 1; PINP: procollagen type 1 amino-terminal propeptide; SCL: sclerostin; TRAP5b: tartrate resistant acid phosphatase isoform 5b.

The reproducibility of the automated assays was established using up to 10 replicates of 2 levels of generic QC material (PeciControl Bone and PeciControl Varia); run in the same batch (intra-assay) and in different batches (inter-assay) to check precision and drift (Table 5). Additionally, nineteen self-reported healthy volunteer samples (11 females 22-61yrs, 8 males 24-53yrs) were used to verify the manufacturer stated reference ranges (Table 4) and to investigate age-related changes in these biomarkers (Figure 10). The blood samples were non-fasting and collected between 9:00 – 10:00, they were centrifuged within one hour of venepuncture and the serum/ plasma was immediately stored at -80°C until analysis. Similarly, for the manual immunoassay kits; up to 8 replicates of QC1 supplied in the kits were included at the beginning, middle and end of the plate in the same batch and in different batches to check precision and drift (Table 4) and the healthy volunteer bloods were used to verify the stated references ranges and age-related changes (Figure 10).

The intra-assay coefficient of variation (CV) was less than 3.1% for the automated assays and less than 5.4% for the manual ELISA's. As expected the inter-assay CV's were higher reflecting the use of different lot numbers of reagents and calibrations but were deemed acceptable for the study.

The mean values for each biomarker were generally consistent with those reported in the kit inserts by the manufacturer; there was an upward trend in results with age. The reference ranges for  $\beta$ CTX, BALP, PINP in pre-menopausal women agreed with values quoted in the literature for identical methods (Glover et al. 2008, Eastell et al. 2012).

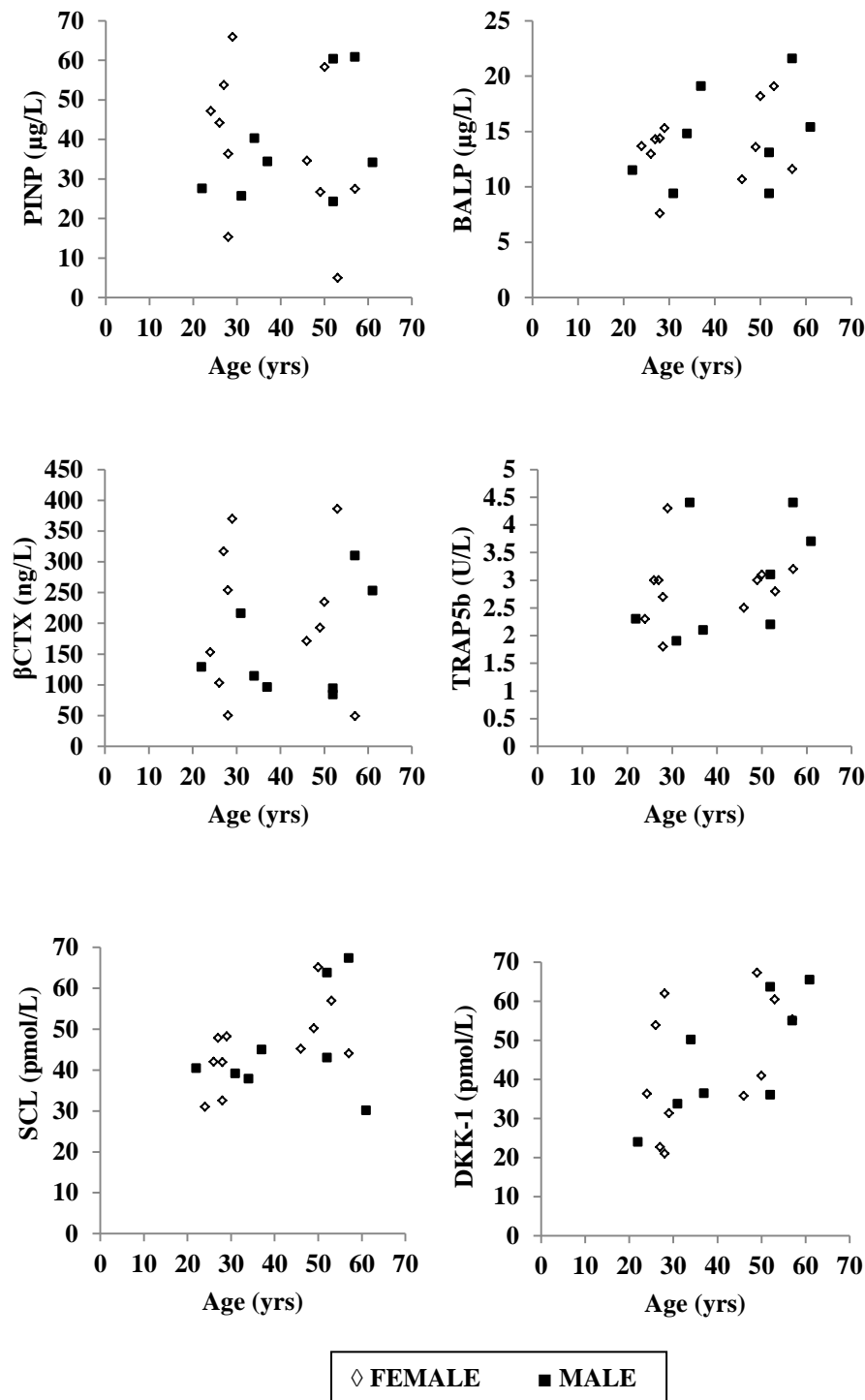


**Figure 10** The effect of age on individual biomarkers for the prospective study

Nineteen self-reported healthy volunteer samples (11 females 22-61yrs, 8 males 24-53yrs) were used to investigate age-related changes in these biomarkers

βCTX: beta-isomerised carboxy terminal telopeptide of type I collagen; BALP: bone specific alkaline phosphatase; DKK-1: dickkopf- related protein 1; PINP: procollagen type 1 amino-terminal propeptide; SCL: sclerostin; TRAP5b: tartrate resistant acid phosphatase isoform 5b.



### 2.2.2 *In vitro* experiments

Unless otherwise stated all the cell culture reagents were prepared under sterile conditions and working reagents were stored at 4°C.

- Heat inactivated FCS for 60mins at 56°C, aliquot and freeze at -20°C until use.
- HBSS + 1% FCS - Add 5ml heat inactivated FCS to 500ml HBSS buffer.
- HBSS + 0.4% EDTA - Add 2ml EDTA to 500ml HBSS buffer (store between 20-25°C)
- $\alpha$ MEM complete - Add 10ml heat-inactivated FCS (10%) + 1ml Glutamax (1%) + 1ml pen/ strep (1%) to 88ml  $\alpha$ MEM

#### Peripheral blood mononuclear cell isolation

Whole blood was collected into EDTA tubes and kept at room temperature (20° to 25°C); samples were always processed within 8hrs. Blood was diluted 1:1 with HBSS+EDTA buffer at room temperature in a 50ml falcon tube. 15ml lymphoprep was added to a second falcon tube and 15-20ml of this diluted blood was slowly layered onto the lymphoprep using a pipette, the tube was then centrifuged at room temperature, 890g for 30mins using the slow acceleration-no brake setting. The PBMC's (the cloudy layer at the interface) were carefully transferred to a new 50ml falcon tube and topped up to 50ml with ice cold HBSS + FCS, mixed gently and centrifuged at 600g, 4°C for 7mins using the no-brake setting. All but a few millimetres of the supernatant was immediately poured off and the cells were resuspended and topped up to 50ml with ice cold HBSS+FCS, then centrifuged at 250g, 4°C for 7mins using the no brake setting. The supernatant was again poured off and the cells resuspended and mixed as before. The tube was kept at 4°C while the number of PBMC's were counted.

20 $\mu$ l of supernatant was added to a solution of 40 $\mu$ l trypan blue and 40 $\mu$ l 3% acetic acid (i.e. 1 in 5 dilution) and mixed well. 10 $\mu$ l of this mixture was loaded onto an 'improved Neubauer' haemocytometer, once the appropriate coverslip was fixed firmly in place to form 'Newton's rings'. The number of viable PBMC's in the 4 outside corner counting grids was recorded. A note was made if large numbers of platelets or cellular debris was present. The number of PBMC's per ml was calculated using a standard formula

(<http://www.hpacultures.org.uk/technical/ccp/cellcounting.aspx>)

$$\text{PBMCs /ml} = (\text{Average of the 4 grids}) \times 10,000 \times 5$$

#### Fluorescence Activated Cell Sorting

All FACS analysis was carried out by qualified Biomedical Scientists in the Haematology laboratory JCUH, to determine the percentages and absolute counts of mature human

monocytes (CD14/64), B lymphocytes (CD19) and T lymphocytes (CD3) in the cell suspension at baseline.

Two separate TruCOUNT tubes were prepared:

- Tube 1 containing 2.5µl CD45 + 5.0µl CD14/64 + 5.0µl CD3, labelled T cell
- Tube 2 containing 2.5µl CD45 + 5.0µl CD14/64 + 5.0µl CD19, labelled B cell

The reagents were added onto the side of the tube just above the stainless steel retainer without touching the pellet, followed by 200µl of cell suspension to each tube. The tubes were capped, mixed gently and incubated for 15mins in the dark at room temperature (20° to 25°C).

The tubes were then thoroughly mixed/ vortexed before analysis on the BD FACSCalibur flow cytometer. Data was acquired and analysed using Cell Quest Pro software and the absolute numbers of monocytes, B cells and T cells calculated manually as per the manufacturer's instructions:

$$\frac{\text{No. of events in region containing cell}}{\text{No. of events in bead region}} \times \frac{\text{No. of beads per test}^*}{\text{Test volume (i.e. 212.5}\mu\text{l)}}$$

\* This value was taken from the TruCOUNT absolute count tube foil pouch label and varied from lot to lot.

### Osteoclast culture

Glass coverslips (13mm diameter) and/or bone slices were sterilised in 70% ethanol for 24hrs, then soaked in  $\alpha$ MEM complete for 60mins prior to use. One coverslip or bone slice was placed using forceps into the bottom of each labelled well, of a 24-well plate and left to dry for a minimum of 30mins before use. Where possible each sample was used in 3 separate replicates of the same experiment to estimate the technical reproducibility.

Mononuclear cells were isolated from fresh peripheral blood (following the PBMC isolation procedure) and the number of PBMC's /ml was recorded. 50ml of the cell suspension was centrifuged at 400g, 4°C for 7mins. The supernatant was poured off and the cell pellet was washed and resuspended in 20ml  $\alpha$ MEM, then centrifuged at 400g, 4°C for 7mins. This time the cells were resuspended in  $x$  ml  $\alpha$ MEM complete (where  $x$ = no. of PBMC's /ml calculated above) giving a final concentration of  $1 \times 10^6$  PBMC's /ml. 500µl of this cell suspension was sent for FACS analysis (following the FACS analysis procedure) and 500µl was layered onto each coverslip or bone slice as appropriate. The plate was incubated in 5% CO<sub>2</sub> at 37°C for up to 21 days. The cells were inspected under the microscope every 2-3 days prior to refreshing the upper 250µl of medium. After 14-21 days, or when there was evidence of osteoclast

formation, the coverslips were stained using the TRAP protocol, the bone slices were stained using the toluidine blue protocol and  $\beta$ CTX was measured, using the Elecsys 2010 assay, in the remaining medium of wells containing the bone slices.

### Osteoclast characterisation

Osteoclasts were characterised by previously established characteristics namely multinuclearity, TRAP expression, actin ring formation that is a prerequisite of cell resorptive activity, also toluidine blue staining of resorption pits and  $\beta$ CTX release by cells cultured on bone slices.

### *Tartrate Resistant Acid Phosphatase stain*

Primary osteoclasts or pre-osteoclasts cultured on glass cover slips were identified morphologically and histochemically using a modified TRAP testing kit from Sigma. Prior to use all reagents were brought to room temperature.

- The citrate/acetone fixative was prepared i.e. 2ml citrate concentrate + 18ml deionised water, mixed thoroughly then 30ml acetone was added.
- A sealed bottle containing 44ml deionised water was pre-heated in a water bath to reach 37°C.
- The following reagents were then added to the pre-warmed water in this order and kept at 37°C until use:

Acetate solution	2.0ml	Mix gently
Naphthol AS-BI Phosphoric Acid	2.0ml	Mix gently
Tartrate solution	2.0ml	Mix gently
Fast Garnet GBC salt	1	Stir for 30-60secs then rapidly filter through a Whatman no. 54

At the end of the culture period the remaining medium was removed and 1ml of PBS was added to each well. One coverslip at a time was removed with forceps and held in a beaker containing the citrate/acetone fixative for 30secs at room temperature, then rinsed carefully in beaker containing deionised water and left on a clean paper towel for at least 15mins to air dry. Once completely dry each coverslip was placed into a single well of a pre-labelled 6 well plate containing 3ml of pre-warmed stain, covered and incubated for 60mins at 37°C in the dark. The remaining stain was then aspirated off and the coverslips were rinsed  $\times 2$  with 1ml deionised water and once with normal tap water. Finally the water was aspirated off and 1ml

acid haematoxylin solution was added to the wells to stain for 5mins. The stain was aspirated off and the coverslips were washed  $\times 3$  with 1ml deionised water and placed on a clean paper towel to air dry. The coverslips were mounted on labelled glass slides and evaluated microscopically. The number of TRAP<sup>+</sup> multinuclear (i.e.  $>3$  nuclei) cells in 9 separate fields were counted and the area and circumference of 3 cells per field was recorded.

#### *Tartrate resistant acid phosphatase positive cell counting procedure*

TRAP<sup>+</sup> cell counting was carried out by a single independent member of staff. A coverslip was chosen if it had; minimum cell clumping, an even distribution of cells and a good uptake of stain, this was to ensure that the count was as accurate as possible.

An Olympus CKX41 microscope with an attached Infinity2 camera was used for the TRAP<sup>+</sup> cell count, initially using  $\times 100$  magnification. The right hand side eyepiece was adapted for measurement purposes by the addition of a fixed, circular glass graticule with a  $10\times 10$  measuring grid etched onto its surface. This grid was used to partition a section of the viewfield for counting. All slides were orientated so that the slide label was on the left hand side and all TRAP<sup>+</sup> cells present in the  $10\times 10$  grid were counted in 9 locations on the coverslip (Figure 11). At each location an image was produced and stored using the Infinity Capture software for later analysis.

Osteoclasts, for the purposes of this procedure, were defined as TRAP<sup>+</sup> cells that displayed evidence of a ruffled border and multiple (i.e.  $>3$ ) nuclei. In each area the  $10\times 10$  grid was orientated, where possible, into the centre of each counting area so that there was a cell in the top left portion of the grid, cells were only counted if the area containing the nuclei was wholly within the grid. Counts were recorded for each area of the coverslip and the mean cell per area was then calculated for each coverslip.

During the counting an image was generated using the Infinity Capture software for each of the 9 counting locations, 3 osteoclasts were selected from each image. Cell selection was based primarily on the presence of a ruffled border and  $>3$  nuclei but was also based on the ability to see the entire perimeter clearly for accuracy of measurement. In addition for each image 3 cells of differing size (i.e. small, medium and large) were selected to give an accurate overall representation. Using the Infinity Analyse software, a line was drawn around the selected cell (Figure 12) and the software automatically calculated the cell area (S) and circumference (P). The cell diameter (d) was calculated using an online calculator (<http://www.onlineconversion.com/circlesolve.htm>) from these measurements using circle theory. The calculation was also manually checked for accuracy i.e.

$$\text{Diameter} = 2 \times \sqrt{\text{area}/\pi}$$

$$\text{Circumference} = \pi d$$

$$(\pi = 3.142)$$

The Infinity Analyse software was initially calibrated in microns ( $\mu\text{m}$ ) using the grid of a Neubauer counting chamber and all measurements were performed in full screen mode.

#### *Actin ring formation*

Actin ring formation is a prerequisite for osteoclast bone resorption. Osteoclasts seeded on glass form podosomes, which are small cylinders of actin surrounded by vinculin. There are three different podosome structures dependent on the stage of osteoclast differentiation; namely clusters, rings and finally belts depicting mature osteoclasts (Saltel et al. 2004). The Invitrogen Life Technologies protocol using Alexa Fluor<sup>®</sup> 488 Phalloidin was optimised. All procedures were carried out inside a fume cupboard and gloves were worn at all times. The reagents were prepared as follows:

- The phalloidin vial was dissolved in 1.5ml methanol to yield a final concentration of 200units/ml, equivalent to approx.  $6.6\mu\text{M}$ , aliquoted into 100 $\mu\text{l}$  amounts and stored at  $-20^{\circ}\text{C}$  until use. A 5 $\mu\text{l}$  stock solution was then added to 200 $\mu\text{l}$  PBS for each coverslip /bone slice to be stained.
- 1ml of 16% methanol-free formaldehyde was mixed with 3ml deionised water to give a 4% working solution.
- 1ml of 1% Triton X-100 was mixed with 9ml PBS to give a 0.1% working solution.
- 20ml of PBS was warmed to room temperature prior to use.

At the end of the culture period the remaining medium was aspirated off and the coverslips and /or bone slices were washed  $\times 3$  with 1ml pre-warmed PBS per well. The PBS was removed and 1ml of 4% formaldehyde was added for 10mins to each well, covering the coverslips /bone slices completely. The wells were then washed  $\times 3$  with 1ml PBS. The PBS was removed and 1ml of 0.1% Triton X-100 was added to each well for 5mins. The wells were again washed  $\times 3$  with 1ml PBS. The PBS was removed and 1ml of the diluted staining solution was added to each well for 20mins at room temperature. The plate was covered to avoid evaporation. The stain was removed and the wells were washed  $\times 3$  with 1ml PBS. The coverslips/ bone slices were then air-dried and mounted on labelled glass slides and evaluated using a fluorescent microscope.

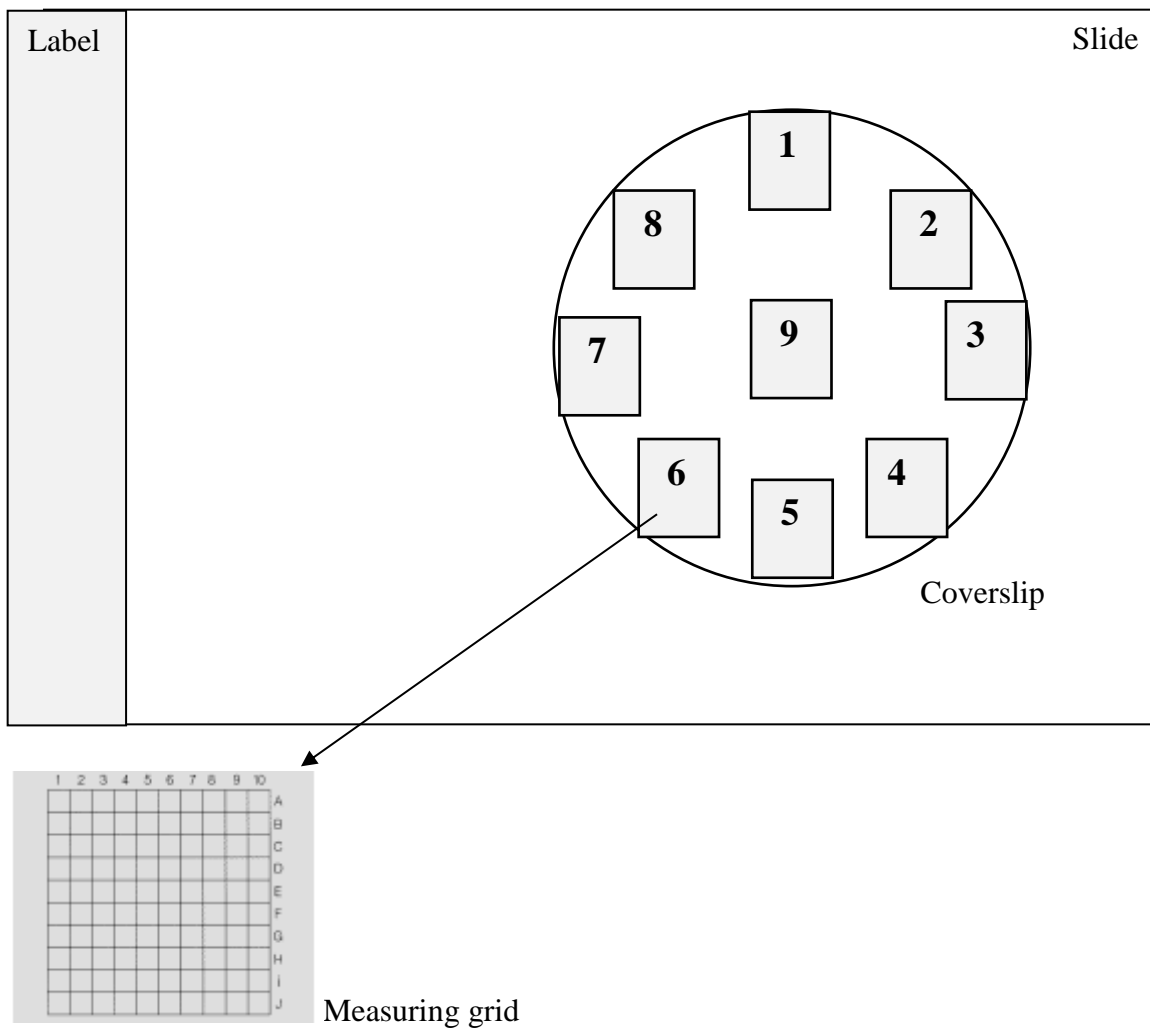


**Figure 11 Diagrammatic representation of the microscope slide showing orientation and counting areas, labelled 1-9 respectively**

The right hand side eyepiece of an Olympus CKX41 microscope was adapted for measurement purposes by the addition of a fixed, circular glass graticule with a 10×10 measuring grid etched onto its surface. The measuring grid was used to partition a section of the viewfield for counting. All slides were orientated so that the slide label was on the left hand side and all TRAP<sup>+</sup> cells present in the 10×10 grid were counted in the 9 locations shown on the coverslip.

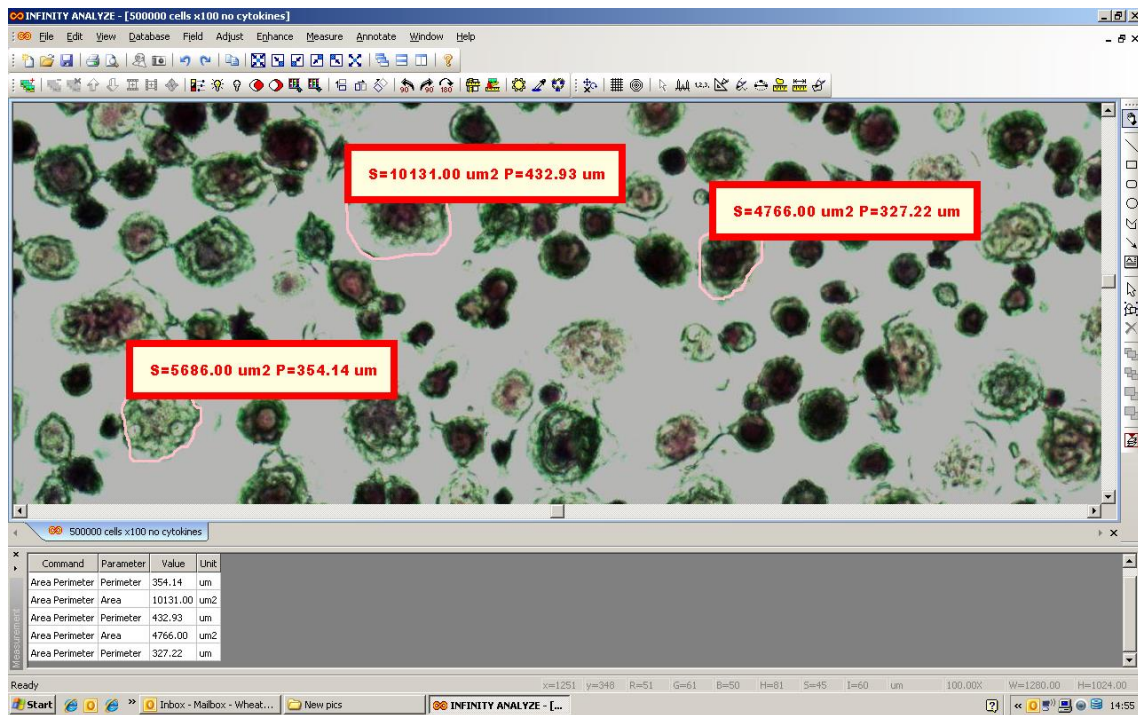


**Figure 12** Infinity analyse software showing the cell area and circumference measurement for 3 TRAP<sup>+</sup> osteoclast-like cells

An image was generated using the Infinity Capture software for each of the 9 counting locations on the glass coverslip and 3 TRAP<sup>+</sup> cells with > 3 nuclei were selected from each image. Using the Infinity Analyse software, a line was drawn around the selected cell and the software then automatically calculated the cell area (S) and cell circumference (P).

### *Toluidine Blue stain for bone slices*

The toluidine blue staining reagents were freshly prepared as follows:

- 100mg toluidine blue was added to 100mg di-sodium tetraborate in 100ml deionised water.
- A 5% sodium hypochlorite solution was made from 1ml concentrate + 15.5ml deionised water.

At the end of the culture period 250µl of medium from each well containing a circular bovine cortical bone slice of 0.4mm thickness and 6mm diameter, was pipetted into a labelled 75x12mm plastic tubes for βCTx analysis. The bone slices were then washed in 1ml of PBS, soaked in 1ml 5% sodium hypochlorite for 5mins, followed by three washes with 1ml deionised water. The water was removed and 300µl 0.1% toluidine blue staining solution was added to each well for 5mins. The bone slice was then removed using forceps and dropped into a labelled beaker containing 300ml deionised water, the water was poured off and fresh water added ×2 until it remained clear. The bone slices were removed and placed on a clean paper towel to air dry before mounting on labelled glass slides to evaluate microscopically.

### *Beta-isomerised Carboxy terminal Telopeptide of type I collagen analysis*

The osteoclast activity was assessed by measuring βCTX in the medium of wells containing bone slices at the end of the culture period. 250µl of cell medium was analysed using the βCTX assay on the Elecsys 2010, described previously in section 2.3.1.

### B cell depletion

B cell depletion was carried out using MACS separation prior to osteoclast culture, unless otherwise stated in a limited number of experiments.

### *Using Magnetic-Activated Cell Sorting*

Cells were always kept cold and pre-cooled solutions were used to prevent capping of antibodies on the cell surface and non-specific cell labelling. The following reagents were prepared prior to use:

- MACS working buffer - 1ml BSA stock solution + 20ml autoMACS rinsing solution, the buffer was then kept cold at 4-8°C

Mononuclear cells were isolated from fresh peripheral blood (refer to the PBMC isolation protocol) and the cell number was determined. 50ml of cell suspension was centrifuged at 300g at 4°C for 10mins and then the supernatant was completely removed. The cell pellet was resuspended in 80µl (per 10<sup>7</sup> cells) of cold MACS buffer and 20µl (per 10<sup>7</sup> total cells) of CD20 microbeads were added, mixed well and then incubated for 15mins at 4-8°C. The cells



were washed with 1-2ml MACS buffer (per  $10^7$  cells) and then centrifuged at 300g at 4 °C for 10mins. While the suspension was spinning the column was prepared as follows:

- A LD column was placed in the magnetic field of a midiMACS separator, making sure the wings face forwards.
- The column was rinsed with 2ml MACS buffer to waste until the liquid was completely removed.

The supernatant was completely removed and resuspended in 500µl MACS buffer (up to  $1.25 \times 10^8$  cells). This solution was added to the column and unlabelled ( $CD20^-$ ) cells were collected into a labelled 15ml falcon tube placed underneath the column. The column was washed  $\times 2$  with 1ml MACS buffer, this was also collected into the falcon tube, and each time the liquid was allowed to pass completely through the column before more buffer was added. The column was removed from the separator and placed over another labelled 15ml falcon tube. 1-2ml MACS buffer was added to the column and the  $CD20^+$  magnetically labelled cells were immediately flushed out into the falcon tube by firmly applying the plunger supplied with the column.

Both tubes were centrifuged at 300g at 4 °C for 10mins and the supernatants were pipetted off completely. Each tube was resuspended in 20ml  $\alpha$ MEM medium and the number of  $CD20^-$  and  $CD20^+$  cells in each respective tube was counted as follows:

20µl of supernatant was added to a solution of 40µl trypan blue and 40µl 3% acetic acid (i.e. 1 in 5 dilution) and mixed well. 10µl of this mixture was loaded onto an 'improved neubauer' haemocytometer, once the appropriate coverslip was fixed firmly in place to form 'Newton's rings'. The number of viable  $CD20^-$  or  $CD20^+$  cells in the 4 outside corner counting grids was calculated using a standard formula

(<http://www.hpacultures.org.uk/technical/ccp/cellcounting.aspx>)

**$CD20^-$  or  $CD20^+$  cells /ml = (Average of the 4 grids)  $\times$  10,000  $\times$  5**

The tubes were then centrifuged at 300g at 4 °C for 10mins. The supernatant was again discarded and the cells were resuspend in  $x$  ml  $\alpha$ MEM complete medium (where  $x$ = no. of  $CD20^-$  or  $CD20^+$  cells/ml) giving a final concentration of  $1 \times 10^6$  cells/ml. 500µl of each fraction was sent for FACS analysis to determine the percentage and absolute numbers of monocytes, T cells and B cells.

*Using rituximab*

RTX is a chimeric monoclonal antibody that binds specifically to CD20 and is an approved therapeutic B cell depleting agent. CD20 is expressed on the surface of B lineage cells from the pre-B cell stage and throughout B cell maturation, but is lost at the final transformation to plasma cells (Cartron et al. 2004). RTX was therefore particularly useful in both *in vitro* and *in vivo* B cell depletion studies.

The RTX working solutions were prepared from serial dilutions of the stock RTX solution (10mg/ml) in  $\alpha$ MEM complete medium immediately prior to use:

- **100 $\mu$ g/ml**; 50 $\mu$ l of stock + 4950 $\mu$ l  $\alpha$ MEM complete
- **10 $\mu$ g/ml**; 500 $\mu$ l of 100 $\mu$ g/ml + 4500 $\mu$ l  $\alpha$ MEM complete
- **1 $\mu$ g/ml**: 500 $\mu$ l of 10 $\mu$ g/ml + 4500 $\mu$ l  $\alpha$ MEM complete
- **0.1 $\mu$ g/ml**: 500 $\mu$ l of 1 $\mu$ g/ml + 4500 $\mu$ l  $\alpha$ MEM complete

Mononuclear cells were isolated from fresh peripheral blood (following the PBMC isolation procedure) and the number of PBMC's /ml was recorded. 50ml of the cell suspension was centrifuged at 400g, 4°C for 7mins. The supernatant was poured off and the cell pellet was washed and resuspended in 20ml  $\alpha$ MEM, then centrifuged at 400g, 4°C for 7mins. This time the cells were resuspended in  $x$  ml  $\alpha$ MEM complete (where  $x$ = no. of PBMC's /ml calculated) giving a final concentration of  $1 \times 10^6$  PBMC's /ml. 500 $\mu$ l of this cell suspension was sent for FACS analysis (following the FACS analysis procedure) and 4 $\times$  2ml fractions were removed to labelled tubes and centrifuged at 400g, 4°C for 7mins. The supernatants were pipetted off completely and the cell pellets were reconstituted in concentrations of rituximab in  $\alpha$ MEM complete medium as follows:

- 2ml suspension reconstituted in 2ml 100 $\mu$ g/ml RTX in medium
- 2ml suspension reconstituted in 2ml 10 $\mu$ g/ml RTX in medium
- 2ml suspension reconstituted in 2ml 1 $\mu$ g/ml RTX in medium
- 2ml suspension reconstituted in 2ml 0.1 $\mu$ g/ml RTX in medium

Giving a final concentration of  $1 \times 10^6$  cells/ml. 500 $\mu$ l of each fraction was sent for FACS analysis to determine the percentage and absolute numbers of monocytes, T cells and B cells.

### 2.3 Subjects

The main characteristics and time-lines of the sub studies are summarised in table 6.

**Table 6** Main characteristics of all the sub studies

Study	Number of participants and site	Gender and menopausal status	Disease state	Samples and analysis	Time-lines
The effects of B cell depletion on bone turnover in patients with rheumatoid arthritis - the pilot study	46 2 Dutch centres	32 Female - 13 pre - 19 post 14 Male	Severe, refractory RA, pre and 6 months post RTX	Serum samples at baseline and 6 months post RTX to measure BTMs, inflammatory markers and DAS28	Recruitment Mar 2005 - Sep 2006 6 - 24 month follow-up 'Last patient last visit' May 2008' Analysed Feb – Jun 2009
The effects of B cell depletion on bone turnover in patients with rheumatoid arthritis - the prospective study	45 10 UK centres	36 Female - 7 pre - 29 post 9 Male	Severe, refractory RA, pre and up to 12 months post RTX	Serum/plasma samples at baseline and 3, 6, 9, 12 months post RTX to measure BTMs, inflammatory markers and DAS28 BMD measured at baseline and 12 months post RTX	Recruitment Aug 2011 - Sep 2012 12 month follow-up 'Last patient last visit' Sept 2013' Analysed Sep – Dec 2013
The effect of <i>in vitro</i> B cell depletion	12 1 UK centre	6 Female 6 Male	Self-reported healthy volunteers with no previous or current history of autoimmune or bone disease	PBMCs isolated from EDTA blood, unfractionated and CD20 depleted fractions cultured to compare the numbers of TRAP <sup>+</sup> cells generated	Recruitment Nov 2012 - Apr 2014 Analysed Nov 2012 – Apr 2014
The effects of <i>ex vivo</i> B cell depletion	5 1 UK centre	4 Female - 4 post 1 Male	Severe, refractory RA, pre and up to 12 months post RTX	PBMCs isolated from EDTA blood at baseline and 3, 6, 12 months post RTX and cultured to determine the numbers of TRAP <sup>+</sup> cells generated at each time point	Recruitment Aug 2011 - Sep 2012 12 month follow-up 'Last patient last visit' Sep 2013' Analysed Apr 2012 – Aug 2013

### **2.3.1 Pilot study**

Serum samples had previously been collected from 46 adult patients who participated in a Dutch, two-centre, open-label clinical trial to investigate the clinical and immunologic effects of treatment with RTX in severe refractory RA (Teng et al. 2009). All patients were older than 18yrs of age, had a clinical diagnosis of RA according to the American College of Rheumatology (ACR) criteria and had failed treatments with a combination(s) of DMARD's and/or TNF blocking agents. RTX was administered as a 1000mg intravenous infusion on days 1 and 15 in conjunction with intravenous methylprednisolone 100mg. TNF blocking agents were discontinued during a washout period of 8 weeks, whereas DMARD's (MTX 2.5-30mg/week; prednisolone 2.5-20mg/day) were continued (Teng et al. 2009). Serum samples were available at baseline (prior to treatment) and 6 months after the RTX infusion. Blood samples were collected between 10:00 -16:00hrs and were non-fasting, all samples were stored at -80°C until analysis. Written informed consent was obtained from all patients and the study was approved by the Ethics Committees of Leiden and Utrecht University Medical Centres in the Netherlands and the Research and Development department at The James Cook University Hospital (Reference no. 2008006) (Wheater et al. 2011).

### **2.3.2 Prospective study**

This was a multicentre, open-label, single treatment arm, prospective clinical trial on a cohort of 45 adult patients with severe RA who started RTX after failure of other DMARDs, including at least one anti-TNF- $\alpha$ . This study did not have a control group; the optimal design would have been a double-blind randomized comparison with placebo. However, as RTX is an approved treatment for refractory RA and is already known to reduce disease activity (Teng et al. 2007), such a control arm would have had to be matched for disease activity and it would have been unethical to have an untreated arm with that level of active disease. The trial was approved by the North East - Newcastle & North Tyneside 1 Research Ethics Committee (REC reference no. 10/H0906/57), the Medicines and Healthcare Products Regulatory Agency (MHRA) (Reference no. 21464/0205/001-0001) and the Research and Development department at The James Cook University Hospital (Reference no. 2010161). This work was funded by a grant from Roche Products Limited (Welwyn Garden City, UK). Recruitment took place in ten UK centres: South Tees Hospitals NHS Foundation Trust; Newcastle Hospitals NHS Foundation Trust; City Hospitals Sunderland NHS Foundation Trust; The Mid Yorkshire Hospitals NHS Trust; Northumbria Healthcare NHS Foundation Trust; County Durham and Darlington NHS Foundation Trust; Gateshead Health NHS

Foundation Trust; North Tees and Hartlepool Hospitals NHS Foundation Trust; South Warwickshire NHS Foundation Trust; and Mid Staffordshire NHS Foundation Trust. Written informed consent was obtained from all patients in compliance with the Declaration of Helsinki. Patients fulfilled the ACR classification criteria 1987 for the diagnosis of RA and the UK National Institute for Health and Care Excellence (NICE) eligibility criteria for treatment with RTX i.e. patients had severe active disease and had an inadequate response to, or were intolerant of, other DMARDs including at least one anti-TNF- $\alpha$ . Patients were excluded if they were younger than 18yrs old, had previously received any B cell depleting agent or had been treated for osteoporosis with bisphosphonates, calcitonin, strontium ranelate, denosumab or teriparatide within the last 3 months. Calcium, vitamin D, corticosteroids, non-biological DMARDs and treatment for concomitant medical conditions were all continued throughout the study at the discretion of the treating physician. RTX was administered following recommended protocol as a 1000mg intravenous infusion on days 1 and 15 in conjunction with intravenous methylprednisolone 100mg. Patients who responded to the first RTX course received a second course at 6 months unless they attained a state of low disease activity, in accordance with clinical practice. Patients were assessed at baseline prior to RTX treatment and then every 3 months over a 12 month follow up period. 25OHD was measured once at the baseline visit, patients were recruited from August 2011 until September 2012 and were spread out evenly throughout the year. Fasting morning blood samples were taken every 3 months into serum separator (SST) and ethylenediaminetetraacetic acid (EDTA) tubes. Serum and plasma were separated within 60mins and immediately stored at  $-80^{\circ}\text{C}$  until analysis. Additionally, in a sub group of patients from Middlesbrough and Newcastle an extra 10ml EDTA blood was collected for *in vitro* osteoclastogenesis at baseline, 3, 6 and 12 months and processed within 8hrs.

### **2.3.3 Osteoclast work**

Blood samples (20mls i.e. 5 $\times$  EDTA blood tubes) were collected by normal venepuncture, by a trained phlebotomist, from self-reported healthy volunteers with no current or previous history of autoimmune or bone disease. The samples were non-fasting and were collected between 9:00 – 10:00. The blood was used to isolate mononuclear cell's following the PBMC isolation procedure (Section 2.2.2) prior to the osteoclast experiments. Volunteers were given an information sheet explaining the study and full written consent to participate was documented. All samples were fully anonymised and identified only by a sample number. The volunteer had no further involvement and individual results were not traceable in any way. The study was approved by the North East - Tyne and Wear South Ethics Committee (REC

reference number 11/NE/0317) and the Research and Development department at The James Cook University Hospital (Reference no. 2011083).

## **2.4 Statistical analysis**

Some statistical tests should only be used on data which are ‘normally’ distributed i.e. follow a Gaussian distribution and are referred to as parametric tests. While non-parametric or ‘distribution-free’ tests can be used with any data however distributed and including outliers. Non-parametric tests are based on fewer assumptions; hence they are generally less powerful than their parametric counterparts. Power being the probability that you will correctly reject the null hypothesis when it is false therefore there is an increased chance of making a Type II error with non-parametric tests and they are less likely to detect an effect or association when one really exists (Bowers et al. 2006). In the case of extremely small sample size, where it is difficult to ascertain the distribution of the data then non-parametric tests are more suitable. In this thesis; if the sample could not be transformed to be normal and the sample size was not sufficient (approximately 30 or more) that a parametric test could be used on a marginally non-normal sample then a non-parametric test was used. To assess the distributional shape and to evaluate if the data collected throughout this thesis were normally distributed, histograms were plotted and their shape visibly assessed. In addition analytical methods such as; ‘sktest’ based on skewness and kurtosis; and ‘swilk’ the Shapiro-Wilk tests for normality of data were used. Each is essentially a goodness of fit test, the null hypothesis for each test is  $H_0$ : data follow a normal distribution versus  $H_1$ : data do not follow a normal distribution. Therefore if the test was statistically significant (e.g.  $p < 0.05$ ) then data do not follow a normal distribution and a non-parametric test was warranted. The complete set of normality tests for variables used throughout this thesis are included in Appendix B and the results are summarised below or in their respective results section. P values  $\leq 0.05$  were considered statistically significant. Statistical analyses were performed using STATA 11 and 12 (StataCorp LP, Texas, USA).

### **2.4.1 Pilot study**

The histograms and tests for normality of data (Appendix B) showed that baseline, 6 month and percent change in  $\beta$ CTX, PINP, osteocalcin, OPG, CRP and ESR and percent change in DAS28 were not normally distributed and so were expressed as medians. However, the absolute change in these variables was normally distributed and so they were expressed as means. Baseline, 6 month and absolute change in DAS28 were normally distributed and so were also expressed as means. Similar results were found for these variables for the

bisphosphonate sub-group analysis. A paired t-test was used to compare change from baseline to 6 months (normally distributed). Spearman's rank correlation coefficient was used to correlate the percentage change from baseline (non-normal distribution) in individual marker.

#### **2.4.2 Prospective study**

The determination of sample size was based on the primary endpoint, change in LS BMD 12 months after the first RTX course. Assuming the true change in LS BMD was  $\geq 0.01 \text{g/cm}^2$  and that the DXA scan was reproducible with a SD of  $0.02 \text{g/cm}^2$ ; the study would have 80% power to detect a statistically significant difference (at the 5% significance level) if 33 patients were included in the final analysis based on a one sample t-test. To allow for a 20% dropout 42 patients should be recruited. The histograms and tests for normality of data (Appendix B) showed generally the BMD data was normally distributed and so they were expressed as means; however, T- and Z- scores were not normally distributed and were expressed as medians. Baseline, 12 month and percent change in  $\beta\text{CTX}$ , TRAP5b, PINP, BALP, SCL, DKK-1, CRP and ESR and percent change in DAS28 were not normally distributed and so were expressed as medians. However, the absolute change in these variables was normally distributed and so they were expressed as means. Baseline, 12 month and absolute change in DAS28 were normally distributed and so were also expressed as means. Similar results were found for all variables for the vitamin D sub-group analysis. The primary endpoint; change in LS BMD and secondary endpoints; change in mean total femur, mean neck of femur and mean forearm BMD, change in BTMs and change in inflammatory markers and DAS28, between baseline and 12 months were investigated using a one sample t-test. The median percentage change from baseline across 4 visits (3, 6, 9 and 12 months) was calculated for BTM's, inflammatory markers and disease activity. Spearman's rank correlation coefficient ( $R_s$ ) was used to correlate percentage change in inflammatory markers with percentage change in BMD site or BTMs. The change over 12 months for each vitamin D category was compared using a Student's t-test or Mann-Whitney test. Missing BMD or biomarker measurements were not imputed at any time point so using a completer analysis approach.

#### **2.4.3 Osteoclast work**

The histograms and tests for normality of data are included in Appendix B, however the sample sizes for the osteoclast cultures were small (*in vitro*  $n=12$  and *ex vivo*  $n=5$ ) and so non-parametric tests were used. Results were expressed as medians and interquartile range. Wilcoxon signed-rank test was used to determine if there was a statistically significant

difference between unfractionated and CD20 depleted PBMC fractions. Spearman's rank correlation coefficient  $R_s$  was used to correlate the initial number of cells and number of TRAP<sup>+</sup> cells generated. The Kruskal-Wallis test was used to determine if there was a statistically significant difference between visits and the nptrend statistic in Stata 11 was used to determine if there was a statistically significant trend in the results from baseline to 12 months for the RA patient data set. Multiple regression analysis was used to investigate which factors predicted osteoclast formation in unfractionated and CD20 depleted blood. Automated stepwise selection was used to create the models and the distribution of the residuals was verified graphically and with the Shapiro-Wilk  $W$  test for normal data (Appendix C).



# **Chapter 3**

## **Pilot Study**



## **Chapter 3. The effects of B cell depletion on bone turnover in patients with rheumatoid arthritis - the pilot study**

### **3.1 Introduction**

Progress has been made towards a greater understanding of the cross-regulation between the immune system and bone. A number of the same family members of cell surface receptors, cytokines and signalling pathways serve a critical role in both systems (Datta et al. 2008) and this is facilitated by their proximity in the bone marrow. The role of the immune system, specifically activated T cells, in inflammatory bone resorption and osteoclastogenesis is well established (Schett 2006, Li et al. 2007), but the role of B cells in osteoclast formation remains controversial. B cells can produce pro-osteoclastogenic cytokines including RANKL (Choi et al. 2001, Manabe et al. 2001) and under pathologic conditions such as RA this process is markedly enhanced by pro-inflammatory cytokines such as TNF- $\alpha$ , IL-1, IL-6 and IL-17 (Schett 2006). B cells also produce cytokines that inhibit osteoclast differentiation from the progenitor cells, such as OPG and TGF- $\beta$  (Li et al. 2007, Neale Weitzmann et al. 2000). The biological implications of these interactions are now being realised and targeted for therapeutic interventions. RA is the most prevalent inflammatory joint disease in which B cells play an important role. Controlled trials have shown that RTX, an antibody directed against CD20, depletes B cells and is an effective biological therapy for RA (Teng et al. 2007). Consequently RA subjects treated with RTX provide an ideal model for examining the effects of B cell depletion on bone turnover. It could be hypothesized that prolonged B cell depletion in patients with RA would affect bone turnover through modulation of osteoclastogenesis. However, some of these effects may be indirect through attenuation of systemic inflammation, while others may be direct as a result of the absence of B cells during osteoclast formation.

The availability of detailed clinical data and serial samples of blood from RA patients, before and after treatment with RTX, who participated in a prior clinical study carried out in The Netherlands (Teng et al. 2009) provided a unique opportunity to examine the role of B cells in inflammatory bone resorption and the results of this pilot study are described in the following Chapter.

### **3.2 Materials and methods**

### **3.2.1 Patient cohort**

The present pilot study involved 46 patients who participated in a prior Dutch, two-centre, open-label clinical trial to investigate the clinical and immunologic effects of treatment with RTX in severe refractory RA (Teng et al. 2009). All patients had failed treatment with a combination of DMARDs and/or TNF blocking agents, the clinical protocol is described in Chapter 2 section 2.3.1. Clinical efficacy had been previously assessed in The Netherlands using DAS28 and all routine laboratory results were available on a database. Menopausal status was confirmed using oestradiol and follicle-stimulating hormone (FSH) results. All patients were depleted of peripheral B cells following treatment with RTX (B-cell lineage marker CD19 analysed by quantitative flow cytometry), (Teng et al. 2009). Blood samples were taken between 1000 and 1600hrs and were non-fasting; all sera were stored at  $-80^{\circ}\text{C}$  until biomarker analysis.

### **3.2.1 Biomarker measurements**

Total PINP, osteocalcin and  $\beta\text{CTX}$  were quantified in serum by ECLIA on the Elecsys 2010 analyser. Both the free and complexed OPG-sRANKL concentration was measured in serum by manual ELISA. Individual assay details are described in Chapter 2 section 2.3.1.

### **3.2.2 Statistical analysis**

Details of the statistical analysis are described in Chapter 2 section 2.4.1.

## **3.3 Results**

### **3.3.1 Demographic and clinical characteristics**

Twenty-six patients (20 females and 6 males) from Leiden and 20 patients (12 females and 8 males) from Utrecht were included in the study. Samples were collected from all patients at baseline and 6 months. Additional blood samples were available at 3, 12, 18 and 24 months from the Leiden cohort; 26 samples were available at 3 months, 2 female patients were withdrawn from the study before their 6 month RTX infusion and at 24 months a further 5 females and 3 males were withdrawn before completing all 3 infusions due to serious adverse events. Only a limited number of samples were collected at the 18 month visit (Figure 13). The baseline characteristics of the 46 RA patients are provided in Table 7. Briefly, their mean age was 54.6yrs and disease duration 15.2yrs, 41 (89%) of patients were positive for IgM-RF and 38 (83%) were positive for ACPA-IgG. The baseline characteristics of patients from

Leiden and Utrecht were compared; there was a significant difference in smoking status and baseline  $\beta$ CTX and OPG, but no significant difference in any other parameters per site (Table 7). Utrecht patients had significantly lower  $\beta$ CTX levels however; fifty percent of these patients were already taking bisphosphonates which would explain the lower values. The effects of anti-osteoporotic medication were examined in Table 9. Additionally, Utrecht patients had significantly lower OPG levels but a greater percentage of these patients were current or former smokers and smoking has been reported to suppress OPG production (Lappin et al. 2007).

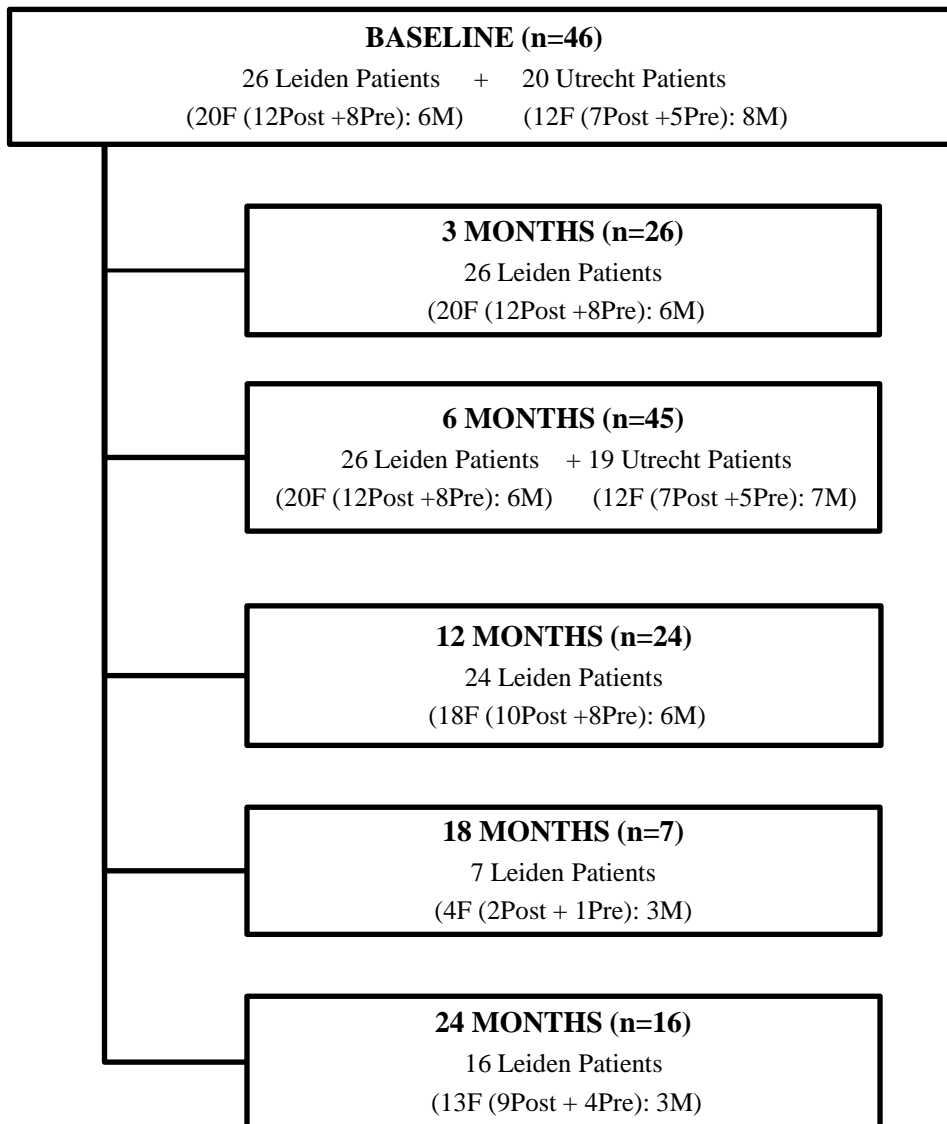


**Figure 13 Flowchart showing the pilot study numbers at each time point**

Patients from two Dutch centres; 26 from Leiden and 20 from Utrecht, were recruited into this pilot study. At 6 months samples were available from 26 Leiden patients and 19 Utrecht patients. Additional samples were collected from the Leiden patients at 3 (n=26), 12 (n=24), 18 (n=7) and 24 months (n=16).

**Table 7 Baseline characteristics of the forty-six rheumatoid arthritis patients**

Baseline characteristic No. (%)	All patients (n=46)	Leiden patients (n=26)	Utrecht patients (n=20)	P value (Difference by site)
Age mean (sd), yrs	54.6 (12.0)	53.2 (12.4)	56.5 (11.6)	0.353
Gender				
- Male	14 (30)	6 (23)	8 (40)	0.216
- Female	32 (70)	20 (77)	12 (60)	
- Pre-menopausal	13 (41)	8 (40)	5 (42)	0.487
- Post-menopausal	19 (59)	12(60)	7 (58)	
Smoking status				
- Current	12 (26)	5 (19)	7 (35)	<b>0.035</b>
- Former	17 (37)	7 (27)	10 (50)	
- Never	17 (37)	14 (54)	3 (15)	
Concomitant medication				
- Methotrexate	32 (70)	21 (81)	11 (55)	0.060
- Prednisolone	28 (61)	14 (54)	14 (70)	0.266
- Bisphosphonate	17 (37)	7 (27)	10 (50)	0.109
Disease duration, mean (sd), yrs	15.2 (11.8)	15.9 (13.2)	14.4 (10.0)	0.691
RF positive	41 (89)	22 (85)	19 (95)	0.262
ACPA positive	38 (83)	21 (81)	17 (85)	0.707
eGFR mean (sd), mls/min/1.73m <sup>2</sup>	88 (23)	89 (20)	87 (28)	0.869
HAQ mean (sd)	1.60 (0.64)	1.66 (0.71)	1.53 (0.55)	0.517
DAS28-CRP median (IQR)	5.62 (5.00-6.64)	5.62 (4.85-6.64)	5.66 (5.00-6.68)	0.673
ESR median (IQR), mm/hr	42 (22-66)	44 (22-66)	39 (18-63)	0.732
CRP median (IQR), mg/L	21.0 (8.0-57.0)	26.0 (15.0-84.0)	16.5 (8.0-44.5)	0.299
TSH median (IQR), mU/L	1.26 (0.69-2.10)	1.62 (0.80-2.24)	0.89 (0.62-1.8)	0.178
LH median (IQR), U/L – females	25.8 (2.0-41.4)	32.9 (4.2-41.4)	21.9 (1.7-37.2)	0.641
FSH median (IQR), U/L – females	47.0 (4.0-61.4)	51.0 (5.2-66.2)	46.5 (2.7-59.2)	0.824
Testosterone median (IQR), nmol/L – males	9.7 (8.3-15.0)	9.0 (8.2-9.7)	13.0 (8.5-20.0)	0.175
βCTX median (IQR), ng/L	224 (114-415)	368 (165-455)	137 (76-252)	<b>0.003</b>
PINP median (IQR), µg/L	35.5 (22.7-46.7)	39.9 (24.8-57.1)	33.4 (18.5-42.3)	0.138
Osteocalcin median (IQR), µg/L	15.2 (9.6-21.4)	16.8 (9.7-30.8)	12.6 (9.6-19.6)	0.150
OPG median (IQR), pmol/L	3.2 (2.2-4.4)	3.9 (2.6-5.5)	2.6 (1.8-3.2)	<b>0.004</b>

Continuous data are presented as means and standard deviation or medians and interquartile range depending on the distribution of the data set; groups were compared using the student's t-test or Mann-Whitney test when appropriate. Categorical variables are displayed as absolute frequencies and percentages; groups were compared using Fisher's exact test. ACPA: Anti-cyclic Citrullinated Peptide Antibody; βCTX: β-isomerised carboxy terminal telopeptide of type I collagen; CRP: C-Reactive Protein; DAS28: Disease Activity Score using 28 tender and swollen joints; eGFR: estimated Glomerular Filtration Rate; ESR: Erythrocyte Sedimentation Rate; FSH: Follicle Stimulating Hormone; HAQ: Health Assessment Questionnaire; LH: Luteinising Hormone; OPG: osteoprotegerin; PINP: procollagen type 1 amino-terminal propeptide; RF: Rheumatoid Factor; TSH: Thyroid Stimulating Hormone.

### 3.3.2 Changes in biomarker levels

Changes in median biomarker concentrations from baseline i.e. before the RTX treatment, to 6 months after the infusion are shown in Table 8. There was a significant reduction in  $\beta$ CTX at 6 months (-97ng/L; 95% CI -147, -47;  $p < 0.001$ ; a reduction of 37%). These results were mirrored by a significant reduction in CRP (-15mg/L; 95% CI -24, -6.8;  $p < 0.001$ ; a reduction of 43%), ESR (-17mm/hr; 95% CI -25, -9;  $p < 0.001$ ; a reduction of 33%) and DAS28 score (-0.94; 95% CI -1.35, -0.52;  $p < 0.001$ ; a reduction of 14%). There was a significant increase in PINP over 6 months (9.7 $\mu$ g/L; 95% CI 3.0, 16.4;  $p = 0.006$ ; an increase of 13%) but no significant change in osteocalcin or OPG levels (Wheater et al. 2011). Additionally, a marker of formation (PINP) and a marker of resorption ( $\beta$ CTX) were expressed as multiples of the median MoM<sub>F</sub> and MoM<sub>R</sub> respectively (described in Chapter 2 section 2.2.1), (Bieglmayer and Kudlacek 2009) and their ratios (MoM<sub>F</sub>/ MoM<sub>R</sub>) plotted before and 6 months after RTX to show the effect of treatment on bone turnover (Figure 14). At baseline 24 (53%) patients had a bone turnover ratio  $< 1$  (i.e. resorption predominated); whereas 6 months post RTX there were only 5 (11%) such patients, the majority had a ratio of  $\geq 1$  (i.e. formation predominated).

### 3.3.3 Time course of change in bone turnover

Additional serial samples were available from a subset of patients (n=26) at 3, 12 and 24 months. There was a wide variance in the changes in biomarker levels, but generally median  $\beta$ CTX levels decreased up until 6 months then gradually returned to baseline values and there was a small increase in bone formation markers; PINP, osteocalcin (Figure 15).



**Table 8 Change in biomarker concentration for the forty-six rheumatoid arthritis patients**

	Baseline	6 Month	Difference ( $\pm 95\%$ CI)	p value	% change ( $\pm 95\%$ CI)
<b><i>Bone Formation</i></b>					
PINP ( $\mu\text{g/L}$ )	35.5	44.4	9.7 (3.0, 16.4)	<b>0.006</b>	13 (-3, 38)
Osteocalcin ( $\mu\text{g/L}$ )	15.2	18.7	2.2 (-0.5, 4.9)	0.113	12 (-5, 31)
<b><i>Bone Resorption</i></b>					
$\beta\text{CTX}$ (ng/L)	224	161	-97 (-147, -47)	<b>&lt;0.001</b>	-37 (-47, -5)
<b><i>Osteocyte marker</i></b>					
OPG (pmol/L)	3.2	2.9	-0.4 (-0.9, 0.1)	0.090	-14 (-32, 10)
<b><i>Inflammatory markers</i></b>					
CRP (mg/L)	21	14	-15 (-24, -6.8)	<b>&lt;0.001</b>	-43 (-55, -5)
ESR (mm/hr)	42	24	-17 (-25, -9)	<b>&lt;0.001</b>	-33 (-46, -15)
<b><i>Disease activity</i></b>					
DAS28 score	5.71	4.78	-0.94 (-1.35, -0.52)	<b>&lt;0.001</b>	-14 (-21, -8)

$\beta\text{CTX}$ :  $\beta$ -isomerised carboxy terminal telopeptide of type I collagen; CRP: C-Reactive Protein; DAS28: Disease Activity Score using 28 tender and swollen joints; ESR: Erythrocyte Sedimentation Rate; OPG: osteoprotegerin; PINP: procollagen type 1 amino-terminal propeptide. Baseline, 6 months and percent change data for PINP, osteocalcin,  $\beta\text{CTX}$ , OPG, CRP, ESR and percent change for DAS28 were not normally distributed therefore results were expressed as medians. Baseline and 6 months DAS28 and all absolute change results were normally distributed and were expressed as means. P values were recorded between baseline and 6 months for all parameters using paired t-tests; p values  $\leq 0.05$  were considered significant.

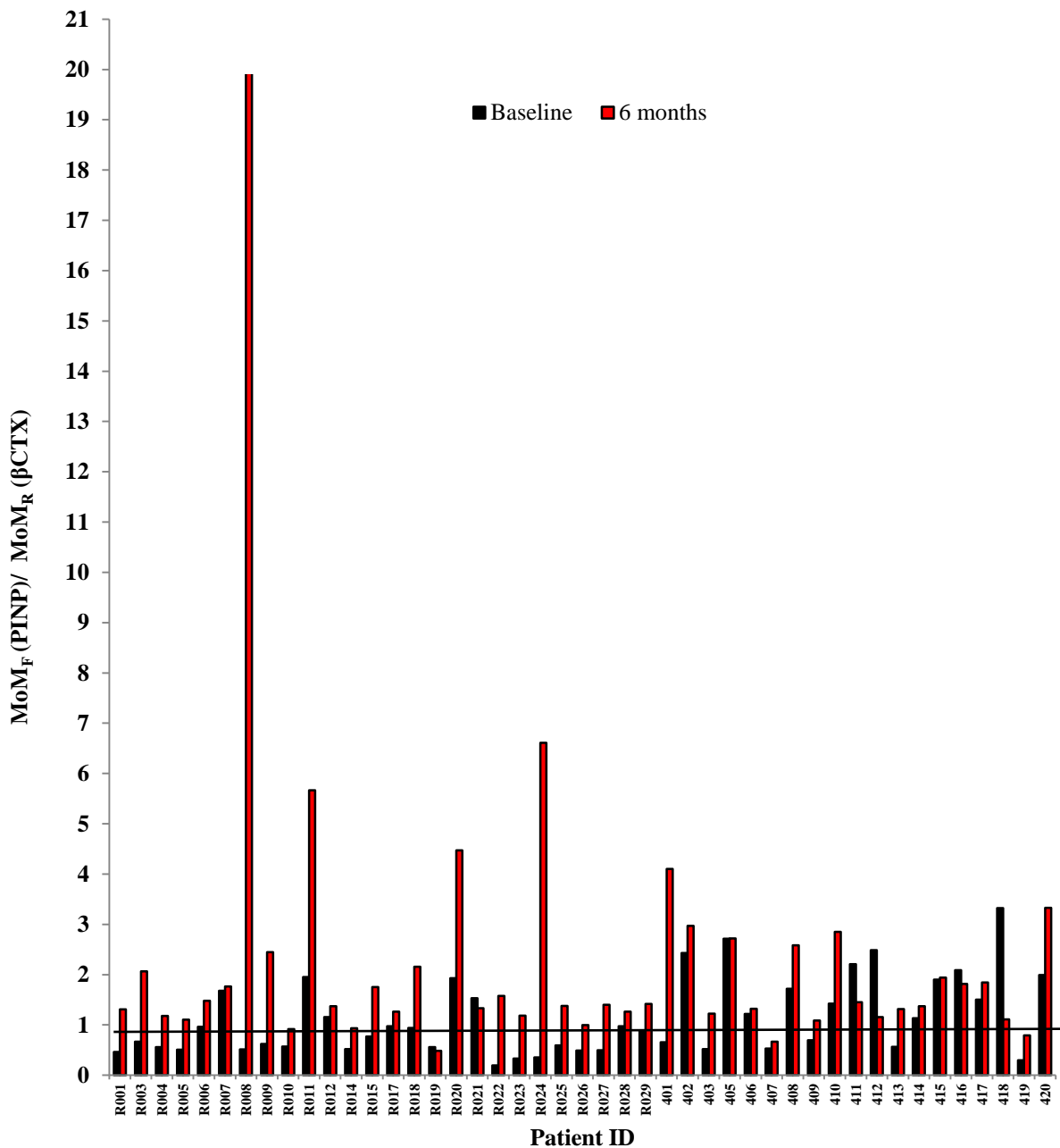
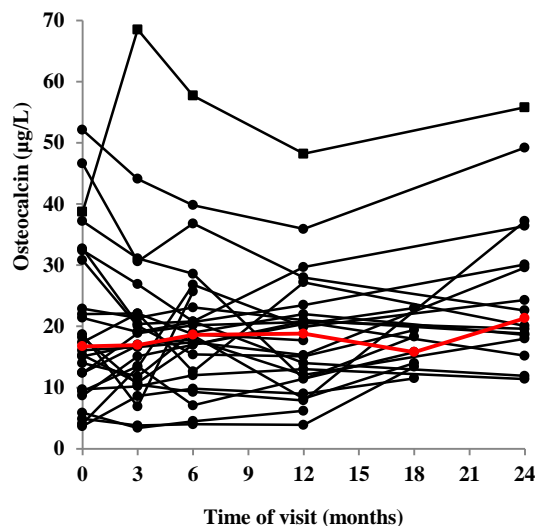
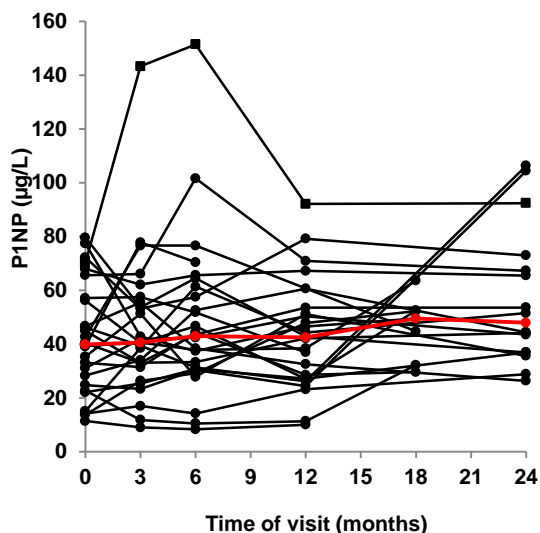


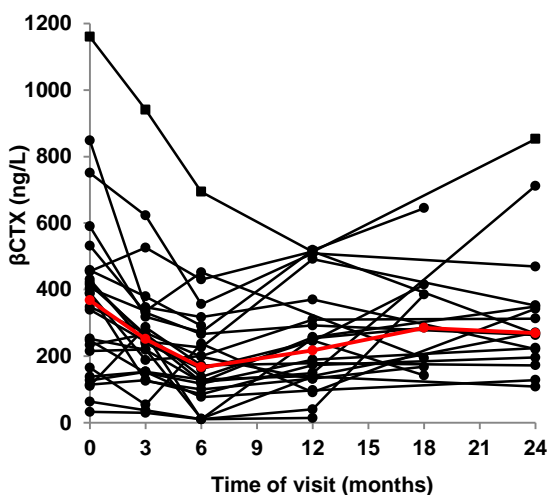
**Figure 14 Ratio of bone marker multiples of the median depicting bone turnover in forty-six rheumatoid arthritis patients' pre and 6 months post rituximab**

Blood samples from 72 healthy volunteers (33 males aged 19 to 62yrs and 39 females aged 20 to 64yrs) were analysed on the Elecsys 2100 for  $\beta$ CTX and PINP to calculate the median of the reference population. Multiples of the median (MoM) were defined as 'individual marker result/ median of the reference population' (Bieglmayer and Kudlacek 2009). Individual  $\beta$ CTX and PINP results from this pilot study looking at 46 patients with refractory RA analysed pre and post RTX, were expressed as ratios of their multiples of the median ( $MoM_F / MoM_R$ ).

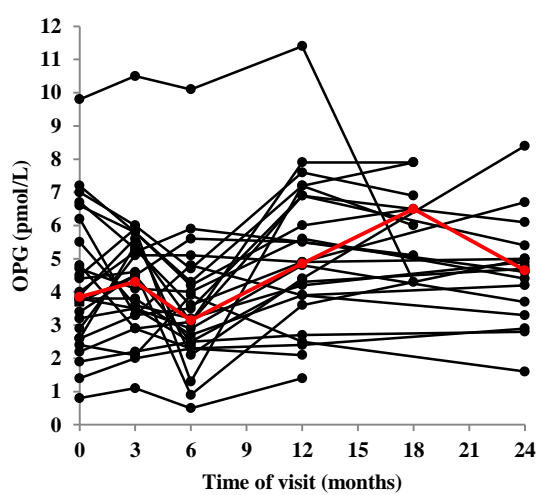
**Bone Formation**



**Bone Resorption**



**Cytokine**



Time of rituximab course:	0	6	12	18 (months)
---------------------------	---	---	----	-------------

**Figure 15** Change in individual bone markers over the course of the study

Serial biomarker results in a subset of RA patients from the pilot study: n= 26 (6M, 8 pre-, 12 post-menopausal F) at 0, 3 and 6 months; n=24 (6M, 8 pre-, 10 post-menopausal F) at 12 months; n=7 (3M, 2 pre-, 2 post-menopausal F) at 18 months; n=16 (3M, 4 pre-, 9 post-menopausal F) at 24 months.

— Indicates the median values.

### **3.3.4 The effect of gender and menopausal status**

As menopausal status is known to markedly affect bone turnover rate and to investigate the wide variance in biomarker results the data was plotted (Figure 16) by gender and menopausal status separately (14 males, 13 pre-menopausal and 19 post-menopausal females). There was a significant decrease in  $\beta$ CTX in males ( $p=0.016$ ) and a borderline significant decrease in postmenopausal females ( $p=0.05$ ), the latter also showed a significant increase in PINP ( $p=0.024$ ) from baseline to 6 months. Premenopausal females had the lowest baseline results overall and least change at 6 months for all bone markers (Wheater et al. 2011). However, the numbers in each group are small and so the gender specific differences should be interpreted with caution.

### **3.3.5 The effect of concomitant medication**

Seventeen patients (4 males; 5 pre- and 8 post-menopausal females) were taking bisphosphonates and prednisolone, a further 11 patients (4 males; 3 pre- and 4 post-menopausal females) were on prednisolone alone and the remaining 18 (6 males; 5 pre- and 7 post-menopausal females) were on neither medication. No patients were on hormone replacement therapy. Results are included in Table 9, there was a significant reduction in  $\beta$ CTX (mean change  $-129\text{ng/L}$  95% CI,  $-191, -67$ ;  $p<0.001$ ; a  $-37\%$  decrease) and OPG (mean change  $-0.7\text{pmol/L}$  95% CI  $-1.3, -0.0$ ;  $p=0.048$ ; a  $16\%$  decrease) at 6 months for patients not taking a bisphosphonates, but no significant change in patients on bisphosphonates.

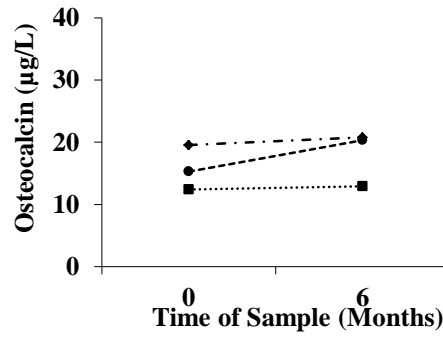
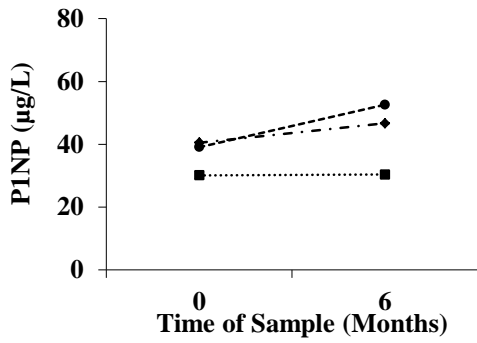
Conversely, there was a significant increase in PINP (mean change  $14.3\mu\text{g/L}$  95% CI,  $3.3, 25.2$ ;  $p=0.014$ ; a  $42\%$  increase) and osteocalcin (mean change  $5.6\mu\text{g/L}$  95% CI,  $1.0, 10.3$ ;  $p=0.021$ ; a  $31\%$  increase) in patients on bisphosphonate, but no significant change on those not taking bisphosphonate (Wheater et al. 2011). Patients on bisphosphonate had increased bone formation at 6 months but no significant change in bone resorption; whereas patients not on bisphosphonate had decreased bone resorption at 6 months but no significant change in bone formation. There was however a significant improvement in the bone turnover ratio 6 months post RTX in bisphosphonate naïve patients (mean change  $0.5$ , 95% CI,  $0.2, 0.8$ ;  $p<0.001$ ), but no significant change in this ratio in patients taking bisphosphonate.

### **3.3.6 Correlations between inflammatory activity and bone turnover**

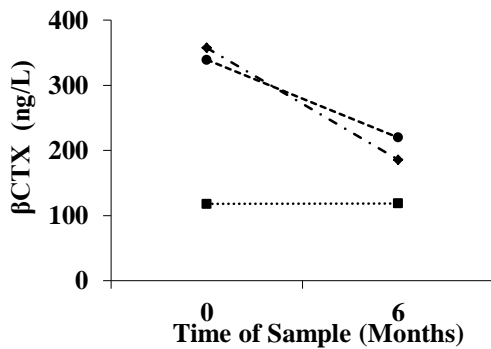
Only the patients not on bisphosphonate or prednisolone ( $n=18$ ) were included in the correlation analysis to examine the effect of RTX on the change in biomarker levels (Table 10). Significant correlations were observed between  $\beta$ CTX and DAS28 ( $R_s=0.570$ ,  $p=0.014$ ) and borderline significant between  $\beta$ CTX and CRP ( $R_s=0.485$ ,  $p=0.057$ ), (Wheater et al.

2011). The significant correlations between the bone turnover markers and between the inflammatory markers were as expected.

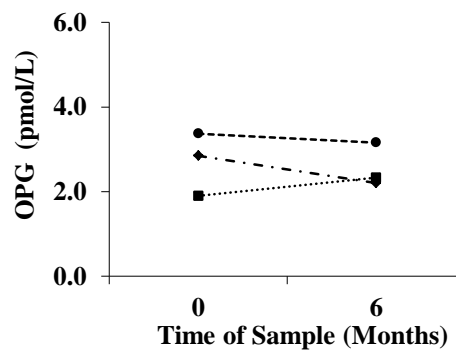
**Bone Formation**



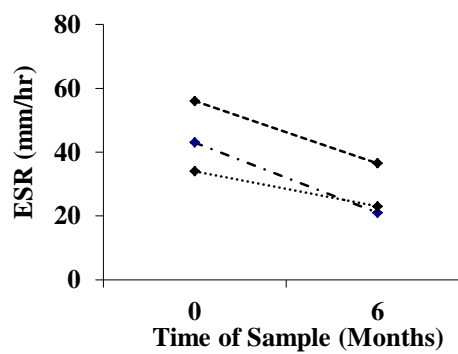
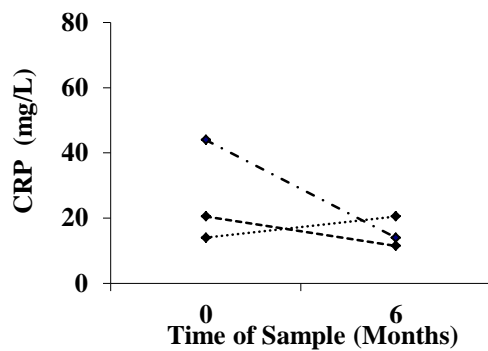
**Bone Resorption**



**Cytokine**



**Inflammatory markers**



**Disease activity**

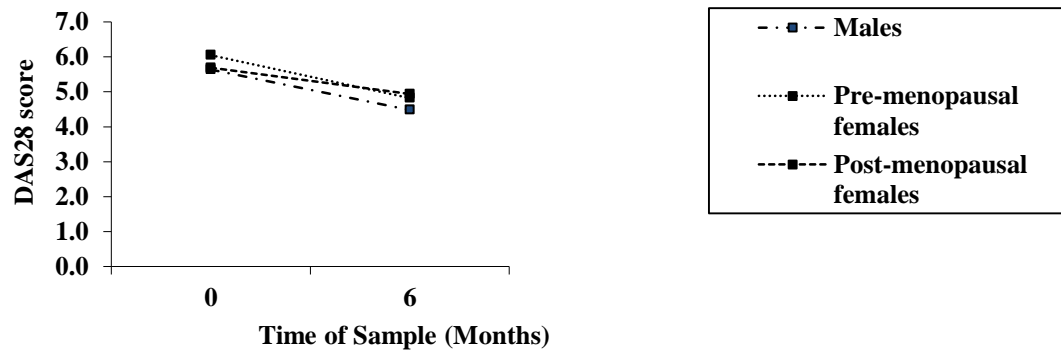


**Figure 16 The effects of gender and menopausal status on median biomarker levels**

Blood samples were taken at baseline before RTX and at 6 months after the infusion in a total of 46 patients with RA. Patients were split by gender and menopausal status (14 males, 13 pre-menopausal and 19 post-menopausal females). Results were expressed as medians.

**Table 9 Effect of bisphosphonate treatment on change in biomarker concentration for forty-six rheumatoid arthritis patients from baseline to six months**

	<i>Baseline</i>	<i>6 Month</i>	<i>Difference ( ±95% CI)</i>	<i>p value</i>	<i>% change ( ±95% CI)</i>
<b>Bone Formation</b>					
<b>PINP (µg/L)</b>					
All Patients (n=46)	35.5	44.4	9.7 (3.0, 16.4)	<b>0.006</b>	13 (-3, 39)
- Bisphosphonate (n=17)	19.8	29.4	14.3 (3.3, 25.2)	<b>0.014</b>	42 (-3, 99)
- No Bisphosphonate (n=29)	44.9	45.6	7.2 (-1.7, 16.1)	0.108	8 (-10, 33)
<b>Osteocalcin (µg/L)</b>					
All Patients (n=46)	15.2	18.7	2.2 (-0.5, 4.9)	0.113	12 (-6, 33)
- Bisphosphonate (n=17)	9.4	11.6	5.6 (1.0, 10.3)	<b>0.021</b>	31 (-7, 127)
- No Bisphosphonate (n=29)	20.1	20.7	0.3 (-3.1, 3.7)	0.850	6 (-16, 21)
<b>Bone Resorption</b>					
<b>βCTX (ng/L)</b>					
All Patients (n=46)	224	161	-97 (-147, -47)	<b>&lt;0.001</b>	-37 (-49, -6)
- Bisphosphonate (n=17)	154	82	-40 (-127, 47)	0.346	-36 (-71, 39)
- No Bisphosphonate (n=29)	328	186	-128 (-191, -67)	<b>&lt;0.001</b>	-37 (-45, -6)
<b>Cytokine</b>					
<b>OPG (pmol/L)</b>					
All Patients (n=46)	3.2	2.9	-0.4 (-0.9, 0.1)	0.090	-14 (-33, 12.5)
- Bisphosphonate (n=17)	2.9	2.9	0.0 (-0.7, 0.7)	0.925	3 (-22, 27)
- No Bisphosphonate (n=29)	3.4	2.7	-0.7 (-1.3, -0.0)	<b>0.048</b>	-16 (-37, 10)

βCTX: β-isomerised carboxy terminal telopeptide of type I collagen; PINP: procollagen type 1 amino-terminal propeptide; OPG: osteoprotegerin. Baseline, 6 months and percent change data for PINP, osteocalcin, βCTX and OPG were not normally distributed therefore results were expressed as medians. All absolute change results were normally distributed and were expressed as means. P values were recorded between baseline and 6 months for all parameters using paired t-tests; p values ≤0.05 were considered significant.

**Table 10 Correlations between the percentage change from baseline of biomarker values for patients not on bisphosphonates or prednisolone (n=18)**

	<b>PINP</b>	<b>Osteocalcin</b>	<b>OPG</b>	<b>CRP</b>	<b>ESR</b>	<b>DAS28</b>
<b>βCTX</b>	0.425	0.567*	-0.020	0.485	0.212	0.570*
<b>PINP</b>		0.715***	0.057	-0.090	-0.020	0.422
<b>Osteocalcin</b>			0.016	-0.004	-0.034	0.348
<b>OPG</b>				0.074	-0.150	0.135
<b>CRP</b>					0.677**	0.596*
<b>ESR</b>						0.628**

βCTX: β-isomerised carboxy terminal telopeptide of type I collagen; PINP: procollagen type 1 amino-terminal propeptide; OPG: osteoprotegerin; CRP: C-Reactive Protein; ESR: Erythrocyte Sedimentation Rate; DAS28: Disease Activity Score using 28 tender and swollen joints. The percent change data was not normally distributed therefore Spearman's rank correlation Rs was used.

\* p<0.05; \*\* p<0.01; \*\*\* p<0.001.



### 3.4 Discussion

The aim of this study was to investigate the effects of B cell depletion with RTX on bone turnover in patients with severe RA. There was a significant suppression of bone resorption depicted by  $\beta$ CTX, along with an increase in PINP a marker of bone formation albeit subjects being treated with a range of therapies, including corticosteroids, which are known to increase bone turnover and bone loss. Glucocorticoids have strong anti-inflammatory effects but their use in RA has been reported to increase the risk of osteoporosis by inducing apoptosis of osteoblasts and osteocytes leading to an uncoupling between bone formation (suppressed) and bone resorption (unchanged or relatively increased), (Lems 2007). This effect can be counteracted by the use of bisphosphonates that induce osteoclast apoptosis (Breuil 2006). Over half of the patients in this study had been on prednisolone alone or in combination with a bisphosphonate for at least six months prior to the start of the study. Bisphosphonates are synthetic analogs of pyrophosphate; they avidly bind to the hydroxyapatite component of the bone matrix and so suppress osteoclast-mediated bone resorption (Goldring and Gravallese 2004). There are two distinct types of bisphosphonates based on the presence or absence of an amino group on the carbon side chain. The amino bisphosphonates; alendronate, risedronate and zoledronate, were commonly used in this pilot study; they inhibit osteoclast recruitment, differentiation, formation of the ruffled border and acid production and induce osteoclast apoptosis (Deal 2005). Typically, bisphosphonates decrease bone resorption rapidly within one to three months and because of the coupling of bone formation and resorption, this inhibition of resorption results in a decrease in formation by six to twelve months (Deal 2005, Brown et al. 2009). There was a significant suppression of bone resorption six months after RTX in this pilot study; however the extent of this decrease was masked by the number of patients already on bisphosphonate; these patients already had suppressed bone resorption at baseline and therefore a non-significant decrease at six months. Interestingly, this group of bisphosphonate treated patients still had a significant increase in bone formation six months after RTX despite the suppressed resorption.

Additionally, there was a significant correlation between the reduction in bone resorption and disease activity in a subset of patients, not on bisphosphonates or prednisolone indicating that the anti-resorptive action and anti-inflammatory therapeutic response may be related. The suppression of bone resorption was possibly due to a combination of factors namely; diminished osteoclast activity resulting from decreased B-cell mediated osteoclastogenesis; decreased systemic inflammatory cytokines; or increased physical activity following RTX treatment (Wheater et al. 2011). The magnitude of difference in the bone markers was difficult to determine because of the heterogeneity of the patients examined in this study with

respect to age, gender and menopausal status. In young adults bone formation and resorption are in balance and reach peak bone mass during the third decade of life, but with ageing there is a net loss of bone (Datta et al. 2008). Additionally, menopausal status is known to markedly affect the rate of bone turnover (Garneo et al. 2000) and so the results were re-assessed by gender and pre- or post-menopause. However, as the numbers per group were small any such differences were interpreted with caution. In general pre-menopausal females had the lowest baseline results overall and showed the least improvement post RTX therapy. Post-menopausal females had higher levels of bone markers at baseline, possibly because bone loss is more rapid post menopause (Garneo et al. 2000). Likewise, the male cohort were older (median age 60.9; range 50.6 – 81.5yrs) and had higher baseline values and an apparent reduction in bone resorption over six months, although the small numbers impacted on the confidence limits and further studies are needed to confirm these observations (Wheater et al. 2011).

Although, several studies have reported that RTX inhibits the progression of structural joint damage in RA (Keystone 2009, Boumans 2012), few studies have reported the effects of a B cell depleting therapy on biochemical markers of bone turnover. These results do however, confirm and extend recent findings with RTX in 13 patients with active RA. The authors reported a significant decrease in bone resorption after 15 months, but no significant change in markers of bone formation (Hein et al. 2010). A review of comparable studies using TNF blocking agents (Barnabe and Hanley 2008), mainly infliximab on markers of bone turnover, show variable results, the majority reporting a similar positive effect on bone six months post therapy.

### 3.5 Conclusion

In conclusion, the results of this pilot study indicated that depletion of B cells with RTX in this RA cohort ameliorated bone turnover, as reflected by the changes in  $\beta$ CTX and PINP six months after treatment. Significant correlations between the percentage decrease from baseline in  $\beta$ CTX and DAS28 suggested that the improvement in disease activity accounted in part for the reduction in bone resorption. However, there were a number of limitations to be addressed in further work. The comparatively small number of subjects impacted on the confidence intervals for the median change from baseline and the study was not powered to adjust for confounders. Additionally, this analysis was not a predefined aim of the original RTX study so thirty-seven percent of patients were already on bisphosphonates, this may have masked the effects of RTX. Furthermore, the blood samples were not all fasted, early morning samples as recommended for markers of bone turnover (Wheater et al. 2013). A further study

---

is needed over a longer follow-up period and after subsequent treatments to confirm these associations, adjust for potential confounders and investigate whether the observed changes in biochemical markers of bone turnover translate into changes in bone mass.



# **Chapter 4**

## **Prospective Study**



## Chapter 4. The effects of B cell depletion on bone turnover in patients with rheumatoid arthritis - the prospective study

### 4.1 Introduction

The results of the pilot study indicated that there was a significant suppression of bone resorption in twenty-nine bisphosphonate naïve patients with severe refractory RA, after a single treatment course of RTX. However, it was evident that the true effect of B cell depletion was masked by including seventeen patients already treated with bisphosphonate in the total cohort. Additionally, the blood samples were not all taken under identical conditions. Bone turnover shows a circadian rhythm, this is most apparent in serum  $\beta$ CTX; levels are highest between 01:30 and 04:30 and may be more than twice that at the nadir between 11:00 and 15:00 (Wichers et al. 1999). Blood samples in the pilot study were all taken between 10:00 and 16:00, the finding that RTX caused the ‘trough’ levels of  $\beta$ CTX to drop was therefore of significance. The disparity in levels can be diminished with fasting and is influenced by variations in serum insulin (Bjarnason et al. 2002). Bone markers are significantly lower in the fed state and dependant on the clearance rate of individual markers or food composition (Clowes et al. 2002). Consequently the timing of the sample collection and fasting status should be tightly controlled in subsequent studies.

Data describing the effect of *in vivo* B cell depletion on general bone loss in patients with RA are still limited. Therefore, a prospective observational study was designed to investigate bone density and biomarkers of bone turnover in RA patients treated with RTX over a 12 month period. The aim of this study was to confirm and extend the results of the pilot study and to address the apparent limitations mentioned above, in a different cohort of patients. It was postulated that the presumed bone-protective effects of RTX on bone density and bone turnover are due either to a direct effect of B cell depletion on osteoclastogenesis, or a reduction in disease activity, or alternatively to both of these effects.

### 4.2 Materials and methods

This was a multicentre, open-label, single treatment arm, prospective clinical trial on a cohort of adult patients with severe RA who started RTX after failure of other DMARDs, including at least one anti-TNF- $\alpha$ . The primary outcome measure was change in lumbar spine BMD. The secondary outcomes were: change in mean total femur, mean neck of femur and mean forearm BMD, change in bone turnover markers, change in inflammatory markers and change in DAS28. Parameters were assessed between baseline and 12 months.

#### **4.2.1 Patient cohort**

All patients were older than 18 years of age and had an established diagnosis of RA according to the American College of Rheumatology (ACR)-criteria and were eligible for treatment with RTX, according to the UK National Institute for Health and Care Excellence (NICE) eligibility criteria. Patients were excluded if they had previously received any B cell depleting agent, or had been treated for osteoporosis with bisphosphonates, calcitonin, strontium ranelate, denosumab or teriparatide. However, calcium, vitamin D, corticosteroids, non-biological DMARDs and treatment for concomitant medical conditions were all continued throughout the study at the discretion of the treating physician. Patients were recruited from 10 UK centres (Figure 17). The clinical protocol is described in Chapter 2 section 2.3.2.

#### **4.2.2 Clinical and laboratory assessments**

Patients were assessed at baseline prior to the first RTX treatment and then every 3 months over a 12 month follow up period. Clinical assessment of disease activity was undertaken using the 28-joint disease activity score and wrCRP (DAS28-CRP). Routine laboratory investigations were performed locally at baseline and every three months. Fresh whole blood samples were analyzed using a flow cytometer (FACS Canto II) to determine the numbers of CD19<sup>+</sup> B cells in a subset of patients as per the study protocol at baseline and 3-monthly visits.



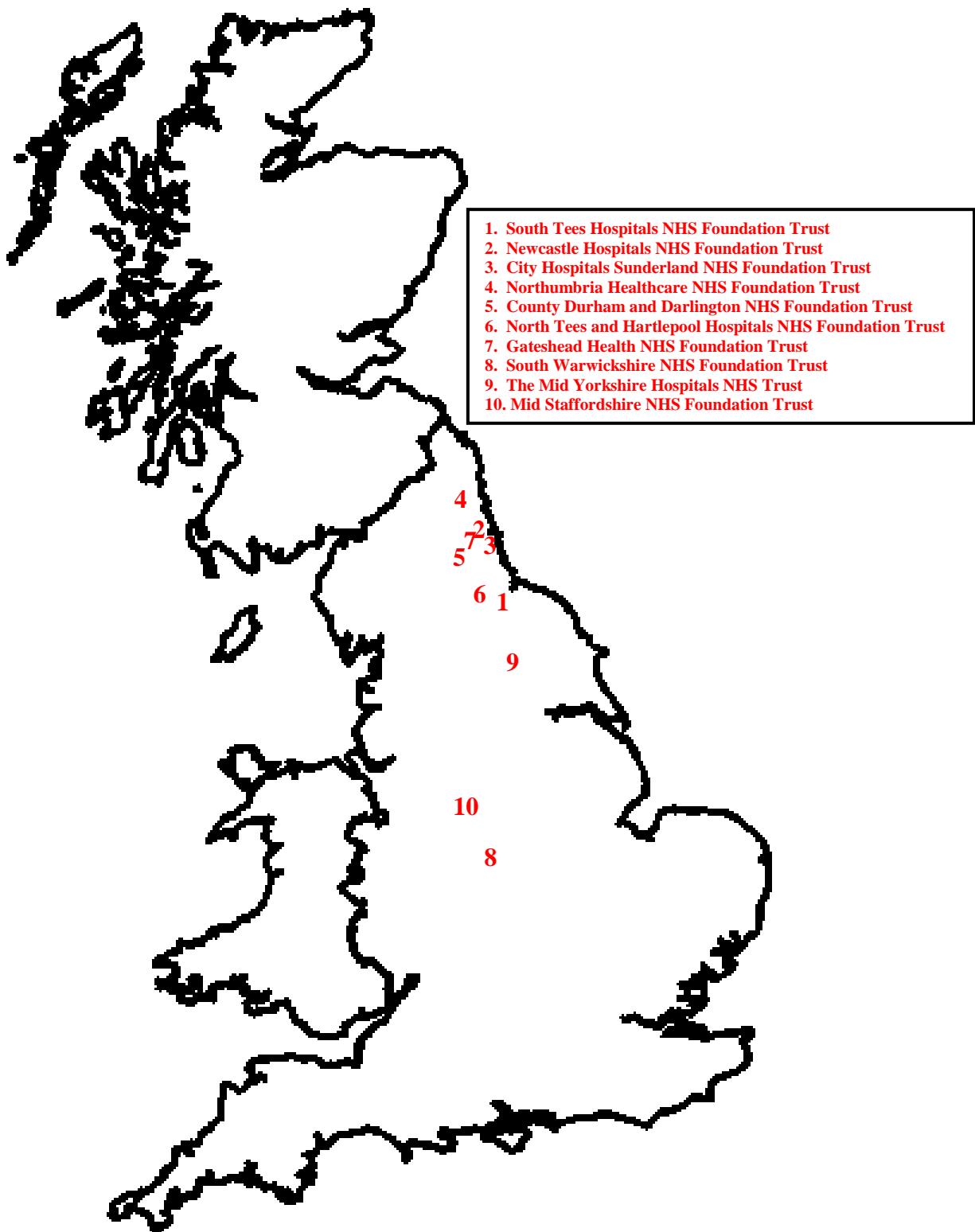


**Figure 17 Location of the ten UK centres recruiting into the prospective study**

Patients were recruited from ten UK Rheumatology centres: South Tees Hospitals n=13; Newcastle Hospitals n=9; City Hospitals Sunderland n=4; Northumbria Healthcare n=3; County Durham and Darlington n=3; North Tees and Hartlepool n=2; Gateshead Health n=3; South Warwickshire n=2; Mid Yorkshire n=4; Mid Staffordshire n=2.

### **4.2.3 Bone mineral density measurements**

BMD was measured at baseline and 12 month by dual-energy X-ray absorptiometry (DXA). Measurements were taken at the lumbar spine (mean L2-L4), also right and left femoral neck, total femur and ultra-distal radius (RUD) forearm; however results were reported as the mean of both sides. Two different DXA machines were used across the 10 centres; 7 centres used GE Lunar Prodigy (Lunar, Madison, Wisconsin, USA) and 3 centres used Hologic Discovery (Hologic, Waltham, Massachusetts, USA). However, in all cases the same machine was used at baseline and follow-up measurement for each patient. The inter-assay coefficient of variation (CV), measured using a local spine phantom, for the different centres were all less than 1.8%.

### **4.2.4 Biomarker measurements**

Fasting morning blood samples were taken every 3 months into SST and EDTA tubes. Serum and plasma were separated within 60mins and immediately stored at -80°C until analysis. All measurements were performed as per manufacturer's instructions and in a centralized laboratory to reduce analytical variation. Total PINP,  $\beta$ CTX and PTH were quantified in plasma by automated ECLIA on the Elecsys 411 analyser. BALP and 25OHD were quantified in serum by chemiluminescence on the iSYS analyser and TRAP5b was measured in serum by a manual ELISA. SCL and DKK-1 were measured in serum using a manual ELISA. Method details are included in Chapter 2 section 2.2.1.

### **4.2.5 Statistical analysis**

Details of the statistical analysis are described in Chapter 2 section 2.4.2.

### 4.3 Results

A total of 45 patients met the eligibility criteria and were enrolled into the study (Figure 18). One patient was subsequently diagnosed with chronic lymphocytic leukaemia (CLL) and excluded; therefore 44 patients received the first RTX infusion. A total of 36 patients completed the 12 month follow up period and were included in the analysis; 32 of these patients received a second course of RTX as per protocol and four patients did not (two patients had low disease activity (DAS28<3.2); one patient had undetectable B cells and one patient refused the second course).

#### 4.3.1 Demographic and clinical characteristics

There was no significant difference in any baseline characteristic (Table 11) between patients who completed the study (n=36) compared to the total number of patients recruited (n=45), or between patients who completed the study (n=36) compared to non-completers (n=9).

Therefore the following analysis included only the 36 patients who completed 12 month follow-up. Seven of these patients were male and 29 were female; 23 females were post-menopausal. Briefly, their mean age was  $58.6 \pm 12.1$  yrs and the mean disease duration was  $10.4 \pm 7.0$  yrs, 33% of patients were current smokers (n=12) consisting of one pre-menopausal, nine post-menopausal and two male patients. Eighty-three percent (n=30) of patients were positive for IgM-RF and 76% (n=25) were ACPA positive. Thirty-nine percent (n=14) of the patients had vitamin D deficiency defined as 25OHD levels below 25nmol/L, only one of these patients was on a calcium and vitamin D supplement at baseline, a further four patients started on supplements during the course of the study. The numbers of CD19<sup>+</sup> B cells were determined in a subset of 16 patients at each visit; all had values less than  $0.01 \times 10^9/L$  at 3 months and four patients had rapid reconstitution of their B cells at 6 months, while the others had long-term depletion.

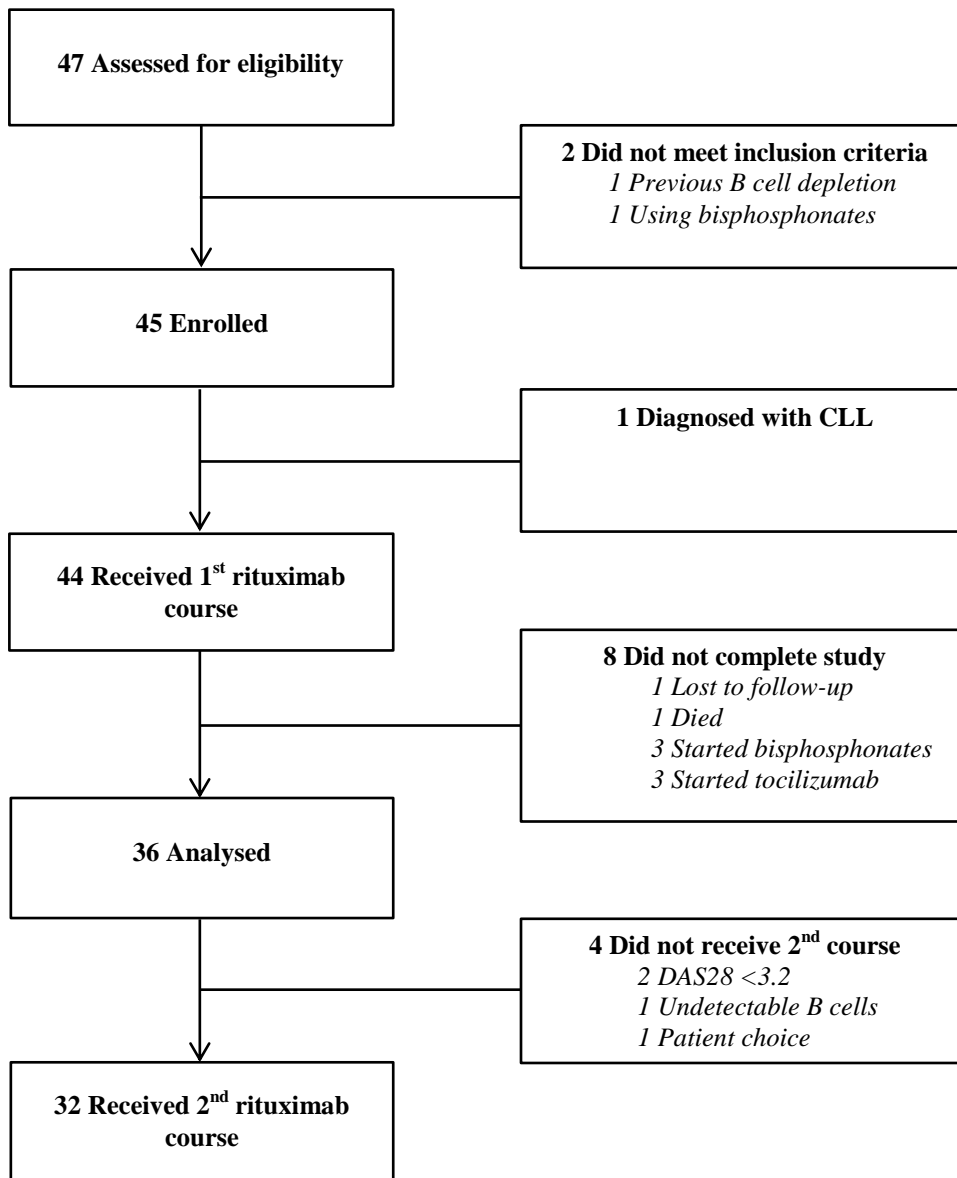


**Figure 18 Consort flow diagram for the prospective study**

Forty-seven patients were screened; 2 patients did not meet the eligibility criteria and so 45 were enrolled onto the study. One patient was subsequently diagnosed with chronic lymphocytic leukaemia therefore only 44 patients received the first course of RTX. A further 8 patients did not complete the study and a total of 36 patients were included in the final analysis; of these only 32 received the second RTX course.

Table 11 Baseline characteristics of the prospective study patients

Characteristics No. (%)	All patients (n=45)	Completed study (n=36)	Did not complete study (n=9)
Age mean (sd), yrs	59.3 (12.2)	58.6(12.1)	62.3 (12.5)
<b>Gender</b>			
- Male	9 (20)	7 (19)	2 (22)
- Female	36 (80)	29 (81)	7 (78)
- Pre-menopausal	7 (19)	6 (21)	1 (14)
- Post-menopausal	29 (81)	23 (79)	6 (86)
<b>Ethnicity</b>			
- White	43 (96)	34 (94)	9 (100)
- Asian	2 (4)	2 (6)	0
<b>Smoking status</b>			
- Current	15 (33)	12 (33)	3 (33)
- Former	14 (31)	11 (31)	3 (33)
- Never	16 (36)	13 (36)	3 (33)
<b>Concomitant medication</b>			
- Hydroxychloroquine	2 (4)	1 (3)	1 (11)
- Leflunomide	5 (11)	3 (8)	2 (22)
- Methotrexate	25 (56)	21 (58)	4 (44)
- Sulfasalazine	5 (11)	5 (14)	0
- Prednisolone	14 (31)	11 (31)	3 (33)
- Calcium/ Vitamin D	5 (11)	4 (11)	1 (11)
BMI mean (sd), kg/m <sup>2</sup>	29.6 (7.5)	29.4 (8.0)	30.5 (5.5)
Disease duration mean (sd), yrs	10.9 (7.8)	10.4 (7.0)	12.9 (10.9)
RF positive	37 (82)	30 (83)	7 (78)
ACPA positive	32 (76)	25 (76)	7 (78)
DAS28-CRP mean (sd)	5.72 (1.32)	5.62 (1.33)	6.10 (1.24)
HAQ mean (sd)	1.94 (0.47)	1.92 (0.43)	2.02 (0.63)
ESR median (IQR), mm/hr	33 (12, 45)	32 (11, 43)	55 (26, 69)
hs-CRP median (IQR), mg/L	12.6 (2.9, 38.1)	11.7 (2.8, 38.8)	29.3 (4.1, 34.0)
eGFR mean (sd), mls/min/1.73m <sup>2</sup>	84 (25)	85 (25)	80 (26)
PTH median (IQR), ng/L	32.1 (27.3, 49.0)	30.2 (26.4, 48.6)	42.4 (28.3, 50.0)
25OHD median (IQR), nmol/L	31.2 (18.3, 64.4)	36.1 (20.6, 74.1)	18.3 (14.0, 34.8)
TSH median (IQR), mU/L	1.43 (1.03, 2.23)	1.45 (1.07, 2.51)	1.40 (0.67, 1.82)
LH median (IQR), U/L – females	30.0 (18.0, 38.0)	30.0 (16.4, 39.8)	27.0 (25.8, 29.3)
FSH median (IQR), U/L – females	59.6 (24.1, 83.7)	59.6 (13.3, 89.8)	60.9 (36.1, 78.0)
Testosterone median (IQR), nmol/L – males	13.4 (10.7, 15.5)	13.4 (9.8, 15.6)	13.5 (11.5, 15.4)
SHBG median (IQR), nmol/L - males	56.5 (21.8, 63.0)	49.7 (21.8, 63.0)	56.5 (56.5, 56.5)
βCTX median (IQR), ng/L	436(269, 555)	423 (257, 511)	578 (336, 627)
PINP median (IQR), µg/L	41.9 (30.9, 52.4)	39.8 (29.6, 46.9)	53.9 (41.7, 65.1)
BALP median (IQR), µg/L	17.9 (14.1, 22.2)	17.2 (13.7, 20.7)	25.2 (18.5, 27.7)
TRAP5b median (IQR), U/L	3.1 (2.6, 3.7)	3.0 (2.5, 4.0)	3.4 (2.9, 3.7)
DKK-1 median (IQR), pmol/L	52.8 (37.9, 68.6)	47.9 (34.9, 67.7)	55.9 (52.8, 74.1)
SCL median (IQR), pmol/L	54.5 (43.8, 63.0)	53.4 (42.0, 63.8)	55.8 (47.7, 60.0)
<b>Lumbar Spine L2-L4</b>			
- BMD mean (sd), g/cm <sup>3</sup>	1.168 (0.23)	1.171 (0.25)	1.158 (0.17)
- T score median (IQR)	-0.4 (-1.1, 0.6)	-0.4 (-1.3, 0.8)	-0.4 (-0.8, -0.2)
- Z score median (IQR)	0.5 (-0.6, 1.7)	0.4 (-0.6, 1.7)	0.8 (0.2, 0.9)
<b>Mean neck of femur</b>			
- BMD mean (sd), g/cm <sup>3</sup>	0.875 (0.15)	0.884 (0.14)	0.840 (0.20)
- T score median (IQR)	-0.8 (-1.4, -0.3)	-0.7 (-1.3, -0.2)	-1.3 (-2.7, -0.5)
- Z score median (IQR)	0.2 (-0.7, 0.8)	0.3 (-0.5, 0.8)	-0.4 (-1.6, 0.3)
<b>Mean total femur</b>			
- BMD mean (sd), g/cm <sup>3</sup>	0.935 (0.16)	0.944 (0.15)	0.901 (0.21)
- T score median (IQR)	-0.6 (-1.7, 0.1)	-0.5 (-1.2, 0.2)	-0.7 (-2.3, -0.5)
- Z score median (IQR)	0.1 (-0.6, 0.8)	0.3 (-0.5, 0.9)	-0.6 (-1.2, 0.4)
<b>Mean radius UD</b>			
- BMD mean (sd), g/cm <sup>3</sup>	0.376 (0.1)	0.381 (0.10)	0.354 (0.07)
- T score median (IQR)	-1.1 (-2.4, 0.2)	-1.1 (-2.4, 0.2)	-1.4 (-2.9, 0.6)
- Z score median (IQR)	-0.6 (-1.4, 1.3)	-0.6 (-1.3, 0.8)	-0.4 (-2.3, 1.6)

Continuous data were presented as means and standard deviation or medians and interquartile range depending on the distribution of the data set; groups were compared using the student's t-test or Mann-Whitney test when appropriate. Categorical variables were displayed as absolute frequencies and percentages, groups were compared using Fisher's exact test. Neck of femur, total femur and radius UD results were reported as the mean of both sides. There was no significant difference in any baseline characteristic for those patients who completed the study (n=36) compared to the total number of patients recruited (n=45) or for those patients who completed the study (n=36) compared to non-completers (n=9).

25OHD: 25Hydroxy vitamin D; ACPA: Anti-cyclic Citrullinated Peptide Antibody; BALP: bone specific alkaline phosphatase;  $\beta$ CTX:  $\beta$ -isomerised carboxy terminal telopeptide of type I collagen; BMI: Body Mass Index; CRP: C-Reactive Protein; DAS28: Disease Activity Score using 28 tender and swollen joints; DKK-1: dickkopf-related protein 1; eGFR: estimated Glomerular Filtration Rate; ESR: Erythrocyte Sedimentation Rate; FSH: Follicle Stimulating Hormone; HAQ: Health Assessment Questionnaire; LH: Luteinising Hormone; PINP: procollagen type 1 amino-terminal propeptide; PTH: Parathyroid Hormone; RA: Rheumatoid Arthritis; RF: Rheumatoid Factor; SCL: sclerostin; SHBG: Sex Hormone Binding Globulin; SJC: Swollen Joint Count; TJC: Tender Joint Count; TRAP5b: tartrate resistant acid phosphatase isoform 5b; TSH: Thyroid Stimulating Hormone.

### 4.3.2 Changes in bone mineral density

There was a significant decrease in mean neck of femur BMD (mean difference  $-0.017\text{g/cm}^2$ , 95% CI  $-0.030, -0.004$  a decrease of  $-2.0\%$ ;  $p=0.011$ ) and mean total femur BMD (mean difference  $-0.016\text{g/cm}^2$ , 95% CI  $-0.025, -0.007$  a decrease of  $-1.7\%$ ;  $p=0.001$ ) after 12 months but no significant change in lumbar spine or ultra-distal forearm BMD (Table 12). Patients were excluded if they had been treated with anti-osteoporotic medication either during or prior to this study and this has had an impact on the T- and Z-scores which were a lot higher than expected for this RA population. Left and right side femoral neck and total femur were analysed separately and comparable decreases were found; femoral neck (left mean difference  $-0.020\text{g/cm}^2$ , 95% CI  $-0.039, -0.002$   $p=0.031$  and right mean difference  $-0.012\text{g/cm}^2$ , 95% CI  $-0.025, 0.000$   $p=0.059$ ) and total femur (left mean difference  $-0.015\text{g/cm}^2$ , 95% CI  $-0.026, -0.005$   $p=0.005$  and right mean difference  $-0.017\text{g/cm}^2$ , 95% CI  $-0.027, -0.007$   $p=0.001$ ). There was no significant difference between each side for either BMD site (femoral neck  $p=0.336$  and total femur  $p=0.690$ ). Despite the general reduction in BMD at all sites, a small percentage of patients did have an increase in BMD after 12 months; 13 (36%) patients (3 males, 4 pre- and 6 post-menopausal females) had an increase (mean change  $0.037 \pm 0.06\text{g/cm}^2$ ;  $2.9 \pm 3.9\%$ ) in LSBMD; 12 (34%) patients (2 males, 4 pre- and 6 post-menopausal females) had an increase (mean change  $0.016 \pm 0.01\text{g/cm}^2$ ;  $1.8 \pm 1.1\%$ ) in MNBMD; 8 (23%) patients (1 male, 2 pre- and 5 post-menopausal females) had an increase (mean change  $0.015 \pm 0.01\text{g/cm}^2$ ;  $1.7 \pm 1.4\%$ ) in MTBMD; and 10 (31%) patients (3 males, 3 pre- and 4 post-menopausal females) had an increase (mean change  $0.031 \pm 0.04\text{g/cm}^2$ ;  $7.0 \pm 8.3\%$ ) in MRUDBMD at 12 months. Although, these positive changes in BMD were not uniformly seen at every site in these patients.

As menopausal status noticeably affected bone turnover in the pilot study, this data was also examined by gender and menopausal status (Table 12). However, as the study was not powered for sub-group analysis these results were interpreted with caution. Seventy nine percent of the women ( $n=23$ ) were post-menopausal, there was a significant decrease in mean neck of femur (mean difference  $-0.018\text{g/cm}^2$ , 95% CI  $-0.036, -0.000$  a decrease of  $-2.1\%$ ;  $p=0.049$ ) and mean total femur BMD (mean difference  $-0.020\text{g/cm}^2$ , 95% CI  $-0.033, -0.008$  a decrease of  $-2.1\%$ ;  $p=0.003$ ) in these women.

Table 12 Change in bone mineral density from baseline to 12 months

	BMD (g/cm <sup>2</sup> ) - Mean (SD)				T score - Median (IQR)				Z score - Median (IQR)			
	Baseline	12 month	Diff (95% CI)	p value	Baseline	12 month	Diff (95% CI)	p value	Baseline	12 month	Diff (95% CI)	p value
<b>Lumbar spine (L2-4)</b>												
All patient (n=36)	1.171 (0.245)	1.161 (0.250)	-0.010 (-0.029, 0.009)	0.302	-0.40 (-1.2,1.00)	-0.20 (-1.2,0.50)	-0.10 (-0.30, 0.00)	0.075	0.50 (-0.60,1.70)	0.30 (-0.70,1.70)	0.00 (-0.30, 0.10)	0.198
<i>Males (n=7)</i>	1.252 (0.188)	1.251 (0.263)	-0.001 (-0.100, 0.098)	0.984	0.20 (-0.40,1.50)	-0.20 (-0.30,1.2)	-0.30 (-0.77, 1.33)	0.499	0.70 (0.20,1.00)	0.40 (-0.20,0.60)	-0.30 (-0.79, 1.71)	0.399
<i>Pre-menopausal (n=6)</i>	1.223 (0.271)	1.219 (0.261)	-0.004 (-0.041, 0.033)	0.790	-0.45 (-0.7,1.7)	-0.35 (-1.10,1.90)	0.05 (-0.39, 0.20)	0.833	-0.30 (-1.80,1.70)	-0.05 (-2.20,1.90)	0.15 (-0.39, 0.29)	0.917
<i>Post-menopausal (n=23)</i>	1.132 (0.255)	1.118 (0.244)	-0.014 (-0.031, 0.003)	0.103	-0.45 (-1.3,0.6)	-0.60 (-1.30,0.40)	-0.10 (-0.31, 0.00)	0.077	0.60 (-0.60,1.80)	0.55 (-0.70,1.70)	0.00 (-0.31, 0.10)	0.311
<b>Mean neck femur</b>												
All patient (n=35)	0.884 (0.140)	0.867 (0.143)	-0.017 (-0.030, -0.004)	<b>0.011</b>	-0.70 (-1.30,-0.20)	-0.75 (-1.50,-0.50)	-0.15 (-0.30, 0.02)	<b>0.007</b>	0.30 (-0.50,0.70)	0.20 (-0.60,0.80)	-0.10 (-0.20, 0.00)	<b>0.043</b>
<i>Males (n=7)</i>	0.920 (0.134)	0.894 (0.154)	-0.026 (-0.058, 0.006)	0.091	-1.30 (-1.60,-0.30)	-1.50 (-1.90,-0.60)	-0.20 (-0.57, 0.17)	0.149	0.05 (-0.50,0.70)	-0.30 (-0.70,0.80)	-0.20 (-0.58, 0.10)	0.116
<i>Pre-menopausal (n=6)</i>	0.917 (0.111)	0.913 (0.093)	-0.004 (-0.039, 0.031)	0.780	-0.55 (-0.80,-0.20)	-0.70 (-0.80,-0.10)	-0.05 (-0.49, 0.28)	0.463	-0.45 (-1.00,-0.10)	-0.35 (-1.00,0.00)	0.05 (-0.38, 0.38)	0.751
<i>Post-menopausal (n=22)</i>	0.863 (0.150)	0.845 (0.152)	-0.018 (-0.036, -0.000)	<b>0.049</b>	-0.70 (-1.40,-0.20)	-0.80 (-1.50,-0.50)	-0.10 (-0.30, 0.01)	<b>0.021</b>	0.50 (0.20,0.80)	0.30 (-0.20,1.00)	-0.10 (-0.20, 0.00)	0.078
<b>Mean total femur</b>												
All patient (n=35)	0.944 (0.153)	0.928 (0.150)	-0.016 (-0.025, -0.007)	<b>0.001</b>	-0.45 (-1.20,0.20)	-0.60 (-1.30,0.20)	-0.10 (-0.20, 0.00)	<b>0.002</b>	0.20 (-0.50,0.90)	0.00 (-0.60,0.80)	-0.10 (-0.20, 0.00)	<b>0.005</b>
<i>Males (n=7)</i>	0.954 (0.171)	0.945 (0.164)	-0.010 (-0.032, 0.013)	0.333	-1.00 (-1.70,-0.40)	-0.90 (-2.00,-0.50)	-0.10 (-0.27, 0.21)	0.344	0.00 (-0.70,0.40)	0.00 (-0.80,0.50)	-0.15 (-0.20, 0.37)	0.463
<i>Pre-menopausal (n=6)</i>	1.021 (0.126)	1.012 (0.137)	-0.009 (-0.031, 0.014)	0.367	0.15 (-0.70, 0.60)	0.00 (-0.70,0.30)	-0.10 (-0.30, 0.18)	0.281	-0.40 (-0.50,0.40)	-0.40 (-0.70,0.40)	-0.05 (-0.19, 0.28)	0.916
<i>Post-menopausal (n=22)</i>	0.920 (0.154)	0.900 (0.145)	-0.020 (-0.033, -0.008)	<b>0.003</b>	-0.40 (-1.60,0.10)	-0.60 (-1.70,0.20)	-0.10 (-0.25, 0.05)	<b>0.004</b>	0.60 (-0.40,1.00)	0.00 (-0.50,0.90)	-0.20 (-0.25, 0.00)	<b>0.004</b>
<b>Mean UD Radius</b>												
All patient (n=32)	0.382 (0.104)	0.380 (0.114)	-0.002 (-0.013, 0.010)	0.787	-1.10 (-2.3, 0.40)	-1.40 (-2.38, 0.63)	-0.10 (-0.33, 0.05)	0.167	-0.50 (-1.20, 0.90)	-0.65 (-1.20, 1.05)	-0.05 (-0.29, 0.09)	0.416
<i>Males (n=7)</i>	0.444 (0.111)	0.456 (0.135)	0.012 (-0.042, 0.066)	0.597	0.20 (-2.60, 2.00)	1.80 (-3.75, 2.15)	-0.10 (-0.88, 2.34)	1.000	1.33 (-1.10, 2.40)	2.13 (-1.20, 3.35)	0.03 (-1.07, 2.89)	0.753
<i>Pre-menopausal (n=6)</i>	0.389 (0.066)	0.393 (0.084)	0.004 (-0.021, 0.030)	0.679	-0.30 (-1.70, 0.60)	-0.33 (-1.80, 0.70)	0.00 (-0.49, 0.35)	0.753	-0.30 (-1.70, 0.90)	-0.33 (-1.80, 1.00)	0.00 (-0.49, 0.39)	0.753
<i>Post-menopausal (n=19)</i>	0.357 (0.105)	0.348 (0.105)	-0.009 (-0.018, 0.001)	0.070	-1.70 (-2.60, -0.70)	-1.65 (-2.40, -0.70)	-0.10 (-0.51, 0.00)	0.067	-0.60 (-1.20, 0.30)	-0.95 (-1.10, 0.60)	-0.05 (-0.49, 0.04)	0.190



Bone mineral density (BMD) was measured in lumbar spine (n=36) mean L2-L4. Also neck of femur (n=35), total femur (n=35) and ultra-distal radius (n=31), the results were reported as mean of both sides. All measured at time 0 before the 1st RTX infusion and after 12 months in patients who completed the study. Results were expressed as mean and standard deviation at baseline and 12 months and mean percentage change from baseline, the mean change from baseline was calculated by paired t-test. T and Z scores for each site were not normally distributed so results were expressed as medians and interquartile range, the median change from baseline was calculated using Wilcoxon signed rank test. Results were also stratified by gender and menopausal status.

### 4.3.3 Changes in biomarker levels

Changes in median biomarker concentration from baseline i.e. before the start of the RTX treatment, to the 12 month visit are shown in Table 13. Additionally, as the markers were measured every 3 months, the median percentage change from baseline across all 4 visits was calculated to estimate the average change over 12 months. There was a significant increase in bone formation over 12 months; PINP (mean change 11.2 $\mu$ g/L; 95% CI -0.4, 22.8;  $p=0.05$ ; 30% increase) and BALP (mean change 3.4 $\mu$ g/L; 95% CI 1.1, 5.8;  $p=0.006$ ; 13% increase). These results were mirrored by a significant reduction in inflammation; CRP (mean change -12.4mg/L; 95% CI -21.1, -3.7;  $p=0.007$ ; 21% decrease), ESR (mean change -15mm/hr; 95% CI -24, -5;  $p=0.003$ ; 20% decrease) and disease activity DAS28-CRP (mean change -1.14; 95% CI -1.70, -0.58;  $p<0.001$ ; 19% decrease) following treatment with RTX. There was no significant change in bone resorption or osteocyte markers. Additionally, the data was reviewed by gender and menopausal status; there was no significant difference in BTMs between men and pre-menopausal women and so they were combined. Post-menopausal women ( $n=23$ ) had higher bone resorption at 12 months, but no difference in bone formation or osteocyte markers compared to the males and pre-menopausal women ( $n=13$ ).

There was a wide variance in the changes in biomarker levels, but generally there was a gradual increase in bone formation markers (PINP, BALP) in a similar pattern to the pilot cohort. However, median  $\beta$ CTX levels decreased to 3 months then gradually returned to baseline values (Figure 19). There was a gradual decrease in median inflammatory markers and disease activity levels (Figure 20).

Furthermore, a marker of formation (PINP) and a marker of resorption ( $\beta$ CTX) were expressed as multiples of the median  $MoM_F$  and  $MoM_R$  respectively (described in Chapter 2 section 2.2.1), (Bieglmayer and Kudlacek 2009) and their ratios ( $MoM_F/MoM_R$ ) plotted at baseline and then every 3 months until the 12 month follow-up visit, to show the effect of treatment on bone turnover (Figure 21). At baseline 25 (83%) patients had a bone turnover ratio  $<1$  (i.e. resorption predominated); at 3 months 21 (70%); at 6 months 23 (77%); at 9 months 24 (80%) and at 12 months 23 (77%) such patients still had ratios  $<1$ . However, 17 (57%) patients (7 patients had ratios  $>1$  but 10 patients still had ratios  $<1$ ) had a small increase in their bone turnover ratio from baseline to 12 months, indicating some albeit minimal improvement in bone turnover.

#### **4.3.4 Correlations between inflammatory activity and bone density or bone turnover**

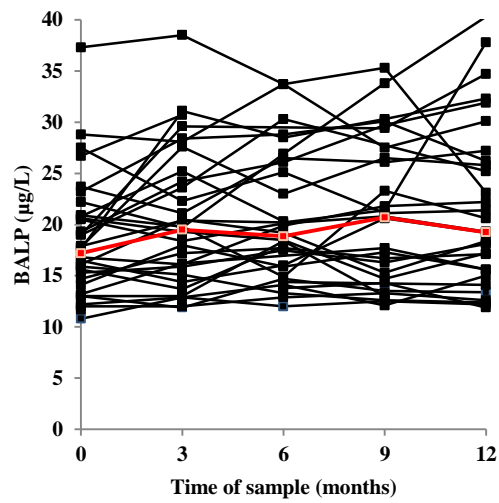
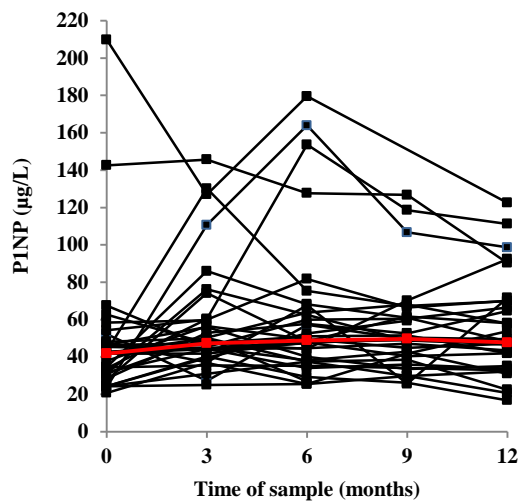
There was a significant positive correlation between median percentage change in ESR and percentage change in mean neck of femur BMD ( $R_s=0.384$ ;  $p=0.030$ ) also between median percentage change in CRP and percentage change in mean neck of femur BMD ( $R_s=0.349$ ;  $p=0.040$ ). Additionally, there was a significant positive correlation between median percentage change in CRP and median percentage change in DKK-1 ( $R_s=0.409$ ;  $p=0.013$ ) and between median percentage change in DAS28 and median percentage change in DKK-1 ( $R_s=0.373$ ;  $p=0.025$ ).

**Table 13 Change in biomarkers from baseline to twelve months**

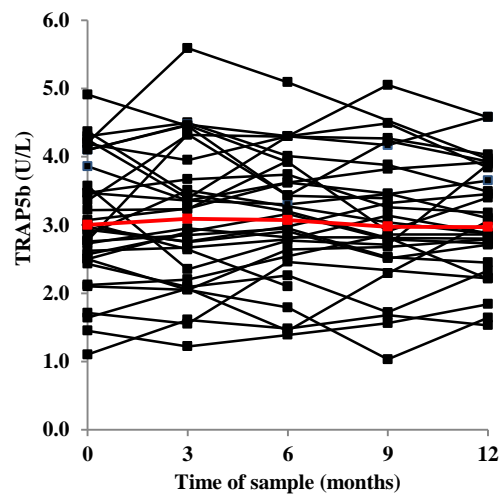
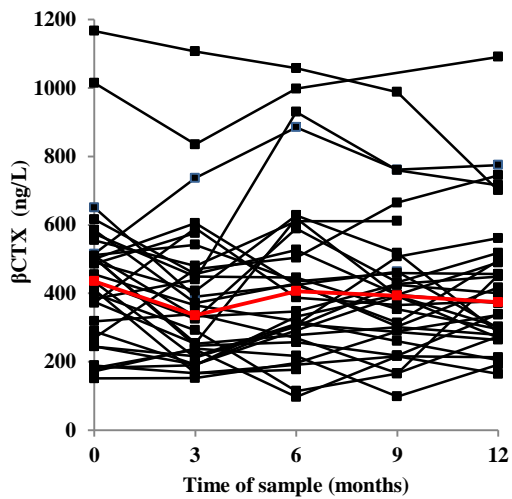
	Baseline	12 Month	Difference (95% CI)	p value	Median % change over 12 month (95% CI)
<b>βCTX (ng/L)</b>					
All patient (n=34)	417 (245, 509)	384 (279, 518)	4 (-72, 80)	0.916	-8 (-23, 15)
<i>Males + Pre-menopausal (n=12)</i>	267 (177, 428)	275 (199, 318)	-33 (-154, 88)	0.562	-6 (-36, 83)
<i>Post-menopausal (n=22)</i>	489 (372, 512)	455 (371, 651)	24 (-78, 127)	0.630	-8 (-23, 27)
<b>TRAP5b (U/L)</b>					
All patient (n=34)	3.0 (2.5, 4.0)	2.9 (2.7, 3.8)	0.0 (-0.2, 0.3)	0.835	0 (-7, 8)
<i>Males + Pre-menopausal (n=12)</i>	2.6 (1.9, 3.7)	2.7 (2.2, 3.3)	0.0 (-0.4, 0.4)	1.000	-0 (-10.6, 22.1)
<i>Post-menopausal (n=22)</i>	3.2 (2.6, 4.1)	3.2 (2.8, 3.9)	0.0 (-0.3, 0.3)	0.804	3.5 (-7.4, 8.0)
<b>PINP (µg/L)</b>					
All patient (n=34)	39.8 (30.9, 46.4)	48.8 (37.8, 70.0)	11.2 (-0.4, 22.8)	<b>0.05</b>	30 (3, 50)
<i>Males + Pre-menopausal (n=12)</i>	35.2 (25.9, 45.1)	46.8 (35.4, 62.3)	15.8 (-1.9, 33.4)	0.076	11.4 (-11.8, 97.6)
<i>Post-menopausal (n=22)</i>	42.0 (31.8, 46.4)	53.6 (41.9, 71.5)	8.7 (-7.4, 24.8)	0.273	32.2 (2.6, 88.1)
<b>BALP (µg/L)</b>					
All patient (n=34)	17.2 (14.1, 20.6)	19.3 (15.6, 26.2)	3.4 (1.1, 5.8)	<b>0.006</b>	13 (4, 19)
<i>Males + Pre-menopausal (n=12)</i>	15.5 (13.1, 17.8)	17.6 (13.5, 19.9)	3.1 (0.3, 5.9)	<b>0.035</b>	10.8 (-5.1, 17.7)
<i>Post-menopausal (n=22)</i>	18.5 (15.9, 23.2)	22.7 (17.2, 27.5)	3.6 (0.1, 7.0)	<b>0.044</b>	14.0 (0.7, 32.3)
<b>SCL (pmol/L)</b>					
All patient (n=34)	53.4 (40.5, 64.4)	55.7 (46.5, 67.6)	4.4 (-0.9, 9.7)	0.100	0.1 (-3, 8)
<i>Males + Pre-menopausal (n=12)</i>	62.6 (44.5, 73.3)	64.5 (51.2, 73.6)	4.6 (-4.7, 13.9)	0.300	-1.1 (-17.1, 15.6)
<i>Post-menopausal (n=22)</i>	52.5 (38.7, 61.1)	54.3 (46.0, 62.5)	4.3 (-2.7, 11.2)	0.217	1.3 (-3.8, 11.7)
<b>DKK-1 (pmol/L)</b>					
All patient (n=34)	47.9 (35.6, 68.6)	51.5 (32.9, 72.8)	2.6 (-4.7, 9.9)	0.479	-2 (-10, 14)
<i>Males + Pre-menopausal (n=12)</i>	44.7 (34.6, 52.2)	44.7 (30.9, 57.6)	1.0 (-7.6, 9.6)	0.803	-13.9 (-23.7, 44.7)
<i>Post-menopausal (n=22)</i>	53.2 (37.9, 77.6)	60.8 (39.8, 90.1)	3.4 (-7.3, 14.2)	0.515	-0.6 (-6.6, 23.8)
<b>CRP (mg/L)</b>					
All patient (n=36)	11.7 (2.8, 38.8)	6.4 (2.5, 14.1)	-12.4 (-21.1, -3.7)	<b>0.007</b>	-21 (-49, 75)
<i>Males + Pre-menopausal (n=13)</i>	14.1 (6.3, 38.1)	4.2 (2.4, 13.0)	-16.0 (-36.4, 4.4)	0.113	-42 (-72, 377)
<i>Post-menopausal (n=23)</i>	7.2 (2.1, 46.7)	7.0 (2.6, 14.7)	-10.4 (-19.3, -1.5)	<b>0.024</b>	-10 (-47, 87)
<b>ESR (mm/hr)</b>					
All patient (n=32)	32 (11, 43)	17 (9, 33)	-15 (-24, -5)	<b>0.003</b>	-20 (-50, 25)
<i>Males + Pre-menopausal (n=11)</i>	39 (28, 62)	13 (6, 33)	-25 (-48, -2)	<b>0.038</b>	-40 (-64, 52)
<i>Post-menopausal (n=21)</i>	30 (10, 39)	19 (11, 27)	-9 (-17, -1)	<b>0.032</b>	-6 (-42, 52)
<b>DAS28 score</b>					
All patient (n=36)	5.62 (1.33)	4.47 (1.44)	-1.14 (-1.70, -0.58)	<b>&lt;0.001</b>	19 (-27, -14)
<i>Males + Pre-menopausal (n=13)</i>	5.67 (1.13)	4.48 (1.33)	-1.19 (-2.26, -0.12)	<b>0.032</b>	-27 (-39, -8)
<i>Post-menopausal (n=23)</i>	5.59 (1.46)	4.48 (1.53)	-1.12 (-1.82, -0.42)	<b>0.003</b>	-17 (-23, -12)

Biomarkers were measured at baseline before the RTX infusion and then at 3, 6, 9 and 12 months in all patients who completed the study. Baseline, 12 months and percent change biomarker data were not normally distributed and were expressed as median and IQR, the median percentage change from baseline across all 4 visits was calculated. Baseline and 12 months DAS28 and all absolute change results were normally distributed and were expressed as means. P values were recorded between baseline and 12 months for all parameters using paired t-tests; p values ≤0.05 were considered significant. Results were also stratified by post-menopausal females and combined males plus pre-menopausal females. BALP: bone specific alkaline phosphatase; βCTX: β-isomerised carboxy terminal telopeptide of type I collagen; DKK-1: dickkopf-related protein 1; ESR: erythrocyte sedimentation rate; DAS28: disease activity score using 28 tender and swollen joints; CRP: high sensitivity -C reactive protein; PINP: procollagen type 1 amino-terminal propeptide; SCL: sclerostin; TRAP5b: tartrate resistant acid phosphatase isoform 5b.

*Bone Formation*



*Bone Resorption*



*Osteocyte markers*

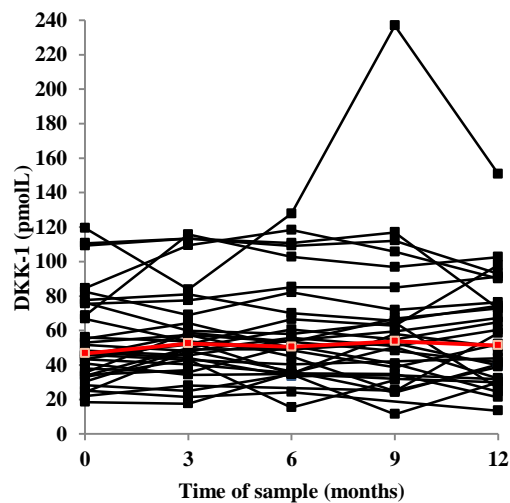
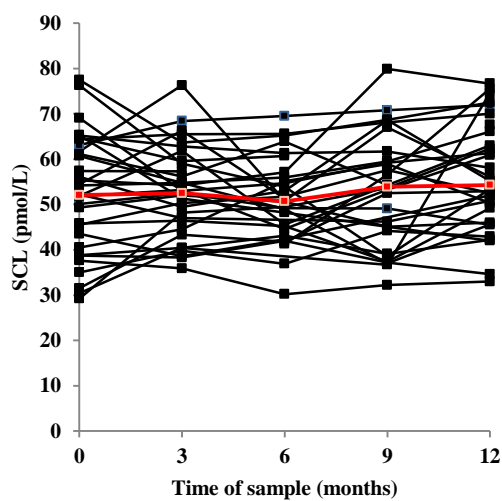
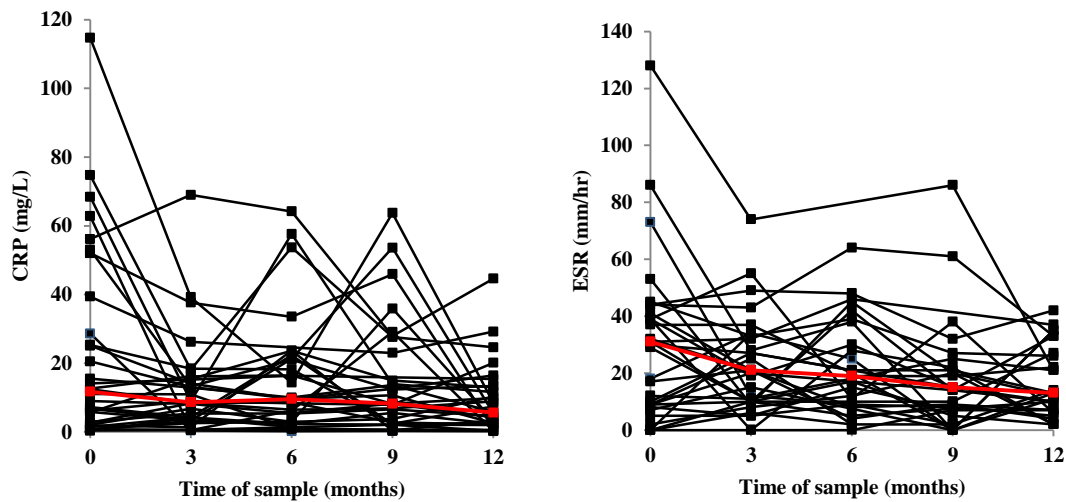
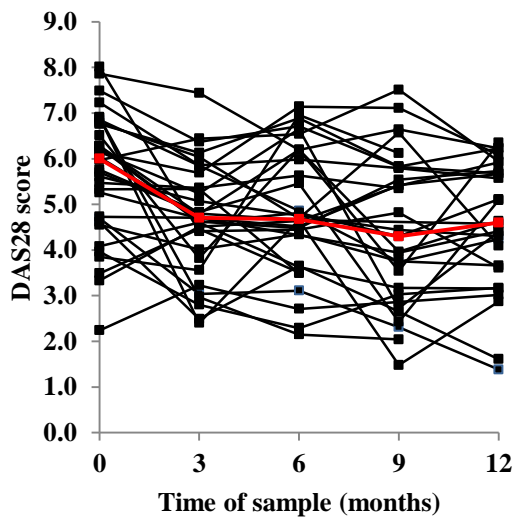


Figure 19 Change in individual bone markers over the course of the study

*Inflammatory markers**Disease activity*

**Figure 20** Change in individual inflammatory markers over the course of the study

Individual patient results for markers of bone resorption, bone formation, osteocytes, inflammation and disease activity were plotted at baseline before the RTX infusion and then at 3, 6, 9 and 12 months in all patients who completed the study.

BALP: bone specific alkaline phosphatase;  $\beta$ CTX:  $\beta$ -isomerised carboxy terminal telopeptide of type I collagen; DKK-1: dickkopf-related protein 1; ESR: erythrocyte sedimentation rate; DAS28: disease activity score using 28 tender and swollen joints; CRP: high sensitivity -C reactive protein; PINP: procollagen type 1 amino-terminal propeptide; SCL: sclerostin; TRAP5b: tartrate resistant acid phosphatase isoform 5b.

— Indicates the median biomarker results

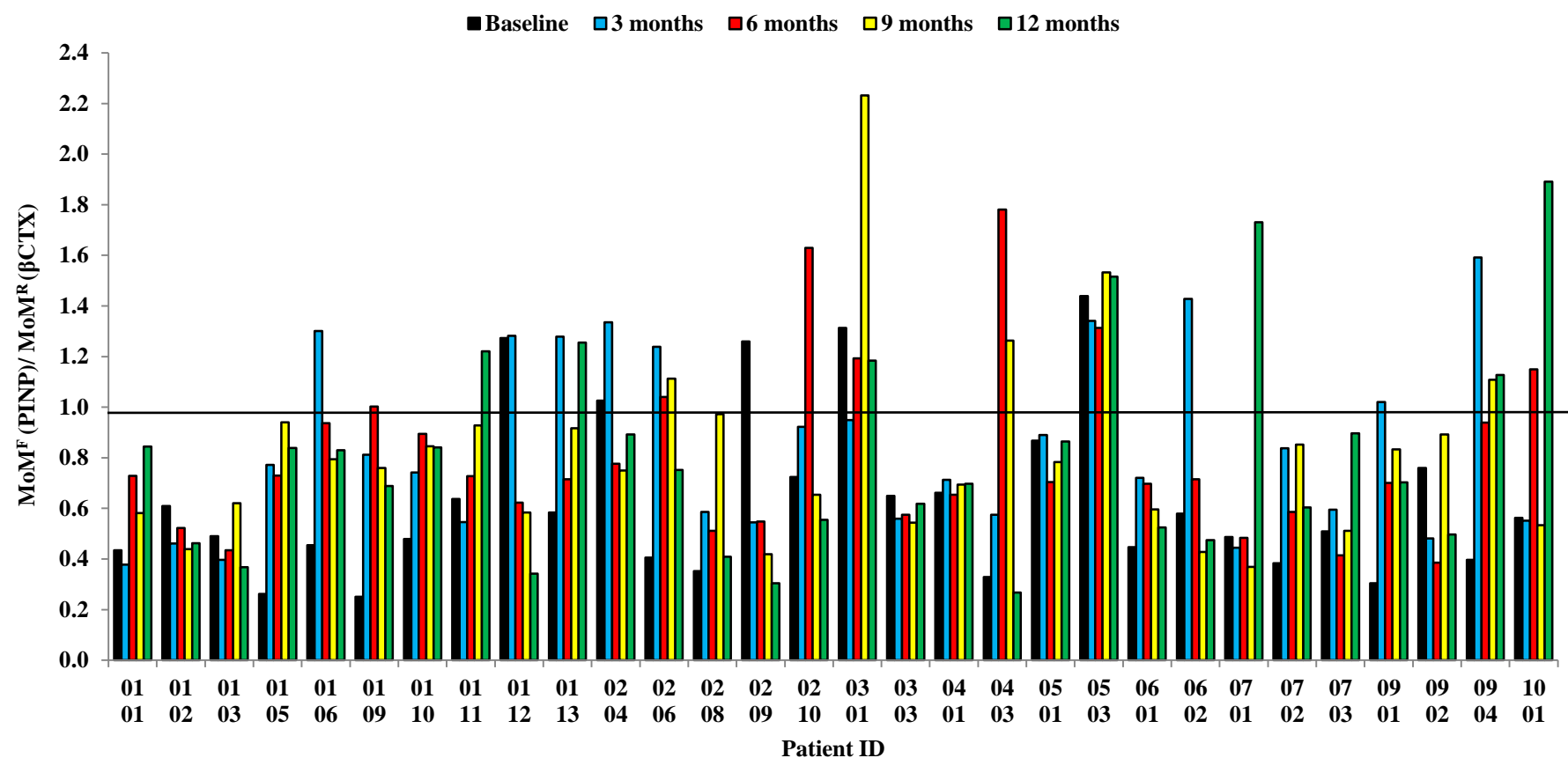


**Figure 21 Ratio of bone marker multiples of the median depicting bone turnover in thirty rheumatoid arthritis patients pre and 3, 6, 9 and 12 months post rituximab**

Blood samples from 72 healthy volunteers (33 males aged 19 to 62yrs and 39 females aged 20 to 64yrs) were analysed on the Elecsys 2010, for  $\beta$ CTX and PINP to calculate the median of the reference population. Multiples of the median (MoM) were defined as 'individual marker result/ median of the reference population' (Bieglmayer and Kudlacek 2009). Individual  $\beta$ CTX and PINP results from this prospective study looking at 30 patients with refractory RA analysed pre and post RTX, were expressed as ratios of their multiples of the median (MoM<sub>F</sub>/ MoM<sub>R</sub>) at each visit.

### 4.3.5 *The effects of vitamin D*

Fourteen (39%) patients (2 males; 2 pre- and 10 post-menopausal females) in this cohort had 25OHD levels below 25nmol/L. There was no significant difference ( $p=0.274$ ) in median 25OHD between males (69nmol/L), pre- (36nmol/L) or post-menopausal females (30nmol/L) at baseline. However, there was a significant difference ( $p=0.001$ ) in median PTH levels (males 19.8; pre- 39.6 and post-menopausal females 33.0ng/L). Total 25OHD was measured due to its effects on disease activity and its critical role in the maintenance of bone health, 25OHD levels could affect the primary and secondary endpoints and so results were stratified by 25OHD concentration; group 1 ( $n=14$ ) included levels below 25nmol/L; group 2 ( $n=22$ ) equal to or greater than 25nmol/L.

The differences between vitamin D group for BMD, BTM and inflammatory biomarkers are included in Table 14. Additionally, there was no significant difference in age, PTH, eGFR, weight, height or BMI at baseline, or HAQ, VAS, tender and swollen joint count at baseline and 12 months between these vitamin D groups.

#### Bone Mineral Density

Vitamin D deficient patients had significantly lower LS BMD at baseline (Group 1: mean 1.048, 95% CI 0.940, 1.156g/cm<sup>2</sup>; Group 2: mean 1.249, 95% CI 1.138, 1.360g/cm<sup>2</sup>;  $p=0.014$ ), but no significant difference in baseline BMD at the femoral neck ( $p=0.272$ ), total femur ( $p=0.174$ ) or forearm ( $p=0.074$ ). However, vitamin D deficient patients had a significantly greater loss ( $p=0.016$ ) of mean neck of femur BMD from baseline to 12 months (mean change -0.036, 95% CI -0.064, -0.007g/cm<sup>2</sup>  $p=0.017$ , a decrease of -4.1%) compared to patients with 25OHD  $\geq 25$  nmol/L (mean change -0.005, 95% CI -0.014, 0.005g/cm<sup>2</sup>  $p=0.314$ , a decrease of -0.6%). Additionally they had a significantly greater loss ( $p=0.015$ ) of mean total femur BMD from baseline to 12 months, (25OHD  $< 25$ nmol/L: mean change -0.029, 95% CI -0.047, -0.010g/cm<sup>2</sup>  $p=0.005$  a decrease of -3.0%; compared to 25OHD  $\geq 25$ nmol/L: -0.008, 95% CI -0.016, 0.000g/cm<sup>2</sup>  $p=0.063$ , a decrease of -0.8%). There was no significant difference in the bone lost at the LS ( $p=0.496$ ) or UD forearm ( $p=0.318$ ) between the two categories (Table 14).

#### Inflammation and disease activity

There was no significant difference in CRP, ESR or DAS28 score between vitamin D groups over 12 months.



Bone turnover markers

There was a significant difference ( $p=0.002$ ) between 25OHD groups in TRAP5b (Group 1: mean change 0.4, 95% CI 0.1, 0.8U/L,  $p=0.011$ , 12.3% increase; Group 2: mean change -0.3, 95% CI -0.5, 0.0U/L,  $p=0.041$ , a -8.6% decrease) from baseline to 12 months. A similar disparity was found in  $\beta$ CTX at several time points; specifically from baseline to 6 months ( $p=0.006$ ); (Group 1: mean change 129, 95% CI 3, 256ng/L, 27% increase; Group 2: mean change -67, 95% CI -135, 1ng/L, a -20% decrease), but there was no significant difference between baseline and 12 months ( $p=0.115$ ). Additionally, there was no significant difference between vitamin D groups for bone formation or osteocyte markers (Table 14).

**Table 14 Change in bone mineral density and biomarkers by vitamin D category from baseline to 12 months**

	Group 1: 25OHD (<25 nmol/L) n=14					Group 2: 25OHD (≥25 nmol/L) n=22					Between group p value (%change)
	Baseline	12 month	Difference (95% CI)	% change	p value Difference	Baseline	12 month	Difference (95% CI)	% change	p value Difference	
Lumbar spine (g/cm <sup>2</sup> )	1.048 (0.187)	1.052 (0.245)	0.004 (-0.040, 0.048)	-0.2 (6.1)	0.845	1.249 (0.250)	1.230 (0.232)	- 0.019 (-0.036, -0.002)	-1.3 (2.8)	<b>0.031</b>	0.496
Mean neck of femur (g/cm <sup>2</sup> )	0.851 (0.160)	0.816 (0.153)	-0.036 (-0.064, -0.007)	-4.1 (5.6)	<b>0.017</b>	0.905 (0.124)	0.900 (0.129)	-0.005 (-0.014, 0.005)	-0.6 (2.4)	0.314	<b>0.016</b>
Mean total femur (g/cm <sup>2</sup> )	0.901 (0.163)	0.872 (0.148)	-0.029 (-0.047, -0.010)	-3.0 (3.2)	<b>0.005</b>	0.973 (0.143)	0.965 (0.142)	-0.008 (-0.016, 0.000)	-0.8 (1.8)	0.063	<b>0.015</b>
Mean UD radius (g/cm <sup>2</sup> )	0.344 (0.072)	0.336 (0.079)	-0.008 (-0.021, 0.006)	-2.4 (5.7)	0.231	0.411 (0.116)	0.414 (0.128)	0.003 (-0.016, 0.022)	0.3 (9.0)	0.763	0.373
βCTX (ng/L)	304 (244,491)	410 (274,626)	95 (-44, 234)	18.5 (-14,169)	0.166	446 (375,555)	384 (287,476)	-60 (-143, 24)	-5.0 (-31,12.5)	0.151	0.115
TRAP5b (U/L)	2.6 (2.1,3.5)	3.0 (2.8,4.0)	0.4 (0.1, 0.8)	12.3 (9.0,31.5)	<b>0.011</b>	3.1 (2.8,4.1)	2.9 (2.6,3.5)	-0.3 (-0.5, 0.0)	-8.6 (-18.0,5.1)	<b>0.041</b>	<b>0.002</b>
PINP (µg/L)	38.3 (33.4,46.4)	47.2 (37.8,70.0)	14.6 (0.2, 28.9)	25.9 (0.0,79.0)	<b>0.047</b>	39.8 (27.5,47.3)	55.8 (38.6,70.8)	8.9 (-9.2, 26.9)	12.7 (-23.8,99.2)	0.317	0.713
BALP (µg/L)	19.2 (15.9,22.2)	27.4 (17.2,32.3)	6.5 (2.0, 11.0)	23.1 (1.7,81.5)	<b>0.009</b>	16.0 (13.2,19.7)	18.2 (15.3,22.7)	1.2 (-1.1, 3.6)	15.3 (4.1,25.2)	0.280	0.310
SCL (pmol/L)	51.8 (40.5,57.4)	56.7 (50.3,74.6)	7.9 (-2.8, 18.7)	15.6 (-10.9,34.4)	0.135	53.5 (45.5,64.4)	54.5 (45.6,65.3)	1.9 (-3.7, 7.5)	3.8 (-9.2,14.7)	0.487	0.421
DKK-1 (pmol/L)	53.2 (37.9,82.6)	59.8 (41.6,76.3)	2.1 (-9.2, 13.5)	14.8 (-14.8,28.9)	0.693	46.4 (33.2,64.2)	49.2 (32.0,66.1)	2.9 (-7.5, 13.3)	2.0 (-25.1,35.4)	0.569	1.000
CRP (mg/L)	17.3 (6.7,46.7)	11.0 (2.6,15.4)	-14.9 (-27.1, -2.7)	-61 (-74.7,9.2)	<b>0.020</b>	7.6 (1.9,28.6)	5.6 (2.2,9.8)	-10.8 (-23.5, 1.9)	-18 (-67.1,69.0)	0.091	0.364
ESR (mm/hr)	31.0 (28.0,41.0)	21.5 (10.0,33.0)	-21 (-41, -2)	-46.3 (-77.4,17.9)	<b>0.037</b>	31.5 (9.0,41.5)	13.0 (7.0,33.0)	-10 (-19, -1)	-5.4 (-66.7,11.1)	<b>0.034</b>	0.443
DAS28 score	5.58 (1.61)	4.66 (1.53)	-0.92 (-1.81, -0.03)	-18.7 (-24.2,-3.2)	<b>0.043</b>	5.65 (1.17)	4.36 (1.41)	-1.28 (-2.05, -0.51)	-18.9 (-38.1,-1.00)	<b>0.002</b>	0.770

Results were stratified by 25OHD status; Group 1 levels up to 24.9 nmol/L; Group 2 levels greater than or equal to 25 nmol/L. Bone mineral density, expressed as mean and standard deviation, was measured in the lumbar spine (mean L2-L4), femoral neck, total femur and UD radius (reported as the mean of both sides), at baseline before the first RTX infusion and after 12 months in all patients who completed the study (n=36). A second RTX cycle was given at 6 months if clinically indicated (n=32). Blood samples taken at baseline and at 12 months were analysed for the following biomarkers: BALP: bone specific alkaline phosphatase; βCTX: β-isomerised carboxy terminal telopeptide

of type I collagen; DKK-1: dickkopf-related protein 1; ESR: erythrocyte sedimentation rate; DAS28: disease activity score using 28 tender and swollen joints ; CRP: high sensitivity -C reactive protein; PINP: procollagen type 1 amino-terminal propeptide; SCL: sclerostin; TRAP5b: tartrate resistant acid phosphatase isoform 5b.

Baseline, 12 months and percent change data for  $\beta$ CTX, TRAP5b, PINP, BALP, SCL, DKK-1, CRP and ESR were not normally distributed therefore results were expressed as medians and interquartile ranges. Baseline and 12 months DAS28 and all absolute change results were normally distributed and were expressed as means. P values were recorded between baseline and 12 months within each group using paired t-tests; p values  $\leq 0.05$  were considered significant. The difference in percentage change from baseline to 12 months for each vitamin D group was compared using a two-sample t-test (for BMD) or Mann-Whitney test (biomarkers).

#### 4.4 Discussion

The aim of this study was to investigate the effects of B cell depletion with RTX on bone density and bone turnover in patients with severe, refractory RA, to confirm and extend the results of the pilot study discussed in the previous Chapter. There was a significant decrease in BMD at the femoral neck (-2%) and total femur (-1.7%) after 12 months, but no significant change in BMD at the lumbar spine or ultra-distal forearm.

There was a significant increase in bone formation in both PINP and BALP biomarkers over 12 months, but no significant change in bone resorption or osteocyte markers. Nevertheless, there was a significant reduction in inflammatory markers and disease activity following treatment with RTX, indicating that the drug was effective in reducing the inflammation of RA in this patient cohort.

Post-menopausal females also had a significant decrease in mean neck (-2.1%) and mean total femur BMD (-2.1%) after 12 months. Additionally, post-menopausal women had the highest levels of bone turnover, specifically  $\beta$ CTX, at baseline and throughout the 12 months, consistent with the results of the pilot study and reflecting the fact that bone loss is more rapid post-menopause (Garnero et al. 2000). Thirty-nine percent of patients in this study (29% males; 33% pre- and 43% post-menopausal females) were classed as vitamin D deficient i.e. 25OHD below 25nmol/L and these patients had significantly lower lumbar spine BMD at baseline compared to patients with 25OHD above 25nmol/L. Furthermore, they had a significantly greater fall in mean femoral neck and total femur BMD after 12 months. Moreover, vitamin D deficient patients had an increase in bone resorption, measured by TRAP5b, whereas patients with higher vitamin D levels had a reduction in TRAP5b. These results are in keeping with a recent Chinese study which reported that serum 25OHD levels in 130 RA patients (95 women and 35 men), were lower in those with osteopenia and osteoporosis than in those with normal BMD (Hong et al. 2014). Vitamin D influences bone quality and is important in maintaining bone density, it has been reported that higher serum 25OHD levels may prevent the occurrence of osteoporosis at the femoral neck, but not at the lumbar spine L2–4 (Yoshimura et al. 2015). However, the precise definition of the vitamin D sufficiency range remains to be established and the methodology and definition of vitamin D deficiency varies widely between studies, many quoting a cut-off value as high as 50nmol/L. While post-menopausal women had the lowest 25OHD concentration in our cohort, there was no significant difference in median levels between males, pre- or post-menopausal women, so vitamin D deficiency may not explain why the post-menopausal women lost BMD more than pre-menopausal women or men.

This is the first longitudinal study investigating the effects of RTX on BMD and bone turnover markers. The effects of TNF inhibitors on bone have typically shown that anti-TNF therapy has a beneficial effect on BMD and BTMs (Barnabe and Hanley 2008). However, results vary by study with regard to the magnitude of the observed change and the time points of the DXA scanning, also on the number and gender of patients included and the concomitant use of prednisolone and/or anti-osteoporotic drugs. A study investigating the effect of RTX on 13 patients with active RA reported a significant decrease in bone resorption after 15 months, but no significant change in markers of bone formation (Hein et al. 2010). Results of the pilot study (Chapter 4) confirmed and extended these results, there was a statistically significant decrease in  $\beta$ CTX mirrored by a reduction in disease activity and a small but statistically significant increase in PINP, in a cohort of 46 RA patients 6 months after a single treatment course of RTX (Wheater et al. 2011), though no BMD data was available and vitamin D levels were not measured. Patients in that cohort had lower bone resorption at baseline compared to patients in this prospective study. However, thirty-seven percent of those patients were taking bisphosphonates and bisphosphonates induce osteoclast apoptosis (Breuil 2006), none of the patients in the current cohort were treated for osteoporosis with bisphosphonates, calcitonin, strontium ranelate, denosumab or teriparatide prior to/ or during the study. The present cohort also contained a higher percentage of postmenopausal females (79% compared to 58% in the pilot) and notably a higher percentage of these women were current smokers (39% compared to 18% in the pilot), above the national average quoted as 19% in 2013 (Office for National Statistics 2013). Smoking may adversely influence the severity of RA (Saag et al. 1997) and RA patients who smoke have a higher need for DMARDs and are reportedly more likely to show a poor response to biologics treatment such as TNF inhibitors (Mattey et al. 2009). Tobacco also increases bone resorption and affects bone mass by alterations in sex hormone metabolism, but also importantly by alterations on the vitamin D-PTH axis (Supervia et al. 2006).

There are still limitations that have not been addressed in this study; the numbers of participants remained relatively small, this limited the power to detect smaller changes in variables such as bone turnover that may have been significant and although all the patients had high disease activity and fulfilled the criteria for treatment with RTX the group was heterogeneous, consisting of men, pre and postmenopausal women and different age groups. Additionally, this study was designed as a single treatment arm trial with no control group, whereas, the optimal design would have been a double-blind randomized comparison with placebo. However, as RTX is an approved treatment for refractory RA and is already known

to reduce disease activity (Teng et al. 2007), such a control arm would have had to be matched for disease activity and it would have been unethical to have an untreated arm with that level of active disease. Patients with active RA would have been expected to have continued bone loss and abnormal bone turnover until the disease activity had been adequately suppressed (Marotte et al. 2007). It is therefore possible that the RTX could have slowed the bone loss that was occurring, but this study would be unable to detect this without a control arm. The duration of the study was also short at only 12 months and it is possible that; a longer evaluation and follow-up of patients after subsequent treatment courses may have shown improvements in BMD and bone turnover. Larger, long-term studies of more clearly defined patient groups are warranted; additionally vitamin D deficiency should be corrected first.

#### **4.5 Conclusion**

The present study revealed that in a cohort of RA patients treated with RTX, BMD fell at the hip sites in postmenopausal women, but was maintained at the lumbar spine and UD radius forearm. The results suggest that treatment with RTX may have slowed down the expected bone loss in these patients and this could be mediated by reduced disease activity or by the reduction of B cells influencing bone cell activity. However, this was hard to quantify without a control group. Men and premenopausal women did not lose BMD and also had lower bone resorption indicating they had lower bone cell activity. Thirty-nine percent of patients had vitamin D deficiency ( $<25\text{nmol/L}$ ), they had significant falls in hip BMD and evidence of higher bone turnover in comparison to patients with vitamin D levels  $\geq 25\text{nmol/L}$ . These data demonstrate that vitamin D deficiency is common in RA patients and contributes to a decrease in BMD. There was an increase in bone formation with RTX as measured with markers of bone turnover, but this did not correspond to an improvement in BMD suggesting a more complex interaction with bone. In conclusion RTX may have had effects on BMD, but this seemed to be influenced by gender, menopausal status, changes in disease activity and vitamin D status and could be confounded by the requirement for prednisolone. A larger study powered to take into account all these factors is required and this will necessitate that vitamin D insufficiency or deficiency be corrected from the start.

## **Chapter 5**

### ***In vitro* osteoclastogenesis**





## Chapter 5. *In vitro* osteoclastogenesis

### 5.1 Introduction

Inflammation and bone resorption are often linked, this is apparent in the joint destruction seen in diseases such as RA where the bone compartment in closest proximity to the inflamed joint suffers the most severe damage (Schett 2006). B cells have a role in both the pathogenesis of RA and the regulation of bone cell activity. A complex relationship exists between B cells and osteoclasts, although the exact nature of this association is still evolving. Osteoclasts are the bone cells solely responsible for breaking down and resorbing the bone matrix, they are end-differentiated multinucleated cells of the myeloid lineage originating from HSC's (Figure 1) and their differentiation pathway is common to that of macrophages and dendritic cells (Väänänen 2000). B cells on the other hand are responsible for the generation and production of immunoglobulins and together with T cells encompass the adaptive immune system (Horowitz et al. 2010). B cells, like osteoclasts, differentiate from HSC's (Figure 1) but from the lymphoid progenitor cells.

Historically murine studies used co-cultures of bone marrow, spleen and stromal cells to yield multinuclear osteoclast-like cells from the fusion of mononuclear precursors (Takahashi et al. 1988); it was thought that close contact between these cells was essential for osteoclastogenesis (Fujikawa et al. 1996). The majority of these systems relied on endogenous stimulators of osteoclastogenesis such as 1, 25(OH)<sub>2</sub>D<sub>3</sub> and PTH via their action on osteoblastic cells. However, it is now recognised that osteoclast formation and activation is critically dependent on two membrane-bound proteins produced by the osteoblasts and stromal cells; M-CSF and RANKL (Datta et al. 2008), that are both essential and sufficient to provide the necessary signals enabling promyeloid precursor cells to differentiate into mature osteoclasts (Figure 7). Moreover, one murine monocytic cell line, RAW 264.7, has been widely used; it only requires stimulation with RANKL to form fully-differentiated osteoclasts as RAW cells already express M-CSF (Collin-Osgdoby et al. 2003).

M-CSF, acting through its receptor c-Fms, stimulates the proliferation and prevents the apoptosis of early osteoclast precursors and RANKL targets specialized osteoclast differentiation specifically in the bone marrow milieu (Datta et al. 2008). RANKL binds and activates its cellular receptor RANK thereby inducing a signalling cascade leading to the differentiation and fusion of osteoclast precursor cells. Multi-nucleation of osteoclasts being essential as mono-nucleated macrophages cannot resorb bone efficiently; the multi-nucleated osteoclasts are formed from this fusion of RANK with mononuclear precursors after contact with RANKL (Yavropoulou and Yovos 2008). The effects of RANKL can be

counterbalanced by OPG, a soluble decoy receptor which binds and neutralises RANKL, thus inhibiting osteoclastogenesis and inducing osteoclast apoptosis (Blair and Zaidi 2006). The production of RANKL and OPG by osteoblasts is influenced by hormones (PTH, oestrogen, glucocorticoids); growth factors (BMP, IGF1, TGF $\beta$ ) and cytokines (TNF- $\alpha$ , IL-1, IL-6, IL-17) and the balance between RANKL and OPG can therefore determine the degree of osteoclastic bone resorption (Geusens 2012). Mature B cells also have the capacity to both inhibit and stimulate osteoclastogenesis by virtue of their ability to secrete these cytokines. B cells produce pro-osteoclastogenic cytokines including RANKL (Choi et al. 2001, Manabe et al. 2001) and under pathologic conditions such as RA this process is markedly enhanced by pro-inflammatory cytokines such as TNF- $\alpha$ , IL-1, IL-6 and IL-17 (Schett 2006). B cells also produce cytokines that inhibit osteoclast differentiation from the progenitor cells, such as OPG and TGF- $\beta$  (Li et al. 2007, Neale Weitzmann et al. 2000). Additionally, some studies have described early developmental stage B-lymphoid lineage cells that have the potential to differentiate into osteoclasts when stimulated with M-CSF and RANKL *in vitro* (Manabe et al. 2001), so it is not surprising that the role of B cells in osteoclastogenesis remains controversial.

Recently, techniques have been described that involve the generation of osteoclasts from human precursor cells, using either fresh bone marrow or peripheral blood. These *in vitro* osteoclastogenesis protocols rely on the isolation of PBMCs to serve as precursors and although this can sometimes be more challenging the results are easier to translate clinically. The protocols described in Table 15 are perhaps typical of this approach (D'Amelio et al. 2004, Nose et al. 2009, Vandooren et al. 2009, Durand et al. 2011), each has certain advantages and disadvantages but the efficiency of osteoclastogenesis *in vitro* is variable. Several systems describe osteoclast formation without additional M-CSF and RANKL i.e. spontaneous osteoclastogenesis. Whilst there is no direct evidence that spontaneous osteoclastogenesis occurs *in vivo*, Vandooren (Vandooren et al. 2009) proposes that it is a potential system to represent osteoclast formation in a variety of conditions associated with bone destruction and loss such as in RA. Furthermore, D'Amelio (D'Amelio et al. 2004) suggests that the essential triggers may already be present in peripheral blood, so the addition of exogenous cytokines could mask endogenous differences in their production making it difficult to distinguish patients from healthy controls. There are wide methodological differences in these culture systems including; the number of mononuclear cells plated; composition of the medium, timeframe plus defining osteoclastogenic characteristics (Table 15). Therefore the protocol described and used in this section had to be optimised to take these variables into account. A standard TRAP stain was most frequently described in these

studies to identify osteoclast-like cells attached to glass cover slips and defining morphological characteristics commonly included; the presence of multiple nuclei (i.e. >3) and a basal ruffled border. Additionally, evidence of osteoclast maturation and activity was assessed using various stains on bone or dentine slices to identify evidence of resorption lacunae.

The aim of this Chapter was therefore to evaluate a protocol for use in the research laboratory at Middlesbrough; to create a robust and reproducible method for osteoclast formation and characterisation from peripheral blood *in vitro*, representative of *in vivo* conditions without the addition of endogenous substances. To use this culture system to investigate the potential role of B cells on osteoclastogenesis; using healthy volunteer blood depleted of B cells *in vitro*, plus blood from RA patients following *in vivo* B cell depletion.

**Table 15 Osteoclast culture techniques described in recent literature**

Reference	D'Amelio et al. 2004	Nose et al. 2009	Vandooren et al. 2009	Durand et al. 2011
<b>PBMC isolation</b>	Ficoll-Paque	Ficoll-Paque Plus	Ficoll-Paque	Ficoll density gradient
<b>No. of cells plated</b>	2× 10 <sup>5</sup> unfractionated PBMCs/well in 96-well plates or 1× 10 <sup>6</sup> PBMCs on dentin slices	5× 10 <sup>4</sup> unfractionated cells/well on an ST2 cell layer in 24-well plates with coverslips or 96-well plates on 6mm dentine slices	7× 10 <sup>5</sup> unfractionated PBMCs/well in 16-well plates with coverslips or 96-well plates on dentine discs	1.5× 10 <sup>6</sup> unfractionated cells/cm <sup>2</sup> in 24-well plates with 12mm coverslips or 48-well plates with bone slices
<b>Medium</b>	α-MEM 10% FBS 100 IU/ml Penicillin 100µg/ml Streptomycin ± 10 <sup>-8</sup> M 1,25(OH) <sub>2</sub> D <sub>3</sub> ± 30ng/ml RANKL ± 25ng/ml M-CSF	α-MEM 10% FBS 50U/ml Penicillin 50µg/ml Streptomycin ST2 cell preparation ± 10 <sup>-8</sup> M 1,25(OH) <sub>2</sub> D <sub>3</sub> ± 10 <sup>-7</sup> M dexamethasone ± 25ng/ml RANKL ± 50ng/ml M-CSF	300µl RPMI 1640 complete ± 40ng/ml RANKL ± 10ng/ml M-CSF	α-MEM 10% FBS 1% Penicillin-Streptomycin 50ng/ml RANKL 10ng/ml M-CSF
<b>Culture conditions</b>	10 days @37°C; 5%CO <sub>2</sub> 21 days for resorption	14 days @37°C; 5%CO <sub>2</sub> 21 days for resorption	14 days @37°C; 5%CO <sub>2</sub> 21 days for resorption	21 days @37°C; 5%CO <sub>2</sub>
<b>Medium change</b>	3 days	3/4 day	3 day	3/4 day
<b>Flow cytometry</b>	Not done	Frequency of OC precursors determined using a limiting dilution assay and quantification by flow cytometry	Not done	Quantification of OC precursors by flow cytometry
<b>Histochem Stain</b>	Sigma TRAP Vitronectin receptor	TRAP	Sigma TRAP	Sigma TRAP Calcitonin receptor
<b>Count</b>	TRAP+ and VNR+ cells/well with >3 nuclei	TRAP+ cells/well with >3 nuclei	TRAP+ cells	TRAP+ cells/well with >3 nuclei
<b>RT-PCR</b>	Not done	RT-PCR for human TRAP (ACP6), human CD51/αv integrin (ITGAV), human β-actin (ACTB) genes	Not done	RT-PCR for Cathepsin K and β-actin
<b>Resorption assay</b>	Dentine slices stained with 0.5% Toluidine blue	Dentine slices stained with Coomassie brilliant blue R250	Dentin resorption assay (IDS) stained with Toluidine blue	Bone slices stained with 0.2% Toluidine blue and resorption area quantified
<b>Other identification</b>	Supernatant level of TNF-α and RANKL Cell viability	N/A	N/A	Osteoclast apoptosis Caspase activity

## 5.2 Osteoclastogenesis protocol

PBMC's, isolated by a standard Ficoll density-gradient centrifugation procedure, were used immediately and without further enhancement to optimise an *in vitro* osteoclast culture system for use in future work in this Chapter. Specifically; the need for exogenous cytokines, PBMC plating density, length of the culture period and osteoclast characterisation was evaluated in this section.

### 5.2.1 Methods

PBMC's were isolated from the fresh peripheral blood (described in Chapter 2 section 2.2.2) of self-reported healthy volunteers (Chapter 2 section 2.3.3). Thereafter, unfractionated cells were cultured in  $\alpha$ MEM complete medium supplemented with recombinant human M-CSF (30ng/ml) and RANKL (25ng/ml), (Chapter 2 section 2.1.2) with the aim of establishing an osteoclast culture system. However, in order to investigate spontaneous osteoclastogenesis *in vitro*, further experiments were carried out without the addition of these two cytokines. To determine the optimum number of mononuclear cell's for the osteoclast culture (Chapter 2 section 2.2.2), varying numbers of PBMC's; 250,000, 500,000, 750,000 and 1,000,000 were re-suspended in 500 $\mu$ l  $\alpha$ MEM complete medium and layered onto glass coverslips in a labelled 24 well plate. The plate was incubated at 37°C in a humidified atmosphere 5% CO<sub>2</sub> for up to 21 days. The medium was refreshed every 2-3 days by replacement of the upper 250 $\mu$ l. Osteoclasts have a limited lifespan and eventually die via apoptosis, therefore to determine the optimal time period for the culture, one set of coverslips was stained using the TRAP protocol described in Chapter 2 section 2.2.2 on day 1, day 7 day 14 and day 21. Additionally bone slices were stained with toluidine blue (Chapter 2 section 2.2.2) to identify any resorption lacunae on day 14 and day 21. All experimental conditions were assayed in triplicate.

Primary osteoclasts were characterised by size, morphology, TRAP and actin staining on glass coverslips and toluidine blue staining on bone slices (Chapter 2 section 2.2.2 for individual osteoclast characterisation methods). Additionally, functional evidence of osteoclast differentiation was determined by measuring the  $\beta$ CTX concentration in the cell supernatant harvested from cells cultured on bone slices for 14 and 21 days. The supernatant was collected three days after the final medium change at the end of the culture period on bone slices. Collagen fragments were quantified using the Roche serum  $\beta$ CTX assay (Chapter 2 section 2.2.1). A control sample consisting of culture medium from a well containing a bone slice but with no added cells was also assayed and the result was subtracted from the values obtained for samples plus cells. Any minus values were adjusted to zero. The within batch

precision of the assay was assessed by measuring  $\beta$ CTX levels in the cell supernatant from 5 separate wells containing control samples after the final medium change at the end of the culture period. The mean  $\beta$ CTX control value was also compared to that obtained from a similar well from the same plate but with added cells. The between batch precision was calculated retrospectively from control results taken from 10 separate plates over several months.

### **5.2.2 Results**

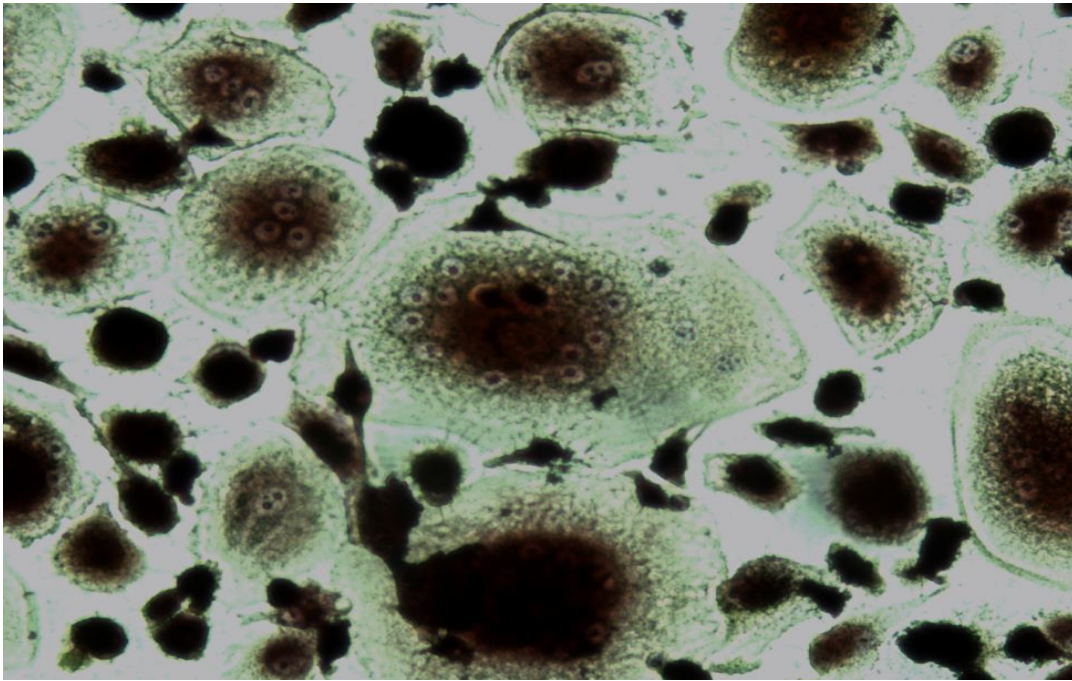
Numerous multi-nucleated osteoclast-like cells developed from the fresh PBMC's, following 14 days culture in  $\alpha$ MEM complete medium supplemented with and without M-CSF plus RANKL (Figure 22), the appropriate medium being replenished every 2-3 days. However, the resulting TRAP<sup>+</sup> cells, from the medium supplemented with cytokines, were more defined, larger and contained more nuclei/cell.

RPMI 1650 medium was also tested but  $\alpha$ MEM complete was found to be the best for supporting optimal growth of osteoclasts. In order to identify the optimum PBMC plating density for spontaneous osteoclastogenesis varying concentrations of mononuclear cells were cultured and the number and quality of the resulting TRAP<sup>+</sup> cells determined. Optimal growth of osteoclast-like cells was obtained at a concentration of  $1 \times 10^6$  cells/ml i.e. 500,000 cells plated in 500 $\mu$ l medium (Figure 23). Increasing the plating density did not further increase the osteoclast yield and at 1,000,000 cells in 500 $\mu$ l medium the cells appeared to be overcrowded. TRAP<sup>+</sup> cells first appeared at day 7 and their number had increased at day 14, however there was some evidence of cell fragmentation on glass coverslips by day 21 (Figure 24). In order to verify the osteoclast-like cells on glass coverslips the Sigma TRAP staining protocol was optimised (Chapter 2 section 2.2.2) and osteoclasts were identified by TRAP staining, morphology (i.e. cell size and presence of a ruffled border) and greater than 3 nuclei (Figure 25), commonly accepted methods of osteoclast identification. In future experiments the number of TRAP<sup>+</sup> cells was also counted (Chapter 2 section 2.2.2), plus the cell diameter and circumference was recorded. Additionally, the Invitrogen Life Technologies protocol using Alexa Fluor<sup>®</sup> 488 Phalloidin was optimised (see 2.2.2) and there was evidence of actin ring formation on the glass coverslips (Figure 26).

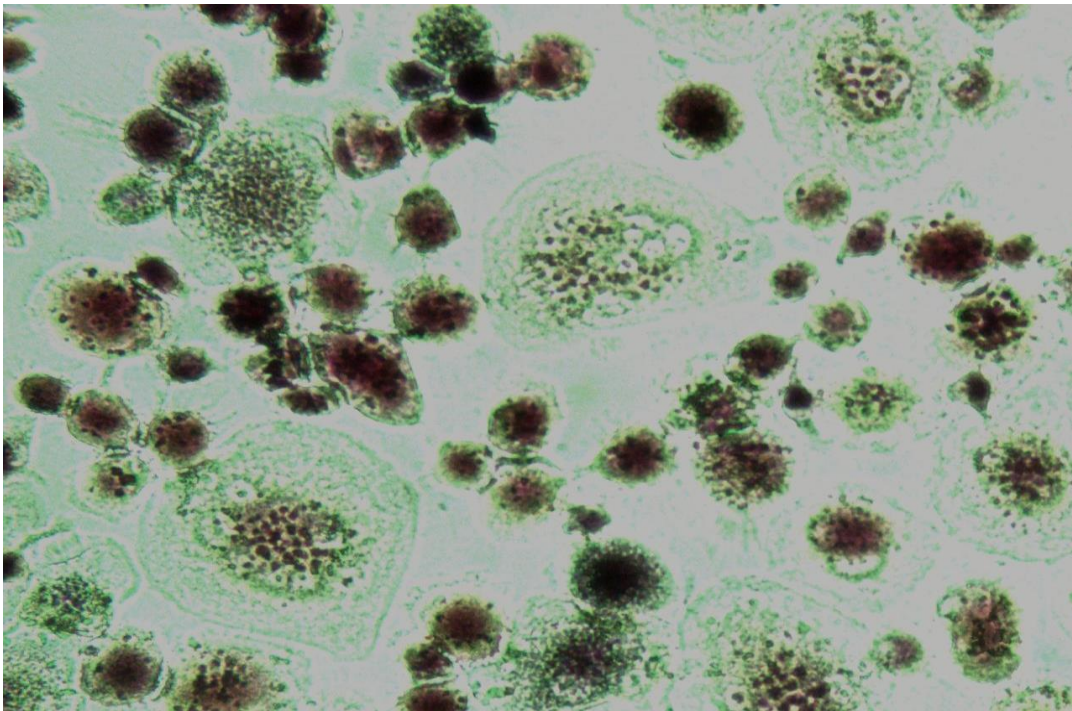
Toluidine blue staining of the bone slice identified areas of resorption after 14 and 21 days (Figure 27). Additionally during bone metabolism, type I collagen is degraded and small fragments of C-terminal telopeptides are released, there was evidence of increased osteoclastic activity on the bone slice as the levels of  $\beta$ CTX in the cell supernatant were also increased. The within batch CV (2.2%) of the  $\beta$ CTX assay after 14 days was calculated from

the mean (88.3ng/L) and SD (2.0ng/L) in 5 separate control wells of cell supernatant from the same plate. In comparison the supernatant  $\beta$ CTX concentration in this plate was 113.4ng/L in the well containing 500,000 cells. The between batch CV (8.7%) of the  $\beta$ CTX assay was calculated retrospectively from the mean (100.9ng/L) and SD (8.8ng/L) in 10 separate control wells containing cell supernatant made up from different batches of  $\alpha$ MEM complete medium over several months.





A. With the addition of M-CSF (30ng/ml) and RANKL (25ng/ml)

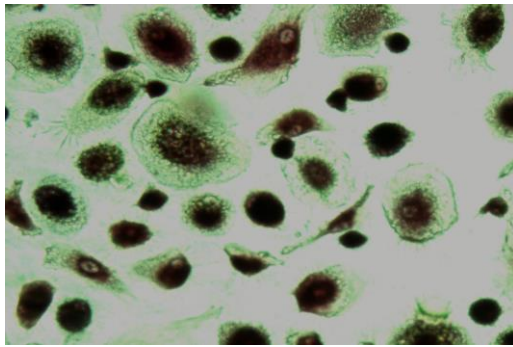


B. Spontaneous osteoclastogenesis

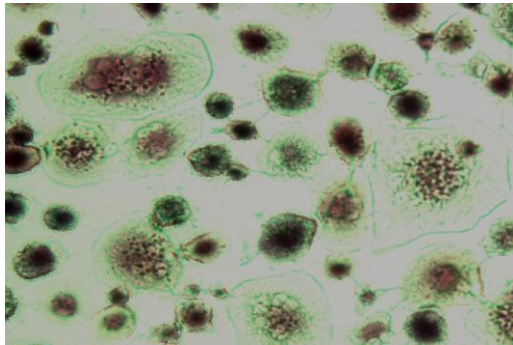
**Figure 22 Comparison with and without the addition of cytokines ( $\times 200$ )**

TRAP stained osteoclast-like cells generated from 500,000 unfractionated, healthy volunteer PBMC's in 500 $\mu$ l  $\alpha$ MEM complete medium containing; A:  $\alpha$ MEM complete supplemented with M-CSF (30ng/ml) and RANKL (25ng/ml); B:  $\alpha$ MEM complete with no added cytokines, after 14 days culture at 37°C in 5% CO<sub>2</sub>, the upper 250 $\mu$ l medium was replenished every 2-3 days. The cells were stained using an optimised Sigma TRAP kit. ( $\times 200$  magnification).

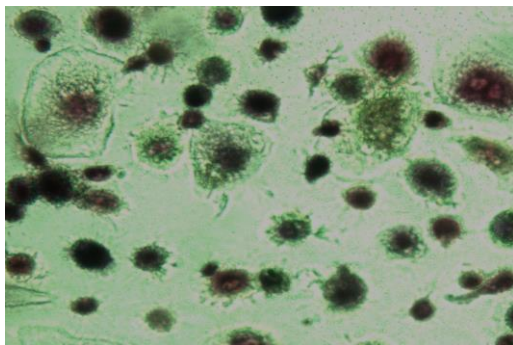




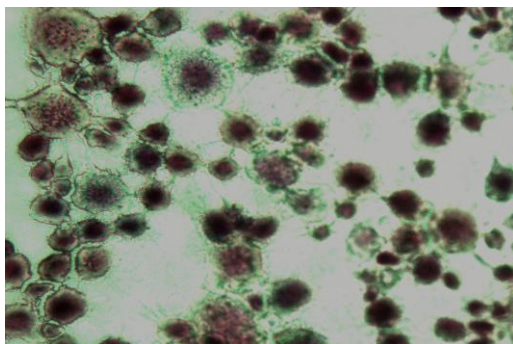
A. 250,000 PBMC's/well



B. 500,000 PBMC's/well



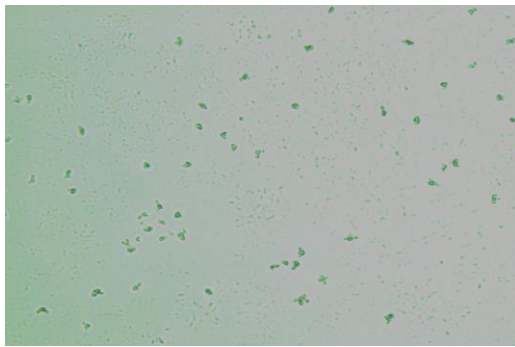
C. 750,000 PBMC's/well



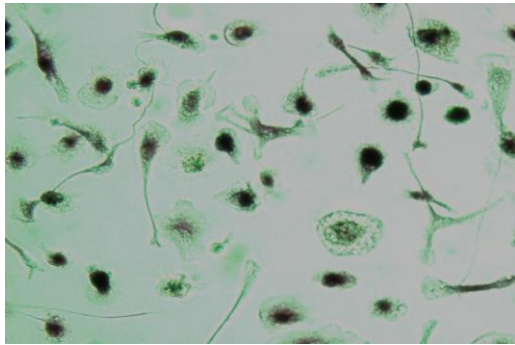
D. 1,000,000 PBMC's/well

**Figure 23 Evaluation of PBMC plating density ( $\times 200$ ) showing typical patterns of TRAP<sup>+</sup> cell formation at each concentration**

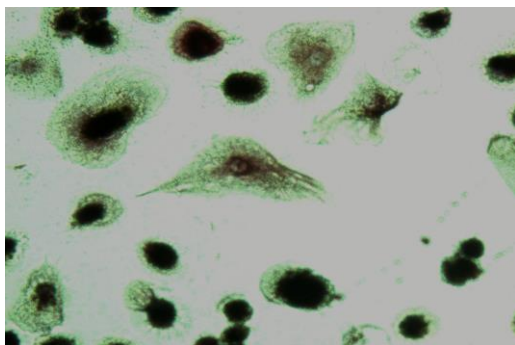
TRAP stained osteoclast-like cells generated from varying numbers of unfractionated, healthy volunteer PBMC's in 500 $\mu$ l  $\alpha$ MEM complete medium. A: 250,000; B: 500,000; C: 750,000; D: 1,000,000 PBMC's/well after 14 days culture at 37°C in 5% CO<sub>2</sub>, the upper 250 $\mu$ l medium was replenished every 2-3 days. The cells were stained using an optimised Sigma TRAP kit. ( $\times 200$  magnification).



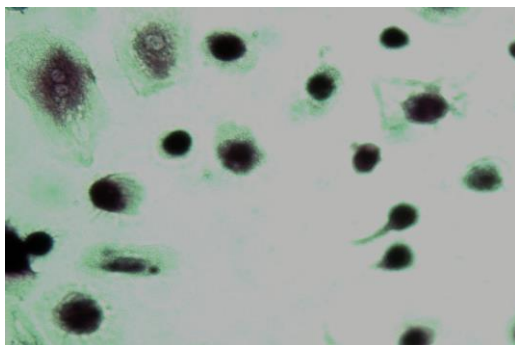
A. Day 1



B. Day 7



C. Day 14



D. Day 21

**Figure 24 Evaluation of the time of culture period ( $\times 200$ ) showing typical patterns of TRAP<sup>+</sup> cell formation at each day**

TRAP stained osteoclast-like cells generated from 500,000 unfractionated, healthy volunteer PBMC's in 500 $\mu$ l  $\alpha$ MEM complete medium with no additional cytokines after; A: 1 day; B: 7 days; C: 14 days; D: 21 days, culture at 37°C in 5% CO<sub>2</sub>, the upper 250 $\mu$ l medium was replenished every 2-3 days. The cells were stained using an optimised Sigma TRAP kit. ( $\times 200$  magnification).

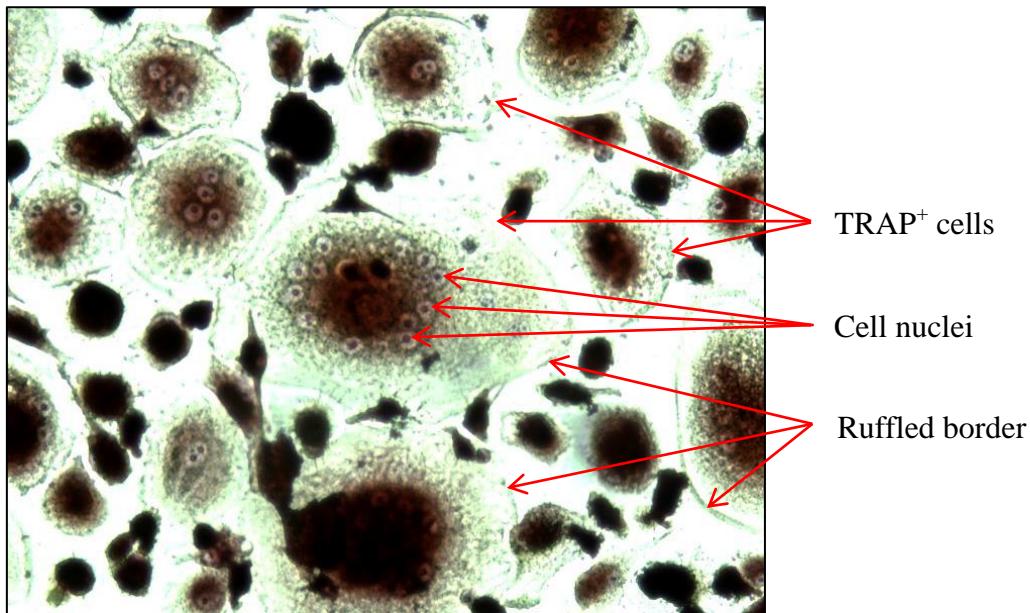


**Figure 25** Representative TRAP<sup>+</sup> multinucleated cells on a glass coverslip

Osteoclasts-like cells on glass coverslips demonstrating TRAP staining. The cells were generated from 500,000 unfractionated, healthy volunteer PBMC's in 500 $\mu$ l  $\alpha$ MEM complete medium with no additional cytokines after 14 days culture at 37°C in 5% CO<sub>2</sub>, the upper 250 $\mu$ l medium was replenished every 2-3 days. The cells were stained using an optimised Sigma TRAP kit. ( $\times$ 200 magnification).

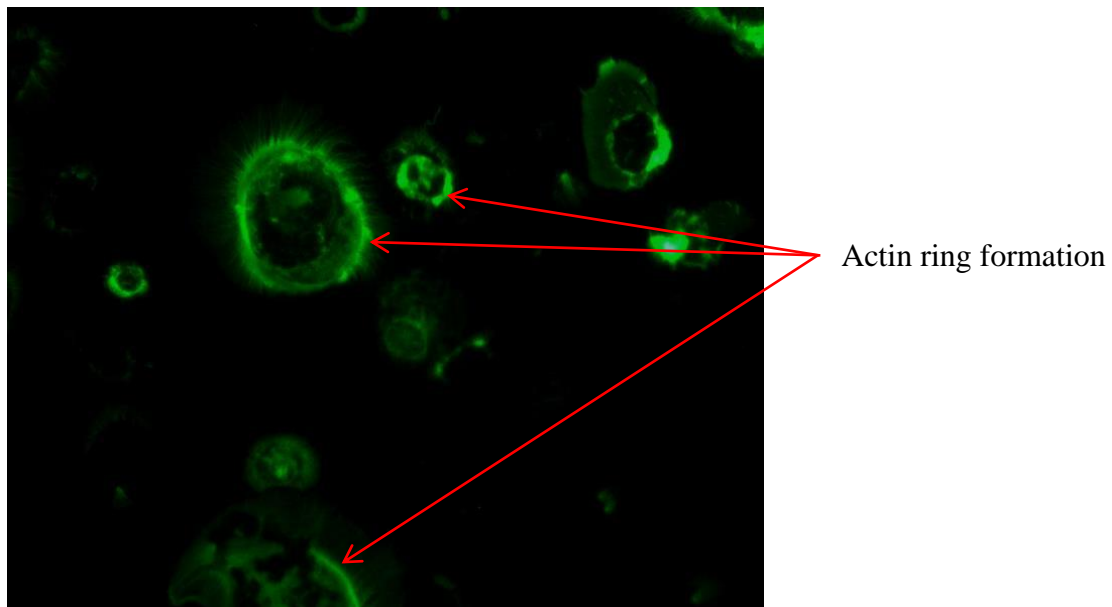


**Figure 26** Representative actin ring formation on a glass coverslip

Osteoclasts-like cells on glass coverslips demonstrating actin ring formation. The cells were generated from 500,000 unfractionated, healthy volunteer PBMC's in 500 $\mu$ l  $\alpha$ MEM complete medium with no additional cytokines after 14 days culture at 37°C in 5% CO<sub>2</sub>, the upper 250 $\mu$ l medium was replenished every 2-3 days. The cells were stained with Alexa Fluor® 488 Phalloidin, using an optimised Invitrogen Life Technologies staining protocol. ( $\times$ 200 magnification).

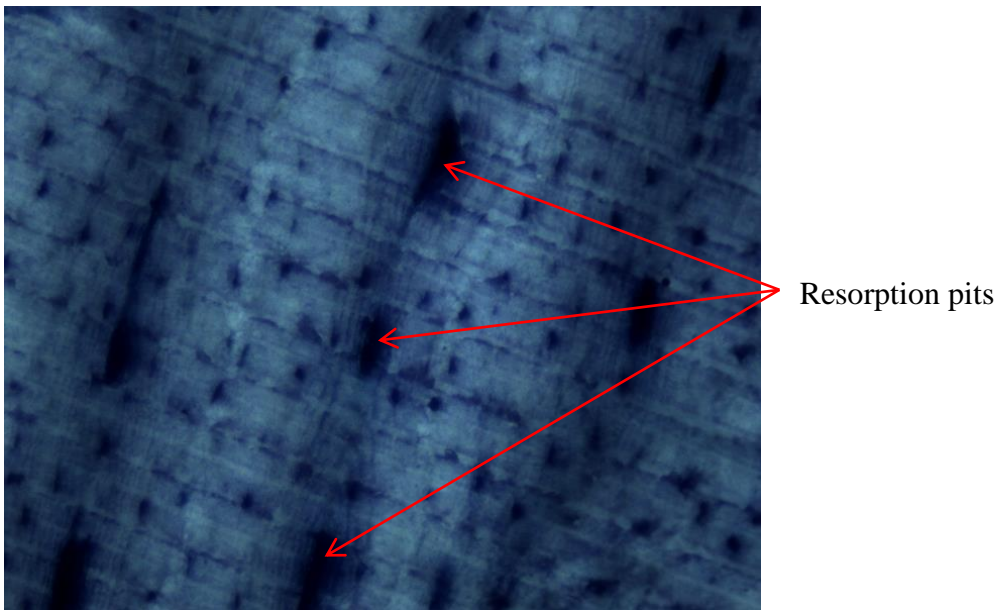


**Figure 27 Representative resorption pits on a bone slice, visualised by toluidine blue staining**

The cells were generated from 500,000 unfractionated, healthy volunteer PBMC's in 500µl  $\alpha$ MEM complete medium with no additional cytokines seeded on bone slices after 14 days culture at 37°C in 5% CO<sub>2</sub>, the upper 250µl medium was replenished every 2-3 days. The bone slices were stained with 0.1% toluidine blue following an optimised protocol. ( $\times 200$  magnification).

### 5.2.3 Discussion

Osteoclast-like cells were generated from peripheral blood using an optimised culture system. It appeared that exogenous cytokines were not essential to the process and spontaneous osteoclastogenesis was observed with unfractionated PBMC's from healthy volunteers. Comparable to the results reported in similar culture systems (D'Amelio et al. 2004, Vandooren et al. 2009). Unfractionated cells were used, allowing the co-culture of monocytes and lymphocytes; additionally the initial medium was not changed for at least 48hrs to mimic *in vivo* conditions as closely as possible. It is likely that there was sufficient endogenous cytokine present in the peripheral blood to stimulate osteoclastogenesis. Although the resulting TRAP<sup>+</sup> cells, from the medium supplemented with M-CSF and RANKL, were more defined, larger and appeared to contain more nuclei. The addition of exogenous cytokines can mask any differences in the amounts of these components in the blood thus making it difficult to distinguish patients from healthy controls (D'Amelio et al. 2004) in future experiments. PBMC plating density did not essentially affect the maximal number of osteoclasts formed.  $1 \times 10^6$  PBMC's/ml was taken as a workable concentration and guaranteed enough cells for all experimental conditions. Furthermore, osteoclasts have a limited lifespan and eventually die via apoptosis if the culture period is too long (Akchurin et al. 2008). Optimal numbers of osteoclast-like cells formed at 14 days on glass cover-slips and measurable resorptive activity was also achieved after 14 days on bone slices, this was consistent with similar osteoclastogenesis protocols (D'Amelio et al. 2004, Nose et al. 2009, Vandooren et al. 2009, Durand et al. 2011). Osteoclasts were identified as multinucleated (more than 3 nuclei) cells that stained positive for TRAP. Actin ring formation is also a prerequisite for osteoclast bone resorption. Osteoclasts seeded on glass form podosomes, which are small cylinders of actin surrounded by vinculin. There are three different podosome structures dependant on the stage of osteoclast differentiation; namely clusters, rings and belts depicting mature osteoclasts (Saltel et al. 2004). After 14 days the osteoclast cells were found to be fully functional; this was confirmed by their ability to form actin rings on glass coverslips, resorption pits on bone slices and by increased  $\beta$ CTX levels in the cell supernatant. However, the Roche crosslaps assay has not been verified for use in cell supernatants. The assay was found to have acceptable precision during the evaluation but there was a lack of sensitivity in subsequent experiments and it was deemed to be semi-quantitative at best.

In conclusion the results demonstrate that using this culture system the multinucleated cells formed from human PBMCs exhibit several characteristics of osteoclasts. Moreover, optimum conditions for detection of a high number of osteoclast-like cells were observed after 14 days

of culture on glass coverslips or bone slices, using 500,000 PBMC's in 500 $\mu$ l  $\alpha$ MEM complete medium.



### 5.3 The effect of *in vitro* B cell depletion

The aim of this section was to investigate the potential role of B cells on osteoclastogenesis specifically using healthy volunteer PBMC's depleted of B cells *in vitro*. B cell depletion *in vitro* can be achieved via; MACS separation with CD20 microbeads; or by using RTX, an approved therapeutic B cell depleting agent that binds to CD20. In each case the antibody recognizes the CD20 antigen, a non-glycosylated transmembrane protein of 33–35kDa (Cartron et al. 2004) that is expressed on the surface of B lineage cells from the pre-B cell stage and throughout B cell maturation, but is lost at the final transformation to plasma cells (Figure 1).

The MACS method allows the cells to be separated by incubating with magnetic nanoparticles coated with antibodies against CD20. The cells expressing CD20 i.e. CD20<sup>+</sup> cells, attach to the magnetic nanoparticles and if this cell solution is then transferred to a column placed in a strong magnetic field, the CD20<sup>+</sup> cells remain on the column, while CD20<sup>-</sup> cells flow straight through. Using either technique *in vitro* results in rapid B cell depletion, however *in vivo* B cell depletion with RTX is much slower. The mechanisms by which RTX actually works *in vivo* still need to be elucidated. A large body of evidence shows that therapeutically RTX induces cell death by different pathways (Cartron et al. 2004); CD20<sup>-</sup> induced apoptosis; complement dependent cytotoxicity; antibody dependent cell-mediated cytotoxicity; and selective targeting and depletion of B cell subsets. It is also likely that the different mechanisms work together, the importance of each one being dependent on the target cell (Clark and Ledbetter 2005).

Additionally, the effect of monocytes on RTX action is uncertain. Pederson et al. report that monocytes compromise RTX treatment *in vivo* in cases such as haematological malignancies with increased numbers of B cells. *In vitro* results in healthy volunteers suggest a monocyte-mediated 'shaving' reaction, leading to complete loss of anti-CD20 antibodies from the surface of B cells (Pederson et al. 2011). Therefore the effect of *in vitro* RTX on unfractionated and CD14<sup>+</sup> purified PBMC's was also explored.

#### 5.3.1 Methods

PBMC's were isolated from the fresh peripheral blood (described in Chapter 2 section 2.2.2) of self-reported healthy volunteers (Chapter 2 section 2.3.3) in this section. Thereafter, 500,000 unfractionated cells were compared to either 500,000 cells subjected to CD20 depletion or CD14 purification in different experiments described below. All cells were suspended in 500µl αMEM complete medium and were layered onto glass coverslips in a labelled 24 well plate, all experimental conditions were assayed in duplicate. The initial

number of monocytes, B cells and T cells was determined in 500µl of this cell suspension by FACS analysis (Chapter 2 section 2.2.2). The plate was incubated at 37°C in a humidified atmosphere 5% CO<sub>2</sub> for 14 days. The medium was refreshed every 2-3 days by replacement of the upper 250µl. The coverslips were stained using the TRAP protocol described in Chapter 2 section 2.2.2 on day 14.

#### Unfractionated vs CD20 depleted PBMC's using magnetic activated cell sorting

PBMC's were isolated from the fresh peripheral blood of 12 self-reported healthy volunteers (Chapter 2 section 2.3.3) and cultured as described above to compare unfractionated to CD20 depleted fractions. B cell depletion was carried out using CD20 microbeads and MACS separation (Miltenyi Biotec) prior to osteoclast culture (described in Chapter 2 section 2.2.2) and the initial numbers of monocytes, B cells and T cells in each fraction was determined by FACS. The number, cell circumference and diameter of the resulting TRAP<sup>+</sup> cells generated after 14 days was also recorded for each fraction.

#### Comparison of CD20 depleted PBMC's using MACS or *in vitro* rituximab

PBMC's were isolated from the fresh peripheral blood of 3 self-reported healthy volunteers (Chapter 2 section 2.2.2) and cultured as described above to compare unfractionated to CD20 depleted fractions. However in this instance, B cell depletion was accomplished simultaneously from the same unfractionated PBMC's, via MACS separation with CD20 microbeads or via the addition of RTX at varying concentrations between 0.1 – 100µg/ml (described in Chapter 2 section 2.2.2) prior to osteoclast culture. Additionally a set of unfractionated PBMC's were cultured and RTX at varying concentrations between 0.1 – 100µg/ml was added at the end of the culture (day 14) for comparison. The initial numbers of monocytes, B cells and T cells in each fraction was determined by FACS after 3, 12 and 24hrs. The number, cell circumference and diameter of the resulting TRAP<sup>+</sup> cells generated after 14 days was also recorded for each fraction.

#### Effect of *in vitro* rituximab on unfractionated and CD14<sup>+</sup> purified PBMC's

PBMC's were isolated from the fresh peripheral blood of 2 self-reported healthy volunteers (Chapter 2 section 2.2.2) and cultured as described above to compare unfractionated to CD14 purified fractions with and without CD20 depletion. B cell depletion was accomplished via the addition of either 1.0 or 10µg/ml RTX added simultaneously on day 1 to unfractionated PBMCs and to MACS purified CD14<sup>+</sup> monocytes. The initial numbers of monocytes, B cells and T cells in each fraction was determined by FACS after 3 and 24hrs. The number, cell



circumference and diameter of the resulting TRAP<sup>+</sup> cells generated after 14 days was also recorded for each fraction.

### Statistical analysis

Details of the statistical analysis are described in Chapter 2 section 2.4.3

### **5.3.2 Results**

#### Unfractionated vs CD20 depleted PBMC's using magnetic activated cell sorting

To investigate whether *in vitro* B cell depletion affects osteoclastogenesis in healthy volunteers unfractionated PBMC's and MACS CD20 depleted PBMC's were cultured, the generation of TRAP<sup>+</sup> osteoclast-like cells and evidence of bone resorption was recorded after 14 days, the results are included in Table 16. The group consisted of 12 self-reported healthy volunteers; 6 females (median age 41 yrs, IQR 31.5-49.0) and 6 males (median age 35.5 yrs; IQR 31.3-46.5), with no history of bone or autoimmune disease. There was a significant difference in the initial number of B cells, between unfractionated and CD20 depleted PBMC fractions as expected (median difference 16650, 95% CI 9101, 31251; p=0.002). But there was no significant difference between the initial number of T cells (median difference 7867, 95% CI -49809, 77228; p=0.875) or monocytes (median difference -8396, 95% CI -42743, 20963; p=0.158) between these fractions. Moreover, there was a significant difference in the absolute numbers of TRAP<sup>+</sup> cells generated (median difference -31, 95% CI -61,-2.9; p=0.023) i.e. there was a greater number of TRAP<sup>+</sup> cells generated from the CD20 depleted compared to the unfractionated PBMC's, yet if these results were analysed by gender the difference was only significant in the male volunteers. However, when the TRAP<sup>+</sup> cell numbers were adjusted to account for any differences in initial monocyte number, there was no significant difference (median difference -0.01, 95% CI -0.08, 0.06; p=0.530) in the cell numbers between these PBMC fractions. There was also no significant difference in TRAP<sup>+</sup> cell circumference (p=0.530) or cell diameter (p=0.454) or the  $\beta$ CTX concentration in the final cell supernatant (p=0.969).

**Table 16 Unfractionated and CD20 depleted cultures in twelve healthy volunteers**

	<b>Unfractionated Cells Median (IQR)</b>	<b>CD20 Depleted Cells Median (IQR)</b>	<b>Median Difference (95%CI)</b>	<b>p value</b>
<b>Initial no. Monocytes</b>				
All samples (n=12)	49227 (41696,65712)	72472 (33641,100783)	-8396 (-42743,20963)	0.158
<i>Female (n=6)</i>	56221 (41530,66665)	72472 (33710,84782)	-6760 (-40197,31116)	0.753
<i>Male (n=6)</i>	46507 (41861,53311)	79811 (33571,109500)	-23328 (-85016,28769)	0.116
<b>Initial no. B cells</b>				
All samples (n=12)	17476 (10541,32009)	1013 (431,2549)	16650 (9101,31251)	<b>0.002</b>
<i>Female (n=6)</i>	19482 (11668,29213)	1083 (565,1522)	16566 (6908,33429)	<b>0.028</b>
<i>Male (n=6)</i>	17476 (9414,35250)	868 (413,3575)	16650 (2424,33897)	<b>0.028</b>
<b>Initial no. T cells</b>				
All samples (n=12)	146028 (107045,227305)	139242 (59800,207437)	7867 (-49809,77228)	0.875
<i>Female (n=6)</i>	143464 (68000,227758)	109266 (41733,196879)	13832 (-37657,102506)	0.345
<i>Male (n=6)</i>	146028 (112665,226851)	169316 (95812,214061)	-8909 (-225391,88228)	0.600
<b>Absolute no. TRAP<sup>+</sup> cells</b>				
All samples (n=12)	60 (42,76)	86 (48,121)	-31 (-61,-2.9)	<b>0.023</b>
<i>Female (n=6)</i>	54 (31,76)	80 (40,87)	-19 (-61,28)	0.345
<i>Male (n=6)</i>	67 (54,75)	109 (56,139)	-39 (-81,-3)	<b>0.028</b>
<b>Monocyte corrected TRAP<sup>+</sup> cells</b>				
All samples (n=12)	0.12 (0.07,0.16)	0.14 (0.08,0.20)	-0.01 (-0.08,0.06)	0.530
<i>Female (n=6)</i>	0.08 (0.07,0.15)	0.12 (0.06,0.23)	-0.02 (-0.20,0.09)	0.463
<i>Male (n=6)</i>	0.15 (0.10,0.17)	0.15 (0.09,0.20)	-0.01 (-0.08,0.11)	0.917
<b>TRAP<sup>+</sup> cell circumference</b>				
All samples (n=12)	329 (293,342)	310 (293,329)	7 (-16,28)	0.530
<i>Female (n=6)</i>	317 (279,332)	310 (295,332)	-7 (-28,7)	0.291
<i>Male (n=6)</i>	334 (320,345)	311 (291,325)	25 (-33,117)	0.249
<b>TRAP<sup>+</sup> cell diameter</b>				
All samples (n=12)	86 (75,89)	81 (75,86)	2 (-4,9)	0.454
<i>Female (n=6)</i>	83 (70,89)	81 (75,86)	-1 (-9,5)	0.673
<i>Male (n=6)</i>	87 (83,88)	81 (74,85)	6 (-7,31)	0.139
<b>Final <math>\beta</math>CTX concentration</b>				
All samples (n=12)	2.2 (0.7,6.5)	0.7 (0,13)	0.2 (-5.1,2.4)	0.969
<i>Female (n=6)</i>	1.8 (1.3,18.3)	0.7 (0,23.8)	0.2 (-9.9,1.8)	0.833
<i>Male (n=6)</i>	3.4 (0,6.5)	0.8 (0,2.2)	1.3 (-19.9,4.3)	0.673

The data were not normally distributed and so results were expressed as medians and interquartile range. Wilcoxon signed-rank test was used to determine if there was a statistically significant difference between unfractionated and CD20 depleted PBMC fractions. P values  $\leq 0.05$  were considered statistically significant.

Collectively examining the unfractionated and CD20 depleted fractions, there was no significant correlation between; the initial number of monocytes and the absolute number of TRAP<sup>+</sup> cells generated ( $R_s = 0.312$ ;  $p = 0.137$ ), (Figure 28); or the initial numbers of B cells and the number of TRAP<sup>+</sup> cells generated corrected for the number of monocytes ( $R_s = -0.086$ ;  $p = 0.689$ ), (Figure 29); or the initial numbers of T cells and the number of TRAP<sup>+</sup> cells generated corrected for the number of monocytes ( $R_s = -0.345$ ;  $p = 0.098$ ), (Figure 30). However, when assessing the unfractionated and CD20 depleted fractions separately; there was a significant positive correlation ( $R_s = 0.671$ ;  $p = 0.017$ ) between the initial number of monocytes and the absolute numbers of TRAP<sup>+</sup> cells generated and a significant negative correlation between the initial number of T cells and the TRAP<sup>+</sup> cells generated corrected for the number of monocytes ( $R_s = -0.627$ ;  $p = 0.029$ ), in CD20 depleted PBMC's. Yet, no significant correlations were found between these parameters and the unfractionated PBMC's, (Figures 28 – 30).

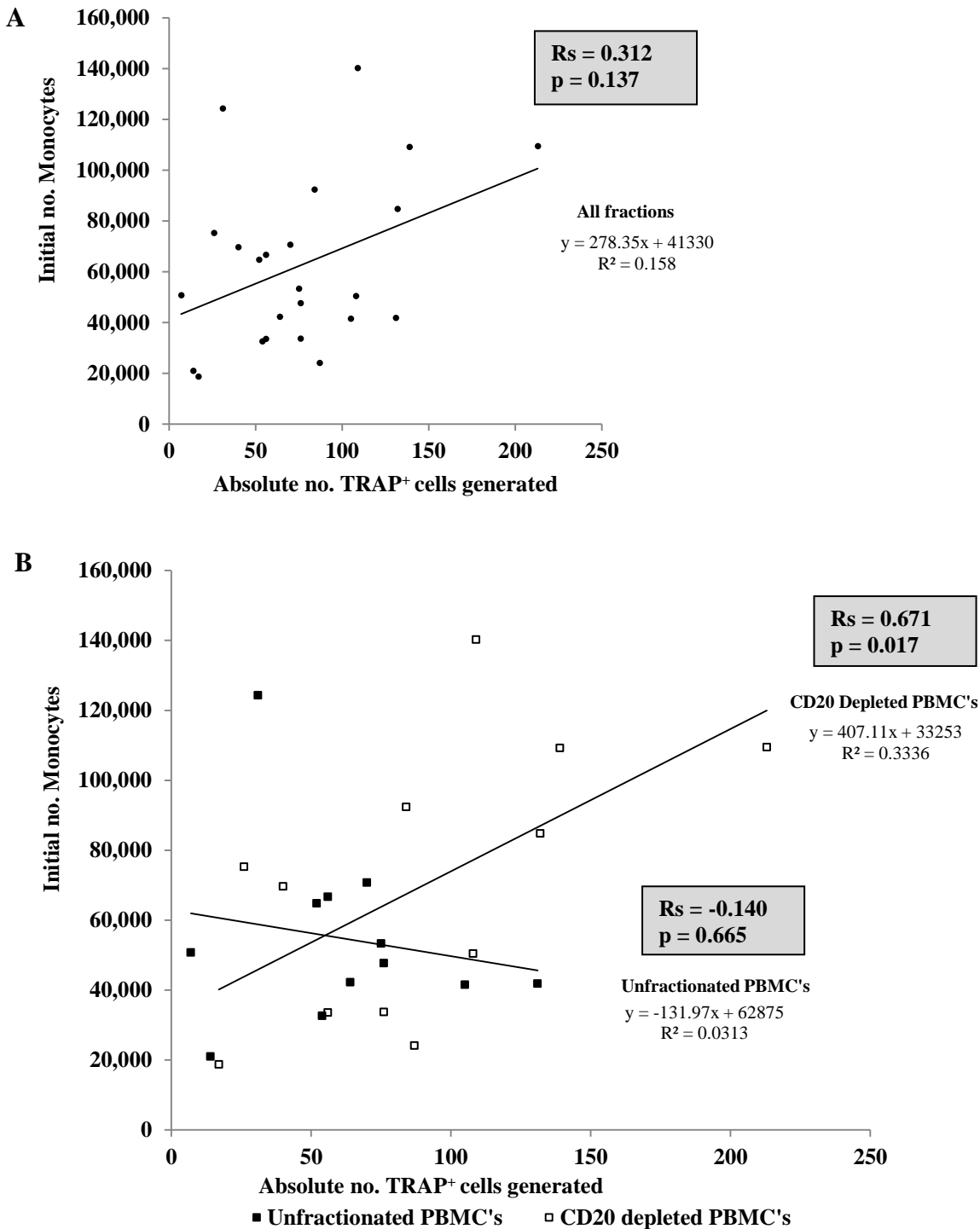


**Figure 28** The effect of the initial number of monocytes on TRAP<sup>+</sup> cells generated from twelve healthy volunteer peripheral blood mononuclear cells

TRAP<sup>+</sup> cells were generated from 500,000 unfractionated PBMC's or MACS CD20 depleted PBMC's, in 500µl αMEM complete medium with no added cytokines, after 14 days culture in 5% CO<sub>2</sub> at 37°C, the upper 250µl medium was replenished every 2-3 days. The absolute number of TRAP<sup>+</sup> cells generated was plotted against the initial number of monocytes for A: all fractions and B: for unfractionated and CD20 depleted PBMC's. The line of best fit/ trendline and equation were generated using Microsoft Excel 2010. Spearman's rank correlation coefficient  $R_s$  was used to correlate these parameters.

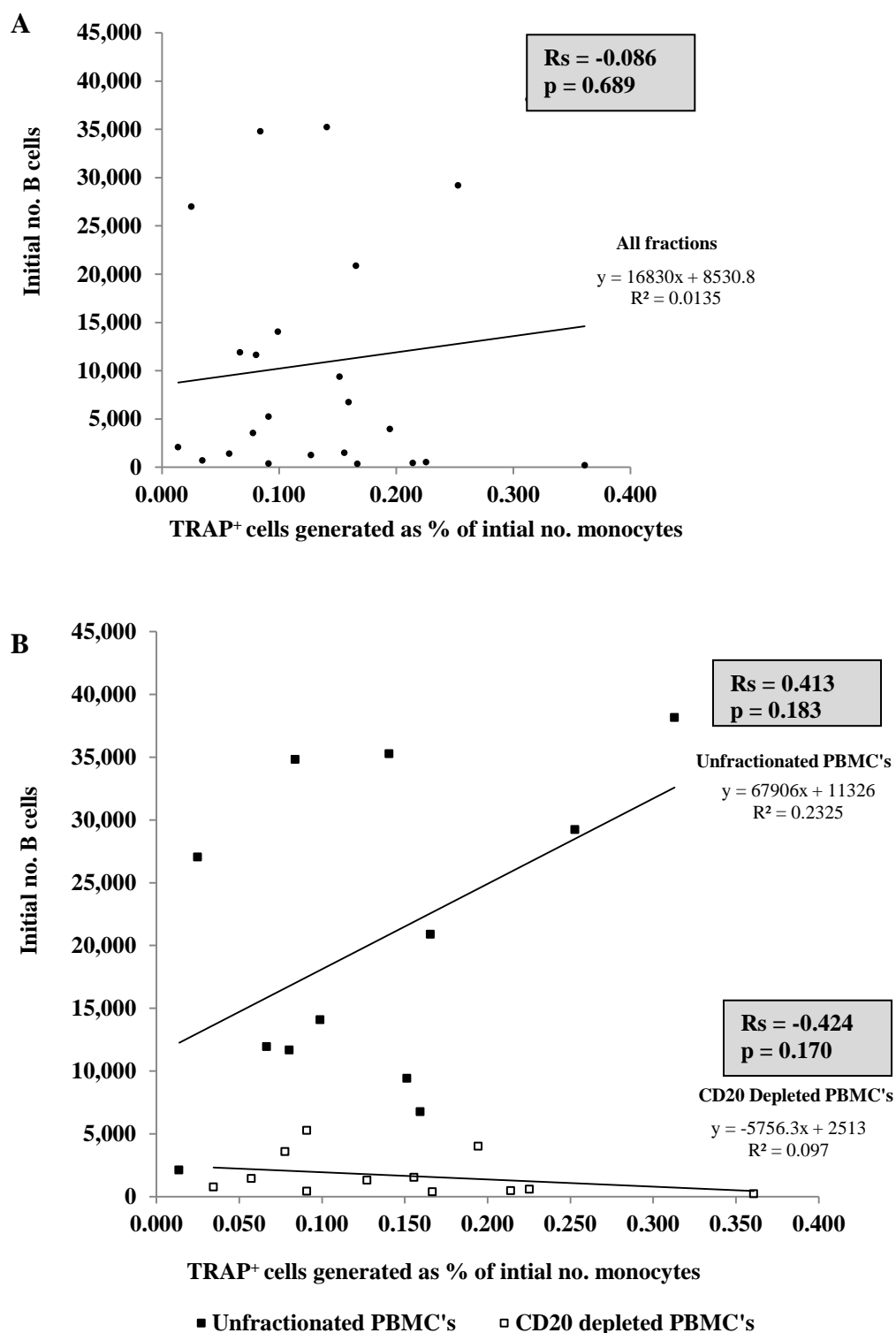


**Figure 29** The effect of the initial number of B cells on TRAP<sup>+</sup> cells generated from twelve healthy volunteer peripheral blood mononuclear cells

TRAP<sup>+</sup> cells were generated from 500,000 unfractionated PBMC's or MACS CD20 depleted PBMC's, in 500 $\mu$ l  $\alpha$ MEM complete medium with no added cytokines, after 14 days culture in 5% CO<sub>2</sub> at 37°C, the upper 250 $\mu$ l medium was replenished every 2-3 days. The absolute number of TRAP<sup>+</sup> cells generated was corrected for the number of monocytes in the initial cell suspension and plotted against the initial number of B cells for A: all fractions and B: for unfractionated and CD20 depleted PBMC's. The line of best fit/ trendline and equation were generated using Microsoft Excel 2010. Spearman's rank correlation coefficient  $R_s$  was used to correlate these parameters.

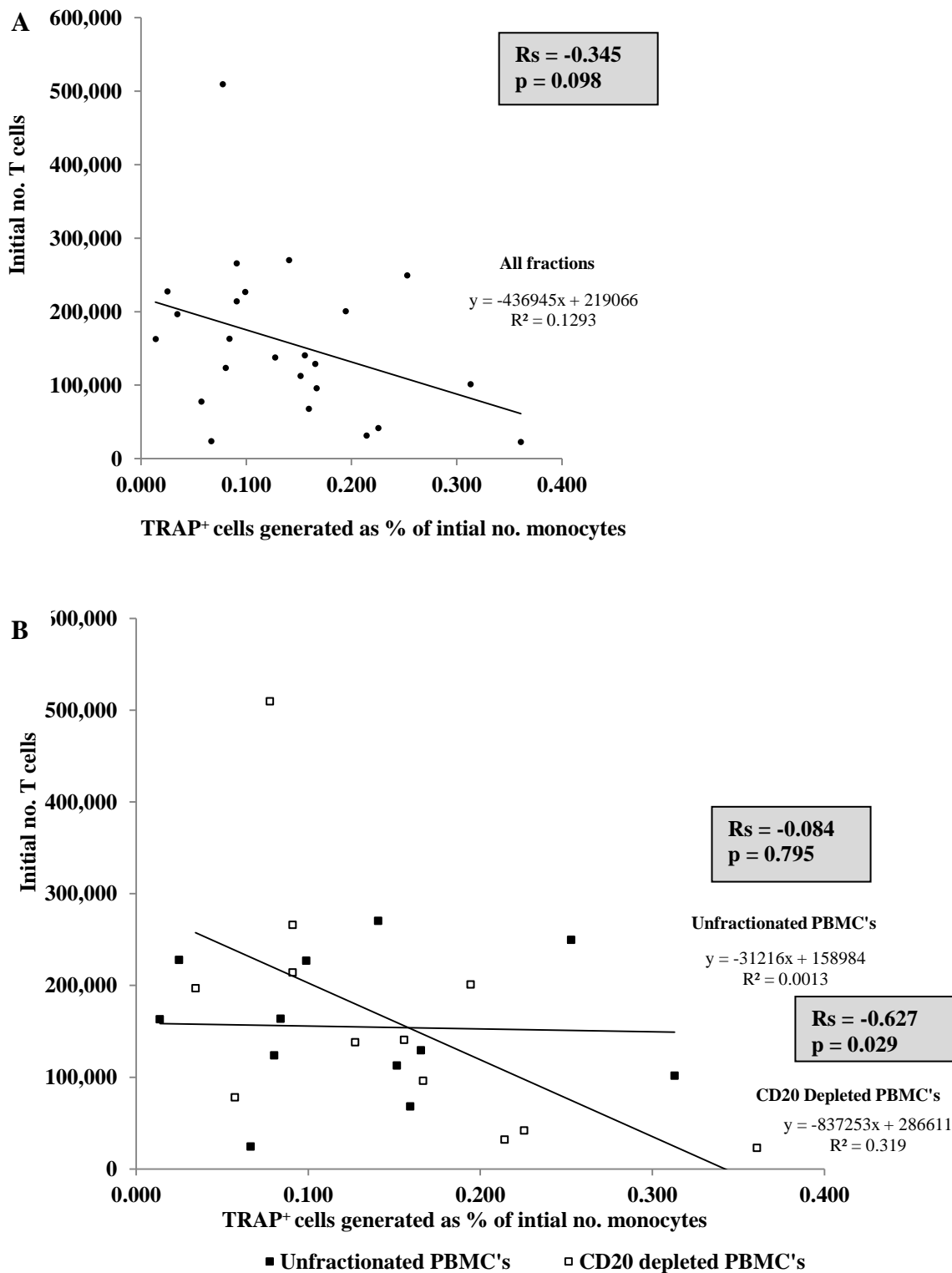


**Figure 30** The effect of the initial number of T cells on TRAP<sup>+</sup> cells generated from twelve healthy volunteer peripheral blood mononuclear cells

TRAP<sup>+</sup> cells were generated from 500,000 unfractionated PBMC's or MACS CD20 depleted PBMC's, in 500 $\mu$ l  $\alpha$ MEM complete medium with no added cytokines, after 14 days culture in 5% CO<sub>2</sub> at 37°C, the upper 250 $\mu$ l medium was replenished every 2-3 days. The absolute number of TRAP<sup>+</sup> cells generated was corrected for the number of monocytes in the initial cell suspension and plotted against the initial number of T cells for A: all fractions and B: for unfractionated and CD20 depleted PBMC's. The line of best fit/ trendline and equation were generated using Microsoft Excel 2010. Spearman's rank correlation coefficient  $R_s$  was used to correlate these parameters.

Comparison of CD20 depleted PBMC's using MACS or in vitro rituximab

B cell depletion was accomplished simultaneously, from the same unfractionated PBMC's, via MACS separation with CD20 microbeads or via the addition of RTX at varying concentrations. Although there were insufficient samples to perform statistical analysis, there was as expected reduced numbers of B cells in the MACS and RTX (at RTX concentrations between 0.1-100µg/ml added on day 1) CD20 depleted PBMC fractions compared to unfractionated PBMC's. Moreover, as previously demonstrated, there were greater numbers of TRAP<sup>+</sup> cells generated and TRAP<sup>+</sup> cell numbers corrected for the initial numbers of monocytes, from the CD20 depleted compared to the unfractionated PBMC's (Table 17). Varying concentrations of RTX (0.1-100µg/ml) were also added at the end of the culture (day 14) but generated a similar number of TRAP<sup>+</sup> cells compared to unfractionated PBMC's. The timing of the FACS analysis was also varied between 3, 12 and 24hrs. The effect of this delay in analysis was minimal on the results of the unfractionated and MACS CD20 depleted PBMC's. However, after 24hrs there was a vast reduction in the initial numbers of monocytes, B cells and T cells counted by FACS in all the tubes containing RTX regardless of the RTX concentration, but this did not seem to affect the eventual numbers of TRAP<sup>+</sup> cells generated after 14 days.

**Table 17 Comparison of CD20 depleted mononuclear cells using either magnetic-activated cell sorting or *in vitro* rituximab**

Sample	Initial no. Monocytes	Initial no. B cells	Initial no. T cells	Absolute no. TRAP <sup>+</sup> cells Mean (SD)	Monocyte corrected TRAP <sup>+</sup> cells	TRAP <sup>+</sup> cell circumference Mean (SD)	TRAP <sup>+</sup> cell diameter Mean (SD)
<b>Sample 1 (Female) FACS done after 3hrs</b>							
Unfractionated (UF)	20,451	24,512	112,436	61 (20)	0.298	310 (58)	80 (15)
MACS CD20 <sup>-</sup> cells	25,129	996	75,432	140 (40)	0.557	291 (66)	77 (18)
MACS CD20 <sup>+</sup> cells	40,794	66,662	67,668				
UF + RTX [0.1µg/ml] added Day 1	16,469	16,756	112,650	160 (32)	0.972	351 (88)	93 (23)
UF + RTX [1.0µg/ml] added Day 1	16,227	14,345	101,789	142 (28)	0.875	326 (72)	86 (19)
UF + RTX [10µg/ml] added Day 1	18,424	14,002	101,163	141 (34)	0.765	333 (118)	88 (30)
UF + RTX [100µg/ml] added Day 1	17,920	14,514	105,150	139 (43)	0.776	304 (81)	82 (22)
UF + RTX [0.1µg/ml] added Day 14	20,451	24,512	112,436	63 (26)	0.308	339 (96)	89 (26)
UF + RTX [1.0µg/ml] added Day 14	20,451	24,512	112,436	49 (19)	0.240	318 (73)	84 (21)
UF + RTX [10µg/ml] added Day 14	20,451	24,512	112,436	43 (17)	0.210	335 (126)	87 (29)
UF + RTX [100µg/ml] added Day 14	20,451	24,512	112,436	50 (25)	0.244	309 (111)	83 (27)
<b>Sample 2 (Female) FACS done after 12hrs</b>							
Unfractionated	124,327	27,031	227,758	31 (11)	0.025	346 (83)	89 (22)
MACS CD20 <sup>-</sup> cells	92,373	5,266	265,879	84 (27)	0.091	359 (100)	93 (100)
MACS CD20 <sup>+</sup> cells	90,597	103,818	87,143				
UF + RTX [1.0µg/ml] added Day 1	69,981	14,775	218,540	26 (13)	0.037	353 (162)	87 (39)
<b>Sample 3 (Male) FACS done after 24hrs</b>							
Unfractionated	32,625	20,880	129,195	54 (21)	0.166	345 (86)	88 (20)
MACS CD20 <sup>-</sup> cells	33,571	366	95,812	56 (26)	0.167	325 (91)	85 (25)
MACS CD20 <sup>+</sup> cells	22,053	47,279	36,440				
UF + RTX [0.1µg/ml] added Day 1	2,610	1,305	6,525	89 (38)	3.410	368 (80)	94 (20)
UF + RTX [1.0µg/ml] added Day 1	2,610	1,305	6,525	85 (40)	3.257	335 (119)	89 (31)
UF + RTX [10µg/ml] added Day 1	2,610	1,305	6,525	70 (23)	2.682	338 (74)	89 (19)

TRAP<sup>+</sup> osteoclast-like cells were generated from 500,000 unfractionated and MACS or varying concentrations of RTX-CD20 depleted PBMC's, all in 500µl αMEM complete medium with no added cytokines, after 14 days culture in 5% CO<sub>2</sub> at 37°C, the upper 250µl medium was replenished every 2-3 days. The absolute number of TRAP<sup>+</sup> cells generated was corrected for the number of monocytes in the initial cell suspension. The TRAP<sup>+</sup> cell circumference and cell diameter was also recorded. The initial numbers of monocytes, B cells and T cells was determined by FACS.

FACS: Fluorescence Activated Cell Sorting MACS: Magnetic-Activated Cell Sorting; RTX: rituximab; UF unfractionated peripheral blood mononuclear cells



Effect of *in vitro* rituximab on unfractionated and CD14<sup>+</sup> purified PBMC's

B cell depletion was accomplished via the addition of RTX added simultaneously on day 1 to unfractionated PBMCs and to MACS purified CD14<sup>+</sup> monocytes and the results are included in Table 18. Although there were insufficient samples to perform statistical analysis, the initial monocyte numbers were increased following MACS CD14<sup>+</sup> purification and these purified monocyte fractions generated the highest absolute numbers of TRAP<sup>+</sup> cells that had the largest cell circumference and diameter. However, even though the CD14<sup>-</sup> fractions generated the lowest numbers of TRAP<sup>+</sup> cells, when they were corrected for the initial numbers of monocytes they actually generated the highest percentage of TRAP<sup>+</sup> cells overall, possibly due to the higher numbers of B and T cells in these fractions. Sample 2 was consistent with previous findings i.e. there were greater numbers of TRAP<sup>+</sup> cells generated from the RTX CD20 depleted fractions, this being true for both the unfractionated and CD14<sup>+</sup> fractions. However, the converse was true for sample 1. Additionally, there was a vast reduction in the initial numbers of monocytes, B cells and T cells in the unfractionated PBMC tube containing RTX when the FACS analysis was delayed for 24 hrs and unfortunately the FACS analysis did not work and so there are no initial monocyte, B and T cell counts for all the tubes containing CD14<sup>+</sup> cells plus RTX.

**Table 18 Effect of *in vitro* rituximab on unfractionated and CD14<sup>+</sup> purified peripheral blood mononuclear cells**

Sample	Initial no. Monocytes	Initial no. B cells	Initial no. T cells	Absolute no. TRAP <sup>+</sup> cells Mean (SD)	Monocyte corrected TRAP <sup>+</sup> cells	TRAP <sup>+</sup> cell circumference Mean (SD)	TRAP <sup>+</sup> cell diameter Mean (SD)
<b>Sample 1 (Male) FACS done after 3hrs</b>							
Unfractionated (UF)	48,478	21,216	251,970	82 (47)	0.169	318 (65)	84 (17)
UF + RTX [10µg/ml] added Day 1	47,295	18,465	223,955	63 (18)	0.133	351 (90)	93 (25)
CD14 <sup>+</sup> cells	139,863	2,593	12,737	74 (22)	0.053	425 (125)	107 (29)
CD14 <sup>+</sup> cells + RTX [10µg/ml] added Day 1				11 (8)		360 (115)	92 (29)
CD14 <sup>-</sup> cells	1,808	26,217	319,777	26 (10)	1.438	320 (74)	84 (20)
<b>Sample 2 (Female) FACS done after 24hrs</b>							
Unfractionated (UF)	45,508	20,753	163,147	48 (19)	0.105	350 (159)	91 (33)
UF + RTX [1.0µg/ml] added Day 1	6,088	1,371	8,840	65 (27)	1.068	366 (66)	99 (19)
CD14 <sup>+</sup> cells	100,548	1,629	19,518	106 (31)	0.105	377 (188)	96 (27)
CD14 <sup>+</sup> cells + RTX [1.0µg/ml] added Day 1				141 (19)		339 (93)	93 (25)
CD14 <sup>-</sup> cells	1,108	21,890	121,489	18 (7)	1.625	318 (79)	85 (21)

TRAP<sup>+</sup> osteoclast-like cells were generated from 500,000 unfractionated or MACS CD14 purified PBMC's, with or without the addition of RTX, also CD14 depleted PBMC's, all in 500µl αMEM complete medium with no added cytokines, after 14 days culture in 5% CO<sub>2</sub> at 37°C, the upper 250µl medium was replenished every 2-3 days. The absolute number of TRAP<sup>+</sup> cells generated was corrected for the number of monocytes in the initial cell suspension. The TRAP<sup>+</sup> cell circumference and cell diameter was also recorded. The initial numbers of monocytes, B cells and T cells was determined by FACS.

FACS: Fluorescence Activated Cell Sorting; MACS: Magnetic-Activated Cell Sorting; PBMC: Peripheral Blood Mononuclear Cells; RTX: rituximab; UF unfractionated peripheral blood mononuclear cells.

### 5.3.3 Discussion

The aim of this section was to investigate *in vitro* B cell depletion on osteoclastogenesis in PBMC's isolated from the blood of self-reported healthy volunteers. There was a significant difference in the initial number of B cells, between unfractionated and MACS CD20 depleted PBMC fractions as expected. But there was no significant difference between the initial number of T cells or monocytes between these fractions. Additionally, there was a greater number of TRAP<sup>+</sup> cells generated from the CD20 depleted compared to unfractionated PBMC's and specifically in male volunteers. However, when the TRAP<sup>+</sup> cell numbers were adjusted to account for any differences in initial monocyte number, there was no significant difference between these PBMC fractions. Moreover, solely in the CD20 depleted fraction as the initial number of monocytes increased more TRAP<sup>+</sup> cells were generated and as the initial number of T cells decreased TRAP<sup>+</sup> cells adjusted for the initial number of monocytes increased. CD14<sup>+</sup> monocytes are known to be osteoclast precursor cells (Costa-Rodrigues et al. 2011, Vandooren et al. 2009) and so with the appropriate stimulus the increased generation of TRAP<sup>+</sup> cells with higher numbers of monocytes was predictable. Osteoclast differentiation is known to be critically controlled by RANKL activating its receptor RANK and thereby inducing a signalling cascade leading to the differentiation and fusion of osteoclast precursor cells (Datta et al. 2008). The catabolic effects of RANKL can be counterbalanced by OPG, a soluble decoy receptor which binds and neutralises RANKL, thus inhibiting osteoclastogenesis and inducing osteoclast apoptosis (Blair and Zaidi 2006). A study in mice by Li et al. reported that B lineage cells were responsible for up to 64% of total bone marrow OPG, 45% of which being derived from mature B cells (Li et al. 2007). Thus by depleting CD20 B cells *in vitro*, OPG may also be suppressed and the RANKL/OPG ratio increased in favour of RANKL activated osteoclastogenesis, generating more TRAP<sup>+</sup> osteoclast-like cells. A further study by Weitzmann et al. using human peripheral blood stem cells, also demonstrated that *in vitro* B cells inhibit osteoclastogenesis, via their ability to secrete TGF- $\beta$  and that TGF- $\beta$  inhibits osteoclast formation through its ability to induce OPG in B cells following CD40 activation (Weitzmann et al. 2000).

The conditions available in the laboratory vary significantly from the clinical environment, therefore to represent therapeutic B cell depletion as closely as possible; RTX was used *in vitro* in an attempt to mirror *in vivo* effects and the working concentration of RTX and timing of the FACS analysis was evaluated. However, although the results were comparable to CD20 depletion by MACS separation, RTX was less efficient in depleting B cells. RTX has been shown to induce apoptosis, complement-mediated lysis and antibody-dependent cellular cytotoxicity *in vitro* to deplete B cells and the different outcomes may be dependent on the B

cell stage amongst other factors (Cartron et al. 2004). Additionally the number of B cells was determined by FACS using CD19 antibodies and this may be inaccurate. A study of the addition of RTX to healthy donor PBMC's *in vitro*, reported a complement independent loss of CD19 without causing B cell death. CD19 was transferred from B cells to monocytes and neutrophils during shaving of the RTX-CD20 complex in an Fc dependent manner, the authors therefore suggest that using CD19<sup>+</sup> cell counts may be compromised by this effect (Jones et al. 2012). Additionally the effect of adding RTX to purified monocytes was inconsistent and the FACS analysis was unreliable. Monocytes reportedly compromise the effects of RTX via a monocyte-mediated 'shaving' reaction, leading to complete loss of anti-CD20 antibodies from the surface of B cells (Pederson et al. 2011). More samples are needed to confirm the effects of adding RTX to purified CD14<sup>+</sup> cells in this osteoclast culture.

#### **5.4 The effects of *ex vivo* B cell depletion**

RA is a chronic systemic inflammatory joint disease, in which B cells play an important role (Edwards and Cambridge 2001). RTX, a chimeric monoclonal antibody directed against the B cell-specific membrane protein CD20, is a successful biologic approved in the UK for treatment of patients with severe refractory RA who have had an inadequate response to, or are intolerant of, other DMARDs including at least one anti-TNF- $\alpha$ . (NICE technology appraisal guidance - TA195, August 2010). Clinical trials have shown that RTX effectively depletes B cells in peripheral blood (Nakou et al. 2009, Teng et al. 2007). Therefore, the RA subjects treated with RTX, in the prospective clinical trial described in Chapter 4, were deemed an ideal *ex vivo* model for determining the role of B cells in osteoclastogenesis.

##### **5.4.1 Methods**

Peripheral blood was collected from 5 adult patients enrolled in the prospective clinical trial, comprising RA patients who started RTX after failure of other DMARDs, previously described in Chapter 4. All patients had severe active disease and had an inadequate response to, or were intolerant of; other DMARDs including at least one anti-TNF- $\alpha$ . RTX was administered following recommended protocol and patients who responded to the first RTX course received a second course at 6 months unless they attained a state of low disease activity, in accordance with clinical practice. Patients were assessed at baseline prior to RTX treatment and then every 3 months over a 12 month follow up period and blood samples were collected at each visit.

To investigate the effect of *ex vivo* B cell depletion on osteoclastogenesis, PBMC's were isolated from 10ml EDTA blood within 6hrs by density-gradient centrifugation (Chapter 2 section 2.2.2). The total number of PBMC's was counted and 500,000 cells, suspended in  $\alpha$ MEM complete medium without the addition of exogenous cytokines, were cultured on glass coverslips and bone slices in 24 well plates in 5% CO<sub>2</sub> at 37°C for 14 days, the medium being replaced every 2-3 days, following the procedures described in Chapter 2 section 2.2.2. Additionally, as PBMC's are heterogeneous consisting of subsets of many cells, the number of monocytes, B cells and T cells in the initial cell suspension was determined by FACS analysis (Chapter 2 section 2.2.2). At the end of the culture period the coverslips were stained for TRAP activity, the number of TRAP<sup>+</sup> cells was counted and the mean cell diameter and circumference calculated. The bone slices were stained with toluidine blue to identify resorption pits and the final medium was analysed for  $\beta$ CTX (All methods are described in Chapter 2 section 2.2.2).

Statistical analysis

Details of the statistical analysis are described in Chapter 2 section 2.4.3

**5.4.2 Results**

Five patients with severe, refractory RA were included, all patients received the first RTX infusion but only 4 patients received the second RTX course and completed the study, one patient dropped out before the 6 month visit. The baseline characteristics are included in Table 19. Briefly the group consisted of 4 post-menopausal females (aged 55-79yrs) and 1 male (aged 47yrs); all 5 patients were RF and ACPA positive. No patient was on prednisolone, however 2 patients received MTX and 1 patient was on a calcium/vitamin D supplement throughout the study period. All patients had normal bone biochemistry; corrected calcium (CCa), phosphate (PO<sub>4</sub>) and total alkaline phosphatase (ALP), but all females had low serum 25OHD, 2 of which also had increased PTH levels, at baseline. The clinical, BMD and bone marker data per patient, per visit is shown in Table 20, this data was collected as part of the prospective clinical trial described in Chapter 4. The change in disease activity, inflammation and bone turnover was variable and the majority of patients seemed to have a slight decrease in BMD over 12 months.

**Table 19** Baseline trial data for five rheumatoid arthritis patients

ID	Age (yrs)	Gender	RA duration (yrs)	Menopause	Smoke Status	BMI (kg/m <sup>2</sup> )	MTX (mg/wk)	Steroid (mg/day)	Ca/Vit D (tab/day)	2nd RTX course	Study complete	ACPA	RF	CCa (mmol/L)	PO <sub>4</sub> (mmol/L)	ALP (U/L)	25OHD (nmol/L)	PTH (ng/L)
0206	55.4	Female	4	Yes	Never	31.5	No	No	2	Yes	Yes	POS	POS	2.16	1.07	86	26.5	83.9
0207	79.8	Female	27	Yes	Former	25.1	No	No	No	No	No	POS	POS	2.23	1.07	91	14.0	73.6
0208	61.6	Female	11	Yes	Never	22.4	No	No	No	Yes	Yes	POS	POS	2.19	1.12	57	17.5	29.2
0209	66.2	Female	17	Yes	Current	25.0	20	No	No	Yes	Yes	POS	POS	2.25	1.06	103	18.8	37.7
0210	47.0	Male	2	N/A	Former	33.3	25	No	No	Yes	Yes	POS	POS	2.20	0.94	75	58.0	27.3

25OHD: 25 Hydroxy Cholecalciferol; ALP: Total Alkaline Phosphatase; ACPA: Anti-cyclic Citrullinated Peptide Antibody; BMI: Body Mass Index; Ca/VitD: Calcium/Vitamin D supplement; CCa: Corrected calcium; MTX: Methotrexate; PTH: Parathyroid Hormone; PO<sub>4</sub>: Phosphate; RA: Rheumatoid Arthritis; RF: Rheumatoid Factor; RTX: Rituximab.

Reference ranges:

ALP 30-120U/L; CCa 2.1-2.6mmol/L; PO<sub>4</sub> 0.8-1.5mmol/L; PTH 12-72ng/L; 25OHD <25nmol/L =deficient, 25-50nmol/L =insufficient, 50-75nmol/L =adequate, >75nmol/L =optimum.

**Table 20 Bone marker and bone mineral density results at each visit for five rheumatoid arthritis patients**

ID	Visit (month)	HAQ	ESR (mm/hr)	CRP (mg/L)	TJC	SJC	VAS (mm)	DAS28	eGFR (ml/min/1.73m <sup>2</sup> )	CD19 (x10 <sup>9</sup> /L)	PINP (µg/L)	BALP (µg/L)	βCTX (ng/L)	TRAP5b (U/L)	SCL (pmol/L)	DKK1 (pmol/L)	LS BMD (g/cm <sup>3</sup> )	MN BMD (g/cm <sup>3</sup> )	MT BMD (g/cm <sup>3</sup> )
0206	0	2.125	37	9.0	16	9	43	5.47	90	0.420	37.8	16.8	504	2.9	31.5	77.6	1.562	1.061	1.092
	3	2.500	37	8.1	18	3	54	5.36	94	0.001	56.5	16.1	247	2.8	43.3	81.0			
	6	2.750	20	5.4	19	6	64	5.63	95	0.370	49.4	19.9	257	3.0	41.8	70.0			
	9	2.625		8.2	20	3	44	5.35	97	0.674	44.8	21.8	218	3.3	52.5	65.7			
	12	2.750	35	9.8	20	11	55	5.99	80		47.1	22.2	339	3.5	52.9	74.3	1.561	1.093	1.074
0207	0	2.500	55	30.9	10	4	52	5.27	80	0.387	52.4	21.2	498	3.5	47.7	65.9	1.122	0.576	0.661
	3	1.625		30.6	1	0	4	2.82	87	0	57.5	15.9	461	3.1	33.2	52.6			
0208	0	1.375	9	0.9	6	4	31	3.33	83	0.384	20.7	11.7	318	2.5	37.6	119.4	1.103	0.965	1.006
	3	1.375	10	2.5	6	8	70	4.51	86	0	36.7		339	2.1	35.9	83.8			
	6	1.500	10	2.9	6	10	72	4.64	102	0.001	25.4	13.8	269	2.6	30.2	127.8			
	9	1.750	10	3.8	14	9	72	5.41	86	0	29.8	14.3	166	2.7	32.2	236.9			
	12	1.625	27	10.3	15	13	65	5.92	93		20.7	11.9	274	2.8	33.0	150.8	1.116	0.916	0.929
0209	0	1.500	29	7.2	22	15	77	6.51	54	0.039	62.6	28.8	269	3.6	55.3	45.4	0.949	0.928	0.940
	3	1.375	10	4.2	5	4	33	3.82	98	0.001	47.3	28.1	470	2.4	64.2	57.4			
	6	1.375	17	22.3	16	11	67	6.2	78	0.002	51.0	33.7	504	2.8	57.1	45.0			
	9	1.625	5	2.2	12	2	20	3.96	72	0	51.5	27.5	665	2.7	79.9	24.7			
	12	1.625	2	2.6	9	13	41	4.63	74	0	41.9	30.1	745	3.9	76.7	58.5	0.941	0.922	0.906
0210	0	2.125	2	0.4	26	11	87	5.97	97	0.370	24.2	15.3	181	2.7	45.5	48.3	1.439	1.153	1.268
	3	2.125	8	0.5	28	24	81	6.44	102	0	40.2	15.9	236	3.0	50.3	45.6			
	6	1.875	12	6.2	24	10	89	6.54	101	0.008	29.2	17.5	97	2.8	51.7	54.3			
	9	2.375	20	29.1	27	23	76	7.51	94		26.1	16.3	216	2.8	57.6	59.5			
	12	2.500	2	0.3	22	21	76	5.94	87	0.001	16.8	18.1	164	2.2	52.5	67.3	1.409	1.171	1.239

βCTX: β-isomerised carboxy terminal telopeptide of type I collagen; BALP: Bone Specific Alkaline Phosphatase; BMD: Bone Mineral Density; CRP: C-Reactive Protein; CD19: Cluster of Differentiation19; DAS28: Disease Activity Score in 28 joints; DKK-1: Dickkopf-related protein 1; ESR: Erythrocyte Sedimentation Rate; eGFR: estimated Glomerular Filtration Rate; HAQ: Health Assessment Questionnaire; LS: Lumbar Spine mean L2-L4; MN: Mean of left and right side neck of femur; MT: Mean of left and right side total femur; PINP: Procollagen type 1 amino-terminal propeptide; SCL: Sclerostin; SJC: Swollen Joint Count; TRAP5b: Tartrate Resistant Acid Phosphatase isoform 5b; TJC: Tender Joint Count; VAS: Visual Analogue Scale.

#### Reference ranges:

All: CRP <5mg/L; eGFR >60ml/min/1.73m<sup>2</sup>.

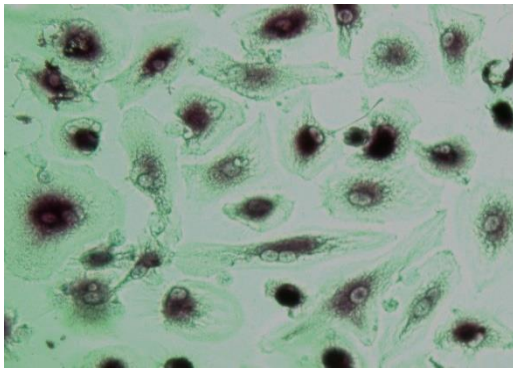
Postmenopausal females: BALP 3.8-22.6µg/L; βCTX 104-1008ng/L; PINP 16.3-73.9µg/L; TRAP5b 1.5-4.9U/L.

Females: DKK-1 12.4-72.2pmol/L; ESR 5-15mm/hr; SCL 21.6-68.1pmol/L.

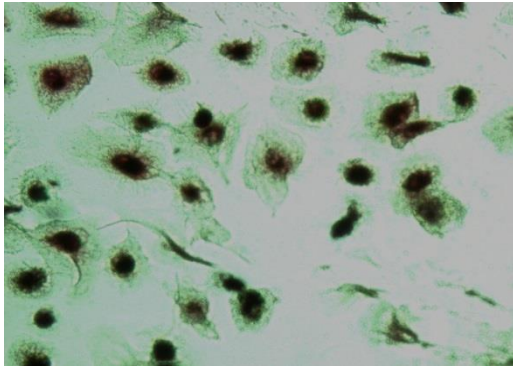
Males: BALP 3.7-20.9µg/L; βCTX 0-854ng/L; DKK-1 15.5-80.8pmol/L; ESR 2-10mm/hr; PINP 15.1-58.6µg/L; SCL 26.4-68.0pmol/L; TRAP5b 1.9-4.8U/L.



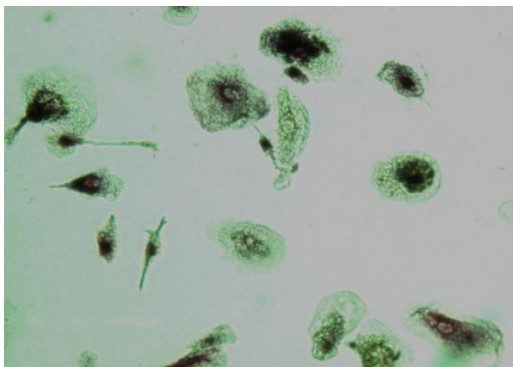
To investigate whether B cell depletion with RTX affects osteoclastogenesis in this subgroup of patients, PBMC's were cultured, without the addition of exogenous cytokines, at each visit and the generation of TRAP<sup>+</sup> osteoclast-like cells and evidence of bone resorption was recorded after 14 days. A typical pattern of change in the number and appearance of TRAP<sup>+</sup> osteoclast-like cells per visit is presented in Figure 31 and results are included in Table 21. There was a significant decrease ( $p=0.046$ ) in the initial number of B cells in the PBMC fraction analysed by FACS, from baseline to 12 months, as expected following RTX therapy in these patients. There was no significant difference in the number of T cells ( $p=0.230$ ) or monocytes ( $p=0.064$ ), however there was a significant upward trend in the number of monocytes ( $p=0.014$ ) from baseline to 12 months but there was a significant negative correlation ( $R_s = -0.638$ ;  $p=0.014$ ) between the initial number of monocytes and the number of TRAP<sup>+</sup> cells generated (Figure 32). Moreover, there was a significant decrease ( $p=0.012$ ) in the absolute numbers of TRAP<sup>+</sup> cells generated over 12 months. TRAP<sup>+</sup> cell numbers were also adjusted to account for any differences in initial monocyte number and there was still a significant decrease ( $p=0.010$ ) over 12 months, individual patient results are illustrated in Figure 33. There was no significant difference in TRAP<sup>+</sup> cell circumference ( $p=0.104$ ) or cell diameter ( $p=0.068$ ) or the  $\beta$ CTX concentration in the final cell supernatant ( $p=0.501$ ). There was a significant positive correlation ( $R_s = 0.583$ ;  $p=0.029$ ) between the initial number of B cells and the number of TRAP<sup>+</sup> cells generated corrected for the number of monocytes. As the number of B cells decreased the number of TRAP<sup>+</sup> cells generated decreased (Figure 34). Conversely, there was a borderline significant negative correlation ( $R_s = -0.533$ ;  $p=0.050$ ) between the initial number of T cells and the number of TRAP<sup>+</sup> cells generated corrected for the number of monocytes. As the number of T cells decreased the number of TRAP<sup>+</sup> cells generated increased (Figure 35).



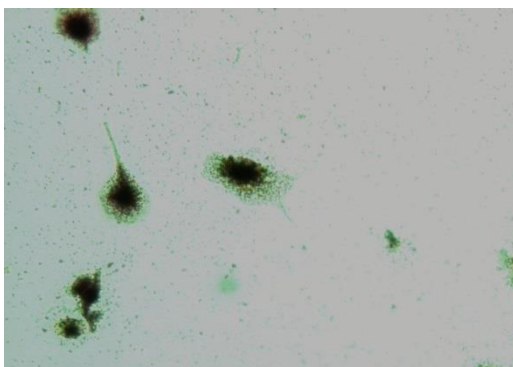
A Baseline



B 3 months



C 6 months



D 12 months

**Figure 31 An example of a patient culture at baseline, 3, 6 and 12 months**

TRAP stained osteoclast-like cells generated from 500,000 unfractionated PBMC's in 500 $\mu$ l  $\alpha$ MEM complete medium with no added cytokines, after 14 days culture in 5% CO<sub>2</sub> at 37°C, the upper 250 $\mu$ l medium was replenished every 2-3 days. The cells were stained using an optimised Sigma TRAP kit. ( $\times$ 200 magnification). Blood was collected at; A: Baseline, prior to RTX infusion; B: after 3 months; C: after 6 months; D: after 12 months treatment.

**Table 21 Median cell counts at baseline and at 3, 6 and 12 month post-rituximab from four rheumatoid arthritis patient cultures**

	<b>Baseline median (IQR)</b>	<b>3 month median (IQR)</b>	<b>6 month median (IQR)</b>	<b>12 month median (IQR)</b>	<b>p value difference by visit</b>	<b>p value trend by visit</b>
<b>Initial no. monocytes</b>	31607 (27838,35169)	50573 (31507,68923)	66761 (47572,85012)	76537 (38901,87097)	0.064	<b>0.014</b>
<b>Initial no. B cells</b>	15457 (10575,20857)	352 (182,525)	433 (96,1276)	197 (194,685)	<b>0.046</b>	<b>0.047</b>
<b>Initial no. T cells</b>	71725 (23750,143603)	124725 (79709,194930)	121741 (25337,294781)	191818 (139331,348075)	0.230	0.053
<b>Absolute no. TRAP<sup>+</sup> cells</b>	137 (132,145)	90 (74,97)	34 (27,34)	21 (12,79)	<b>0.012</b>	<b>0.003</b>
<b>Monocyte corrected TRAP<sup>+</sup> cells</b>	0.44 (0.38,0.51)	0.19 (0.13,0.25)	0.04 (0.04,0.07)	0.05 (0.01,0.10)	<b>0.010</b>	<b>0.003</b>
<b>TRAP<sup>+</sup> cell circumference</b>	361 (344,391)	348 (308,375)	330 (289,335)	299 (251,322)	0.104	<b>0.014</b>
<b>TRAP<sup>+</sup> cell diameter</b>	90 (85,99)	89 (79,98)	81 (72,83)	77 (60,82)	0.068	<b>0.012</b>
<b>Final <math>\beta</math>CTX concentration</b>	5.4 (1.0,9.8)	7.2 (4.2,14.1)	3.3 (3.1,6.5)	2.0 (1.3,4.9)	0.501	0.279

The data were not normally distributed and so results were expressed as medians and interquartile range. The Kruskal-Wallis test was used to determine if there was a statistically significant difference between visits and the nptrend statistic in Stata 11 was used to determine if there was a statistically significant trend in the results from baseline to 12 months. P values  $\leq 0.05$  were considered statistically significant.

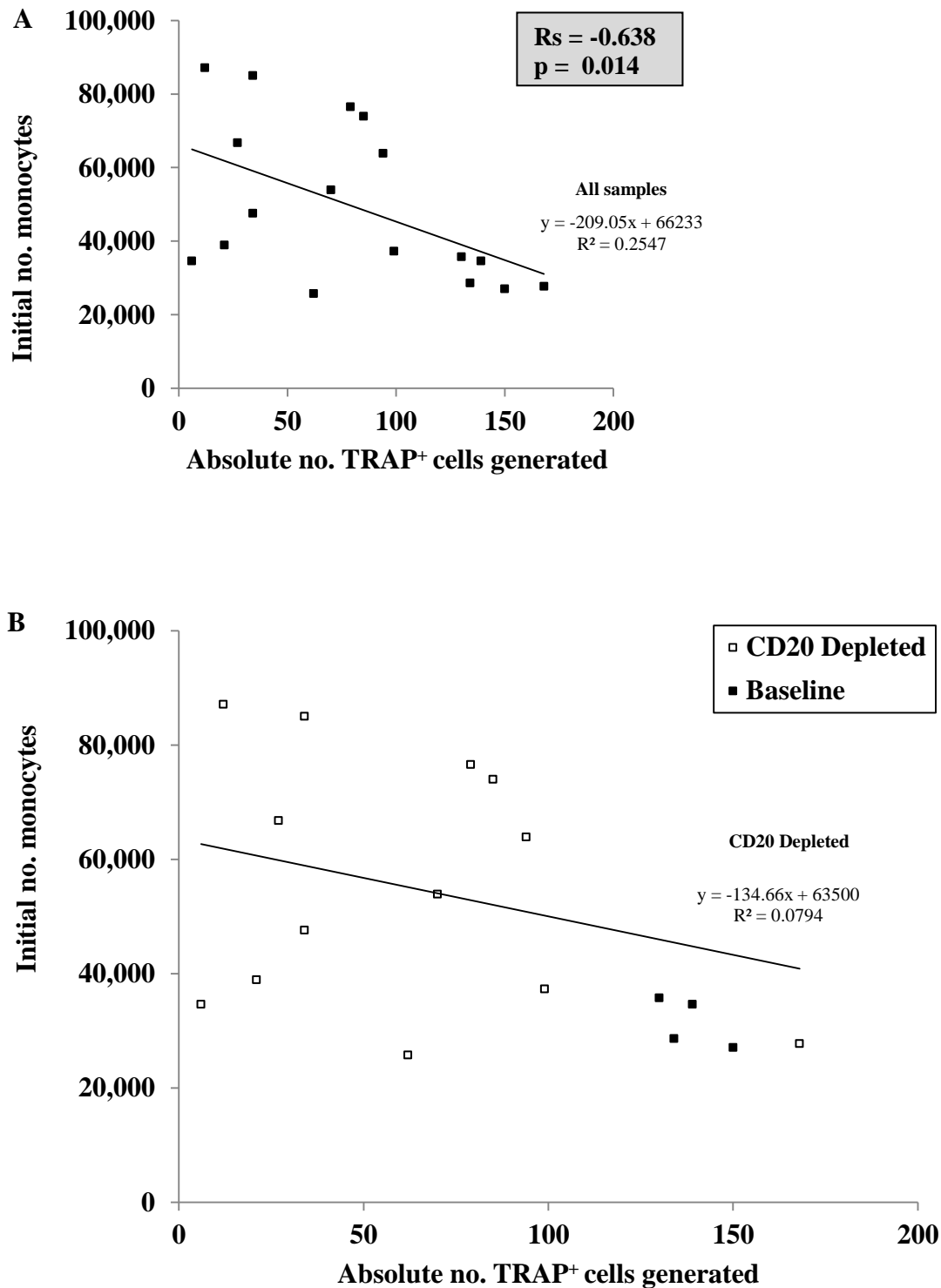


**Figure 32** The effect of the initial number of monocytes on TRAP<sup>+</sup> cells generated from four rheumatoid arthritis patient cultures

TRAP<sup>+</sup> osteoclast-like cells were generated from 500,000 unfractionated PBMC's in 500µl αMEM complete medium with no added cytokines, after 14 days culture in 5% CO<sub>2</sub> at 37°C, the upper 250µl medium was replenished every 2-3 days. The absolute number of TRAP<sup>+</sup> cells generated each visit was plotted against the initial number of monocytes for A: All samples and B: Baseline and following CD20 depletion. The line of best fit/ trendline and equation were generated using Microsoft Excel 2010. Spearman's rank correlation coefficient  $R_s$  was used to correlate these parameters.

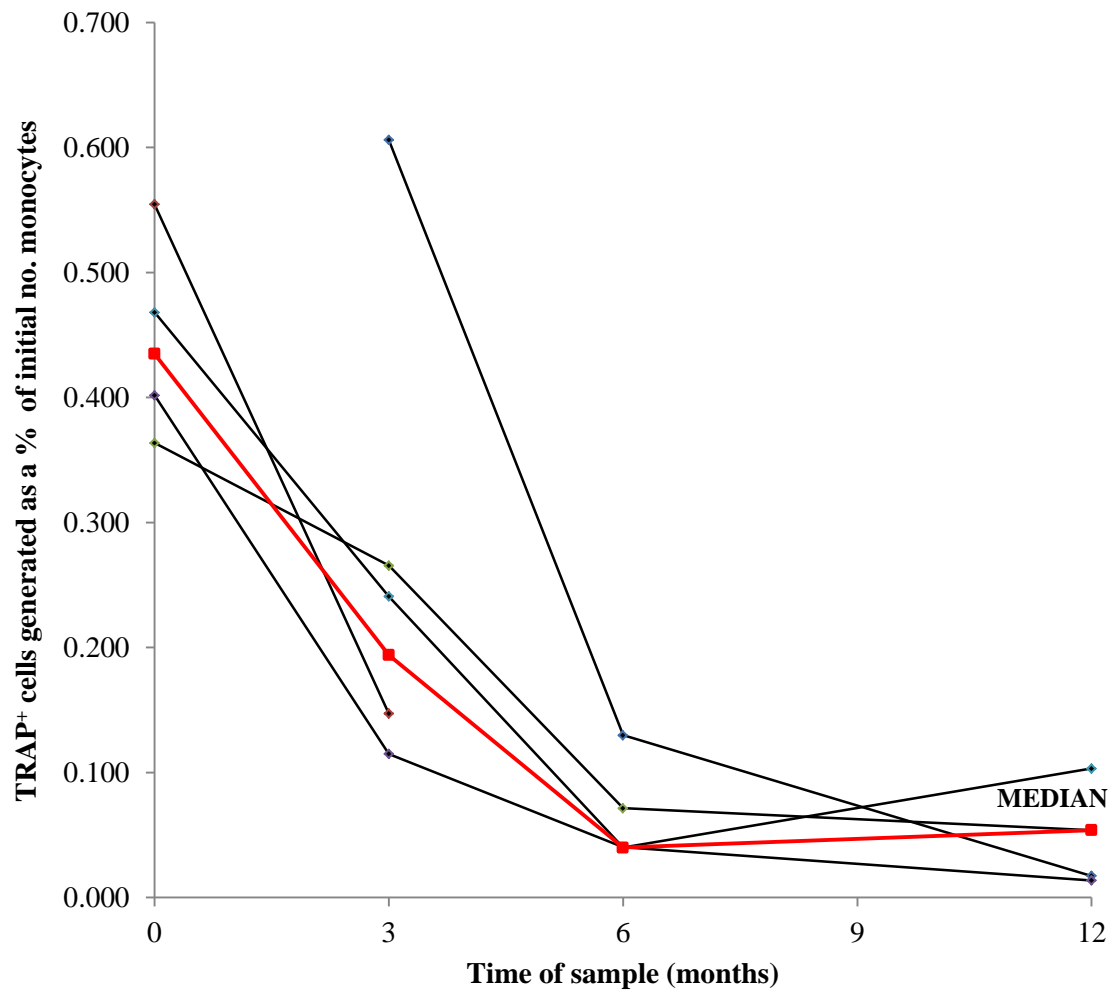


**Figure 33 TRAP<sup>+</sup> cells generated from five rheumatoid arthritis patient cultures before and 3, 6, 12 months post rituximab**

TRAP<sup>+</sup> osteoclast-like cells were generated from 500,000 unfractionated PBMC's in 500 $\mu$ l  $\alpha$ MEM complete medium with no added cytokines, after 14 days culture in 5% CO<sub>2</sub> at 37°C, the upper 250 $\mu$ l medium was replenished every 2-3 days. The absolute number of TRAP<sup>+</sup> cells generated each visit was corrected for the number of monocytes in the initial cell suspension. The dotted line represents the median values.

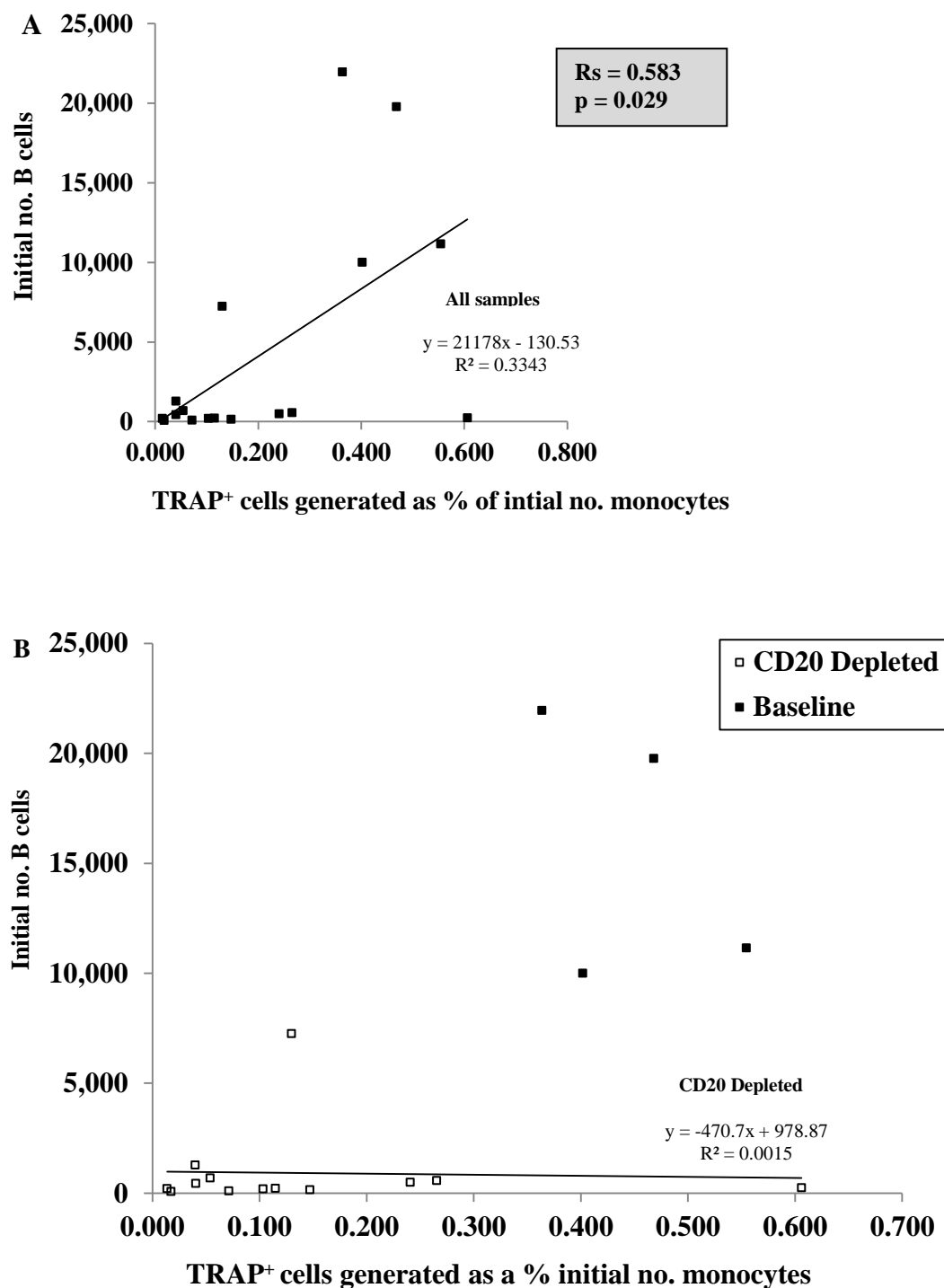


**Figure 34** The effect of the initial number of B cells on TRAP<sup>+</sup> cells generated from four rheumatoid arthritis patient cultures

TRAP<sup>+</sup> osteoclast-like cells were generated from 500,000 unfractionated PBMC's in 500 $\mu$ l  $\alpha$ MEM complete medium with no added cytokines, after 14 days culture in 5% CO<sub>2</sub> at 37°C, the upper 250 $\mu$ l medium was replenished every 2-3 days. The absolute number of TRAP<sup>+</sup> cells generated each visit was corrected for the number of monocytes in the initial cell suspension and plotted against the initial number of B cells for A: All samples and B: Baseline and following CD20 depletion. The line of best fit/trendline and equation were generated using Microsoft Excel 2010. Spearman's rank correlation coefficient Rs was used to correlate these parameters.

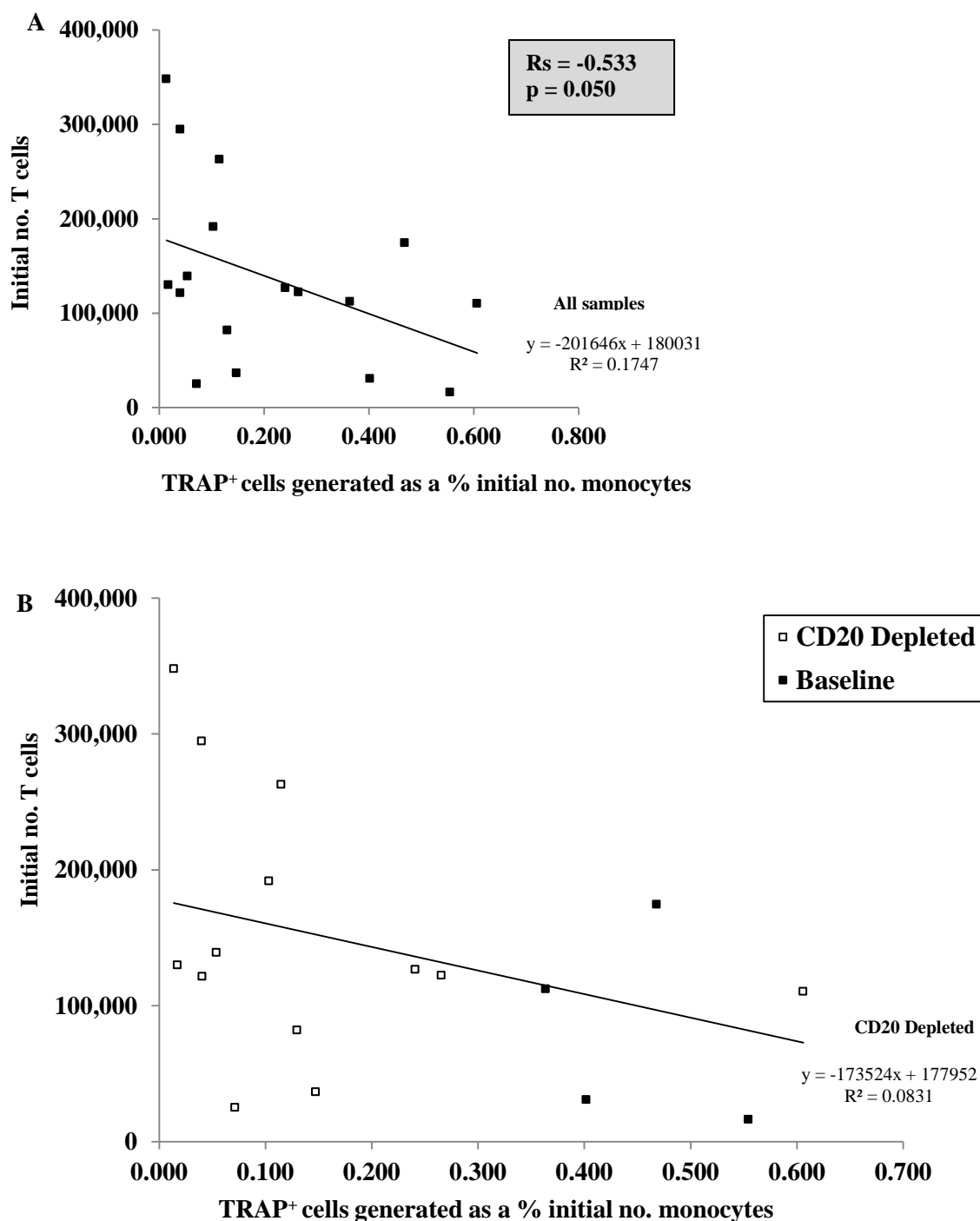


**Figure 35** The effect of the initial numbers of T cells on TRAP<sup>+</sup> cells generated from four rheumatoid arthritis patient cultures

TRAP<sup>+</sup> osteoclast-like cells were generated from 500,000 unfractionated PBMC's in 500 $\mu$ l  $\alpha$ MEM complete medium with no added cytokines, after 14 days culture in 5% CO<sub>2</sub> at 37°C, the upper 250 $\mu$ l medium was replenished every 2-3 days. The absolute number of TRAP<sup>+</sup> cells generated each visit was corrected for the number of monocytes in the initial cell suspension and plotted against the initial number of T cells for A: All samples and B: Baseline and following CD20 depletion. The line of best fit/trendline and equation were generated using Microsoft Excel 2010. Spearman's rank correlation coefficient was used to correlate these parameters.

### **5.4.3 Multiple regression analysis to explore factors affecting osteoclastogenesis**

There were not enough samples to carry out multiple regression analysis on the healthy volunteer and RA patient samples separately so the data were combined to explore predictors of osteoclastogenesis in two multiple regression models (Stepwise analysis for each model included in Appendix C).

**Model 1:** the model investigated the effect of the following variables; initial numbers of monocytes, B cells, T cells, age and gender, on the outcome i.e. TRAP<sup>+</sup> cells generated from unfractionated PBMCs from healthy volunteers and baseline RA patient samples.

In this model it was found that in unfractionated cells, B cells were borderline significant predictors of osteoclastogenesis ( $p=0.045$ ) but this effect was predominantly dependent on the subject i.e. healthy volunteer or RA patient ( $p<0.001$ ).

**Model 2:** the model investigated the effect of the following variables; initial numbers of monocytes, B cells, T cells, age and gender, on the outcome i.e. TRAP<sup>+</sup> cells generated from *in vitro* CD20 depleted PBMCs in healthy volunteers and RA patient samples 12 months after RTX.

In this model it was found that when cells are CD20 depleted, monocytes significantly increase osteoclastogenesis ( $p=0.002$ ) and to a lesser extent T cells suppress osteoclastogenesis ( $p=0.016$ ).

In summary these results indicate that in CD20 depleted cells, monocytes increase and T cells suppress osteoclastogenesis. However, at baseline i.e. in the presence of CD20 cells these effects are not significant and it is the disease state itself that has the most significant effect on osteoclastogenesis.



#### 5.4.4 Discussion

The aim of this section was to investigate B cell depletion with RTX, *ex vivo*, on osteoclastogenesis in PBMC's isolated from the blood of patients with refractory RA. There was a significant decrease in B cells in the PBMC fraction following RTX therapy, this was verified by the CD19 results in peripheral blood and confirmed B cell depletion as expected in these patients consistent with the results of other clinical trials using RTX (Nakou et al. 2009, Teng et al. 2007). There was, however, no significant difference in the number of T cells or monocytes in the PBMC fraction from baseline to 12 months, although as the B cells decreased there was an apparent increase in the percentage of monocytes in the fraction counted by FACS. Since CD14<sup>+</sup> monocytes are known to be osteoclast precursor cells (Costa-Rodrigues et al. 2011, Vandooren et al. 2009), with the appropriate stimulus an increase in the resulting number of TRAP<sup>+</sup> cells might have been expected. Yet, there was a significant decrease in both the absolute numbers of TRAP<sup>+</sup> cells and TRAP<sup>+</sup> cells adjusted to account for any differences in initial monocyte number, from baseline to 12 months in these patients. Additionally, there was a significant positive correlation between the initial number of B cells and the number of TRAP<sup>+</sup> cells generated corrected for the number of monocytes. As the number of B cells decreased the number of TRAP<sup>+</sup> cells generated also decreased. Conversely, there was a borderline significant negative correlation between the initial number of T cells and the number of TRAP<sup>+</sup> cells generated corrected for the number of monocytes. As the number of T cells decreased the number of TRAP<sup>+</sup> cells generated increased. The differentiation and activation of osteoclasts requires the binding of RANKL to its receptor RANK on osteoclast precursors (Lacey et al. 1998). Activated B cells, involved in the development of inflammatory arthritis, are known to express RANKL as well as other cytokines that are involved in bone resorption (Horowitz et al. 2010, Yeo 2011), switched memory B cells (CD27<sup>+</sup>IgD<sup>-</sup>) having the highest propensity (Meednu et al. 2015). These results suggest that depletion of RANKL-expressing B cells may contribute to the inhibition of bone erosion by RTX. However, there are several limitations to this work; the extent to which *in vitro* osteoclastogenesis reflects the *in vivo* situation in the inflamed joint remains in question and as this was a small patient sample, these results would have to be replicated in a much larger group. Although, several studies have reported that the B cell-targeted therapy, RTX, inhibits the progression of structural joint damage in RA (Keystone 2009, Boumans 2012).

## 5.5 Conclusion

The initial aim of this Chapter was to create a robust and reproducible protocol for osteoclast formation and characterisation from peripheral blood *in vitro*, without the addition of endogenous substances. Subsequently to use this culture system to investigate the potential role of B cells on osteoclastogenesis; using healthy volunteer blood depleted of B cells *in vitro*, plus blood from RA patients following *in vivo* B cell depletion.

Predictably, there was a significant difference in the initial number of B cells; between unfractionated and CD20 depleted PBMC fractions in the healthy volunteers, also between baseline and following RTX therapy in the RA patients; but no significant difference between the initial number of T cells or monocytes in either group. Interestingly, significantly greater numbers of TRAP<sup>+</sup> cells were generated from *in vitro* CD20 depleted compared to unfractionated PBMCs in healthy volunteer blood, however this was not significant after adjustment for initial monocyte number. Moreover, as the initial number of monocytes increased more TRAP<sup>+</sup> cells were generated and as the initial number of T cells decreased TRAP<sup>+</sup> cells adjusted for the initial number of monocytes increased, specifically in the CD20 depleted fraction. Whereas, in RA patients following *ex vivo* CD20 depletion with RTX, there were significantly reduced numbers of TRAP<sup>+</sup> cells generated and this number remained significant even after adjustment for the initial number of monocytes, when compared to baseline. Furthermore, as the initial number of monocytes decreased more TRAP<sup>+</sup> cells were generated and as the initial number of T cells decreased TRAP<sup>+</sup> cells adjusted for the initial number of monocytes increased. Although the trendline for all samples and CD20 depleted samples were comparable there were too few samples to correlate the fractions separately. Additionally, *in vitro* osteoclastogenesis was significantly higher in the baseline RA samples compared to unfractionated PBMC's from healthy controls. These results were consistent with the IODA study; *in vitro* osteoclastogenesis varied among healthy individuals and the authors hypothesized that increased osteoclastogenesis was a potential marker for the presence of RA, also osteoclasts from RA patients showed lower apoptotic rates and there was no difference in bone resorptive activity between RA patients and controls. (Durand et al. 2011). In summary the multiple linear regression results indicate that in CD20 depleted cells, monocytes increase and T cells suppress osteoclastogenesis. However, at baseline i.e. in the presence of CD20 cells these effects are not significant and it is the disease state itself that has the most significant effect on osteoclastogenesis.

# **Chapter 6**

## **Discussion**



## Chapter 6. Discussion

### 6.1 Discussion

The aim of this project was to address the role of human B cells in bone turnover. Given the impact of B-cells in the pathogenesis of RA and apparent importance in regulating bone cell activity it was postulated that prolonged B cell depletion in patients with RA may have a beneficial effect on the bone loss that would otherwise be expected in active disease. It was proposed to initially explore the effects of *in vivo* B cell depletion on serum BTMs before and after RTX treatment in a cohort of patients with severe RA. Subsequently to confirm and extend these findings in a second cohort of RA patients; to additionally measure the change in bone density and to explore factors that may influence the outcome such as change in disease activity and vitamin D status. Finally to evaluate and create a robust, reproducible protocol for osteoclast formation and characterisation from peripheral blood *in vitro*, representative of *in vivo* conditions without the addition of endogenous substances and to use this culture system to investigate the potential role of B cells on osteoclastogenesis; using healthy volunteer blood depleted of B cells *in vitro*, plus blood from RA patients following B cell depletion *ex vivo*.

Preliminary results from the pilot study indicated that there was a significant suppression in bone resorption accompanied to a lesser degree by an increase in bone formation in RA patients six months after B cell depletion. The fact that there was a significant correlation between the change from baseline in  $\beta$ CTX and DAS28 in this cohort indicated that the anti-resorptive action and anti-inflammatory therapeutic response were related. This was expected as decreased bone resorption is likely to be due to a combination of diminished osteoclast activity, which results from decreased B-cell mediated osteoclastogenesis, decreased systemic inflammatory cytokines and increased physical activity following RTX treatment. However, this significant reduction in bone resorption was not replicated in a second group of RA patients treated with RTX over twelve months. Although there was a significant increase in bone formation, BMD fell at the femur sites but was maintained at the lumbar spine and forearm. Nevertheless, there was still a significant reduction in inflammatory markers and disease activity following B cell depletion with RTX, indicating that the drug was effective in reducing the inflammation of RA in this patient cohort. There were several differences between the two cohorts to explain these results. Patients in the pilot study had lower bone resorption at baseline and 37% of these patients were taking bisphosphonates which are known to induce osteoclast apoptosis (Lems 2007); none of the patients in the prospective

study were treated for osteoporosis with bisphosphonates, calcitonin, strontium ranelate, denosumab or teriparatide prior to/ or during the study. However, there was a higher percentage of post-menopausal women in the prospective cohort; 79% compared to 58% and the loss of BMD at the femur sites was more pronounced in these women. Oestrogen decline post-menopause induces accelerated bone loss (Garnero et al. 2000) and although oestrogen withdrawal is associated with a significant expansion in the mature B cell population, the role of these cells as mediators of the bone loss remains unclear.

Ageing is also a risk factor; the development of an inflammatory environment during ageing can also lead to increased bone resorption and loss of BMD (Li et al. 2014). Furthermore, a higher percentage of the post-menopausal women were current smokers (39% compared to 18% in the pilot study). Smoking may adversely influence the severity of RA (Saag et al. 1997) and RA patients who smoke have a higher need for DMARDs and are reportedly more likely to show a poor response to biologics treatment such as TNF inhibitors (Mattey et al. 2009). Tobacco also increases bone resorption and affects bone mass by alterations in sex hormone metabolism, but also importantly by alterations on the vitamin D-PTH axis (Supervia et al. 2006). The prospective study results were confounded by a high prevalence of vitamin D deficiency and these patients had a significant decrease in femur BMD and evidence of higher bone turnover i.e. an increase in serum TRAP5b compared to decreased levels over 12 months in patients with 'normal' 25OHD. Vitamin D influences bone quality and is important for maintaining bone density, research indicates that higher vitamin D levels may prevent the occurrence of osteoporosis at the femoral neck, but not at the lumbar spine L2–4 (Yoshimura et al. 2015). Although post-menopausal women had the lowest median 25OHD concentration in this cohort, there was no significant difference in median levels between males, pre- or post-menopausal women, so vitamin D deficiency may not explain why the post-menopausal women lost BMD more than pre-menopausal women or men. Additionally, as there were no control groups it was difficult to establish whether depletion of B cells had in fact slowed down the expected bone loss in the prospective cohort. The relatively short duration of follow-up and small number of participants limited the power of the study and the reduction in inflammation and disease activity could increase mobility and possibly reduce the need of drugs such as glucocorticoid which may then improve bone health.

Results of the *in vitro* osteoclastogenesis indicated that significantly greater numbers of TRAP<sup>+</sup> cells were generated from *in vitro* CD20 depleted when compared to unfractionated PBMCs in healthy volunteer blood. Moreover, as the initial number of monocytes increased

more TRAP<sup>+</sup> cells were generated and as the initial number of T cells decreased TRAP<sup>+</sup> cells adjusted for the initial number of monocytes increased, specifically after B cell depletion. In contrast, there were significantly reduced numbers of TRAP<sup>+</sup> cells generated in PBMCs from RA patients following *ex vivo* CD20 depletion with RTX compared to baseline. Furthermore, as the initial number of monocytes decreased more TRAP<sup>+</sup> cells were generated and as the initial number of T cells decreased TRAP<sup>+</sup> cells adjusted for the initial number of monocytes increased. Additionally, *in vitro* osteoclastogenesis was significantly higher in the baseline RA samples compared to unfractionated PBMC's from healthy controls. In summary multiple regression analysis indicated that in CD20 depleted cells, monocytes increase and T cells suppress osteoclastogenesis. However, at baseline i.e. in the presence of CD20 cells these effects are not significant and it is the disease state itself that has the most significant effect on osteoclastogenesis. These results were consistent with the IODA study; the authors hypothesized that increased osteoclastogenesis was a potential marker for the presence of RA (Durand et al. 2011). CD14<sup>+</sup> monocytes are known to be osteoclast precursor cells (Costa-Rodrigues et al. 2011, Vandooren et al. 2009) and so with the appropriate stimulus the increased generation of TRAP<sup>+</sup> cells with higher numbers of monocytes was predictable in healthy volunteers. B cells are an important source of OPG (Li et al. 2007), thus by depleting CD20 B cells *in vitro*, OPG may also be suppressed and the RANKL/OPG ratio increased in favour of RANKL activated osteoclastogenesis, generating more TRAP<sup>+</sup> osteoclast-like cells. This is consistent with the fact that B-cell KO mice were observed to be osteoporotic and deficient in OPG, suggesting that the production of OPG by B cells outweighs the production of RANKL under basal conditions (Li et al. 2007). RANKL is required for osteoclastogenesis and plays a key role in mediating bone erosion. It is now known that B cells also contribute to RANKL production in the inflamed rheumatoid joint (Yeo et al. 2011) and in particular switched memory B cells have the greatest propensity to produce RANKL (Meednu et al. 2015). Meednu et al. also hypothesise that the role of B cells in bone erosion is developmental and stage-dependent; they confirmed that stimulated B cells promote *in vitro* osteoclastogenesis from monocytes in a RANKL dependent manner (Meednu et al. 2015). Recently a subset of B cells, expressing FcRL4, has been identified in the rheumatoid synovium that are capable of producing RANKL and TNF- $\alpha$  and these pathogenic B cells are reportedly not found in healthy individuals (Yeo et al. 2015). FcRL4<sup>+</sup> B cells also express high levels of CD20 and are therefore significantly reduced with RTX (Yeo et al. 2015).

## 6.2 Conclusion

Preliminary results indicated that there was a significant suppression in bone resorption accompanied to a lesser degree by an increase in bone formation in RA patients six months after RTX, possibly due to a direct effect on osteoclasts and osteoblasts, respectively, or at least partially explained by the decreased inflammation and disease activity. However, the significant reduction in bone resorption was not replicated in a second cohort of RA patients treated with RTX over twelve months. Nevertheless there was a significant reduction in inflammatory markers and disease activity following B cell depletion, indicating that the drug was effective in reducing the inflammation of RA. Additionally, despite a significant increase in bone formation, BMD fell at the femur sites in postmenopausal women, but was maintained at the lumbar spine and forearm. Men and premenopausal women did not lose BMD and also had lower bone resorption indicating they had lower bone cell activity. But the results were confounded by a high prevalence of vitamin D deficiency and these patients had significant falls in femur BMD and evidence of higher bone turnover. Furthermore, as there were no control groups it was difficult to establish whether depletion of B cells had in fact slowed down the expected bone loss in these patients. Results of *in vitro* osteoclastogenesis indicated that in healthy subjects B cell depletion tended to increase osteoclast formation, suggesting that the production of OPG by B cells outweighed the production of RANKL under basal conditions. In contrast, in pro-inflammatory states, where B cells are activated e.g. RA, B cells produce cytokines like RANKL that stimulate osteoclastogenesis resulting in an increased production of osteoclasts. In summary when B cells are depleted, monocytes increase and T cells suppress osteoclastogenesis. However, in the presence of B cells these effects are not significant and it is the disease state itself that has the most significant effect on osteoclastogenesis.

## 6.3 Future perspective

On reflection there are many things that could have been improved; although BMD was measured and the pre-analytical blood collection was standardised in the prospective cohort any improvement in bone turnover was hard to establish. This study was designed as a single treatment arm trial with no control group, whereas, the optimal design would have been a double-blind randomized comparison with placebo. However, as RTX is an approved treatment for refractory RA and is already known to reduce disease activity, such a control arm would have had to be matched for disease activity and it would have been unethical to have an untreated arm with that level of active disease. A possible follow-on study could



include RA patients naive to biologic treatment; to compare the change in bone density and bone turnover between B cell depletion and TNF- $\alpha$  inhibition, over 24 months in postmenopausal women with optimal vitamin D status. Additionally, the *in vitro* osteoclastic potential of this new cohort of patients should be investigated and FACS performed to identify subsets of pathogenic B cells specific to inflammatory bone erosion.



# References



## References

- Agrawal S, Misra R, Aggarwal A (2007) Autoantibodies in rheumatoid arthritis: association with severity of disease in established RA. *Clin Rheumatol*, 26:201-204.
- Akchurin T, Aissiou T, Kemeny N, Prosk E, Nigam N, Komarova SV (2008) Complex dynamics of osteoclast formation and death in long-term cultures. *PLoS One*, 3(5):1-11. e2104. doi:10.1371/journal.pone.0002104.
- Allman D, Pillai S (2008) Peripheral B cell subsets. *Curr Opin Immunol*, 20:149-157.
- Alatalo SL, Ivaska KK, Waguespack SG, Econs MJ, Väänänen HK, Halleen JM (2004) Osteoclast-derived serum tartrate-resistant acid phosphatase 5b in Albers-Schönberg disease (Type II autosomal dominant osteoporosis). *Clin Chem*, 50(5):883-890.
- Amrein K, Amrein S, Drexler C, Dimai HP, Dobnig H, Pfeifer K, Tomaschitz A, Pieber TR, Fahrleitner-Pammer A (2012) Sclerostin and its association with physical activity, age, gender, body composition and bone mineral content in healthy adults. *J Clin Endocrinol Metab*, 97(1):148–154.
- Asagiri M, Takayanagi H (2007) The molecular understanding of osteoclast differentiation. *Bone*, 40:251-264.
- Asma GEM, van den Bergh RL, Vossen JM (1983) Development of pre-B and B lymphocytes in the human fetus. *Clin Exp Immunol*, 56:407-414.
- Avbersek-Luznik I, Stopar TG, Marc J (2007) Activity or mass concentration of bone-specific alkaline phosphatase as a marker of bone formation. *Clin Chem Lab Med*, 45(8):1014-1018.
- Bakker MF, Jacobs JWJ, Verstappen SMM, Bijlsma JWJ (2007) Tight control in the treatment of rheumatoid arthritis: efficacy and feasibility. *Ann Rheum Dis*, 66(Suppl III):iii56-iii60.
- Barnabe C, Hanley DA (2008) Effect of Tumour Necrosis Factor Alpha Inhibition on Bone Density and Turnover Markers in Patients with Rheumatoid Arthritis and Spondyloarthritis. *Semin Arthritis Rheum*, 39:116-122.
- Barrow AD, Raynal N, Andersen TL, Slatter DA, Bihan D, Pugh N, Cella M, Kim T, Rho J, Negishi-Koga T, Delaisse J-M, Takayanagi H, Lorenzo J, Colonna M, Farndale RW, Choi Y, Trowsdale J (2011) OSCAR is a collagen receptor that costimulates osteoclastogenesis in DAP12-deficient humans and mice. *J Clin Invest*, 121(9):3505-3516.
- Bauer D, Krege J, Lane N, Leary E, Libanati C, Miller P, Myers G, Silverman S, Vesper HW, Lee D, Payette M, Randall S (2012) National Bone Health Alliance bone turnover

marker project: current practices and the need for US harmonization, standardization, and common reference ranges. *Osteoporos Int*, 23:2425-2433.

- Bellido T, Saini V, Pajevic PD (2013) Effects of PTH on osteocyte function. *Bone*, 54(2):250-257.
- Bergmann P, Body JJ, Boonen S, Boutsen Y, Devogelaer JP, Goemaere S, Kaufman JM, Reginster JY, Gangji V, Members of the Advisory Board on Bone Markers (2009) Evidence-based guidelines for the use of biochemical markers of bone turnover in the selection and monitoring of bisphosphonate treatment in osteoporosis: a consensus document of the Belgian bone club. *Int J Clin Pract*, 63(1):19–26.
- Bieglmayer C, Kudlacek S (2009) The bone marker plot: an innovative method to assess bone turnover in women. *Eur J Clin Invest*, 39:230-238.
- Bjarnason NH, Henriksen EEG, Alexandersen P, Christgau S, Henriksen DB, Christiansen C (2002) Mechanism of circadian variation in bone resorption. *Bone*, 30:307-313.
- Blair HC, Zaidi M (2006) Osteoclastic differentiation and function regulated by old and new pathways. *Rev Endocr Metab Disord*, 7:23-32.
- Blake GM, Fogelman I (2009) The clinical role of dual energy X-ray absorptiometry. *Eur J Radiol*, 71:406-414.
- Blake GM, Fogelman I (2010) An update on Dual-Energy X-Ray absorptiometry. *Semin Nucl Med*, 40:62-73.
- Blank RD, Malone DG, Christian RC, Vallarta-Ast NL, Krueger DC, Drezner MK, Binkley NC, Hansen KE (2006) Patient variables impact lumbar spine dual energy X-ray absorptiometry precision. *Osteoporos Int*, 17:768-774.
- Bowers D, House A, Owens D (2006) Identifying the characteristics of data. In: *Understanding clinical papers*. West Sussex: J Wiley & Sons Ltd. pp 63-72.
- Blumsohn A, Hannon RA, Eastell R (1995) Apparent instability of osteocalcin in serum as measured with different commercially available immunoassays. *Clin Chem*, 41:318–319.
- Bonewald LF (2011) The amazing osteocyte. *J Bone Miner Res*, 26(2):229-238.
- Boumans MJH, Thurlings RM, Yeo L, Scheel-Toellner D, Vos K, Gerlag DM, Tak PP (2012) Rituximab abrogates joint destruction in rheumatoid arthritis by inhibiting osteoclastogenesis. *Ann Rheum Dis*, 71:108–113.
- Bowsher RR, Sailstad JM (2008) Insights in the application of research-grade diagnostic kits for biomarker assessments in support of clinical drug development: Bioanalysis of circulating concentrations of soluble receptor activator of nuclear factor  $\kappa$ B ligand. *J Pharm Biomed Anal*, 48:1282-1289.

- Brandt J, Krogh TN, Jensen CH, Frederiksen JK, Teisner B (1999) Thermal Instability of the Trimeric Structure of the N-terminal Propeptide of Human Procollagen Type I in Relation to Assay Technology. *Clin Chem*, 45(1): 47-53.
- Breuil V, Euller-Ziegler L (2006) Bisphosphonate therapy in rheumatoid arthritis. *Joint Bone Spine*. 73:349-354.
- Brown JP, Albert C, Nassar BA, Adachi JD, Cole D, Davison KS, Dooley KC, Don-Wauchope A, Douville P, Hanley DA, Jamal SA, Josse R, Kaiser S, Krahn J, Krause R, Kremer R, Lepage R, Letendre E, Morin S, Ooi DS, Papaioannou A, Ste-Marie L-G (2009) Bone turnover markers in the management of osteoporosis. *Clin Biochem*, 42:929–942.
- Brown JP, Prince RL, Deal C, Recker RR, Kiel DP, de Gregorio LH, Hadji P, Hofbauer LC, Alvaro-Gracia JM, Wang H, Austin M, Wagman RB, Newmark R, Libanati C, San Martin J, Bone HG (2009) Comparison of the effect of denosumab and alendronate on BMD and biochemical markers of bone turnover in postmenopausal women with low bone mass: A randomised, blinded, phase 3 trial. *J Bone Miner Res*, 24(1):153-161.
- Bueznli PR, Sims NA (2015) Quantifying the osteocyte network in the human skeleton. *Bone*, 75:144-150.
- Carey JJ, Licata AA, Delaney MF (2006) Biochemical markers of bone turnover. *Clin Rev Bone Miner Metab*, 4(3):197–212.
- Cartron G, Watier H, Golay J, Solal-Celigny P (2004) From the bench to the bedside: ways to improve rituximab efficacy. *Blood*, 104(9):2635-2642.
- Choi Y, Woo KM, Ko S-H, Lee YJ, Park S-J, Kim H-M, Kwon BS (2001) Osteoclastogenesis is enhanced by activated B cells but suppressed by activated CD8<sup>+</sup> T cells. *Eur J Immunol*, 31:2179-2188.
- Clark EA, Ledbetter JA (2005) How does B cell depletion therapy work, and how can it be improved? *Ann Rheum Dis*, 64:iv77-iv80.
- Clowes JA, Hannon RA, Yap TS, Hoyle NR, Blumsohn A, Eastell R (2002) Effect of feeding on bone turnover markers and its impact on biological variability of measurements. *Bone*, 30(6):886-890.
- Cohen SB, Emery P, Greenwald MW, Dougados M, Furie RA, Genovese MC, Keystone EC, Loveless JE, Burmester G-R, Cravets MW, Hessey EW, Shaw T, Totoritis MC for the REFLEX Trial Group (2006) Rituximab for rheumatoid arthritis refractory to anti-tumor necrosis factor therapy. Results of a multicentre, randomised, double-blind, placebo-controlled, phase III trial evaluating primary efficacy and safety at twenty-four weeks. *Arthritis and Rheum*, 54(9):2793-2806.

- Collin-Osgodby P, Yu X, Zheng H, Osgodby P (2003) RANKL-mediated osteoclast formation from murine RAW 264.7 cells. *Methods Mol Med*, 80:153–166.
- Compston J (2015) FRAX – Where are we now? *Maturitas*, 284-287.
- D’Amelio P, Grimaldi A, Pescarmona GP, Tamone C, Roato I, Isaia G (December 20<sup>th</sup> 2004) Spontaneous osteoclast formation from peripheral blood mononuclear cells in postmenopausal osteoporosis. *FASEB J*, doi:10.1096/fj.04-2214fje.
- Dalakas MC (2008) B cells as therapeutic targets in autoimmune neurological disorders. *Nature Clin Pract*, 4(10):557-567.
- Dallas SL, Bonewald LF (2010) Dynamics of the transition from osteoblast to osteocyte. *Ann N Y Acad Sci*, 1192:437-443.
- Datta HK, Ng FW, Walker JA, Tuck SP, Varanasi SS (2008) The cell biology of bone metabolism. *J Clin Pathol*, 61:577-587.
- Deal C (2005) The use of bisphosphonates in rheumatic disease and osteoporosis. In: M Maricic, OS Gluck, eds. *Bone Disease in Rheumatology*. Arizona: Lippincott Williams and Wilkens, pp 141-149.
- Deal C (2012) Bone loss in rheumatoid arthritis: Systemic, periarticular and focal. *Curr Rheumatol Rep*, 14(3):231-237.
- Diarra D, Stolina M, Polzer K, Zwerina J, Ominsky MS, Dwyer D, Korb A, Smolen J, Hoffmann M, Scheinecker C, van der Heide D, Landewe R, Lacey D, Richards WG, Schett G (2007) Dickkopf-1 is a master regulator of joint remodeling. *Nat Med*, 13(2):156-163.
- Durand M, Boire G, Komarova SV, Dixon SJ, Sims SM, Harrison RE, Nabavi N, Maria O, Manolson MF, Mizianty M, Kurgan L, de Brum-Fernandes AJ (2011) The increased *in vitro* osteoclastogenesis in patients with rheumatoid arthritis is due to increased percentage of precursors and decreased apoptosis – The *In Vitro* Osteoclast Differentiation in Arthritis (IODA) study. *Bone*, 48(3):588-596.
- Eastell R, Garnero P, Audebert C, Cahall DL (2012) Reference intervals of bone turnover markers in healthy premenopausal women: Results from a cross-sectional European study. *Bone*, 50:1141-1147.
- Edwards JCW, Cambridge G (2001) Sustained improvement in rheumatoid arthritis following a protocol designed to deplete B lymphocytes. *Rheumatology (Oxford)*, 40:205-211.
- Emery P, Fleischmann R, Filipowicz-Sosnowska A, Schechtman J, Szczepanski L, Kavanaugh A, Racewicz AJ, van Vollenhoven RF, Li NF, Agarwal S, Hessey EW, Shaw TM for the DANCER Study Group (2006) The efficacy and safety of rituximab in patients



with active rheumatoid arthritis despite methotrexate treatment. Results of a phase IIb randomised, double-blind, placebo-controlled, dose-ranging trial. *Arthritis and Rheum*, 54(5):1390-1400.

- Fillatreau S (2012) Cytokine-producing B cells as regulators of pathogenic and protective immune responses. *Ann Rheum Dis*, 0:1-5.
- Franck H, Gottwalt J (2009) Peripheral bone density in patients with rheumatoid arthritis. *Clin Rheumatol* 28:1141-1145.
- Franz-Odenaal TA, Hall BK, Witten PE (2006) Buried alive: How osteoblasts become osteocytes. *Dev Dyn*, 235:176-190.
- Fujikawa Y, Quinn JMW, Sabokbar A, McGee JO'D, Athanasou A (1996) The human osteoclast precursor circulates in the monocyte fraction. *Endocrinology*, 137(9):4058-4060.
- Garcia-Pérez MA, Noguera I, Hermenegildo C, Martínez-Romero A, Tarín JJ, Cano A (2006) Alterations in the phenotype and function of immune cells in ovariectomy-induced osteopenic mice. *Hum Reprod*, 21(4):880-887.
- Garnero P, Sornay-Rendu E, Claustrat B, Delmas PD (2000) Biochemical markers of bone turnover, endogenous hormones and the risk of fractures in postmenopausal women: The OFELY study. *J Bone Miner Res* 15(8):1526–1536.
- Geusens P (2012) The role of RANK ligand/ osteoprotegerin in rheumatoid arthritis. *Ther Adv Musculoskel Dis*, 4(4):225-233.
- Glover SJ, Garnero P, Naylor K, Rogers A, Eastell R (2008) Establishing a reference range for bone turnover markers in young, healthy women. *Bone* 42:623-630.
- Goldring SR, Gravallesse EM (2004) Bisphosphonates: Environmental protection for the joint. *Arthritis Rheum*, 50(7):2044-2047.
- Gonciulea A, Jan de Beur S (2015) The dynamic skeleton. *Rev Endocr Metab Disord*, 16:79-91.
- Gough AK, Lilley J, Eyre S, Holder RL, Emery P (1994) Generalised bone loss in patients with early rheumatoid arthritis. *Lancet* 344:23-27.
- Gross TS, King KA, Rabaia NA, Pathare P, Srinivasan S (2005) Upregulation of osteopontin by osteocytes deprived of mechanical loading or oxygen. *J Bone Miner Res*, 20(2):250-256.
- Halleen JM, Alatalo SL, Suominen H, Cheng S, Janckila AJ, Väänänen HK (2000) Tartrate-resistant acid phosphatase 5b: a novel serum marker of bone resorption. *J Bone Miner Res*, 15(7):1337–1345.

- Hannon RA, Eastell R (2000) Preanalytical variability of biochemical markers of bone turnover. *Osteoporos Int*, 11(Suppl 6):S30-44.
- Hannon RA, Eastell R (2006) Bone markers and current laboratory assays. *Cancer treatment reviews*, 32(Suppl 1):7-14.
- Harnett MM, Katz E, Ford CA (2005) Differential signalling during B-cell Maturation. *Immunol Lett*, 98:33-44.
- Harris DP, Haynes L, Sayles PC, Duso DK, Eaton SM, Lepak NM, Johnson LL, Swain SL, Lund FE (2000) Reciprocal regulation of polarized cytokine production by effector B and T cells. *Nat Immunol*, 1(6):475-482.
- Hayer S, Polzer K, Brandl A, Zwerina J, Kireva T, Smolen JS, Schett G (2008) B cell infiltrates induce endosteal bone formation in inflammatory arthritis. *J Bone Miner Res*, 23(10):1650-1660.
- Haynes DR, Crotti TN, Loric M, Bain GI, Atkins GJ, Findlay DM (2001) Osteoprotegerin and receptor activator of nuclear factor kappaB ligand (RANKL) regulate osteoclast formation by cells in the human rheumatoid arthritic joint. *Rheumatology (Oxford)*, 40:623-630.
- Hein G, Eidner T, Oelzner P, Rose M, Wilke A, Wolf G, Franke S (2011) Influence of rituximab on markers of bone remodeling in patients with rheumatoid arthritis: a prospective open-label pilot study. *Rheumatol Int*, 31(2):269-272.
- Holmbeck K, Bianco P, Pidoux I, Inoue S, Billingham RC, Wu W, Chrysovergis K, Yamada S, Birkedal-Hansen H, Poole AR (2005) The metalloproteinase MT1-MMP is required for normal development and maintenance of osteocyte processes in bone. *J Cell Sci*, 118:147-156.
- Hong Q, Xu J, Xu S, Lian L, Zhang M, Ding C (2014) Associations between serum 25-hydroxyvitamin D and disease activity, inflammatory cytokines and bone loss in patients with rheumatoid arthritis. *Rheumatology (Oxford)*, 53:1994-2001.
- Horowitz MC, Xi Y, Pflugh DL, Hesslein DGT, Schatz DG, Lorenzo JA, Bothwell ALM (2004) Pax5-Deficient mice exhibit early onset osteopenia with increased osteoclast progenitors. *J Immunol*, 173:6583-6591.
- Horowitz MC, Fretz JA, Lorenzo JA (2010) How B cells influence bone biology in health and disease. *Bone*, 47(3):472-479.
- <http://www.onlineconversion.com/circlesolve.htm>
- International Society for Clinical Densitometry (2007) Official position- Adults <https://iscd.app.box.com/v/op-iscd-2007-adult-eng>

- Jacquin C, Gran DE, Lee SK, Lorenzo JA, Aguila HL (2006) Identification of multiple osteoclast precursor populations in murine bone marrow. *J Bone Miner Res*, 21(1):67-77.
- Jimenez-Boj E, Redlich K, Türk B, Hanslik-Schnabel B, Wanivenhaus A, Chott A, Smolen JS, Schett G (2005) Interaction between synovial inflammatory tissue and bone marrow in rheumatoid arthritis. *J Immunol*, 175:2579-2588.
- Johnsen HE, Bergkvist KS, Schmitz A, Kjeldsen MK, Hansen SM, Gaihede M, Nørgaard MA, Bæch J, Grønholdt M-L, Jensen FS, Johansen P, Bødker JS, Bøgsted M, Dybkær K for the Myeloma Stem Cell Network (MSCNET) 2014 Cell of origin associated classification of B-cell malignancies by gene signatures of the normal B-cell hierarchy. *Leuk Lymphoma*, 55(6):1251-1260.
- Jones JD, Hamilton BJ, Rigby WFC (2012) Rituximab mediates loss of CD19 on B cells in the absence of cell death. *Arthritis Rheum*, 64(10):3111-3118.
- Kanis J (2004) Assessment of osteoporosis at the primary health-care level. Technical Report WHO, in: Collaborating Centre, University of Sheffield, UK Summary Meeting Report Brussels, Belgium, 5–7 May 2004, <http://www.who.int/chp/topics/Osteoporosis.pdf> (accessed 04.05.17).
- Kanis JA, McCloskey EV, Johansson H, Oden A, Melton LJ, Khaltsev N (2008) A reference standard for the description of osteoporosis. *Bone*, 42:467-475.
- Kearns AE, Khosla S, Kostenuik PJ (2008) Receptor activator of nuclear factor  $\kappa$ B ligand and osteoprotegerin regulation of bone remodelling in health and disease. *Endocr Rev*, 29(2):155–192.
- Kelly CA, Bartholomew P, Lapworth A, Basu A, Hamilton J, Heycock C (2002) Peripheral bone density in patients with rheumatoid arthritis and factors which influence it. *Eur J Intern Med*, 13:423-427.
- Keystone E, Emery P, Peterfy CG, Tak PP, Cohen S, Genovese MC, Dougados M, Burmester GR, Greenwald M, Kvien TK, Williams S, Hagerty D, Cravets MW, Shaw T (2009) Rituximab inhibits structural joint damage in patients with rheumatoid arthritis with an inadequate response to tumour necrosis factor inhibitor therapies. *Ann Rheum Dis*, 68:216–221.
- Kosinski M, Kujawski SC, Martin R, Wanke LA, Buatti MC, Ware JE, Perfetto EM (2002) Health-related quality of life in early rheumatoid arthritis: Impact of disease and treatment response. *Am J Manag Care*, 8:231-240.
- Kostoglou-Athanassiou I, Athanassiou P, Lyraki A, Raftakis I, Antoniadis C (2012) Vitamin D and rheumatoid arthritis. *Ther Adv Endocrinol Metab*, 3(6):181-187.

- Kramer I, Halleux C, Keller H, Pegurri M, Gooi JH, Weber PB, Feng JQ, Bonewald LF, Kneissel M (2010) Osteocyte Wnt/ $\beta$ -Catenin signalling is required for normal bone homeostasis. *Mol Cell Biol*, 30(12):3071-3085.
- Kudlacek S, Schneider B, Woloszczuk W, Pietschmann P, Willvonseder R for the Austrian study group on normative values of bone metabolism (2003) Serum levels of osteoprotegerin increase with age in a healthy adult population. *Bone*, 32:681-686.
- Lacey DL, Timms E, Tan H-L, Kelley MJ, Dunstan CR, Burgess T, Elliott R, Colombero A, Elliott G, Scully S, Hsu H, Sullivan J, Hawkins N, Davy E, Capparelli C, Eli A, Qian Y-X, Kaufman S, Sarosi I, Shalhoub V, Senaldi G, Guo J, Delaney J, Boyle WJ (1998) Osteoprotegerin Ligand is a Cytokine that regulates Osteoclast Differentiation and Activation. *Cell*, 93:165-176.
- Lappin DF, Sherrabeh S, Jenkins WMM, Macpherson LMD (2007) Effect of smoking on serum RANKL and OPG in sex, age and clinically matched supportive-therapy periodontitis patients. *J Clin Periodontol*, 34:271-277.
- LeBien TW, Tedder TF (2008) B lymphocytes: how they develop and function. *Blood*, 112(5):1570-1580.
- Lems WF (2007) Bisphosphonates and Glucocorticoids: Effects on Bone Quality. *Arthritis Rheum*, 56:3518-3522.
- Li X, Zhang Y, Kang H, Liu W, Liu P, Zhang J, Harris S, Wu D (2005) Sclerostin binds to LRP5/6 and antagonizes canonical Wnt signaling. *J Biol Chem*, 280:19883–19887.
- Li Y, Toraldo G, Li A, Yang X, Zhang H, Qian W-P, Neale Weitzmann M (2007) B cells and T cells are critical for the preservation of bone homeostasis and attainment of peak bone mass in vivo. *Blood*, 109:3839-3848.
- Li Y, Terauchi M, Vikulina T, Roser-Page S, Weitzmann MN (2014) B cell production of both OPG and RANKL is significantly increased in aged mice. *Open Bone J*, 6:8-17.
- Lipsky PE (2001) Systemic lupus erythematosus: an autoimmune disease of B cell hyperactivity. *Nat Immunol*, 2:764-766.
- Lund FE (2008) Cytokine-producing B lymphocytes – key regulators of immunity. *Curr Opin Immunol*, 20:332-338.
- Manabe N, Kawaguchi H, Chikuda H, Miyaura C, Inada M, Nagai R, Nabeshima Y-i, Nakamura K, Sinclair AM, Scheuermann RH, Kuro-o M (2001) Connection between B lymphocyte and osteoclast differentiation pathways. *J Immunol*, 167:2625-2631.
- Mansour A, Anginot A, Mancini SJC, Schiff C, Carle GF, Wakkach A, Blin-Wakkach C (2011) Osteoclast activity modulates B-cell development in the bone marrow. *Cell Res*, 21:1102-1115.

- Marin L, Koivula M-K, Jukkola-Vuorinen A, Leino A, Risteli J (2011) Comparison of total and intact aminoterminal propeptide of type 1 procollagen assays in patients with breast cancer with or without bone metastases. *Ann Clin Biochem*, 48:447–451.
- Marotte H, Pallot-Prades B, Grange L, Gaudin P, Alexandre C, Miossec P (2007) A 1-year case-control study in patients with rheumatoid arthritis indicates prevention of loss of bone mineral density in both responders and nonresponders to infliximab. *Arthritis Res Ther*, 9(3):R61 (doi:10.1186/ar2219).
- Mattey DL, Brownfield A, Dawes PT (2009) Relationship between pack-year history of smoking and response to tumour necrosis factor antagonists in patients with rheumatoid arthritis. *J Rheumatol*, 36(6):1180-1187.
- Mauri C, Ehrenstein MR (2007) Cells of the synovium in rheumatoid arthritis. B cells. *Arthritis Res Ther*, 9:205 (doi:10.1186/ar2125).
- Mauri C, Gray D, Mushtaq N, Londei M (2003) Prevention of arthritis by interleukin 10 producing B cells. *J Exp Med*, 197:489-501.
- McInnes IB, Schett G (2011) The pathogenesis of rheumatoid arthritis. *N Engl J Med*, 365:2205-2219.
- Meednu N, Zhang H, Owen T, Sun W, Wang V, Cistrone C, Rangel-Moreno J, Xing L, Anolik JH (2015) A link between B cells and bone erosion in rheumatoid arthritis: Receptor activator of nuclear factor kappa-B ligand production by memory B cells. *Arthritis Rheumatol*, 'Accepted Article', doi: 10.1002/art.39489.
- Mewar D, Wilson AG (2006) Autoantibodies in rheumatoid arthritis: a review. *Biomed Pharmacother*, 60(10):648-655.
- Mirza FS, Padhi ID, Raisz LG, Lorenzo JA (2010) Serum sclerostin levels negatively correlate with parathyroid hormone levels and free estrogen index in postmenopausal women. *J Clin Endocrinol Metab*, 95(4):1991–1997.
- Nakashima T, Hayashi M, Fukunaga T, Kurata K, Oh-hora M, Feng JQ, Bonewald LF, Kodama T, Wutz A, Wagner EF, Penninger JM, Takayanagi H (2011) Evidence for osteocyte regulation of bone homeostasis through RANKL expression. *Nat Med*, 17(10):1231-1234.
- Nakou M, Katsikas G, Sidiropoulos P, Bertsiias G, Papadimitraki E, Raptopoulou A, Koutala H, Papadaki HA, Kritikos H, Boumpas DT (2009) Rituximab therapy reduces activated B cells in both the peripheral blood and bone marrow of patients with rheumatoid arthritis: depletion of memory B cells correlates with clinical response. *Arthritis Res Ther*, 11(4):R131 (doi:10.1186/ar2798).

- Neale Weitzmann M, Cenci S, Haug J, Brown C, DiPersio J, Pacifici R (2000) B lymphocytes inhibit human osteoclastogenesis by secretion of TGF $\beta$ . *J Cell Biochem*, 78:318-24.
- Nelson DA, Welgert JM, Mosley-Williams AD (2005) Measurement of bone mineral density: DXA and QCT. In: M Maricic, OS Gluck, eds. *Bone Disease in Rheumatology*. Arizona: Lippincott Williams and Wilkens, pp 35-44.
- Nera K-P, Kyläniemi MK, Lassila O (2015) Regulation of B cell to plasma cell transition within the follicular B cell response. *Scand J Immunol*, 82:225-234.
- NICE technology appraisal guidance - TA195, (issued August 2010) Adalimumab, etanercept, infliximab, rituximab and abatacept for the treatment of rheumatoid arthritis after the failure of a TNF inhibitor. <http://www.nice.org.uk/guidance/ta195> Assessed February 2016.
- Noble BS, Peet N, Stevens HY, Brabbs A, Mosley JR, Reilly GC, Reave J, Skerry TM, Lanyon LE (2003) Mechanical loading: Biphasic osteocyte survival and targeting of osteoclasts for bone destruction in rat cortical bone. *Am J Physiol Cell Physiol*, 284:C934-C943.
- Nose M, Yamazaki H, Hagino H, Morio Y, Hayashi S-I, Teshima R (2009) Comparison of osteoclast precursors in peripheral blood mononuclear cells from rheumatoid arthritis and osteoporosis patients. *J Bone Miner Metab*, 27:57-65.
- Office for National Statistics (dated November 25 2014) Adult smoking habits in Great Britain, 2013. [http://www.ons.gov.uk/ons/dcp171778\\_386291.pdf](http://www.ons.gov.uk/ons/dcp171778_386291.pdf). Assessed 20 March 2015.
- Panaroni C, Wu JY (2013) Interactions between B lymphocytes and the osteoblast lineage in bone marrow. *Calcif Tissue Int*, 93(3):261-268.
- Panayi GS (2005) B cells: a fundamental role in the pathogenesis of rheumatoid arthritis? *Rheumatology (Oxford)*, 44(Suppl 2):ii3-ii7.
- Pederson AE, Jungersen MB, Pedersen CD (2011) Monocytes mediate shaving of B cell-bound anti-CD20 antibodies. *Immunology*, 133:239-245.
- Polyzos SA, Anastasilakis AD, Bratengeier C, Woloszczuk W, Papatheodorou A, Terpos E (2012) Serum sclerostin levels positively correlate with lumbar spinal bone mineral density in postmenopausal women – the six-month effect of risedronate and teriparatide. *Osteoporos Int*, 23:1171–1176.
- Public Health England - Cell Counting Using a Haemocytometer. <http://www.hpacultures.org.uk/technical/ccp/cellcounting.aspx>. Assessed 9 May 2016.

- Qvist P, Munk M, Hoyle N, Christiansen C (2004) Serum and plasma fragments of C-telopeptides of type I collagen (CTX) are stable during storage at low temperatures for 3 years. *Clin Chim Acta*, 350(1–2):167–173.
- Rabinda V, Bruyère O, Reginster JY (2011) Relationship between bone mineral density changes and risk of fractures among patients receiving calcium with or without vitamin D supplementation: a meta-regression. *Osteoporos Int*, 22:893-901.
- Ritterhouse LL, Crowe SR, Niewold TB, Kamen DL, Macwana SR, Roberts VC, Dedeker AB, Harley JB, Scofield RH, Guthridge JM, James JA (2011) Vitamin D deficiency is associated with an increased autoimmune response in healthy individuals and in patients with systemic lupus erythematosus. *Ann Rheum Dis*, 70:1569-1574.
- Rogers RS, Dawson AW, Wang Z, Thyfault JP, Hinton PS (2011) Acute response of plasma markers of bone turnover to a single bout of resistance training or plyometrics. *J Appl Physiol*, 111:1353–1360.
- Rosenquist C, Qvist P, Bjarnason N, Christiansen C (1995) Measurement of a more stable region of Osteocalcin in serum by ELISA with two monoclonal antibodies. *Clin Chem*, 41(10):1439-45.
- Rosenquist C, Fiedelius C, Christgau S, Pedersen BJ, Bonde M, Quist P (1998) Serum Crosslaps One Step ELISA. First application of monoclonal antibodies for measurement in serum of bone-related degradation products from C-terminal telopeptides of type I collagen. *Clin Chem*, 44(11): 2281-2289.
- Saag KG, Cerhan JR, Kolluri S, Ohashi K, Hunninghake GW, Schwartz DA (1997) Cigarette smoking and rheumatoid arthritis severity. *Ann Rheum Dis*, 56:463–469.
- Saltel F, Destaing O, Bard F, Eichert D, Jurdic P (2004) Apatite-mediated Actin Dynamics in Resorbing Osteoclasts. *Mol Biol Cell*, 15:5231–5241.
- Schafer AL, Vittinghoff E, Ramachandran R, Mahmoudi N, Bauer DC (2010) Laboratory reproducibility of biochemical markers of bone turnover in clinical practice. *Osteoporos Int*, 21: 439-445.
- Schett G (2006) Rheumatoid arthritis: inflammation and bone loss. *Wien Med Wochenschr*, 156(1–2):34–41.
- Schett G (2007) Cells of the synovium in rheumatoid arthritis: Osteoclasts. *Arthritis Res Ther*, 9(1):203.
- Schuit SC, van der Klift M, Weel AE, de Laet CE, Burger H, Seeman E, Hofman A, Uitterlinden AG, van Leeuwen JP, Pols HA (2004) Fracture incidence and association with bone mineral density in elderly men and women: The Rotterdam study. *Bone*, 34:195-202.

- Scott DL, Coulton BL, Symmons DPM, Popert AJ (1987) Long-term outcome of treating rheumatoid arthritis: results after 20 years. *Lancet*, 329(8542):1108-1111.
- Seibel MJ, Lang M, Geilenkeuser W-J (2001) Interlaboratory variation of biochemical markers of bone turnover. *Clin Chem*, 47(8):1443-1450.
- Seibel MJ (2005) Biochemical markers of bone turnover Part 1: Biochemistry and variability. *Clin Biochem Rev*, 26:97-122.
- Silman AJ, Pearson JE (2002) Epidemiology and genetics of rheumatoid arthritis. *Arthritis Res*, 4(Suppl 3):S265-S272.
- Silverman GJ (2006) Therapeutic B cell depletion and regeneration in rheumatoid arthritis. Emerging patterns and paradigms. *Arthritis and Rheum*, 54(8):2356-2367.
- Silverman GJ, Carson DA (2003) Roles of B cells in rheumatoid arthritis. *Arthritis Res Ther*, 5(Suppl 4):S1-S6.
- Stokes FJ, Ivanov P, Bailey LM, Fraser WD (2011) The effects of sampling procedures and storage conditions on short-term stability of blood-based biochemical markers of bone metabolism. *Clin Chem*, 57(1): 138-140.
- Supervia A, Nogués X, Enjuanes A, Vila J, Mellibovsky L, Serrano S, Aubía J, Díez-Pérez A (2006) Effect of smoking and smoking cessation on bone mass, bone remodelling, vitamin D, PTH and sex hormones. *J Musculoskelet Neuronal Interact*, 6(3):234-241.
- Swaminathan R (2001) Biochemical markers of bone turnover. *Clinica Chimica Acta*, 313:95-105.
- Symmons D, Turner G, Webb R, Asten P, Barrett E, Lunt M, Scott D, Silman A (2002) The prevalence of rheumatoid arthritis in the United Kingdom: new estimates for a new century. *Rheumatology (Oxford)*, 41:793-800.
- Tak PP, Rigby WF, Rubbert-Roth A, Peterfy CG, van Vollenhoven RF, Stohl W, Hessey E, Chen A, Tyrrell H, Shaw TM for the IMAGE Investigators (2011) Inhibition of joint damage and improved clinical outcomes with rituximab plus methotrexate in early active rheumatoid arthritis: the IMAGE trial. *Ann Rheum Dis*, 70:39-46.
- Takahashi N, Yamana H, Yoshiki S, Roodman GD, Mundy GR, Jones SJ, Boyde A, Suda T (1988) Osteoclast-like cell formation and its regulation by osteotropic hormones in mouse bone marrow cultures. *Endocrinol*, 122:1373-1382.
- Takemura S, Klimiuk PA, Braun A, Goronzy JJ, Weyand CM (2001) T cell activation in rheumatoid synovium is B cell dependent. *J Immunol*, 167:4710-4718.



- Teng YKO, Levarht EWN, Hashemi M, Bajema IM, Toes REM, Huizinga TWJ, van Laar JM (2007) Immunohistochemical Analysis as a Means to Predict Responsiveness to Rituximab Treatment. *Arthritis and Rheum*, 56(12):3909-3918.
- Teng YKO, Tekstra J, Breedveld FC, Lafeber F, Bijlsma JWJ, van Laar JM (2009) Rituximab fixed retreatment versus on-demand retreatment in refractory rheumatoid arthritis: comparison of two B cell depleting treatment strategies. *Ann Rheum Dis*, 68:1075-1077.
- Väänänen HK, Zhao H, Mulari M, Halleen JM (2000) The cell biology of osteoclast function. *J Cell Sci*, 113: 377-381.
- Vandooren B, Melis L, Veys EM, Tak PP, Baeten D (2009) *In Vitro* spontaneous osteoclastogenesis of human peripheral blood mononuclear cells is not crucially dependent on T lymphocytes. *Arthritis and Rheum*, 60(4):1020-1025.
- van Staa TP, Geusens P, Bijlsma JWJ, Leufkens HGM, Cooper C (2006) Clinical assessment of the long-term risk of fracture in patients with rheumatoid arthritis. *Arthritis and Rheum*, 54(10):3104-3112.
- Vasikaran S, Eastell R, Bruyère O, Foldes AJ, Garnero P, Griesmacher A, McClung M, Morris HA, Silverman S, Trenti T, Wahl DA, Cooper C, Kanis JA, for the IOF-IFCC Bone Marker Standards Working Group (2011) Markers of bone turnover for the prediction of fracture risk and monitoring of osteoporosis treatment: a need for international reference standards. *Osteoporos Int*, 22: 391-420.
- Vazquez MI, Catalan-Dibene J, Zlotnik A (2015) B cell responses and cytokine production are regulated by their immune microenvironment. *Cytokine*, 74:318-326.
- Weinblatt ME, Keystone EC, Furst DE, Moreland LW, Weisman MH, Birbara CA, Teoh LA, Fischkoff SA, Chartash EK (2003) Adalimumab, a fully anti-tumour necrosis factor  $\alpha$  monoclonal antibody, for the treatment of rheumatoid arthritis in patients taking concomitant methotrexate. The ARMADA trial. *Arthritis Rheum*, 48(1):35-45.
- Weitzmann MN, Cenci S, Haug J, Brown C, DiPersio J, Pacifici R (2000) B lymphocytes inhibit human osteoclastogenesis by secretion of TGF $\beta$ . *J Cell Biochem*, 78:318-324.
- Wheeler G, Hogan VE, Teng YKO, Tekstra J, Tuck SP, Lafeber FP, Huizinga TWJ, Bijlsma JWJ, Francis RM, Datta HK, van Laar JM (2011) Suppression of bone turnover by B-cell depletion in patients with rheumatoid arthritis. *Osteoporos Int*, 22(12):3067-3072.
- Wheeler G, Elshahaly M, Tuck SP, Datta HK, van Laar JM (2013) The clinical utility of bone marker measurements in osteoporosis. *J Transl Med*, 11:201.

- Wheater G, Goodrum C, Tuck SP, Datta HK, van Laar JM (2014) Method-specific differences in  $\beta$ -isomerised carboxy-terminal cross-linking telopeptide of type I collagen and procollagen type I aminoterminal propeptide using two fully automated immunoassays. *Clin Chem Lab Med*, 52(7):e135–e138.
- Wichers M, Schmidt E, Bidlingmaier F, Klingmüller D (1999) Diurnal rhythm of cross laps in human serum. *Clin Chem*, 45:1858-1860.
- Wu JY, Purton LE, Rodda SJ, Chen M, Weinstein LS, McMahon AP, Scadden DT, Kronenberg HM (2008) Osteoblastic regulation of B lymphopoiesis is mediated by  $G_{\beta\alpha}$ -dependent signalling pathways. *Proc Natl Acad Sci USA*, 105(44):16976-16981.
- Xu S, Wang Y, Lu J (2012) Osteoprotegerin and RANKL in the pathogenesis of rheumatoid arthritis-induced osteoporosis. *Rheumatol Int*, 32:3397-3403.
- Yavropoulou MP, Yovos JG (2008) Osteoclastogenesis – Current knowledge and future perspectives. *J Musculoskelet Neuronal Interact*, 8(3):204-216.
- Yeo L, Toellner K-M, Salmon M, Filer A, Buckley CD, Raza K, Scheel-Toellner D (2011) Cytokine mRNA profiling identifies B cells as a major source of RANKL in rheumatoid arthritis. *Ann Rheum Dis*, 70:2022-2028.
- Yeo L, Lom H, Juarez M, Snow M, Buckley CD, Filer A, Raza K, Scheel-Toellner D (2015) Expression of FcRL4 defines a pro-inflammatory, RANKL-producing B cell subset in rheumatoid arthritis. *Ann Rheum Dis*, 74:928-935.
- Yoshimura N, Muraki S, Oka H, Nakamura K, Kawaguchi H, Tanaka S, Akune T (2015) Serum levels of 25-hydroxyvitamin D and the occurrence of musculoskeletal diseases: a 3-year follow-up to the road study. *Osteoporos Int*, 26:151-161.
- You L, Temiyasathit S, Lee P, Kim CH, Tummala P, Yao W, Kingery W, Malone AM, Kwon RY, Jacobs CR (2008) Osteocytes as mechanosensors in the inhibition of bone resorption due to mechanical loading. *Bone*, 42(1):172-179.
- Youinou P, Taher TE, Pers J-O, Mageed RA, Renaudineau Y (2009) B Lymphocyte cytokines and rheumatic autoimmune disease. *Arthritis Rheum*, 60(7):1873-1880.
- Zhu J, Garrett R, Jung Y, Zhang Y, Kim N, Wang J, Joe GJ, Hexner E, Choi Y, Taichman RS, Emerson SG (2007) Osteoblasts support B-lymphocyte commitment and differentiation from hematopoietic stem cells. *Blood*, 109(9):3706-3712.

# Appendices



## Appendix A. Generic Materials

### General reagents

- Glacial Acetic acid (99.8-100.5%); product code 27225 (2.5L), Acetone ( $\geq 99.5\%$ ); product code SIGM650501 (1L), Ethyl Alcohol -pure ( $\geq 99.5\%$ ); product code 459844 (2.5L), Ethylene Diamine Tetraacetic Acid - disodium salt solution (EDTA); product code E7889 (100ml; 0.5M in H<sub>2</sub>O), Fetal Calf Serum (FCS); product code F7524 (100ml), Hank's Balanced Salt Solution (HBSS); product code H9394 (500ml), Methyl Alcohol -pure ( $\geq 99.8\%$ ); product code 32213(2.5L), Penicillin/ Streptomycin (pen/strep); product code P0781 (100ml; with 10,000units penicillin and 10mg streptomycin per ml in 0.9% saline), were purchased from LabShop<sup>®</sup> (Hartlepool, Cleveland, TS25 2DL, UK), a UK distributor for Sigma-Aldrich Company Ltd. (Gillingham, SP8 4XT, UK).
- Sterile Phosphate Buffered Saline (PBS); product code 10010-015 (500ml) and Triton X-100; product code HFH-10 (10ml; 1% solution) were purchased from Invitrogen Life Technologies (Paisley PA4 9RF, UK).
- Di-Sodium tetraborate; product code 102674E (500g), was purchased from VWR International - UK Ltd (Lutterworth, Leicestershire, LE17 4XN, UK).
- Sodium Hypochlorite solution; product code 129905 (0.82mol/L), was purchased from Siemens Healthcare Diagnostics (Camberley, Surrey, GU16 8QD, UK).
- Formaldehyde 16% (methanol-free solution); product code 28908 (10ml), was purchased from Fischer Scientific UK Ltd. (Loughborough, Leicestershire, LE11 5RG, UK).

### General consumables

- Coverslips for counting chamber; product code HAE2130, coverslips for microscope slides (22×26mm, 22×32mm, 22×50mm); product codes MIC3200, MIC3202, MIC3206, Eppendorf tubes (1.5ml); product code E0030108051, Eppendorf sterile pipette tips (0.1-20 $\mu$ l, 2-200 $\mu$ l, 50-1000 $\mu$ l); product codes EPPE0030075005, EPPE0030075021, EPPE0030075064, Eppendorf pipette tips (0.1-20 $\mu$ l, 2-200 $\mu$ l, 50-1000 $\mu$ l); product codes E0030000838, E0030000870, E0030000919, microscope slides (76×26mm); product code MIC2152, multichannel pipette reservoirs; product code PIP5704, Pasteur pipettes (0.5, 1.0, 3.0ml); product codes PIP4216, PIP4236, PIP4210, sterile 15ml and 50ml BD falcon tubes; product codes 352096, 352098, sterile 75×12mm polypropylene tubes (5ml); product code TIS5402, sterile

serological pipettes (5, 10 and 25ml); product codes SLS4010, SLS4020, SLS4030 and Whatman No.54 filter paper; product code FIL2272, were purchased from LabShop<sup>®</sup> (Hartlepool, Cleveland, TS25 2DL, UK).

### **General equipment**

- Advia 2400; automated clinical chemistry analyser (Siemens Healthcare Diagnostics, Camberley, Surrey, GU16 8QD, UK).
- Elecsys 2010 analyser and updated version E411; automated electrochemiluminescent immunoassay (ECLIA) systems (Roche Diagnostics Ltd. Burgess Hill, West Sussex, RH15 9RY, UK).
- iSYS analyser; a fully-automated system based on chemiluminescence and absorbency technology (IDS Ltd, Boldon, Tyne and Wear, NE35 9PD, UK).
- Eppendorf Mixmate; a microplate mixer; product code E535300030, supplied by Scientific Laboratory Supplies Ltd. (Hessle, East Riding of Yorkshire, HU13 0AE, UK).
- Microplate reader LT-4000 with Manta software for data analysis and management and Strip Washer LT-3000 (Labtech International Ltd. Uckfield, East Sussex, TN22 1QQ, UK).
- FACSCalibur<sup>™</sup> Flow Cytometer- 4 Colour: (BD BioSciences, Oxford, OX4 4DQ UK).
- MiniMACS and MidiMACS separators (Miltenyi Biotec, Bisley, Surrey GU24 9DR, UK).
- Olympus CKX41 inverted microscope with a fixed Infinity2 camera and Lumenera Infinity image software, supplied by J.B Microscopes Ltd. (Rothbury, Northumberland, NE65 7YG, UK).
- Sanyo CO<sub>2</sub> incubator at 5% CO<sub>2</sub> and 37°C; product code MCO-18AIC (Panasonic Biomedical Sales Europe BV, Loughborough, Leicestershire, LE11 1QJ, UK).
- Esco Airstream class 2 biological safety cabinet AC2-4E1, Forceps; product code INS4356, Grant water bath; product code BAT3060, Improved Neubauer haemocytometer; product code HAE2118, Rota-filler 5000 pipette filler; product code PIP7595, Tally Counter; product code COU2000 and Techne NOICE; product code FNOICE, were supplied by Scientific Laboratory Supplies Ltd. (Hessle, East Riding of Yorkshire, HU13 0AE, UK).
- Eppendorf 8 channel pipette (10-100µl); product code E114000131. (30-300µl); product code E3114000158. (0.5-10µl); product code E3111000122. Eppendorf

pipette (10-100 $\mu$ l); product code E3111000149 and (100-1000 $\mu$ l); product code E3111000165, were supplied by Scientific Laboratory Supplies Ltd. (Hessle, East Riding of Yorkshire, HU13 0AE, UK). All annually calibrated by Pipette Doctor (Sartorius Ltd, Epsom, Surrey, KT19 9QQ, UK).

- Biocold upright lab refrigerator; product code BIO280FRS, lab freezer -20°C; product code BIO245FZS, Brunswick Scientific freezer -80°C; product code FRE6010, filter funnel (100mm diameter); product code FUN1060, glass beakers (50 and 100ml); product codes BEA1004 and BEA1006, measuring cylinders (100ml, 500ml); product codes CYL2006, CYL2010, Select vortex mixer; product code SLS5100, Sigma refrigerated centrifuge (2-16PK); product code 10160 and timer; product code TIM0280, were supplied by Scientific Laboratory Supplies Ltd. (Hessle, East Riding of Yorkshire, HU13 0AE, UK).
- ELGA deionised water system and Purelab UHQ (Veolia, High Wycombe, Buckinghamshire, HP11 1JU, UK).



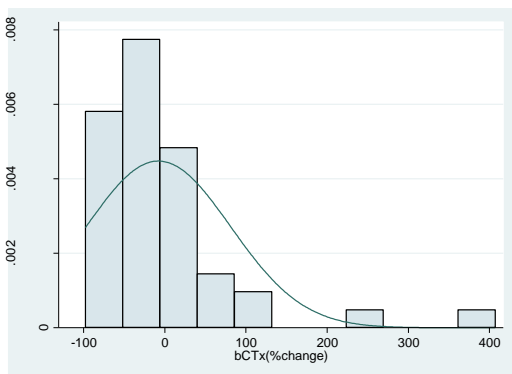
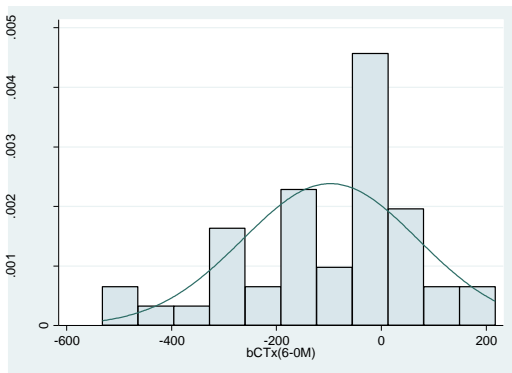
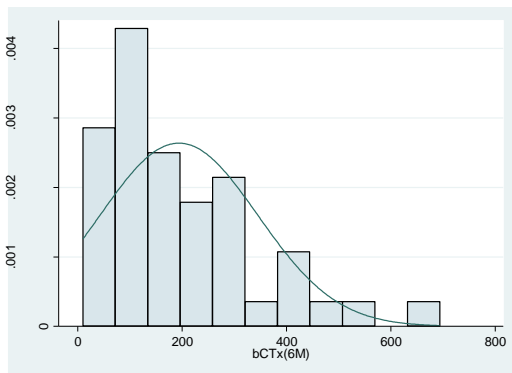
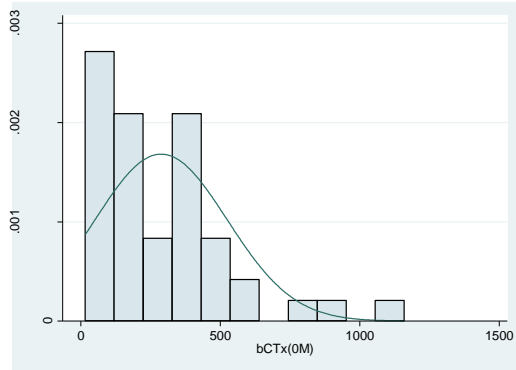


## Appendix B. Tests for normality of data

### Pilot Study

#### $\beta$ CTX

- All



. sktest boctx

Skewness/Kurtosis tests for Normality

Variable	Obs	Pr(Skewness)	Pr(Kurtosis)	adj chi2(2)	joint Prob>chi2
boctx	46	0.0003	0.0069	15.82	0.0004

. swilk boctx

Shapiro-wilk w test for normal data

Variable	Obs	W	V	z	Prob>z
boctx	46	0.87306	5.592	3.653	0.00013

. sktest ctx6m

Skewness/Kurtosis tests for Normality

Variable	Obs	Pr(Skewness)	Pr(Kurtosis)	adj chi2(2)	joint Prob>chi2
ctx6m	45	0.0021	0.0571	10.69	0.0048

. swilk ctx6m

Shapiro-wilk w test for normal data

Variable	Obs	W	V	z	Prob>z
ctx6m	45	0.90476	4.124	3.003	0.00134

. sktest ctxchange

Skewness/Kurtosis tests for Normality

Variable	Obs	Pr(Skewness)	Pr(Kurtosis)	adj chi2(2)	joint Prob>chi2
ctxchange	45	0.0566	0.6348	4.05	0.1322

. swilk ctxchange

Shapiro-wilk w test for normal data

Variable	Obs	W	V	z	Prob>z
ctxchange	45	0.95446	1.972	1.439	0.07504

. sktest ctxperchange

Skewness/Kurtosis tests for Normality

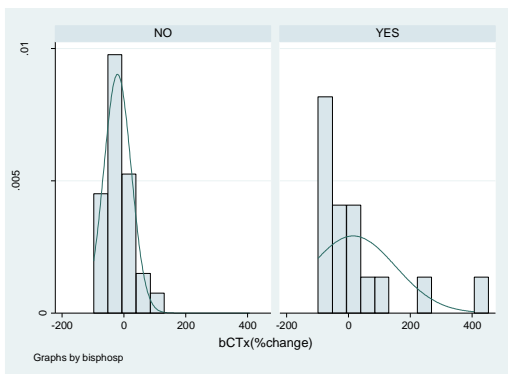
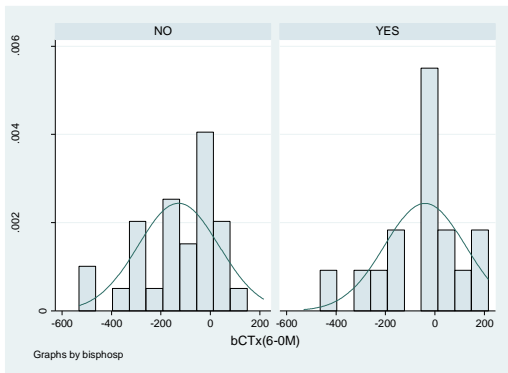
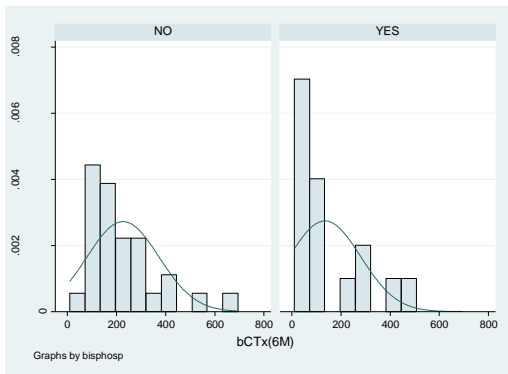
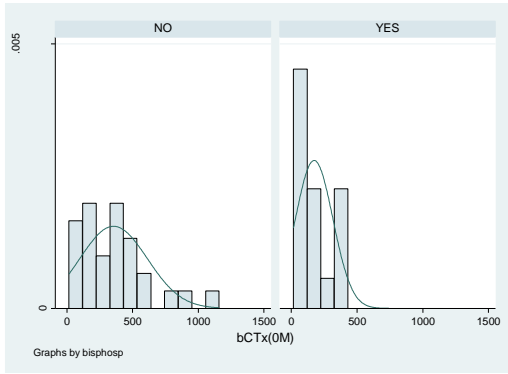
Variable	Obs	Pr(Skewness)	Pr(Kurtosis)	adj chi2(2)	joint Prob>chi2
ctxperchange	45	0.0000	0.0000	35.33	0.0000

. swilk ctxperchange

Shapiro-wilk w test for normal data

Variable	Obs	W	V	z	Prob>z
ctxperchange	45	0.69897	13.036	5.442	0.00000

- **By bisphosphonate medication**



. sktest bctx0m if bisphos ==0

Skewness/Kurtosis tests for Normality

Variable	Obs	Pr(Skewness)	Pr(Kurtosis)	adj chi2(2)	joint Prob>chi2
bctx0m	29	0.0048	0.0474	9.75	0.0076

. swilk bctx0m if bisphos ==0

Shapiro-wilk W test for normal data

Variable	Obs	W	V	z	Prob>z
bctx0m	29	0.88114	3.684	2.691	0.00357

. sktest bctx6m if bisphos ==0

Skewness/Kurtosis tests for Normality

Variable	Obs	Pr(Skewness)	Pr(Kurtosis)	adj chi2(2)	joint Prob>chi2
bctx6m	29	0.0013	0.0236	12.12	0.0023

. swilk bctx6m if bisphos ==0

Shapiro-wilk W test for normal data

Variable	Obs	W	V	z	Prob>z
bctx6m	29	0.85619	4.457	3.084	0.00102

. sktest bctx60m if bisphos ==0

Skewness/Kurtosis tests for Normality

Variable	Obs	Pr(Skewness)	Pr(Kurtosis)	adj chi2(2)	joint Prob>chi2
bctx60m	29	0.0500	0.7492	4.14	0.1261

. swilk bctx60m if bisphos ==0

Shapiro-wilk W test for normal data

Variable	Obs	W	V	z	Prob>z
bctx60m	29	0.92571	2.302	1.721	0.04264

. sktest bctxchange if bisphos ==0

Skewness/Kurtosis tests for Normality

Variable	Obs	Pr(Skewness)	Pr(Kurtosis)	adj chi2(2)	joint Prob>chi2
bctxchange	29	0.0023	0.0150	11.93	0.0026

. swilk bctxchange if bisphos ==0

Shapiro-wilk W test for normal data

Variable	Obs	W	V	z	Prob>z
bctxchange	29	0.89000	3.409	2.531	0.00569

. sktest bctx0m if bisphos ==1

Skewness/Kurtosis tests for Normality

Variable	Obs	Pr(Skewness)	Pr(Kurtosis)	adj chi2(2)	joint Prob>chi2
bctx0m	17	0.2284	0.2196	3.42	0.1806

. swilk bctx0m if bisphos ==1

Shapiro-wilk W test for normal data

Variable	Obs	W	V	z	Prob>z
bctx0m	17	0.87116	2.722	1.997	0.02292

. sktest bctx6m if bisphos ==1

Skewness/Kurtosis tests for Normality

Variable	Obs	Pr(Skewness)	Pr(Kurtosis)	adj chi2(2)	joint Prob>chi2
bctx6m	16	0.0572	0.8417	3.98	0.1364

. swilk bctx6m if bisphos ==1

Shapiro-wilk W test for normal data

Variable	Obs	W	V	z	Prob>z
bctx6m	16	0.82085	3.630	2.561	0.00522

. sktest bctx60m if bisphos ==1

Skewness/Kurtosis tests for Normality

Variable	Obs	Pr(Skewness)	Pr(Kurtosis)	adj chi2(2)	joint Prob>chi2
bctx60m	16	0.2523	0.5257	1.95	0.3777

. swilk bctx60m if bisphos ==1

Shapiro-wilk W test for normal data

Variable	Obs	W	V	z	Prob>z
bctx60m	16	0.95974	0.816	-0.404	0.65707

. sktest bctxchange if bisphos ==1

Skewness/Kurtosis tests for Normality

Variable	Obs	Pr(Skewness)	Pr(Kurtosis)	adj chi2(2)	joint Prob>chi2
bctxchange	16	0.0017	0.0153	11.92	0.0026

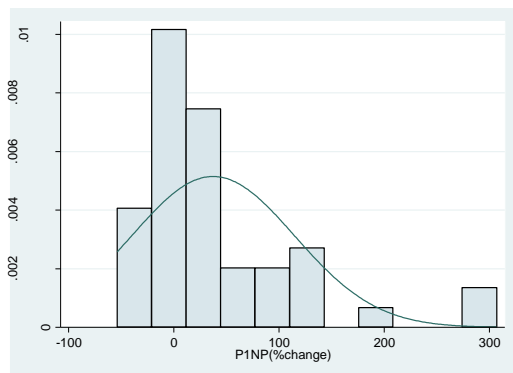
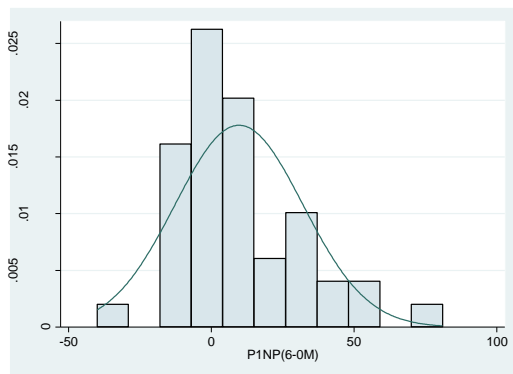
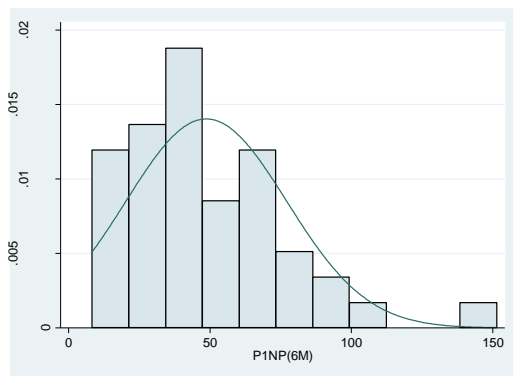
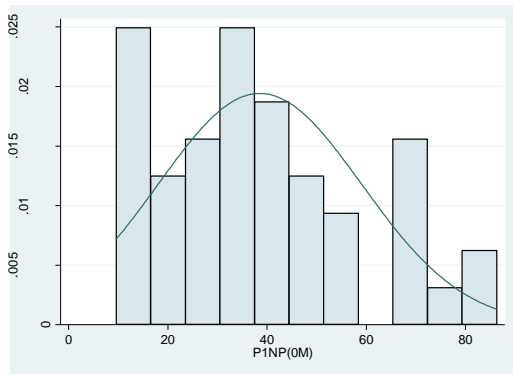
. swilk bctxchange if bisphos ==1

Shapiro-wilk W test for normal data

Variable	Obs	W	V	z	Prob>z
bctxchange	16	0.75909	4.881	3.149	0.00082

# PINP

- All



. sktest bop1np

Skewness/Kurtosis tests for Normality

Variable	Obs	Pr(Skewness)	Pr(Kurtosis)	adj chi2(2)	joint Prob>chi2
bop1np	46	0.1039	0.5403	3.21	0.2007

. swilk bop1np

Shapiro-Wilk W test for normal data

Variable	Obs	W	V	z	Prob>z
bop1np	46	0.94717	2.327	1.793	0.03651

. sktest p1np6m

Skewness/Kurtosis tests for Normality

Variable	Obs	Pr(Skewness)	Pr(Kurtosis)	adj chi2(2)	joint Prob>chi2
p1np6m	45	0.0018	0.0124	12.67	0.0018

. swilk p1np6m

Shapiro-Wilk W test for normal data

Variable	Obs	W	V	z	Prob>z
p1np6m	45	0.91979	3.473	2.639	0.00416

. sktest p1npchange

Skewness/Kurtosis tests for Normality

Variable	Obs	Pr(Skewness)	Pr(Kurtosis)	adj chi2(2)	joint Prob>chi2
p1npchange	45	0.0122	0.0822	8.08	0.0176

. swilk p1npchange

Shapiro-Wilk W test for normal data

Variable	Obs	W	V	z	Prob>z
p1npchange	45	0.92570	3.218	2.477	0.00663

. sktest p1npchange

Skewness/Kurtosis tests for Normality

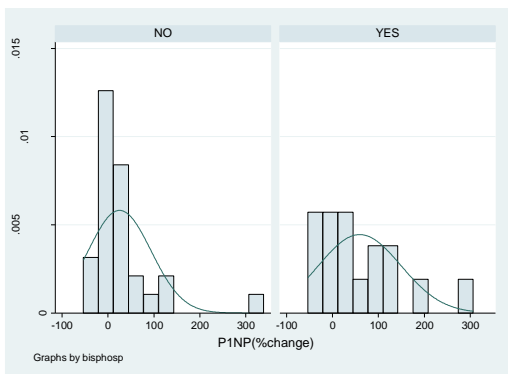
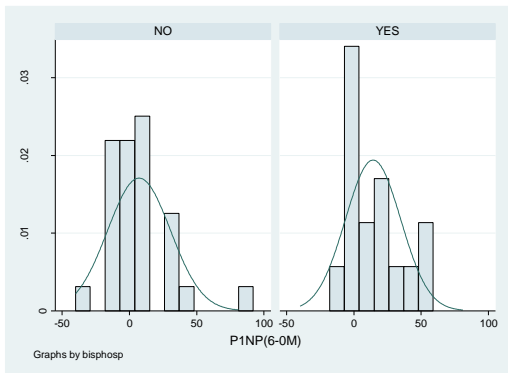
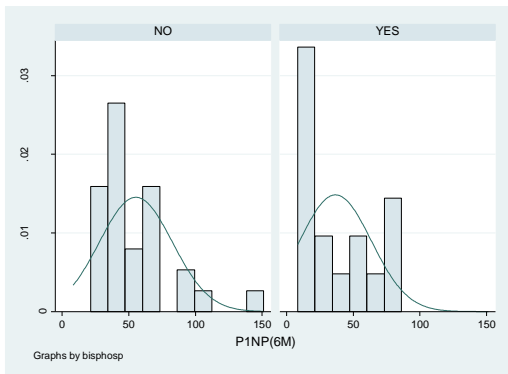
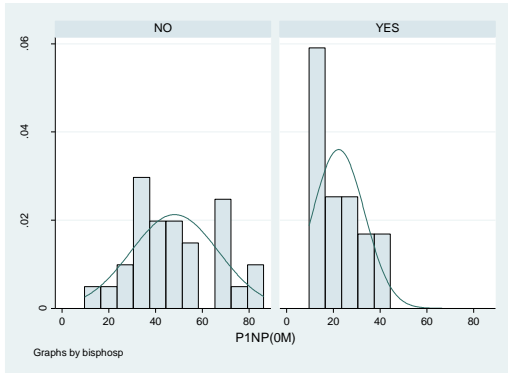
Variable	Obs	Pr(Skewness)	Pr(Kurtosis)	adj chi2(2)	joint Prob>chi2
p1npchange	45	0.0000	0.0020	20.49	0.0000

. swilk p1npchange

Shapiro-Wilk W test for normal data

Variable	Obs	W	V	z	Prob>z
p1npchange	45	0.80818	8.306	4.487	0.00000

- **By bisphosphonate medication**



. sktest p1np0m if bisphos ==0

Skewness/Kurtosis tests for Normality

Variable	Obs	Pr(Skewness)	Pr(Kurtosis)	adj chi2(2)	joint Prob>chi2
p1np0m	29	0.3785	0.2855	2.09	0.3525

. swilk p1np0m if bisphos ==0

Shapiro-wilk W test for normal data

Variable	Obs	W	V	z	Prob>z
p1np0m	29	0.96228	1.169	0.323	0.37352

. sktest p1np6m if bisphos ==0

Skewness/Kurtosis tests for Normality

Variable	Obs	Pr(Skewness)	Pr(Kurtosis)	adj chi2(2)	joint Prob>chi2
p1np6m	29	0.0003	0.0042	16.00	0.0003

. swilk p1np6m if bisphos ==0

Shapiro-wilk W test for normal data

Variable	Obs	W	V	z	Prob>z
p1np6m	29	0.80544	6.030	3.707	0.00010

. sktest p1np60m if bisphos ==0

Skewness/Kurtosis tests for Normality

Variable	Obs	Pr(Skewness)	Pr(Kurtosis)	adj chi2(2)	joint Prob>chi2
p1np60m	29	0.0129	0.0260	9.25	0.0098

. swilk p1np60m if bisphos ==0

Shapiro-wilk W test for normal data

Variable	Obs	W	V	z	Prob>z
p1np60m	29	0.91002	2.789	2.116	0.01717

. sktest p1npchange if bisphos ==0

Skewness/Kurtosis tests for Normality

Variable	Obs	Pr(Skewness)	Pr(Kurtosis)	adj chi2(2)	joint Prob>chi2
p1npchange	29	0.0000	0.0001	25.74	0.0000

. swilk p1npchange if bisphos ==0

Shapiro-wilk W test for normal data

Variable	Obs	W	V	z	Prob>z
p1npchange	29	0.72795	8.432	4.399	0.00001

. sktest p1np0m if bisphos ==1

Skewness/Kurtosis tests for Normality

Variable	Obs	Pr(Skewness)	Pr(Kurtosis)	adj chi2(2)	joint Prob>chi2
p1np0m	17	0.3318	0.1683	3.28	0.1938

. swilk p1np0m if bisphos ==1

Shapiro-wilk W test for normal data

Variable	Obs	W	V	z	Prob>z
p1np0m	17	0.90626	1.980	1.362	0.08653

. sktest p1np6m if bisphos ==1

Skewness/Kurtosis tests for Normality

Variable	Obs	Pr(Skewness)	Pr(Kurtosis)	adj chi2(2)	joint Prob>chi2
p1np6m	16	0.2955	0.1247	3.83	0.1473

. swilk p1np6m if bisphos ==1

Shapiro-wilk W test for normal data

Variable	Obs	W	V	z	Prob>z
p1np6m	16	0.86834	2.668	1.949	0.02565

. sktest p1np60m if bisphos ==1

Skewness/Kurtosis tests for Normality

Variable	Obs	Pr(Skewness)	Pr(Kurtosis)	adj chi2(2)	joint Prob>chi2
p1np60m	16	0.1492	0.5353	2.85	0.2406

. swilk p1np60m if bisphos ==1

Shapiro-wilk W test for normal data

Variable	Obs	W	V	z	Prob>z
p1np60m	16	0.87485	2.536	1.848	0.03229

. sktest p1npchange if bisphos ==1

Skewness/Kurtosis tests for Normality

Variable	Obs	Pr(Skewness)	Pr(Kurtosis)	adj chi2(2)	joint Prob>chi2
p1npchange	16	0.0427	0.2251	5.38	0.0680

. swilk p1npchange if bisphos ==1

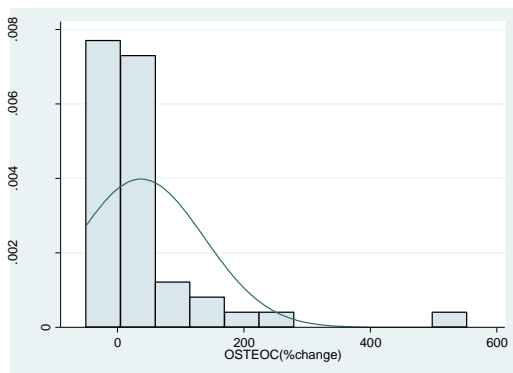
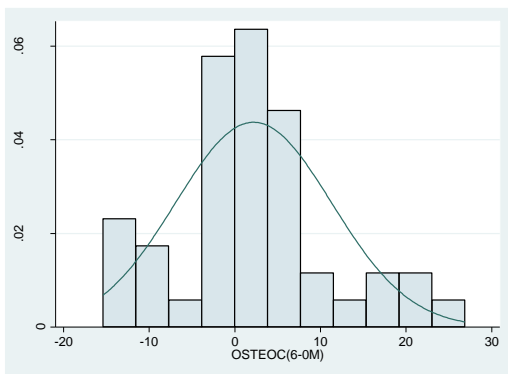
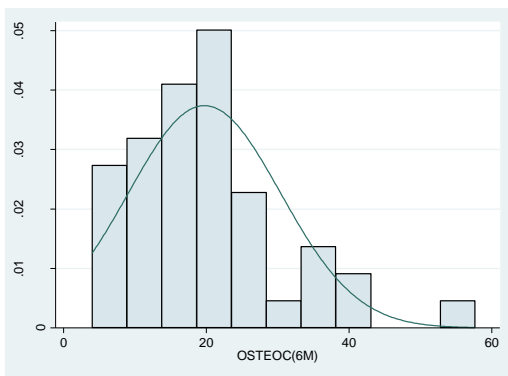
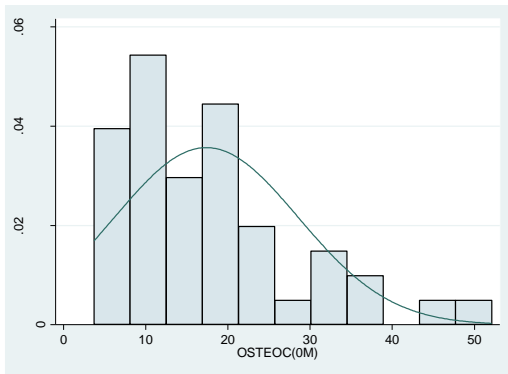
Shapiro-wilk W test for normal data

Variable	Obs	W	V	z	Prob>z
p1npchange	16	0.90982	1.827	1.197	0.11560



# Osteocalcin

- All



. sktest boosteoc

Skewness/Kurtosis tests for Normality					
Variable	Obs	Pr(Skewness)	Pr(Kurtosis)	adj chi2(2)	joint Prob>chi2
boosteoc	46	0.0014	0.0641	11.11	0.0039

. swilk boosteoc

Shapiro-wilk w test for normal data					
Variable	Obs	W	V	z	Prob>z
boosteoc	46	0.89328	4.701	3.285	0.00051

. sktest osteoc6m

Skewness/Kurtosis tests for Normality					
Variable	Obs	Pr(Skewness)	Pr(Kurtosis)	adj chi2(2)	joint Prob>chi2
osteoc6m	45	0.0030	0.0163	11.74	0.0028

. swilk osteoc6m

Shapiro-wilk w test for normal data					
Variable	Obs	W	V	z	Prob>z
osteoc6m	45	0.92736	3.145	2.429	0.00758

. sktest osteocchange

Skewness/Kurtosis tests for Normality					
Variable	Obs	Pr(Skewness)	Pr(Kurtosis)	adj chi2(2)	joint Prob>chi2
osteocchange	45	0.0597	0.1704	5.26	0.0722

. swilk osteocchange

Shapiro-wilk w test for normal data					
Variable	Obs	W	V	z	Prob>z
osteocchange	45	0.94227	2.500	1.942	0.02609

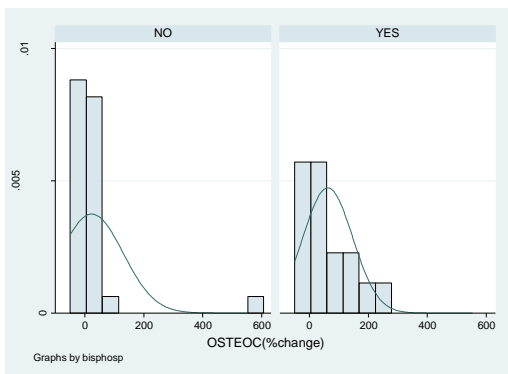
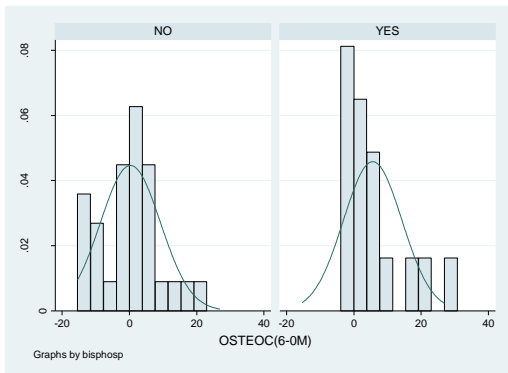
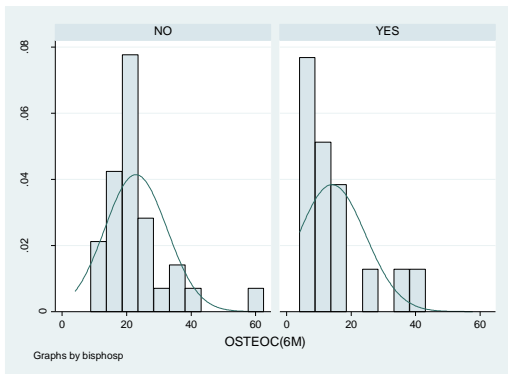
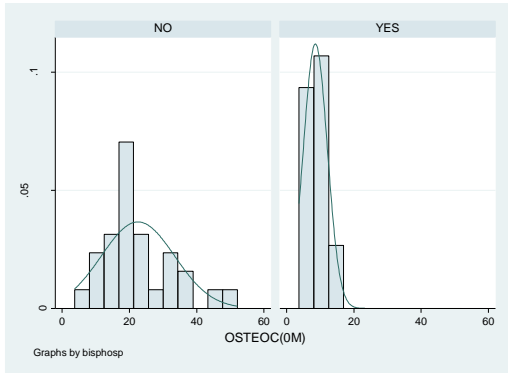
. sktest osteocperchange

Skewness/Kurtosis tests for Normality					
Variable	Obs	Pr(Skewness)	Pr(Kurtosis)	adj chi2(2)	joint Prob>chi2
osteocperc~e	45	0.0000	0.0000	41.83	0.0000

. swilk osteocperchange

Shapiro-wilk w test for normal data					
Variable	Obs	W	V	z	Prob>z
osteocperc~e	45	0.63713	15.714	5.838	0.00000

- **By bisphosphonate medication**



. sktest osteoc0m if bisphos ==0

Skewness/Kurtosis tests for Normality

Variable	Obs	Pr(Skewness)	Pr(Kurtosis)	adj chi2(2)	joint Prob>chi2
osteoc0m	29	0.0164	0.1860	6.75	0.0342

. swilk osteoc0m if bisphos ==0

Shapiro-wilk W test for normal data

Variable	Obs	w	V	z	Prob>z
osteoc0m	29	0.91034	2.779	2.109	0.01748

. sktest osteoc6m if bisphos ==0

Skewness/Kurtosis tests for Normality

Variable	Obs	Pr(Skewness)	Pr(Kurtosis)	adj chi2(2)	joint Prob>chi2
osteoc6m	29	0.0003	0.0018	17.05	0.0002

. swilk osteoc6m if bisphos ==0

Shapiro-wilk W test for normal data

Variable	Obs	w	V	z	Prob>z
osteoc6m	29	0.84289	4.869	3.266	0.00055

. sktest osteoc60m if bisphos ==0

Skewness/Kurtosis tests for Normality

Variable	Obs	Pr(Skewness)	Pr(Kurtosis)	adj chi2(2)	joint Prob>chi2
osteoc60m	29	0.2845	0.4404	1.89	0.3888

. swilk osteoc60m if bisphos ==0

Shapiro-wilk W test for normal data

Variable	Obs	w	V	z	Prob>z
osteoc60m	29	0.96297	1.148	0.284	0.38807

. sktest osteocchange if bisphos ==0

Skewness/Kurtosis tests for Normality

Variable	Obs	Pr(Skewness)	Pr(Kurtosis)	adj chi2(2)	joint Prob>chi2
osteocchange	29	0.0000	0.0000	41.17	0.0000

. swilk osteocchange if bisphos ==0

Shapiro-wilk W test for normal data

Variable	Obs	w	V	z	Prob>z
osteocchange	29	0.45372	16.931	5.838	0.00000

. sktest osteoc0m if bisphos ==1

Skewness/Kurtosis tests for Normality

Variable	Obs	Pr(Skewness)	Pr(Kurtosis)	adj chi2(2)	joint Prob>chi2
osteoc0m	17	0.6362	0.2743	1.59	0.4518

. swilk osteoc0m if bisphos ==1

Shapiro-wilk W test for normal data

Variable	Obs	w	V	z	Prob>z
osteoc0m	17	0.93632	1.345	0.592	0.27707

. sktest osteoc6m if bisphos ==1

Skewness/Kurtosis tests for Normality

Variable	Obs	Pr(Skewness)	Pr(Kurtosis)	adj chi2(2)	joint Prob>chi2
osteoc6m	16	0.0247	0.2821	5.80	0.0549

. swilk osteoc6m if bisphos ==1

Shapiro-wilk W test for normal data

Variable	Obs	w	V	z	Prob>z
osteoc6m	16	0.84608	3.119	2.259	0.01194

. sktest osteoc60m if bisphos ==1

Skewness/Kurtosis tests for Normality

Variable	Obs	Pr(Skewness)	Pr(Kurtosis)	adj chi2(2)	joint Prob>chi2
osteoc60m	16	0.0091	0.1481	7.60	0.0224

. swilk osteoc60m if bisphos ==1

Shapiro-wilk W test for normal data

Variable	Obs	w	V	z	Prob>z
osteoc60m	16	0.79200	4.214	2.857	0.00214

. sktest osteocchange if bisphos ==1

Skewness/Kurtosis tests for Normality

Variable	Obs	Pr(Skewness)	Pr(Kurtosis)	adj chi2(2)	joint Prob>chi2
osteocchange	16	0.1171	0.7400	2.97	0.2264

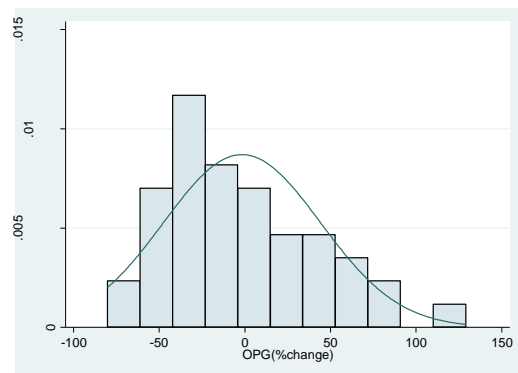
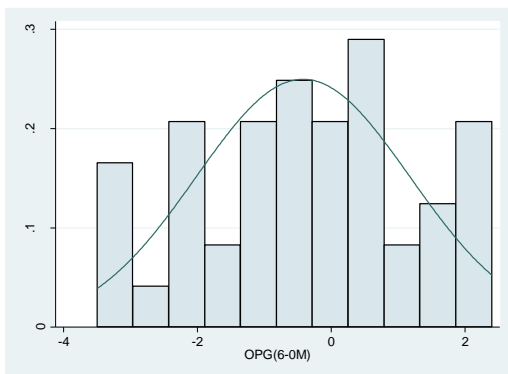
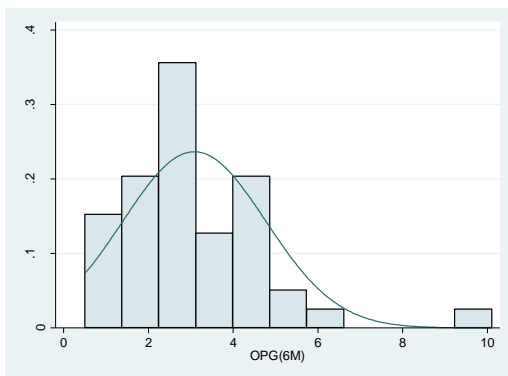
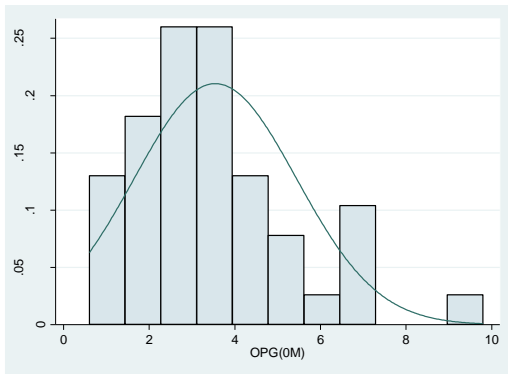
. swilk osteocchange if bisphos ==1

Shapiro-wilk W test for normal data

Variable	Obs	w	V	z	Prob>z
osteocchange	16	0.87617	2.509	1.827	0.03384

# OPG

1 All



. sktest boopg

Skewness/Kurtosis tests for Normality

Variable	Obs	Pr(Skewness)	Pr(Kurtosis)	adj	chi2(2)	joint	Prob>chi2
boopg	46	0.0041	0.0724		9.61		0.0082

. swilk boopg

Shapiro-wilk w test for normal data

Variable	Obs	W	V	z	Prob>z
boopg	46	0.93138	3.023	2.347	0.00945

. sktest opg6m

Skewness/Kurtosis tests for Normality

Variable	Obs	Pr(Skewness)	Pr(Kurtosis)	adj	chi2(2)	joint	Prob>chi2
opg6m	45	0.0001	0.0004		20.33		0.0000

. swilk opg6m

Shapiro-wilk w test for normal data

Variable	Obs	W	V	z	Prob>z
opg6m	45	0.89003	4.762	3.308	0.00047

. sktest opgchange

Skewness/Kurtosis tests for Normality

Variable	Obs	Pr(Skewness)	Pr(Kurtosis)	adj	chi2(2)	joint	Prob>chi2
opgchange	45	0.7335	0.1660		2.15		0.3405

. swilk opgchange

Shapiro-wilk w test for normal data

Variable	Obs	W	V	z	Prob>z
opgchange	45	0.97237	1.197	0.380	0.35183

. sktest ogpperchange

Skewness/Kurtosis tests for Normality

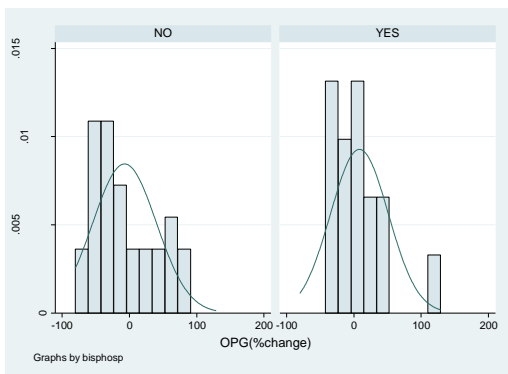
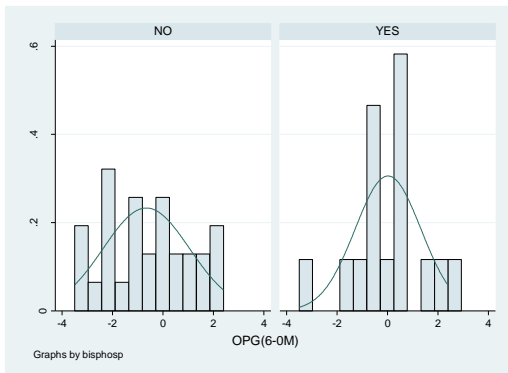
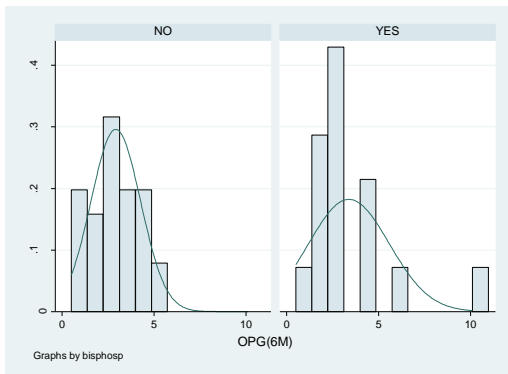
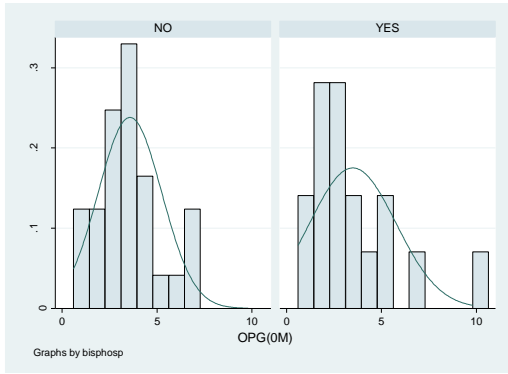
Variable	Obs	Pr(Skewness)	Pr(Kurtosis)	adj	chi2(2)	joint	Prob>chi2
ogpperchange	45	0.0493	0.6822		4.18		0.1234

. swilk ogpperchange

Shapiro-wilk w test for normal data

Variable	Obs	W	V	z	Prob>z
ogpperchange	45	0.95375	2.003	1.472	0.07050

- **By bisphosphonate medication**



. sktest opg0m if bisphos ==0

Skewness/Kurtosis tests for Normality

Variable	Obs	Pr(Skewness)	Pr(Kurtosis)	adj chi2(2)	joint Prob>chi2
opg0m	29	0.2688	0.8450	1.36	0.5078

. swilk opg0m if bisphos ==0

Shapiro-wilk W test for normal data

Variable	Obs	W	V	z	Prob>z
opg0m	29	0.96126	1.201	0.377	0.35304

. sktest opg6m if bisphos ==0

Skewness/Kurtosis tests for Normality

Variable	Obs	Pr(Skewness)	Pr(Kurtosis)	adj chi2(2)	joint Prob>chi2
opg6m	29	0.6945	0.2952	1.34	0.5110

. swilk opg6m if bisphos ==0

Shapiro-wilk W test for normal data

Variable	Obs	W	V	z	Prob>z
opg6m	29	0.97981	0.626	-0.967	0.83326

. sktest opg60m if bisphos ==0

Skewness/Kurtosis tests for Normality

Variable	Obs	Pr(Skewness)	Pr(Kurtosis)	adj chi2(2)	joint Prob>chi2
opg60m	29	0.7617	0.0849	3.37	0.1856

. swilk opg60m if bisphos ==0

Shapiro-wilk W test for normal data

Variable	Obs	W	V	z	Prob>z
opg60m	29	0.98789	0.375	-2.023	0.97844

. sktest opgchange if bisphos ==0

Skewness/Kurtosis tests for Normality

Variable	Obs	Pr(Skewness)	Pr(Kurtosis)	adj chi2(2)	joint Prob>chi2
opgchange	29	0.1900	0.1915	3.73	0.1547

. swilk opgchange if bisphos ==0

Shapiro-wilk W test for normal data

Variable	Obs	W	V	z	Prob>z
opgchange	29	0.92333	2.376	1.786	0.03707

. sktest opg0m if bisphos ==1

Skewness/Kurtosis tests for Normality

Variable	Obs	Pr(Skewness)	Pr(Kurtosis)	adj chi2(2)	joint Prob>chi2
opg0m	17	0.0066	0.0459	9.21	0.0100

. swilk opg0m if bisphos ==1

Shapiro-wilk W test for normal data

Variable	Obs	W	V	z	Prob>z
opg0m	17	0.85224	3.122	2.270	0.01160

. sktest opg6m if bisphos ==1

Skewness/Kurtosis tests for Normality

Variable	Obs	Pr(Skewness)	Pr(Kurtosis)	adj chi2(2)	joint Prob>chi2
opg6m	16	0.0013	0.0039	13.64	0.0011

. swilk opg6m if bisphos ==1

Shapiro-wilk W test for normal data

Variable	Obs	W	V	z	Prob>z
opg6m	16	0.80690	3.913	2.710	0.00337

. sktest opg60m if bisphos ==1

Skewness/Kurtosis tests for Normality

Variable	Obs	Pr(Skewness)	Pr(Kurtosis)	adj chi2(2)	joint Prob>chi2
opg60m	16	0.4887	0.2502	2.05	0.3583

. swilk opg60m if bisphos ==1

Shapiro-wilk W test for normal data

Variable	Obs	W	V	z	Prob>z
opg60m	16	0.96434	0.723	-0.646	0.74071

. sktest opgchange if bisphos ==1

Skewness/Kurtosis tests for Normality

Variable	Obs	Pr(Skewness)	Pr(Kurtosis)	adj chi2(2)	joint Prob>chi2
opgchange	16	0.0139	0.0339	8.67	0.0131

. swilk opgchange if bisphos ==1

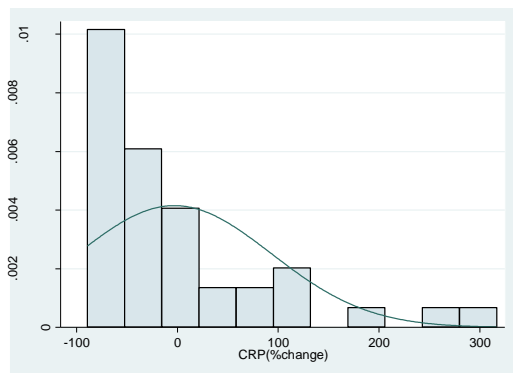
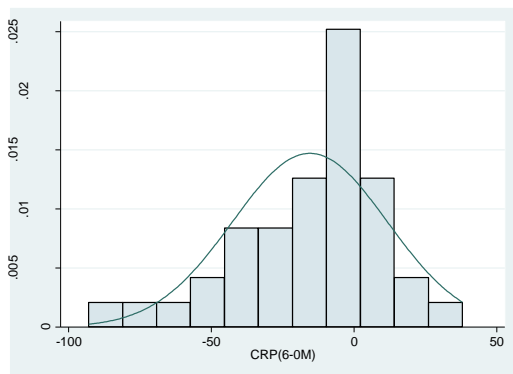
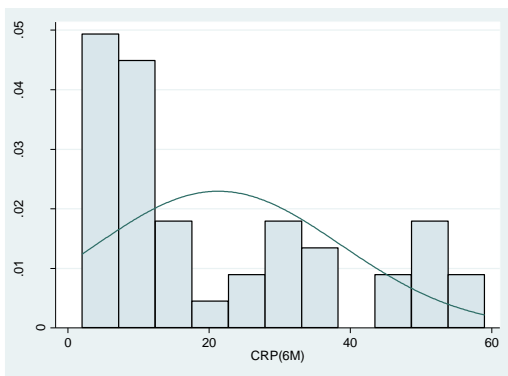
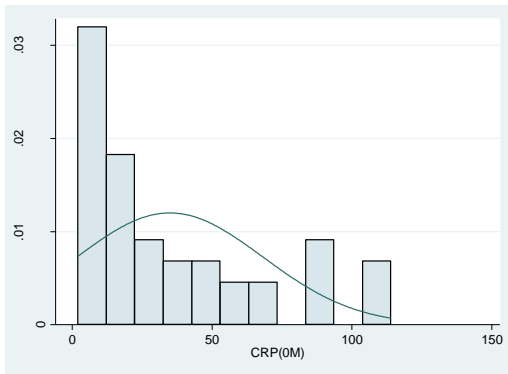
Shapiro-wilk W test for normal data

Variable	Obs	W	V	z	Prob>z
opgchange	16	0.88231	2.385	1.726	0.04217



# CRP

- All



. sktest bocrp

Skewness/Kurtosis tests for Normality

Variable	Obs	Pr(Skewness)	Pr(Kurtosis)	adj	chi2(2)	joint Prob>chi2
bocrp	43	0.0066	0.9128		6.70	0.0351

. swilk bocrp

Shapiro-wilk w test for normal data

Variable	Obs	W	V	z	Prob>z
bocrp	43	0.84063	6.661	4.008	0.00003

. sktest crp6m

Skewness/Kurtosis tests for Normality

Variable	Obs	Pr(Skewness)	Pr(Kurtosis)	adj	chi2(2)	joint Prob>chi2
crp6m	43	0.0302	0.2586		5.67	0.0588

. swilk crp6m

Shapiro-wilk w test for normal data

Variable	Obs	W	V	z	Prob>z
crp6m	43	0.86768	5.531	3.615	0.00015

. sktest crpchange

Skewness/Kurtosis tests for Normality

Variable	Obs	Pr(Skewness)	Pr(Kurtosis)	adj	chi2(2)	joint Prob>chi2
crpchange	40	0.0234	0.1816		6.36	0.0416

. swilk crpchange

Shapiro-wilk w test for normal data

Variable	Obs	W	V	z	Prob>z
crpchange	40	0.93852	2.430	1.869	0.03084

. sktest crpperchange

Skewness/Kurtosis tests for Normality

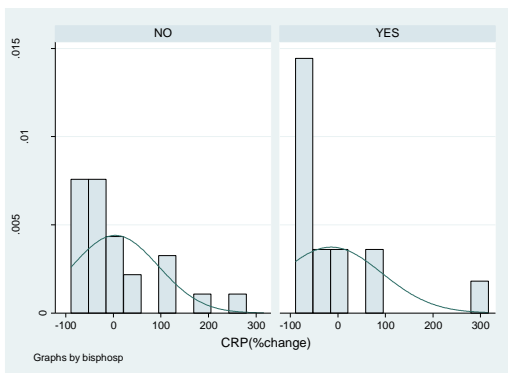
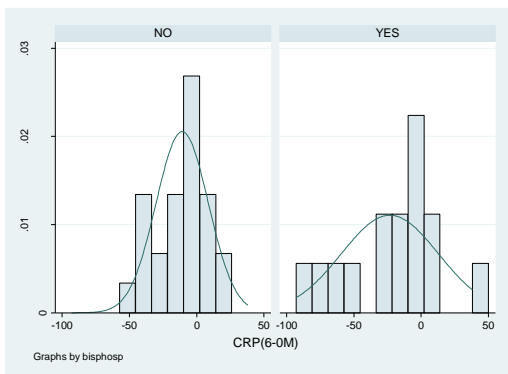
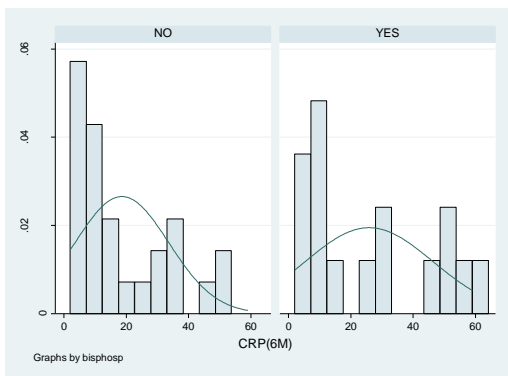
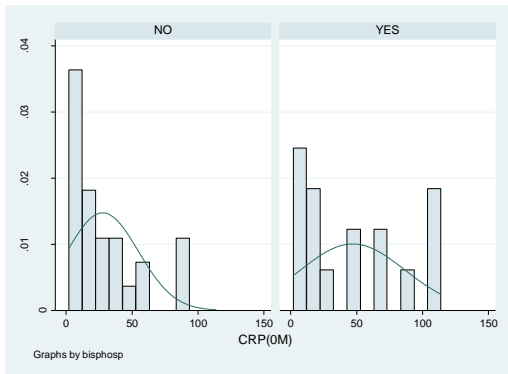
Variable	Obs	Pr(Skewness)	Pr(Kurtosis)	adj	chi2(2)	joint Prob>chi2
crpperchange	40	0.0001	0.0091		16.75	0.0002

. swilk crpperchange

Shapiro-wilk w test for normal data

Variable	Obs	W	V	z	Prob>z
crpperchange	40	0.78260	8.593	4.527	0.00000

## By bisphosphonate medication



. sktest crp0m if bisphos ==0

Skewness/Kurtosis tests for Normality					
Variable	Obs	Pr(Skewness)	Pr(Kurtosis)	adj chi2(2)	joint Prob>chi2
crp0m	27	0.0123	0.4583	6.26	0.0438

. swilk crp0m if bisphos ==0

Shapiro-wilk W test for normal data					
Variable	Obs	w	V	z	Prob>z
crp0m	27	0.83313	4.906	3.267	0.00054

. sktest crp6m if bisphos ==0

Skewness/Kurtosis tests for Normality					
Variable	Obs	Pr(Skewness)	Pr(Kurtosis)	adj chi2(2)	joint Prob>chi2
crp6m	27	0.0457	0.6576	4.34	0.1144

. swilk crp6m if bisphos ==0

Shapiro-wilk W test for normal data					
Variable	Obs	w	V	z	Prob>z
crp6m	27	0.86372	4.006	2.851	0.00218

. sktest crp60m if bisphos ==0

Skewness/Kurtosis tests for Normality					
Variable	Obs	Pr(Skewness)	Pr(Kurtosis)	adj chi2(2)	joint Prob>chi2
crp60m	25	0.3406	0.7085	1.13	0.5689

. swilk crp60m if bisphos ==0

Shapiro-wilk W test for normal data					
Variable	Obs	w	V	z	Prob>z
crp60m	25	0.93414	1.830	1.235	0.10833

. sktest crpchange if bisphos ==0

Skewness/Kurtosis tests for Normality					
Variable	Obs	Pr(Skewness)	Pr(Kurtosis)	adj chi2(2)	joint Prob>chi2
crpchange	25	0.0037	0.0946	9.27	0.0097

. swilk crpchange if bisphos ==0

Shapiro-wilk W test for normal data					
Variable	Obs	w	V	z	Prob>z
crpchange	25	0.82241	4.935	3.263	0.00055

. sktest crp0m if bisphos ==1

Skewness/Kurtosis tests for Normality					
Variable	Obs	Pr(Skewness)	Pr(Kurtosis)	adj chi2(2)	joint Prob>chi2
crp0m	16	0.2513	0.1368	3.89	0.1430

. swilk crp0m if bisphos ==1

Shapiro-wilk W test for normal data					
Variable	Obs	w	V	z	Prob>z
crp0m	16	0.84350	3.171	2.292	0.01095

. sktest crp6m if bisphos ==1

Skewness/Kurtosis tests for Normality					
Variable	Obs	Pr(Skewness)	Pr(Kurtosis)	adj chi2(2)	joint Prob>chi2
crp6m	16	0.3634	0.0779	4.19	0.1229

. swilk crp6m if bisphos ==1

Shapiro-wilk W test for normal data					
Variable	Obs	w	V	z	Prob>z
crp6m	16	0.88298	2.371	1.715	0.04320

. sktest crp60m if bisphos ==1

Skewness/Kurtosis tests for Normality					
Variable	Obs	Pr(Skewness)	Pr(Kurtosis)	adj chi2(2)	joint Prob>chi2
crp60m	15	0.3808	0.9369	0.84	0.6574

. swilk crp60m if bisphos ==1

Shapiro-wilk W test for normal data					
Variable	Obs	w	V	z	Prob>z
crp60m	15	0.95440	0.884	-0.243	0.59614

. sktest crpchange if bisphos ==1

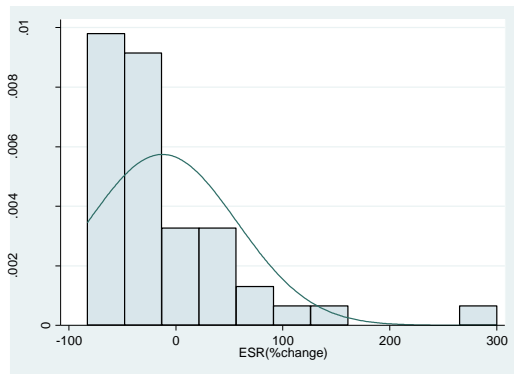
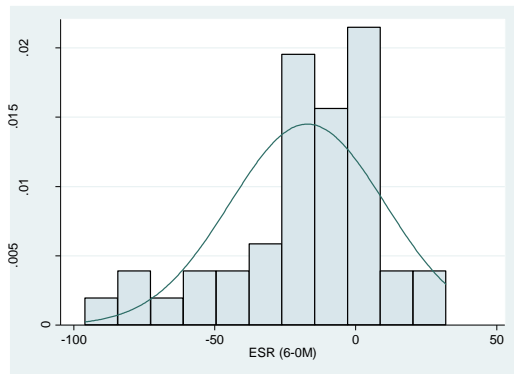
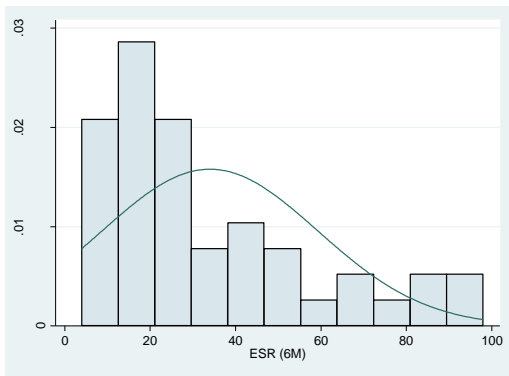
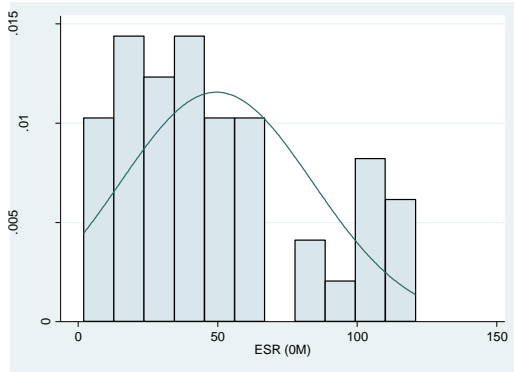
Skewness/Kurtosis tests for Normality					
Variable	Obs	Pr(Skewness)	Pr(Kurtosis)	adj chi2(2)	joint Prob>chi2
crpchange	15	0.0004	0.0021	15.64	0.0004

. swilk crpchange if bisphos ==1

Shapiro-wilk W test for normal data					
Variable	Obs	w	V	z	Prob>z
crpchange	15	0.69088	5.994	3.542	0.00020

# ESR

- All



. sktest boesr

Skewness/Kurtosis tests for Normality

Variable	Obs	Pr(Skewness)	Pr(Kurtosis)	adj	joint	
				chi2(2)	Prob>chi2	
boesr	45	0.0451	0.4120	4.69	0.0957	

. swilk boesr

Shapiro-wilk w test for normal data

Variable	Obs	W	V	z	Prob>z
boesr	45	0.91057	3.872	2.869	0.00206

. sktest esr6m

Skewness/Kurtosis tests for Normality

Variable	Obs	Pr(Skewness)	Pr(Kurtosis)	adj	joint	
				chi2(2)	Prob>chi2	
esr6m	45	0.0040	0.5597	7.60	0.0223	

. swilk esr6m

Shapiro-wilk w test for normal data

Variable	Obs	W	V	z	Prob>z
esr6m	45	0.86568	5.816	3.731	0.00010

. sktest esrchage

Skewness/Kurtosis tests for Normality

Variable	Obs	Pr(Skewness)	Pr(Kurtosis)	adj	joint	
				chi2(2)	Prob>chi2	
esrchage	44	0.0084	0.1712	7.74	0.0209	

. swilk esrchage

Shapiro-wilk w test for normal data

Variable	Obs	W	V	z	Prob>z
esrchage	44	0.92996	2.980	2.311	0.01041

. sktest esrperchange

Skewness/Kurtosis tests for Normality

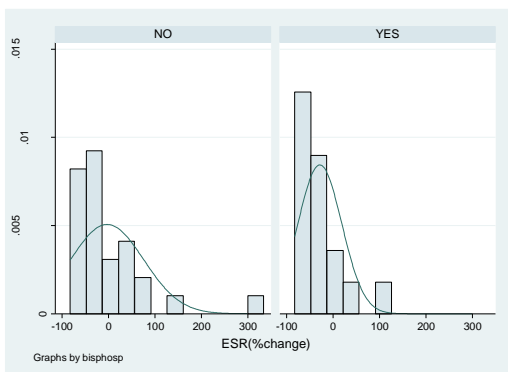
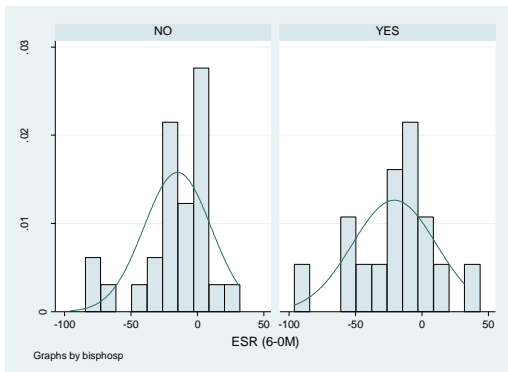
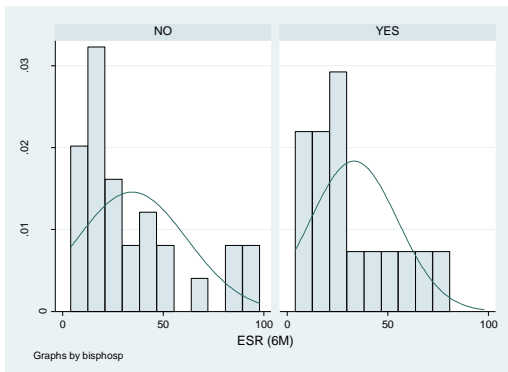
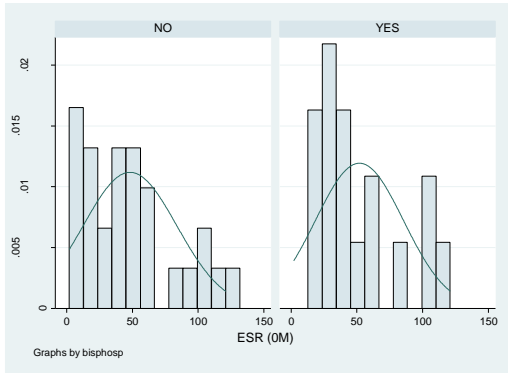
Variable	Obs	Pr(Skewness)	Pr(Kurtosis)	adj	joint	
				chi2(2)	Prob>chi2	
esrperchange	44	0.0000	0.0000	29.66	0.0000	

. swilk esrperchange

Shapiro-wilk w test for normal data

Variable	Obs	W	V	z	Prob>z
esrperchange	44	0.77525	9.564	4.779	0.00000

- **By bisphosphonate medication**



. sktest esr0m if bisphos ==0

Skewness/Kurtosis tests for Normality

Variable	Obs	Pr(Skewness)	Pr(Kurtosis)	adj chi2(2)	joint Prob>chi2
esr0m	28	0.1175	0.6323	2.95	0.2291

. swilk esr0m if bisphos ==0

Shapiro-wilk W test for normal data

Variable	Obs	W	V	z	Prob>z
esr0m	28	0.91907	2.444	1.840	0.03289

. sktest esr6m if bisphos ==0

Skewness/Kurtosis tests for Normality

Variable	Obs	Pr(Skewness)	Pr(Kurtosis)	adj chi2(2)	joint Prob>chi2
esr6m	29	0.0123	0.5735	6.10	0.0473

. swilk esr6m if bisphos ==0

Shapiro-wilk W test for normal data

Variable	Obs	W	V	z	Prob>z
esr6m	29	0.84629	4.764	3.221	0.00064

. sktest esr60m if bisphos ==0

Skewness/Kurtosis tests for Normality

Variable	Obs	Pr(Skewness)	Pr(Kurtosis)	adj chi2(2)	joint Prob>chi2
esr60m	28	0.0102	0.1421	7.62	0.0221

. swilk esr60m if bisphos ==0

Shapiro-wilk W test for normal data

Variable	Obs	W	V	z	Prob>z
esr60m	28	0.89180	3.267	2.438	0.00739

. sktest esrchange if bisphos ==0

Skewness/Kurtosis tests for Normality

Variable	Obs	Pr(Skewness)	Pr(Kurtosis)	adj chi2(2)	joint Prob>chi2
esrchange	28	0.0000	0.0003	21.29	0.0000

. swilk esrchange if bisphos ==0

Shapiro-wilk W test for normal data

Variable	Obs	W	V	z	Prob>z
esrchange	28	0.78250	6.568	3.875	0.00005

. sktest esr0m if bisphos ==1

Skewness/Kurtosis tests for Normality

Variable	Obs	Pr(Skewness)	Pr(Kurtosis)	adj chi2(2)	joint Prob>chi2
esr0m	17	0.0903	0.7336	3.46	0.1776

. swilk esr0m if bisphos ==1

Shapiro-wilk W test for normal data

Variable	Obs	W	V	z	Prob>z
esr0m	17	0.85703	3.020	2.204	0.01375

. sktest esr6m if bisphos ==1

Skewness/Kurtosis tests for Normality

Variable	Obs	Pr(Skewness)	Pr(Kurtosis)	adj chi2(2)	joint Prob>chi2
esr6m	16	0.0993	0.8536	3.20	0.2024

. swilk esr6m if bisphos ==1

Shapiro-wilk W test for normal data

Variable	Obs	W	V	z	Prob>z
esr6m	16	0.87463	2.540	1.852	0.03204

. sktest esr60m if bisphos ==1

Skewness/Kurtosis tests for Normality

Variable	Obs	Pr(Skewness)	Pr(Kurtosis)	adj chi2(2)	joint Prob>chi2
esr60m	16	0.1703	0.3146	3.37	0.1859

. swilk esr60m if bisphos ==1

Shapiro-wilk W test for normal data

Variable	Obs	W	V	z	Prob>z
esr60m	16	0.95721	0.867	-0.284	0.61161

. sktest esrchange if bisphos ==1

Skewness/Kurtosis tests for Normality

Variable	Obs	Pr(Skewness)	Pr(Kurtosis)	adj chi2(2)	joint Prob>chi2
esrchange	16	0.0030	0.0120	11.50	0.0032

. swilk esrchange if bisphos ==1

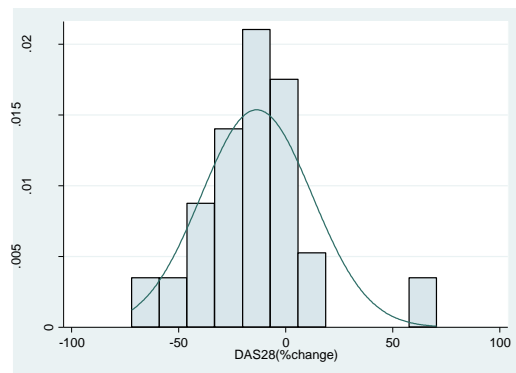
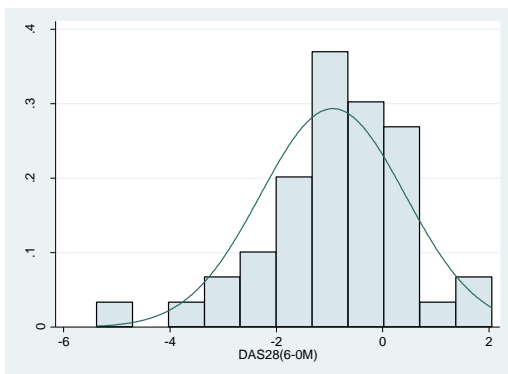
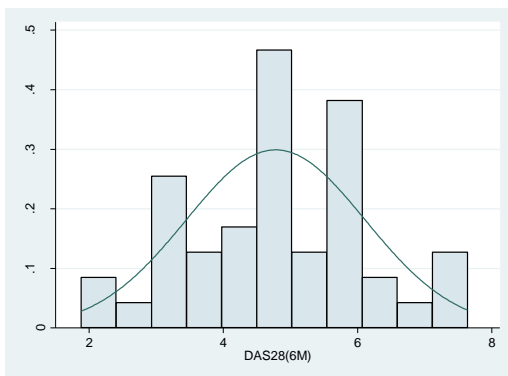
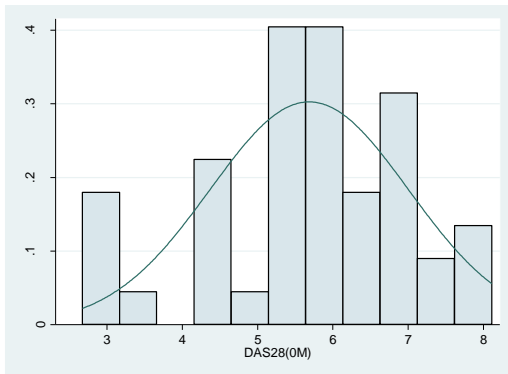
Shapiro-wilk W test for normal data

Variable	Obs	W	V	z	Prob>z
esrchange	16	0.83302	3.383	2.421	0.00774



# DAS28 score

- All



. sktest bodas28

Skewness/Kurtosis tests for Normality					
Variable	Obs	Pr(Skewness)	Pr(Kurtosis)	adj chi2(2)	joint Prob>chi2
bodas28	45	0.0935	0.7054	3.15	0.2072

. swilk bodas28

Shapiro-wilk w test for normal data					
Variable	Obs	W	V	z	Prob>z
bodas28	45	0.95539	1.932	1.395	0.08145

. sktest das286m

Skewness/Kurtosis tests for Normality					
Variable	Obs	Pr(Skewness)	Pr(Kurtosis)	adj chi2(2)	joint Prob>chi2
das286m	45	0.8802	0.8921	0.04	0.9797

. swilk das286m

Shapiro-wilk w test for normal data					
Variable	Obs	W	V	z	Prob>z
das286m	45	0.98416	0.686	-0.799	0.78794

. sktest das28change

Skewness/Kurtosis tests for Normality					
Variable	Obs	Pr(Skewness)	Pr(Kurtosis)	adj chi2(2)	joint Prob>chi2
das28change	44	0.0684	0.0430	6.73	0.0346

. swilk das28change

Shapiro-wilk w test for normal data					
Variable	Obs	W	V	z	Prob>z
das28change	44	0.96265	1.589	0.980	0.16344

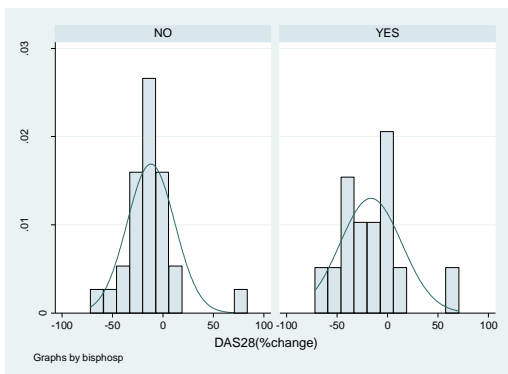
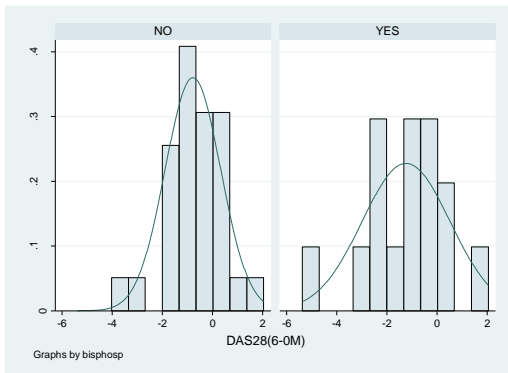
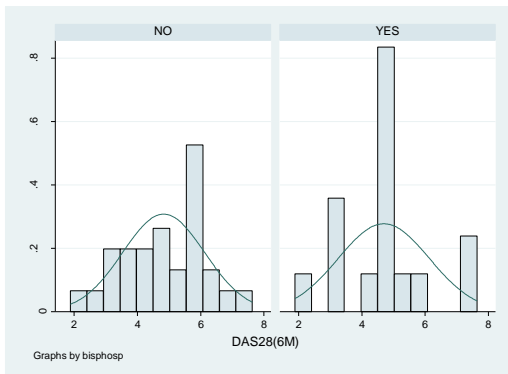
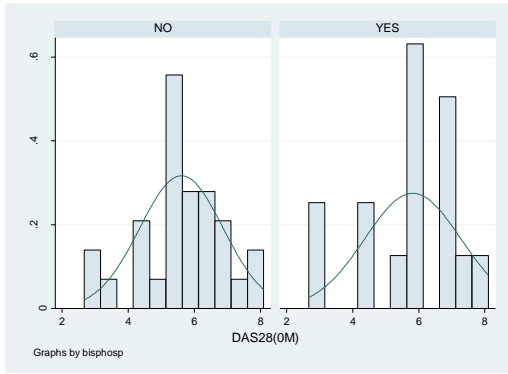
. sktest das28perchange

Skewness/Kurtosis tests for Normality					
Variable	Obs	Pr(Skewness)	Pr(Kurtosis)	adj chi2(2)	joint Prob>chi2
das28perch~e	44	0.0330	0.0098	9.42	0.0090

. swilk das28perchange

Shapiro-wilk w test for normal data					
Variable	Obs	W	V	z	Prob>z
das28perch~e	44	0.92752	3.084	2.384	0.00857

- **By bisphosphonate medication**



. sktest das280m if bisphos ==0

Skewness/Kurtosis tests for Normality

Variable	Obs	Pr(Skewness)	Pr(Kurtosis)	adj chi2(2)	joint Prob>chi2
das280m	29	0.1595	0.4926	2.68	0.2615

. swilk das280m if bisphos ==0

Shapiro-Wilk W test for normal data

Variable	Obs	W	V	z	Prob>z
das280m	29	0.95890	1.274	0.499	0.30873

. sktest das286m if bisphos ==0

Skewness/Kurtosis tests for Normality

Variable	Obs	Pr(Skewness)	Pr(Kurtosis)	adj chi2(2)	joint Prob>chi2
das286m	29	0.3249	0.5759	1.38	0.5020

. swilk das286m if bisphos ==0

Shapiro-Wilk W test for normal data

Variable	Obs	W	V	z	Prob>z
das286m	29	0.96582	1.059	0.119	0.45267

. sktest das2860m if bisphos ==0

Skewness/Kurtosis tests for Normality

Variable	Obs	Pr(Skewness)	Pr(Kurtosis)	adj chi2(2)	joint Prob>chi2
das2860m	29	0.8177	0.1338	2.52	0.2842

. swilk das2860m if bisphos ==0

Shapiro-Wilk W test for normal data

Variable	Obs	W	V	z	Prob>z
das2860m	29	0.96932	0.951	-0.104	0.54133

. sktest das28change if bisphos ==0

Skewness/Kurtosis tests for Normality

Variable	Obs	Pr(Skewness)	Pr(Kurtosis)	adj chi2(2)	joint Prob>chi2
das28change	29	0.0172	0.0025	11.71	0.0029

. swilk das28change if bisphos ==0

Shapiro-Wilk W test for normal data

Variable	Obs	W	V	z	Prob>z
das28change	29	0.89989	3.103	2.336	0.00974

. sktest das280m if bisphos ==1

Skewness/Kurtosis tests for Normality

Variable	Obs	Pr(Skewness)	Pr(Kurtosis)	adj chi2(2)	joint Prob>chi2
das280m	16	0.1937	0.6868	2.11	0.3476

. swilk das280m if bisphos ==1

Shapiro-Wilk W test for normal data

Variable	Obs	W	V	z	Prob>z
das280m	16	0.93522	1.312	0.540	0.29456

. sktest das286m if bisphos ==1

Skewness/Kurtosis tests for Normality

Variable	Obs	Pr(Skewness)	Pr(Kurtosis)	adj chi2(2)	joint Prob>chi2
das286m	16	0.3547	0.3666	1.90	0.3872

. swilk das286m if bisphos ==1

Shapiro-Wilk W test for normal data

Variable	Obs	W	V	z	Prob>z
das286m	16	0.92040	1.613	0.949	0.17123

. sktest das2860m if bisphos ==1

Skewness/Kurtosis tests for Normality

Variable	Obs	Pr(Skewness)	Pr(Kurtosis)	adj chi2(2)	joint Prob>chi2
das2860m	15	0.2609	0.2995	2.72	0.2570

. swilk das2860m if bisphos ==1

Shapiro-Wilk W test for normal data

Variable	Obs	W	V	z	Prob>z
das2860m	15	0.96240	0.729	-0.625	0.73408

. sktest das28change if bisphos ==1

Skewness/Kurtosis tests for Normality

Variable	Obs	Pr(Skewness)	Pr(Kurtosis)	adj chi2(2)	joint Prob>chi2
das28change	15	0.2350	0.1303	4.02	0.1337

. swilk das28change if bisphos ==1

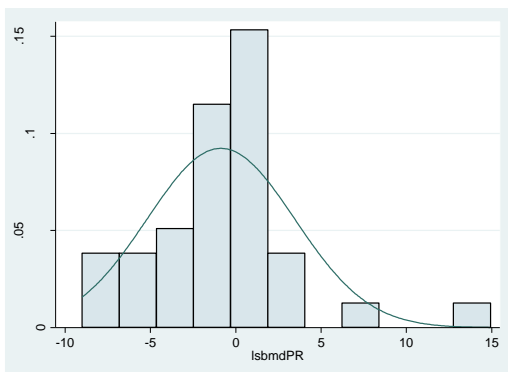
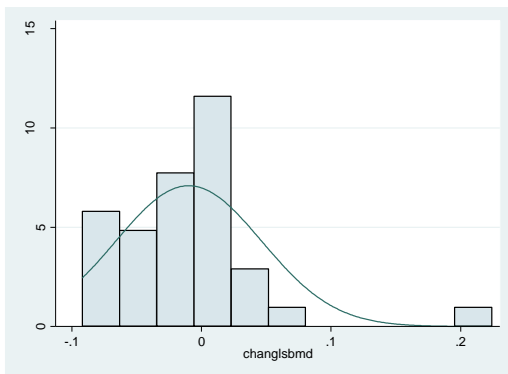
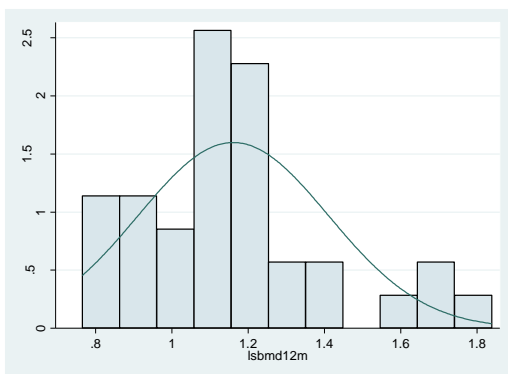
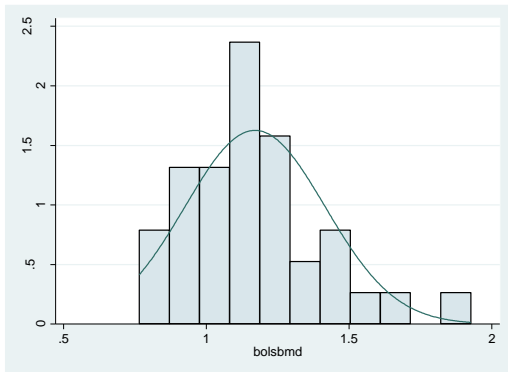
Shapiro-Wilk W test for normal data

Variable	Obs	W	V	z	Prob>z
das28change	15	0.95637	0.846	-0.331	0.62956

# Prospective Study

## LSBMD

- All



. sktest bolsbmd

Skewness/Kurtosis tests for Normality					
Variable	Obs	Pr(Skewness)	Pr(Kurtosis)	adj chi2(2)	joint Prob>chi2
bolsbmd	36	0.0158	0.0802	7.75	0.0207

. swilk bolsbmd

Shapiro-wilk W test for normal data					
Variable	Obs	W	V	z	Prob>z
bolsbmd	36	0.94493	2.008	1.458	0.07244

. sktest lsbmd12m

Skewness/Kurtosis tests for Normality					
Variable	Obs	Pr(Skewness)	Pr(Kurtosis)	adj chi2(2)	joint Prob>chi2
lsbmd12m	36	0.0269	0.2036	6.05	0.0484

. swilk lsbmd12m

Shapiro-wilk W test for normal data					
Variable	Obs	W	V	z	Prob>z
lsbmd12m	36	0.93321	2.435	1.861	0.03135

. sktest changlsbmd

Skewness/Kurtosis tests for Normality					
Variable	Obs	Pr(Skewness)	Pr(Kurtosis)	adj chi2(2)	joint Prob>chi2
changlsbmd	36	0.0001	0.0001	21.30	0.0000

. swilk changlsbmd

Shapiro-wilk W test for normal data					
Variable	Obs	W	V	z	Prob>z
changlsbmd	36	0.82720	6.301	3.849	0.00006

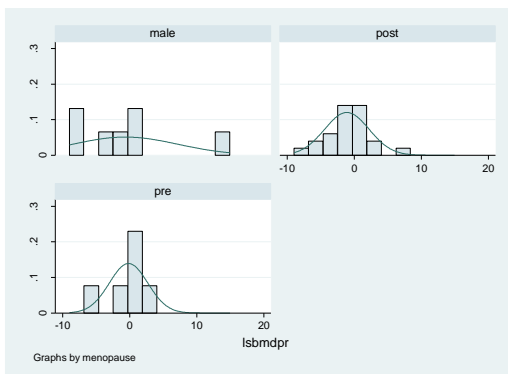
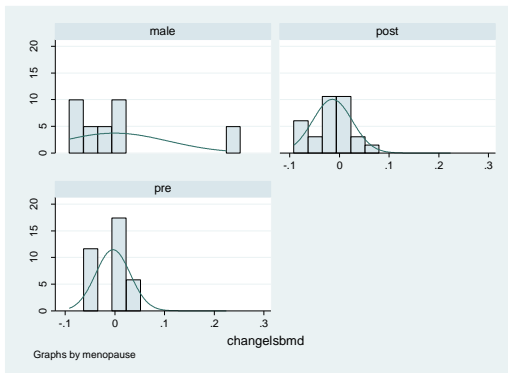
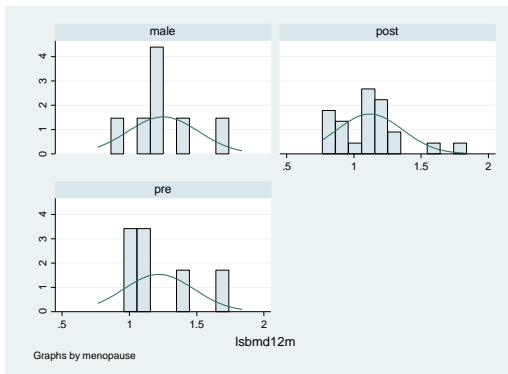
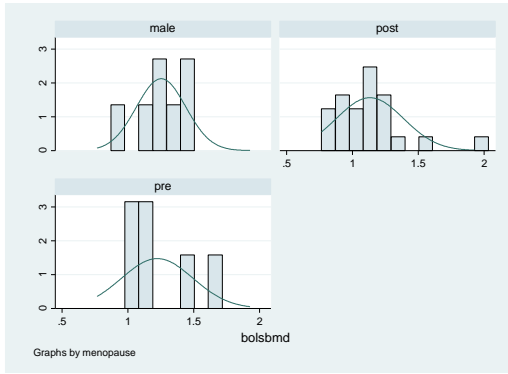
. sktest lsbmdpr

Skewness/Kurtosis tests for Normality					
Variable	Obs	Pr(Skewness)	Pr(Kurtosis)	adj chi2(2)	joint Prob>chi2
lsbmdpr	36	0.0108	0.0027	12.23	0.0022

. swilk lsbmdpr

Shapiro-wilk W test for normal data					
Variable	Obs	W	V	z	Prob>z
lsbmdpr	36	0.90344	3.521	2.632	0.00424

- **By gender and menopausal status**



. sktest bolsbmd if menopausal ==0

Skewness/Kurtosis tests for Normality

Variable	Obs	Pr(Skewness)	Pr(Kurtosis)	adj chi2(2)	joint Prob>chi2
bolsbmd	6	.	.	.	.

. swilk bolsbmd if menopausal ==0

Shapiro-wilk W test for normal data

Variable	Obs	W	V	z	Prob>z
bolsbmd	6	0.84945	1.864	1.012	0.15580

. sktest lsbmd12m if menopausal ==0

Skewness/Kurtosis tests for Normality

Variable	Obs	Pr(Skewness)	Pr(Kurtosis)	adj chi2(2)	joint Prob>chi2
lsbmd12m	6	.	.	.	.

. swilk lsbmd12m if menopausal ==0

Shapiro-wilk W test for normal data

Variable	Obs	W	V	z	Prob>z
lsbmd12m	6	0.84061	1.974	1.117	0.13190

. sktest changelsbmd if menopausal ==0

Skewness/Kurtosis tests for Normality

Variable	Obs	Pr(Skewness)	Pr(Kurtosis)	adj chi2(2)	joint Prob>chi2
changelsbmd	6	.	.	.	.

. swilk changelsbmd if menopausal ==0

Shapiro-wilk W test for normal data

Variable	Obs	W	V	z	Prob>z
changelsbmd	6	0.80502	2.415	1.513	0.06518

. sktest lsbmdpr if menopausal ==0

Skewness/Kurtosis tests for Normality

Variable	Obs	Pr(Skewness)	Pr(Kurtosis)	adj chi2(2)	joint Prob>chi2
lsbmdpr	6	.	.	.	.

. swilk lsbmdpr if menopausal ==0

Shapiro-wilk W test for normal data

Variable	Obs	W	V	z	Prob>z
lsbmdpr	6	0.82021	2.227	1.349	0.08863



. sktest bolsbmd if menopausal ==1

Skewness/Kurtosis tests for Normality

Variable	Obs	Pr(Skewness)	Pr(Kurtosis)	adj chi2(2)	joint Prob>chi2
bolsbmd	23	0.0080	0.0175	10.19	0.0061

. swilk bolsbmd if menopausal ==1

Shapiro-wilk W test for normal data

Variable	Obs	W	V	Z	Prob>z
bolsbmd	23	0.89874	2.649	1.981	0.02381

. sktest lsbmd12m if menopausal ==1

Skewness/Kurtosis tests for Normality

Variable	Obs	Pr(Skewness)	Pr(Kurtosis)	adj chi2(2)	joint Prob>chi2
lsbmd12m	23	0.0237	0.0423	7.92	0.0191

. swilk lsbmd12m if menopausal ==1

Shapiro-wilk W test for normal data

Variable	Obs	W	V	Z	Prob>z
lsbmd12m	23	0.90820	2.401	1.781	0.03743

. sktest changelsbmd if menopausal ==1

Skewness/Kurtosis tests for Normality

Variable	Obs	Pr(Skewness)	Pr(Kurtosis)	adj chi2(2)	joint Prob>chi2
changelsbmd	23	0.5905	0.4477	0.93	0.6287

. swilk changelsbmd if menopausal ==1

Shapiro-wilk W test for normal data

Variable	Obs	W	V	Z	Prob>z
changelsbmd	23	0.93795	1.623	0.985	0.16239

. sktest lsbmdpr if menopausal ==1

Skewness/Kurtosis tests for Normality

Variable	Obs	Pr(Skewness)	Pr(Kurtosis)	adj chi2(2)	joint Prob>chi2
lsbmdpr	23	0.6643	0.2108	1.94	0.3795

. swilk lsbmdpr if menopausal ==1

Shapiro-wilk W test for normal data

Variable	Obs	W	V	Z	Prob>z
lsbmdpr	23	0.96745	0.851	-0.327	0.62826

. sktest bolsbmd if menopausal ==2

Skewness/Kurtosis tests for Normality

Variable	Obs	Pr(Skewness)	Pr(Kurtosis)	joint	
				adj chi2(2)	Prob>chi2
bolsbmd	7	.	.	.	.

. swilk bolsbmd if menopausal ==2

Shapiro-wilk W test for normal data

Variable	Obs	W	V	z	Prob>z
bolsbmd	7	0.97833	0.285	-1.655	0.95105

. sktest lsbmd12m if menopausal ==2

Skewness/Kurtosis tests for Normality

Variable	Obs	Pr(Skewness)	Pr(Kurtosis)	joint	
				adj chi2(2)	Prob>chi2
lsbmd12m	7	.	.	.	.

. swilk lsbmd12m if menopausal ==2

Shapiro-wilk W test for normal data

Variable	Obs	W	V	z	Prob>z
lsbmd12m	7	0.94816	0.681	-0.562	0.71293

. sktest changelsbmd if menopausal ==2

Skewness/Kurtosis tests for Normality

Variable	Obs	Pr(Skewness)	Pr(Kurtosis)	joint	
				adj chi2(2)	Prob>chi2
changelsbmd	7	.	.	.	.

. swilk changelsbmd if menopausal ==2

Shapiro-wilk W test for normal data

Variable	Obs	W	V	z	Prob>z
changelsbmd	7	0.79159	2.737	1.828	0.03379

. sktest lsbmdpr if menopausal ==2

Skewness/Kurtosis tests for Normality

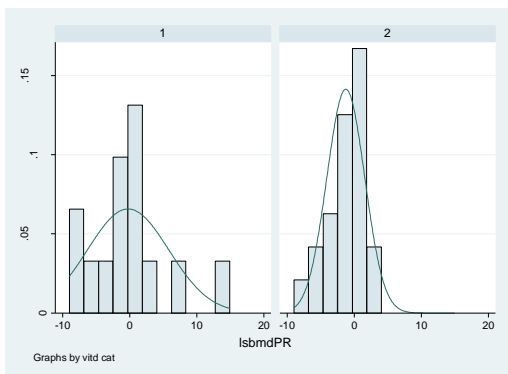
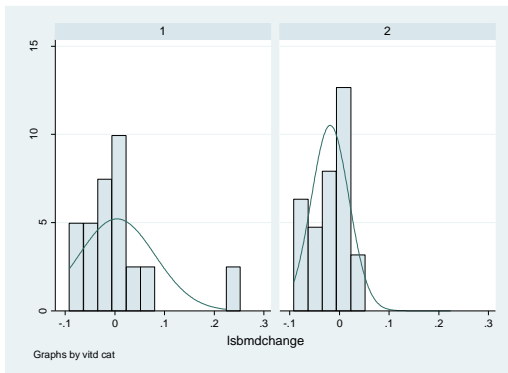
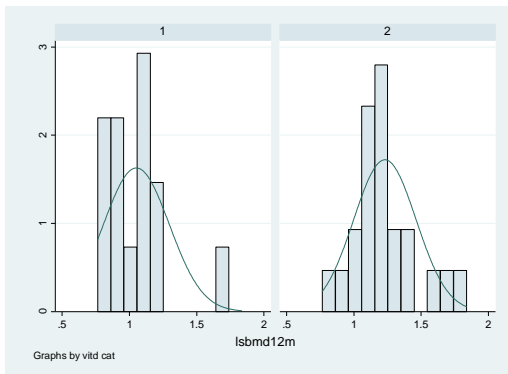
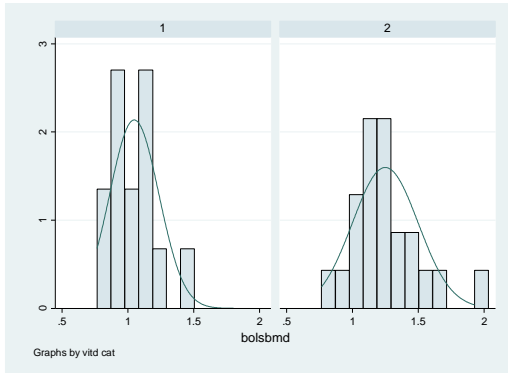
Variable	Obs	Pr(Skewness)	Pr(Kurtosis)	joint	
				adj chi2(2)	Prob>chi2
lsbmdpr	7	.	.	.	.

. swilk lsbmdpr if menopausal ==2

Shapiro-wilk W test for normal data

Variable	Obs	W	V	z	Prob>z
lsbmdpr	7	0.87377	1.658	0.841	0.20019

- **By vitamin D category**



. sktest bolsbmd if vitdcat ==1

Skewness/Kurtosis tests for Normality

Variable	Obs	Pr(Skewness)	Pr(Kurtosis)	adj chi2(2)	joint Prob>chi2
bolsbmd	14	0.1510	0.1908	4.09	0.1296

. swilk bolsbmd if vitdcat ==1

Shapiro-wilk W test for normal data

Variable	Obs	W	V	z	Prob>z
bolsbmd	14	0.94973	0.930	-0.142	0.55651

. sktest lsbmd12m if vitdcat ==1

Skewness/Kurtosis tests for Normality

Variable	Obs	Pr(Skewness)	Pr(Kurtosis)	adj chi2(2)	joint Prob>chi2
lsbmd12m	14	0.0127	0.0240	9.07	0.0107

. swilk lsbmd12m if vitdcat ==1

Shapiro-wilk W test for normal data

Variable	Obs	W	V	z	Prob>z
lsbmd12m	14	0.87166	2.375	1.703	0.04428

. sktest lsbmdchange if vitdcat ==1

Skewness/Kurtosis tests for Normality

Variable	Obs	Pr(Skewness)	Pr(Kurtosis)	adj chi2(2)	joint Prob>chi2
lsbmdchange	14	0.0042	0.0073	11.55	0.0031

. swilk lsbmdchange if vitdcat ==1

Shapiro-wilk W test for normal data

Variable	Obs	W	V	z	Prob>z
lsbmdchange	14	0.81682	3.390	2.403	0.00812

. sktest lsbmdpr if vitdcat ==1

Skewness/Kurtosis tests for Normality

Variable	Obs	Pr(Skewness)	Pr(Kurtosis)	adj chi2(2)	joint Prob>chi2
lsbmdpr	14	0.1095	0.0877	5.30	0.0707

. swilk lsbmdpr if vitdcat ==1

Shapiro-wilk W test for normal data

Variable	Obs	W	V	z	Prob>z
lsbmdpr	14	0.90423	1.772	1.127	0.12990

. sktest bolsbmd if vitdcat ==2

Skewness/Kurtosis tests for Normality

Variable	Obs	Pr(Skewness)	Pr(Kurtosis)	adj chi2(2)	joint Prob>chi2
bolsbmd	22	0.0432	0.1268	5.97	0.0505

. swilk bolsbmd if vitdcat ==2

Shapiro-wilk W test for normal data

Variable	Obs	W	V	z	Prob>z
bolsbmd	22	0.94076	1.501	0.823	0.20518

. sktest lsbmd12m if vitdcat ==2

Skewness/Kurtosis tests for Normality

Variable	Obs	Pr(Skewness)	Pr(Kurtosis)	adj chi2(2)	joint Prob>chi2
lsbmd12m	22	0.0476	0.1696	5.54	0.0626

. swilk lsbmd12m if vitdcat ==2

Shapiro-wilk W test for normal data

Variable	Obs	W	V	z	Prob>z
lsbmd12m	22	0.92819	1.819	1.213	0.11250

. sktest lsbmdchange if vitdcat ==2

Skewness/Kurtosis tests for Normality

Variable	Obs	Pr(Skewness)	Pr(Kurtosis)	adj chi2(2)	joint Prob>chi2
lsbmdchange	22	0.1419	0.8173	2.47	0.2909

. swilk lsbmdchange if vitdcat ==2

Shapiro-wilk W test for normal data

Variable	Obs	W	V	z	Prob>z
lsbmdchange	22	0.92537	1.891	1.292	0.09826

. sktest lsbmdpr if vitdcat ==2

Skewness/Kurtosis tests for Normality

Variable	Obs	Pr(Skewness)	Pr(Kurtosis)	adj chi2(2)	joint Prob>chi2
lsbmdpr	22	0.3035	0.6847	1.34	0.5125

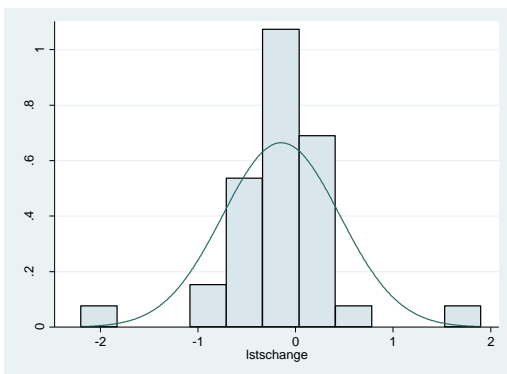
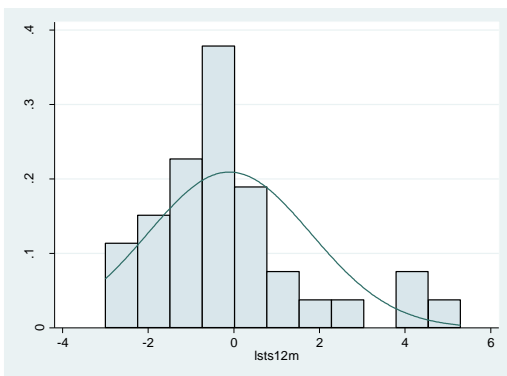
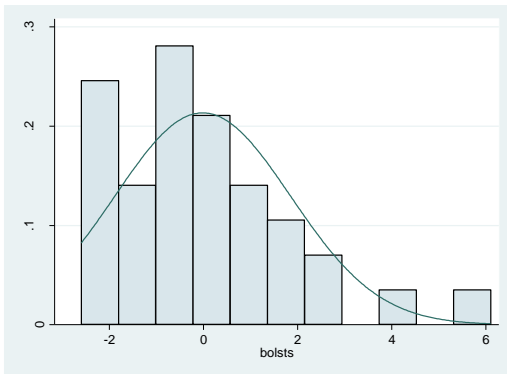
. swilk lsbmdpr if vitdcat ==2

Shapiro-wilk W test for normal data

Variable	Obs	W	V	z	Prob>z
----------	-----	---	---	---	--------

# LS t score

- All



. sktest bo1sts

Skewness/Kurtosis tests for Normality					
Variable	Obs	Pr(Skewness)	Pr(Kurtosis)	adj chi2(2)	joint Prob>chi2
bo1sts	36	0.0038	0.0316	10.59	0.0050

. swilk bo1sts

Shapiro-wilk w test for normal data					
Variable	Obs	w	V	z	Prob>z
bo1sts	36	0.91575	3.072	2.347	0.00947

. sktest 1sts12m

Skewness/Kurtosis tests for Normality					
Variable	Obs	Pr(Skewness)	Pr(Kurtosis)	adj chi2(2)	joint Prob>chi2
1sts12m	35	0.0071	0.0927	8.58	0.0137

. swilk 1sts12m

Shapiro-wilk w test for normal data					
Variable	Obs	w	V	z	Prob>z
1sts12m	35	0.90871	3.258	2.466	0.00684

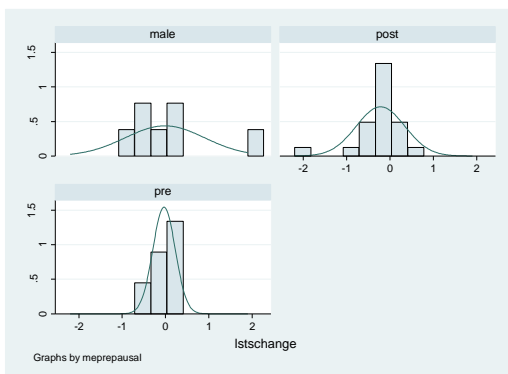
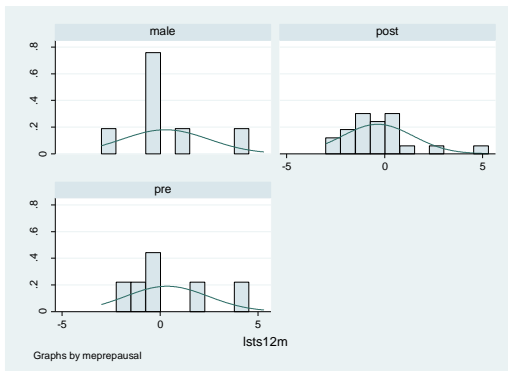
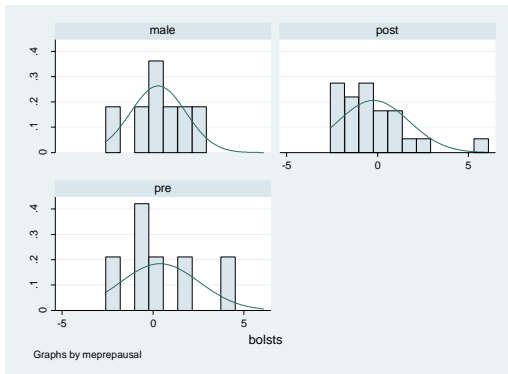
. sktest 1stschange

Skewness/Kurtosis tests for Normality					
Variable	Obs	Pr(Skewness)	Pr(Kurtosis)	adj chi2(2)	joint Prob>chi2
1stschange	35	0.8283	0.0004	10.37	0.0056

. swilk 1stschange

Shapiro-wilk w test for normal data					
Variable	Obs	w	V	z	Prob>z
1stschange	35	0.84083	5.681	3.626	0.00014

## - By gender and menopausal status



. sktest bolsts if menopause ==0

Skewness/Kurtosis tests for Normality					
Variable	Obs	Pr(Skewness)	Pr(Kurtosis)	adj chi2(2)	joint Prob>chi2
bolsts	6	.	.	.	.

. swilk bolsts if menopause ==0

Shapiro-wilk W test for normal data					
Variable	Obs	W	V	z	Prob>z
bolsts	6	0.90216	1.212	0.288	0.38685

. sktest lsts12m if menopause ==0

Skewness/Kurtosis tests for Normality					
Variable	Obs	Pr(Skewness)	Pr(Kurtosis)	adj chi2(2)	joint Prob>chi2
lsts12m	6	.	.	.	.

. swilk lsts12m if menopause ==0

Shapiro-wilk W test for normal data					
Variable	Obs	W	V	z	Prob>z
lsts12m	6	0.90565	1.168	0.232	0.40843

. sktest lstschange if menopause ==0

Skewness/Kurtosis tests for Normality					
Variable	Obs	Pr(Skewness)	Pr(Kurtosis)	adj chi2(2)	joint Prob>chi2
lstschange	6	.	.	.	.

. swilk lstschange if menopause ==0

Shapiro-wilk W test for normal data					
Variable	Obs	W	V	z	Prob>z
lstschange	6	0.85856	1.752	0.899	0.18428

. sktest bolsts if menopause ==1

Skewness/Kurtosis tests for Normality					
Variable	Obs	Pr(Skewness)	Pr(Kurtosis)	adj chi2(2)	joint Prob>chi2
bolsts	23	0.0021	0.0081	12.60	0.0018

. swilk bolsts if menopause ==1

Shapiro-wilk W test for normal data					
Variable	Obs	W	V	z	Prob>z
bolsts	23	0.87087	3.377	2.475	0.00666

. sktest lsts12m if menopause ==1

Skewness/Kurtosis tests for Normality					
Variable	Obs	Pr(Skewness)	Pr(Kurtosis)	adj chi2(2)	joint Prob>chi2
lsts12m	22	0.0040	0.0128	11.35	0.0034

. swilk lsts12m if menopause ==1

Shapiro-wilk W test for normal data					
Variable	Obs	W	V	z	Prob>z
lsts12m	22	0.87536	3.158	2.331	0.00986

. sktest lstschange if menopause ==1

Skewness/Kurtosis tests for Normality					
Variable	Obs	Pr(Skewness)	Pr(Kurtosis)	adj chi2(2)	joint Prob>chi2
lstschange	22	0.0003	0.0008	17.60	0.0002

. swilk lstschange if menopause ==1

Shapiro-wilk W test for normal data					
Variable	Obs	W	V	z	Prob>z
lstschange	22	0.79978	5.072	3.293	0.00050



. sktest bolsts if menopause ==2

Skewness/Kurtosis tests for Normality

Variable	Obs	Pr(Skewness)	Pr(Kurtosis)	adj chi2(2)	joint Prob>chi2
bolsts	7	.	.	.	.

. swilk bolsts if menopause ==2

Shapiro-wilk w test for normal data

Variable	Obs	W	V	z	Prob>z
bolsts	7	0.97439	0.336	-1.462	0.92814

. sktest lsts12m if menopause ==2

Skewness/Kurtosis tests for Normality

Variable	Obs	Pr(Skewness)	Pr(Kurtosis)	adj chi2(2)	joint Prob>chi2
lsts12m	7	.	.	.	.

. swilk lsts12m if menopause ==2

Shapiro-wilk w test for normal data

Variable	Obs	W	V	z	Prob>z
lsts12m	7	0.89113	1.430	0.581	0.28062

. sktest lstschange if menopause ==2

Skewness/Kurtosis tests for Normality

Variable	Obs	Pr(Skewness)	Pr(Kurtosis)	adj chi2(2)	joint Prob>chi2
lstschange	7	.	.	.	.

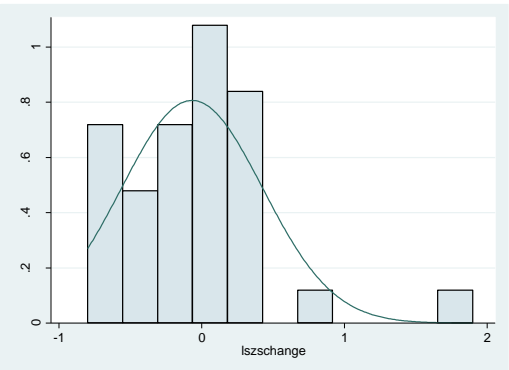
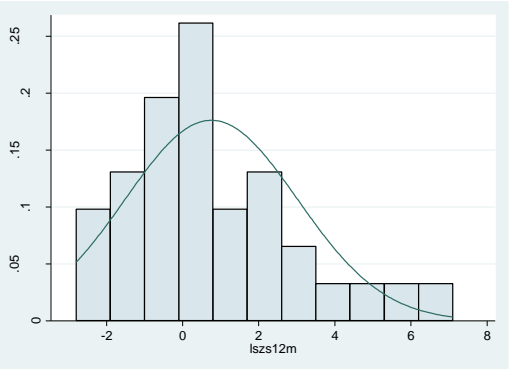
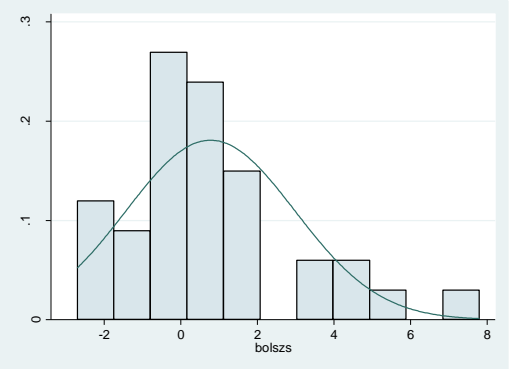
. swilk lstschange if menopause ==2

Shapiro-wilk w test for normal data

Variable	Obs	W	V	z	Prob>z
lstschange	7	0.79493	2.693	1.793	0.03649

# LS z score

- All



. sktest bolszs

Skewness/Kurtosis tests for Normality					
Variable	Obs	Pr(Skewness)	Pr(Kurtosis)	adj chi2(2)	joint Prob>chi2
bolszs	35	0.0074	0.0564	9.09	0.0106

. swilk bolszs

Shapiro-wilk w test for normal data					
Variable	Obs	W	V	z	Prob>z
bolszs	35	0.92779	2.577	1.976	0.02406

. sktest lszs12m

Skewness/Kurtosis tests for Normality					
Variable	Obs	Pr(Skewness)	Pr(Kurtosis)	adj chi2(2)	joint Prob>chi2
lszs12m	34	0.0194	0.1519	6.77	0.0338

. swilk lszs12m

Shapiro-wilk w test for normal data					
Variable	Obs	W	V	z	Prob>z
lszs12m	34	0.93688	2.204	1.647	0.04979

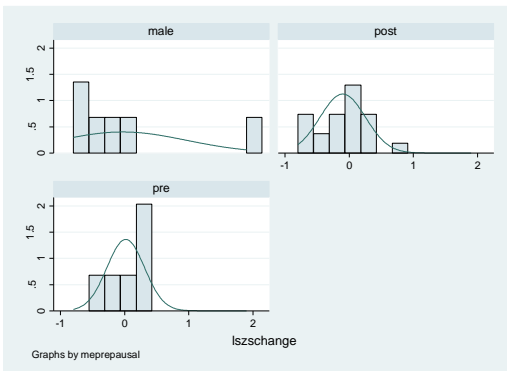
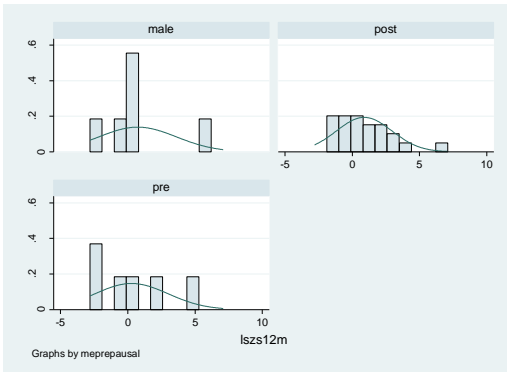
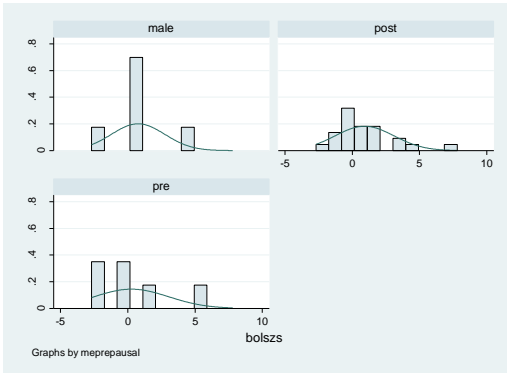
. sktest lszschange

Skewness/Kurtosis tests for Normality					
Variable	Obs	Pr(Skewness)	Pr(Kurtosis)	adj chi2(2)	joint Prob>chi2
lszschange	34	0.0003	0.0004	19.05	0.0001

. swilk lszschange

Shapiro-wilk w test for normal data					
Variable	Obs	W	V	z	Prob>z
lszschange	34	0.84887	5.277	3.466	0.00026

- **By gender and menopausal status**



. sktest bolszs if menopause ==0

Skewness/Kurtosis tests for Normality						
Variable	Obs	Pr(Skewness)	Pr(Kurtosis)	adj	chi2(2)	joint Prob>chi2
bolszs	6	.	.	.	.	.

. swilk bolszs if menopause ==0

Shapiro-Wilk W test for normal data					
Variable	Obs	W	V	z	Prob>z
bolszs	6	0.93437	0.813	-0.290	0.61422

. sktest lszs12m if menopause ==0

Skewness/Kurtosis tests for Normality						
Variable	Obs	Pr(Skewness)	Pr(Kurtosis)	adj	chi2(2)	joint Prob>chi2
lszs12m	6	.	.	.	.	.

. swilk lszs12m if menopause ==0

Shapiro-Wilk W test for normal data					
Variable	Obs	W	V	z	Prob>z
lszs12m	6	0.93853	0.761	-0.378	0.64740

. sktest lszschang if menopause ==0

Skewness/Kurtosis tests for Normality						
Variable	Obs	Pr(Skewness)	Pr(Kurtosis)	adj	chi2(2)	joint Prob>chi2
lszschang	6	.	.	.	.	.

. swilk lszschang if menopause ==0

Shapiro-Wilk W test for normal data					
Variable	Obs	W	V	z	Prob>z
lszschang	6	0.83840	2.001	1.143	0.12644

. sktest bolszs if menopause ==1

Skewness/Kurtosis tests for Normality						
Variable	Obs	Pr(Skewness)	Pr(Kurtosis)	adj	chi2(2)	joint Prob>chi2
bolszs	23	0.0038	0.0188	11.00	0.0041	0.0041

. swilk bolszs if menopause ==1

Shapiro-Wilk W test for normal data					
Variable	Obs	W	V	z	Prob>z
bolszs	23	0.88208	3.084	2.290	0.01100

. sktest lszs12m if menopause ==1

Skewness/Kurtosis tests for Normality						
Variable	Obs	Pr(Skewness)	Pr(Kurtosis)	adj	chi2(2)	joint Prob>chi2
lszs12m	22	0.0111	0.0380	8.92	0.0116	0.0116

. swilk lszs12m if menopause ==1

Shapiro-Wilk W test for normal data					
Variable	Obs	W	V	z	Prob>z
lszs12m	22	0.90668	2.364	1.745	0.04052

. sktest lszschang if menopause ==1

Skewness/Kurtosis tests for Normality						
Variable	Obs	Pr(Skewness)	Pr(Kurtosis)	adj	chi2(2)	joint Prob>chi2
lszschang	22	0.8667	0.8242	0.08	0.9620	0.9620

. swilk lszschang if menopause ==1

Shapiro-Wilk W test for normal data					
Variable	Obs	W	V	z	Prob>z
lszschang	22	0.94819	1.313	0.551	0.29067

. sktest bolszs if menopause ==2

Skewness/Kurtosis tests for Normality					
Variable	Obs	Pr(Skewness)	Pr(Kurtosis)	adj chi2(2)	joint Prob>chi2
bolszs	6	.	.	.	.

. swilk bolszs if menopause ==2

Shapiro-Wilk W test for normal data					
Variable	Obs	W	V	z	Prob>z
bolszs	6	0.90615	1.162	0.223	0.41157

. sktest lszs12m if menopause ==2

Skewness/Kurtosis tests for Normality					
Variable	Obs	Pr(Skewness)	Pr(Kurtosis)	adj chi2(2)	joint Prob>chi2
lszs12m	6	.	.	.	.

. swilk lszs12m if menopause ==2

Shapiro-Wilk W test for normal data					
Variable	Obs	W	V	z	Prob>z
lszs12m	6	0.88426	1.433	0.556	0.28918

. sktest lszschang if menopause ==2

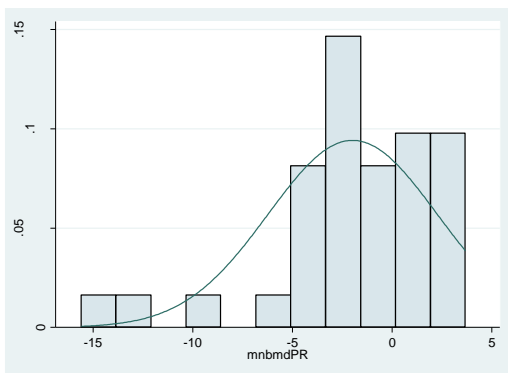
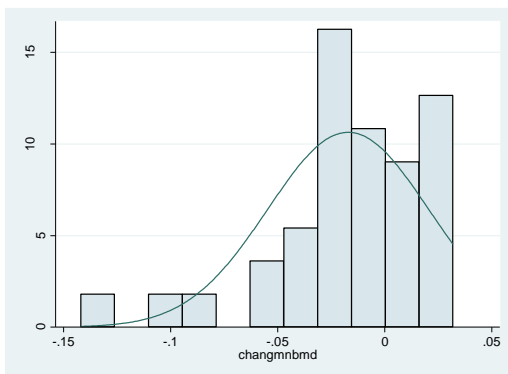
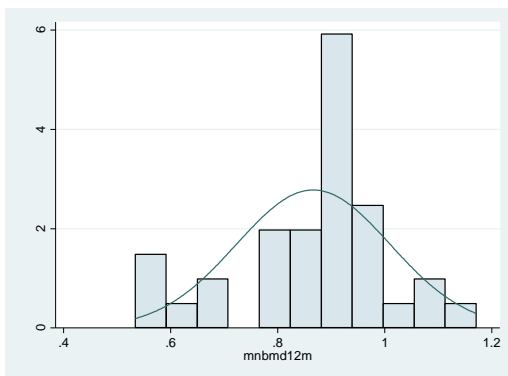
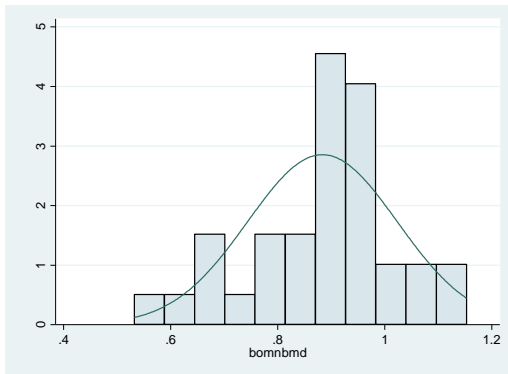
Skewness/Kurtosis tests for Normality					
Variable	Obs	Pr(Skewness)	Pr(Kurtosis)	adj chi2(2)	joint Prob>chi2
lszschang	6	.	.	.	.

. swilk lszschang if menopause ==2

Shapiro-Wilk W test for normal data					
Variable	Obs	W	V	z	Prob>z
lszschang	6	0.77091	2.837	1.857	0.03167

# MNBMD

1 All



. sktest bomnbmd

Skewness/Kurtosis tests for Normality

Variable	Obs	Pr(Skewness)	Pr(Kurtosis)	adj chi2(2)	joint Prob>chi2
bomnbmd	35	0.1505	0.4884	2.75	0.2526

. swilk bomnbmd

Shapiro-wilk W test for normal data

Variable	Obs	W	V	z	Prob>z
bomnbmd	35	0.95849	1.482	0.821	0.20591

. sktest mnbmd12m

Skewness/Kurtosis tests for Normality

Variable	Obs	Pr(Skewness)	Pr(Kurtosis)	adj chi2(2)	joint Prob>chi2
mnbmd12m	35	0.1270	0.4143	3.24	0.1974

. swilk mnbmd12m

Shapiro-wilk W test for normal data

Variable	Obs	W	V	z	Prob>z
mnbmd12m	35	0.93644	2.269	1.710	0.04362

. sktest changmnbmd

Skewness/Kurtosis tests for Normality

Variable	Obs	Pr(Skewness)	Pr(Kurtosis)	adj chi2(2)	joint Prob>chi2
changmnbmd	35	0.0008	0.0102	13.78	0.0010

. swilk changmnbmd

Shapiro-wilk W test for normal data

Variable	Obs	W	V	z	Prob>z
changmnbmd	35	0.87251	4.551	3.163	0.00078

. sktest mnbmdpr

Skewness/Kurtosis tests for Normality

Variable	Obs	Pr(Skewness)	Pr(Kurtosis)	adj chi2(2)	joint Prob>chi2
mnbmdpr	35	0.0011	0.0145	13.02	0.0015

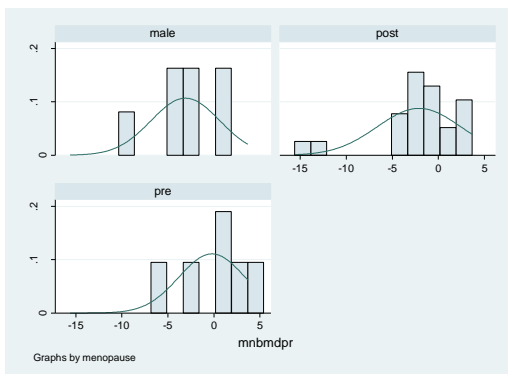
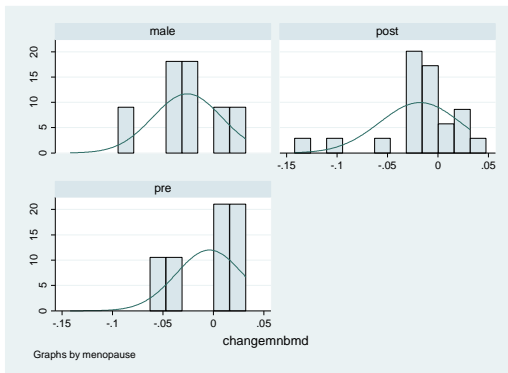
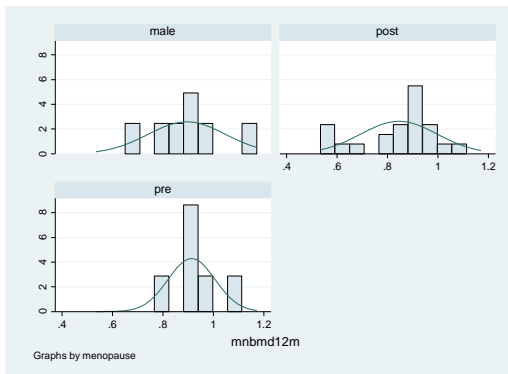
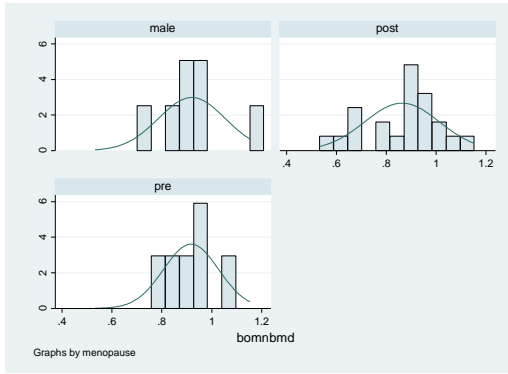
. swilk mnbmdpr

Shapiro-wilk W test for normal data

Variable	Obs	W	V	z	Prob>z
mnbmdpr	35	0.87864	4.331	3.060	0.00111



- **By gender and menopausal status**



. sktest bomnbmd if menopausal ==0

Skewness/Kurtosis tests for Normality

Variable	Obs	Pr(Skewness)	Pr(Kurtosis)	adj chi2(2)	joint Prob>chi2
bomnbmd	6	.	.	.	.

. swilk bomnbmd if menopausal ==0

Shapiro-wilk W test for normal data

Variable	Obs	W	V	z	Prob>z
bomnbmd	6	0.96973	0.375	-1.230	0.89061

. sktest mnbmd12m if menopausal ==0

Skewness/Kurtosis tests for Normality

Variable	Obs	Pr(Skewness)	Pr(Kurtosis)	adj chi2(2)	joint Prob>chi2
mnbmd12m	6	.	.	.	.

. swilk mnbmd12m if menopausal ==0

Shapiro-wilk W test for normal data

Variable	Obs	W	V	z	Prob>z
mnbmd12m	6	0.95474	0.560	-0.767	0.77846

. sktest changemnbmd if menopausal ==0

Skewness/Kurtosis tests for Normality

Variable	Obs	Pr(Skewness)	Pr(Kurtosis)	adj chi2(2)	joint Prob>chi2
changemnbmd	6	.	.	.	.

. swilk changemnbmd if menopausal ==0

Shapiro-wilk W test for normal data

Variable	Obs	W	V	z	Prob>z
changemnbmd	6	0.92131	0.974	-0.037	0.51487

. sktest mnbmdpr if menopausal ==0

Skewness/Kurtosis tests for Normality

Variable	Obs	Pr(Skewness)	Pr(Kurtosis)	adj chi2(2)	joint Prob>chi2
mnbmdpr	6	.	.	.	.

. swilk mnbmdpr if menopausal ==0

Shapiro-wilk W test for normal data

Variable	Obs	W	V	z	Prob>z
mnbmdpr	6	0.93594	0.793	-0.323	0.62670

. sktest bomnbmd if menopausal ==1

Skewness/Kurtosis tests for Normality

Variable	Obs	Pr(Skewness)	Pr(Kurtosis)	adj	chi2(2)	joint	Prob>chi2
bomnbmd	22	0.1685	0.9455		2.11		0.3476

. swilk bomnbmd if menopausal ==1

Shapiro-Wilk W test for normal data

Variable	Obs	W	V	z	Prob>z
bomnbmd	22	0.94821	1.312	0.551	0.29089

. sktest mnbmd12m if menopausal ==1

Skewness/Kurtosis tests for Normality

Variable	Obs	Pr(Skewness)	Pr(Kurtosis)	adj	chi2(2)	joint	Prob>chi2
mnbmd12m	22	0.0944	0.9955		3.15		0.2071

. swilk mnbmd12m if menopausal ==1

Shapiro-Wilk W test for normal data

Variable	Obs	W	V	z	Prob>z
mnbmd12m	22	0.89335	2.702	2.015	0.02194

. sktest changemnbmd if menopausal ==1

Skewness/Kurtosis tests for Normality

Variable	Obs	Pr(Skewness)	Pr(Kurtosis)	adj	chi2(2)	joint	Prob>chi2
changemnbmd	22	0.0008	0.0069		13.85		0.0010

. swilk changemnbmd if menopausal ==1

Shapiro-Wilk W test for normal data

Variable	Obs	W	V	z	Prob>z
changemnbmd	22	0.80009	5.064	3.289	0.00050

. sktest mnbmdpr if menopausal ==1

Skewness/Kurtosis tests for Normality

Variable	Obs	Pr(Skewness)	Pr(Kurtosis)	adj	chi2(2)	joint	Prob>chi2
mnbmdpr	22	0.0012	0.0114		12.86		0.0016

. swilk mnbmdpr if menopausal ==1

Shapiro-Wilk W test for normal data

Variable	Obs	W	V	z	Prob>z
mnbmdpr	22	0.80990	4.816	3.187	0.00072

. sktest bomnbmd if menopausal ==2

Skewness/Kurtosis tests for Normality

Variable	Obs	Pr(Skewness)	Pr(Kurtosis)	adj chi2(2)	joint Prob>chi2
bomnbmd	7	.	.	.	.

. swilk bomnbmd if menopausal ==2

Shapiro-Wilk W test for normal data

Variable	Obs	W	V	z	Prob>z
bomnbmd	7	0.94015	0.786	-0.359	0.64004

. sktest mnbmd12m if menopausal ==2

Skewness/Kurtosis tests for Normality

Variable	Obs	Pr(Skewness)	Pr(Kurtosis)	adj chi2(2)	joint Prob>chi2
mnbmd12m	7	.	.	.	.

. swilk mnbmd12m if menopausal ==2

Shapiro-Wilk W test for normal data

Variable	Obs	W	V	z	Prob>z
mnbmd12m	7	0.95638	0.573	-0.797	0.78717

. sktest changemnbmd if menopausal ==2

Skewness/Kurtosis tests for Normality

Variable	Obs	Pr(Skewness)	Pr(Kurtosis)	adj chi2(2)	joint Prob>chi2
changemnbmd	7	.	.	.	.

. swilk changemnbmd if menopausal ==2

Shapiro-Wilk W test for normal data

Variable	Obs	W	V	z	Prob>z
changemnbmd	7	0.92151	1.031	0.047	0.48123

. sktest mnbmdpr if menopausal ==2

Skewness/Kurtosis tests for Normality

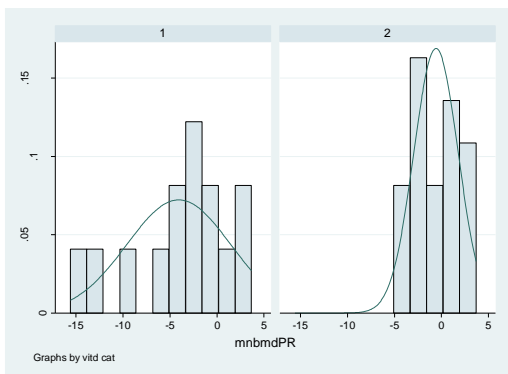
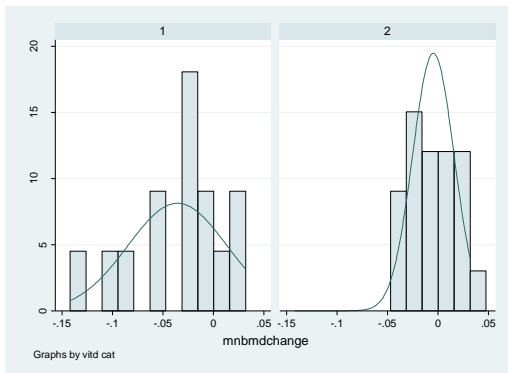
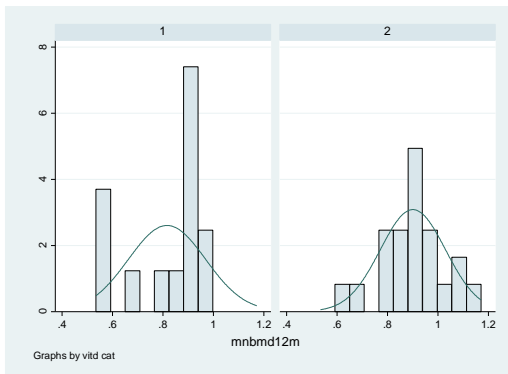
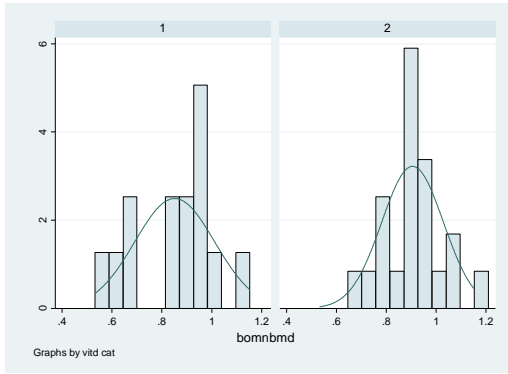
Variable	Obs	Pr(Skewness)	Pr(Kurtosis)	adj chi2(2)	joint Prob>chi2
mnbmdpr	7	.	.	.	.

. swilk mnbmdpr if menopausal ==2

Shapiro-Wilk W test for normal data

Variable	Obs	W	V	z	Prob>z
mnbmdpr	7	0.95184	0.633	-0.663	0.74644

- **By vitamin D category**



. sktest bomnbmd if vitdcat ==1

Skewness/Kurtosis tests for Normality					
Variable	Obs	Pr(Skewness)	Pr(Kurtosis)	adj chi2(2)	joint Prob>chi2
bomnbmd	14	0.2060	0.9371	1.84	0.3990

. swilk bomnbmd if vitdcat ==1

Shapiro-wilk W test for normal data					
Variable	Obs	W	V	z	Prob>z
bomnbmd	14	0.91531	1.567	0.885	0.18818

. sktest mnbmd12m if vitdcat ==1

Skewness/Kurtosis tests for Normality					
Variable	Obs	Pr(Skewness)	Pr(Kurtosis)	adj chi2(2)	joint Prob>chi2
mnbmd12m	14	0.0984	0.5762	3.53	0.1708

. swilk mnbmd12m if vitdcat ==1

Shapiro-wilk W test for normal data					
Variable	Obs	W	V	z	Prob>z
mnbmd12m	14	0.80644	3.582	2.512	0.00600

. sktest mnbmdchange if vitdcat ==1

Skewness/Kurtosis tests for Normality					
Variable	Obs	Pr(Skewness)	Pr(Kurtosis)	adj chi2(2)	joint Prob>chi2
mnbmdchange	14	0.1409	0.6155	2.83	0.2425

. swilk mnbmdchange if vitdcat ==1

Shapiro-wilk W test for normal data					
Variable	Obs	W	V	z	Prob>z
mnbmdchange	14	0.93559	1.192	0.346	0.36469

. sktest mnbmdpr if vitdcat ==1

Skewness/Kurtosis tests for Normality					
Variable	Obs	Pr(Skewness)	Pr(Kurtosis)	adj chi2(2)	joint Prob>chi2
mnbmdpr	14	0.1633	0.6811	2.46	0.2930

. swilk mnbmdpr if vitdcat ==1

Shapiro-wilk W test for normal data					
Variable	Obs	W	V	z	Prob>z
mnbmdpr	14	0.93741	1.158	0.289	0.38618

. sktest bomnbmd if vitdcat ==2

Skewness/Kurtosis tests for Normality					
Variable	Obs	Pr(Skewness)	Pr(Kurtosis)	adj chi2(2)	joint Prob>chi2
bomnbmd	21	0.8663	0.6660	0.21	0.8982

. swilk bomnbmd if vitdcat ==2

Shapiro-wilk W test for normal data					
Variable	Obs	W	V	z	Prob>z
bomnbmd	21	0.98336	0.408	-1.814	0.96513

. sktest mnbmd12m if vitdcat ==2

Skewness/Kurtosis tests for Normality					
Variable	Obs	Pr(Skewness)	Pr(Kurtosis)	adj chi2(2)	joint Prob>chi2
mnbmd12m	21	0.8358	0.4440	0.66	0.7172

. swilk mnbmd12m if vitdcat ==2

Shapiro-wilk W test for normal data					
Variable	Obs	W	V	z	Prob>z
mnbmd12m	21	0.98209	0.439	-1.665	0.95200

. sktest mnbmdchange if vitdcat ==2

Skewness/Kurtosis tests for Normality					
Variable	Obs	Pr(Skewness)	Pr(Kurtosis)	adj chi2(2)	joint Prob>chi2
mnbmdchange	21	0.7448	0.0775	3.62	0.1640

. swilk mnbmdchange if vitdcat ==2

Shapiro-wilk W test for normal data					
Variable	Obs	W	V	z	Prob>z
mnbmdchange	21	0.94678	1.304	0.537	0.29570

. sktest mnbmdpr if vitdcat ==2

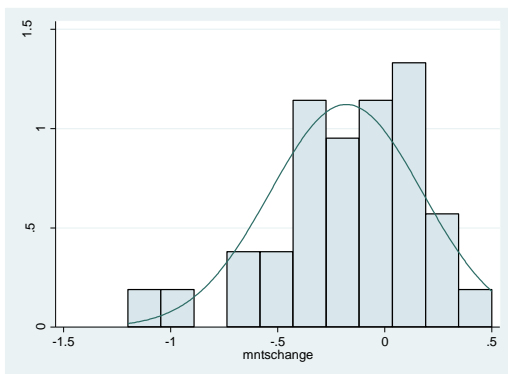
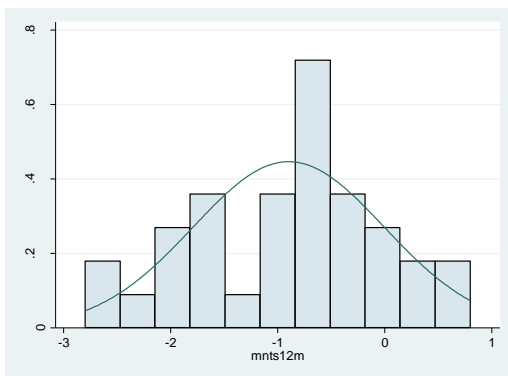
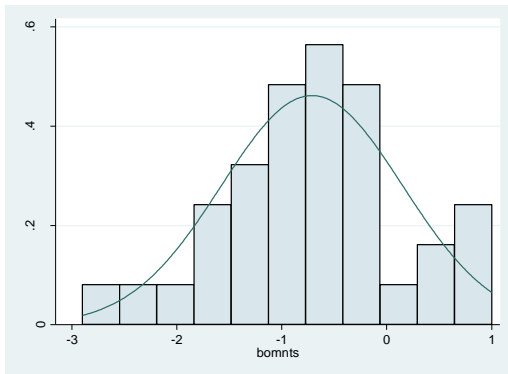
Skewness/Kurtosis tests for Normality					
Variable	Obs	Pr(Skewness)	Pr(Kurtosis)	adj chi2(2)	joint Prob>chi2
mnbmdpr	21	0.9521	0.1128	2.84	0.2420

. swilk mnbmdpr if vitdcat ==2

Shapiro-wilk W test for normal data					
Variable	Obs	W	V	z	Prob>z

# MN t score

- All



. sktest bomnts

Skewness/Kurtosis tests for Normality					
Variable	Obs	Pr(Skewness)	Pr(Kurtosis)	adj chi2(2)	joint Prob>chi2
bomnts	35	0.7847	0.5250	0.49	0.7816

. swilk bomnts

Shapiro-wilk w test for normal data					
Variable	Obs	w	V	z	Prob>z
bomnts	35	0.98409	0.568	-1.181	0.88121

. sktest mnts12m

Skewness/Kurtosis tests for Normality					
Variable	Obs	Pr(Skewness)	Pr(Kurtosis)	adj chi2(2)	joint Prob>chi2
mnts12m	34	0.6027	0.7935	0.34	0.8439

. swilk mnts12m

Shapiro-wilk w test for normal data					
Variable	Obs	w	V	z	Prob>z
mnts12m	34	0.98189	0.632	-0.955	0.83034

. sktest mntschange

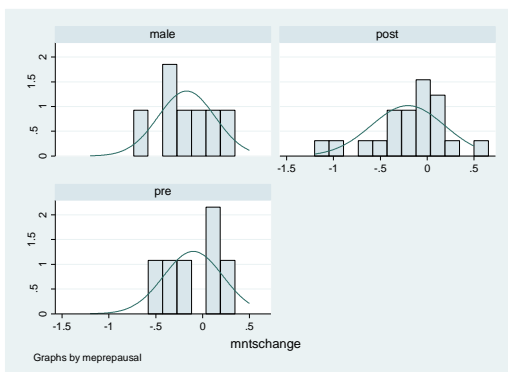
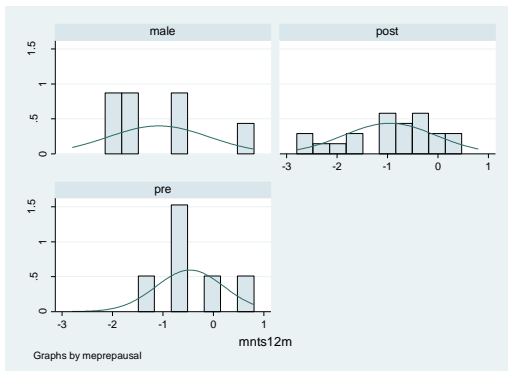
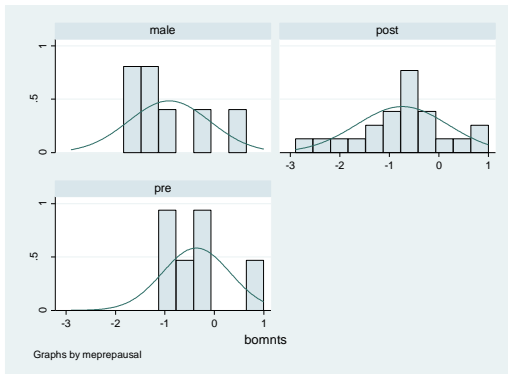
Skewness/Kurtosis tests for Normality					
Variable	Obs	Pr(Skewness)	Pr(Kurtosis)	adj chi2(2)	joint Prob>chi2
mntschange	34	0.0269	0.1125	6.70	0.0350

. swilk mntschange

Shapiro-wilk w test for normal data					
Variable	Obs	w	V	z	Prob>z
mntschange	34	0.93899	2.130	1.576	0.05752



- **By gender and menopausal status**



. sktest bomnts if menopause ==0

Skewness/Kurtosis tests for Normality					
Variable	Obs	Pr(Skewness)	Pr(Kurtosis)	adj chi2(2)	joint Prob>chi2
bomnts	6	.	.	.	.

. swilk bomnts if menopause ==0

Shapiro-wilk W test for normal data					
Variable	Obs	W	V	z	Prob>z
bomnts	6	0.85998	1.734	0.881	0.18908

. sktest mnts12m if menopause ==0

Skewness/Kurtosis tests for Normality					
Variable	Obs	Pr(Skewness)	Pr(Kurtosis)	adj chi2(2)	joint Prob>chi2
mnts12m	6	.	.	.	.

. swilk mnts12m if menopause ==0

Shapiro-wilk W test for normal data					
Variable	Obs	W	V	z	Prob>z
mnts12m	6	0.97743	0.280	-1.539	0.93810

. sktest mntschange if menopause ==0

Skewness/Kurtosis tests for Normality					
Variable	Obs	Pr(Skewness)	Pr(Kurtosis)	adj chi2(2)	joint Prob>chi2
mntschange	6	.	.	.	.

. swilk mntschange if menopause ==0

Shapiro-wilk W test for normal data					
Variable	Obs	W	V	z	Prob>z
mntschange	6	0.92809	0.891	-0.165	0.56544

. sktest bomnts if menopause ==1

Skewness/Kurtosis tests for Normality					
Variable	Obs	Pr(Skewness)	Pr(Kurtosis)	adj chi2(2)	joint Prob>chi2
bomnts	22	0.4688	0.5103	1.03	0.5961

. swilk bomnts if menopause ==1

Shapiro-wilk W test for normal data					
Variable	Obs	W	V	z	Prob>z
bomnts	22	0.98409	0.403	-1.843	0.96731

. sktest mnts12m if menopause ==1

Skewness/Kurtosis tests for Normality					
Variable	Obs	Pr(Skewness)	Pr(Kurtosis)	adj chi2(2)	joint Prob>chi2
mnts12m	21	0.2413	0.7533	1.63	0.4436

. swilk mnts12m if menopause ==1

Shapiro-wilk W test for normal data					
Variable	Obs	W	V	z	Prob>z
mnts12m	21	0.94917	1.246	0.444	0.32852

. sktest mntschange if menopause ==1

Skewness/Kurtosis tests for Normality					
Variable	Obs	Pr(Skewness)	Pr(Kurtosis)	adj chi2(2)	joint Prob>chi2
mntschange	21	0.0467	0.1382	5.79	0.0554

. swilk mntschange if menopause ==1

Shapiro-wilk W test for normal data					
Variable	Obs	W	V	z	Prob>z
mntschange	21	0.90991	2.208	1.601	0.05470

. sktest bomnts if menopause ==2

Skewness/Kurtosis tests for Normality

Variable	Obs	Pr(Skewness)	Pr(Kurtosis)	adj	chi2(2)	joint	Prob>chi2
bomnts	7	.	.	.	.	.	.

. swilk bomnts if menopause ==2

Shapiro-Wilk W test for normal data

Variable	Obs	W	V	z	Prob>z
bomnts	7	0.89300	1.405	0.551	0.29070

. sktest mnts12m if menopause ==2

Skewness/Kurtosis tests for Normality

Variable	Obs	Pr(Skewness)	Pr(Kurtosis)	adj	chi2(2)	joint	Prob>chi2
mnts12m	7	.	.	.	.	.	.

. swilk mnts12m if menopause ==2

Shapiro-Wilk W test for normal data

Variable	Obs	W	V	z	Prob>z
mnts12m	7	0.86786	1.736	0.924	0.17779

. sktest mntschange if menopause ==2

Skewness/Kurtosis tests for Normality

Variable	Obs	Pr(Skewness)	Pr(Kurtosis)	adj	chi2(2)	joint	Prob>chi2
mntschange	7	.	.	.	.	.	.

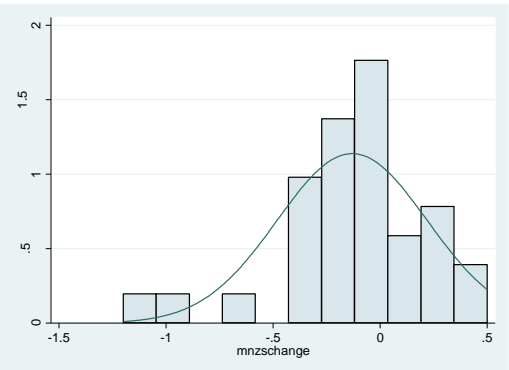
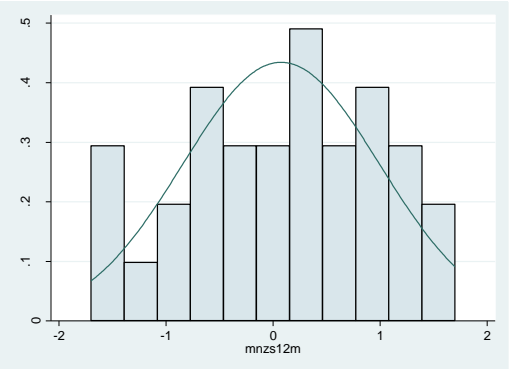
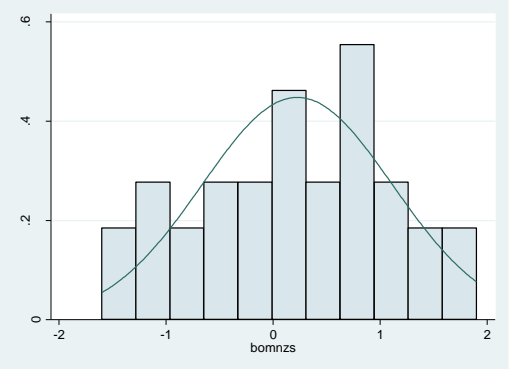
. swilk mntschange if menopause ==2

Shapiro-Wilk W test for normal data

Variable	Obs	W	V	z	Prob>z
mntschange	7	0.94657	0.702	-0.520	0.69843

# MN z score

- All



. sktest bomnzs

Skewness/Kurtosis tests for Normality					
Variable	Obs	Pr(Skewness)	Pr(Kurtosis)	adj chi2(2)	joint Prob>chi2
bomnzs	34	0.5425	0.4045	1.13	0.5685

. swilk bomnzs

Shapiro-wilk w test for normal data					
Variable	Obs	w	v	z	Prob>z
bomnzs	34	0.98142	0.649	-0.902	0.81640

. sktest mnzs12m

Skewness/Kurtosis tests for Normality					
Variable	Obs	Pr(Skewness)	Pr(Kurtosis)	adj chi2(2)	joint Prob>chi2
mnzs12m	33	0.5488	0.2514	1.80	0.4064

. swilk mnzs12m

Shapiro-wilk w test for normal data					
Variable	Obs	w	v	z	Prob>z
mnzs12m	33	0.97598	0.820	-0.412	0.65994

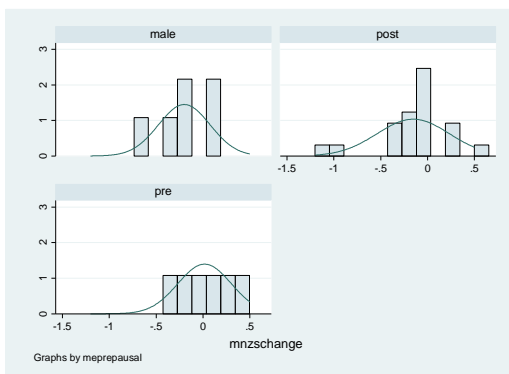
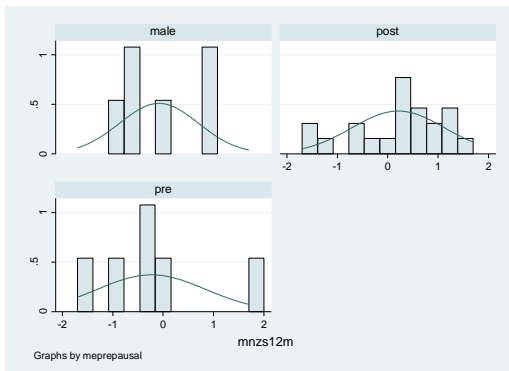
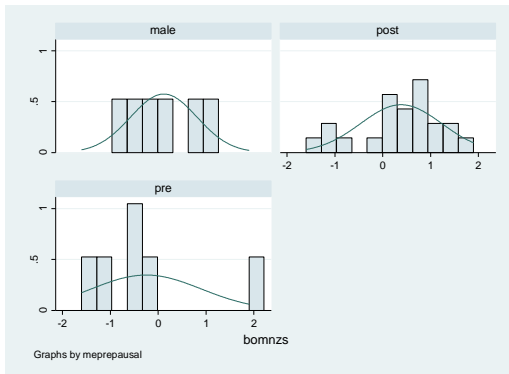
. sktest mnzschange

Skewness/Kurtosis tests for Normality					
Variable	Obs	Pr(Skewness)	Pr(Kurtosis)	adj chi2(2)	joint Prob>chi2
mnzschange	33	0.0135	0.0291	9.10	0.0106

. swilk mnzschange

Shapiro-wilk w test for normal data					
Variable	Obs	w	v	z	Prob>z
mnzschange	33	0.92175	2.671	2.044	0.02049

- **By gender and menopausal status**



. sktest bomnzs if menopause ==0

Skewness/Kurtosis tests for Normality

Variable	Obs	Pr(Skewness)	Pr(Kurtosis)	adj	chi2(2)	joint	Prob>chi2
bomnzs	6	.	.	.	.	.	.

. swilk bomnzs if menopause ==0

Shapiro-Wilk W test for normal data

Variable	Obs	W	V	z	Prob>z
bomnzs	6	0.85865	1.751	0.898	0.18459

. sktest mnzs12m if menopause ==0

Skewness/Kurtosis tests for Normality

Variable	Obs	Pr(Skewness)	Pr(Kurtosis)	adj	chi2(2)	joint	Prob>chi2
mnzs12m	6	.	.	.	.	.	.

. swilk mnzs12m if menopause ==0

Shapiro-Wilk W test for normal data

Variable	Obs	W	V	z	Prob>z
mnzs12m	6	0.90259	1.206	0.281	0.38945

. sktest mnzschange if menopause ==0

Skewness/Kurtosis tests for Normality

Variable	Obs	Pr(Skewness)	Pr(Kurtosis)	adj	chi2(2)	joint	Prob>chi2
mnzschange	6	.	.	.	.	.	.

. swilk mnzschange if menopause ==0

Shapiro-Wilk W test for normal data

Variable	Obs	W	V	z	Prob>z
mnzschange	6	0.98901	0.136	-2.215	0.98661

. sktest bomnzs if menopause ==1

Skewness/Kurtosis tests for Normality

Variable	Obs	Pr(Skewness)	Pr(Kurtosis)	adj	chi2(2)	joint	Prob>chi2
bomnzs	22	0.0837	0.5772		3.67		0.1596

. swilk bomnzs if menopause ==1

Shapiro-Wilk W test for normal data

Variable	Obs	W	V	z	Prob>z
bomnzs	22	0.92913	1.795	1.187	0.11770

. sktest mnzs12m if menopause ==1

Skewness/Kurtosis tests for Normality

Variable	Obs	Pr(Skewness)	Pr(Kurtosis)	adj	chi2(2)	joint	Prob>chi2
mnzs12m	21	0.1122	0.8973		2.86		0.2390

. swilk mnzs12m if menopause ==1

Shapiro-Wilk W test for normal data

Variable	Obs	W	V	z	Prob>z
mnzs12m	21	0.92374	1.869	1.264	0.10310

. sktest mnzschange if menopause ==1

Skewness/Kurtosis tests for Normality

Variable	Obs	Pr(Skewness)	Pr(Kurtosis)	adj	chi2(2)	joint	Prob>chi2
mnzschange	21	0.0201	0.0406		8.14		0.0171

. swilk mnzschange if menopause ==1

Shapiro-Wilk W test for normal data

Variable	Obs	W	V	z	Prob>z
mnzschange	21	0.86060	3.416	2.483	0.00651

. sktest bomnzs if menopause ==2

Skewness/Kurtosis tests for Normality					
Variable	Obs	Pr(Skewness)	Pr(Kurtosis)	adj chi2(2)	joint Prob>chi2
bomnzs	6	.	.	.	.

. swilk bomnzs if menopause ==2

Shapiro-wilk W test for normal data					
Variable	Obs	W	V	z	Prob>z
bomnzs	6	0.96019	0.493	-0.920	0.82123

. sktest mnzs12m if menopause ==2

Skewness/Kurtosis tests for Normality					
Variable	Obs	Pr(Skewness)	Pr(Kurtosis)	adj chi2(2)	joint Prob>chi2
mnzs12m	6	.	.	.	.

. swilk mnzs12m if menopause ==2

Shapiro-wilk W test for normal data					
Variable	Obs	W	V	z	Prob>z
mnzs12m	6	0.86736	1.643	0.786	0.21590

. sktest mnzschang if menopause ==2

Skewness/Kurtosis tests for Normality					
Variable	Obs	Pr(Skewness)	Pr(Kurtosis)	adj chi2(2)	joint Prob>chi2
mnzschang	6	.	.	.	.

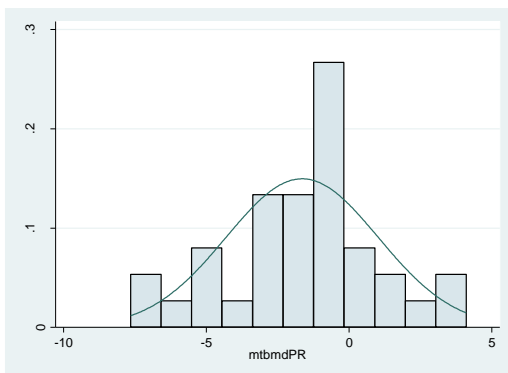
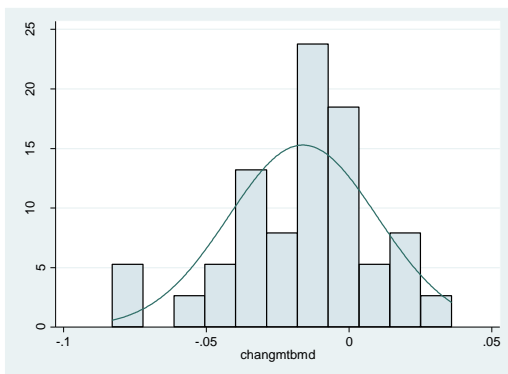
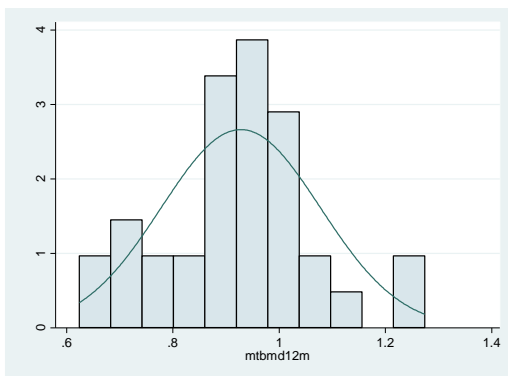
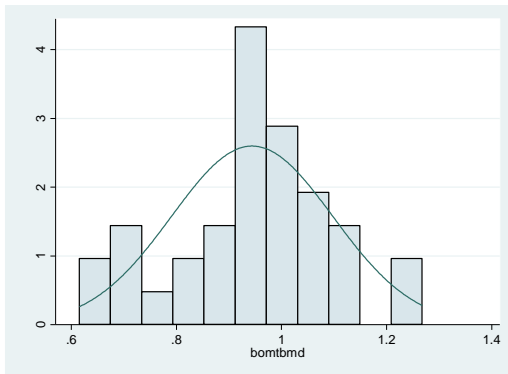
. swilk mnzschang if menopause ==2

Shapiro-wilk W test for normal data					
Variable	Obs	W	V	z	Prob>z
mnzschang	6	0.91741	1.023	0.033	0.48689



# MTBMD

- All



. sktest bomtbmd

Skewness/Kurtosis tests for Normality					
Variable	Obs	Pr(Skewness)	Pr(Kurtosis)	adj chi2(2)	joint Prob>chi2
bomtbmd	35	0.6838	0.7554	0.26	0.8768

. swilk bomtbmd

Shapiro-wilk W test for normal data					
Variable	Obs	W	V	z	Prob>z
bomtbmd	35	0.97506	0.890	-0.243	0.59601

. sktest mtbmd12m

Skewness/Kurtosis tests for Normality					
Variable	Obs	Pr(Skewness)	Pr(Kurtosis)	adj chi2(2)	joint Prob>chi2
mtbmd12m	35	0.9476	0.5136	0.44	0.8018

. swilk mtbmd12m

Shapiro-wilk W test for normal data					
Variable	Obs	W	V	z	Prob>z
mtbmd12m	35	0.96245	1.340	0.611	0.27048

. sktest changmtbmd

Skewness/Kurtosis tests for Normality					
Variable	Obs	Pr(Skewness)	Pr(Kurtosis)	adj chi2(2)	joint Prob>chi2
changmtbmd	35	0.1478	0.2759	3.56	0.1685

. swilk changmtbmd

Shapiro-wilk W test for normal data					
Variable	Obs	W	V	z	Prob>z
changmtbmd	35	0.96779	1.150	0.291	0.38553

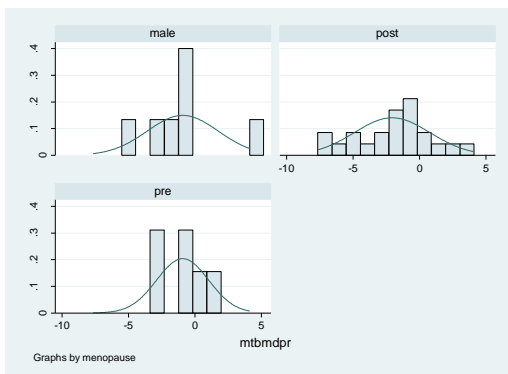
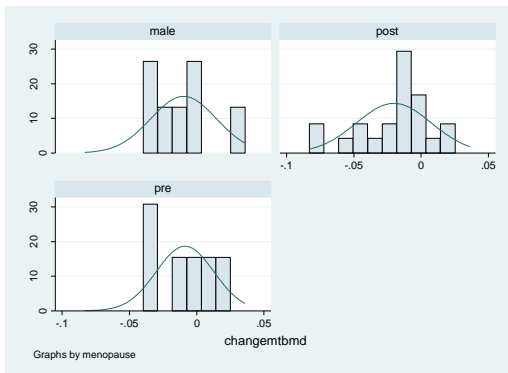
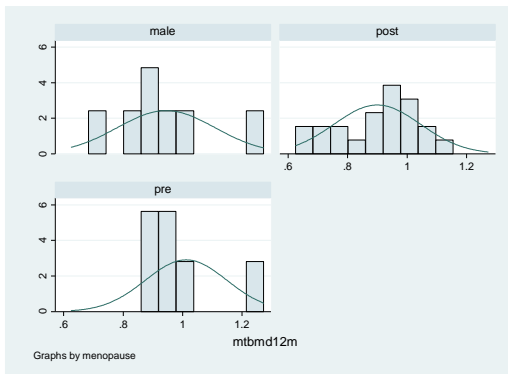
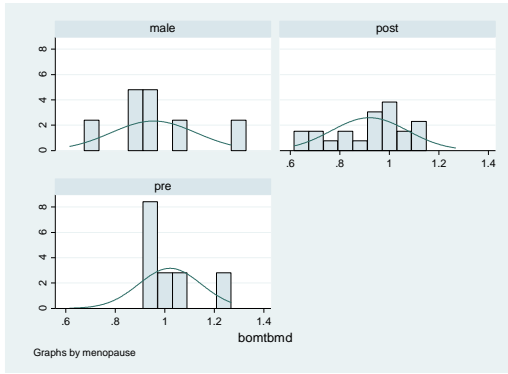
. sktest mtbmdpr

Skewness/Kurtosis tests for Normality					
Variable	Obs	Pr(Skewness)	Pr(Kurtosis)	adj chi2(2)	joint Prob>chi2
mtbmdpr	35	0.4731	0.5129	0.99	0.6083

. swilk mtbmdpr

Shapiro-wilk W test for normal data					
Variable	Obs	W	V	z	Prob>z
mtbmdpr	35	0.97811	0.781	-0.515	0.69670

- **By gender and menopausal status**



. sktest bomtbmd if menopausal ==0

Skewness/Kurtosis tests for Normality

Variable	Obs	Pr(Skewness)	Pr(Kurtosis)	adj chi2(2)	joint Prob>chi2
bomtbmd	6	.	.	.	.

. swilk bomtbmd if menopausal ==0

Shapiro-wilk W test for normal data

Variable	Obs	W	V	z	Prob>z
bomtbmd	6	0.86239	1.704	0.851	0.19751

. sktest mtbmd12m if menopausal ==0

Skewness/Kurtosis tests for Normality

Variable	Obs	Pr(Skewness)	Pr(Kurtosis)	adj chi2(2)	joint Prob>chi2
mtbmd12m	6	.	.	.	.

. swilk mtbmd12m if menopausal ==0

Shapiro-wilk W test for normal data

Variable	Obs	W	V	z	Prob>z
mtbmd12m	6	0.79451	2.545	1.622	0.05242

. sktest changembmd if menopausal ==0

Skewness/Kurtosis tests for Normality

Variable	Obs	Pr(Skewness)	Pr(Kurtosis)	adj chi2(2)	joint Prob>chi2
changembmd	6	.	.	.	.

. swilk changembmd if menopausal ==0

Shapiro-wilk W test for normal data

Variable	Obs	W	V	z	Prob>z
changembmd	6	0.95839	0.515	-0.868	0.80728

. sktest mtbmdpr if menopausal ==0

Skewness/Kurtosis tests for Normality

Variable	Obs	Pr(Skewness)	Pr(Kurtosis)	adj chi2(2)	joint Prob>chi2
mtbmdpr	6	.	.	.	.

. swilk mtbmdpr if menopausal ==0

Shapiro-wilk W test for normal data

Variable	Obs	W	V	z	Prob>z
mtbmdpr	6	0.96969	0.375	-1.228	0.89034

. sktest bomtbmd if menopausal ==1

Skewness/Kurtosis tests for Normality

Variable	Obs	Pr(Skewness)	Pr(Kurtosis)	adj	chi2(2)	joint	Prob>chi2
bomtbmd	22	0.2922	0.5021		1.72		0.4230

. swilk bomtbmd if menopausal ==1

Shapiro-Wilk W test for normal data

Variable	Obs	W	V	z	Prob>z
bomtbmd	22	0.94649	1.356	0.617	0.26865

. sktest mtbmd12m if menopausal ==1

Skewness/Kurtosis tests for Normality

Variable	Obs	Pr(Skewness)	Pr(Kurtosis)	adj	chi2(2)	joint	Prob>chi2
mtbmd12m	22	0.3127	0.5691		1.47		0.4787

. swilk mtbmd12m if menopausal ==1

Shapiro-Wilk W test for normal data

Variable	Obs	W	V	z	Prob>z
mtbmd12m	22	0.94908	1.290	0.516	0.30281

. sktest changemtmd if menopausal ==1

Skewness/Kurtosis tests for Normality

Variable	Obs	Pr(Skewness)	Pr(Kurtosis)	adj	chi2(2)	joint	Prob>chi2
changemtmd	22	0.1105	0.5845		3.20		0.2014

. swilk changemtmd if menopausal ==1

Shapiro-Wilk W test for normal data

Variable	Obs	W	V	z	Prob>z
changemtmd	22	0.93905	1.544	0.881	0.18916

. sktest mtbmdpr if menopausal ==1

Skewness/Kurtosis tests for Normality

Variable	Obs	Pr(Skewness)	Pr(Kurtosis)	adj	chi2(2)	joint	Prob>chi2
mtbmdpr	22	0.4040	0.9903		0.74		0.6908

. swilk mtbmdpr if menopausal ==1

Shapiro-Wilk W test for normal data

Variable	Obs	W	V	z	Prob>z
mtbmdpr	22	0.96754	0.822	-0.396	0.65411

. sktest bomtbmd if menopausal ==2

Skewness/Kurtosis tests for Normality

Variable	Obs	Pr(Skewness)	Pr(Kurtosis)	adj chi2(2)	joint Prob>chi2
bomtbmd	7	.	.	.	.

. swilk bomtbmd if menopausal ==2

Shapiro-Wilk W test for normal data

Variable	Obs	W	V	z	Prob>z
bomtbmd	7	0.94712	0.695	-0.534	0.70340

. sktest mtbmd12m if menopausal ==2

Skewness/Kurtosis tests for Normality

Variable	Obs	Pr(Skewness)	Pr(Kurtosis)	adj chi2(2)	joint Prob>chi2
mtbmd12m	7	.	.	.	.

. swilk mtbmd12m if menopausal ==2

Shapiro-Wilk W test for normal data

Variable	Obs	W	V	z	Prob>z
mtbmd12m	7	0.96313	0.484	-1.016	0.84510

. sktest changemtmd if menopausal ==2

Skewness/Kurtosis tests for Normality

Variable	Obs	Pr(Skewness)	Pr(Kurtosis)	adj chi2(2)	joint Prob>chi2
changemtmd	7	.	.	.	.

. swilk changemtmd if menopausal ==2

Shapiro-Wilk W test for normal data

Variable	Obs	W	V	z	Prob>z
changemtmd	7	0.92780	0.948	-0.081	0.53237

. sktest mtbmdpr if menopausal ==2

Skewness/Kurtosis tests for Normality

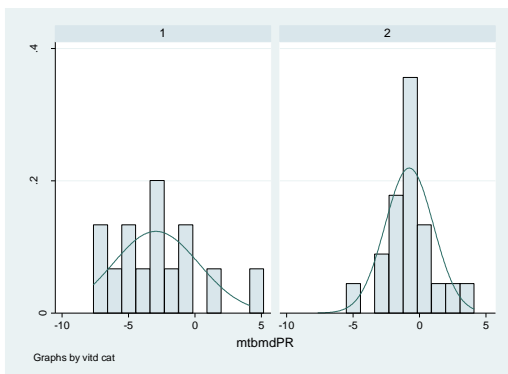
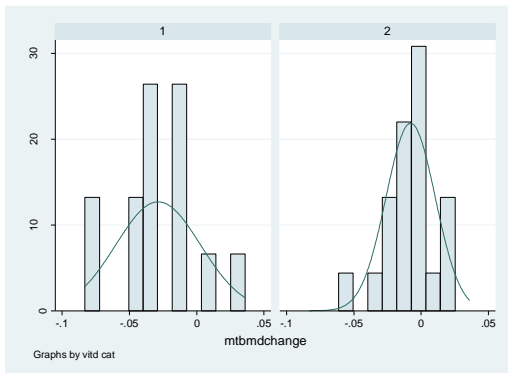
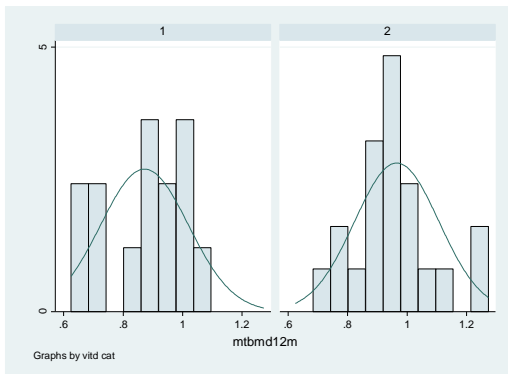
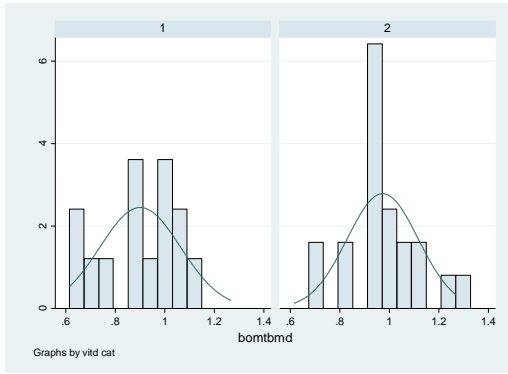
Variable	Obs	Pr(Skewness)	Pr(Kurtosis)	adj chi2(2)	joint Prob>chi2
mtbmdpr	7	.	.	.	.

. swilk mtbmdpr if menopausal ==2

Shapiro-Wilk W test for normal data

Variable	Obs	W	V	z	Prob>z
mtbmdpr	7	0.92010	1.049	0.075	0.47017

- **By vitamin D category**



. sktest bomtbmd if vitdcat ==1

Skewness/Kurtosis tests for Normality

Variable	Obs	Pr(Skewness)	Pr(Kurtosis)	adj chi2(2)	joint Prob>chi2
bomtbmd	14	0.4216	0.4225	1.45	0.4832

. swilk bomtbmd if vitdcat ==1

Shapiro-wilk W test for normal data

Variable	Obs	W	V	z	Prob>z
bomtbmd	14	0.94460	1.025	0.049	0.48037

. sktest mtbmd12m if vitdcat ==1

Skewness/Kurtosis tests for Normality

Variable	Obs	Pr(Skewness)	Pr(Kurtosis)	adj chi2(2)	joint Prob>chi2
mtbmd12m	14	0.3134	0.2947	2.46	0.2925

. swilk mtbmd12m if vitdcat ==1

Shapiro-wilk W test for normal data

Variable	Obs	W	V	z	Prob>z
mtbmd12m	14	0.89887	1.872	1.234	0.10862

. sktest mtbmdchange if vitdcat ==1

Skewness/Kurtosis tests for Normality

Variable	Obs	Pr(Skewness)	Pr(Kurtosis)	adj chi2(2)	joint Prob>chi2
mtbmdchange	14	0.7995	0.5381	0.46	0.7956

. swilk mtbmdchange if vitdcat ==1

Shapiro-wilk W test for normal data

Variable	Obs	W	V	z	Prob>z
mtbmdchange	14	0.97525	0.458	-1.537	0.93788

. sktest mtbmdpr if vitdcat ==1

Skewness/Kurtosis tests for Normality

Variable	Obs	Pr(Skewness)	Pr(Kurtosis)	adj chi2(2)	joint Prob>chi2
mtbmdpr	14	0.3193	0.5064	1.63	0.4430

. swilk mtbmdpr if vitdcat ==1

Shapiro-wilk W test for normal data

Variable	Obs	W	V	z	Prob>z
mtbmdpr	14	0.95895	0.760	-0.541	0.70577

. sktest bomtbmd if vitdcat ==2

Skewness/Kurtosis tests for Normality

Variable	Obs	Pr(Skewness)	Pr(Kurtosis)	adj chi2(2)	joint Prob>chi2
bomtbmd	21	0.5697	0.5455	0.73	0.6935

. swilk bomtbmd if vitdcat ==2

Shapiro-wilk W test for normal data

Variable	Obs	W	V	z	Prob>z
bomtbmd	21	0.95173	1.183	0.339	0.36717

. sktest mtbmd12m if vitdcat ==2

Skewness/Kurtosis tests for Normality

Variable	Obs	Pr(Skewness)	Pr(Kurtosis)	adj chi2(2)	joint Prob>chi2
mtbmd12m	21	0.3666	0.4949	1.41	0.4950

. swilk mtbmd12m if vitdcat ==2

Shapiro-wilk W test for normal data

Variable	Obs	W	V	z	Prob>z
mtbmd12m	21	0.95286	1.155	0.292	0.38525

. sktest mtbmdchange if vitdcat ==2

Skewness/Kurtosis tests for Normality

Variable	Obs	Pr(Skewness)	Pr(Kurtosis)	adj chi2(2)	joint Prob>chi2
mtbmdchange	21	0.4204	0.1985	2.59	0.2743

. swilk mtbmdchange if vitdcat ==2

Shapiro-wilk W test for normal data

Variable	Obs	W	V	z	Prob>z
mtbmdchange	21	0.95344	1.141	0.266	0.39496

. sktest mtbmdpr if vitdcat ==2

Skewness/Kurtosis tests for Normality

Variable	Obs	Pr(Skewness)	Pr(Kurtosis)	adj chi2(2)	joint Prob>chi2
mtbmdpr	21	0.9112	0.2604	1.40	0.4956

. swilk mtbmdpr if vitdcat ==2

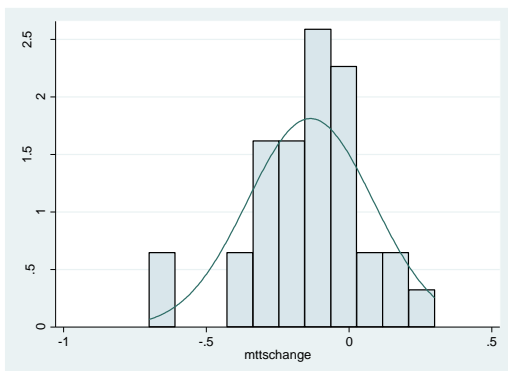
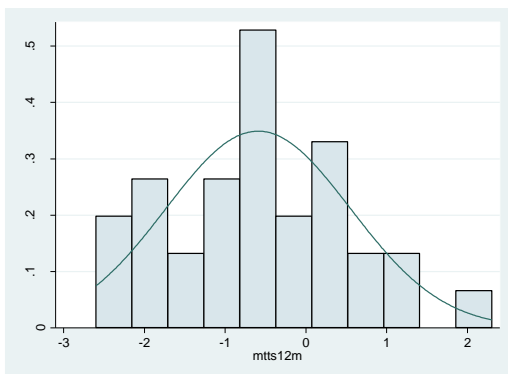
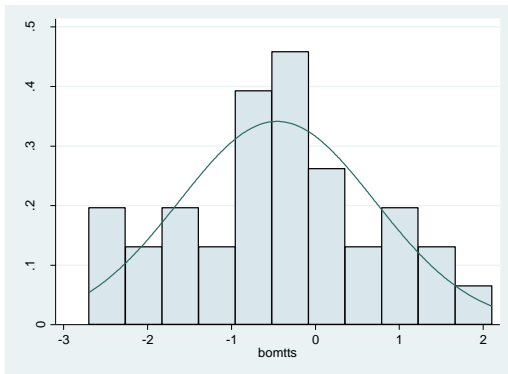
Shapiro-wilk W test for normal data

Variable	Obs	W	V	z	Prob>z
----------	-----	---	---	---	--------



# MT t score

1 All



. sktest bomtts

Skewness/Kurtosis tests for Normality					
Variable	Obs	Pr(Skewness)	Pr(Kurtosis)	adj chi2(2)	joint Prob>chi2
bomtts	35	0.8512	0.6675	0.22	0.8960

. swilk bomtts

Shapiro-wilk w test for normal data					
Variable	Obs	w	V	z	Prob>z
bomtts	35	0.98495	0.537	-1.297	0.90272

. sktest mtts12m

Skewness/Kurtosis tests for Normality					
Variable	Obs	Pr(Skewness)	Pr(Kurtosis)	adj chi2(2)	joint Prob>chi2
mtts12m	34	0.5100	0.8056	0.51	0.7748

. swilk mtts12m

Shapiro-wilk w test for normal data					
Variable	Obs	w	V	z	Prob>z
mtts12m	34	0.97758	0.783	-0.510	0.69506

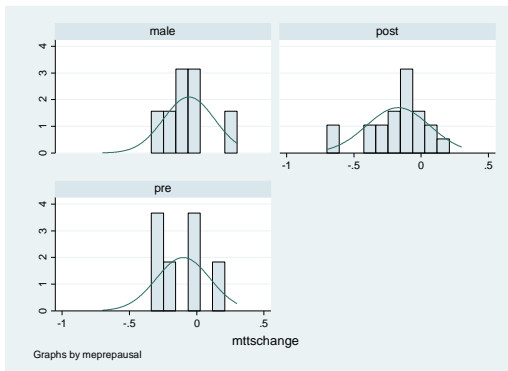
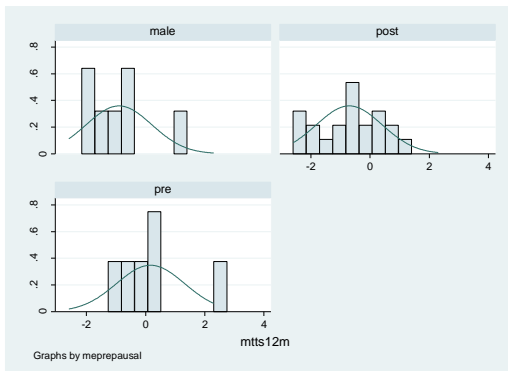
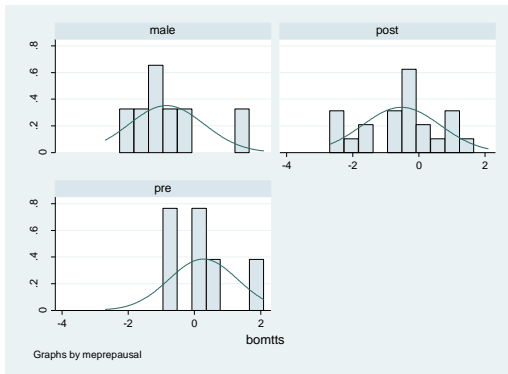
. sktest mttschange

Skewness/Kurtosis tests for Normality					
Variable	Obs	Pr(Skewness)	Pr(Kurtosis)	adj chi2(2)	joint Prob>chi2
mttschange	34	0.0978	0.1575	4.74	0.0935

. swilk mttschange

Shapiro-wilk w test for normal data					
Variable	Obs	w	V	z	Prob>z
mttschange	34	0.95125	1.702	1.108	0.13388

- **By gender and menopausal status**



. sktest bomtts if menopause ==0

Skewness/Kurtosis tests for Normality					
Variable	Obs	Pr(Skewness)	Pr(Kurtosis)	adj chi2(2)	joint Prob>chi2
bomtts	6	.	.	.	.

. swilk bomtts if menopause ==0

Shapiro-wilk W test for normal data					
Variable	Obs	W	V	z	Prob>z
bomtts	6	0.87653	1.529	0.664	0.25350

. sktest mtts12m if menopause ==0

Skewness/Kurtosis tests for Normality					
Variable	Obs	Pr(Skewness)	Pr(Kurtosis)	adj chi2(2)	joint Prob>chi2
mtts12m	6	.	.	.	.

. swilk mtts12m if menopause ==0

Shapiro-wilk W test for normal data					
Variable	Obs	W	V	z	Prob>z
mtts12m	6	0.85444	1.803	0.951	0.17089

. sktest mttschange if menopause ==0

Skewness/Kurtosis tests for Normality					
Variable	Obs	Pr(Skewness)	Pr(Kurtosis)	adj chi2(2)	joint Prob>chi2
mttschange	6	.	.	.	.

. swilk mttschange if menopause ==0

Shapiro-wilk W test for normal data					
Variable	Obs	W	V	z	Prob>z
mttschange	6	0.87155	1.591	0.731	0.23246

. sktest bomtts if menopause ==1

Skewness/Kurtosis tests for Normality					
Variable	Obs	Pr(Skewness)	Pr(Kurtosis)	adj chi2(2)	joint Prob>chi2
bomtts	22	0.5981	0.4241	0.99	0.6102

. swilk bomtts if menopause ==1

Shapiro-wilk W test for normal data					
Variable	Obs	W	V	z	Prob>z
bomtts	22	0.95619	1.110	0.211	0.41631

. sktest mtts12m if menopause ==1

Skewness/Kurtosis tests for Normality					
Variable	Obs	Pr(Skewness)	Pr(Kurtosis)	adj chi2(2)	joint Prob>chi2
mtts12m	21	0.7106	0.3405	1.14	0.5662

. swilk mtts12m if menopause ==1

Shapiro-wilk W test for normal data					
Variable	Obs	W	V	z	Prob>z
mtts12m	21	0.96425	0.876	-0.268	0.60553

. sktest mttschange if menopause ==1

Skewness/Kurtosis tests for Normality					
Variable	Obs	Pr(Skewness)	Pr(Kurtosis)	adj chi2(2)	joint Prob>chi2
mttschange	21	0.0683	0.3201	4.45	0.1081

. swilk mttschange if menopause ==1

Shapiro-wilk W test for normal data					
Variable	Obs	W	V	z	Prob>z
mttschange	21	0.92068	1.944	1.344	0.08953

. sktest bomtts if menopause ==2

Skewness/Kurtosis tests for Normality

Variable	Obs	Pr(Skewness)	Pr(Kurtosis)	adj	chi2(2)	joint	Prob>chi2
bomtts	7	.	.	.	.	.	.

. swilk bomtts if menopause ==2

Shapiro-Wilk W test for normal data

Variable	Obs	W	V	Z	Prob>z
bomtts	7	0.88986	1.447	0.601	0.27395

. sktest mtts12m if menopause ==2

Skewness/Kurtosis tests for Normality

Variable	Obs	Pr(Skewness)	Pr(Kurtosis)	adj	chi2(2)	joint	Prob>chi2
mtts12m	7	.	.	.	.	.	.

. swilk mtts12m if menopause ==2

Shapiro-Wilk W test for normal data

Variable	Obs	W	V	Z	Prob>z
mtts12m	7	0.90787	1.210	0.302	0.38133

. sktest mttschange if menopause ==2

Skewness/Kurtosis tests for Normality

Variable	Obs	Pr(Skewness)	Pr(Kurtosis)	adj	chi2(2)	joint	Prob>chi2
mttschange	7	.	.	.	.	.	.

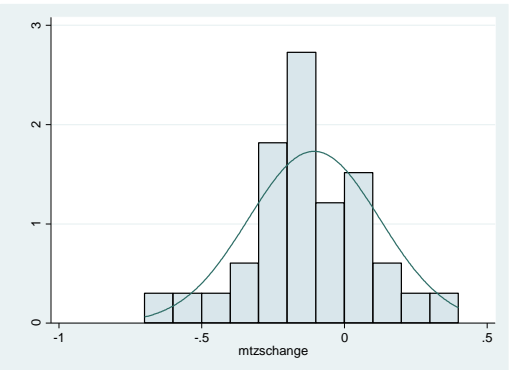
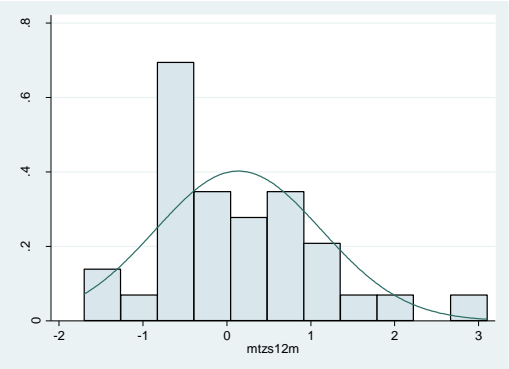
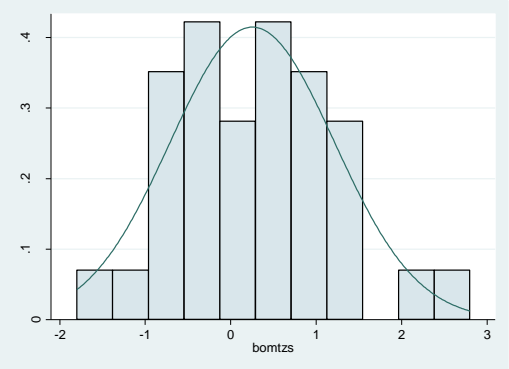
. swilk mttschange if menopause ==2

Shapiro-Wilk W test for normal data

Variable	Obs	W	V	Z	Prob>z
mttschange	7	0.93201	0.893	-0.172	0.56816

# MT z score

- All



. sktest bomtzs

Skewness/Kurtosis tests for Normality					
Variable	Obs	Pr(Skewness)	Pr(Kurtosis)	adj chi2(2)	joint Prob>chi2
bomtzs	34	0.3425	0.5238	1.39	0.4981

. swilk bomtzs

Shapiro-wilk w test for normal data					
Variable	Obs	w	v	z	Prob>z
bomtzs	34	0.98359	0.573	-1.161	0.87709

. sktest mtzs12m

Skewness/Kurtosis tests for Normality					
Variable	Obs	Pr(Skewness)	Pr(Kurtosis)	adj chi2(2)	joint Prob>chi2
mtzs12m	33	0.0446	0.1213	5.99	0.0499

. swilk mtzs12m

Shapiro-wilk w test for normal data					
Variable	Obs	w	v	z	Prob>z
mtzs12m	33	0.95471	1.546	0.906	0.18234

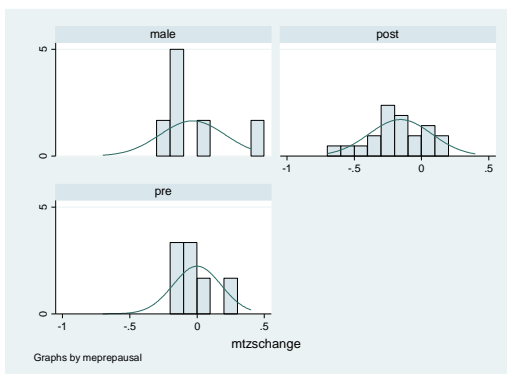
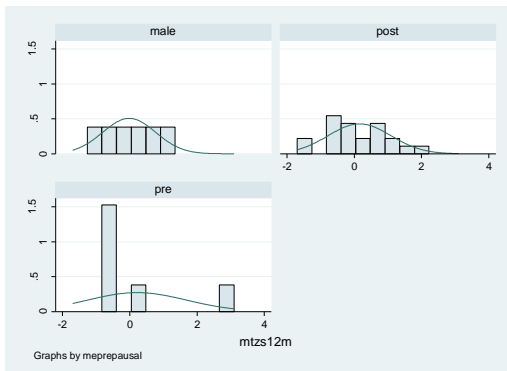
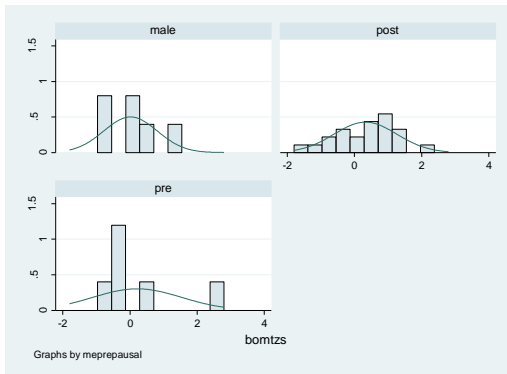
. sktest mtzschange

Skewness/Kurtosis tests for Normality					
Variable	Obs	Pr(Skewness)	Pr(Kurtosis)	adj chi2(2)	joint Prob>chi2
mtzschange	33	0.7615	0.3921	0.87	0.6479

. swilk mtzschange

Shapiro-wilk w test for normal data					
Variable	Obs	w	v	z	Prob>z
mtzschange	33	0.96891	1.061	0.124	0.45069

# - By gender and menopausal status





. sktest bomtzs if menopause ==0

Skewness/Kurtosis tests for Normality

Variable	Obs	Pr(Skewness)	Pr(Kurtosis)	adj	chi2(2)	joint	Prob>chi2
bomtzs	6	.	.	.	.	.	.

. swilk bomtzs if menopause ==0

Shapiro-Wilk W test for normal data

Variable	Obs	W	V	z	Prob>z
bomtzs	6	0.71138	3.574	2.403	0.00813

. sktest mtzs12m if menopause ==0

Skewness/Kurtosis tests for Normality

Variable	Obs	Pr(Skewness)	Pr(Kurtosis)	adj	chi2(2)	joint	Prob>chi2
mtzs12m	6	.	.	.	.	.	.

. swilk mtzs12m if menopause ==0

Shapiro-Wilk W test for normal data

Variable	Obs	W	V	z	Prob>z
mtzs12m	6	0.71258	3.560	2.393	0.00837

. sktest mtzschange if menopause ==0

Skewness/Kurtosis tests for Normality

Variable	Obs	Pr(Skewness)	Pr(Kurtosis)	adj	chi2(2)	joint	Prob>chi2
mtzschange	6	.	.	.	.	.	.

. swilk mtzschange if menopause ==0

Shapiro-Wilk W test for normal data

Variable	Obs	W	V	z	Prob>z
mtzschange	6	0.93341	0.825	-0.271	0.60671

. sktest bomtzs if menopause ==1

Skewness/Kurtosis tests for Normality

Variable	Obs	Pr(Skewness)	Pr(Kurtosis)	adj	chi2(2)	joint	Prob>chi2
bomtzs	22	0.3033	0.9484		1.15		0.5614

. swilk bomtzs if menopause ==1

Shapiro-Wilk W test for normal data

Variable	Obs	W	V	z	Prob>z
bomtzs	22	0.97248	0.697	-0.732	0.76779

. sktest mtzs12m if menopause ==1

Skewness/Kurtosis tests for Normality

Variable	Obs	Pr(Skewness)	Pr(Kurtosis)	adj	chi2(2)	joint	Prob>chi2
mtzs12m	21	0.9817	0.9189		0.01		0.9946

. swilk mtzs12m if menopause ==1

Shapiro-Wilk W test for normal data

Variable	Obs	W	V	z	Prob>z
mtzs12m	21	0.98589	0.346	-2.146	0.98408

. sktest mtzschange if menopause ==1

Skewness/Kurtosis tests for Normality

Variable	Obs	Pr(Skewness)	Pr(Kurtosis)	adj	chi2(2)	joint	Prob>chi2
mtzschange	21	0.4400	0.8023		0.70		0.7051

. swilk mtzschange if menopause ==1

Shapiro-Wilk W test for normal data

Variable	Obs	W	V	z	Prob>z
mtzschange	21	0.95893	1.006	0.013	0.49488

. sktest bomtzs if menopause ==2

Skewness/Kurtosis tests for Normality					
Variable	Obs	Pr(Skewness)	Pr(Kurtosis)	adj chi2(2)	joint Prob>chi2
bomtzs	6	.	.	.	.

. swilk bomtzs if menopause ==2

Shapiro-Wilk W test for normal data					
Variable	Obs	W	V	z	Prob>z
bomtzs	6	0.95665	0.537	-0.819	0.79357

. sktest mtzs12m if menopause ==2

Skewness/Kurtosis tests for Normality					
Variable	Obs	Pr(Skewness)	Pr(Kurtosis)	adj chi2(2)	joint Prob>chi2
mtzs12m	6	.	.	.	.

. swilk mtzs12m if menopause ==2

Shapiro-Wilk W test for normal data					
Variable	Obs	W	V	z	Prob>z
mtzs12m	6	0.93999	0.743	-0.410	0.65912

. sktest mtzschange if menopause ==2

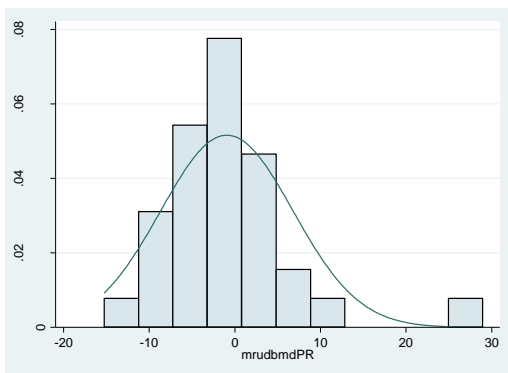
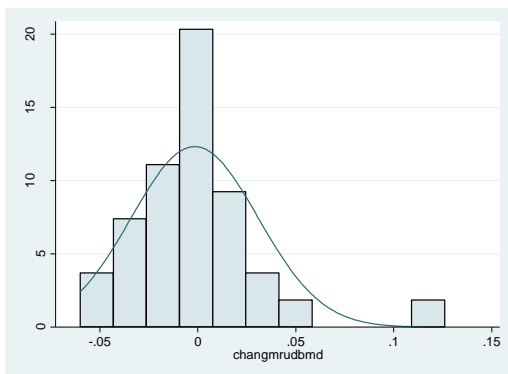
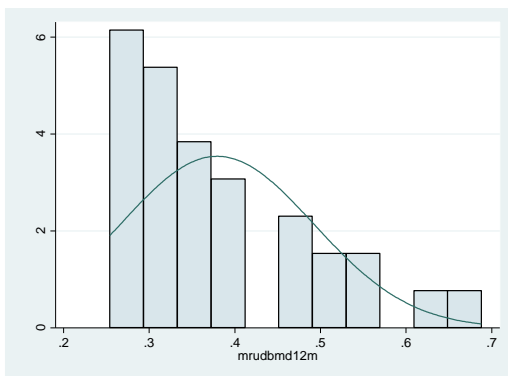
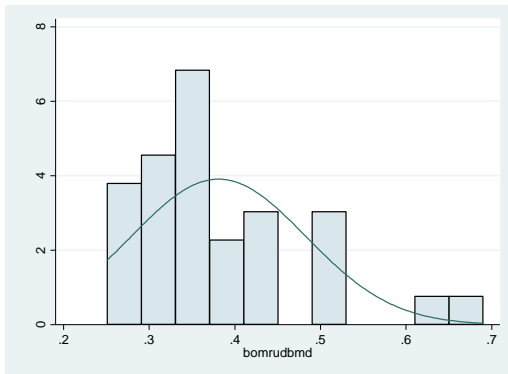
Skewness/Kurtosis tests for Normality					
Variable	Obs	Pr(Skewness)	Pr(Kurtosis)	adj chi2(2)	joint Prob>chi2
mtzschange	6	.	.	.	.

. swilk mtzschange if menopause ==2

Shapiro-Wilk W test for normal data					
Variable	Obs	W	V	z	Prob>z
mtzschange	6	0.78160	2.705	1.752	0.03989

# MRUDBMD

- All



. sktest bomrubmd

Skewness/Kurtosis tests for Normality					
Variable	Obs	Pr(Skewness)	Pr(Kurtosis)	adj chi2(2)	joint Prob>chi2
bomrubmd	33	0.0044	0.0721	9.42	0.0090

. swilk bomrubmd

Shapiro-wilk W test for normal data					
Variable	Obs	W	V	z	Prob>z
bomrubmd	33	0.89630	3.540	2.629	0.00428

. sktest mrubmd12m

Skewness/Kurtosis tests for Normality					
Variable	Obs	Pr(Skewness)	Pr(Kurtosis)	adj chi2(2)	joint Prob>chi2
mrubmd12m	33	0.0091	0.3311	6.94	0.0312

. swilk mrubmd12m

Shapiro-wilk W test for normal data					
Variable	Obs	W	V	z	Prob>z
mrubmd12m	33	0.87973	4.106	2.938	0.00165

. sktest changmrubmd

Skewness/Kurtosis tests for Normality					
Variable	Obs	Pr(Skewness)	Pr(Kurtosis)	adj chi2(2)	joint Prob>chi2
changmrubmd	32	0.0001	0.0003	19.98	0.0000

. swilk changmrubmd

Shapiro-wilk W test for normal data					
Variable	Obs	W	V	z	Prob>z
changmrubmd	32	0.83496	5.505	3.541	0.00020

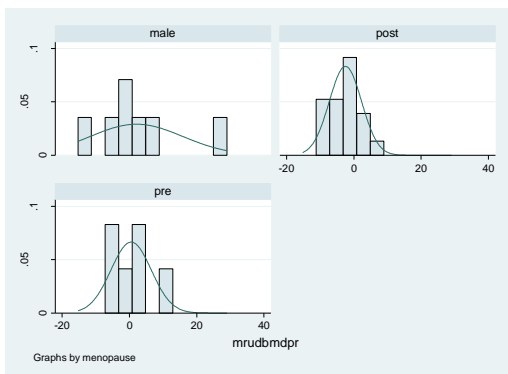
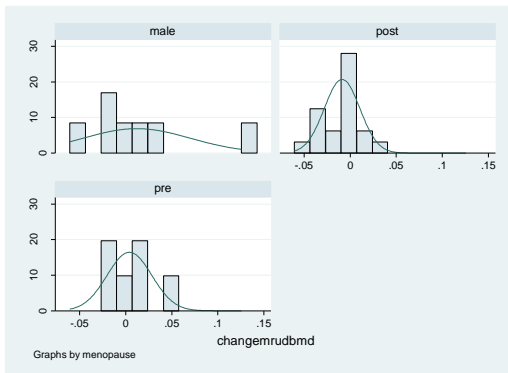
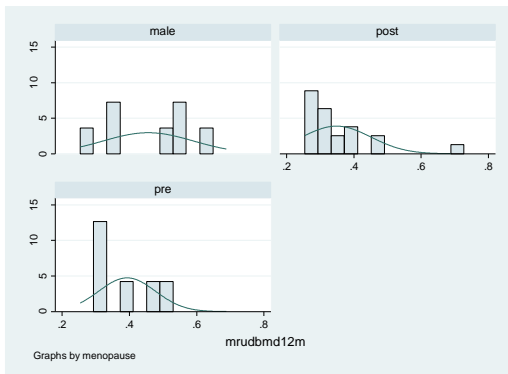
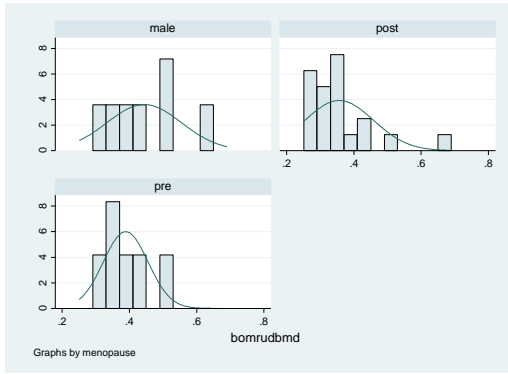
. sktest mrubmdpr

Skewness/Kurtosis tests for Normality					
Variable	Obs	Pr(Skewness)	Pr(Kurtosis)	adj chi2(2)	joint Prob>chi2
mrubmdpr	32	0.0003	0.0005	18.57	0.0001

. swilk mrubmdpr

Shapiro-wilk W test for normal data					
Variable	Obs	W	V	z	Prob>z
mrubmdpr	32	0.85884	4.709	3.217	0.00065

- **By gender and menopausal status**



. sktest bomrubmd if menopausal ==0

Skewness/Kurtosis tests for Normality

Variable	Obs	Pr(Skewness)	Pr(Kurtosis)	adj chi2(2)	joint Prob>chi2
bomrubmd	6	.	.	.	.

. swilk bomrubmd if menopausal ==0

Shapiro-Wilk W test for normal data

Variable	Obs	W	V	z	Prob>z
bomrubmd	6	0.92470	0.933	-0.100	0.53982

. sktest mrubmd12m if menopausal ==0

Skewness/Kurtosis tests for Normality

Variable	Obs	Pr(Skewness)	Pr(Kurtosis)	adj chi2(2)	joint Prob>chi2
mrubmd12m	6	.	.	.	.

. swilk mrubmd12m if menopausal ==0

Shapiro-Wilk W test for normal data

Variable	Obs	W	V	z	Prob>z
mrubmd12m	6	0.85162	1.838	0.985	0.16222

. sktest changemrubmd if menopausal ==0

Skewness/Kurtosis tests for Normality

Variable	Obs	Pr(Skewness)	Pr(Kurtosis)	adj chi2(2)	joint Prob>chi2
changemrud-d	6	.	.	.	.

. swilk changemrubmd if menopausal ==0

Shapiro-Wilk W test for normal data

Variable	Obs	W	V	z	Prob>z
changemrud-d	6	0.94421	0.691	-0.505	0.69325

. sktest mrubmdpr if menopausal ==0

Skewness/Kurtosis tests for Normality

Variable	Obs	Pr(Skewness)	Pr(Kurtosis)	adj chi2(2)	joint Prob>chi2
mrubmdpr	6	.	.	.	.

. swilk mrubmdpr if menopausal ==0

Shapiro-Wilk W test for normal data

Variable	Obs	W	V	z	Prob>z
mrubmdpr	6	0.96303	0.458	-1.006	0.84278

. sktest bomrubmd if menopausal ==1

Skewness/Kurtosis tests for Normality

Variable	Obs	Pr(Skewness)	Pr(Kurtosis)	adj chi2(2)	joint Prob>chi2
bomrubmd	20	0.0007	0.0034	14.76	0.0006

. swilk bomrubmd if menopausal ==1

Shapiro-Wilk W test for normal data

Variable	Obs	W	V	z	Prob>z
bomrubmd	20	0.81036	4.489	3.026	0.00124

. sktest mrubmd12m if menopausal ==1

Skewness/Kurtosis tests for Normality

Variable	Obs	Pr(Skewness)	Pr(Kurtosis)	adj chi2(2)	joint Prob>chi2
mrubmd12m	20	0.0005	0.0027	15.31	0.0005

. swilk mrubmd12m if menopausal ==1

Shapiro-Wilk W test for normal data

Variable	Obs	W	V	z	Prob>z
mrubmd12m	20	0.79622	4.823	3.171	0.00076

. sktest changemrubmd if menopausal ==1

Skewness/Kurtosis tests for Normality

Variable	Obs	Pr(Skewness)	Pr(Kurtosis)	adj chi2(2)	joint Prob>chi2
changemrud~d	19	0.6089	0.2345	1.88	0.3916

. swilk changemrubmd if menopausal ==1

Shapiro-Wilk W test for normal data

Variable	Obs	W	V	z	Prob>z
changemrud~d	19	0.94880	1.169	0.313	0.37701

. sktest mrubmdpr if menopausal ==1

Skewness/Kurtosis tests for Normality

Variable	Obs	Pr(Skewness)	Pr(Kurtosis)	adj chi2(2)	joint Prob>chi2
mrubmdpr	19	0.4313	0.6112	0.95	0.6218

. swilk mrubmdpr if menopausal ==1

Shapiro-Wilk W test for normal data

Variable	Obs	W	V	z	Prob>z
mrubmdpr	19	0.94945	1.154	0.288	0.38678

. sktest bomrubmd if menopausal ==2

Skewness/Kurtosis tests for Normality

Variable	Obs	Pr(Skewness)	Pr(Kurtosis)	adj chi2(2)	joint Prob>chi2
bomrubmd	7	.	.	.	.

. swilk bomrubmd if menopausal ==2

Shapiro-wilk W test for normal data

Variable	Obs	W	V	z	Prob>z
bomrubmd	7	0.97548	0.322	-1.513	0.93486

. sktest mrudbmd12m if menopausal ==2

Skewness/Kurtosis tests for Normality

Variable	Obs	Pr(Skewness)	Pr(Kurtosis)	adj chi2(2)	joint Prob>chi2
mrudbmd12m	7	.	.	.	.

. swilk mrudbmd12m if menopausal ==2

Shapiro-wilk W test for normal data

Variable	Obs	W	V	z	Prob>z
mrudbmd12m	7	0.89259	1.411	0.558	0.28846

. sktest changemrubmd if menopausal ==2

Skewness/Kurtosis tests for Normality

Variable	Obs	Pr(Skewness)	Pr(Kurtosis)	adj chi2(2)	joint Prob>chi2
changemrud-d	7	.	.	.	.

. swilk changemrubmd if menopausal ==2

Shapiro-wilk W test for normal data

Variable	Obs	W	V	z	Prob>z
changemrud-d	7	0.89147	1.425	0.576	0.28242

. sktest mrudbmdpr if menopausal ==2

Skewness/Kurtosis tests for Normality

Variable	Obs	Pr(Skewness)	Pr(Kurtosis)	adj chi2(2)	joint Prob>chi2
mrudbmdpr	7	.	.	.	.

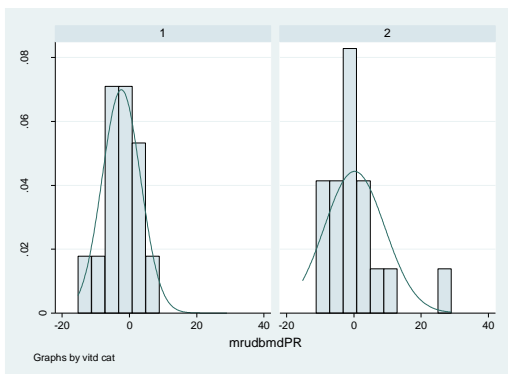
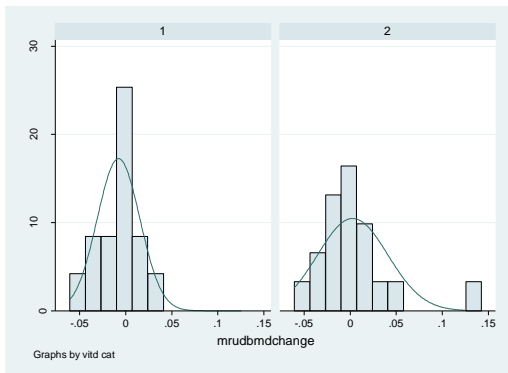
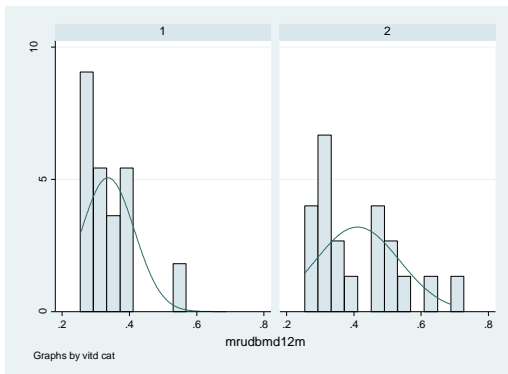
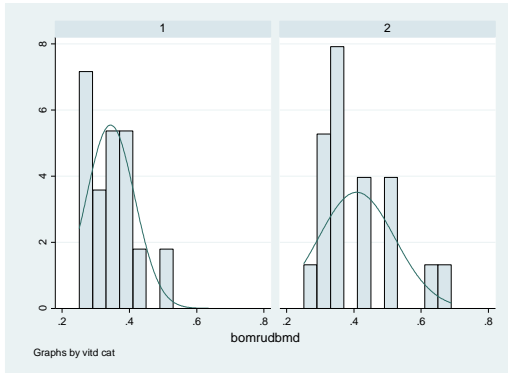
. swilk mrudbmdpr if menopausal ==2

Shapiro-wilk W test for normal data

Variable	Obs	W	V	z	Prob>z
mrudbmdpr	7	0.89319	1.403	0.548	0.29173



- **By vitamin D category**



```
. sktest bomrubmd if vitdcat ==1
      Skewness/Kurtosis tests for Normality
+-----+-----+-----+-----+-----+
Variable | Obs  Pr(Skewness)  Pr(Kurtosis)  adj chi2(2)  joint Prob>chi2
-----+-----+-----+-----+-----+
bomrubmd | 14   0.2347         0.5800         1.97         0.3726
```

```
. swilk bomrubmd if vitdcat ==1
      Shapiro-wilk W test for normal data
+-----+-----+-----+-----+-----+
Variable | Obs    W         V         z         Prob>z
-----+-----+-----+-----+-----+
bomrubmd | 14   0.94984     0.928     -0.146     0.55818
```

```
. sktest mrubmd12m if vitdcat ==1
      Skewness/Kurtosis tests for Normality
+-----+-----+-----+-----+-----+
Variable | Obs  Pr(Skewness)  Pr(Kurtosis)  adj chi2(2)  joint Prob>chi2
-----+-----+-----+-----+-----+
mrubmd12m | 14   0.0233         0.0628         7.37         0.0251
```

```
. swilk mrubmd12m if vitdcat ==1
      Shapiro-wilk W test for normal data
+-----+-----+-----+-----+-----+
Variable | Obs    W         V         z         Prob>z
-----+-----+-----+-----+-----+
mrubmd12m | 14   0.87238     2.362     1.692     0.04532
```

```
. sktest mrubmdchange if vitdcat ==1
      Skewness/Kurtosis tests for Normality
+-----+-----+-----+-----+-----+
Variable | Obs  Pr(Skewness)  Pr(Kurtosis)  adj chi2(2)  joint Prob>chi2
-----+-----+-----+-----+-----+
mrubmdcha~e | 14   0.5499         0.1361         3.03         0.2199
```

```
. swilk mrubmdchange if vitdcat ==1
      Shapiro-wilk W test for normal data
+-----+-----+-----+-----+-----+
Variable | Obs    W         V         z         Prob>z
-----+-----+-----+-----+-----+
mrubmdcha~e | 14   0.95379     0.855     -0.308     0.62086
```

```
. sktest mrubmdpr if vitdcat ==1
      Skewness/Kurtosis tests for Normality
+-----+-----+-----+-----+-----+
Variable | Obs  Pr(Skewness)  Pr(Kurtosis)  adj chi2(2)  joint Prob>chi2
-----+-----+-----+-----+-----+
mrubmdpr | 14   0.3587         0.2855         2.30         0.3169
```

```
. swilk mrubmdpr if vitdcat ==1
      Shapiro-wilk W test for normal data
+-----+-----+-----+-----+-----+
Variable | Obs    W         V         z         Prob>z
-----+-----+-----+-----+-----+
mrubmdpr | 14   0.97013     0.553     -1.167     0.87844
```

```
. sktest bomrubmd if vitdcat ==2
      Skewness/Kurtosis tests for Normality
+-----+-----+-----+-----+-----+
Variable | Obs  Pr(Skewness)  Pr(Kurtosis)  adj chi2(2)  joint Prob>chi2
-----+-----+-----+-----+-----+
bomrubmd | 19   0.0362         0.3358         5.19         0.0747
```

```
. swilk bomrubmd if vitdcat ==2
      Shapiro-wilk W test for normal data
+-----+-----+-----+-----+-----+
Variable | Obs    W         V         z         Prob>z
-----+-----+-----+-----+-----+
bomrubmd | 19   0.89326     2.437     1.789     0.03680
```

```
. sktest mrubmd12m if vitdcat ==2
      Skewness/Kurtosis tests for Normality
+-----+-----+-----+-----+-----+
Variable | Obs  Pr(Skewness)  Pr(Kurtosis)  adj chi2(2)  joint Prob>chi2
-----+-----+-----+-----+-----+
mrubmd12m | 19   0.1134         0.9235         2.86         0.2391
```

```
. swilk mrubmd12m if vitdcat ==2
      Shapiro-wilk W test for normal data
+-----+-----+-----+-----+-----+
Variable | Obs    W         V         z         Prob>z
-----+-----+-----+-----+-----+
mrubmd12m | 19   0.89877     2.311     1.683     0.04623
```

```
. sktest mrubmdchange if vitdcat ==2
      Skewness/Kurtosis tests for Normality
+-----+-----+-----+-----+-----+
Variable | Obs  Pr(Skewness)  Pr(Kurtosis)  adj chi2(2)  joint Prob>chi2
-----+-----+-----+-----+-----+
mrubmdcha~e | 18   0.0008         0.0025         14.76         0.0006
```

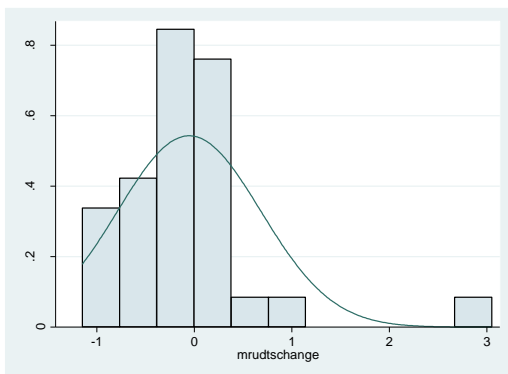
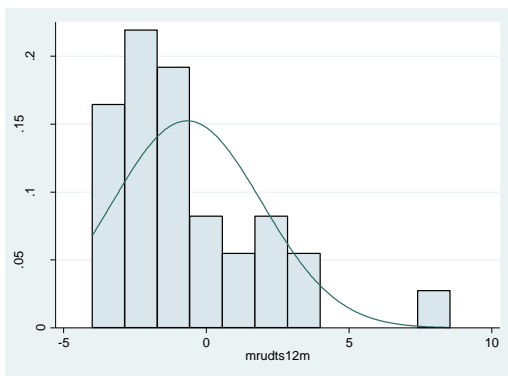
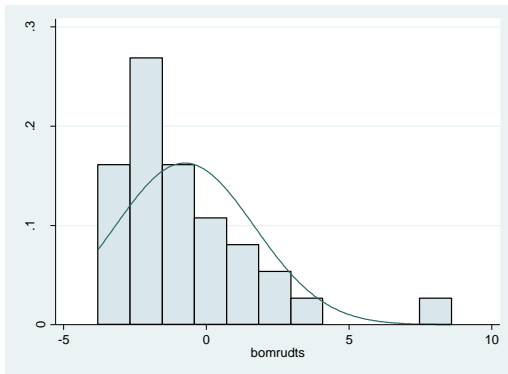
```
. swilk mrubmdchange if vitdcat ==2
      Shapiro-wilk W test for normal data
+-----+-----+-----+-----+-----+
Variable | Obs    W         V         z         Prob>z
-----+-----+-----+-----+-----+
mrubmdcha~e | 18   0.80818     4.217     2.880     0.00199
```

```
. sktest mrubmdpr if vitdcat ==2
      Skewness/Kurtosis tests for Normality
+-----+-----+-----+-----+-----+
Variable | Obs  Pr(Skewness)  Pr(Kurtosis)  adj chi2(2)  joint Prob>chi2
-----+-----+-----+-----+-----+
mrubmdpr | 18   0.0009         0.0032         14.41         0.0007
```

```
. swilk mrubmdpr if vitdcat ==2
      Shapiro-wilk W test for normal data
+-----+-----+-----+-----+-----+
Variable | Obs    W         V         z         Prob>z
```

# MRUD t score

- All



. sktest bomrudts

Skewness/Kurtosis tests for Normality					
Variable	Obs	Pr(Skewness)	Pr(Kurtosis)	adj chi2(2)	joint Prob>chi2
bomrudts	33	0.0001	0.0011	18.49	0.0001

. swilk bomrudts

Shapiro-wilk w test for normal data					
Variable	Obs	w	V	z	Prob>z
bomrudts	33	0.84953	5.137	3.404	0.00033

. sktest mrudts12m

Skewness/Kurtosis tests for Normality					
Variable	Obs	Pr(Skewness)	Pr(Kurtosis)	adj chi2(2)	joint Prob>chi2
mrudts12m	32	0.0009	0.0071	14.01	0.0009

. swilk mrudts12m

Shapiro-wilk w test for normal data					
Variable	Obs	w	V	z	Prob>z
mrudts12m	32	0.87765	4.081	2.920	0.00175

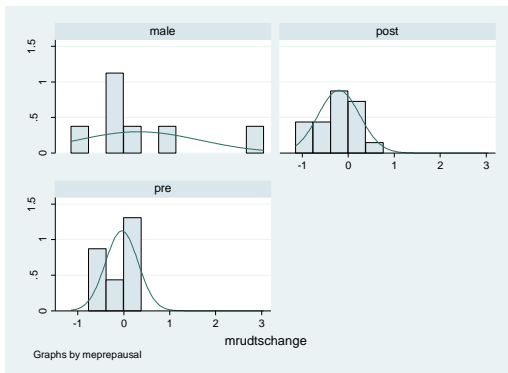
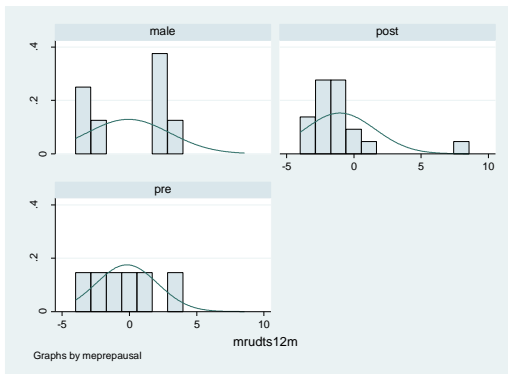
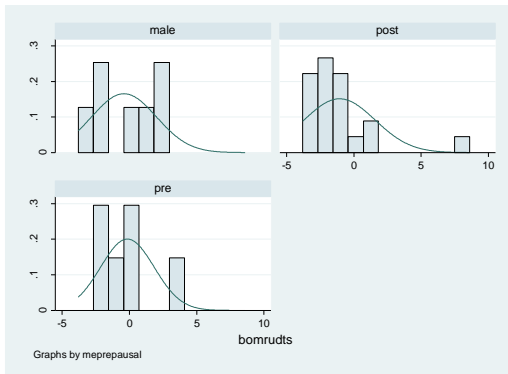
. sktest mrudtschange

Skewness/Kurtosis tests for Normality					
Variable	Obs	Pr(Skewness)	Pr(Kurtosis)	adj chi2(2)	joint Prob>chi2
mrudtschange	31	0.0000	0.0000	25.18	0.0000

. swilk mrudtschange

Shapiro-wilk w test for normal data					
Variable	Obs	w	V	z	Prob>z
mrudtschange	31	0.78485	7.008	4.034	0.00003

- **By gender and menopausal status**



. sktest bomrudts if menopause ==0

Skewness/Kurtosis tests for Normality

Variable	Obs	Pr(Skewness)	Pr(Kurtosis)	adj chi2(2)	joint Prob>chi2
bomrudts	6	.	.	.	.

. swilk bomrudts if menopause ==0

Shapiro-wilk W test for normal data

Variable	Obs	W	V	z	Prob>z
bomrudts	6	0.94914	0.630	-0.623	0.73328

. sktest mrudts12m if menopause ==0

Skewness/Kurtosis tests for Normality

Variable	Obs	Pr(Skewness)	Pr(Kurtosis)	adj chi2(2)	joint Prob>chi2
mrudts12m	6	.	.	.	.

. swilk mrudts12m if menopause ==0

Shapiro-wilk W test for normal data

Variable	Obs	W	V	z	Prob>z
mrudts12m	6	0.95373	0.573	-0.740	0.77038

. sktest mrudtschange if menopause ==0

Skewness/Kurtosis tests for Normality

Variable	Obs	Pr(Skewness)	Pr(Kurtosis)	adj chi2(2)	joint Prob>chi2
mrudtschange	6	.	.	.	.

. swilk mrudtschange if menopause ==0

Shapiro-wilk W test for normal data

Variable	Obs	W	V	z	Prob>z
mrudtschange	6	0.91543	1.047	0.068	0.47305

. sktest bomrudts if menopause ==1

Skewness/Kurtosis tests for Normality

Variable	Obs	Pr(Skewness)	Pr(Kurtosis)	adj chi2(2)	joint Prob>chi2
bomrudts	20	0.0000	0.0002	21.70	0.0000

. swilk bomrudts if menopause ==1

Shapiro-wilk W test for normal data

Variable	Obs	W	V	z	Prob>z
bomrudts	20	0.70650	6.947	3.906	0.00005

. sktest mrudts12m if menopause ==1

Skewness/Kurtosis tests for Normality

Variable	Obs	Pr(Skewness)	Pr(Kurtosis)	adj chi2(2)	joint Prob>chi2
mrudts12m	19	0.0000	0.0001	22.54	0.0000

. swilk mrudts12m if menopause ==1

Shapiro-wilk W test for normal data

Variable	Obs	W	V	z	Prob>z
mrudts12m	19	0.67920	7.324	3.999	0.00003

. sktest mrudtschange if menopause ==1

Skewness/Kurtosis tests for Normality

Variable	Obs	Pr(Skewness)	Pr(Kurtosis)	adj chi2(2)	joint Prob>chi2
mrudtschange	18	0.9741	0.9537	0.00	0.9978

. swilk mrudtschange if menopause ==1

Shapiro-wilk W test for normal data

Variable	Obs	W	V	z	Prob>z
mrudtschange	18	0.96372	0.797	-0.453	0.67471

. sktest bomrudts if menopause ==2

Skewness/Kurtosis tests for Normality

Variable	Obs	Pr(Skewness)	Pr(Kurtosis)	adj	chi2(2)	joint	Prob>chi2
bomrudts	7	.	.	.	.	.	.

. swilk bomrudts if menopause ==2

Shapiro-Wilk W test for normal data

Variable	Obs	W	V	z	Prob>z
bomrudts	7	0.92513	0.983	-0.026	0.51028

. sktest mrudts12m if menopause ==2

Skewness/Kurtosis tests for Normality

Variable	Obs	Pr(Skewness)	Pr(Kurtosis)	adj	chi2(2)	joint	Prob>chi2
mrudts12m	7	.	.	.	.	.	.

. swilk mrudts12m if menopause ==2

Shapiro-Wilk W test for normal data

Variable	Obs	W	V	z	Prob>z
mrudts12m	7	0.83095	2.220	1.394	0.08169

. sktest mrudtschange if menopause ==2

Skewness/Kurtosis tests for Normality

Variable	Obs	Pr(Skewness)	Pr(Kurtosis)	adj	chi2(2)	joint	Prob>chi2
mrudtschange	7	.	.	.	.	.	.

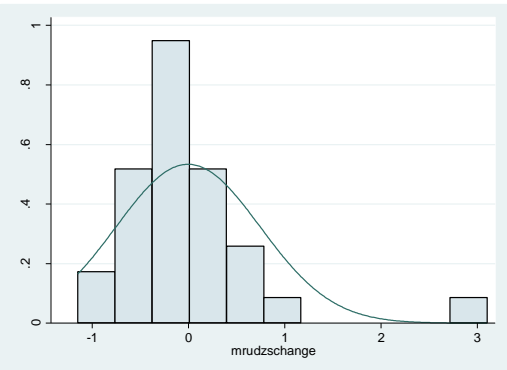
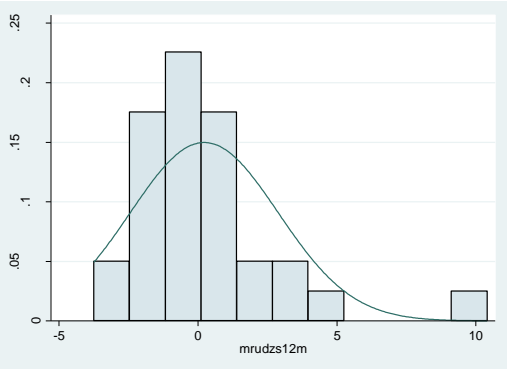
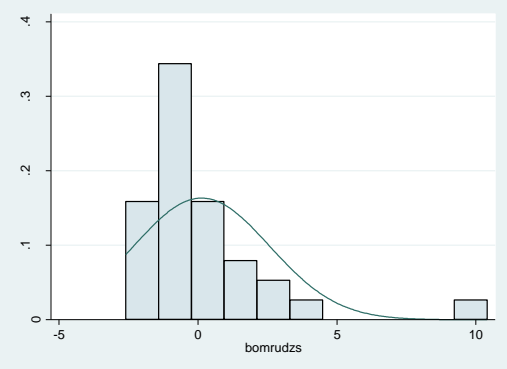
. swilk mrudtschange if menopause ==2

Shapiro-Wilk W test for normal data

Variable	Obs	W	V	z	Prob>z
mrudtschange	7	0.84065	2.093	1.277	0.10076

# MRUD z score

- All





. sktest bomrudzs

Skewness/Kurtosis tests for Normality

Variable	Obs	Pr(Skewness)	Pr(Kurtosis)	adj chi2(2)	joint Prob>chi2
bomrudzs	32	0.0000	0.0001	25.61	0.0000

. swilk bomrudzs

Shapiro-wilk w test for normal data

Variable	Obs	w	V	z	Prob>z
bomrudzs	32	0.77488	7.509	4.186	0.00001

. sktest mrudzs12m

Skewness/Kurtosis tests for Normality

Variable	Obs	Pr(Skewness)	Pr(Kurtosis)	adj chi2(2)	joint Prob>chi2
mrudzs12m	31	0.0001	0.0007	19.00	0.0001

. swilk mrudzs12m

Shapiro-wilk w test for normal data

Variable	Obs	w	V	z	Prob>z
mrudzs12m	31	0.83916	5.239	3.431	0.00030

. sktest mrudzschange

Skewness/Kurtosis tests for Normality

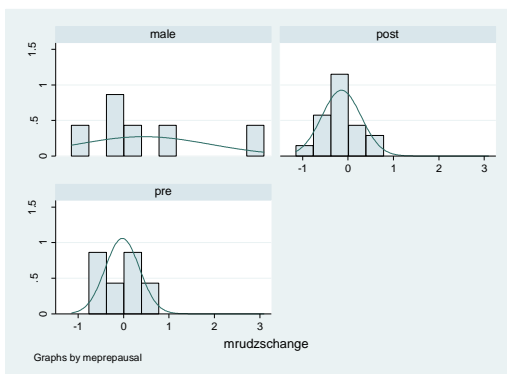
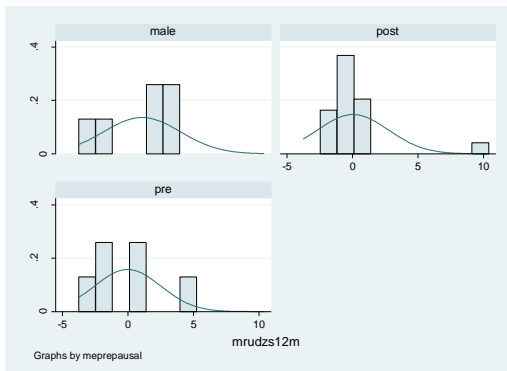
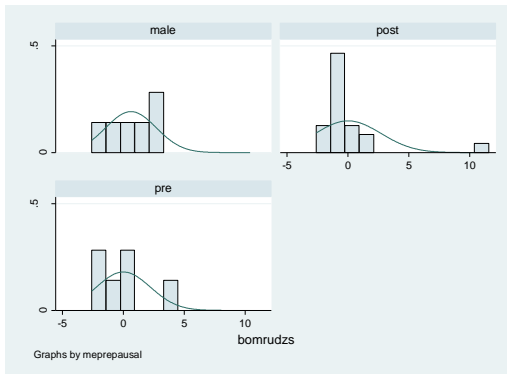
Variable	Obs	Pr(Skewness)	Pr(Kurtosis)	adj chi2(2)	joint Prob>chi2
mrudzschange	30	0.0000	0.0001	24.46	0.0000

. swilk mrudzschange

Shapiro-wilk w test for normal data

Variable	Obs	w	V	z	Prob>z
mrudzschange	30	0.78967	6.685	3.929	0.00004

- **By gender and menopausal status**



. sktest bomrudzs if menopause ==0

Skewness/Kurtosis tests for Normality						
Variable	Obs	Pr(Skewness)	Pr(Kurtosis)	adj	chi2(2)	joint Prob>chi2
bomrudzs	6	.	.	.	.	.

. swilk bomrudzs if menopause ==0

Shapiro-Wilk W test for normal data					
Variable	Obs	W	V	z	Prob>z
bomrudzs	6	0.93912	0.754	-0.391	0.65209

. sktest mrudzs12m if menopause ==0

Skewness/Kurtosis tests for Normality						
Variable	Obs	Pr(Skewness)	Pr(Kurtosis)	adj	chi2(2)	joint Prob>chi2
mrudzs12m	6	.	.	.	.	.

. swilk mrudzs12m if menopause ==0

Shapiro-Wilk W test for normal data					
Variable	Obs	W	V	z	Prob>z
mrudzs12m	6	0.94637	0.664	-0.556	0.71078

. sktest mrudzschang if menopause ==0

Skewness/Kurtosis tests for Normality						
Variable	Obs	Pr(Skewness)	Pr(Kurtosis)	adj	chi2(2)	joint Prob>chi2
mrudzschang	6	.	.	.	.	.

. swilk mrudzschang if menopause ==0

Shapiro-Wilk W test for normal data					
Variable	Obs	W	V	z	Prob>z
mrudzschang	6	0.91855	1.009	0.013	0.49497

. sktest bomrudzs if menopause ==1

Skewness/Kurtosis tests for Normality						
Variable	Obs	Pr(Skewness)	Pr(Kurtosis)	adj	chi2(2)	joint Prob>chi2
bomrudzs	20	0.0000	0.0000	25.67	0.0000	0.0000

. swilk bomrudzs if menopause ==1

Shapiro-Wilk W test for normal data					
Variable	Obs	W	V	z	Prob>z
bomrudzs	20	0.61890	9.021	4.433	0.00000

. sktest mrudzs12m if menopause ==1

Skewness/Kurtosis tests for Normality						
Variable	Obs	Pr(Skewness)	Pr(Kurtosis)	adj	chi2(2)	joint Prob>chi2
mrudzs12m	19	0.0000	0.0000	25.55	0.0000	0.0000

. swilk mrudzs12m if menopause ==1

Shapiro-Wilk W test for normal data					
Variable	Obs	W	V	z	Prob>z
mrudzs12m	19	0.59993	9.133	4.443	0.00000

. sktest mrudzschang if menopause ==1

Skewness/Kurtosis tests for Normality						
Variable	Obs	Pr(Skewness)	Pr(Kurtosis)	adj	chi2(2)	joint Prob>chi2
mrudzschang	18	0.8406	0.8461	0.08	0.9617	0.9617

. swilk mrudzschang if menopause ==1

Shapiro-Wilk W test for normal data					
Variable	Obs	W	V	z	Prob>z
mrudzschang	18	0.95209	1.053	0.104	0.45874

. sktest bomrudzs if menopause ==2

Skewness/Kurtosis tests for Normality

Variable	Obs	Pr(Skewness)	Pr(Kurtosis)	adj chi2(2)	joint Prob>chi2
bomrudzs	6	.	.	.	.

. swilk bomrudzs if menopause ==2

Shapiro-wilk W test for normal data

Variable	Obs	W	V	z	Prob>z
bomrudzs	6	0.89160	1.342	0.449	0.32666

. sktest mrudzs12m if menopause ==2

Skewness/Kurtosis tests for Normality

Variable	Obs	Pr(Skewness)	Pr(Kurtosis)	adj chi2(2)	joint Prob>chi2
mrudzs12m	6	.	.	.	.

. swilk mrudzs12m if menopause ==2

Shapiro-wilk W test for normal data

Variable	Obs	W	V	z	Prob>z
mrudzs12m	6	0.86660	1.652	0.796	0.21299

. sktest mrudzschange if menopause ==2

Skewness/Kurtosis tests for Normality

Variable	Obs	Pr(Skewness)	Pr(Kurtosis)	adj chi2(2)	joint Prob>chi2
mrudzschange	6	.	.	.	.

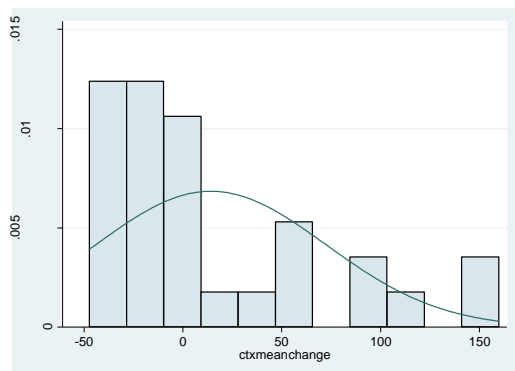
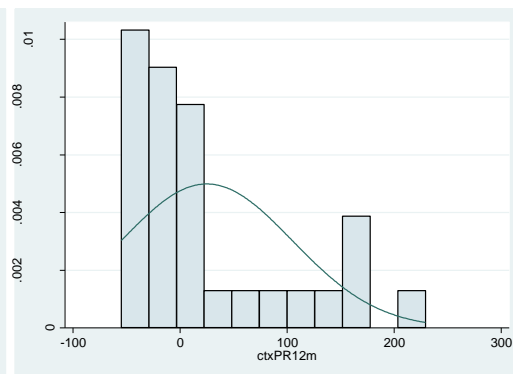
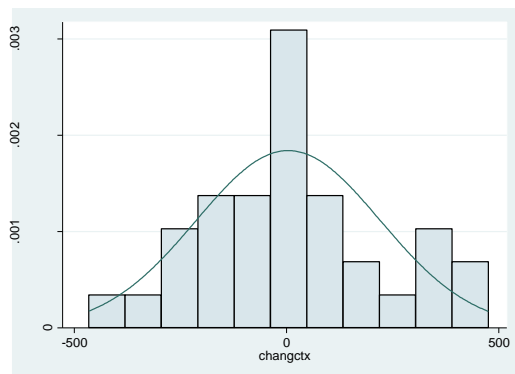
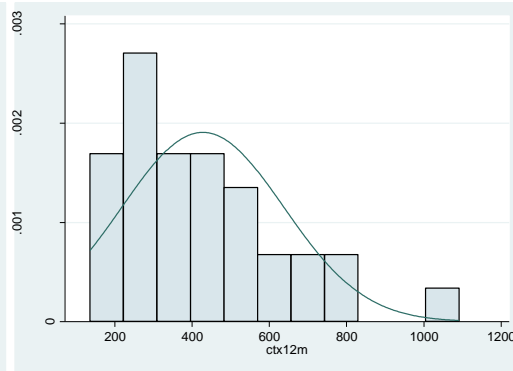
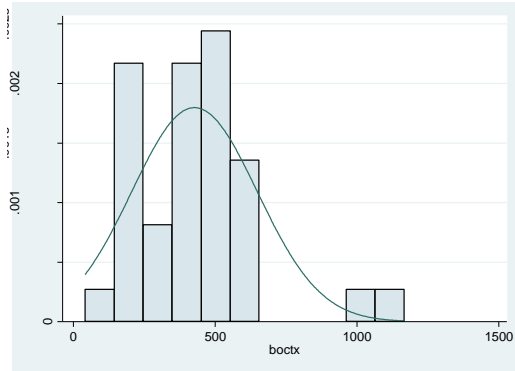
. swilk mrudzschange if menopause ==2

Shapiro-wilk W test for normal data

Variable	Obs	W	V	z	Prob>z
mrudzschange	6	0.89409	1.312	0.412	0.34018

# $\beta$ CTX

- All



. sktest boctx

Skewness/Kurtosis tests for Normality					
Variable	Obs	Pr(Skewness)	Pr(Kurtosis)	adj chi2(2)	joint Prob>chi2
boctx	36	0.0026	0.0082	12.61	0.0018

. swilk boctx

Shapiro-wilk w test for normal data					
Variable	Obs	W	V	z	Prob>z
boctx	36	0.89407	3.863	2.826	0.00236

. sktest ctx12m

Skewness/Kurtosis tests for Normality					
Variable	Obs	Pr(Skewness)	Pr(Kurtosis)	adj chi2(2)	joint Prob>chi2
ctx12m	34	0.0075	0.0797	8.67	0.0131

. swilk ctx12m

Shapiro-wilk w test for normal data					
Variable	Obs	W	V	z	Prob>z
ctx12m	34	0.91746	2.882	2.206	0.01370

. sktest ctxc12m

Skewness/Kurtosis tests for Normality					
Variable	Obs	Pr(Skewness)	Pr(Kurtosis)	adj chi2(2)	joint Prob>chi2
ctxc12m	30	0.5805	0.7713	0.40	0.8192

. swilk ctxc12m

Shapiro-wilk w test for normal data					
Variable	Obs	W	V	z	Prob>z
ctxc12m	30	0.97998	0.636	-0.935	0.82515

. sktest ctxpr12m

Skewness/Kurtosis tests for Normality					
Variable	Obs	Pr(Skewness)	Pr(Kurtosis)	adj chi2(2)	joint Prob>chi2
ctxpr12m	30	0.0066	0.4575	7.05	0.0295

. swilk ctxpr12m

Shapiro-wilk w test for normal data					
Variable	Obs	W	V	z	Prob>z
ctxpr12m	30	0.82071	5.699	3.598	0.00016

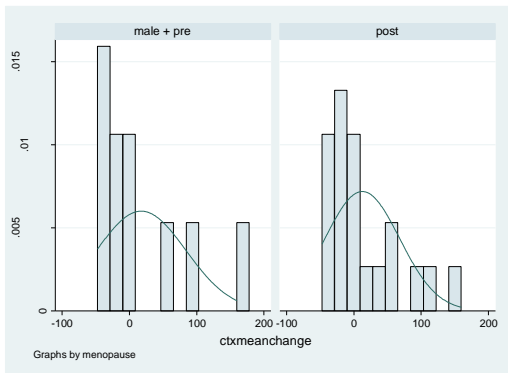
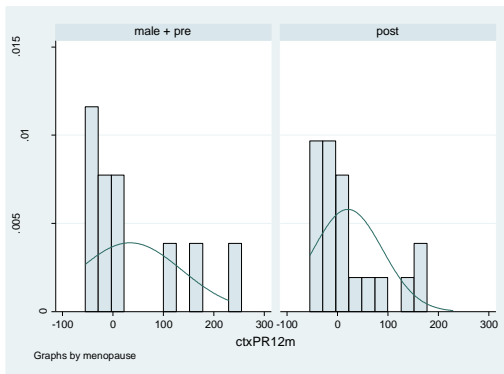
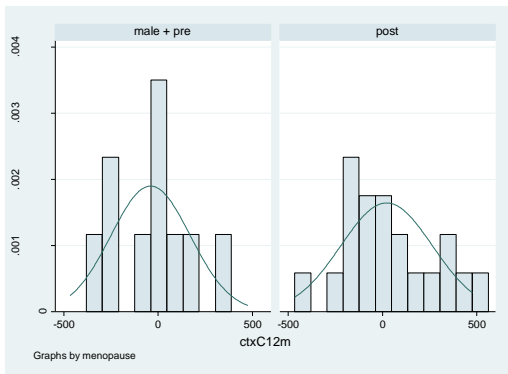
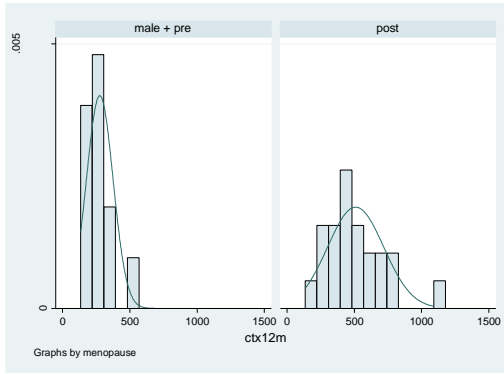
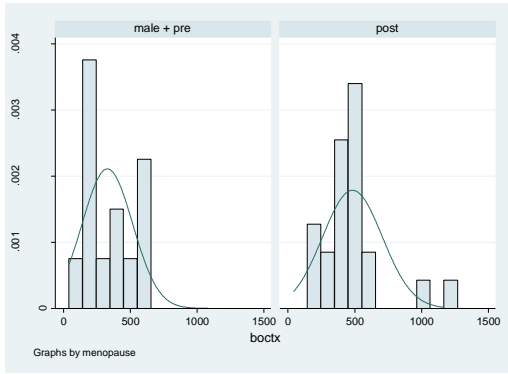
. sktest ctxmeanchange

Skewness/Kurtosis tests for Normality					
Variable	Obs	Pr(Skewness)	Pr(Kurtosis)	adj chi2(2)	joint Prob>chi2
ctxmeancha~e	30	0.0055	0.3040	7.63	0.0221

. swilk ctxmeanchange

Shapiro-wilk w test for normal data					
Variable	Obs	W	V	z	Prob>z
ctxmeancha~e	30	0.83240	5.327	3.459	0.00027

- **By gender and menopausal status**



. sktest boctx if menopausal ==0

Skewness/Kurtosis tests for Normality					
Variable	Obs	Pr(Skewness)	Pr(Kurtosis)	adj chi2(2)	joint Prob>chi2
boctx	13	0.5816	0.3276	1.43	0.4898

. swilk boctx if menopausal ==0

Shapiro-Wilk w test for normal data					
Variable	Obs	W	V	z	Prob>z
boctx	13	0.94699	0.934	-0.135	0.55352

. sktest ctx12m if menopausal ==0

Skewness/Kurtosis tests for Normality					
Variable	Obs	Pr(Skewness)	Pr(Kurtosis)	adj chi2(2)	joint Prob>chi2
ctx12m	12	0.2647	0.4590	2.09	0.3517

. swilk ctx12m if menopausal ==0

Shapiro-Wilk w test for normal data					
Variable	Obs	W	V	z	Prob>z
ctx12m	12	0.95598	0.735	-0.599	0.72534

. sktest ctxc12m if menopausal ==0

Skewness/Kurtosis tests for Normality					
Variable	Obs	Pr(Skewness)	Pr(Kurtosis)	adj chi2(2)	joint Prob>chi2
ctxc12m	10	0.9618	0.6590	0.20	0.9062

. swilk ctxc12m if menopausal ==0

Shapiro-Wilk w test for normal data					
Variable	Obs	W	V	z	Prob>z
ctxc12m	10	0.96847	0.486	-1.157	0.87633

. sktest ctxpr12m if menopausal ==0

Skewness/Kurtosis tests for Normality					
Variable	Obs	Pr(Skewness)	Pr(Kurtosis)	adj chi2(2)	joint Prob>chi2
ctxpr12m	10	0.1115	0.9874	3.07	0.2155

. swilk ctxpr12m if menopausal ==0

Shapiro-Wilk w test for normal data					
Variable	Obs	W	V	z	Prob>z
ctxpr12m	10	0.82243	2.737	1.925	0.02711

. sktest ctxmeanchange if menopausal ==0

Skewness/Kurtosis tests for Normality					
Variable	Obs	Pr(Skewness)	Pr(Kurtosis)	adj chi2(2)	joint Prob>chi2
ctxmeanchange	10	0.0551	0.3796	4.56	0.1024

. swilk ctxmeanchange if menopausal ==0

Shapiro-Wilk w test for normal data					
Variable	Obs	W	V	z	Prob>z
ctxmeanchange	10	0.83212	2.587	1.806	0.03549



. sktest boctx if menopausal ==1

Skewness/Kurtosis tests for Normality					
Variable	Obs	Pr(Skewness)	Pr(Kurtosis)	adj chi2(2)	joint Prob>chi2
boctx	23	0.0011	0.0077	13.40	0.0012

. swilk boctx if menopausal ==1

Shapiro-wilk w test for normal data					
Variable	Obs	W	V	z	Prob>z
boctx	23	0.80825	5.016	3.279	0.00052

. sktest ctx12m if menopausal ==1

Skewness/Kurtosis tests for Normality					
Variable	Obs	Pr(Skewness)	Pr(Kurtosis)	adj chi2(2)	joint Prob>chi2
ctx12m	22	0.0423	0.1727	5.66	0.0589

. swilk ctx12m if menopausal ==1

Shapiro-wilk w test for normal data					
Variable	Obs	W	V	z	Prob>z
ctx12m	22	0.93224	1.717	1.096	0.13663

. sktest ctxc12m if menopausal ==1

Skewness/Kurtosis tests for Normality					
Variable	Obs	Pr(Skewness)	Pr(Kurtosis)	adj chi2(2)	joint Prob>chi2
ctxc12m	20	0.6559	0.8972	0.22	0.8980

. swilk ctxc12m if menopausal ==1

Shapiro-wilk w test for normal data					
Variable	Obs	W	V	z	Prob>z
ctxc12m	20	0.96645	0.794	-0.465	0.67896

. sktest ctxpr12m if menopausal ==1

Skewness/Kurtosis tests for Normality					
Variable	Obs	Pr(Skewness)	Pr(Kurtosis)	adj chi2(2)	joint Prob>chi2
ctxpr12m	20	0.0116	0.2988	6.68	0.0354

. swilk ctxpr12m if menopausal ==1

Shapiro-wilk w test for normal data					
Variable	Obs	W	V	z	Prob>z
ctxpr12m	20	0.80583	4.596	3.074	0.00106

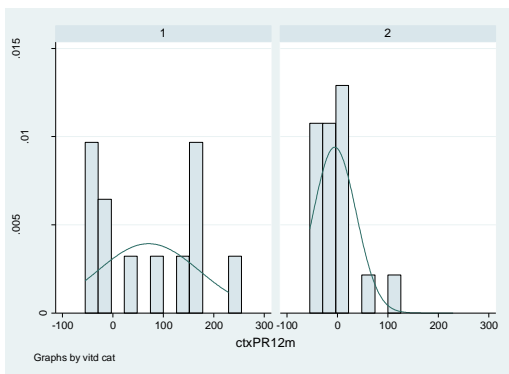
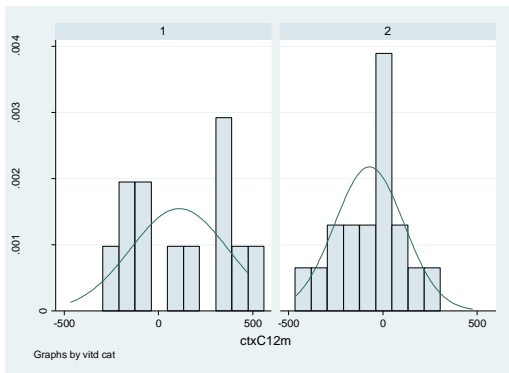
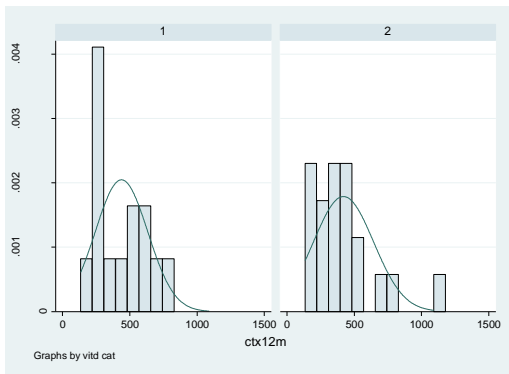
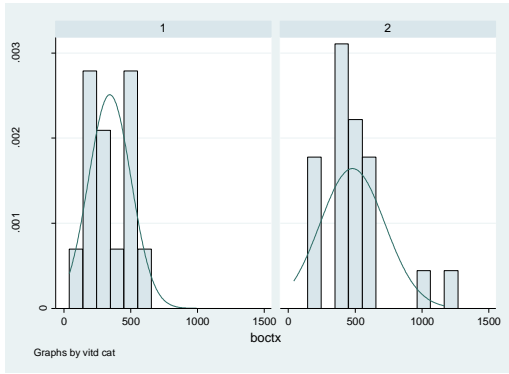
. sktest ctxmeanchange if menopausal ==1

Skewness/Kurtosis tests for Normality					
Variable	Obs	Pr(Skewness)	Pr(Kurtosis)	adj chi2(2)	joint Prob>chi2
ctxmeancha~e	20	0.0121	0.2193	6.92	0.0314

. swilk ctxmeanchange if menopausal ==1

Shapiro-wilk w test for normal data					
Variable	Obs	W	V	z	Prob>z
ctxmeancha~e	20	0.84265	3.725	2.650	0.00402

- By vitamin D category



. sktest boctx if vitdcat ==1

Skewness/Kurtosis tests for Normality

Variable	Obs	Pr(Skewness)	Pr(Kurtosis)	adj	chi2(2)	joint	Prob>chi2
boctx	14	0.9697	0.7319		0.12		0.9423

. swilk boctx if vitdcat ==1

Shapiro-Wilk W test for normal data

Variable	Obs	W	V	z	Prob>z
boctx	14	0.95211	0.886	-0.237	0.59384

. sktest ctx12m if vitdcat ==1

Skewness/Kurtosis tests for Normality

Variable	Obs	Pr(Skewness)	Pr(Kurtosis)	adj	chi2(2)	joint	Prob>chi2
ctx12m	14	0.6794	0.1487		2.63		0.2681

. swilk ctx12m if vitdcat ==1

Shapiro-Wilk W test for normal data

Variable	Obs	W	V	z	Prob>z
ctx12m	14	0.92876	1.318	0.544	0.29314

. sktest ctxc12m if vitdcat ==1

Skewness/Kurtosis tests for Normality

Variable	Obs	Pr(Skewness)	Pr(Kurtosis)	adj	chi2(2)	joint	Prob>chi2
ctxc12m	12	0.9070	0.0708		3.73		0.1548

. swilk ctxc12m if vitdcat ==1

Shapiro-Wilk W test for normal data

Variable	Obs	W	V	z	Prob>z
ctxc12m	12	0.91550	1.412	0.672	0.25082

. sktest ctxpr12m if vitdcat ==1

Skewness/Kurtosis tests for Normality

Variable	Obs	Pr(Skewness)	Pr(Kurtosis)	adj	chi2(2)	joint	Prob>chi2
ctxpr12m	12	0.7165	0.0354		4.65		0.0978

. swilk ctxpr12m if vitdcat ==1

Shapiro-Wilk W test for normal data

Variable	Obs	W	V	z	Prob>z
ctxpr12m	12	0.87360	2.112	1.457	0.07261

. sktest boctx if vitdcat ==2

Skewness/Kurtosis tests for Normality					
Variable	Obs	Pr(Skewness)	Pr(Kurtosis)	adj chi2(2)	joint Prob>chi2
boctx	22	0.0107	0.0333	9.10	0.0105

. swilk boctx if vitdcat ==2

Shapiro-Wilk W test for normal data					
Variable	Obs	W	V	z	Prob>z
boctx	22	0.85939	3.562	2.576	0.00500

. sktest ctx12m if vitdcat ==2

Skewness/Kurtosis tests for Normality					
Variable	Obs	Pr(Skewness)	Pr(Kurtosis)	adj chi2(2)	joint Prob>chi2
ctx12m	20	0.0035	0.0204	10.92	0.0043

. swilk ctx12m if vitdcat ==2

Shapiro-Wilk W test for normal data					
Variable	Obs	W	V	z	Prob>z
ctx12m	20	0.85394	3.457	2.500	0.00621

. sktest ctxc12m if vitdcat ==2

Skewness/Kurtosis tests for Normality					
Variable	Obs	Pr(Skewness)	Pr(Kurtosis)	adj chi2(2)	joint Prob>chi2
ctxc12m	18	0.4166	0.6884	0.89	0.6417

. swilk ctxc12m if vitdcat ==2

Shapiro-Wilk W test for normal data					
Variable	Obs	W	V	z	Prob>z
ctxc12m	18	0.96981	0.664	-0.821	0.79412

. sktest ctxpr12m if vitdcat ==2

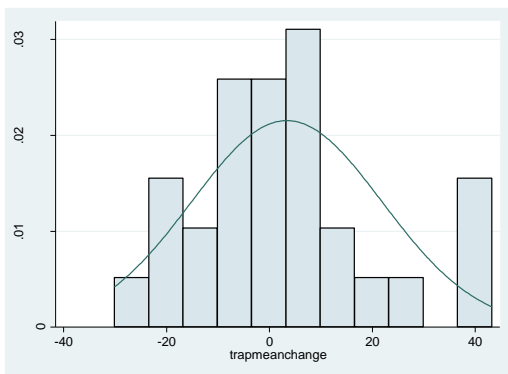
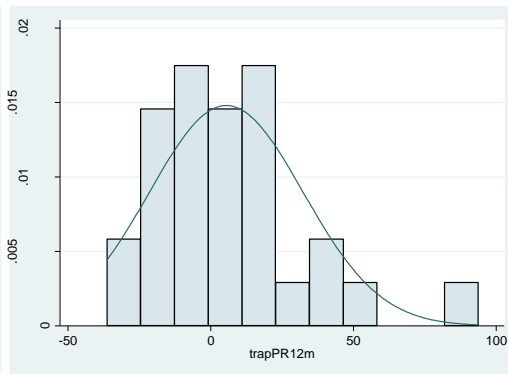
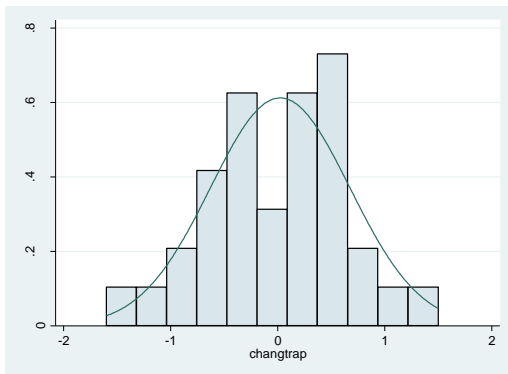
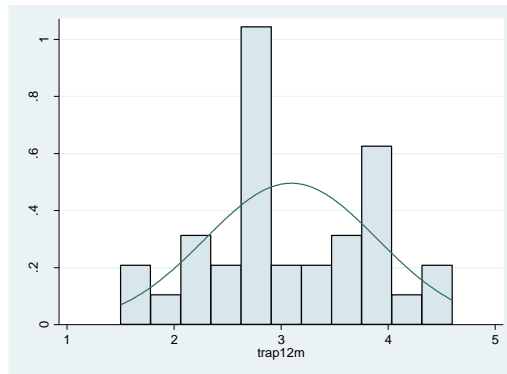
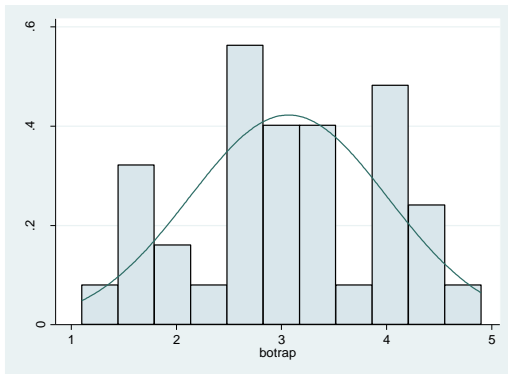
Skewness/Kurtosis tests for Normality					
Variable	Obs	Pr(Skewness)	Pr(Kurtosis)	adj chi2(2)	joint Prob>chi2
ctxpr12m	18	0.0046	0.0111	11.20	0.0037

. swilk ctxpr12m if vitdcat ==2

Shapiro-Wilk W test for normal data					
Variable	Obs	W	V	z	Prob>z
ctxpr12m	18	0.86049	3.067	2.243	0.01245

# TRAP

- All



. sktest botrap

Skewness/Kurtosis tests for Normality					
Variable	Obs	Pr(Skewness)	Pr(Kurtosis)	adj chi2(2)	joint Prob>chi2
botrap	36	0.7475	0.3184	1.16	0.5592

. swilk botrap

Shapiro-wilk w test for normal data					
Variable	Obs	W	V	z	Prob>z
botrap	36	0.97743	0.823	-0.407	0.65803

. sktest trap12m

Skewness/Kurtosis tests for Normality					
Variable	Obs	Pr(Skewness)	Pr(Kurtosis)	adj chi2(2)	joint Prob>chi2
trap12m	34	0.9499	0.5316	0.40	0.8171

. swilk trap12m

Shapiro-wilk w test for normal data					
Variable	Obs	W	V	z	Prob>z
trap12m	34	0.98591	0.492	-1.478	0.93036

. sktest trapc12m

Skewness/Kurtosis tests for Normality					
Variable	Obs	Pr(Skewness)	Pr(Kurtosis)	adj chi2(2)	joint Prob>chi2
trapc12m	29	0.6143	0.6668	0.45	0.7976

. swilk trapc12m

Shapiro-wilk w test for normal data					
Variable	Obs	W	V	z	Prob>z
trapc12m	29	0.98651	0.418	-1.800	0.96404

. sktest trappr12m

Skewness/Kurtosis tests for Normality					
Variable	Obs	Pr(Skewness)	Pr(Kurtosis)	adj chi2(2)	joint Prob>chi2
trappr12m	29	0.0071	0.0215	10.18	0.0062

. swilk trappr12m

Shapiro-wilk w test for normal data					
Variable	Obs	W	V	z	Prob>z
trappr12m	29	0.91718	2.567	1.945	0.02588

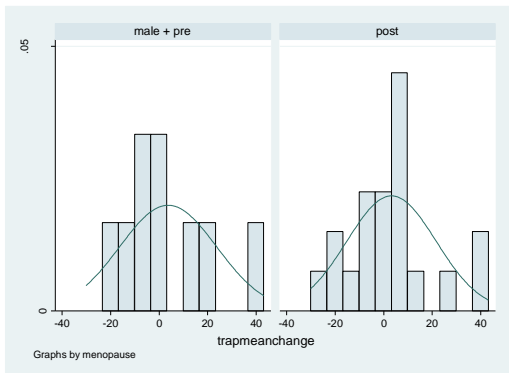
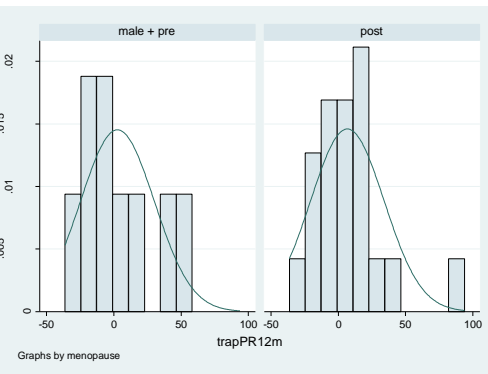
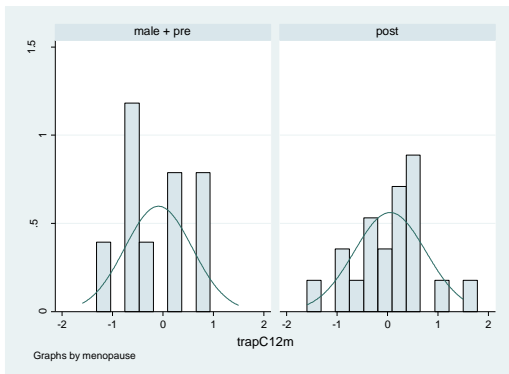
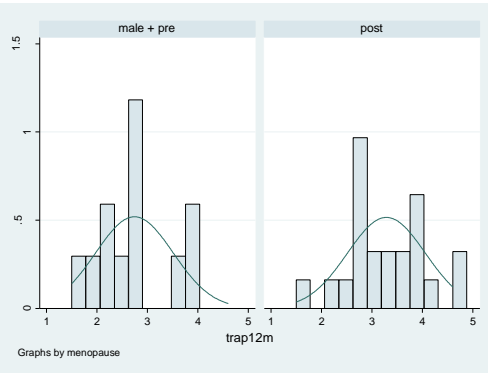
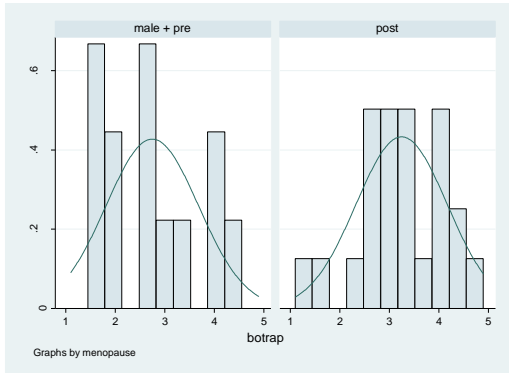
. sktest trapmeanchange

Skewness/Kurtosis tests for Normality					
Variable	Obs	Pr(Skewness)	Pr(Kurtosis)	adj chi2(2)	joint Prob>chi2
trapmeanch~e	29	0.1060	0.5625	3.24	0.1978

. swilk trapmeanchange

Shapiro-wilk w test for normal data					
Variable	Obs	W	V	z	Prob>z
trapmeanch~e	29	0.94046	1.845	1.264	0.10312

- **By gender and menopausal status**



. sktest botrap if menopausal ==0

Skewness/Kurtosis tests for Normality					
Variable	Obs	Pr(Skewness)	Pr(Kurtosis)	adj chi2(2)	joint Prob>chi2
botrap	13	0.5679	0.2707	1.77	0.4135

. swilk botrap if menopausal ==0

Shapiro-Wilk w test for normal data					
Variable	Obs	W	V	z	Prob>z
botrap	13	0.94582	0.954	-0.092	0.53650

. sktest trap12m if menopausal ==0

Skewness/Kurtosis tests for Normality					
Variable	Obs	Pr(Skewness)	Pr(Kurtosis)	adj chi2(2)	joint Prob>chi2
trap12m	12	0.5791	0.5901	0.63	0.7288

. swilk trap12m if menopausal ==0

Shapiro-Wilk w test for normal data					
Variable	Obs	W	V	z	Prob>z
trap12m	12	0.94421	0.932	-0.137	0.55452

. sktest trapc12m if menopausal ==0

Skewness/Kurtosis tests for Normality					
Variable	Obs	Pr(Skewness)	Pr(Kurtosis)	adj chi2(2)	joint Prob>chi2
trapc12m	9	0.9421	0.7015	0.15	0.9267

. swilk trapc12m if menopausal ==0

Shapiro-Wilk w test for normal data					
Variable	Obs	W	V	z	Prob>z
trapc12m	9	0.93222	0.996	-0.007	0.50279

. sktest trappr12m if menopausal ==0

Skewness/Kurtosis tests for Normality					
Variable	Obs	Pr(Skewness)	Pr(Kurtosis)	adj chi2(2)	joint Prob>chi2
trappr12m	9	0.4335	0.4379	1.38	0.5007

. swilk trappr12m if menopausal ==0

Shapiro-Wilk w test for normal data					
Variable	Obs	W	V	z	Prob>z
trappr12m	9	0.93021	1.025	0.042	0.48335

. sktest trapmeanchange if menopausal ==0

Skewness/Kurtosis tests for Normality					
Variable	Obs	Pr(Skewness)	Pr(Kurtosis)	adj chi2(2)	joint Prob>chi2
trapmeanch~e	9	0.2146	0.6038	2.15	0.3417

. swilk trapmeanchange if menopausal ==0

Shapiro-Wilk w test for normal data					
Variable	Obs	W	V	z	Prob>z
trapmeanch~e	9	0.93230	0.995	-0.009	0.50359



. sktest botrap if menopausal ==1

Skewness/Kurtosis tests for Normality					
Variable	Obs	Pr(Skewness)	Pr(Kurtosis)	adj chi2(2)	joint Prob>chi2
botrap	23	0.4122	0.7114	0.86	0.6489

. swilk botrap if menopausal ==1

Shapiro-wilk w test for normal data					
Variable	Obs	W	V	z	Prob>z
botrap	23	0.96980	0.790	-0.479	0.64814

. sktest trap12m if menopausal ==1

Skewness/Kurtosis tests for Normality					
Variable	Obs	Pr(Skewness)	Pr(Kurtosis)	adj chi2(2)	joint Prob>chi2
trap12m	22	0.7996	0.8145	0.12	0.9420

. swilk trap12m if menopausal ==1

Shapiro-wilk w test for normal data					
Variable	Obs	W	V	z	Prob>z
trap12m	22	0.96729	0.829	-0.381	0.64843

. sktest trapc12m if menopausal ==1

Skewness/Kurtosis tests for Normality					
Variable	Obs	Pr(Skewness)	Pr(Kurtosis)	adj chi2(2)	joint Prob>chi2
trapc12m	20	0.5289	0.3759	1.30	0.5233

. swilk trapc12m if menopausal ==1

Shapiro-wilk w test for normal data					
Variable	Obs	W	V	z	Prob>z
trapc12m	20	0.96961	0.719	-0.664	0.74651

. sktest trappr12m if menopausal ==1

Skewness/Kurtosis tests for Normality					
Variable	Obs	Pr(Skewness)	Pr(Kurtosis)	adj chi2(2)	joint Prob>chi2
trappr12m	20	0.0039	0.0060	12.14	0.0023

. swilk trappr12m if menopausal ==1

Shapiro-wilk w test for normal data					
Variable	Obs	W	V	z	Prob>z
trappr12m	20	0.86749	3.137	2.304	0.01062

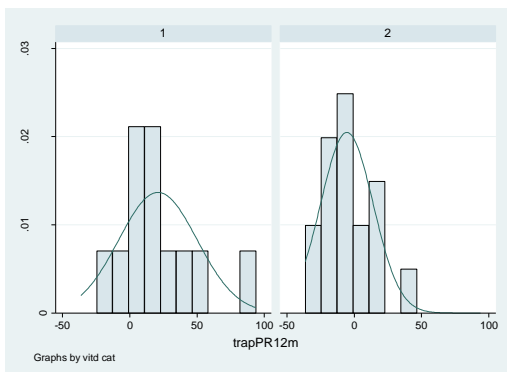
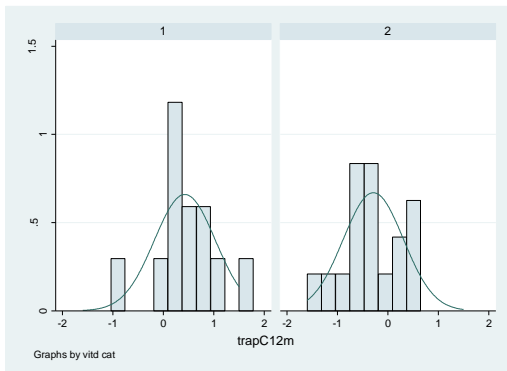
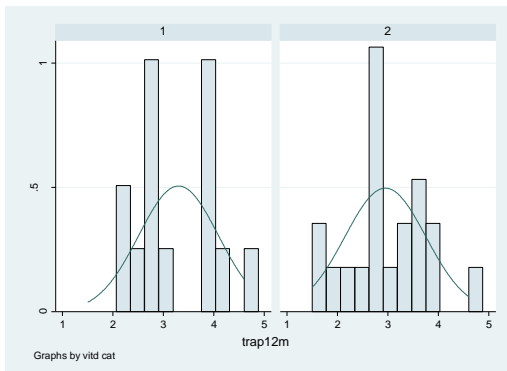
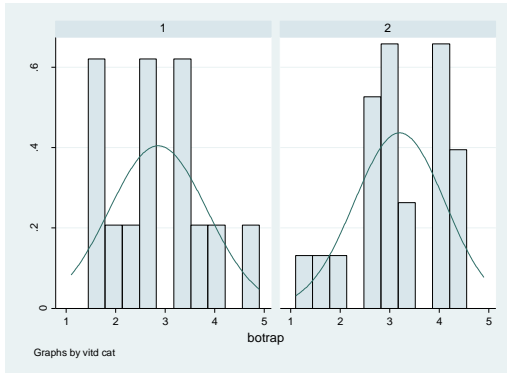
. sktest trapmeanchange if menopausal ==1

Skewness/Kurtosis tests for Normality					
Variable	Obs	Pr(Skewness)	Pr(Kurtosis)	adj chi2(2)	joint Prob>chi2
trapmeanch~e	20	0.1790	0.3771	2.93	0.2311

. swilk trapmeanchange if menopausal ==1

Shapiro-wilk w test for normal data					
Variable	Obs	W	V	z	Prob>z
trapmeanch~e	20	0.93424	1.557	0.892	0.18626

## - By vitamin D category



. sktest botrap if vitdcat ==1

Skewness/Kurtosis tests for Normality					
Variable	Obs	Pr(Skewness)	Pr(Kurtosis)	adj chi2(2)	joint Prob>chi2
botrap	14	0.3201	0.9727	1.10	0.5782

. swilk botrap if vitdcat ==1

Shapiro-Wilk W test for normal data					
Variable	Obs	W	V	z	Prob>z
botrap	14	0.95053	0.916	-0.174	0.56898

. sktest trap12m if vitdcat ==1

Skewness/Kurtosis tests for Normality					
Variable	Obs	Pr(Skewness)	Pr(Kurtosis)	adj chi2(2)	joint Prob>chi2
trap12m	14	0.7268	0.0845	3.58	0.1673

. swilk trap12m if vitdcat ==1

Shapiro-Wilk W test for normal data					
Variable	Obs	W	V	z	Prob>z
trap12m	14	0.92034	1.474	0.764	0.22240

. sktest trapc12m if vitdcat ==1

Skewness/Kurtosis tests for Normality					
Variable	Obs	Pr(Skewness)	Pr(Kurtosis)	adj chi2(2)	joint Prob>chi2
trapc12m	12	0.5020	0.2011	2.46	0.2929

. swilk trapc12m if vitdcat ==1

Shapiro-Wilk W test for normal data					
Variable	Obs	W	V	z	Prob>z
trapc12m	12	0.94469	0.924	-0.154	0.56115

. sktest trappr12m if vitdcat ==1

Skewness/Kurtosis tests for Normality					
Variable	Obs	Pr(Skewness)	Pr(Kurtosis)	adj chi2(2)	joint Prob>chi2
trappr12m	12	0.0282	0.0605	7.13	0.0283

. swilk trappr12m if vitdcat ==1

Shapiro-Wilk W test for normal data					
Variable	Obs	W	V	z	Prob>z
trappr12m	12	0.86397	2.273	1.600	0.05483

. sktest botrap if vitdcat ==2

Skewness/Kurtosis tests for Normality					
Variable	Obs	Pr(Skewness)	Pr(Kurtosis)	adj chi2(2)	joint Prob>chi2
botrap	22	0.2232	0.8725	1.66	0.4353

. swilk botrap if vitdcat ==2

Shapiro-Wilk W test for normal data					
Variable	Obs	W	V	z	Prob>z
botrap	22	0.92299	1.951	1.355	0.08770

. sktest trap12m if vitdcat ==2

Skewness/Kurtosis tests for Normality					
Variable	Obs	Pr(Skewness)	Pr(Kurtosis)	adj chi2(2)	joint Prob>chi2
trap12m	20	0.9126	0.9418	0.02	0.9914

. swilk trap12m if vitdcat ==2

Shapiro-Wilk W test for normal data					
Variable	Obs	W	V	z	Prob>z
trap12m	20	0.98009	0.471	-1.516	0.93522

. sktest trapc12m if vitdcat ==2

Skewness/Kurtosis tests for Normality					
Variable	Obs	Pr(Skewness)	Pr(Kurtosis)	adj chi2(2)	joint Prob>chi2
trapc12m	17	0.3772	0.7539	0.96	0.6201

. swilk trapc12m if vitdcat ==2

Shapiro-Wilk W test for normal data					
Variable	Obs	W	V	z	Prob>z
trapc12m	17	0.96426	0.755	-0.561	0.71244

. sktest trappr12m if vitdcat ==2

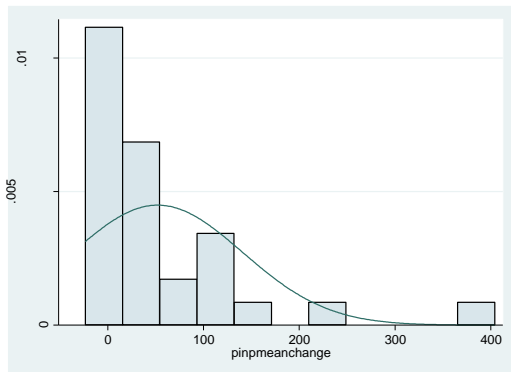
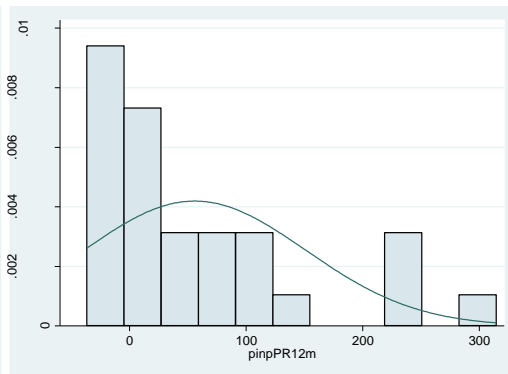
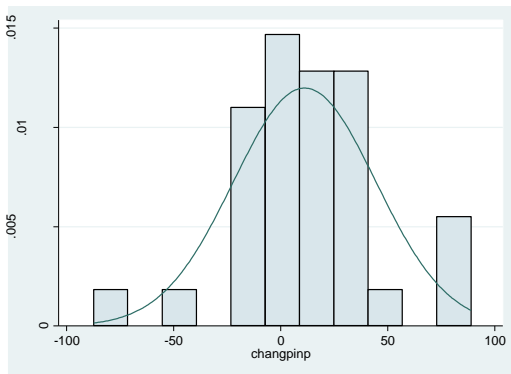
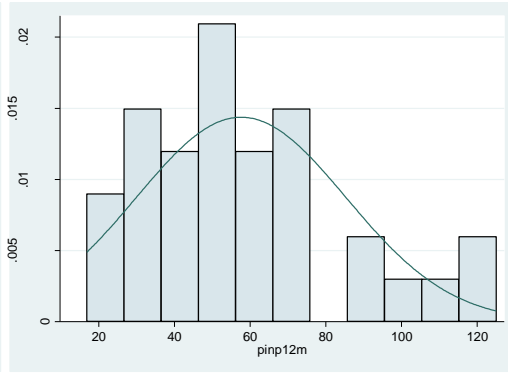
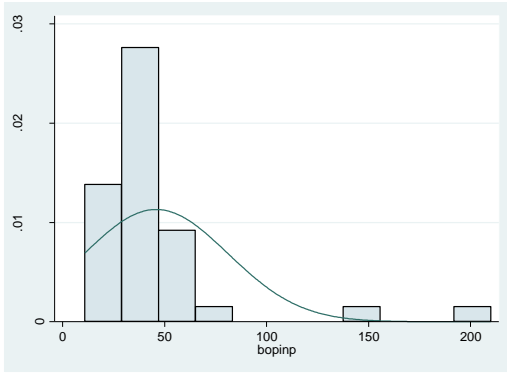
Skewness/Kurtosis tests for Normality					
Variable	Obs	Pr(Skewness)	Pr(Kurtosis)	adj chi2(2)	joint Prob>chi2
trappr12m	17	0.2861	0.9405	1.27	0.5312

. swilk trappr12m if vitdcat ==2

Shapiro-Wilk W test for normal data					
Variable	Obs	W	V	z	Prob>z
trappr12m	17	0.96248	0.793	-0.463	0.67841

# PINP

- All



. sktest bopin

Skewness/Kurtosis tests for Normality					
Variable	Obs	Pr(Skewness)	Pr(Kurtosis)	adj chi2(2)	joint Prob>chi2
bopin	36	0.0000	0.0000	36.57	0.0000

. swilk bopin

Shapiro-wilk w test for normal data					
Variable	Obs	W	V	z	Prob>z
bopin	36	0.58280	15.213	5.692	0.00000

. sktest pinp12m

Skewness/Kurtosis tests for Normality					
Variable	Obs	Pr(Skewness)	Pr(Kurtosis)	adj chi2(2)	joint Prob>chi2
pinp12m	34	0.0240	0.4607	5.41	0.0668

. swilk pinp12m

Shapiro-wilk w test for normal data					
Variable	Obs	W	V	z	Prob>z
pinp12m	34	0.92111	2.755	2.111	0.01737

. sktest pinpc12m

Skewness/Kurtosis tests for Normality					
Variable	Obs	Pr(Skewness)	Pr(Kurtosis)	adj chi2(2)	joint Prob>chi2
pinpc12m	30	0.1176	0.2019	4.24	0.1199

. swilk pinpc12m

Shapiro-wilk w test for normal data					
Variable	Obs	W	V	z	Prob>z
pinpc12m	30	0.93596	2.036	1.470	0.07081

. sktest pinppr12m

Skewness/Kurtosis tests for Normality					
Variable	Obs	Pr(Skewness)	Pr(Kurtosis)	adj chi2(2)	joint Prob>chi2
pinppr12m	30	0.0041	0.1933	8.45	0.0146

. swilk pinppr12m

Shapiro-wilk w test for normal data					
Variable	Obs	W	V	z	Prob>z
pinppr12m	30	0.83141	5.359	3.471	0.00026

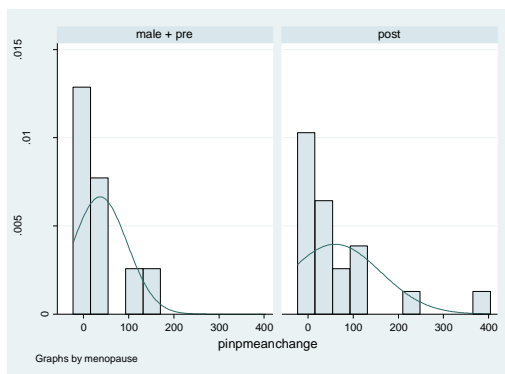
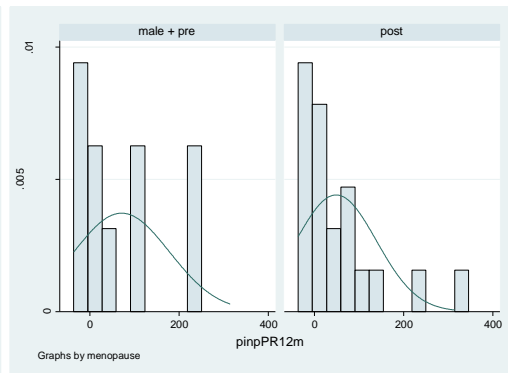
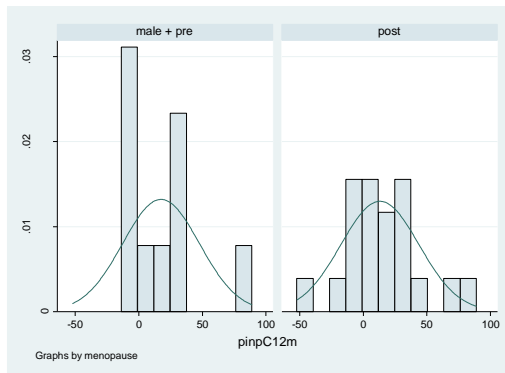
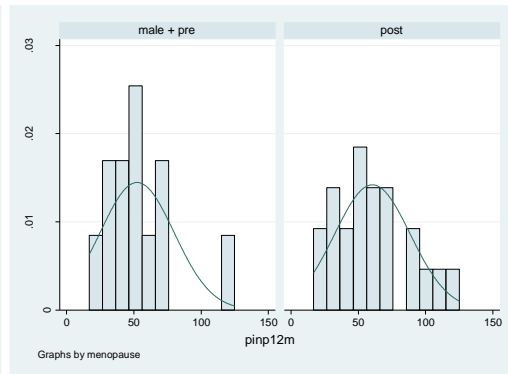
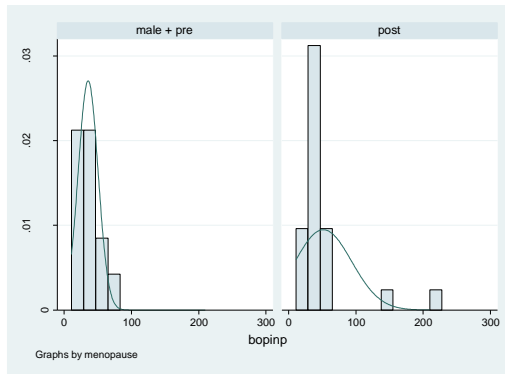
. sktest pinpmeanchange

Skewness/Kurtosis tests for Normality					
Variable	Obs	Pr(Skewness)	Pr(Kurtosis)	adj chi2(2)	joint Prob>chi2
pinpmeanchange~e	30	0.0000	0.0002	23.52	0.0000

. swilk pinpmeanchange

Shapiro-wilk w test for normal data					
Variable	Obs	W	V	z	Prob>z
pinpmeanchange~e	30	0.73171	8.528	4.432	0.00000

- By gender and menopausal status



. sktest bopinp if menopausal ==0

Skewness/Kurtosis tests for Normality					
Variable	Obs	Pr(Skewness)	Pr(Kurtosis)	adj chi2(2)	joint Prob>chi2
bopinp	13	0.3415	0.4703	1.63	0.4431

. swilk bopinp if menopausal ==0

Shapiro-wilk W test for normal data					
Variable	Obs	W	V	z	Prob>z
bopinp	13	0.96516	0.614	-0.957	0.83068

. sktest pinp12m if menopausal ==0

Skewness/Kurtosis tests for Normality					
Variable	Obs	Pr(Skewness)	Pr(Kurtosis)	adj chi2(2)	joint Prob>chi2
pinp12m	12	0.0115	0.0195	9.27	0.0097

. swilk pinp12m if menopausal ==0

Shapiro-wilk W test for normal data					
Variable	Obs	W	V	z	Prob>z
pinp12m	12	0.86295	2.290	1.614	0.05323

. sktest pinpc12m if menopausal ==0

Skewness/Kurtosis tests for Normality					
Variable	Obs	Pr(Skewness)	Pr(Kurtosis)	adj chi2(2)	joint Prob>chi2
pinpc12m	10	0.0278	0.0666	6.94	0.0312

. swilk pinpc12m if menopausal ==0

Shapiro-wilk W test for normal data					
Variable	Obs	W	V	z	Prob>z
pinpc12m	10	0.82375	2.716	1.909	0.02813

. sktest pinppr12m if menopausal ==0

Skewness/Kurtosis tests for Normality					
Variable	Obs	Pr(Skewness)	Pr(Kurtosis)	adj chi2(2)	joint Prob>chi2
pinppr12m	10	0.1918	0.6961	2.20	0.3334

. swilk pinppr12m if menopausal ==0

Shapiro-wilk W test for normal data					
Variable	Obs	W	V	z	Prob>z
pinppr12m	10	0.83524	2.539	1.766	0.03869

. sktest pinpmeanchange if menopausal ==0

Skewness/Kurtosis tests for Normality					
Variable	Obs	Pr(Skewness)	Pr(Kurtosis)	adj chi2(2)	joint Prob>chi2
pinpmeanch~e	10	0.0503	0.4042	4.61	0.0998

. swilk pinpmeanchange if menopausal ==0

Shapiro-wilk W test for normal data					
Variable	Obs	W	V	z	Prob>z
pinpmeanch~e	10	0.81887	2.791	1.968	0.02456



. sktest bopinp if menopausal ==1

Skewness/Kurtosis tests for Normality

Variable	Obs	Pr(Skewness)	Pr(Kurtosis)	adj chi2(2)	joint Prob>chi2
bopinp	23	0.0000	0.0001	24.58	0.0000

. swilk bopinp if menopausal ==1

Shapiro-wilk w test for normal data

Variable	Obs	W	V	z	Prob>z
bopinp	23	0.57850	11.025	4.881	0.00000

. sktest pinp12m if menopausal ==1

Skewness/Kurtosis tests for Normality

Variable	Obs	Pr(Skewness)	Pr(Kurtosis)	adj chi2(2)	joint Prob>chi2
pinp12m	22	0.1508	0.9631	2.30	0.3161

. swilk pinp12m if menopausal ==1

Shapiro-wilk w test for normal data

Variable	Obs	W	V	z	Prob>z
pinp12m	22	0.94326	1.437	0.736	0.23097

. sktest pinpc12m if menopausal ==1

Skewness/Kurtosis tests for Normality

Variable	Obs	Pr(Skewness)	Pr(Kurtosis)	adj chi2(2)	joint Prob>chi2
pinpc12m	20	0.4384	0.3280	1.73	0.4210

. swilk pinpc12m if menopausal ==1

Shapiro-wilk w test for normal data

Variable	Obs	W	V	z	Prob>z
pinpc12m	20	0.95714	1.014	0.029	0.48849

. sktest pinppr12m if menopausal ==1

Skewness/Kurtosis tests for Normality

Variable	Obs	Pr(Skewness)	Pr(Kurtosis)	adj chi2(2)	joint Prob>chi2
pinppr12m	20	0.0022	0.0232	11.33	0.0035

. swilk pinppr12m if menopausal ==1

Shapiro-wilk w test for normal data

Variable	Obs	W	V	z	Prob>z
pinppr12m	20	0.81195	4.451	3.009	0.00131

. sktest pinpmeanch~e if menopausal ==1

Skewness/Kurtosis tests for Normality

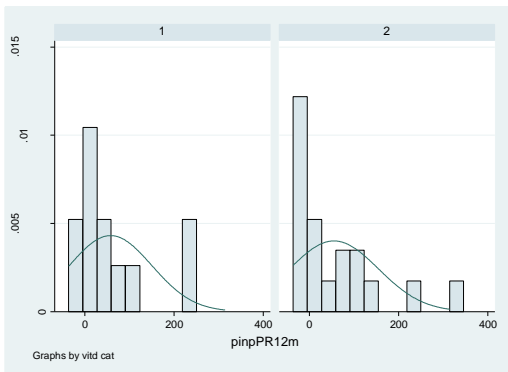
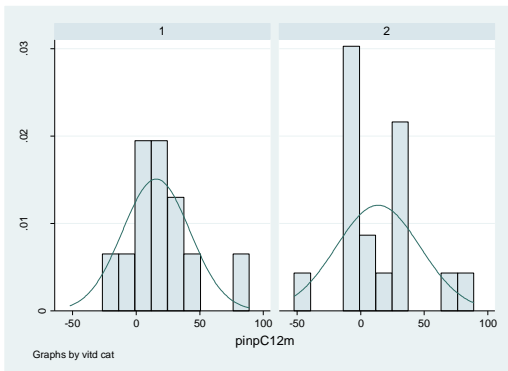
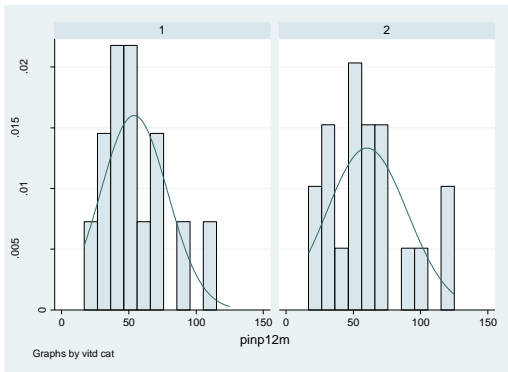
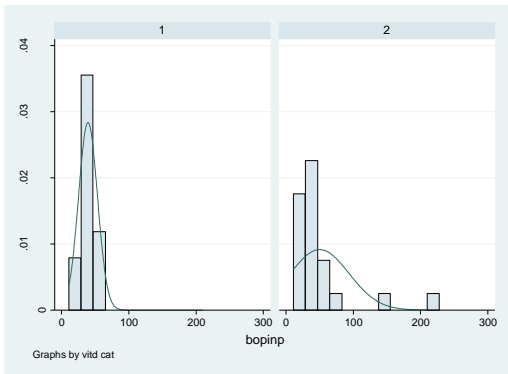
Variable	Obs	Pr(Skewness)	Pr(Kurtosis)	adj chi2(2)	joint Prob>chi2
pinpmeanch~e	20	0.0001	0.0010	18.19	0.0001

. swilk pinpmeanch~e if menopausal ==1

Shapiro-wilk w test for normal data

Variable	Obs	W	V	z	Prob>z
pinpmeanch~e	20	0.71890	6.654	3.819	0.00007

- By vitamin D category



. sktest bopinp if vitdcat ==1

Skewness/Kurtosis tests for Normality					
Variable	Obs	Pr(Skewness)	Pr(Kurtosis)	adj chi2(2)	joint Prob>chi2
bopinp	14	0.6651	0.7566	0.28	0.8678

. swilk bopinp if vitdcat ==1

Shapiro-Wilk W test for normal data					
Variable	Obs	W	V	z	Prob>z
bopinp	14	0.97006	0.554	-1.162	0.87740

. sktest pinp12m if vitdcat ==1

Skewness/Kurtosis tests for Normality					
Variable	Obs	Pr(Skewness)	Pr(Kurtosis)	adj chi2(2)	joint Prob>chi2
pinp12m	14	0.0686	0.3528	4.38	0.1117

. swilk pinp12m if vitdcat ==1

Shapiro-Wilk W test for normal data					
Variable	Obs	W	V	z	Prob>z
pinp12m	14	0.91100	1.647	0.982	0.16293

. sktest pinpc12m if vitdcat ==1

Skewness/Kurtosis tests for Normality					
Variable	Obs	Pr(Skewness)	Pr(Kurtosis)	adj chi2(2)	joint Prob>chi2
pinpc12m	12	0.0892	0.1850	4.71	0.0947

. swilk pinpc12m if vitdcat ==1

Shapiro-Wilk W test for normal data					
Variable	Obs	W	V	z	Prob>z
pinpc12m	12	0.92735	1.214	0.378	0.35286

. sktest pinppr12m if vitdcat ==1

Skewness/Kurtosis tests for Normality					
Variable	Obs	Pr(Skewness)	Pr(Kurtosis)	adj chi2(2)	joint Prob>chi2
pinppr12m	12	0.0361	0.3802	5.07	0.0793

. swilk pinppr12m if vitdcat ==1

Shapiro-Wilk W test for normal data					
Variable	Obs	W	V	z	Prob>z
pinppr12m	12	0.81579	3.078	2.190	0.01424

. sktest bopinp if vitdcat ==2

Skewness/Kurtosis tests for Normality					
Variable	Obs	Pr(Skewness)	Pr(Kurtosis)	adj chi2(2)	joint Prob>chi2
bopinp	22	0.0000	0.0002	23.26	0.0000

. swilk bopinp if vitdcat ==2

Shapiro-Wilk W test for normal data					
Variable	Obs	W	V	z	Prob>z
bopinp	22	0.57007	10.892	4.842	0.00000

. sktest pinp12m if vitdcat ==2

Skewness/Kurtosis tests for Normality					
Variable	Obs	Pr(Skewness)	Pr(Kurtosis)	adj chi2(2)	joint Prob>chi2
pinp12m	20	0.0903	0.5717	3.59	0.1657

. swilk pinp12m if vitdcat ==2

Shapiro-Wilk W test for normal data					
Variable	Obs	W	V	z	Prob>z
pinp12m	20	0.92885	1.684	1.051	0.14673

. sktest pinpc12m if vitdcat ==2

Skewness/Kurtosis tests for Normality					
Variable	Obs	Pr(Skewness)	Pr(Kurtosis)	adj chi2(2)	joint Prob>chi2
pinpc12m	18	0.2553	0.2482	3.01	0.2220

. swilk pinpc12m if vitdcat ==2

Shapiro-Wilk W test for normal data					
Variable	Obs	W	V	z	Prob>z
pinpc12m	18	0.92607	1.625	0.972	0.16558

. sktest pinppr12m if vitdcat ==2

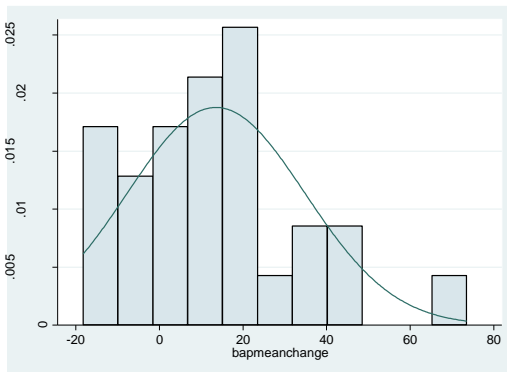
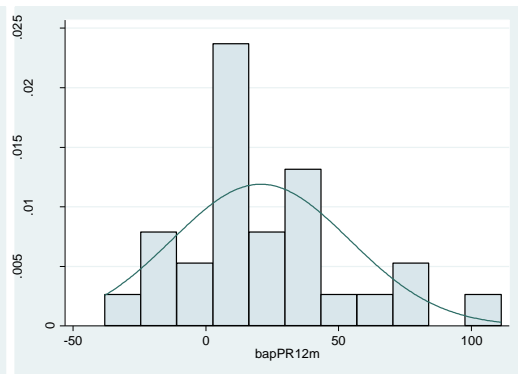
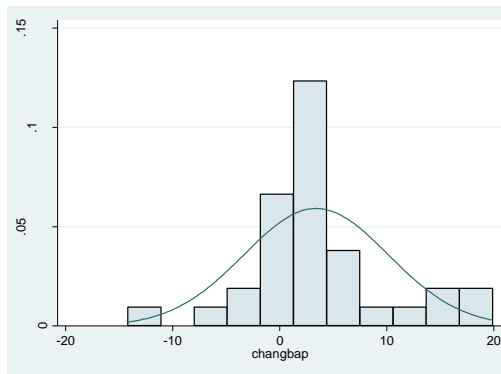
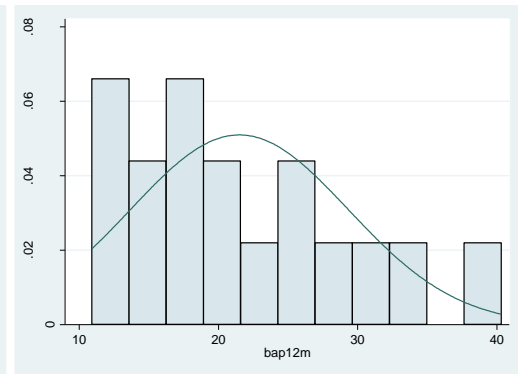
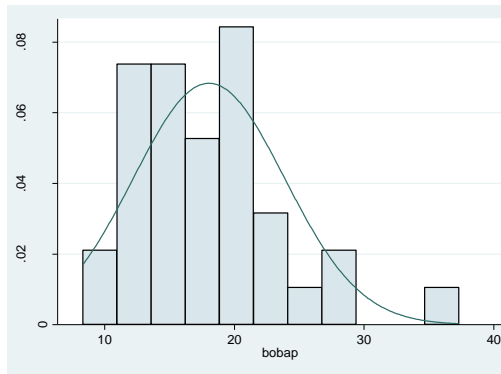
Skewness/Kurtosis tests for Normality					
Variable	Obs	Pr(Skewness)	Pr(Kurtosis)	adj chi2(2)	joint Prob>chi2
pinppr12m	18	0.0109	0.1248	7.60	0.0224

. swilk pinppr12m if vitdcat ==2

Shapiro-Wilk W test for normal data					
Variable	Obs	W	V	z	Prob>z
pinppr12m	18	0.82603	3.824	2.685	0.00363

# BALP

- All



. sktest bobap

Skewness/Kurtosis tests for Normality					
Variable	Obs	Pr(Skewness)	Pr(Kurtosis)	adj chi2(2)	joint Prob>chi2
bobap	36	0.0065	0.0345	9.82	0.0074

. swilk bobap

Shapiro-wilk w test for normal data					
Variable	Obs	W	V	z	Prob>z
bobap	36	0.93330	2.432	1.859	0.03154

. sktest bap12m

Skewness/Kurtosis tests for Normality					
Variable	Obs	Pr(Skewness)	Pr(Kurtosis)	adj chi2(2)	joint Prob>chi2
bap12m	34	0.0744	0.8943	3.48	0.1755

. swilk bap12m

Shapiro-wilk w test for normal data					
Variable	Obs	W	V	z	Prob>z
bap12m	34	0.93746	2.184	1.627	0.05184

. sktest bapc12m

Skewness/Kurtosis tests for Normality					
Variable	Obs	Pr(Skewness)	Pr(Kurtosis)	adj chi2(2)	joint Prob>chi2
bapc12m	28	0.3192	0.0854	4.15	0.1256

. swilk bapc12m

Shapiro-wilk w test for normal data					
Variable	Obs	W	V	z	Prob>z
bapc12m	28	0.91472	2.575	1.947	0.02574

. sktest bappr12m

Skewness/Kurtosis tests for Normality					
Variable	Obs	Pr(Skewness)	Pr(Kurtosis)	adj chi2(2)	joint Prob>chi2
bappr12m	28	0.0412	0.1890	5.60	0.0609

. swilk bappr12m

Shapiro-wilk w test for normal data					
Variable	Obs	W	V	z	Prob>z
bappr12m	28	0.93201	2.053	1.481	0.06931

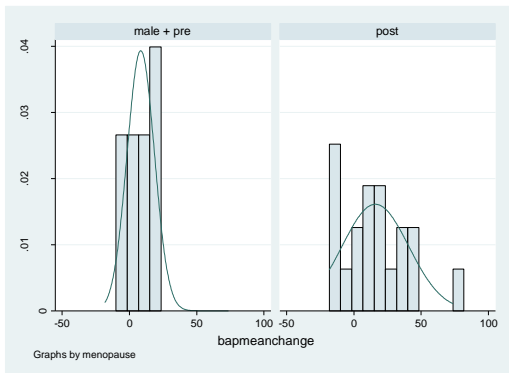
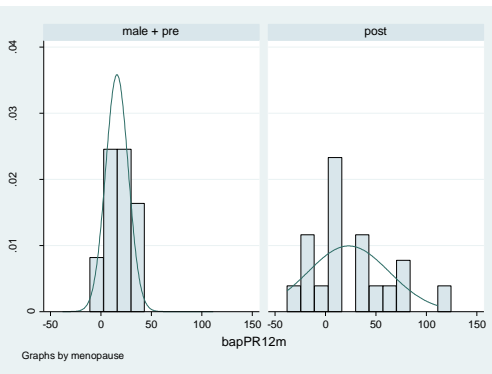
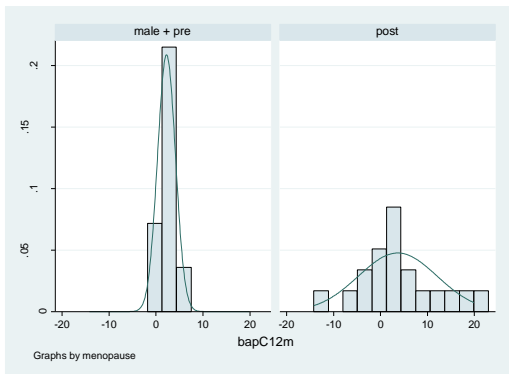
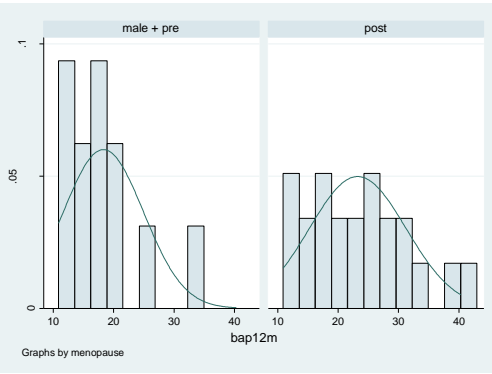
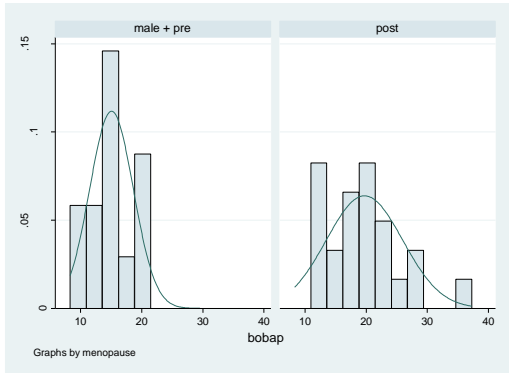
. sktest bapmeanchange

Skewness/Kurtosis tests for Normality					
Variable	Obs	Pr(Skewness)	Pr(Kurtosis)	adj chi2(2)	joint Prob>chi2
bapmeanchange	28	0.0821	0.2294	4.54	0.1031

. swilk bapmeanchange

Shapiro-wilk w test for normal data					
Variable	Obs	W	V	z	Prob>z
bapmeanchange	28	0.95174	1.457	0.775	0.21906

- **By gender and menopausal status**



. sktest bobap if menopausal ==0

Skewness/Kurtosis tests for Normality					
Variable	Obs	Pr(Skewness)	Pr(Kurtosis)	adj chi2(2)	joint Prob>chi2
bobap	13	0.8207	0.9656	0.05	0.9737

. swilk bobap if menopausal ==0

Shapiro-Wilk w test for normal data					
Variable	Obs	W	V	z	Prob>z
bobap	13	0.98096	0.335	-2.140	0.98384

. sktest bap12m if menopausal ==0

Skewness/Kurtosis tests for Normality					
Variable	Obs	Pr(Skewness)	Pr(Kurtosis)	adj chi2(2)	joint Prob>chi2
bap12m	12	0.0239	0.0780	7.05	0.0294

. swilk bap12m if menopausal ==0

Shapiro-Wilk w test for normal data					
Variable	Obs	W	V	z	Prob>z
bap12m	12	0.87285	2.124	1.468	0.07104

. sktest bapc12m if menopausal ==0

Skewness/Kurtosis tests for Normality					
Variable	Obs	Pr(Skewness)	Pr(Kurtosis)	adj chi2(2)	joint Prob>chi2
bapc12m	9	0.0754	0.0696	5.80	0.0551

. swilk bapc12m if menopausal ==0

Shapiro-Wilk w test for normal data					
Variable	Obs	W	V	z	Prob>z
bapc12m	9	0.88261	1.725	0.965	0.16726

. sktest bappr12m if menopausal ==0

Skewness/Kurtosis tests for Normality					
Variable	Obs	Pr(Skewness)	Pr(Kurtosis)	adj chi2(2)	joint Prob>chi2
bappr12m	9	0.7125	0.9930	0.14	0.9343

. swilk bappr12m if menopausal ==0

Shapiro-Wilk w test for normal data					
Variable	Obs	W	V	z	Prob>z
bappr12m	9	0.94686	0.781	-0.401	0.65563

. sktest bapmeanchange if menopausal ==0

Skewness/Kurtosis tests for Normality					
Variable	Obs	Pr(Skewness)	Pr(Kurtosis)	adj chi2(2)	joint Prob>chi2
bapmeanchange	9	0.2262	0.7729	1.81	0.4047

. swilk bapmeanchange if menopausal ==0

Shapiro-Wilk w test for normal data					
Variable	Obs	W	V	z	Prob>z
bapmeanchange	9	0.87095	1.896	1.146	0.12586



. sktest bobap if menopausal ==1

Skewness/Kurtosis tests for Normality					
Variable	Obs	Pr(Skewness)	Pr(Kurtosis)	adj chi2(2)	joint Prob>chi2
bobap	23	0.0417	0.1447	5.87	0.0531

. swilk bobap if menopausal ==1

Shapiro-wilk w test for normal data					
Variable	Obs	W	V	z	Prob>z
bobap	23	0.93494	1.702	1.081	0.13979

. sktest bap12m if menopausal ==1

Skewness/Kurtosis tests for Normality					
Variable	Obs	Pr(Skewness)	Pr(Kurtosis)	adj chi2(2)	joint Prob>chi2
bap12m	22	0.3164	0.7203	1.23	0.5400

. swilk bap12m if menopausal ==1

Shapiro-wilk w test for normal data					
Variable	Obs	W	V	z	Prob>z
bap12m	22	0.96015	1.010	0.019	0.49235

. sktest bapc12m if menopausal ==1

Skewness/Kurtosis tests for Normality					
Variable	Obs	Pr(Skewness)	Pr(Kurtosis)	adj chi2(2)	joint Prob>chi2
bapc12m	19	0.6947	0.5381	0.56	0.7562

. swilk bapc12m if menopausal ==1

Shapiro-wilk w test for normal data					
Variable	Obs	W	V	z	Prob>z
bapc12m	19	0.96210	0.865	-0.291	0.61440

. sktest bappr12m if menopausal ==1

Skewness/Kurtosis tests for Normality					
Variable	Obs	Pr(Skewness)	Pr(Kurtosis)	adj chi2(2)	joint Prob>chi2
bappr12m	19	0.2002	0.9482	1.84	0.3985

. swilk bappr12m if menopausal ==1

Shapiro-wilk w test for normal data					
Variable	Obs	W	V	z	Prob>z
bappr12m	19	0.95188	1.099	0.189	0.42508

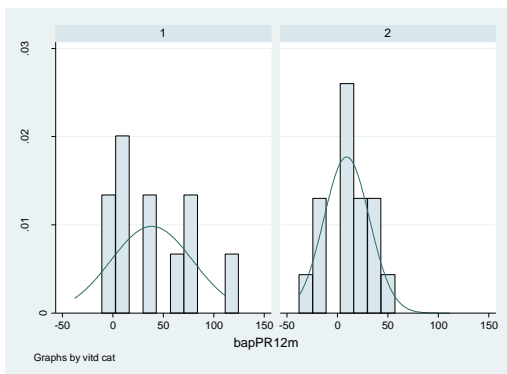
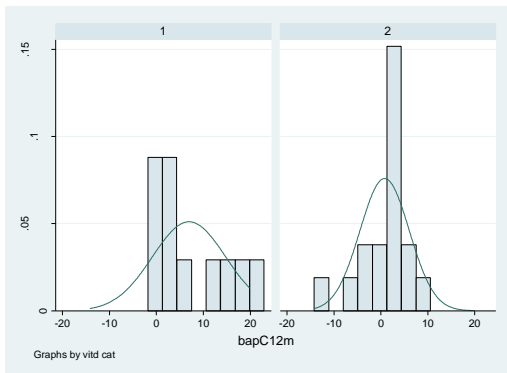
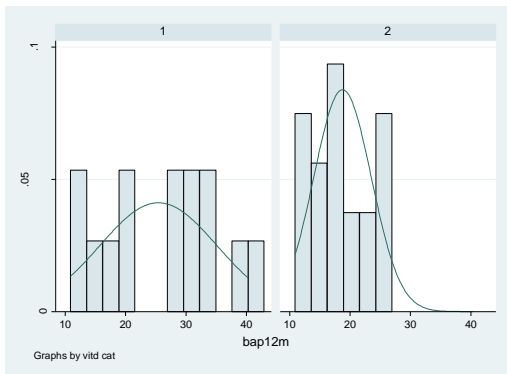
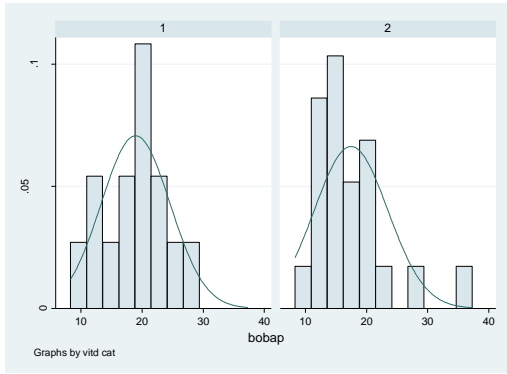
. sktest bapmeanchange if menopausal ==1

Skewness/Kurtosis tests for Normality					
Variable	Obs	Pr(Skewness)	Pr(Kurtosis)	adj chi2(2)	joint Prob>chi2
bapmeanchange	19	0.3159	0.8421	1.14	0.5646

. swilk bapmeanchange if menopausal ==1

Shapiro-wilk w test for normal data					
Variable	Obs	W	V	z	Prob>z
bapmeanchange	19	0.95783	0.963	-0.076	0.53039

## - By vitamin D category



. sktest bobap if vitdcat ==1

Skewness/Kurtosis tests for Normality

Variable	Obs	Pr(Skewness)	Pr(Kurtosis)	adj	chi2(2)	joint	Prob>chi2
bobap	14	0.8033	0.9056		0.08		0.9627

. swilk bobap if vitdcat ==1

Shapiro-Wilk W test for normal data

Variable	Obs	W	V	z	Prob>z
bobap	14	0.98474	0.282	-2.490	0.99360

. sktest bap12m if vitdcat ==1

Skewness/Kurtosis tests for Normality

Variable	Obs	Pr(Skewness)	Pr(Kurtosis)	adj	chi2(2)	joint	Prob>chi2
bap12m	14	0.8459	0.1404		2.58		0.2757

. swilk bap12m if vitdcat ==1

Shapiro-Wilk W test for normal data

Variable	Obs	W	V	z	Prob>z
bap12m	14	0.94571	1.005	0.009	0.49634

. sktest bapc12m if vitdcat ==1

Skewness/Kurtosis tests for Normality

Variable	Obs	Pr(Skewness)	Pr(Kurtosis)	adj	chi2(2)	joint	Prob>chi2
bapc12m	11	0.2774	0.2329		3.13		0.2088

. swilk bapc12m if vitdcat ==1

Shapiro-Wilk W test for normal data

Variable	Obs	W	V	z	Prob>z
bapc12m	11	0.85351	2.372	1.670	0.04741

. sktest bappr12m if vitdcat ==1

Skewness/Kurtosis tests for Normality

Variable	Obs	Pr(Skewness)	Pr(Kurtosis)	adj	chi2(2)	joint	Prob>chi2
bappr12m	11	0.3522	0.3593		1.99		0.3690

. swilk bappr12m if vitdcat ==1

Shapiro-Wilk W test for normal data

Variable	Obs	W	V	z	Prob>z
bappr12m	11	0.89729	1.663	0.949	0.17126

. sktest bobap if vitdcat ==2

Skewness/Kurtosis tests for Normality					
Variable	Obs	Pr(Skewness)	Pr(Kurtosis)	adj chi2(2)	joint Prob>chi2
bobap	22	0.0007	0.0044	14.48	0.0007

. swilk bobap if vitdcat ==2

Shapiro-Wilk W test for normal data					
Variable	Obs	W	V	z	Prob>z
bobap	22	0.82998	4.307	2.961	0.00153

. sktest bap12m if vitdcat ==2

Skewness/Kurtosis tests for Normality					
Variable	Obs	Pr(Skewness)	Pr(Kurtosis)	adj chi2(2)	joint Prob>chi2
bap12m	20	0.5494	0.1197	3.16	0.2063

. swilk bap12m if vitdcat ==2

Shapiro-Wilk W test for normal data					
Variable	Obs	W	V	z	Prob>z
bap12m	20	0.95129	1.153	0.287	0.38707

. sktest bapc12m if vitdcat ==2

Skewness/Kurtosis tests for Normality					
Variable	Obs	Pr(Skewness)	Pr(Kurtosis)	adj chi2(2)	joint Prob>chi2
bapc12m	17	0.0092	0.0277	9.39	0.0092

. swilk bapc12m if vitdcat ==2

Shapiro-Wilk W test for normal data					
Variable	Obs	W	V	z	Prob>z
bapc12m	17	0.87097	2.726	2.000	0.02277

. sktest bappr12m if vitdcat ==2

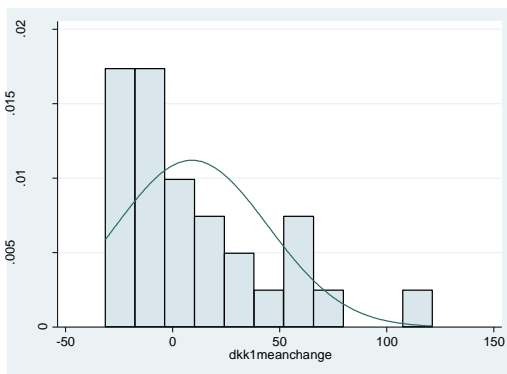
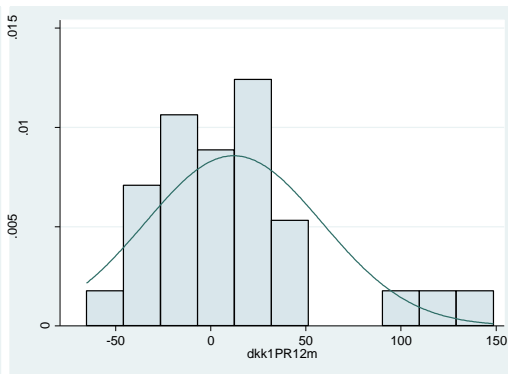
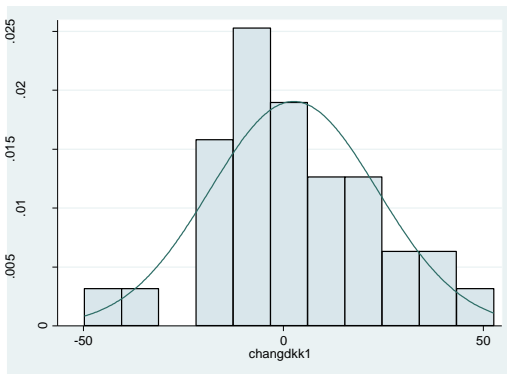
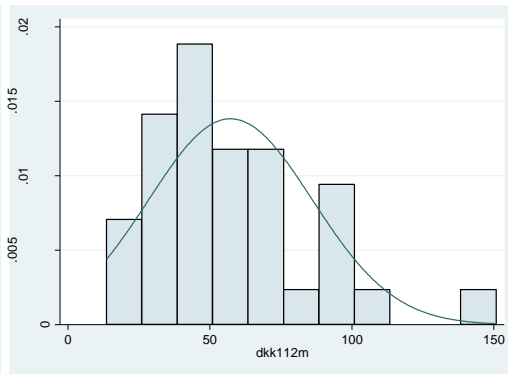
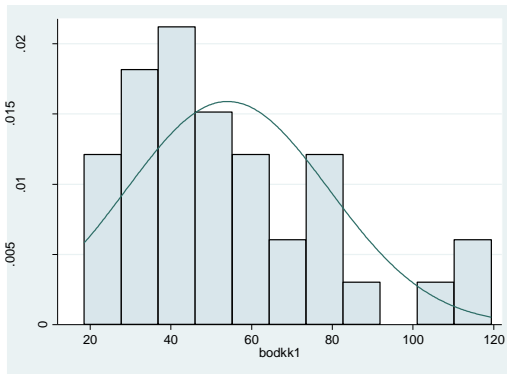
Skewness/Kurtosis tests for Normality					
Variable	Obs	Pr(Skewness)	Pr(Kurtosis)	adj chi2(2)	joint Prob>chi2
bappr12m	17	0.2715	0.9459	1.35	0.5098

. swilk bappr12m if vitdcat ==2

Shapiro-Wilk W test for normal data					
Variable	Obs	W	V	z	Prob>z
bappr12m	17	0.93661	1.339	0.582	0.28019

# DKK-1

- All



. sktest bodkk1

Skewness/Kurtosis tests for Normality					
Variable	Obs	Pr(Skewness)	Pr(Kurtosis)	adj chi2(2)	joint Prob>chi2
bodkk1	36	0.0166	0.3311	6.18	0.0455

. swilk bodkk1

Shapiro-wilk w test for normal data					
Variable	Obs	W	V	z	Prob>z
bodkk1	36	0.92298	2.809	2.159	0.01541

. sktest dkk112m

Skewness/Kurtosis tests for Normality					
Variable	Obs	Pr(Skewness)	Pr(Kurtosis)	adj chi2(2)	joint Prob>chi2
dkk112m	34	0.0107	0.0579	8.59	0.0136

. swilk dkk112m

Shapiro-wilk w test for normal data					
Variable	Obs	W	V	z	Prob>z
dkk112m	34	0.93082	2.416	1.838	0.03305

. sktest dkk1c12m

Skewness/Kurtosis tests for Normality					
Variable	Obs	Pr(Skewness)	Pr(Kurtosis)	adj chi2(2)	joint Prob>chi2
dkk1c12m	29	0.9777	0.4539	0.58	0.7464

. swilk dkk1c12m

Shapiro-wilk w test for normal data					
Variable	Obs	W	V	z	Prob>z
dkk1c12m	29	0.97838	0.670	-0.826	0.79550

. sktest dkk1pr12m

Skewness/Kurtosis tests for Normality					
Variable	Obs	Pr(Skewness)	Pr(Kurtosis)	adj chi2(2)	joint Prob>chi2
dkk1pr12m	29	0.0072	0.0554	9.08	0.0107

. swilk dkk1pr12m

Shapiro-wilk w test for normal data					
Variable	Obs	W	V	z	Prob>z
dkk1pr12m	29	0.90395	2.977	2.251	0.01219

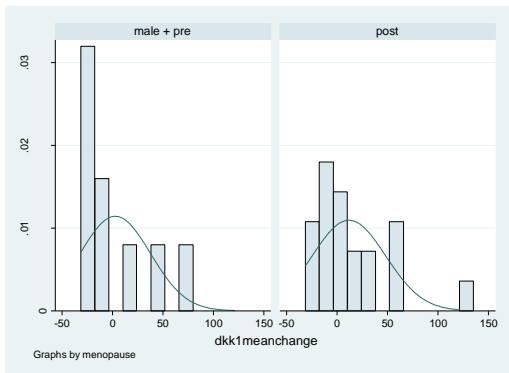
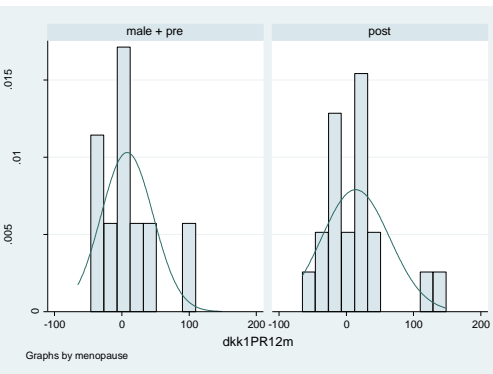
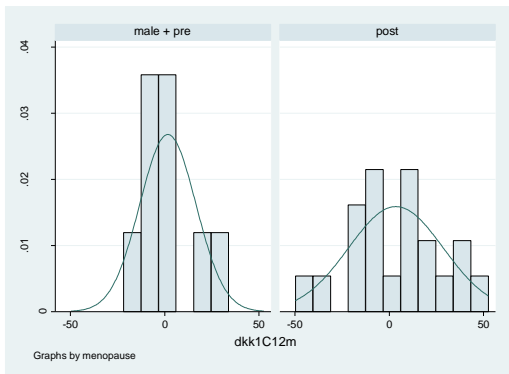
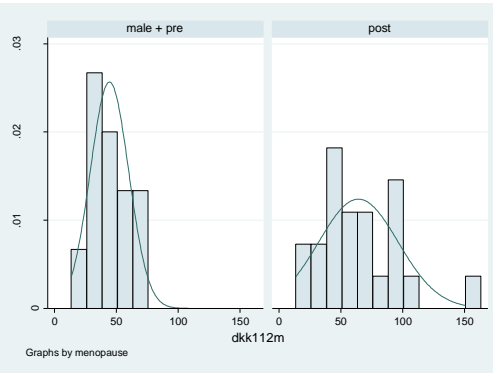
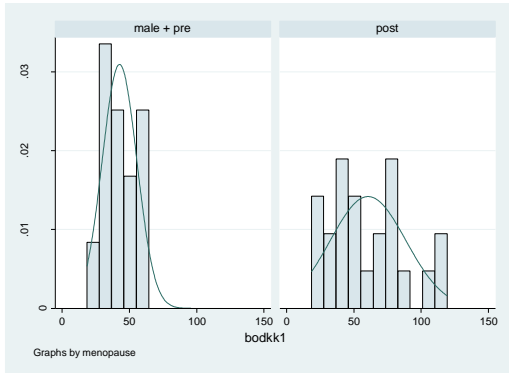
. sktest dkk1meanchange

Skewness/Kurtosis tests for Normality					
Variable	Obs	Pr(Skewness)	Pr(Kurtosis)	adj chi2(2)	joint Prob>chi2
dkk1meanchange	29	0.0029	0.0460	10.39	0.0055

. swilk dkk1meanchange

Shapiro-wilk w test for normal data					
Variable	Obs	W	V	z	Prob>z
dkk1meanchange	29	0.86450	4.199	2.961	0.00153

- **By gender and menopausal status**



. sktest bodkk1 if menopausal ==0

Skewness/Kurtosis tests for Normality					
Variable	Obs	Pr(Skewness)	Pr(Kurtosis)	adj chi2(2)	joint Prob>chi2
bodkk1	13	0.8876	0.9291	0.03	0.9861

. swilk bodkk1 if menopausal ==0

Shapiro-Wilk w test for normal data					
Variable	Obs	W	V	z	Prob>z
bodkk1	13	0.98519	0.261	-2.632	0.99576

. sktest dkk112m if menopausal ==0

Skewness/Kurtosis tests for Normality					
Variable	Obs	Pr(Skewness)	Pr(Kurtosis)	adj chi2(2)	joint Prob>chi2
dkk112m	12	0.7884	0.1686	2.31	0.3153

. swilk dkk112m if menopausal ==0

Shapiro-Wilk w test for normal data					
Variable	Obs	W	V	z	Prob>z
dkk112m	12	0.92829	1.198	0.352	0.36234

. sktest dkk1c12m if menopausal ==0

Skewness/Kurtosis tests for Normality					
Variable	Obs	Pr(Skewness)	Pr(Kurtosis)	adj chi2(2)	joint Prob>chi2
dkk1c12m	9	0.1171	0.4634	3.53	0.1714

. swilk dkk1c12m if menopausal ==0

Shapiro-Wilk w test for normal data					
Variable	Obs	W	V	z	Prob>z
dkk1c12m	9	0.90307	1.424	0.612	0.27033

. sktest dkk1pr12m if menopausal ==0

Skewness/Kurtosis tests for Normality					
Variable	Obs	Pr(Skewness)	Pr(Kurtosis)	adj chi2(2)	joint Prob>chi2
dkk1pr12m	9	0.0430	0.1186	5.84	0.0538

. swilk dkk1pr12m if menopausal ==0

Shapiro-Wilk w test for normal data					
Variable	Obs	W	V	z	Prob>z
dkk1pr12m	9	0.87944	1.771	1.016	0.15490

. sktest dkk1meanchange if menopausal ==0

Skewness/Kurtosis tests for Normality					
Variable	Obs	Pr(Skewness)	Pr(Kurtosis)	adj chi2(2)	joint Prob>chi2
dkk1meanch~e	9	0.0684	0.6214	3.93	0.1399

. swilk dkk1meanchange if menopausal ==0

Shapiro-Wilk w test for normal data					
Variable	Obs	W	V	z	Prob>z
dkk1meanch~e	9	0.78491	3.160	2.205	0.01372



. sktest bodkk1 if menopausal ==1

Skewness/Kurtosis tests for Normality					
Variable	Obs	Pr(Skewness)	Pr(Kurtosis)	adj chi2(2)	joint Prob>chi2
bodkk1	23	0.2097	0.7637	1.83	0.3996

. swilk bodkk1 if menopausal ==1

Shapiro-wilk w test for normal data					
Variable	Obs	W	V	z	Prob>z
bodkk1	23	0.94188	1.520	0.852	0.19721

. sktest dkk112m if menopausal ==1

Skewness/Kurtosis tests for Normality					
Variable	Obs	Pr(Skewness)	Pr(Kurtosis)	adj chi2(2)	joint Prob>chi2
dkk112m	22	0.1237	0.2714	3.89	0.1431

. swilk dkk112m if menopausal ==1

Shapiro-wilk w test for normal data					
Variable	Obs	W	V	z	Prob>z
dkk112m	22	0.95434	1.157	0.295	0.38396

. sktest dkk1c12m if menopausal ==1

Skewness/Kurtosis tests for Normality					
Variable	Obs	Pr(Skewness)	Pr(Kurtosis)	adj chi2(2)	joint Prob>chi2
dkk1c12m	20	0.7587	0.7403	0.20	0.9029

. swilk dkk1c12m if menopausal ==1

Shapiro-wilk w test for normal data					
Variable	Obs	W	V	z	Prob>z
dkk1c12m	20	0.98311	0.400	-1.847	0.96764

. sktest dkk1pr12m if menopausal ==1

Skewness/Kurtosis tests for Normality					
Variable	Obs	Pr(Skewness)	Pr(Kurtosis)	adj chi2(2)	joint Prob>chi2
dkk1pr12m	20	0.0234	0.0840	7.14	0.0281

. swilk dkk1pr12m if menopausal ==1

Shapiro-wilk w test for normal data					
Variable	Obs	W	V	z	Prob>z
dkk1pr12m	20	0.90230	2.313	1.690	0.04556

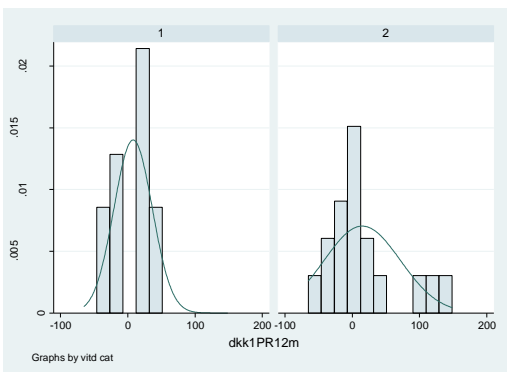
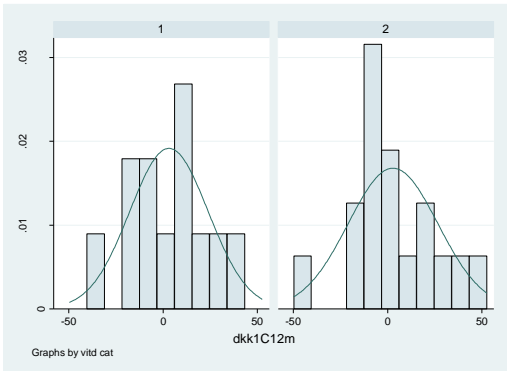
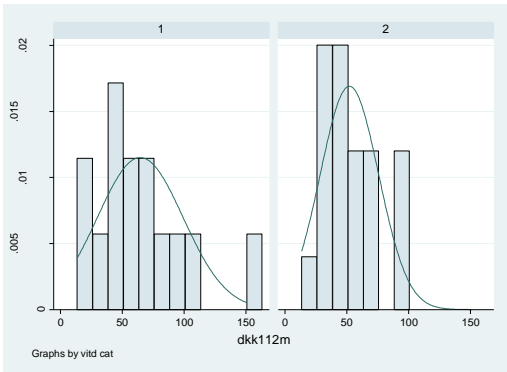
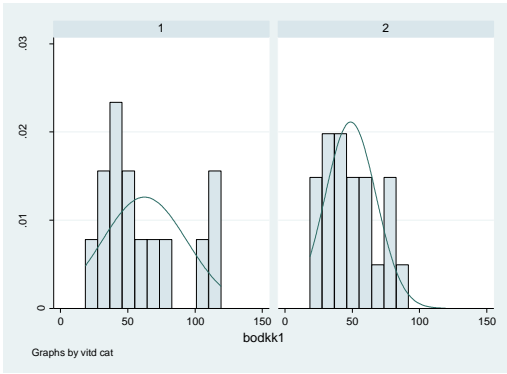
. sktest dkk1meanchange if menopausal ==1

Skewness/Kurtosis tests for Normality					
Variable	Obs	Pr(Skewness)	Pr(Kurtosis)	adj chi2(2)	joint Prob>chi2
dkk1meanch~e	20	0.0047	0.0250	10.35	0.0057

. swilk dkk1meanchange if menopausal ==1

Shapiro-wilk w test for normal data					
Variable	Obs	W	V	z	Prob>z
dkk1meanch~e	20	0.85141	3.517	2.535	0.00563

- By vitamin D category



. sktest bodkk1 if vitdcat ==1

Skewness/Kurtosis tests for Normality					
Variable	Obs	Pr(Skewness)	Pr(Kurtosis)	adj chi2(2)	joint Prob>chi2
bodkk1	14	0.2103	0.6616	2.03	0.3631

. swilk bodkk1 if vitdcat ==1

Shapiro-Wilk W test for normal data					
Variable	Obs	W	V	z	Prob>z
bodkk1	14	0.90342	1.787	1.143	0.12646

. sktest dkk112m if vitdcat ==1

Skewness/Kurtosis tests for Normality					
Variable	Obs	Pr(Skewness)	Pr(Kurtosis)	adj chi2(2)	joint Prob>chi2
dkk112m	14	0.0607	0.1510	5.37	0.0682

. swilk dkk112m if vitdcat ==1

Shapiro-Wilk W test for normal data					
Variable	Obs	W	V	z	Prob>z
dkk112m	14	0.92408	1.405	0.670	0.25159

. sktest dkk1c12m if vitdcat ==1

Skewness/Kurtosis tests for Normality					
Variable	Obs	Pr(Skewness)	Pr(Kurtosis)	adj chi2(2)	joint Prob>chi2
dkk1c12m	12	0.6248	0.8735	0.26	0.8761

. swilk dkk1c12m if vitdcat ==1

Shapiro-Wilk W test for normal data					
Variable	Obs	W	V	z	Prob>z
dkk1c12m	12	0.97470	0.423	-1.678	0.95330

. sktest dkk1pr12m if vitdcat ==1

Skewness/Kurtosis tests for Normality					
Variable	Obs	Pr(Skewness)	Pr(Kurtosis)	adj chi2(2)	joint Prob>chi2
dkk1pr12m	12	0.6425	0.2377	1.86	0.3940

. swilk dkk1pr12m if vitdcat ==1

Shapiro-Wilk W test for normal data					
Variable	Obs	W	V	z	Prob>z
dkk1pr12m	12	0.93154	1.144	0.262	0.39671

. sktest bodkk1 if vitdcat ==2

Skewness/Kurtosis tests for Normality					
Variable	Obs	Pr(Skewness)	Pr(Kurtosis)	adj chi2(2)	joint Prob>chi2
bodkk1	22	0.4136	0.2525	2.20	0.3326

. swilk bodkk1 if vitdcat ==2

Shapiro-Wilk W test for normal data					
Variable	Obs	W	V	z	Prob>z
bodkk1	22	0.94642	1.357	0.620	0.26771

. sktest dkk112m if vitdcat ==2

Skewness/Kurtosis tests for Normality					
Variable	Obs	Pr(Skewness)	Pr(Kurtosis)	adj chi2(2)	joint Prob>chi2
dkk112m	20	0.3183	0.6087	1.38	0.5005

. swilk dkk112m if vitdcat ==2

Shapiro-Wilk W test for normal data					
Variable	Obs	W	V	z	Prob>z
dkk112m	20	0.95035	1.175	0.325	0.37249

. sktest dkk1c12m if vitdcat ==2

Skewness/Kurtosis tests for Normality					
Variable	Obs	Pr(Skewness)	Pr(Kurtosis)	adj chi2(2)	joint Prob>chi2
dkk1c12m	17	0.8220	0.2985	1.25	0.5350

. swilk dkk1c12m if vitdcat ==2

Shapiro-Wilk W test for normal data					
Variable	Obs	W	V	z	Prob>z
dkk1c12m	17	0.96175	0.808	-0.425	0.66464

. sktest dkk1pr12m if vitdcat ==2

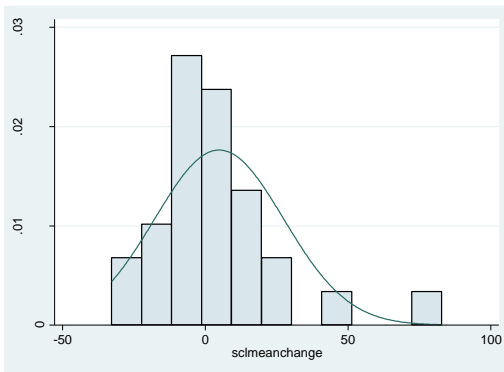
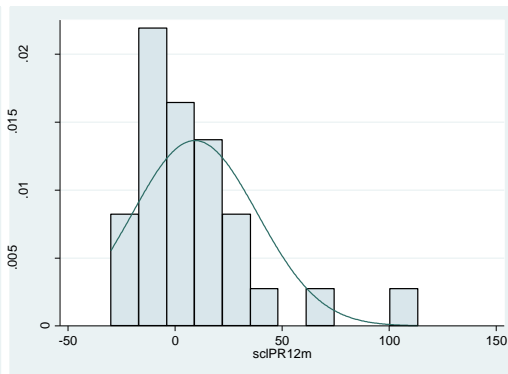
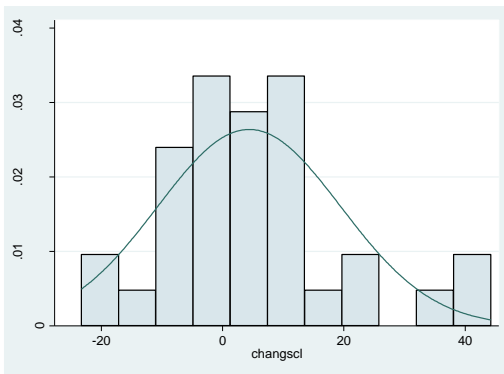
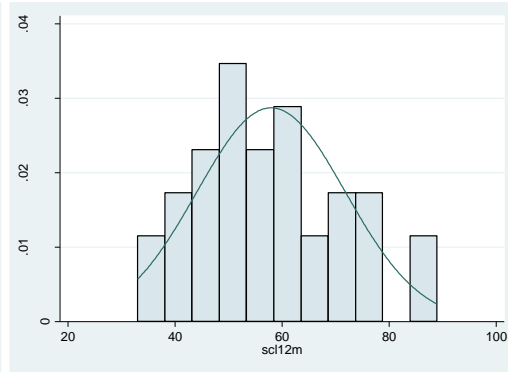
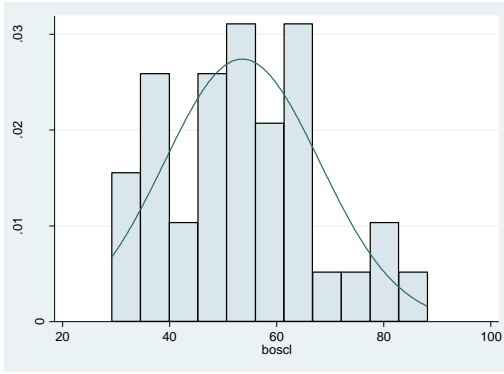
Skewness/Kurtosis tests for Normality					
Variable	Obs	Pr(Skewness)	Pr(Kurtosis)	adj chi2(2)	joint Prob>chi2
dkk1pr12m	17	0.0359	0.3085	5.28	0.0715

. swilk dkk1pr12m if vitdcat ==2

Shapiro-Wilk W test for normal data					
Variable	Obs	W	V	z	Prob>z
dkk1pr12m	17	0.88229	2.487	1.817	0.03464

# SCL

- All



. sktest bosc1

Skewness/Kurtosis tests for Normality					
Variable	Obs	Pr(Skewness)	Pr(Kurtosis)	adj chi2(2)	joint Prob>chi2
bosc1	36	0.4359	0.7464	0.74	0.6898

. swilk bosc1

Shapiro-wilk w test for normal data					
Variable	Obs	W	V	z	Prob>z
bosc1	36	0.97769	0.814	-0.431	0.66690

. sktest scl12m

Skewness/Kurtosis tests for Normality					
Variable	Obs	Pr(Skewness)	Pr(Kurtosis)	adj chi2(2)	joint Prob>chi2
scl12m	34	0.3036	0.8427	1.16	0.5587

. swilk scl12m

Shapiro-wilk w test for normal data					
Variable	Obs	W	V	z	Prob>z
scl12m	34	0.97414	0.903	-0.213	0.58420

. sktest sclc12m

Skewness/Kurtosis tests for Normality					
Variable	Obs	Pr(Skewness)	Pr(Kurtosis)	adj chi2(2)	joint Prob>chi2
sclc12m	28	0.3965	0.3347	1.79	0.4082

. swilk sclc12m

Shapiro-wilk w test for normal data					
Variable	Obs	W	V	z	Prob>z
sclc12m	28	0.98087	0.578	-1.130	0.87074

. sktest sclpr12m

Skewness/Kurtosis tests for Normality					
Variable	Obs	Pr(Skewness)	Pr(Kurtosis)	adj chi2(2)	joint Prob>chi2
sclpr12m	28	0.0003	0.0020	16.72	0.0002

. swilk sclpr12m

Shapiro-wilk w test for normal data					
Variable	Obs	W	V	z	Prob>z
sclpr12m	28	0.84212	4.768	3.216	0.00065

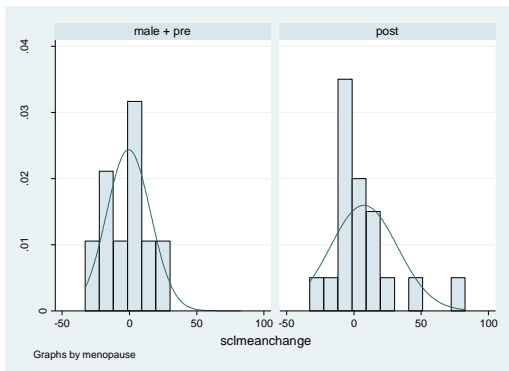
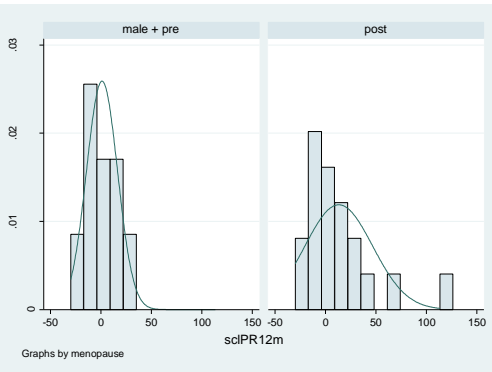
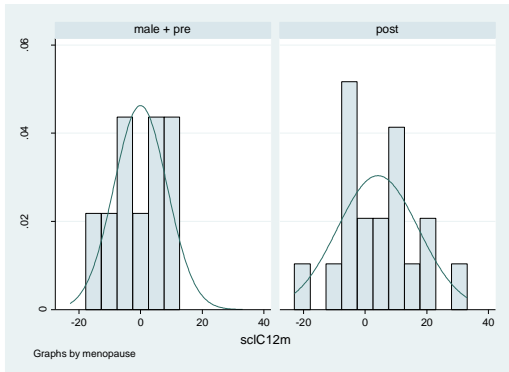
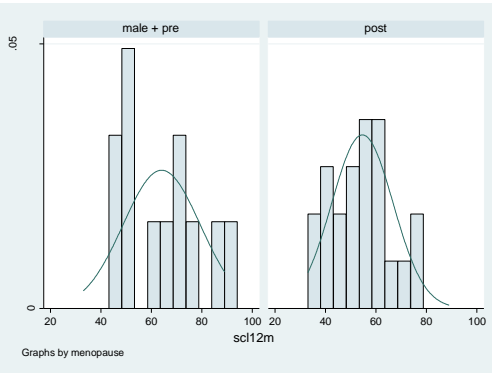
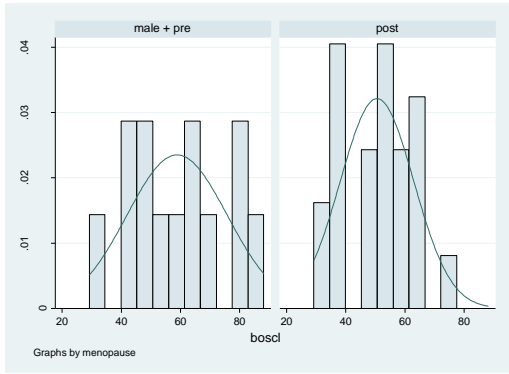
. sktest sclmeanchange

Skewness/Kurtosis tests for Normality					
Variable	Obs	Pr(Skewness)	Pr(Kurtosis)	adj chi2(2)	joint Prob>chi2
sclmeancha~e	28	0.0009	0.0033	14.86	0.0006

. swilk sclmeanchange

Shapiro-wilk w test for normal data					
Variable	Obs	W	V	z	Prob>z
sclmeancha~e	28	0.86399	4.107	2.909	0.00182

- **By gender and menopausal status**



. sktest boscl if menopausal ==0

Skewness/Kurtosis tests for Normality					
Variable	Obs	Pr(Skewness)	Pr(Kurtosis)	adj chi2(2)	joint Prob>chi2
boscl	13	0.8730	0.5349	0.42	0.8112

. swilk boscl if menopausal ==0

Shapiro-Wilk w test for normal data					
Variable	Obs	W	V	z	Prob>z
boscl	13	0.97790	0.389	-1.848	0.96770

. sktest scl12m if menopausal ==0

Skewness/Kurtosis tests for Normality					
Variable	Obs	Pr(Skewness)	Pr(Kurtosis)	adj chi2(2)	joint Prob>chi2
scl12m	12	0.5443	0.3357	1.47	0.4788

. swilk scl12m if menopausal ==0

Shapiro-Wilk w test for normal data					
Variable	Obs	W	V	z	Prob>z
scl12m	12	0.91789	1.372	0.616	0.26892

. sktest sclc12m if menopausal ==0

Skewness/Kurtosis tests for Normality					
Variable	Obs	Pr(Skewness)	Pr(Kurtosis)	adj chi2(2)	joint Prob>chi2
sclc12m	9	0.4996	0.5632	0.85	0.6528

. swilk sclc12m if menopausal ==0

Shapiro-Wilk w test for normal data					
Variable	Obs	W	V	z	Prob>z
sclc12m	9	0.92729	1.068	0.111	0.45596

. sktest sclpr12m if menopausal ==0

Skewness/Kurtosis tests for Normality					
Variable	Obs	Pr(Skewness)	Pr(Kurtosis)	adj chi2(2)	joint Prob>chi2
sclpr12m	9	0.8235	0.7606	0.14	0.9312

. swilk sclpr12m if menopausal ==0

Shapiro-Wilk w test for normal data					
Variable	Obs	W	V	z	Prob>z
sclpr12m	9	0.97939	0.303	-1.763	0.96106

. sktest sclmeanchange if menopausal ==0

Skewness/Kurtosis tests for Normality					
Variable	Obs	Pr(Skewness)	Pr(Kurtosis)	adj chi2(2)	joint Prob>chi2
sclmeancha~e	9	0.5123	0.8861	0.45	0.7996

. swilk sclmeanchange if menopausal ==0

Shapiro-Wilk w test for normal data					
Variable	Obs	W	V	z	Prob>z
sclmeancha~e	9	0.96538	0.509	-1.048	0.85260



. sktest boscl if menopausal ==1

Skewness/Kurtosis tests for Normality					
Variable	Obs	Pr(Skewness)	Pr(Kurtosis)	adj chi2(2)	joint Prob>chi2
boscl	23	0.9721	0.4573	0.58	0.7484

. swilk boscl if menopausal ==1

Shapiro-wilk w test for normal data					
Variable	Obs	W	V	z	Prob>z
boscl	23	0.96759	0.848	-0.336	0.63156

. sktest scl12m if menopausal ==1

Skewness/Kurtosis tests for Normality					
Variable	Obs	Pr(Skewness)	Pr(Kurtosis)	adj chi2(2)	joint Prob>chi2
scl12m	22	0.8386	0.5955	0.32	0.8507

. swilk scl12m if menopausal ==1

Shapiro-wilk w test for normal data					
Variable	Obs	W	V	z	Prob>z
scl12m	22	0.97744	0.572	-1.134	0.87166

. sktest sclc12m if menopausal ==1

Skewness/Kurtosis tests for Normality					
Variable	Obs	Pr(Skewness)	Pr(Kurtosis)	adj chi2(2)	joint Prob>chi2
sclc12m	19	0.5968	0.5237	0.73	0.6935

. swilk sclc12m if menopausal ==1

Shapiro-wilk w test for normal data					
Variable	Obs	W	V	z	Prob>z
sclc12m	19	0.98628	0.313	-2.331	0.99014

. sktest sclpr12m if menopausal ==1

Skewness/Kurtosis tests for Normality					
Variable	Obs	Pr(Skewness)	Pr(Kurtosis)	adj chi2(2)	joint Prob>chi2
sclpr12m	19	0.0038	0.0181	10.91	0.0043

. swilk sclpr12m if menopausal ==1

Shapiro-wilk w test for normal data					
Variable	Obs	W	V	z	Prob>z
sclpr12m	19	0.86171	3.157	2.309	0.01047

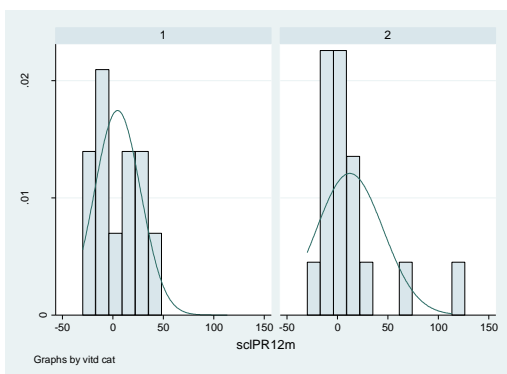
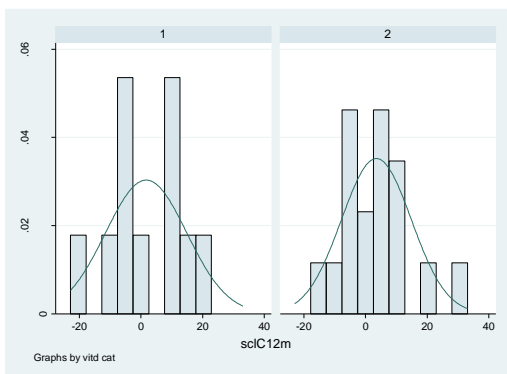
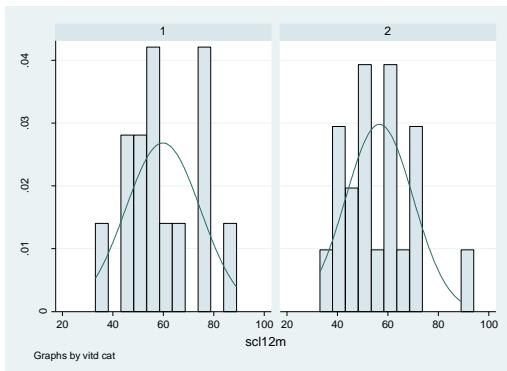
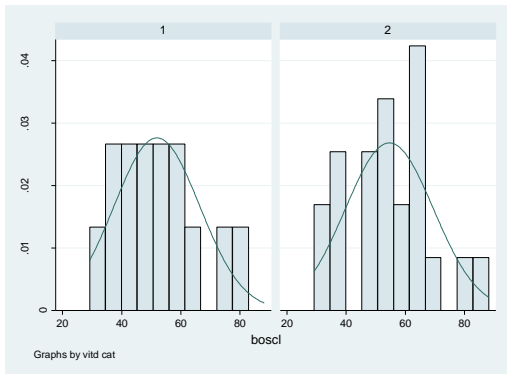
. sktest sclmeanchange if menopausal ==1

Skewness/Kurtosis tests for Normality					
Variable	Obs	Pr(Skewness)	Pr(Kurtosis)	adj chi2(2)	joint Prob>chi2
sclmeancha~e	19	0.0033	0.0101	11.73	0.0028

. swilk sclmeanchange if menopausal ==1

Shapiro-wilk w test for normal data					
Variable	Obs	W	V	z	Prob>z
sclmeancha~e	19	0.83744	3.711	2.634	0.00422

## - By vitamin D category



. sktest boscl if vitdcat ==1

Skewness/Kurtosis tests for Normality					
Variable	Obs	Pr(Skewness)	Pr(Kurtosis)	adj chi2(2)	joint Prob>chi2
boscl	14	0.3857	0.8857	0.84	0.6574

. swilk boscl if vitdcat ==1

Shapiro-Wilk W test for normal data					
Variable	Obs	W	V	z	Prob>z
boscl	14	0.95527	0.828	-0.372	0.64508

. sktest scl12m if vitdcat ==1

Skewness/Kurtosis tests for Normality					
Variable	Obs	Pr(Skewness)	Pr(Kurtosis)	adj chi2(2)	joint Prob>chi2
scl12m	14	0.7150	0.8814	0.16	0.9251

. swilk scl12m if vitdcat ==1

Shapiro-Wilk W test for normal data					
Variable	Obs	W	V	z	Prob>z
scl12m	14	0.97216	0.515	-1.305	0.90412

. sktest sclc12m if vitdcat ==1

Skewness/Kurtosis tests for Normality					
Variable	Obs	Pr(Skewness)	Pr(Kurtosis)	adj chi2(2)	joint Prob>chi2
sclc12m	11	0.6538	0.8569	0.23	0.8898

. swilk sclc12m if vitdcat ==1

Shapiro-Wilk W test for normal data					
Variable	Obs	W	V	z	Prob>z
sclc12m	11	0.96938	0.496	-1.176	0.88020

. sktest sclpr12m if vitdcat ==1

Skewness/Kurtosis tests for Normality					
Variable	Obs	Pr(Skewness)	Pr(Kurtosis)	adj chi2(2)	joint Prob>chi2
sclpr12m	11	0.8124	0.2298	1.73	0.4204

. swilk sclpr12m if vitdcat ==1

Shapiro-Wilk W test for normal data					
Variable	Obs	W	V	z	Prob>z
sclpr12m	11	0.94770	0.847	-0.292	0.61473

. sktest boscl if vitdcat ==2

Skewness/Kurtosis tests for Normality					
Variable	Obs	Pr(Skewness)	Pr(Kurtosis)	adj chi2(2)	joint Prob>chi2
boscl	22	0.6814	0.8850	0.19	0.9096

. swilk boscl if vitdcat ==2

Shapiro-Wilk W test for normal data					
Variable	Obs	W	V	z	Prob>z
boscl	22	0.97436	0.650	-0.875	0.80910

. sktest scl12m if vitdcat ==2

Skewness/Kurtosis tests for Normality					
Variable	Obs	Pr(Skewness)	Pr(Kurtosis)	adj chi2(2)	joint Prob>chi2
scl12m	20	0.2602	0.6655	1.61	0.4468

. swilk scl12m if vitdcat ==2

Shapiro-Wilk W test for normal data					
Variable	Obs	W	V	z	Prob>z
scl12m	20	0.96483	0.832	-0.369	0.64411

. sktest sclc12m if vitdcat ==2

Skewness/Kurtosis tests for Normality					
Variable	Obs	Pr(Skewness)	Pr(Kurtosis)	adj chi2(2)	joint Prob>chi2
sclc12m	17	0.0576	0.0976	5.91	0.0520

. swilk sclc12m if vitdcat ==2

Shapiro-Wilk W test for normal data					
Variable	Obs	W	V	z	Prob>z
sclc12m	17	0.92282	1.630	0.975	0.16483

. sktest sclpr12m if vitdcat ==2

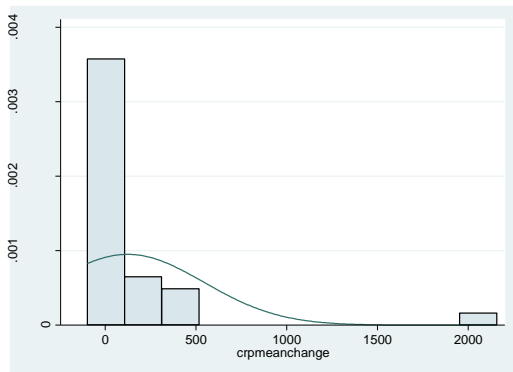
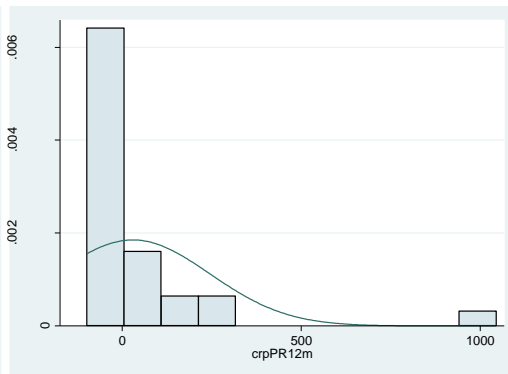
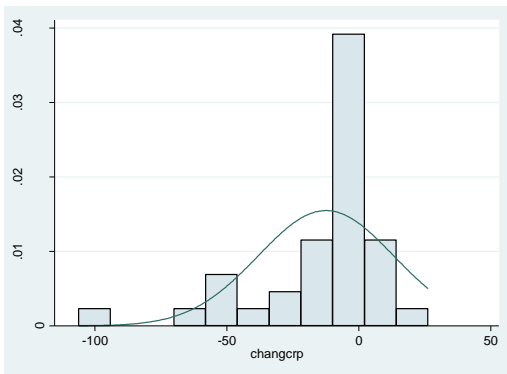
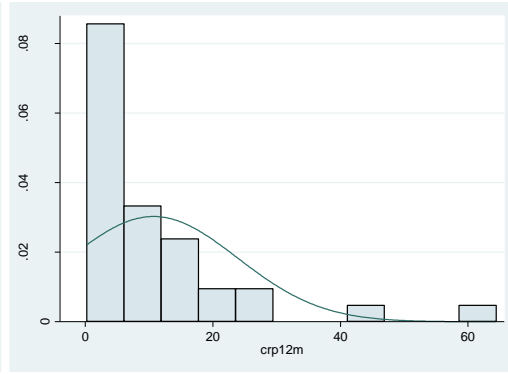
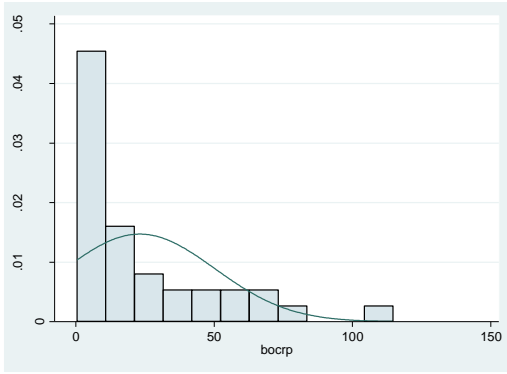
Skewness/Kurtosis tests for Normality					
Variable	Obs	Pr(Skewness)	Pr(Kurtosis)	adj chi2(2)	joint Prob>chi2
sclpr12m	17	0.0007	0.0046	14.22	0.0008

. swilk sclpr12m if vitdcat ==2

Shapiro-Wilk W test for normal data					
Variable	Obs	W	V	z	Prob>z
sclpr12m	17	0.75949	5.081	3.242	0.00059

# CRP

- All



. sktest bocrp

Skewness/Kurtosis tests for Normality					
Variable	Obs	Pr(Skewness)	Pr(Kurtosis)	adj chi2(2)	joint Prob>chi2
bocrp	36	0.0006	0.0266	13.01	0.0015

. swilk bocrp

Shapiro-wilk w test for normal data					
Variable	Obs	W	V	z	Prob>z
bocrp	36	0.80123	7.248	4.142	0.00002

. sktest crp12m

Skewness/Kurtosis tests for Normality					
Variable	Obs	Pr(Skewness)	Pr(Kurtosis)	adj chi2(2)	joint Prob>chi2
crp12m	36	0.0000	0.0001	26.08	0.0000

. swilk crp12m

Shapiro-wilk w test for normal data					
Variable	Obs	W	V	z	Prob>z
crp12m	36	0.71408	10.426	4.902	0.00000

. sktest crpc12m

Skewness/Kurtosis tests for Normality					
Variable	Obs	Pr(Skewness)	Pr(Kurtosis)	adj chi2(2)	joint Prob>chi2
crpc12m	30	0.0003	0.0036	15.92	0.0003

. swilk crpc12m

Shapiro-wilk w test for normal data					
Variable	Obs	W	V	z	Prob>z
crpc12m	30	0.83265	5.319	3.456	0.00027

. sktest crppr12m

Skewness/Kurtosis tests for Normality					
Variable	Obs	Pr(Skewness)	Pr(Kurtosis)	adj chi2(2)	joint Prob>chi2
crppr12m	30	0.0000	0.0000	36.34	0.0000

. swilk crppr12m

Shapiro-wilk w test for normal data					
Variable	Obs	W	V	z	Prob>z
crppr12m	30	0.54401	14.494	5.528	0.00000

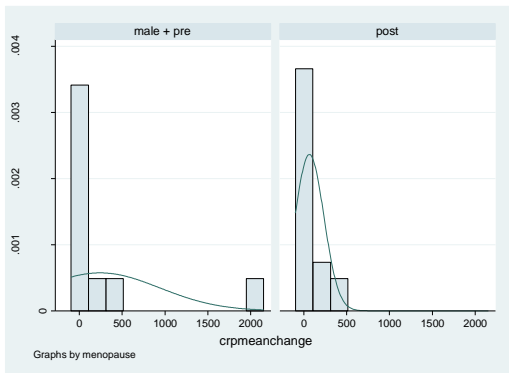
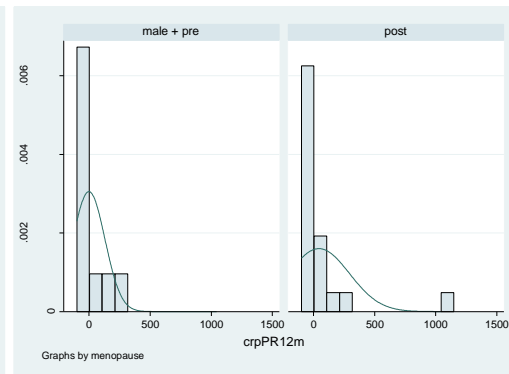
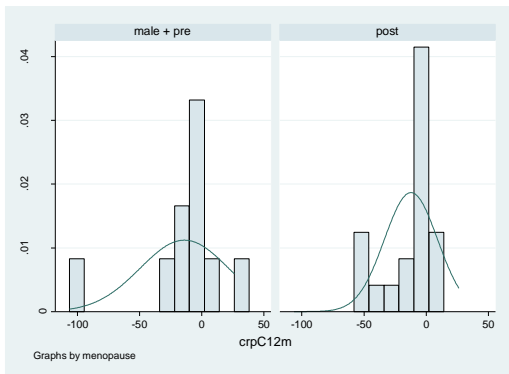
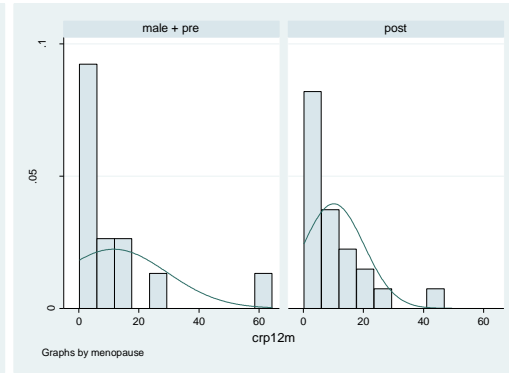
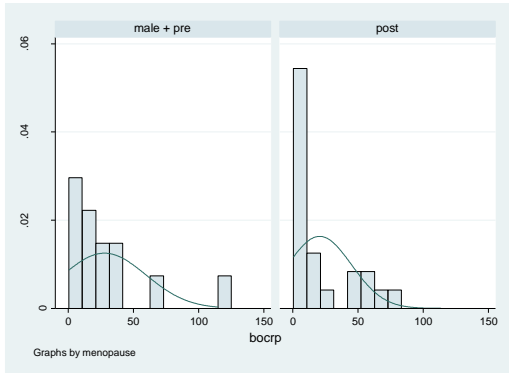
. sktest crpmeanchange

Skewness/Kurtosis tests for Normality					
Variable	Obs	Pr(Skewness)	Pr(Kurtosis)	adj chi2(2)	joint Prob>chi2
crpmeanchange	30	0.0000	0.0000	38.75	0.0000

. swilk crpmeanchange

Shapiro-wilk w test for normal data					
Variable	Obs	W	V	z	Prob>z
crpmeanchange	30	0.47901	16.560	5.804	0.00000

- **By gender and menopausal status**



. sktest bocrp if menopausal ==0

Skewness/Kurtosis tests for Normality					joint
Variable	Obs	Pr(Skewness)	Pr(Kurtosis)	adj chi2(2)	Prob>chi2
bocrp	13	0.0039	0.0166	10.67	0.0048

. swilk bocrp if menopausal ==0

Shapiro-Wilk w test for normal data					
Variable	Obs	W	V	z	Prob>z
bocrp	13	0.79126	3.677	2.551	0.00538

. sktest crp12m if menopausal ==0

Skewness/Kurtosis tests for Normality					joint
Variable	Obs	Pr(Skewness)	Pr(Kurtosis)	adj chi2(2)	Prob>chi2
crp12m	13	0.0004	0.0021	15.21	0.0005

. swilk crp12m if menopausal ==0

Shapiro-Wilk w test for normal data					
Variable	Obs	W	V	z	Prob>z
crp12m	13	0.66383	5.921	3.484	0.00025

. sktest crpc12m if menopausal ==0

Skewness/Kurtosis tests for Normality					joint
Variable	Obs	Pr(Skewness)	Pr(Kurtosis)	adj chi2(2)	Prob>chi2
crpc12m	10	0.0031	0.0058	11.60	0.0030

. swilk crpc12m if menopausal ==0

Shapiro-Wilk w test for normal data					
Variable	Obs	W	V	z	Prob>z
crpc12m	10	0.76660	3.597	2.531	0.00569

. sktest crppr12m if menopausal ==0

Skewness/Kurtosis tests for Normality					joint
Variable	Obs	Pr(Skewness)	Pr(Kurtosis)	adj chi2(2)	Prob>chi2
crppr12m	10	0.0191	0.1186	6.77	0.0339

. swilk crppr12m if menopausal ==0

Shapiro-Wilk w test for normal data					
Variable	Obs	W	V	z	Prob>z
crppr12m	10	0.77142	3.523	2.483	0.00651

. sktest crpmeanchange if menopausal ==0

Skewness/Kurtosis tests for Normality					joint
Variable	Obs	Pr(Skewness)	Pr(Kurtosis)	adj chi2(2)	Prob>chi2
crpmeanchange	10	0.0003	0.0011	15.73	0.0004

. swilk crpmeanchange if menopausal ==0

Shapiro-Wilk w test for normal data					
Variable	Obs	W	V	z	Prob>z
crpmeanchange	10	0.54210	7.057	4.236	0.00001



. sktest bocrp if menopausal ==1

Skewness/Kurtosis tests for Normality					
Variable	Obs	Pr(Skewness)	Pr(Kurtosis)	adj chi2(2)	joint Prob>chi2
bocrp	23	0.0245	0.9613	5.00	0.0821

. swilk bocrp if menopausal ==1

Shapiro-wilk w test for normal data					
Variable	Obs	W	V	z	Prob>z
bocrp	23	0.77723	5.827	3.584	0.00017

. sktest crp12m if menopausal ==1

Skewness/Kurtosis tests for Normality					
Variable	Obs	Pr(Skewness)	Pr(Kurtosis)	adj chi2(2)	joint Prob>chi2
crp12m	23	0.0005	0.0030	15.49	0.0004

. swilk crp12m if menopausal ==1

Shapiro-wilk w test for normal data					
Variable	Obs	W	V	z	Prob>z
crp12m	23	0.80822	5.016	3.279	0.00052

. sktest crpc12m if menopausal ==1

Skewness/Kurtosis tests for Normality					
Variable	Obs	Pr(Skewness)	Pr(Kurtosis)	adj chi2(2)	joint Prob>chi2
crpc12m	20	0.0462	0.9233	4.21	0.1220

. swilk crpc12m if menopausal ==1

Shapiro-wilk w test for normal data					
Variable	Obs	W	V	z	Prob>z
crpc12m	20	0.85556	3.419	2.478	0.00661

. sktest crppr12m if menopausal ==1

Skewness/Kurtosis tests for Normality					
Variable	Obs	Pr(Skewness)	Pr(Kurtosis)	adj chi2(2)	joint Prob>chi2
crppr12m	20	0.0000	0.0000	28.78	0.0000

. swilk crppr12m if menopausal ==1

Shapiro-wilk w test for normal data					
Variable	Obs	W	V	z	Prob>z
crppr12m	20	0.50908	11.620	4.943	0.00000

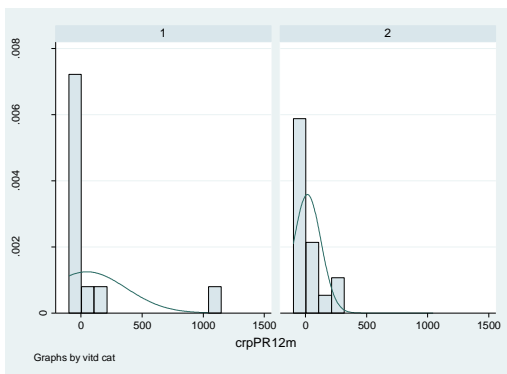
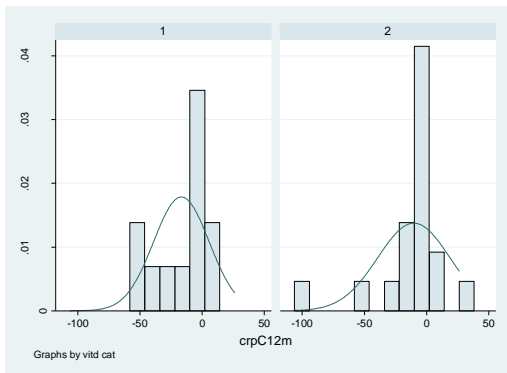
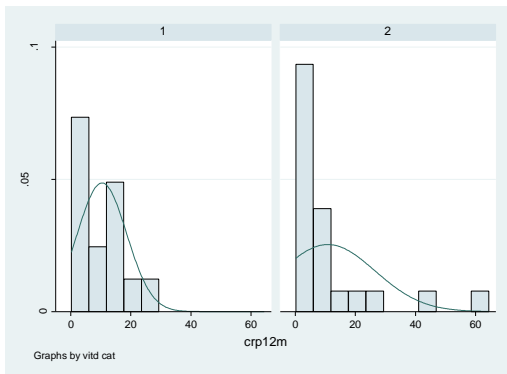
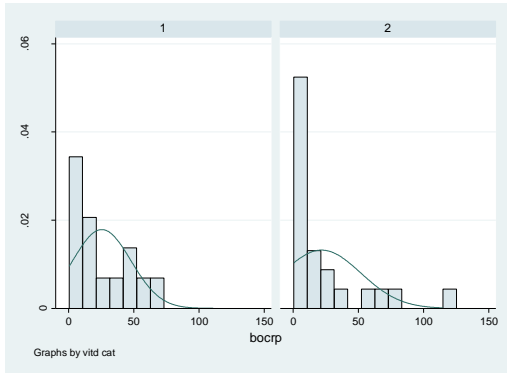
. sktest crpmeanchange if menopausal ==1

Skewness/Kurtosis tests for Normality					
Variable	Obs	Pr(Skewness)	Pr(Kurtosis)	adj chi2(2)	joint Prob>chi2
crpmeancha~e	20	0.0055	0.1637	8.15	0.0170

. swilk crpmeanchange if menopausal ==1

Shapiro-wilk w test for normal data					
Variable	Obs	W	V	z	Prob>z
crpmeancha~e	20	0.76021	5.676	3.499	0.00023

- By vitamin D category



. sktest bocrp if vitdcat ==1

Skewness/Kurtosis tests for Normality					
Variable	Obs	Pr(Skewness)	Pr(Kurtosis)	adj chi2(2)	joint Prob>chi2
bocrp	14	0.2525	0.3590	2.50	0.2861

. swilk bocrp if vitdcat ==1

Shapiro-Wilk W test for normal data					
Variable	Obs	W	V	z	Prob>z
bocrp	14	0.88856	2.062	1.425	0.07706

. sktest crp12m if vitdcat ==1

Skewness/Kurtosis tests for Normality					
Variable	Obs	Pr(Skewness)	Pr(Kurtosis)	adj chi2(2)	joint Prob>chi2
crp12m	14	0.1860	0.5993	2.35	0.3090

. swilk crp12m if vitdcat ==1

Shapiro-Wilk W test for normal data					
Variable	Obs	W	V	z	Prob>z
crp12m	14	0.89638	1.918	1.282	0.09994

. sktest crpc12m if vitdcat ==1

Skewness/Kurtosis tests for Normality					
Variable	Obs	Pr(Skewness)	Pr(Kurtosis)	adj chi2(2)	joint Prob>chi2
crpc12m	12	0.2397	0.6158	1.89	0.3881

. swilk crpc12m if vitdcat ==1

Shapiro-Wilk W test for normal data					
Variable	Obs	W	V	z	Prob>z
crpc12m	12	0.90528	1.583	0.895	0.18553

. sktest crppr12m if vitdcat ==1

Skewness/Kurtosis tests for Normality					
Variable	Obs	Pr(Skewness)	Pr(Kurtosis)	adj chi2(2)	joint Prob>chi2
crppr12m	12	0.0000	0.0002	19.91	0.0000

. swilk crppr12m if vitdcat ==1

Shapiro-Wilk W test for normal data					
Variable	Obs	W	V	z	Prob>z
crppr12m	12	0.47860	8.712	4.218	0.00001

. sktest bocrp if vitdcat ==2

Skewness/Kurtosis tests for Normality					
Variable	obs	Pr(Skewness)	Pr(Kurtosis)	adj chi2(2)	joint Prob>chi2
bocrp	22	0.0010	0.0190	12.55	0.0019

. swilk bocrp if vitdcat ==2

Shapiro-wilk W test for normal data					
Variable	Obs	W	V	z	Prob>z
bocrp	22	0.73292	6.766	3.877	0.00005

. sktest crp12m if vitdcat ==2

Skewness/Kurtosis tests for Normality					
Variable	obs	Pr(Skewness)	Pr(Kurtosis)	adj chi2(2)	joint Prob>chi2
crp12m	22	0.0001	0.0012	18.89	0.0001

. swilk crp12m if vitdcat ==2

Shapiro-wilk W test for normal data					
Variable	Obs	W	V	z	Prob>z
crp12m	22	0.65551	8.727	4.393	0.00001

. sktest crpc12m if vitdcat ==2

Skewness/Kurtosis tests for Normality					
Variable	obs	Pr(Skewness)	Pr(Kurtosis)	adj chi2(2)	joint Prob>chi2
crpc12m	18	0.0003	0.0012	16.89	0.0002

. swilk crpc12m if vitdcat ==2

Shapiro-wilk W test for normal data					
Variable	Obs	W	V	z	Prob>z
crpc12m	18	0.74530	5.599	3.448	0.00028

. sktest crppr12m if vitdcat ==2

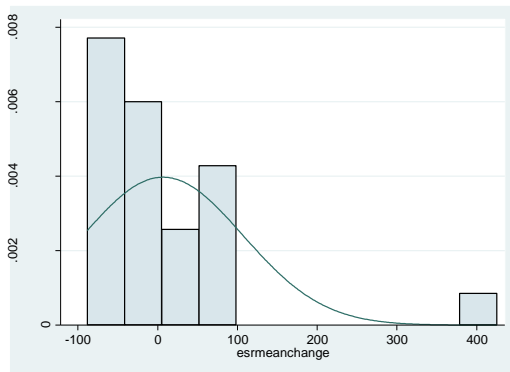
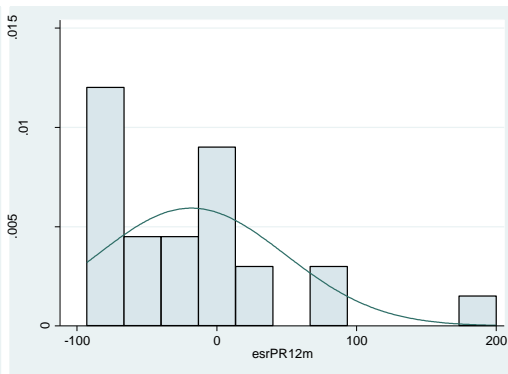
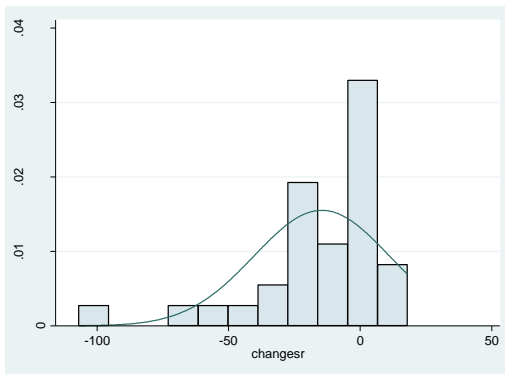
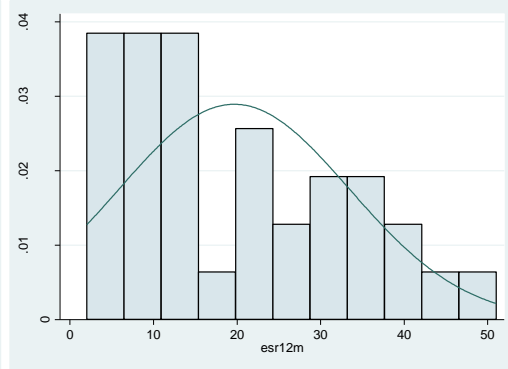
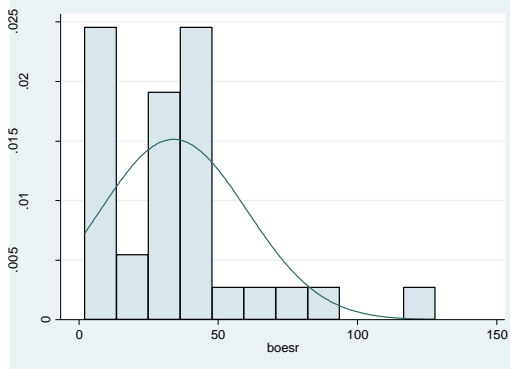
Skewness/Kurtosis tests for Normality					
Variable	obs	Pr(Skewness)	Pr(Kurtosis)	adj chi2(2)	joint Prob>chi2
crppr12m	18	0.0176	0.1754	6.68	0.0354

. swilk crppr12m if vitdcat ==2

Shapiro-wilk W test for normal data					
Variable	Obs	W	V	z	Prob>z
crppr12m	18	0.86483	2.971	2.180	0.01464

# ESR

- All



. sktest boesr

Skewness/Kurtosis tests for Normality					
Variable	Obs	Pr(Skewness)	Pr(Kurtosis)	adj chi2(2)	joint Prob>chi2
boesr	33	0.0006	0.0039	15.32	0.0005

. swilk boesr

Shapiro-wilk w test for normal data					
Variable	Obs	W	V	z	Prob>z
boesr	33	0.85760	4.861	3.289	0.00050

. sktest esr12m

Skewness/Kurtosis tests for Normality					
Variable	Obs	Pr(Skewness)	Pr(Kurtosis)	adj chi2(2)	joint Prob>chi2
esr12m	35	0.1670	0.1534	4.13	0.1269

. swilk esr12m

Shapiro-wilk w test for normal data					
Variable	Obs	W	V	z	Prob>z
esr12m	35	0.92415	2.707	2.079	0.01881

. sktest esrc12m

Skewness/Kurtosis tests for Normality					
Variable	Obs	Pr(Skewness)	Pr(Kurtosis)	adj chi2(2)	joint Prob>chi2
esrc12m	25	0.0003	0.0027	16.08	0.0003

. swilk esrc12m

Shapiro-wilk w test for normal data					
Variable	Obs	W	V	z	Prob>z
esrc12m	25	0.81836	5.047	3.309	0.00047

. sktest esrpr12m

Skewness/Kurtosis tests for Normality					
Variable	Obs	Pr(Skewness)	Pr(Kurtosis)	adj chi2(2)	joint Prob>chi2
esrpr12m	25	0.0035	0.0150	11.38	0.0034

. swilk esrpr12m

Shapiro-wilk w test for normal data					
Variable	Obs	W	V	z	Prob>z
esrpr12m	25	0.87611	3.443	2.527	0.00575

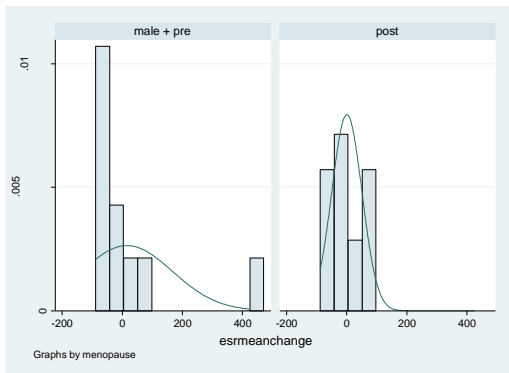
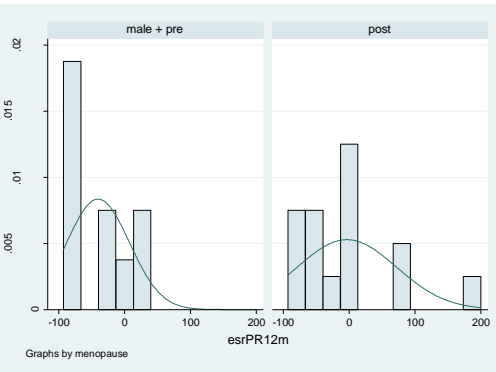
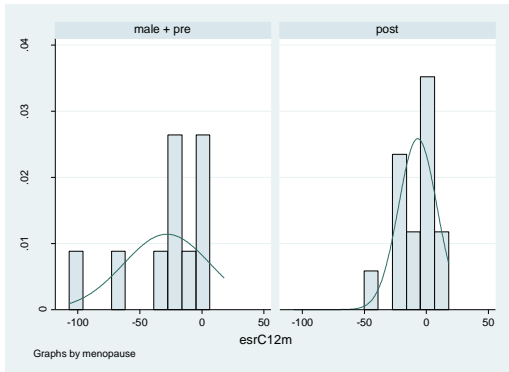
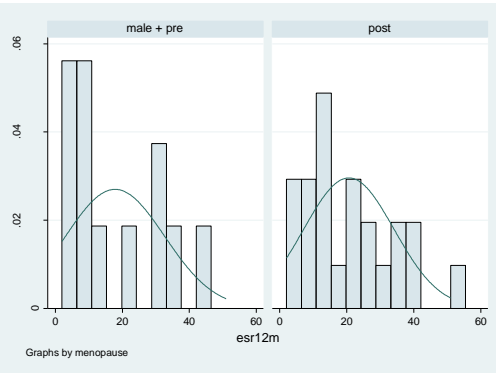
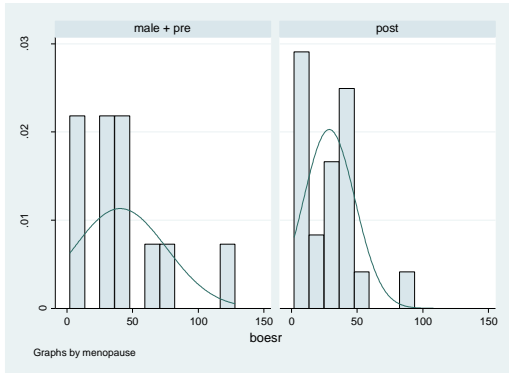
. sktest esrmeanchange

Skewness/Kurtosis tests for Normality					
Variable	Obs	Pr(Skewness)	Pr(Kurtosis)	adj chi2(2)	joint Prob>chi2
esrmeanchange	25	0.0000	0.0000	27.83	0.0000

. swilk esrmeanchange

Shapiro-wilk w test for normal data					
Variable	Obs	W	V	z	Prob>z
esrmeanchange	25	0.66685	9.257	4.549	0.00000

- **By gender and menopausal status**



. sktest boesr if menopausal ==0

Skewness/Kurtosis tests for Normality					
Variable	Obs	Pr(Skewness)	Pr(Kurtosis)	adj chi2(2)	joint Prob>chi2
boesr	12	0.0333	0.0698	6.81	0.0333

. swilk boesr if menopausal ==0

Shapiro-Wilk w test for normal data					
Variable	Obs	W	V	z	Prob>z
boesr	12	0.87354	2.113	1.458	0.07247

. sktest esr12m if menopausal ==0

Skewness/Kurtosis tests for Normality					
Variable	Obs	Pr(Skewness)	Pr(Kurtosis)	adj chi2(2)	joint Prob>chi2
esr12m	12	0.3155	0.1394	3.67	0.1600

. swilk esr12m if menopausal ==0

Shapiro-Wilk w test for normal data					
Variable	Obs	W	V	z	Prob>z
esr12m	12	0.85098	2.490	1.777	0.03775

. sktest esrc12m if menopausal ==0

Skewness/Kurtosis tests for Normality					
Variable	Obs	Pr(Skewness)	Pr(Kurtosis)	adj chi2(2)	joint Prob>chi2
esrc12m	10	0.0330	0.1485	5.97	0.0505

. swilk esrc12m if menopausal ==0

Shapiro-Wilk w test for normal data					
Variable	Obs	W	V	z	Prob>z
esrc12m	10	0.84386	2.406	1.654	0.04907

. sktest esrpr12m if menopausal ==0

Skewness/Kurtosis tests for Normality					
Variable	Obs	Pr(Skewness)	Pr(Kurtosis)	adj chi2(2)	joint Prob>chi2
esrpr12m	10	0.4428	0.2893	2.01	0.3657

. swilk esrpr12m if menopausal ==0

Shapiro-Wilk w test for normal data					
Variable	Obs	W	V	z	Prob>z
esrpr12m	10	0.90035	1.536	0.769	0.22105

. sktest esrmeanchange if menopausal ==0

Skewness/Kurtosis tests for Normality					
Variable	Obs	Pr(Skewness)	Pr(Kurtosis)	adj chi2(2)	joint Prob>chi2
esrmeanchange	10	0.0005	0.0017	14.61	0.0007

. swilk esrmeanchange if menopausal ==0

Shapiro-Wilk w test for normal data					
Variable	Obs	W	V	z	Prob>z
esrmeanchange	10	0.63686	5.596	3.611	0.00015



. sktest boesr if menopausal ==1

Skewness/Kurtosis tests for Normality					
Variable	Obs	Pr(Skewness)	Pr(Kurtosis)	adj chi2(2)	joint Prob>chi2
boesr	21	0.0278	0.0753	7.07	0.0292

. swilk boesr if menopausal ==1

Shapiro-wilk w test for normal data					
Variable	Obs	W	V	z	Prob>z
boesr	21	0.88261	2.877	2.136	0.01633

. sktest esr12m if menopausal ==1

Skewness/Kurtosis tests for Normality					
Variable	Obs	Pr(Skewness)	Pr(Kurtosis)	adj chi2(2)	joint Prob>chi2
esr12m	23	0.2130	0.7195	1.85	0.3961

. swilk esr12m if menopausal ==1

Shapiro-wilk w test for normal data					
Variable	Obs	W	V	z	Prob>z
esr12m	23	0.94705	1.385	0.662	0.25395

. sktest esrc12m if menopausal ==1

Skewness/Kurtosis tests for Normality					
Variable	Obs	Pr(Skewness)	Pr(Kurtosis)	adj chi2(2)	joint Prob>chi2
esrc12m	15	0.2695	0.6737	1.58	0.4546

. swilk esrc12m if menopausal ==1

Shapiro-wilk w test for normal data					
Variable	Obs	W	V	z	Prob>z
esrc12m	15	0.96034	0.769	-0.520	0.69836

. sktest esrpr12m if menopausal ==1

Skewness/Kurtosis tests for Normality					
Variable	Obs	Pr(Skewness)	Pr(Kurtosis)	adj chi2(2)	joint Prob>chi2
esrpr12m	15	0.0168	0.0518	7.97	0.0186

. swilk esrpr12m if menopausal ==1

Shapiro-wilk w test for normal data					
Variable	Obs	W	V	z	Prob>z
esrpr12m	15	0.88217	2.285	1.634	0.05112

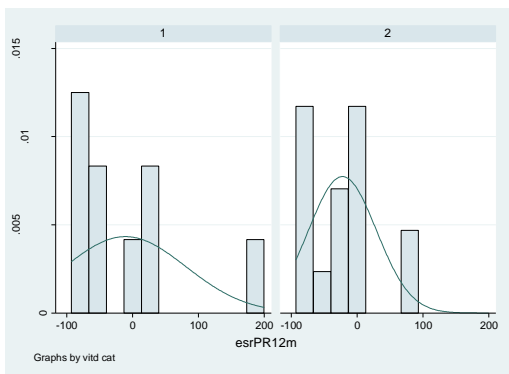
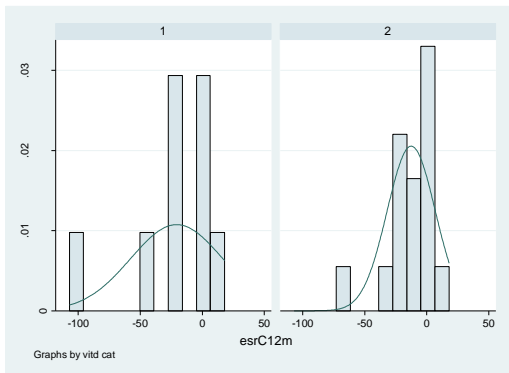
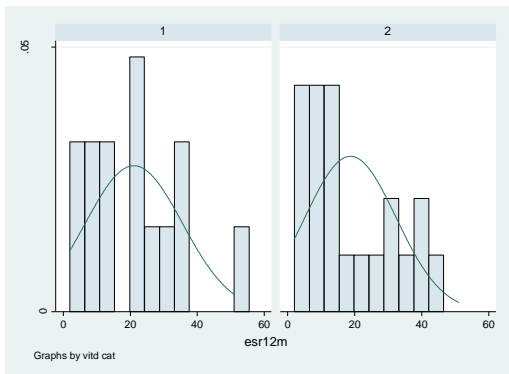
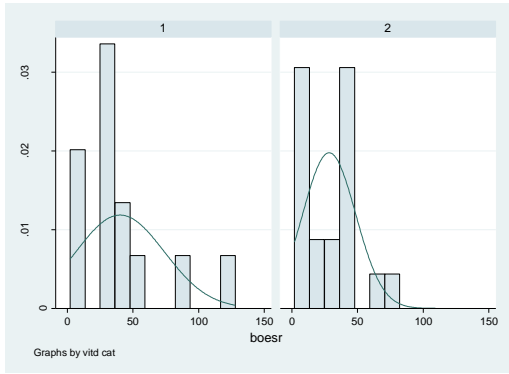
. sktest esrmeanchange if menopausal ==1

Skewness/Kurtosis tests for Normality					
Variable	Obs	Pr(Skewness)	Pr(Kurtosis)	adj chi2(2)	joint Prob>chi2
esrmeancha~e	15	0.6199	0.1093	3.29	0.1930

. swilk esrmeanchange if menopausal ==1

Shapiro-wilk w test for normal data					
Variable	Obs	W	V	z	Prob>z
esrmeancha~e	15	0.93680	1.225	0.402	0.34379

- By vitamin D category



. sktest boesr if vitdcat ==1

Skewness/Kurtosis tests for Normality

Variable	Obs	Pr(Skewness)	Pr(Kurtosis)	adj	chi2(2)	joint	Prob>chi2
boesr	13	0.0085	0.0370		9.00		0.0111

. swilk boesr if vitdcat ==1

Shapiro-Wilk W test for normal data

Variable	Obs	W	V	z	Prob>z
boesr	13	0.81552	3.249	2.309	0.01048

. sktest esr12m if vitdcat ==1

Skewness/Kurtosis tests for Normality

Variable	Obs	Pr(Skewness)	Pr(Kurtosis)	adj	chi2(2)	joint	Prob>chi2
esr12m	14	0.4028	0.9108		0.77		0.6812

. swilk esr12m if vitdcat ==1

Shapiro-Wilk W test for normal data

Variable	Obs	W	V	z	Prob>z
esr12m	14	0.95480	0.836	-0.352	0.63744

. sktest esrc12m if vitdcat ==1

Skewness/Kurtosis tests for Normality

Variable	Obs	Pr(Skewness)	Pr(Kurtosis)	adj	chi2(2)	joint	Prob>chi2
esrc12m	9	0.0171	0.0376		7.88		0.0195

. swilk esrc12m if vitdcat ==1

Shapiro-Wilk W test for normal data

Variable	Obs	W	V	z	Prob>z
esrc12m	9	0.83739	2.389	1.607	0.05401

. sktest esrpr12m if vitdcat ==1

Skewness/Kurtosis tests for Normality

Variable	Obs	Pr(Skewness)	Pr(Kurtosis)	adj	chi2(2)	joint	Prob>chi2
esrpr12m	9	0.0213	0.0589		7.23		0.0269

. swilk esrpr12m if vitdcat ==1

Shapiro-Wilk W test for normal data

Variable	Obs	W	V	z	Prob>z
esrpr12m	9	0.82729	2.537	1.732	0.04163

. sktest boesr if vitdcat ==2

Skewness/Kurtosis tests for Normality					
Variable	Obs	Pr(Skewness)	Pr(Kurtosis)	adj chi2(2)	joint Prob>chi2
boesr	20	0.3267	0.7539	1.16	0.5607

. swilk boesr if vitdcat ==2

Shapiro-Wilk W test for normal data					
Variable	Obs	W	V	z	Prob>z
boesr	20	0.92783	1.708	1.079	0.14026

. sktest esr12m if vitdcat ==2

Skewness/Kurtosis tests for Normality					
Variable	Obs	Pr(Skewness)	Pr(Kurtosis)	adj chi2(2)	joint Prob>chi2
esr12m	21	0.2072	0.1187	4.23	0.1204

. swilk esr12m if vitdcat ==2

Shapiro-Wilk W test for normal data					
Variable	Obs	W	V	z	Prob>z
esr12m	21	0.88770	2.752	2.047	0.02035

. sktest esrc12m if vitdcat ==2

Skewness/Kurtosis tests for Normality					
Variable	Obs	Pr(Skewness)	Pr(Kurtosis)	adj chi2(2)	joint Prob>chi2
esrc12m	16	0.0078	0.0257	9.62	0.0082

. swilk esrc12m if vitdcat ==2

Shapiro-Wilk W test for normal data					
Variable	Obs	W	V	z	Prob>z
esrc12m	16	0.85971	2.842	2.075	0.01899

. sktest esrpr12m if vitdcat ==2

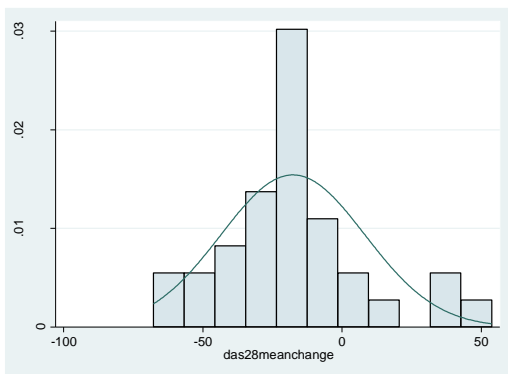
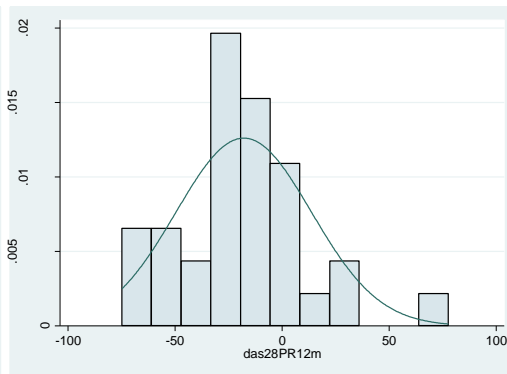
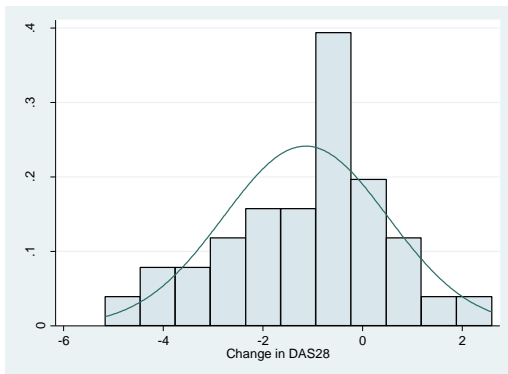
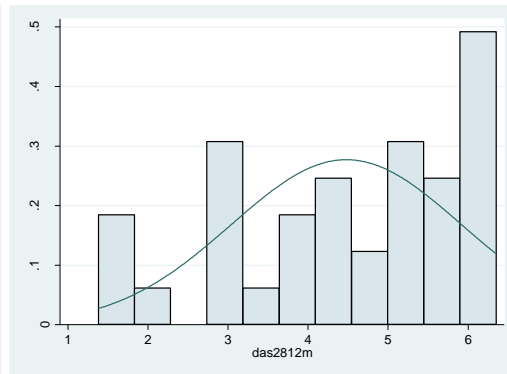
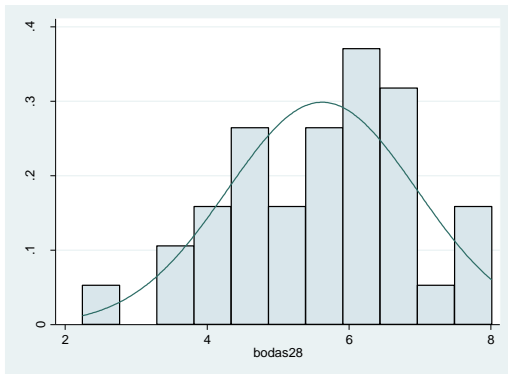
Skewness/Kurtosis tests for Normality					
Variable	Obs	Pr(Skewness)	Pr(Kurtosis)	adj chi2(2)	joint Prob>chi2
esrpr12m	16	0.3500	0.9620	0.96	0.6202

. swilk esrpr12m if vitdcat ==2

Shapiro-Wilk W test for normal data					
Variable	Obs	W	V	z	Prob>z
esrpr12m	16	0.95042	1.004	0.009	0.49645

# DAS28 score

- All



. sktest bodas28

Skewness/Kurtosis tests for Normality					
Variable	Obs	Pr(Skewness)	Pr(Kurtosis)	adj chi2(2)	joint Prob>chi2
bodas28	36	0.2656	0.9371	1.32	0.5163

. swilk bodas28

Shapiro-wilk w test for normal data					
Variable	Obs	W	V	z	Prob>z
bodas28	36	0.98072	0.703	-0.737	0.76945

. sktest das2812m

Skewness/Kurtosis tests for Normality					
Variable	Obs	Pr(Skewness)	Pr(Kurtosis)	adj chi2(2)	joint Prob>chi2
das2812m	36	0.1302	0.3531	3.41	0.1816

. swilk das2812m

Shapiro-wilk w test for normal data					
Variable	Obs	W	V	z	Prob>z
das2812m	36	0.92791	2.629	2.021	0.02164

. sktest das28c12m

Skewness/Kurtosis tests for Normality					
Variable	Obs	Pr(Skewness)	Pr(Kurtosis)	adj chi2(2)	joint Prob>chi2
das28c12m	33	0.3720	0.5723	1.19	0.5526

. swilk das28c12m

Shapiro-wilk w test for normal data					
Variable	Obs	W	V	z	Prob>z
das28c12m	33	0.97627	0.810	-0.438	0.66920

. sktest das28pr12m

Skewness/Kurtosis tests for Normality					
Variable	Obs	Pr(Skewness)	Pr(Kurtosis)	adj chi2(2)	joint Prob>chi2
das28pr12m	33	0.1323	0.0769	5.23	0.0731

. swilk das28pr12m

Shapiro-wilk w test for normal data					
Variable	Obs	W	V	z	Prob>z
das28pr12m	33	0.94203	1.979	1.420	0.07784

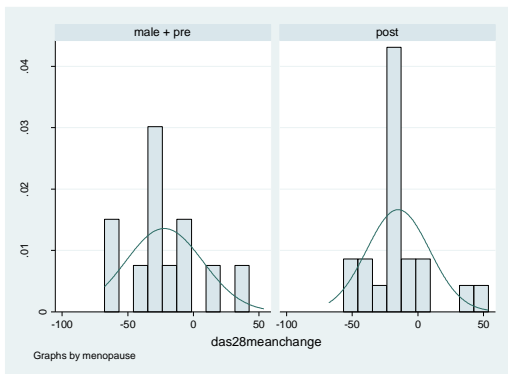
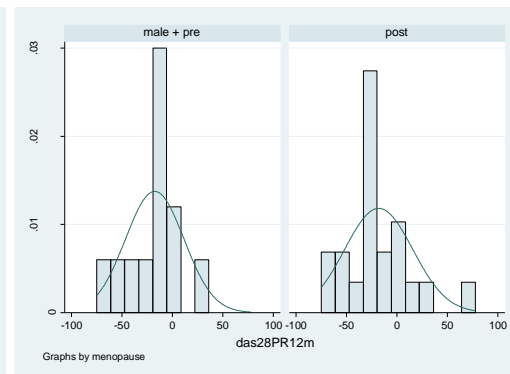
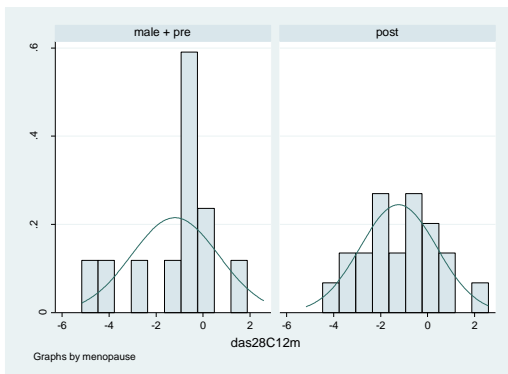
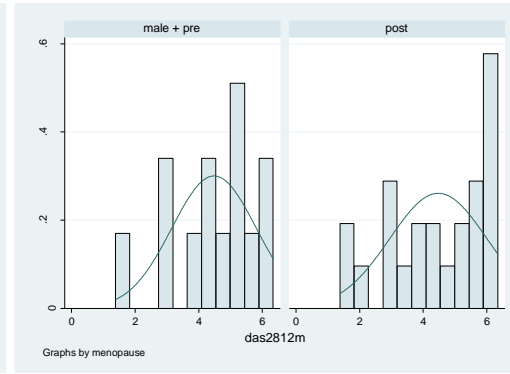
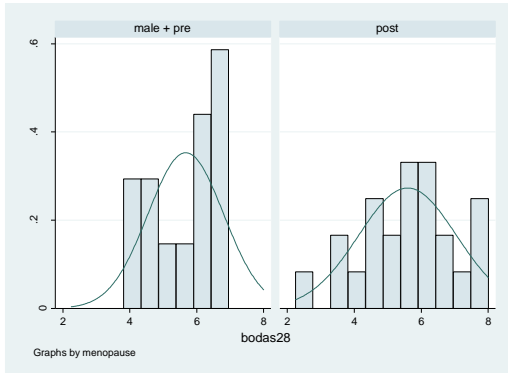
. sktest das28meanchange

Skewness/Kurtosis tests for Normality					
Variable	Obs	Pr(Skewness)	Pr(Kurtosis)	adj chi2(2)	joint Prob>chi2
das28meanc~e	33	0.0385	0.0949	6.45	0.0397

. swilk das28meanchange

Shapiro-wilk w test for normal data					
Variable	Obs	W	V	z	Prob>z
das28meanc~e	33	0.93243	2.307	1.739	0.04106

# - By gender and menopausal status



. sktest bodas28 if menopausal ==0

Skewness/Kurtosis tests for Normality

Variable	Obs	Pr(Skewness)	Pr(Kurtosis)	adj chi2(2)	joint Prob>chi2
bodas28	13	0.4278	0.1638	3.04	0.2190

. swilk bodas28 if menopausal ==0

Shapiro-Wilk w test for normal data

Variable	Obs	W	V	z	Prob>z
bodas28	13	0.89243	1.895	1.252	0.10530

. sktest das2812m if menopausal ==0

Skewness/Kurtosis tests for Normality

Variable	Obs	Pr(Skewness)	Pr(Kurtosis)	adj chi2(2)	joint Prob>chi2
das2812m	13	0.2580	0.9426	1.46	0.4830

. swilk das2812m if menopausal ==0

Shapiro-Wilk w test for normal data

Variable	Obs	W	V	z	Prob>z
das2812m	13	0.95371	0.815	-0.400	0.65540

. sktest das28c12m if menopausal ==0

Skewness/Kurtosis tests for Normality

Variable	Obs	Pr(Skewness)	Pr(Kurtosis)	adj chi2(2)	joint Prob>chi2
das28c12m	12	0.0763	0.3814	4.19	0.1230

. swilk das28c12m if menopausal ==0

Shapiro-Wilk w test for normal data

Variable	Obs	W	V	z	Prob>z
das28c12m	12	0.87920	2.018	1.368	0.08561

. sktest das28pr12m if menopausal ==0

Skewness/Kurtosis tests for Normality

Variable	Obs	Pr(Skewness)	Pr(Kurtosis)	adj chi2(2)	joint Prob>chi2
das28pr12m	12	0.4649	0.3980	1.42	0.4925

. swilk das28pr12m if menopausal ==0

Shapiro-Wilk w test for normal data

Variable	Obs	W	V	z	Prob>z
das28pr12m	12	0.94441	0.929	-0.144	0.55722

. sktest das28meanchange if menopausal ==0

Skewness/Kurtosis tests for Normality

Variable	Obs	Pr(Skewness)	Pr(Kurtosis)	adj chi2(2)	joint Prob>chi2
das28meanc~e	12	0.2915	0.3147	2.50	0.2859

. swilk das28meanchange if menopausal ==0

Shapiro-Wilk w test for normal data

Variable	Obs	W	V	z	Prob>z
das28meanc~e	12	0.95846	0.694	-0.712	0.76170



. sktest bodas28 if menopausal ==1

Skewness/Kurtosis tests for Normality					
Variable	Obs	Pr(Skewness)	Pr(Kurtosis)	adj chi2(2)	joint Prob>chi2
bodas28	23	0.3932	0.8145	0.84	0.6582

. swilk bodas28 if menopausal ==1

Shapiro-wilk w test for normal data					
Variable	Obs	W	V	z	Prob>z
bodas28	23	0.97766	0.584	-1.092	0.86263

. sktest das2812m if menopausal ==1

Skewness/Kurtosis tests for Normality					
Variable	Obs	Pr(Skewness)	Pr(Kurtosis)	adj chi2(2)	joint Prob>chi2
das2812m	23	0.2143	0.3937	2.53	0.2824

. swilk das2812m if menopausal ==1

Shapiro-wilk w test for normal data					
Variable	Obs	W	V	z	Prob>z
das2812m	23	0.92097	2.067	1.477	0.06987

. sktest das28c12m if menopausal ==1

Skewness/Kurtosis tests for Normality					
Variable	Obs	Pr(Skewness)	Pr(Kurtosis)	adj chi2(2)	joint Prob>chi2
das28c12m	21	0.6848	0.5452	0.56	0.7575

. swilk das28c12m if menopausal ==1

Shapiro-wilk w test for normal data					
Variable	Obs	W	V	z	Prob>z
das28c12m	21	0.98465	0.376	-1.977	0.97596

. sktest das28pr12m if menopausal ==1

Skewness/Kurtosis tests for Normality					
Variable	Obs	Pr(Skewness)	Pr(Kurtosis)	adj chi2(2)	joint Prob>chi2
das28pr12m	21	0.0537	0.0591	6.57	0.0374

. swilk das28pr12m if menopausal ==1

Shapiro-wilk w test for normal data					
Variable	Obs	W	V	z	Prob>z
das28pr12m	21	0.92105	1.935	1.334	0.09106

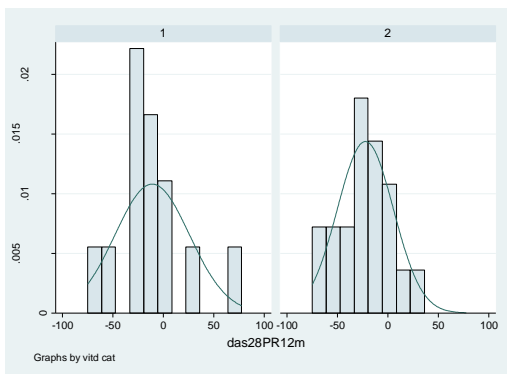
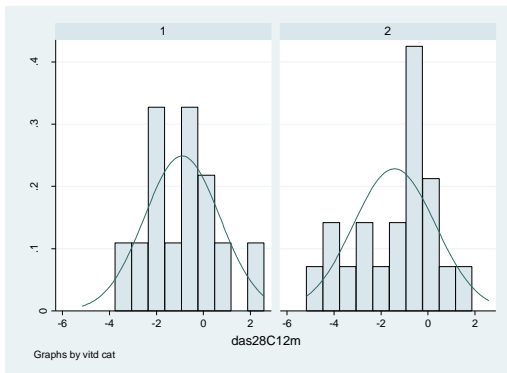
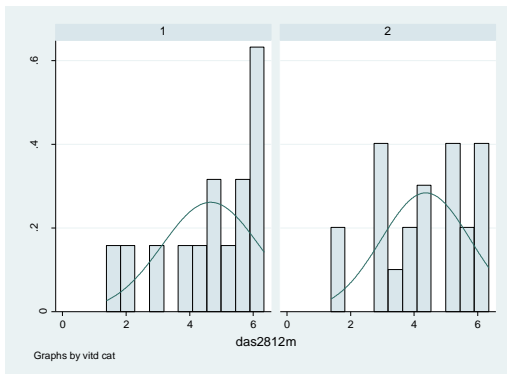
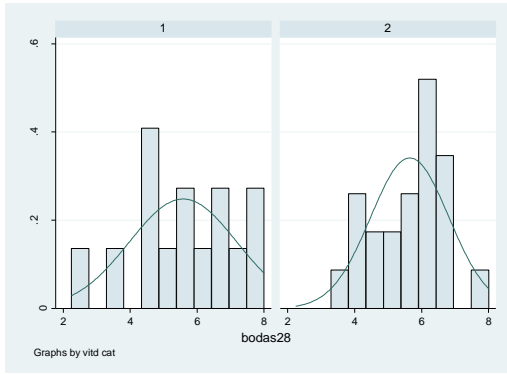
. sktest das28meanchange if menopausal ==1

Skewness/Kurtosis tests for Normality					
Variable	Obs	Pr(Skewness)	Pr(Kurtosis)	adj chi2(2)	joint Prob>chi2
das28meanc~e	21	0.0112	0.0359	8.95	0.0114

. swilk das28meanchange if menopausal ==1

Shapiro-wilk w test for normal data					
Variable	Obs	W	V	z	Prob>z
das28meanc~e	21	0.86766	3.243	2.378	0.00869

# - By vitamin D category



. sktest bodas28 if vitdcat ==1

Skewness/Kurtosis tests for Normality

Variable	Obs	Pr(Skewness)	Pr(Kurtosis)	adj	chi2(2)	joint	Prob>chi2
bodas28	14	0.3335	0.9057		1.05		0.5923

. swilk bodas28 if vitdcat ==1

Shapiro-Wilk W test for normal data

Variable	Obs	W	V	z	Prob>z
bodas28	14	0.96614	0.627	-0.920	0.82127

. sktest das2812m if vitdcat ==1

Skewness/Kurtosis tests for Normality

Variable	Obs	Pr(Skewness)	Pr(Kurtosis)	adj	chi2(2)	joint	Prob>chi2
das2812m	14	0.1780	0.8575		2.13		0.3445

. swilk das2812m if vitdcat ==1

Shapiro-Wilk W test for normal data

Variable	Obs	W	V	z	Prob>z
das2812m	14	0.89946	1.861	1.223	0.11076

. sktest das28c12m if vitdcat ==1

Skewness/Kurtosis tests for Normality

Variable	Obs	Pr(Skewness)	Pr(Kurtosis)	adj	chi2(2)	joint	Prob>chi2
das28c12m	13	0.3978	0.4244		1.54		0.4634

. swilk das28c12m if vitdcat ==1

Shapiro-Wilk W test for normal data

Variable	Obs	W	V	z	Prob>z
das28c12m	13	0.96566	0.605	-0.985	0.83771

. sktest das28pr12m if vitdcat ==1

Skewness/Kurtosis tests for Normality

Variable	Obs	Pr(Skewness)	Pr(Kurtosis)	adj	chi2(2)	joint	Prob>chi2
das28pr12m	13	0.1026	0.1115		5.10		0.0781

. swilk das28pr12m if vitdcat ==1

Shapiro-Wilk W test for normal data

Variable	Obs	W	V	z	Prob>z
das28pr12m	13	0.90252	1.717	1.059	0.14480

. sktest bodas28 if vitdcat ==2

Skewness/Kurtosis tests for Normality

Variable	Obs	Pr(Skewness)	Pr(Kurtosis)	adj chi2(2)	joint Prob>chi2
bodas28	22	0.6918	0.7140	0.29	0.8644

. swilk bodas28 if vitdcat ==2

Shapiro-Wilk W test for normal data

Variable	Obs	W	V	z	Prob>z
bodas28	22	0.96625	0.855	-0.317	0.62455

. sktest das2812m if vitdcat ==2

Skewness/Kurtosis tests for Normality

Variable	Obs	Pr(Skewness)	Pr(Kurtosis)	adj chi2(2)	joint Prob>chi2
das2812m	22	0.2538	0.6100	1.72	0.4222

. swilk das2812m if vitdcat ==2

Shapiro-Wilk W test for normal data

Variable	Obs	W	V	z	Prob>z
das2812m	22	0.93319	1.693	1.067	0.14295

. sktest das28c12m if vitdcat ==2

Skewness/Kurtosis tests for Normality

Variable	Obs	Pr(Skewness)	Pr(Kurtosis)	adj chi2(2)	joint Prob>chi2
das28c12m	20	0.1554	0.9887	2.27	0.3219

. swilk das28c12m if vitdcat ==2

Shapiro-Wilk W test for normal data

Variable	Obs	W	V	z	Prob>z
das28c12m	20	0.93820	1.463	0.767	0.22166

. sktest das28pr12m if vitdcat ==2

Skewness/Kurtosis tests for Normality

Variable	Obs	Pr(Skewness)	Pr(Kurtosis)	adj chi2(2)	joint Prob>chi2
das28pr12m	20	0.6584	0.8192	0.25	0.8835

. swilk das28pr12m if vitdcat ==2

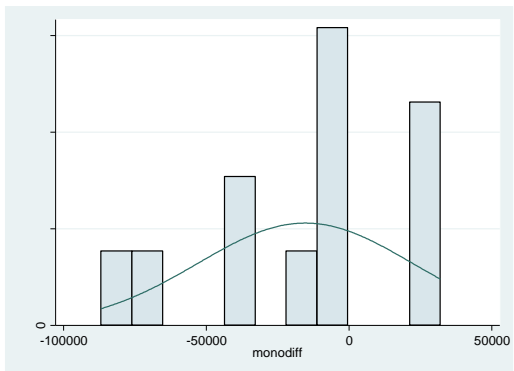
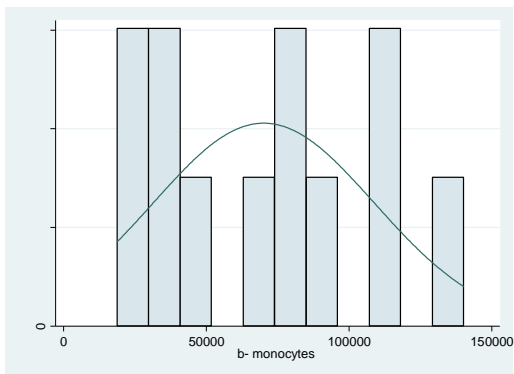
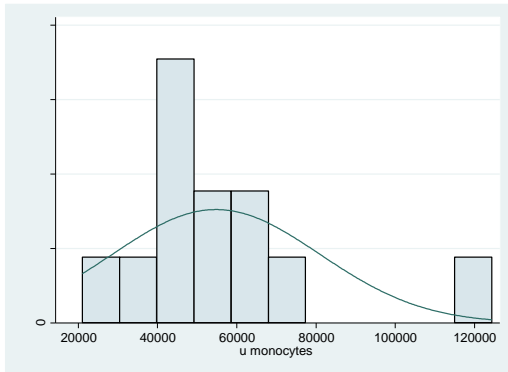
Shapiro-Wilk W test for normal data

Variable	Obs	W	V	z	Prob>z
das28pr12m	20	0.97138	0.678	-0.785	0.78364

## In vitro unfractionated and CD20 depleted PBMC comparisons

### Initial number of monocytes

- All



. sktest umonocytes

Skewness/Kurtosis tests for Normality					
Variable	Obs	Pr(Skewness)	Pr(Kurtosis)	adj chi2(2)	joint Prob>chi2
umonocytes	12	0.0096	0.0155	9.71	0.0078

. swilk umonocytes

Shapiro-wilk w test for normal data					
Variable	Obs	w	V	z	Prob>z
umonocytes	12	0.84724	2.552	1.826	0.03394

. sktest bmonocytes

Skewness/Kurtosis tests for Normality					
Variable	Obs	Pr(Skewness)	Pr(Kurtosis)	adj chi2(2)	joint Prob>chi2
bmonocytes	12	0.6643	0.4327	0.88	0.6449

. swilk bmonocytes

Shapiro-wilk w test for normal data					
Variable	Obs	w	V	z	Prob>z
bmonocytes	12	0.94967	0.841	-0.337	0.63211

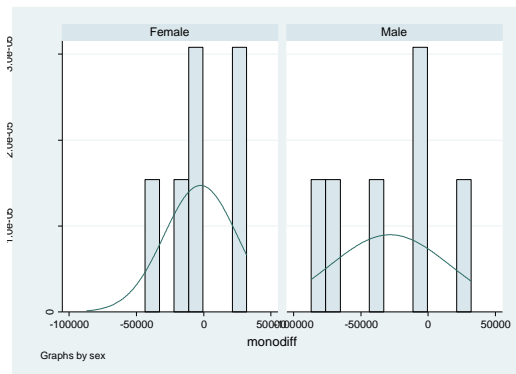
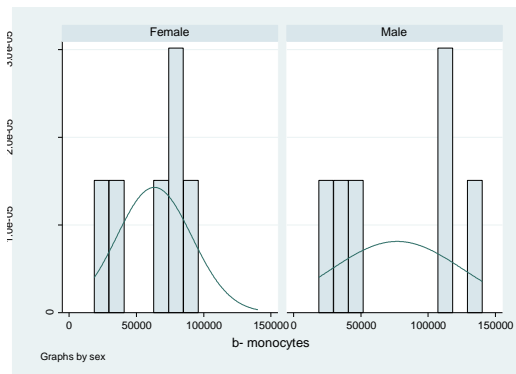
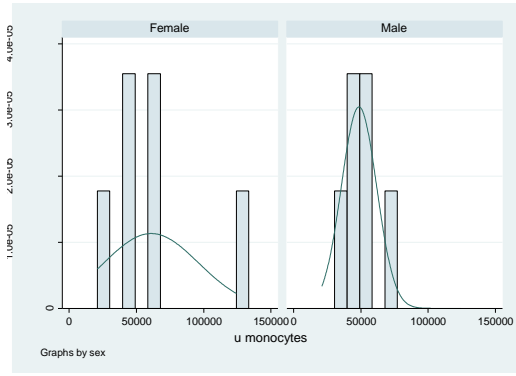
. sktest monodiff

Skewness/Kurtosis tests for Normality					
Variable	Obs	Pr(Skewness)	Pr(Kurtosis)	adj chi2(2)	joint Prob>chi2
monodiff	12	0.3728	0.9168	0.88	0.6445

. swilk monodiff

Shapiro-wilk w test for normal data					
Variable	Obs	w	V	z	Prob>z
monodiff	12	0.93331	1.114	0.211	0.41657

- **By gender**



. sktest umonocytes if gender ==0

Skewness/Kurtosis tests for Normality

Variable	Obs	Pr(Skewness)	Pr(Kurtosis)	adj chi2(2)	joint Prob>chi2
umonocytes	6	.	.	.	.

. swilk umonocytes if gender ==0

Shapiro-wilk W test for normal data

Variable	Obs	W	V	z	Prob>z
umonocytes	6	0.94492	0.682	-0.522	0.69904

. sktest bmonocytes if gender ==0

Skewness/Kurtosis tests for Normality

Variable	Obs	Pr(Skewness)	Pr(Kurtosis)	adj chi2(2)	joint Prob>chi2
bmonocytes	6	.	.	.	.

. swilk bmonocytes if gender ==0

Shapiro-wilk W test for normal data

Variable	Obs	W	V	z	Prob>z
bmonocytes	6	0.90635	1.160	0.220	0.41285

. sktest monodiff if gender ==0

Skewness/Kurtosis tests for Normality

Variable	Obs	Pr(Skewness)	Pr(Kurtosis)	adj chi2(2)	joint Prob>chi2
monodiff	6	.	.	.	.

. swilk monodiff if gender ==0

Shapiro-wilk W test for normal data

Variable	Obs	W	V	z	Prob>z
monodiff	6	0.96969	0.375	-1.228	0.89032

. sktest umonocytes if gender ==1

Skewness/Kurtosis tests for Normality

Variable	Obs	Pr(Skewness)	Pr(Kurtosis)	adj chi2(2)	joint Prob>chi2
umonocytes	6	.	.	.	.

. swilk umonocytes if gender ==1

Shapiro-wilk W test for normal data

Variable	Obs	W	V	z	Prob>z
umonocytes	6	0.90532	1.173	0.237	0.40634

. sktest bmonocytes if gender ==1

Skewness/Kurtosis tests for Normality

Variable	Obs	Pr(Skewness)	Pr(Kurtosis)	adj chi2(2)	joint Prob>chi2
bmonocytes	6	.	.	.	.

. swilk bmonocytes if gender ==1

Shapiro-wilk W test for normal data

Variable	Obs	W	V	z	Prob>z
bmonocytes	6	0.88370	1.440	0.564	0.28649

. sktest monodiff if gender ==1

Skewness/Kurtosis tests for Normality

Variable	Obs	Pr(Skewness)	Pr(Kurtosis)	adj chi2(2)	joint Prob>chi2
monodiff	6	.	.	.	.

. swilk monodiff if gender ==1

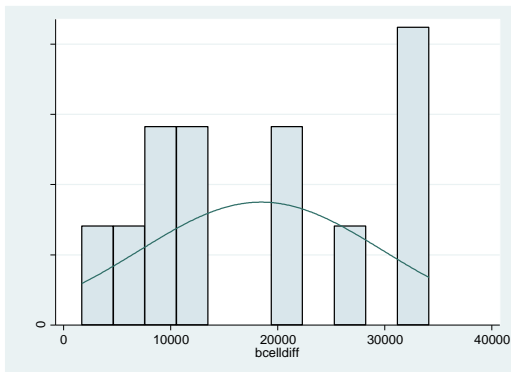
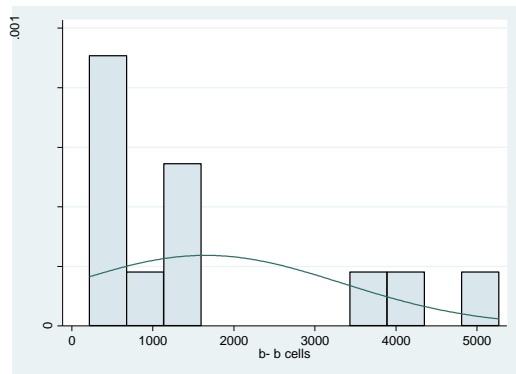
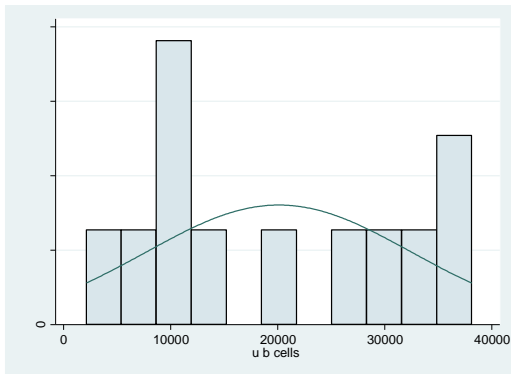
Shapiro-wilk W test for normal data

Variable	Obs	W	V	z	Prob>z
monodiff	6	0.94297	0.706	-0.477	0.68319



# Initial number of b cells

- All



. sktest ubcells

Skewness/Kurtosis tests for Normality					
Variable	Obs	Pr(Skewness)	Pr(Kurtosis)	adj chi2(2)	joint Prob>chi2
ubcells	12	0.7923	0.0882	3.50	0.1736

. swilk ubcells

Shapiro-wilk w test for normal data					
Variable	Obs	w	V	z	Prob>z
ubcells	12	0.92370	1.275	0.473	0.31805

. sktest bbcells

Skewness/Kurtosis tests for Normality					
Variable	Obs	Pr(Skewness)	Pr(Kurtosis)	adj chi2(2)	joint Prob>chi2
bbcells	12	0.0459	0.5659	4.48	0.1064

. swilk bbcells

Shapiro-wilk w test for normal data					
Variable	Obs	w	V	z	Prob>z
bbcells	12	0.79580	3.412	2.391	0.00840

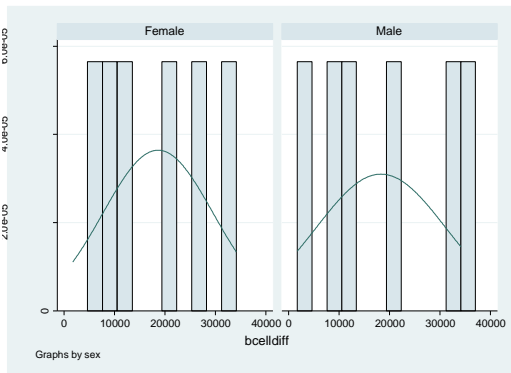
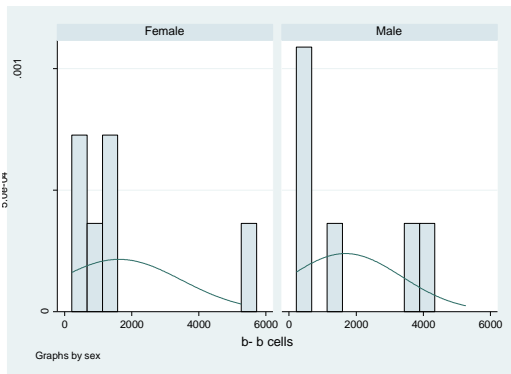
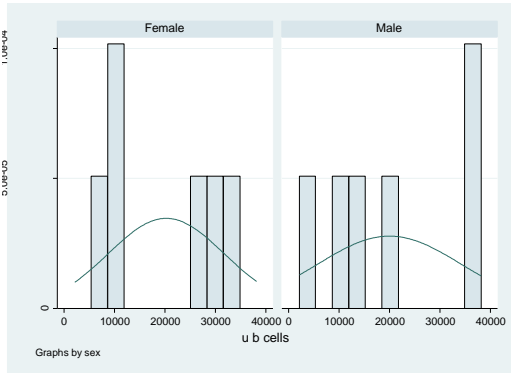
. sktest bcelldiff

Skewness/Kurtosis tests for Normality					
Variable	Obs	Pr(Skewness)	Pr(Kurtosis)	adj chi2(2)	joint Prob>chi2
bcelldiff	12	0.7648	0.1108	3.14	0.2076

. swilk bcelldiff

Shapiro-wilk w test for normal data					
Variable	Obs	w	V	z	Prob>z
bcelldiff	12	0.91836	1.364	0.605	0.27260

- **By gender**



. sktest ubcells if gender ==0

Skewness/Kurtosis tests for Normality

Variable	Obs	Pr(Skewness)	Pr(Kurtosis)	adj chi2(2)	joint Prob>chi2
ubcells	6	.	.	.	.

. swilk ubcells if gender ==0

Shapiro-wilk W test for normal data

Variable	Obs	W	V	z	Prob>z
ubcells	6	0.93448	0.811	-0.293	0.61509

. sktest bcells if gender ==0

Skewness/Kurtosis tests for Normality

Variable	Obs	Pr(Skewness)	Pr(Kurtosis)	adj chi2(2)	joint Prob>chi2
bcells	6	.	.	.	.

. swilk bcells if gender ==0

Shapiro-wilk W test for normal data

Variable	Obs	W	V	z	Prob>z
bcells	6	0.77791	2.750	1.788	0.03685

. sktest bcelldiff if gender ==0

Skewness/Kurtosis tests for Normality

Variable	Obs	Pr(Skewness)	Pr(Kurtosis)	adj chi2(2)	joint Prob>chi2
bcelldiff	6	.	.	.	.

. swilk bcelldiff if gender ==0

Shapiro-wilk W test for normal data

Variable	Obs	W	V	z	Prob>z
bcelldiff	6	0.94138	0.726	-0.441	0.67034

. sktest ubcells if gender ==1

Skewness/Kurtosis tests for Normality

Variable	Obs	Pr(Skewness)	Pr(Kurtosis)	adj chi2(2)	joint Prob>chi2
ubcells	6	.	.	.	.

. swilk ubcells if gender ==1

Shapiro-wilk W test for normal data

Variable	Obs	W	V	z	Prob>z
ubcells	6	0.88997	1.363	0.473	0.31803

. sktest bcells if gender ==1

Skewness/Kurtosis tests for Normality

Variable	Obs	Pr(Skewness)	Pr(Kurtosis)	adj chi2(2)	joint Prob>chi2
bcells	6	.	.	.	.

. swilk bcells if gender ==1

Shapiro-wilk W test for normal data

Variable	Obs	W	V	z	Prob>z
bcells	6	0.74360	3.175	2.115	0.01723

. sktest bcelldiff if gender ==1

Skewness/Kurtosis tests for Normality

Variable	Obs	Pr(Skewness)	Pr(Kurtosis)	adj chi2(2)	joint Prob>chi2
bcelldiff	6	.	.	.	.

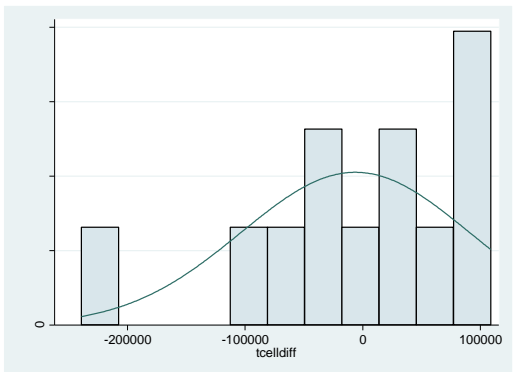
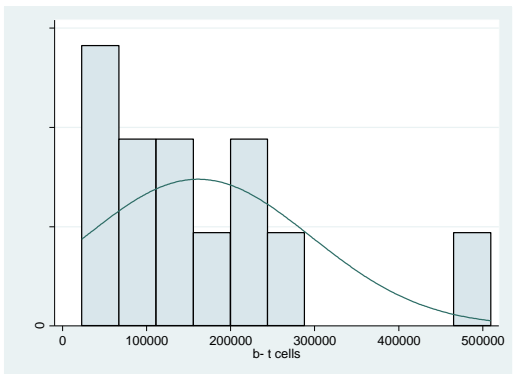
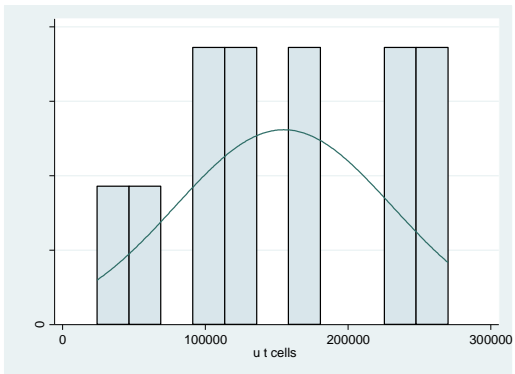
. swilk bcelldiff if gender ==1

Shapiro-wilk W test for normal data

Variable	Obs	W	V	z	Prob>z
bcelldiff	6	0.92236	0.962	-0.056	0.52252

# Initial number of t cells

- All



. sktest utcells

Skewness/Kurtosis tests for Normality					
Variable	Obs	Pr(Skewness)	Pr(Kurtosis)	adj chi2(2)	joint Prob>chi2
utcells	12	0.9858	0.4831	0.51	0.7750

. swilk utcells

Shapiro-wilk w test for normal data					
Variable	Obs	w	V	z	Prob>z
utcells	12	0.96038	0.662	-0.804	0.78922

. sktest btcells

Skewness/Kurtosis tests for Normality					
Variable	Obs	Pr(Skewness)	Pr(Kurtosis)	adj chi2(2)	joint Prob>chi2
btcells	12	0.0156	0.0350	8.34	0.0155

. swilk btcells

Shapiro-wilk w test for normal data					
Variable	Obs	w	V	z	Prob>z
btcells	12	0.85458	2.430	1.730	0.04184

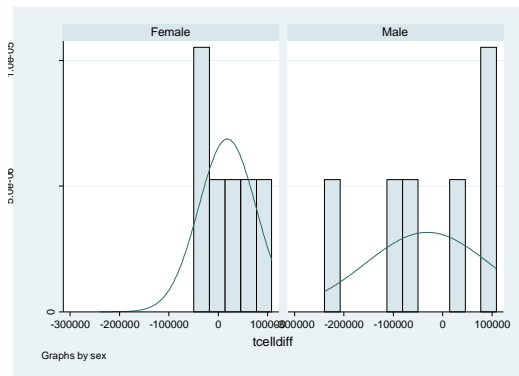
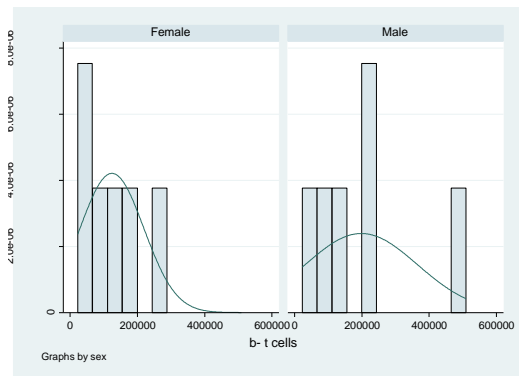
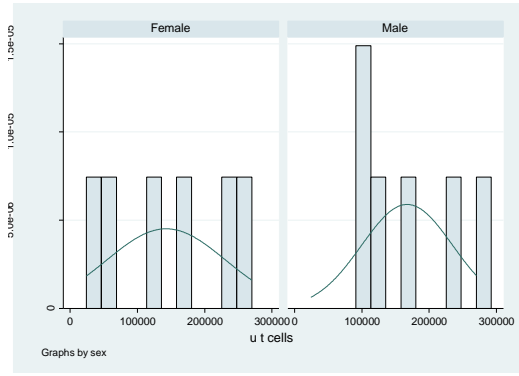
. sktest tcellldiff

Skewness/Kurtosis tests for Normality					
Variable	Obs	Pr(Skewness)	Pr(Kurtosis)	adj chi2(2)	joint Prob>chi2
tcellldiff	12	0.0585	0.1424	5.45	0.0655

. swilk tcellldiff

Shapiro-wilk w test for normal data					
Variable	Obs	w	V	z	Prob>z
tcellldiff	12	0.90470	1.592	0.906	0.18238

- **By gender**



. sktest utcells if gender ==0

Skewness/Kurtosis tests for Normality

Variable	Obs	Pr(Skewness)	Pr(Kurtosis)	adj chi2(2)	joint Prob>chi2
utcells	6	.	.	.	.

. swilk utcells if gender ==0

Shapiro-wilk W test for normal data

Variable	Obs	W	V	z	Prob>z
utcells	6	0.89854	1.256	0.344	0.36538

. sktest btcells if gender ==0

Skewness/Kurtosis tests for Normality

Variable	Obs	Pr(Skewness)	Pr(Kurtosis)	adj chi2(2)	joint Prob>chi2
btcells	6	.	.	.	.

. swilk btcells if gender ==0

Shapiro-wilk W test for normal data

Variable	Obs	W	V	z	Prob>z
btcells	6	0.86100	1.721	0.868	0.19262

. sktest tcelldiff if gender ==0

Skewness/Kurtosis tests for Normality

Variable	Obs	Pr(Skewness)	Pr(Kurtosis)	adj chi2(2)	joint Prob>chi2
tcelldiff	6	.	.	.	.

. swilk tcelldiff if gender ==0

Shapiro-wilk W test for normal data

Variable	Obs	W	V	z	Prob>z
tcelldiff	6	0.91078	1.105	0.147	0.44157

. sktest utcells if gender ==1

Skewness/Kurtosis tests for Normality

Variable	Obs	Pr(Skewness)	Pr(Kurtosis)	adj chi2(2)	joint Prob>chi2
utcells	6	.	.	.	.

. swilk utcells if gender ==1

Shapiro-wilk W test for normal data

Variable	Obs	W	V	z	Prob>z
utcells	6	0.95593	0.546	-0.799	0.78793

. sktest btcells if gender ==1

Skewness/Kurtosis tests for Normality

Variable	Obs	Pr(Skewness)	Pr(Kurtosis)	adj chi2(2)	joint Prob>chi2
btcells	6	.	.	.	.

. swilk btcells if gender ==1

Shapiro-wilk W test for normal data

Variable	Obs	W	V	z	Prob>z
btcells	6	0.94061	0.736	-0.424	0.66412

. sktest tcelldiff if gender ==1

Skewness/Kurtosis tests for Normality

Variable	Obs	Pr(Skewness)	Pr(Kurtosis)	adj chi2(2)	joint Prob>chi2
tcelldiff	6	.	.	.	.

. swilk tcelldiff if gender ==1

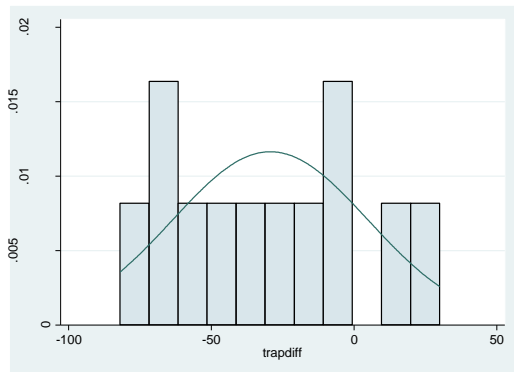
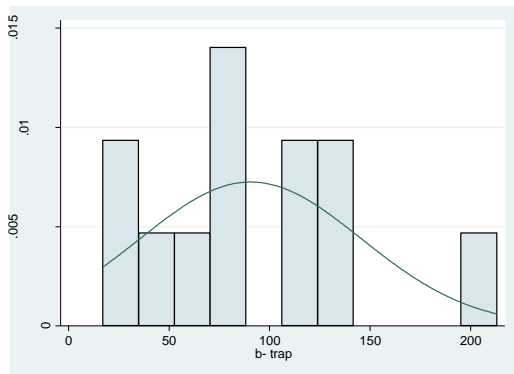
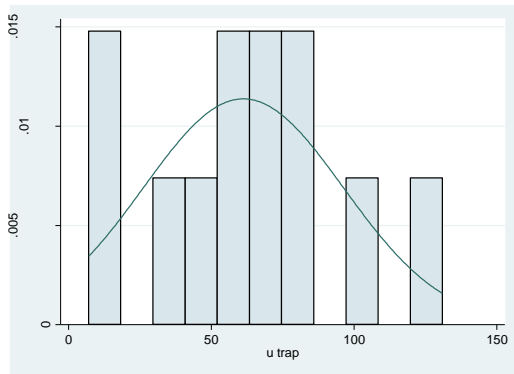
Shapiro-wilk W test for normal data

Variable	Obs	W	V	z	Prob>z
tcelldiff	6	0.88808	1.386	0.501	0.30824



# Absolute number of TRAP<sup>+</sup> cells generated

- All



. sktest utrap

Skewness/Kurtosis tests for Normality					
Variable	Obs	Pr(Skewness)	Pr(Kurtosis)	adj chi2(2)	joint Prob>chi2
utrap	12	0.5748	0.6245	0.58	0.7475

. swilk utrap

Shapiro-wilk w test for normal data					
Variable	Obs	w	V	z	Prob>z
utrap	12	0.96208	0.634	-0.889	0.81308

. sktest btrap

Skewness/Kurtosis tests for Normality					
Variable	Obs	Pr(Skewness)	Pr(Kurtosis)	adj chi2(2)	joint Prob>chi2
btrap	12	0.2112	0.3671	2.82	0.2439

. swilk btrap

Shapiro-wilk w test for normal data					
Variable	Obs	w	V	z	Prob>z
btrap	12	0.95075	0.823	-0.380	0.64794

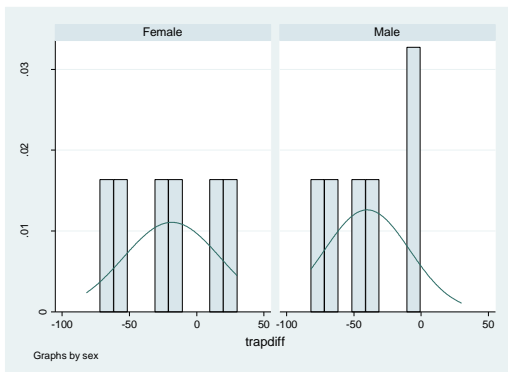
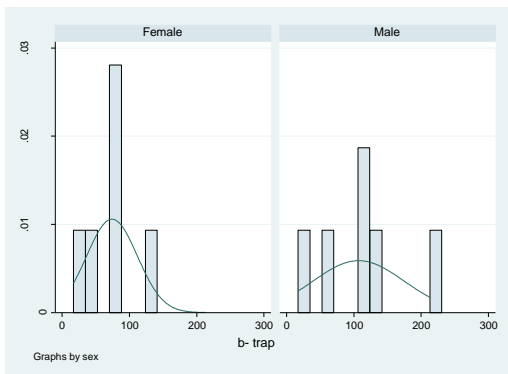
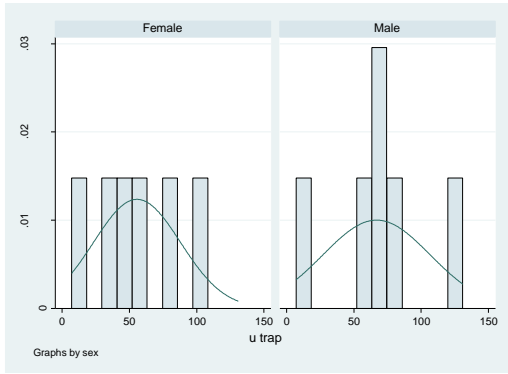
. sktest trapdiff

Skewness/Kurtosis tests for Normality					
Variable	Obs	Pr(Skewness)	Pr(Kurtosis)	adj chi2(2)	joint Prob>chi2
trapdiff	12	0.8114	0.5036	0.52	0.7696

. swilk trapdiff

Shapiro-wilk w test for normal data					
Variable	Obs	w	V	z	Prob>z
trapdiff	12	0.97946	0.343	-2.083	0.98139

## - By gender



. sktest utrap if gender ==0

Skewness/Kurtosis tests for Normality

Variable	Obs	Pr(Skewness)	Pr(Kurtosis)	adj chi2(2)	joint Prob>chi2
utrap	6	.	.	.	.

. swilk utrap if gender ==0

Shapiro-wilk W test for normal data

Variable	Obs	W	V	z	Prob>z
utrap	6	0.93400	0.817	-0.283	0.61131

. sktest btrap if gender ==0

Skewness/Kurtosis tests for Normality

Variable	Obs	Pr(Skewness)	Pr(Kurtosis)	adj chi2(2)	joint Prob>chi2
btrap	6	.	.	.	.

. swilk btrap if gender ==0

Shapiro-wilk W test for normal data

Variable	Obs	W	V	z	Prob>z
btrap	6	0.97201	0.347	-1.315	0.90568

. sktest trapdiff if gender ==0

Skewness/Kurtosis tests for Normality

Variable	Obs	Pr(Skewness)	Pr(Kurtosis)	adj chi2(2)	joint Prob>chi2
trapdiff	6	.	.	.	.

. swilk trapdiff if gender ==0

Shapiro-wilk W test for normal data

Variable	Obs	W	V	z	Prob>z
trapdiff	6	0.94880	0.634	-0.614	0.73051

. sktest utrap if gender ==1

Skewness/Kurtosis tests for Normality

Variable	Obs	Pr(Skewness)	Pr(Kurtosis)	adj chi2(2)	joint Prob>chi2
utrap	6	.	.	.	.

. swilk utrap if gender ==1

Shapiro-wilk W test for normal data

Variable	Obs	W	V	z	Prob>z
utrap	6	0.98199	0.223	-1.763	0.96102

. sktest btrap if gender ==1

Skewness/Kurtosis tests for Normality

Variable	Obs	Pr(Skewness)	Pr(Kurtosis)	adj chi2(2)	joint Prob>chi2
btrap	6	.	.	.	.

. swilk btrap if gender ==1

Shapiro-wilk W test for normal data

Variable	Obs	W	V	z	Prob>z
btrap	6	0.94872	0.635	-0.613	0.72993

. sktest trapdiff if gender ==1

Skewness/Kurtosis tests for Normality

Variable	Obs	Pr(Skewness)	Pr(Kurtosis)	adj chi2(2)	joint Prob>chi2
trapdiff	6	.	.	.	.

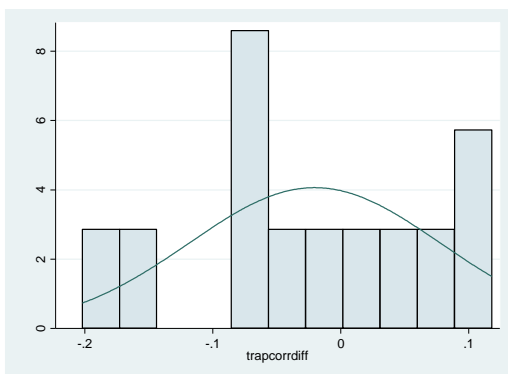
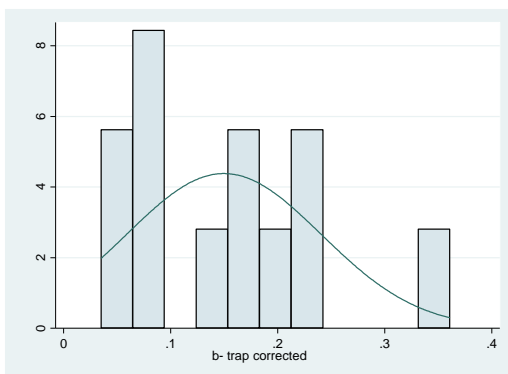
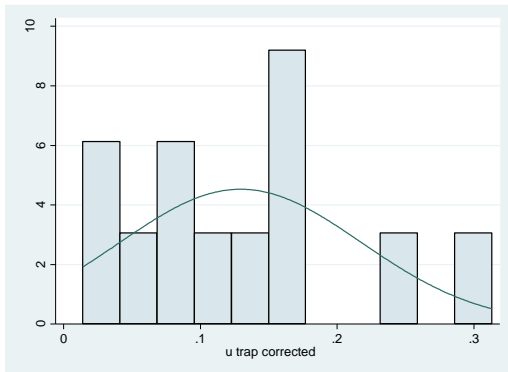
. swilk trapdiff if gender ==1

Shapiro-wilk W test for normal data

Variable	Obs	W	V	z	Prob>z
trapdiff	6	0.95654	0.538	-0.816	0.79271

# Number of TRAP<sup>+</sup> cells generated corrected for the initial numbers of monocytes

- All



. sktest utrapcorr

Skewness/Kurtosis tests for Normality					
Variable	Obs	Pr(Skewness)	Pr(Kurtosis)	adj chi2(2)	joint Prob>chi2
utrapcorre-d	12	0.2006	0.5903	2.26	0.3232

. swilk utrapcorr

Shapiro-wilk W test for normal data					
Variable	Obs	W	V	z	Prob>z
utrapcorre-d	12	0.93693	1.054	0.102	0.45940

. sktest btrapcorr

Skewness/Kurtosis tests for Normality					
Variable	Obs	Pr(Skewness)	Pr(Kurtosis)	adj chi2(2)	joint Prob>chi2
btrapcorre-d	12	0.1038	0.2459	4.25	0.1193

. swilk btrapcorr

Shapiro-wilk W test for normal data					
Variable	Obs	W	V	z	Prob>z
btrapcorre-d	12	0.92874	1.191	0.340	0.36699

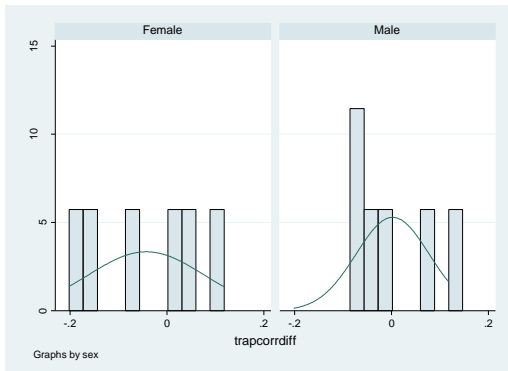
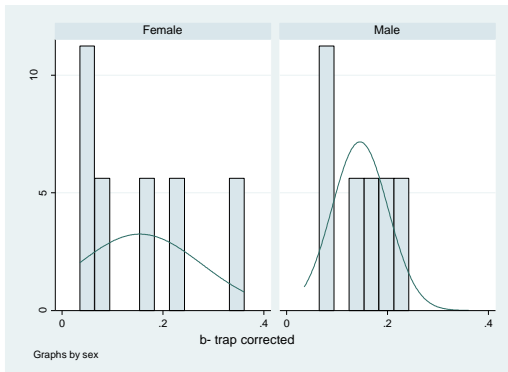
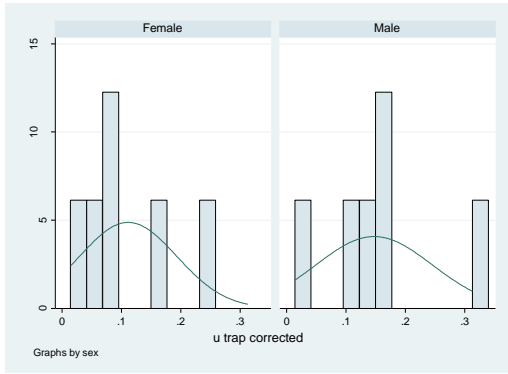
. sktest trapcorrdiff

Skewness/Kurtosis tests for Normality					
Variable	Obs	Pr(Skewness)	Pr(Kurtosis)	adj chi2(2)	joint Prob>chi2
trapcorrdiff	12	0.4866	0.8129	0.57	0.7538

. swilk trapcorrdiff

Shapiro-wilk W test for normal data					
Variable	Obs	W	V	z	Prob>z
trapcorrdiff	12	0.96505	0.584	-1.048	0.85278

# - By gender



. sktest utrapcorr if gender ==0

Skewness/Kurtosis tests for Normality

Variable	Obs	Pr(Skewness)	Pr(Kurtosis)	adj chi2(2)	joint Prob>chi2
utrapcorre-d	6	.	.	.	.

. swilk utrapcorr if gender ==0

Shapiro-wilk W test for normal data

Variable	Obs	W	V	z	Prob>z
utrapcorre-d	6	0.93717	0.778	-0.349	0.63646

. sktest btrapcorr if gender ==0

Skewness/Kurtosis tests for Normality

Variable	Obs	Pr(Skewness)	Pr(Kurtosis)	adj chi2(2)	joint Prob>chi2
btrapcorre-d	6	.	.	.	.

. swilk btrapcorr if gender ==0

Shapiro-wilk W test for normal data

Variable	Obs	W	V	z	Prob>z
btrapcorre-d	6	0.93325	0.827	-0.267	0.60539

. sktest trapcorrdiff if gender ==0

Skewness/Kurtosis tests for Normality

Variable	Obs	Pr(Skewness)	Pr(Kurtosis)	adj chi2(2)	joint Prob>chi2
trapcorrdiff	6	.	.	.	.

. swilk trapcorrdiff if gender ==0

Shapiro-wilk W test for normal data

Variable	Obs	W	V	z	Prob>z
trapcorrdiff	6	0.93307	0.829	-0.264	0.60402

. sktest utrapcorr if gender ==1

Skewness/Kurtosis tests for Normality

Variable	Obs	Pr(Skewness)	Pr(Kurtosis)	adj chi2(2)	joint Prob>chi2
utrapcorre-d	6	.	.	.	.

. swilk utrapcorr if gender ==1

Shapiro-wilk W test for normal data

Variable	Obs	W	V	z	Prob>z
utrapcorre-d	6	0.89137	1.345	0.453	0.32545

. sktest btrapcorr if gender ==1

Skewness/Kurtosis tests for Normality

Variable	Obs	Pr(Skewness)	Pr(Kurtosis)	adj chi2(2)	joint Prob>chi2
btrapcorre-d	6	.	.	.	.

. swilk btrapcorr if gender ==1

Shapiro-wilk W test for normal data

Variable	Obs	W	V	z	Prob>z
btrapcorre-d	6	0.91351	1.071	0.101	0.45990

. sktest trapcorrdiff if gender ==1

Skewness/Kurtosis tests for Normality

Variable	Obs	Pr(Skewness)	Pr(Kurtosis)	adj chi2(2)	joint Prob>chi2
trapcorrdiff	6	.	.	.	.

. swilk trapcorrdiff if gender ==1

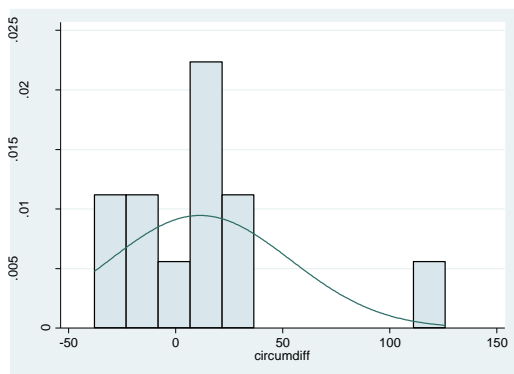
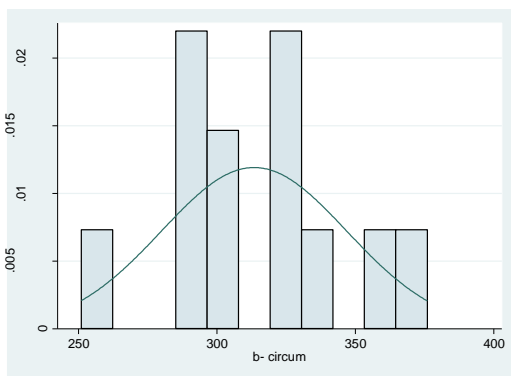
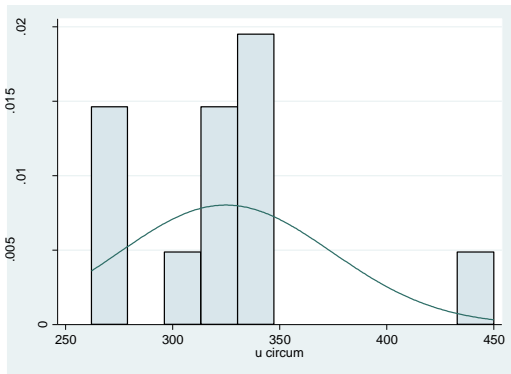
Shapiro-wilk W test for normal data

Variable	Obs	W	V	z	Prob>z
trapcorrdiff	6	0.93307	0.829	-0.264	0.60403



# TRAP<sup>+</sup> cell circumference

- All



. sktest ucircum

Skewness/Kurtosis tests for Normality

Variable	Obs	Pr(Skewness)	Pr(Kurtosis)	adj chi2(2)	joint Prob>chi2
ucircum	12	0.0552	0.0412	6.82	0.0330

. swilk ucircum

Shapiro-wilk W test for normal data

Variable	Obs	W	V	z	Prob>z
ucircum	12	0.85798	2.373	1.684	0.04612

. sktest bcircum

Skewness/Kurtosis tests for Normality

Variable	Obs	Pr(Skewness)	Pr(Kurtosis)	adj chi2(2)	joint Prob>chi2
bcircum	12	0.7361	0.5621	0.46	0.7942

. swilk bcircum

Shapiro-wilk W test for normal data

Variable	Obs	W	V	z	Prob>z
bcircum	12	0.95240	0.795	-0.446	0.67225

. sktest circumdiff

Skewness/Kurtosis tests for Normality

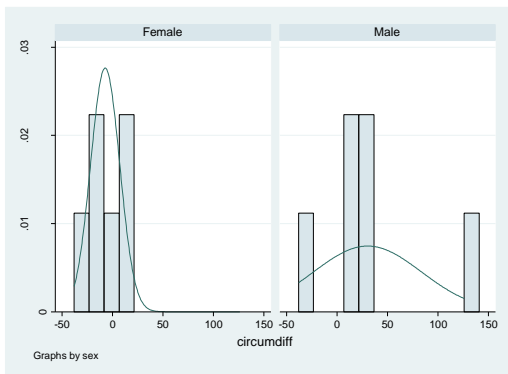
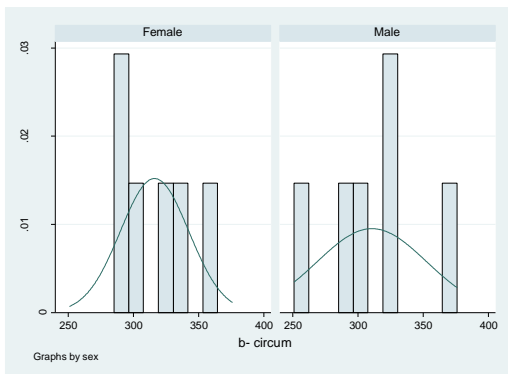
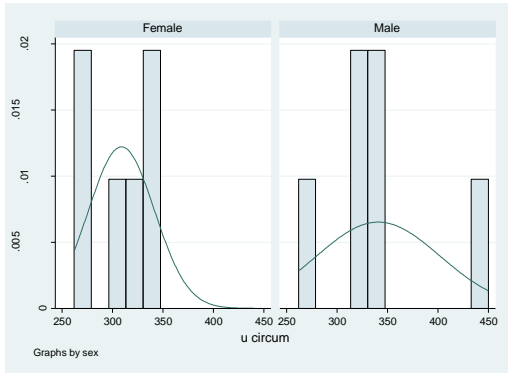
Variable	Obs	Pr(Skewness)	Pr(Kurtosis)	adj chi2(2)	joint Prob>chi2
circumdiff	12	0.0057	0.0093	10.78	0.0046

. swilk circumdiff

Shapiro-wilk W test for normal data

Variable	Obs	W	V	z	Prob>z
circumdiff	12	0.82845	2.866	2.052	0.02010

# - By gender



. sktest ucircum if gender ==0

Skewness/Kurtosis tests for Normality

Variable	Obs	Pr(Skewness)	Pr(Kurtosis)	adj chi2(2)	joint Prob>chi2
ucircum	6	.	.	.	.

. swilk ucircum if gender ==0

Shapiro-wilk W test for normal data

Variable	Obs	W	V	z	Prob>z
ucircum	6	0.88400	1.437	0.559	0.28793

. sktest bcircum if gender ==0

Skewness/Kurtosis tests for Normality

Variable	Obs	Pr(Skewness)	Pr(Kurtosis)	adj chi2(2)	joint Prob>chi2
bcircum	6	.	.	.	.

. swilk bcircum if gender ==0

Shapiro-wilk W test for normal data

Variable	Obs	W	V	z	Prob>z
bcircum	6	0.96968	0.375	-1.228	0.89031

. sktest circumdiff if gender ==0

Skewness/Kurtosis tests for Normality

Variable	Obs	Pr(Skewness)	Pr(Kurtosis)	adj chi2(2)	joint Prob>chi2
circumdiff	6	.	.	.	.

. swilk circumdiff if gender ==0

Shapiro-wilk W test for normal data

Variable	Obs	W	V	z	Prob>z
circumdiff	6	0.88308	1.448	0.572	0.28351

. sktest ucircum if gender ==1

Skewness/Kurtosis tests for Normality

Variable	Obs	Pr(Skewness)	Pr(Kurtosis)	adj chi2(2)	joint Prob>chi2
ucircum	6	.	.	.	.

. swilk ucircum if gender ==1

Shapiro-wilk W test for normal data

Variable	Obs	W	V	z	Prob>z
ucircum	6	0.93569	0.796	-0.318	0.62472

. sktest bcircum if gender ==1

Skewness/Kurtosis tests for Normality

Variable	Obs	Pr(Skewness)	Pr(Kurtosis)	adj chi2(2)	joint Prob>chi2
bcircum	6	.	.	.	.

. swilk bcircum if gender ==1

Shapiro-wilk W test for normal data

Variable	Obs	W	V	z	Prob>z
bcircum	6	0.90677	1.155	0.214	0.41546

. sktest circumdiff if gender ==1

Skewness/Kurtosis tests for Normality

Variable	Obs	Pr(Skewness)	Pr(Kurtosis)	adj chi2(2)	joint Prob>chi2
circumdiff	6	.	.	.	.

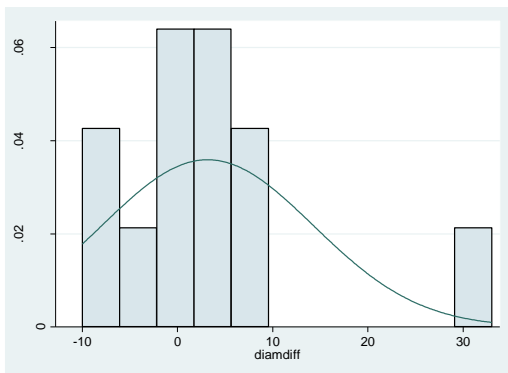
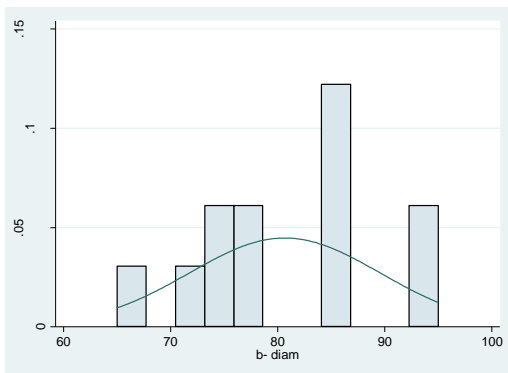
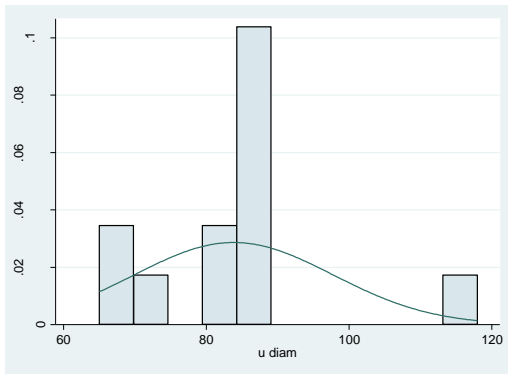
. swilk circumdiff if gender ==1

Shapiro-wilk W test for normal data

Variable	Obs	W	V	z	Prob>z
circumdiff	6	0.92006	0.990	-0.014	0.50577

# TRAP<sup>+</sup> cell diameter

- All



. sktest udiam

Skewness/Kurtosis tests for Normality					
Variable	Obs	Pr(Skewness)	Pr(Kurtosis)	adj chi2(2)	joint Prob>chi2
udiam	12	0.1074	0.0637	5.65	0.0593

. swilk udiam

Shapiro-wilk w test for normal data					
Variable	Obs	w	V	z	Prob>z
udiam	12	0.85443	2.432	1.732	0.04165

. sktest bdiam

Skewness/Kurtosis tests for Normality					
Variable	Obs	Pr(Skewness)	Pr(Kurtosis)	adj chi2(2)	joint Prob>chi2
bdiam	12	0.9816	0.6872	0.16	0.9219

. swilk bdiam

Shapiro-wilk w test for normal data					
Variable	Obs	w	V	z	Prob>z
bdiam	12	0.96127	0.647	-0.848	0.80178

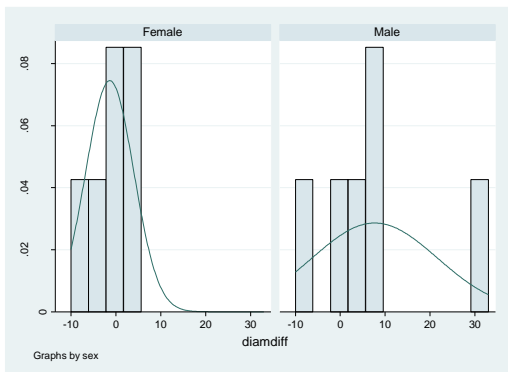
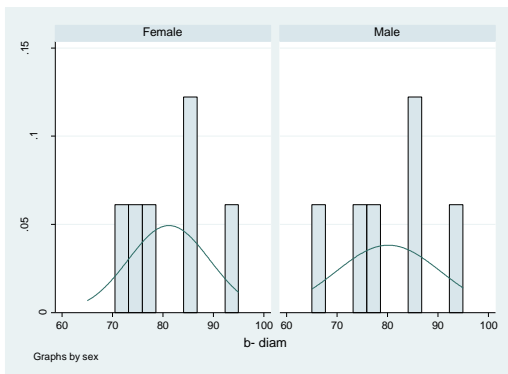
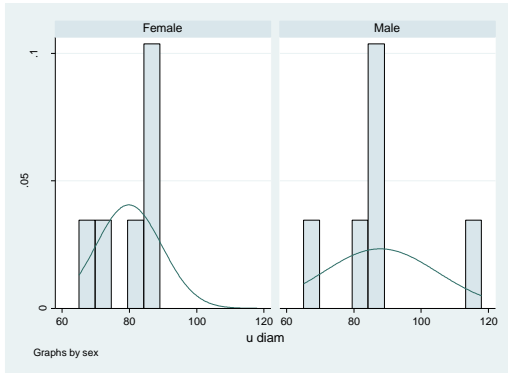
. sktest diamdifff

Skewness/Kurtosis tests for Normality					
Variable	Obs	Pr(Skewness)	Pr(Kurtosis)	adj chi2(2)	joint Prob>chi2
diamdifff	12	0.0076	0.0122	10.19	0.0061

. swilk diamdifff

Shapiro-wilk w test for normal data					
Variable	Obs	w	V	z	Prob>z
diamdifff	12	0.84457	2.597	1.859	0.03148

## - By gender



. sktest udiam if gender ==0

Skewness/Kurtosis tests for Normality

Variable	Obs	Pr(Skewness)	Pr(Kurtosis)	adj chi2(2)	joint Prob>chi2
udiam	6	.	.	.	.

. swilk udiam if gender ==0

Shapiro-wilk W test for normal data

Variable	Obs	W	V	z	Prob>z
udiam	6	0.86725	1.644	0.788	0.21546

. sktest bdiam if gender ==0

Skewness/Kurtosis tests for Normality

Variable	Obs	Pr(Skewness)	Pr(Kurtosis)	adj chi2(2)	joint Prob>chi2
bdiam	6	.	.	.	.

. swilk bdiam if gender ==0

Shapiro-wilk W test for normal data

Variable	Obs	W	V	z	Prob>z
bdiam	6	0.98916	0.134	-2.227	0.98702

. sktest diamdiff if gender ==0

Skewness/Kurtosis tests for Normality

Variable	Obs	Pr(Skewness)	Pr(Kurtosis)	adj chi2(2)	joint Prob>chi2
diamdiff	6	.	.	.	.

. swilk diamdiff if gender ==0

Shapiro-wilk W test for normal data

Variable	Obs	W	V	z	Prob>z
diamdiff	6	0.90783	1.142	0.196	0.42225

. sktest udiam if gender ==1

Skewness/Kurtosis tests for Normality

Variable	Obs	Pr(Skewness)	Pr(Kurtosis)	adj chi2(2)	joint Prob>chi2
udiam	6	.	.	.	.

. swilk udiam if gender ==1

Shapiro-wilk W test for normal data

Variable	Obs	W	V	z	Prob>z
udiam	6	0.94600	0.669	-0.547	0.70779

. sktest bdiam if gender ==1

Skewness/Kurtosis tests for Normality

Variable	Obs	Pr(Skewness)	Pr(Kurtosis)	adj chi2(2)	joint Prob>chi2
bdiam	6	.	.	.	.

. swilk bdiam if gender ==1

Shapiro-wilk W test for normal data

Variable	Obs	W	V	z	Prob>z
bdiam	6	0.92469	0.933	-0.100	0.53980

. sktest diamdiff if gender ==1

Skewness/Kurtosis tests for Normality

Variable	Obs	Pr(Skewness)	Pr(Kurtosis)	adj chi2(2)	joint Prob>chi2
diamdiff	6	.	.	.	.

. swilk diamdiff if gender ==1

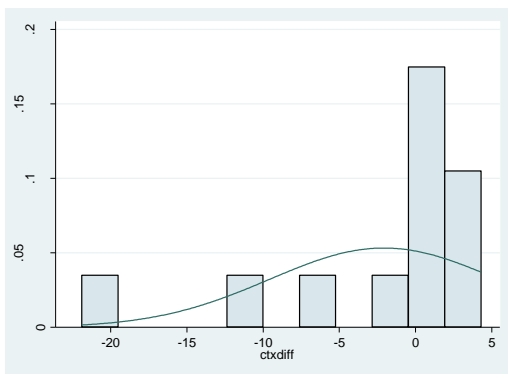
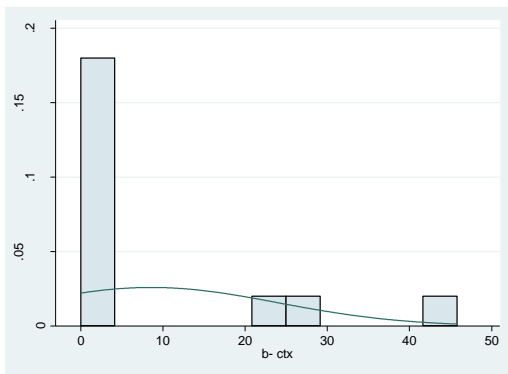
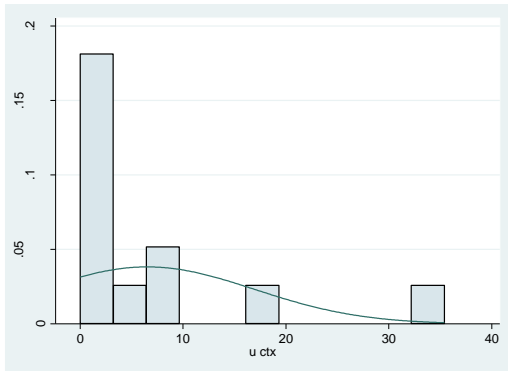
Shapiro-wilk W test for normal data

Variable	Obs	W	V	z	Prob>z
diamdiff	6	0.96915	0.382	-1.209	0.88666



# $\beta$ CTX concentration of supernatant

- All



. sktest uctx

Skewness/Kurtosis tests for Normality					
Variable	Obs	Pr(Skewness)	Pr(Kurtosis)	adj chi2(2)	joint Prob>chi2
uctx	12	0.0010	0.0059	13.10	0.0014

. swilk uctx

Shapiro-wilk w test for normal data					
Variable	Obs	w	V	z	Prob>z
uctx	12	0.66419	5.611	3.360	0.00039

. sktest bctx

Skewness/Kurtosis tests for Normality					
Variable	Obs	Pr(Skewness)	Pr(Kurtosis)	adj chi2(2)	joint Prob>chi2
bctx	12	0.0095	0.1205	7.63	0.0220

. swilk bctx

Shapiro-wilk w test for normal data					
Variable	Obs	w	V	z	Prob>z
bctx	12	0.64116	5.996	3.490	0.00024

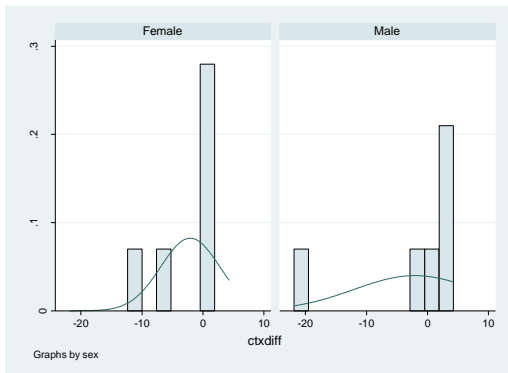
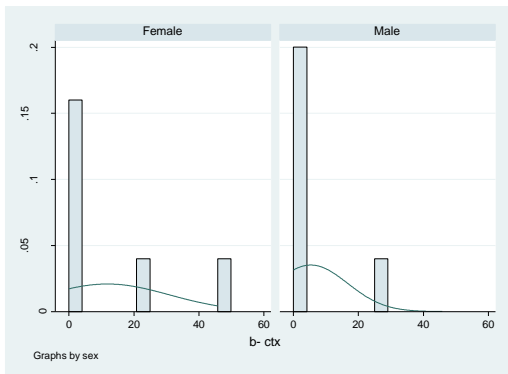
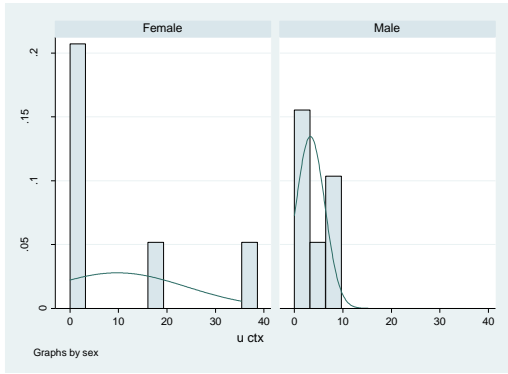
. sktest ctxdiff

Skewness/Kurtosis tests for Normality					
Variable	Obs	Pr(Skewness)	Pr(Kurtosis)	adj chi2(2)	joint Prob>chi2
ctxdiff	12	0.0039	0.0191	10.44	0.0054

. swilk ctxdiff

Shapiro-wilk w test for normal data					
Variable	Obs	w	V	z	Prob>z
ctxdiff	12	0.72797	4.545	2.950	0.00159

- **By gender**



. sktest uctx if gender ==0

Skewness/Kurtosis tests for Normality

Variable	Obs	Pr(Skewness)	Pr(Kurtosis)	adj chi2(2)	joint Prob>chi2
uctx	6	.	.	.	.

. swilk uctx if gender ==0

Shapiro-wilk W test for normal data

Variable	Obs	W	V	z	Prob>z
uctx	6	0.99522	0.059	-2.885	0.99804

. sktest bctx if gender ==0

Skewness/Kurtosis tests for Normality

Variable	Obs	Pr(Skewness)	Pr(Kurtosis)	adj chi2(2)	joint Prob>chi2
bctx	6	.	.	.	.

. swilk bctx if gender ==0

Shapiro-wilk W test for normal data

Variable	Obs	W	V	z	Prob>z
bctx	6	0.58356	5.157	3.442	0.00029

. sktest ctxdiff if gender ==0

Skewness/Kurtosis tests for Normality

Variable	Obs	Pr(Skewness)	Pr(Kurtosis)	adj chi2(2)	joint Prob>chi2
ctxdiff	6	.	.	.	.

. swilk ctxdiff if gender ==0

Shapiro-wilk W test for normal data

Variable	Obs	W	V	z	Prob>z
ctxdiff	6	0.55393	5.524	3.667	0.00012

. sktest uctx if gender ==1

Skewness/Kurtosis tests for Normality

Variable	Obs	Pr(Skewness)	Pr(Kurtosis)	adj chi2(2)	joint Prob>chi2
uctx	6	.	.	.	.

. swilk uctx if gender ==1

Shapiro-wilk W test for normal data

Variable	Obs	W	V	z	Prob>z
uctx	6	0.73971	3.224	2.150	0.01577

. sktest bctx if gender ==1

Skewness/Kurtosis tests for Normality

Variable	Obs	Pr(Skewness)	Pr(Kurtosis)	adj chi2(2)	joint Prob>chi2
bctx	6	.	.	.	.

. swilk bctx if gender ==1

Shapiro-wilk W test for normal data

Variable	Obs	W	V	z	Prob>z
bctx	6	0.76076	2.963	1.954	0.02534

. sktest ctxdiff if gender ==1

Skewness/Kurtosis tests for Normality

Variable	Obs	Pr(Skewness)	Pr(Kurtosis)	adj chi2(2)	joint Prob>chi2
ctxdiff	6	.	.	.	.

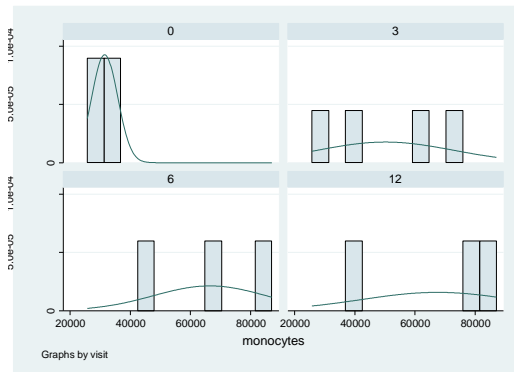
. swilk ctxdiff if gender ==1

Shapiro-wilk W test for normal data

Variable	Obs	W	V	z	Prob>z
ctxdiff	6	0.81473	2.294	1.409	0.07941

## Ex vivo number of TRAP<sup>+</sup> cells generated per visit

### Initial number of monocytes



```
. swilk monocytes if visit ==0
```

Shapiro-Wilk w test for normal data

Variable	Obs	w	V	z	Prob>z
monocytes	4	0.87298	1.465	0.497	0.30953

```
. swilk monocytes if visit ==3
```

Shapiro-Wilk w test for normal data

Variable	Obs	w	V	z	Prob>z
monocytes	4	0.93036	0.803	-0.244	0.59650

```
. swilk monocytes if visit ==6
```

Shapiro-Wilk w test for normal data

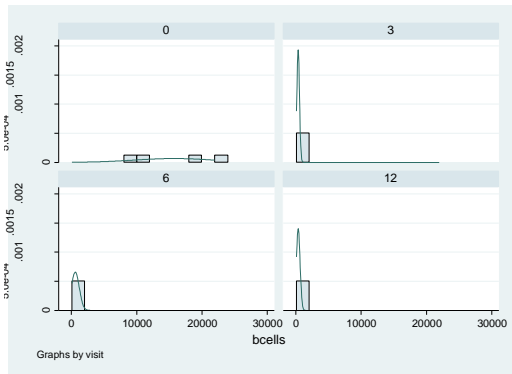
Variable	Obs	w	V	z	Prob>z
monocytes	3	0.99979	0.003	-1.917	0.97238

```
. swilk monocytes if visit ==12
```

Shapiro-Wilk w test for normal data

Variable	Obs	w	V	z	Prob>z
monocytes	3	0.90481	1.421	0.251	0.40098

# Initial number of b cells



```
. swilk bcells if visit ==0
```

Shapiro-wilk W test for normal data

Variable	Obs	W	V	z	Prob>z
bcells	4	0.85540	1.668	0.693	0.24413

```
. swilk bcells if visit ==3
```

Shapiro-wilk W test for normal data

Variable	Obs	W	V	z	Prob>z
bcells	4	0.90165	1.134	0.153	0.43929

```
. swilk bcells if visit ==6
```

Shapiro-wilk W test for normal data

Variable	Obs	W	V	z	Prob>z
bcells	3	0.94225	0.862	-0.092	0.53649

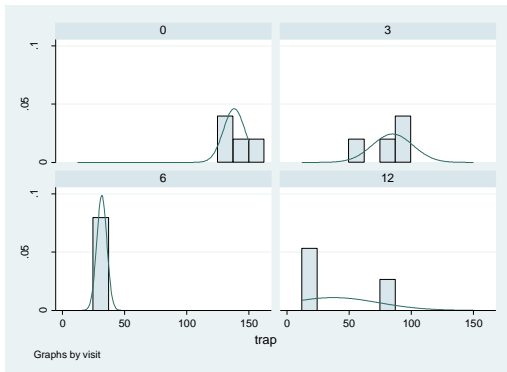
```
. swilk bcells if visit ==12
```

Shapiro-wilk W test for normal data

Variable	Obs	W	V	z	Prob>z
bcells	3	0.75458	3.664	2.323	0.01009



## Absolute number of TRAP<sup>+</sup> cells generated



```
. swilk trap if visit ==0
```

Shapiro-wilk W test for normal data

Variable	Obs	W	V	z	Prob>z
trap	4	0.94544	0.629	-0.490	0.68777

```
. swilk trap if visit ==3
```

Shapiro-wilk W test for normal data

Variable	Obs	W	V	z	Prob>z
trap	4	0.89950	1.159	0.180	0.42859

```
. swilk trap if visit ==6
```

Shapiro-wilk W test for normal data

Variable	Obs	W	V	z	Prob>z
trap	3	0.75000	3.732	.	-0.00005

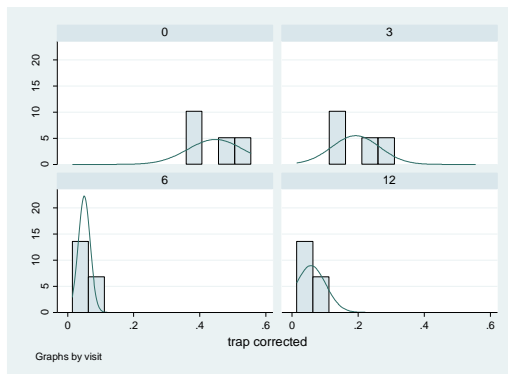
```
. swilk trap if visit ==12
```

Shapiro-wilk W test for normal data

Variable	Obs	W	V	z	Prob>z
trap	3	0.84869	2.259	0.716	0.23693



## Number of TRAP<sup>+</sup> cells generated corrected for the initial numbers of monocytes



```
. swilk trapcorrected if visit ==0
```

Shapiro-Wilk w test for normal data

Variable	Obs	W	V	z	Prob>z
trapcorrec~d	4	0.96266	0.431	-0.826	0.79561

```
. swilk trapcorrected if visit ==3
```

Shapiro-Wilk w test for normal data

Variable	Obs	W	V	z	Prob>z
trapcorrec~d	4	0.90074	1.145	0.164	0.43473

```
. swilk trapcorrected if visit ==6
```

Shapiro-Wilk w test for normal data

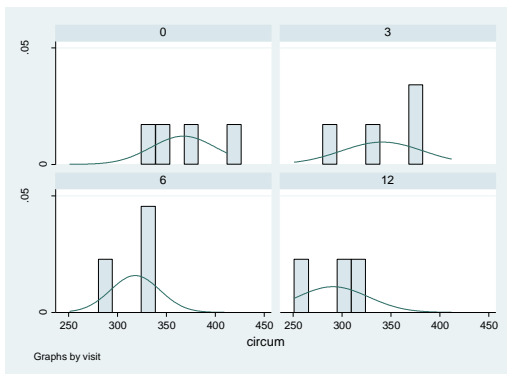
Variable	Obs	W	V	z	Prob>z
trapcorrec~d	3	0.75000	3.732	.	-0.00005

```
. swilk trapcorrected if visit ==12
```

Shapiro-Wilk w test for normal data

Variable	Obs	W	V	z	Prob>z
trapcorrec~d	3	0.99660	0.051	-1.219	0.88863

# TRAP<sup>+</sup> cell circumference



```
. swilk circum if visit ==0
```

Shapiro-wilk W test for normal data

Variable	Obs	W	V	z	Prob>z
circum	4	0.95089	0.566	-0.588	0.72171

```
. swilk circum if visit ==3
```

Shapiro-wilk W test for normal data

Variable	Obs	W	V	z	Prob>z
circum	4	0.91769	0.949	-0.060	0.52409

```
. swilk circum if visit ==6
```

Shapiro-wilk W test for normal data

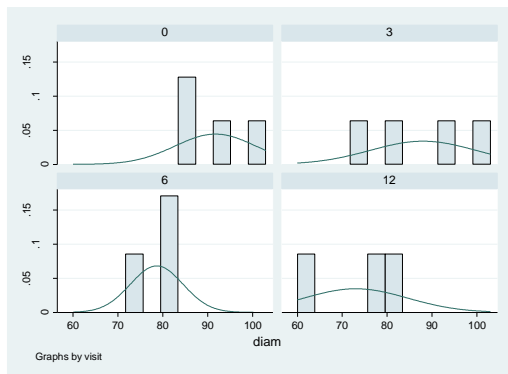
Variable	Obs	W	V	z	Prob>z
circum	3	0.83046	2.531	0.880	0.18946

```
. swilk circum if visit ==12
```

Shapiro-wilk W test for normal data

Variable	Obs	W	V	z	Prob>z
circum	3	0.96031	0.592	-0.298	0.61697

## TRAP<sup>+</sup> cell diameter



```
. swilk diam if visit ==0
      Shapiro-wilk w test for normal data
```

Variable	Obs	w	V	z	Prob>z
diam	4	0.89277	1.237	0.264	0.39603

```
. swilk diam if visit ==3
      Shapiro-wilk w test for normal data
```

Variable	Obs	w	V	z	Prob>z
diam	4	0.95318	0.540	-0.631	0.73600

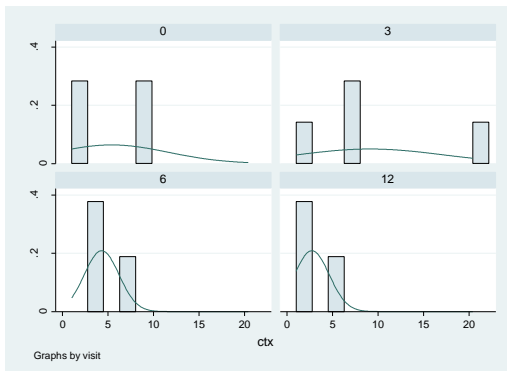
```
. swilk diam if visit ==6
      Shapiro-wilk w test for normal data
```

Variable	Obs	w	V	z	Prob>z
diam	3	0.88107	1.775	0.447	0.32754

```
. swilk diam if visit ==12
      Shapiro-wilk w test for normal data
```

Variable	Obs	w	V	z	Prob>z
diam	3	0.90977	1.347	0.209	0.41732

## $\beta$ CTX concentration of supernatant



```
. swilk ctx if visit ==0
```

Shapiro-wilk W test for normal data

Variable	Obs	W	V	z	Prob>z
ctx	2	.	.	.	.

```
. swilk ctx if visit ==3
```

Shapiro-wilk W test for normal data

Variable	Obs	W	V	z	Prob>z
ctx	4	0.89470	1.214	0.240	0.40523

```
. swilk ctx if visit ==6
```

Shapiro-wilk W test for normal data

Variable	Obs	W	V	z	Prob>z
ctx	3	0.79396	3.076	1.281	0.10011

```
. swilk ctx if visit ==12
```

Shapiro-wilk W test for normal data

Variable	Obs	W	V	z	Prob>z
ctx	3	0.88930	1.653	0.379	0.35219

## Appendix C. Multiple regression analysis

### Stepwise regression model 1 – unfractionated mononuclear cells

```
. stepwise, pe(.05):regress trap monocytes bcells tcells subject age gender
begin with empty model
p = 0.0008 < 0.0500 adding subject
p = 0.0451 < 0.0500 adding bcells
```

Source	SS	df	MS	Number of obs =
Model	21558.9076	2	10779.4538	16
Residual	9979.09242	13	767.622493	F( 2, 13) = 14.04
Total	31538	15	2102.53333	Prob > F = 0.0006
				R-squared = 0.6836
				Adj R-squared = 0.6349
				Root MSE = 27.706

trap	Coef.	Std. Err.	t	P> t	[95% Conf. Interval]
subject	83.35144	16.25066	5.13	0.000	48.24402 118.4589
bcells	.0014469	.0006527	2.22	0.045	.0000368 .0028571
_cons	32.15892	15.36872	2.09	0.057	-1.043189 65.36102

```
. stepwise, pr(.05):regress trap monocytes bcells tcells subject age gender
begin with full model
p = 0.8149 >= 0.0500 removing monocytes
p = 0.5291 >= 0.0500 removing tcells
p = 0.5213 >= 0.0500 removing gender
p = 0.2700 >= 0.0500 removing age
```

Source	SS	df	MS	Number of obs =
Model	21558.9076	2	10779.4538	16
Residual	9979.09242	13	767.622493	F( 2, 13) = 14.04
Total	31538	15	2102.53333	Prob > F = 0.0006
				R-squared = 0.6836
				Adj R-squared = 0.6349
				Root MSE = 27.706

trap	Coef.	Std. Err.	t	P> t	[95% Conf. Interval]
subject	83.35144	16.25066	5.13	0.000	48.24402 118.4589
bcells	.0014469	.0006527	2.22	0.045	.0000368 .0028571
_cons	32.15892	15.36872	2.09	0.057	-1.043189 65.36102

```
. stepwise, pr(.0500001)pe(.05)forward:regress trap monocytes bcells tcells subject age gender
begin with empty model
p = 0.0008 < 0.0500 adding subject
p = 0.0451 < 0.0500 adding bcells
```

Source	SS	df	MS	Number of obs =
Model	21558.9076	2	10779.4538	16
Residual	9979.09242	13	767.622493	F( 2, 13) = 14.04
Total	31538	15	2102.53333	Prob > F = 0.0006
				R-squared = 0.6836
				Adj R-squared = 0.6349
				Root MSE = 27.706

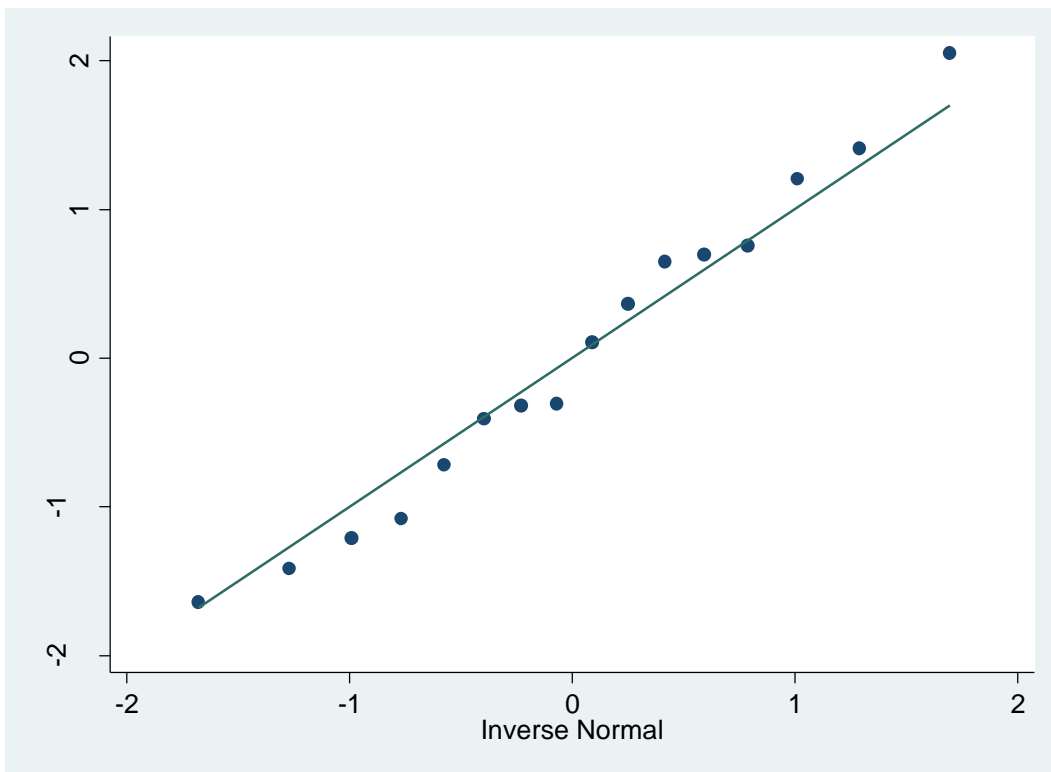
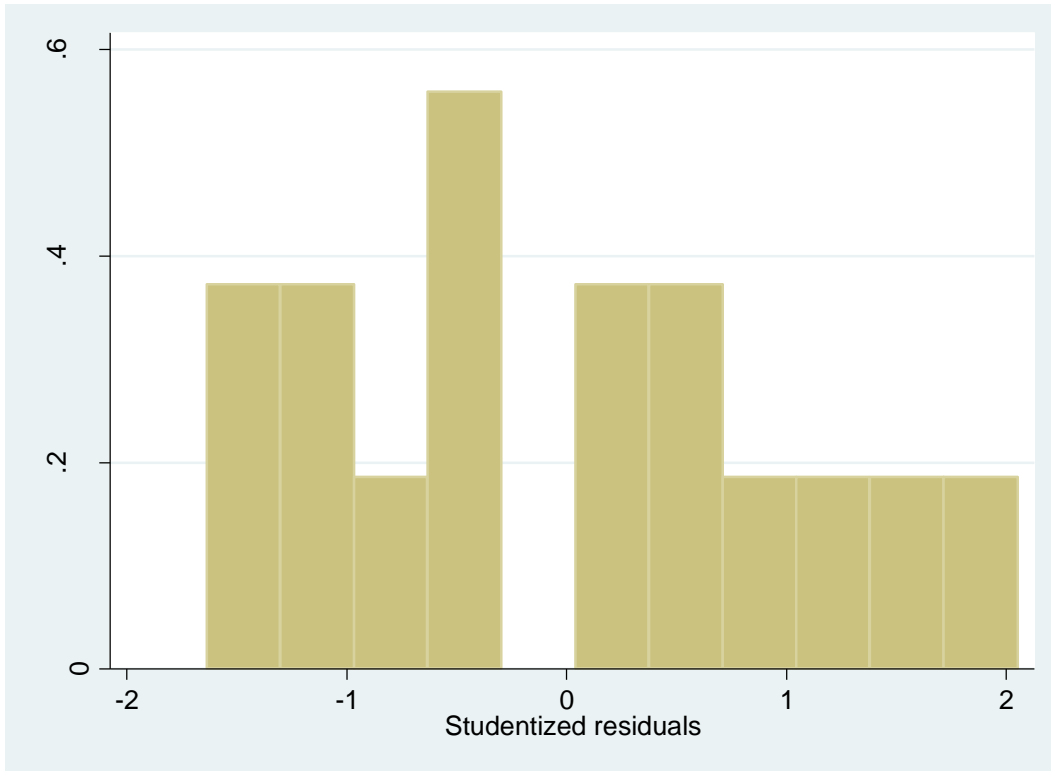
trap	Coef.	Std. Err.	t	P> t	[95% Conf. Interval]
subject	83.35144	16.25066	5.13	0.000	48.24402 118.4589
bcells	.0014469	.0006527	2.22	0.045	.0000368 .0028571
_cons	32.15892	15.36872	2.09	0.057	-1.043189 65.36102

```
. stepwise, pr(.0500001)pe(.05):regress trap monocytes bcells tcells subject age gender
begin with full model
p = 0.8149 >= 0.0500 removing monocytes
p = 0.5291 >= 0.0500 removing tcells
p = 0.5213 >= 0.0500 removing gender
p = 0.2700 >= 0.0500 removing age
```

Source	SS	df	MS	Number of obs =
Model	21558.9076	2	10779.4538	16
Residual	9979.09242	13	767.622493	F( 2, 13) = 14.04
Total	31538	15	2102.53333	Prob > F = 0.0006
				R-squared = 0.6836
				Adj R-squared = 0.6349
				Root MSE = 27.706

trap	Coef.	Std. Err.	t	P> t	[95% Conf. Interval]
subject	83.35144	16.25066	5.13	0.000	48.24402 118.4589
bcells	.0014469	.0006527	2.22	0.045	.0000368 .0028571
_cons	32.15892	15.36872	2.09	0.057	-1.043189 65.36102

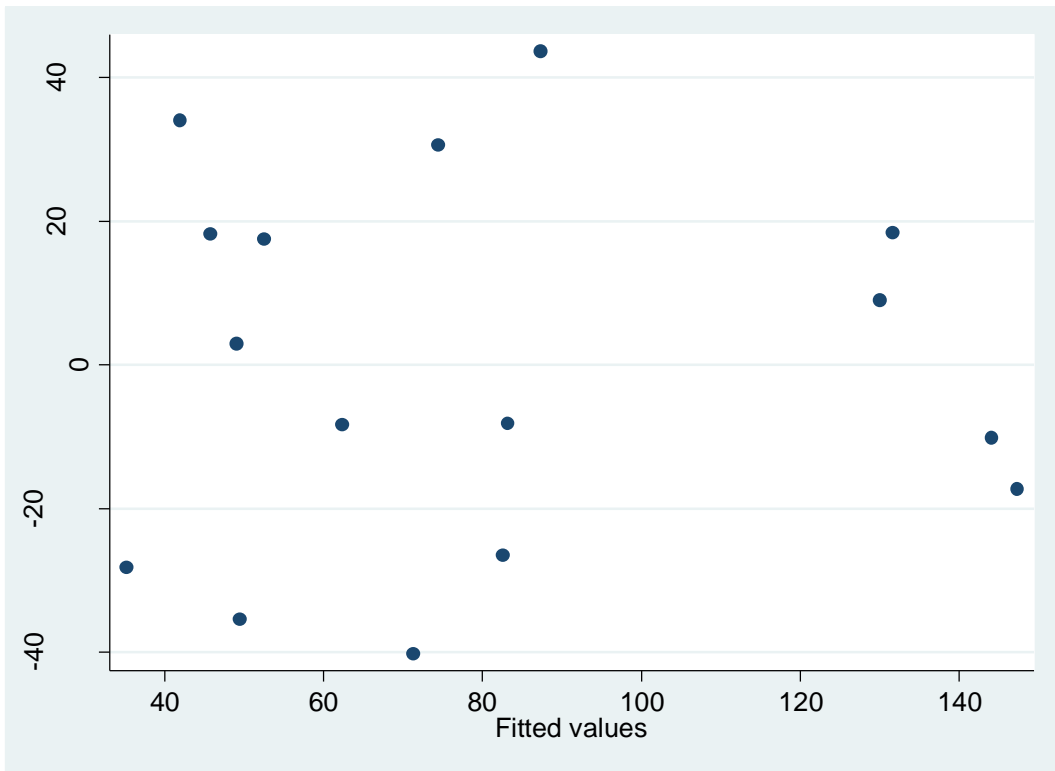
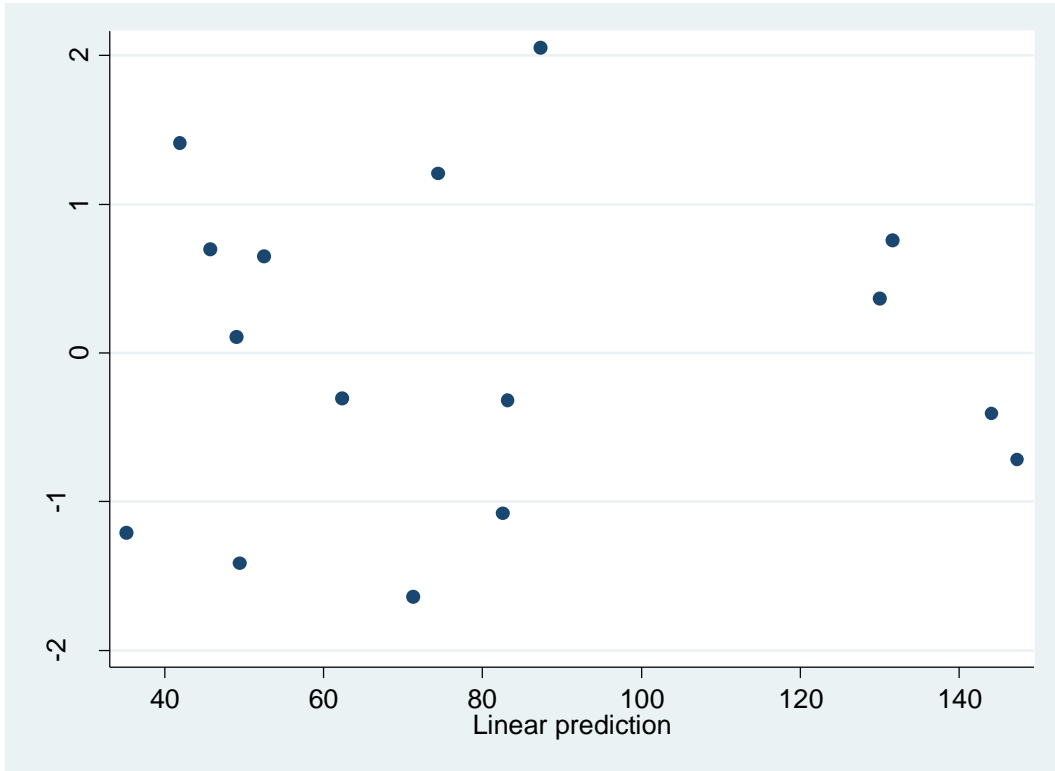
Check validity of model i.e. residuals normally distributed



. swilk resid

Shapiro-Wilk w test for normal data

Variable	Obs	W	V	z	Prob>z
resids	16	0.97172	0.573	-1.106	0.86557



## Stepwise regression model 2 – CD20 depleted mononuclear cells

```
. stepwise, pe(.05):regress trap monocytes bcells tcells gender age subject
begin with empty model
p = 0.0430 < 0.0500 adding monocytes
p = 0.0163 < 0.0500 adding tcells
```

Source	SS	df	MS	Number of obs = 16		
Model	22932.2993	2	11466.1497	F( 2, 13) = 7.45		
Residual	20000.1382	13	1538.47217	Prob > F = 0.0070		
Total	42932.4375	15	2862.1625	R-squared = 0.5341		
				Adj R-squared = 0.4625		
				Root MSE = 39.223		

trap	Coef.	Std. Err.	t	P> t	[95% Conf. Interval]	
monocytes	.0015291	.0003967	3.85	0.002	.0006721	.0023862
tcells	-.0002916	.0001057	-2.76	0.016	-.00052	-.0000633
_cons	23.25103	22.57972	1.03	0.322	-25.5295	72.03156

```
. stepwise, pr(.05):regress trap monocytes bcells tcells gender age subject
begin with full model
p = 0.5554 >= 0.0500 removing subject
p = 0.4101 >= 0.0500 removing age
p = 0.0635 >= 0.0500 removing bcells
p = 0.0647 >= 0.0500 removing gender
```

Source	SS	df	MS	Number of obs = 16		
Model	22932.2993	2	11466.1497	F( 2, 13) = 7.45		
Residual	20000.1382	13	1538.47217	Prob > F = 0.0070		
Total	42932.4375	15	2862.1625	R-squared = 0.5341		
				Adj R-squared = 0.4625		
				Root MSE = 39.223		

trap	Coef.	Std. Err.	t	P> t	[95% Conf. Interval]	
monocytes	.0015291	.0003967	3.85	0.002	.0006721	.0023862
tcells	-.0002916	.0001057	-2.76	0.016	-.00052	-.0000633
_cons	23.25103	22.57972	1.03	0.322	-25.5295	72.03156

```
. stepwise, pr(.0500001) pe(.05) forward:regress trap monocytes bcells tcells gender age subject
begin with empty model
p = 0.0430 < 0.0500 adding monocytes
p = 0.0163 < 0.0500 adding tcells
```

Source	SS	df	MS	Number of obs = 16		
Model	22932.2993	2	11466.1497	F( 2, 13) = 7.45		
Residual	20000.1382	13	1538.47217	Prob > F = 0.0070		
Total	42932.4375	15	2862.1625	R-squared = 0.5341		
				Adj R-squared = 0.4625		
				Root MSE = 39.223		

trap	Coef.	Std. Err.	t	P> t	[95% Conf. Interval]	
monocytes	.0015291	.0003967	3.85	0.002	.0006721	.0023862
tcells	-.0002916	.0001057	-2.76	0.016	-.00052	-.0000633
_cons	23.25103	22.57972	1.03	0.322	-25.5295	72.03156

```
. stepwise, pr(.0500001) pe(.05) :regress trap monocytes bcells tcells gender age subject
begin with full model
p = 0.5554 >= 0.0500 removing subject
p = 0.4101 >= 0.0500 removing age
p = 0.0635 >= 0.0500 removing bcells
p = 0.0647 >= 0.0500 removing gender
```

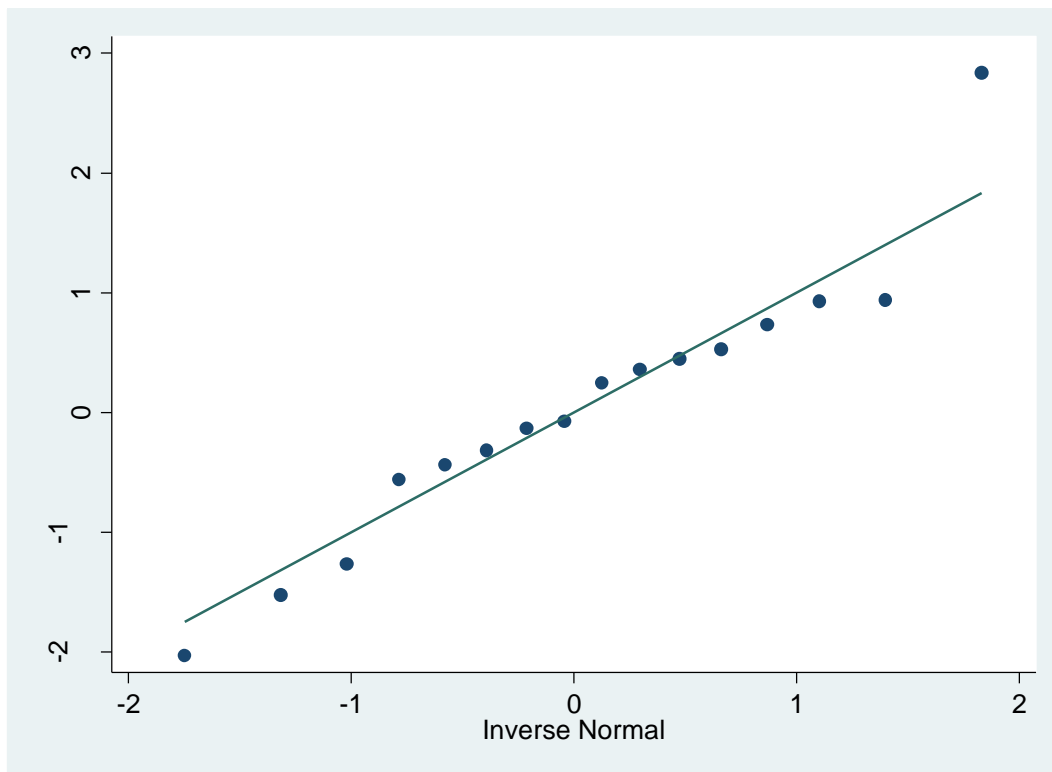
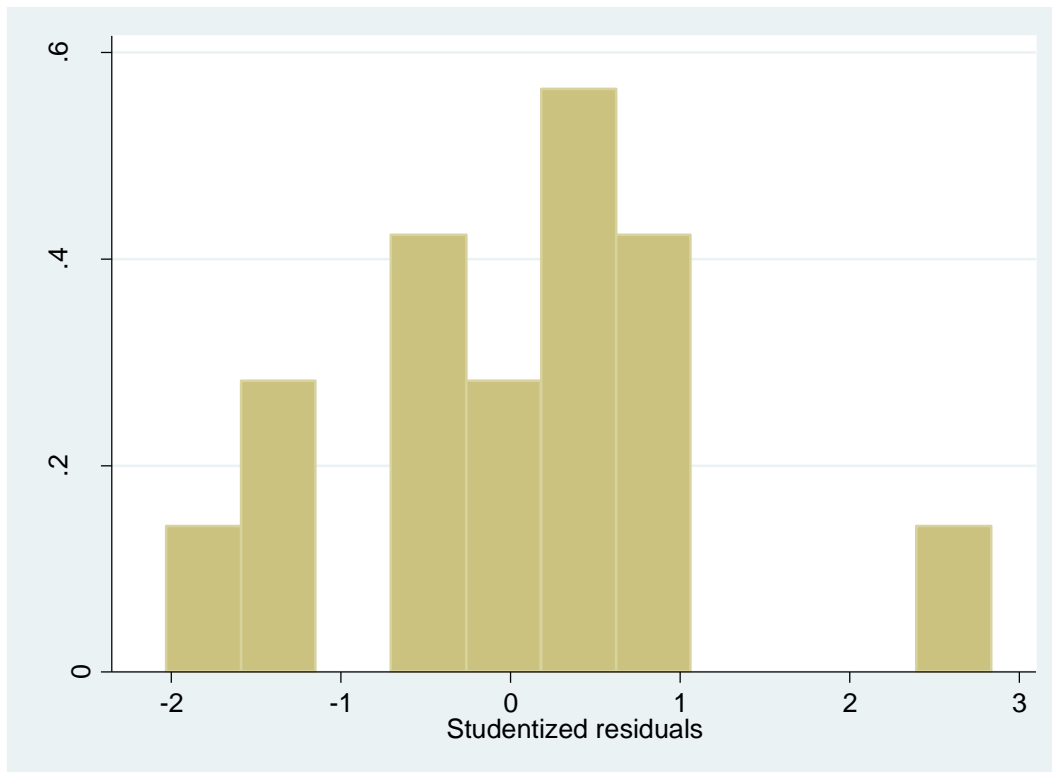
Source	SS	df	MS	Number of obs = 16		
Model	22932.2993	2	11466.1497	F( 2, 13) = 7.45		
Residual	20000.1382	13	1538.47217	Prob > F = 0.0070		
Total	42932.4375	15	2862.1625	R-squared = 0.5341		
				Adj R-squared = 0.4625		
				Root MSE = 39.223		

trap	Coef.	Std. Err.	t	P> t	[95% Conf. Interval]	
monocytes	.0015291	.0003967	3.85	0.002	.0006721	.0023862
tcells	-.0002916	.0001057	-2.76	0.016	-.00052	-.0000633
_cons	23.25103	22.57972	1.03	0.322	-25.5295	72.03156



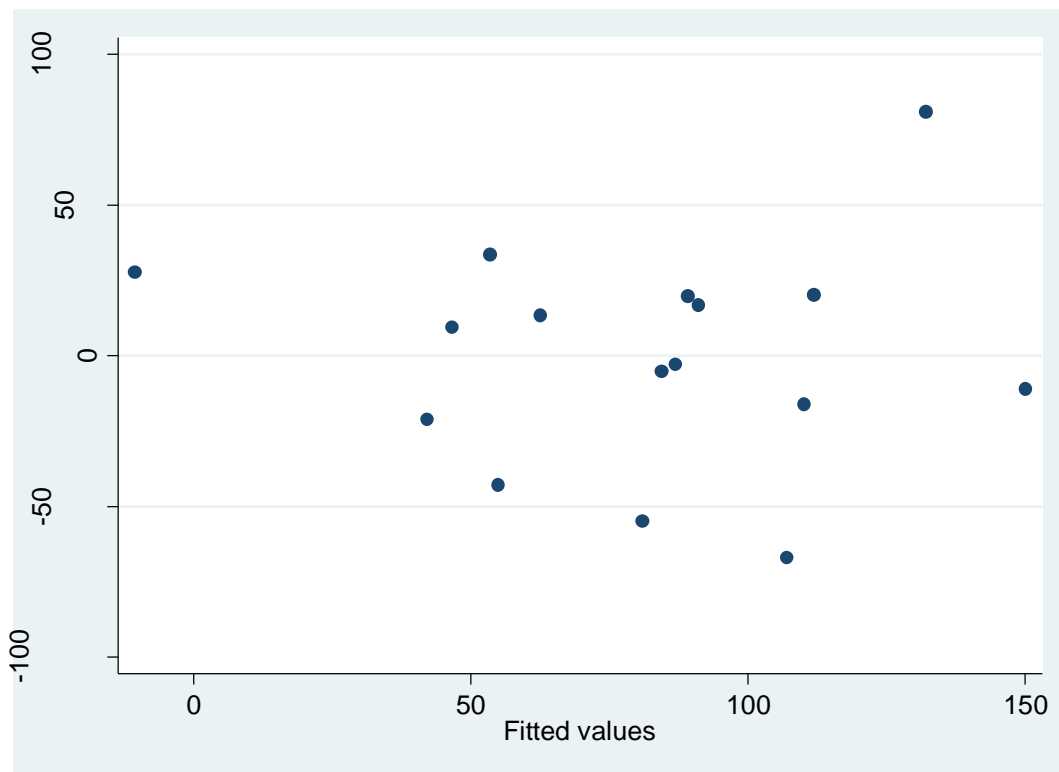
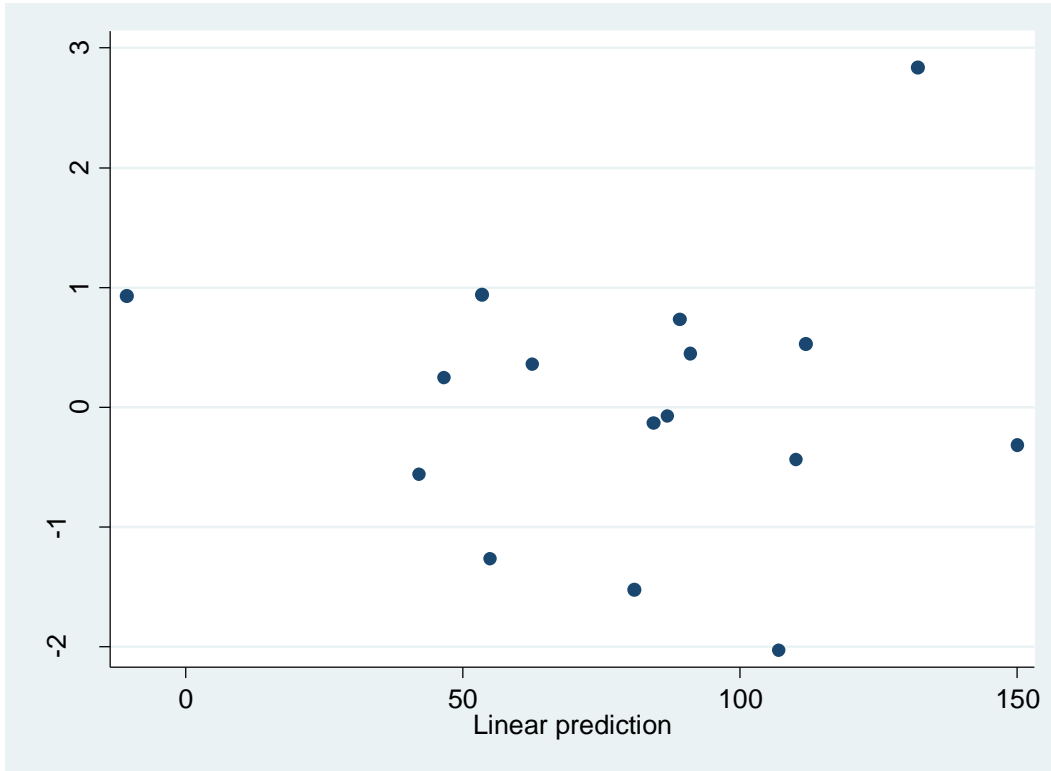
Check validity of model i.e. residuals normally distributed



. swilk resid

Shapiro-wilk w test for normal data

variable	Obs	W	V	z	Prob>z
resids	16	0.95322	0.948	-0.106	0.54232



## Appendix D. Publications arising from this thesis

### Original publication in peer reviewed journals

- Hogan VE, Wheeler G, Huigens C, Hügle T, van Laar JM (2010) Role of B-cells in rheumatic autoimmune disease. *The Open Arthritis Journal*, 3:32-36.
- Wheeler G, Hogan VE, Teng YKO, Tekstra J, Tuck SP, Lafeber FP, Huizinga TWJ, Bijlsma JWJ, Francis RM, Datta HK, van Laar JM (2011) Suppression of bone turnover by B-cell depletion in patients with rheumatoid arthritis. *Osteoporos Int*, 22(12):3067-3072.
- Elshahaly M, Wheeler G, Tuck SP, Datta HK, van Laar JM (2012) The role of B-cells in bone turnover in rheumatoid arthritis. *International Journal of Clinical Rheumatology*, 7(2):167-177.
- Teng YKO, Wheeler G, Hogan VE, Stocks P, Levarht EWN, Huizinga TWJ, Toes REM, van Laar JM (2012) Induction of long-term B-cell depletion in refractory rheumatoid arthritis patients preferentially affects autoreactive more than protective humoral immunity. *Arthritis Res Ther*, 14(2):R57.
- Wheeler G, Elshahaly M, Tuck SP, Datta HK, van Laar JM (2013) The clinical utility of bone marker measurements in osteoporosis. *J Transl Med*, 11:201.
- Wheeler G, Goodrum C, Tuck SP, Datta HK, van Laar JM (2014) Method-specific differences in  $\beta$ -isomerised carboxy-terminal cross-linking telopeptide of type I collagen and procollagen type I aminoterminal propeptide using two fully automated immunoassays. *Clin Chem Lab Med*, 52(7):e135–e138.

### Submitted for publication

- Wheeler G, Elshahaly M, Naraghi K, Tuck SP, Datta HK, van Laar JM, on behalf of the HORUS trial investigator group (2017) Changes in bone density and bone turnover in patients with rheumatoid arthritis treated with rituximab, results from an open-label, single treatment arm, prospective clinical trial.

## Abstracts

- Wheater G, Hogan VE, Teng YKO, Tekstra J, Tuck SP, Lafeber FP, Bijlsma JWJ, Francis RM, Datta HK, van Laar JM (2010) Effects of rituximab on bone turnover in patients with rheumatoid arthritis. *Osteoporos Int*, 21(supplement3):P156:iii101.
- Wheater G, Hogan VE, Teng YKO, Tekstra J, Tuck SP, Lafeber FP, Bijlsma JWJ, Francis RM, Datta HK, van Laar JM (2010) Effects of rituximab on bone turnover in patients with rheumatoid arthritis. *Ann Rheum Dis*, EULAR poster June 2010.
- Wheater G, Hogan VE, Teng YKO, Tekstra J, Tuck SP, Lafeber FP, Bijlsma JWJ, Francis RM, Datta HK, van Laar JM (2011) Effects of rituximab on bone turnover in patients with rheumatoid arthritis. *Rheumatology (Oxford)*, 50(supplement 3):P6:S463
- Wheater G, Elshahaly M, Tuck SP, Drury J, van Laar JM (2013) Bone marker reference range study: a comparison of the manufacturer's reference range and laboratory healthy volunteer results to patients with rheumatoid arthritis. *BMC Musculoskeletal Disorders*, 14(supplement 1):A3.